PROCEEDINGS OF THE 21st INTERNATIONAL MINING CONGRESS OF TURKEY

MAY 6-8, 2009 Antalya/Turkey

Editors
Dr. Nejat TAMZOK Dr. Bülent TOKA

UCTEA
THE CHAMBER OF MINING ENGINEERS OF TURKEY

PROCEEDINGS OF THE 21ST INTERNATIONAL MINING CONGRESS AND EXHIBITION OF TURKEY

Edited by

Dr. Nejat TAMZOK
Dr. Bülent TOKA

THE CHAMBER OF MINING
ENGINEERS OF TURKEY

The volume of proceeding was sponsored by DEMİR EXPORT CO.

This Congress is supported by TÜBİTAK (The Scientific and Technological Research Council of Turkey)

Published by Grup Matbaacılık, Ankara, Turkey
Phone: +90 (312) 384 73 44 Fax: +90 (312) 384 73 46

Publication No: 156
ISBN 978-9944-89-715-0

Address: Selanik Cad. No:19/3 06650 – Kızılay, Ankara-Turkey
Phone : +90 (312) 425 10 80
Fax : +90 (312) 417 52 90
Web : www.maden.org.tr
E-mail : maden@maden.org.tr

FOREWORD

"We assume this Congress as the beginning of the great many perfect mining congresses in our country." These words were from the foreword of the First Scientific and Technical Mining Congress of Turkey in 1969. To realize this aim, mining congresses of Turkey have been transformed into an international platform in which legal, economic and social subjects related with the mining industry as well as scientific and technological advancements in the sector could be discussed within the forty years. Today, our mining congresses generate a suitable environment for our colleagues and industry representatives in every two years.

In this congress, the papers those took part in the proceedings' book have been accepted among approximately 170 papers submitted by scientists and practitioners. All papers have been reviewed accurately by the members of the scientific committee and finally 114 papers have been accepted to publish in the Congress' Book. In addition, totally 28 mining companies, state owned or private, have participated in the exhibition realized together with the Congress.

We should like to offer our thanks to the members of the Executive Committee and Scientific Committee for their tremendous contribution, to all authors, to the keynote speakers and also to all companies that sponsored the Congress.

Asım KUTLUATA
Chairman
Executive Committee

Mehmet TORUN
Chairman
The Chamber of Mining
Engineers of Turkey

Member of Boards of the Chamber

President	: Mehmet TORUN
II. President	: Fatma Berna VATAN
Secretary	: Nahit ARI
Treasurer	: Cemalettin Sağtekin
	Niyazi KARADENİZ
	İbrahim YILMAZOĞLU
	Mehmet GÜLER

Executive Committee of the Congress

President	: Asım KUTLUATA
Secretary	: Nadir AVŞAROĞLU
Members	: Yusuf Ziya AKGÖK
	Nahit ARI
	Ali ÖNEMLİ
	Nejat TAMZOK
	Bülent TOKA
	İbrahim YILMAZOĞLU

Scientific Committee

Dr. Ali AKAR
Dr. Hamdi AKÇAKOCA
Dr. Ata Utku AKÇIL
Dr. Nuri Ali AKÇİN
Dr. Hürriyet AKDAŞ
Yusuf Ziya AKGÖL
Dr. Raşit ALTINDAĞ
Dr. Mesut ANIL
Dr. Ergin ARIOĞLU
Dr. Ali İhsan AROL
Dr. A. Fatma ARSLAN
Dr. Vedat ARSLAN
Dr. M. Ümit ATALAY
Dr. Ümit ATICI
Nadir AVŞAROĞLU
Dr. Hamit AYDIN
Yusuf AYDIN
Dr. Kerim AYDINER
Dr. Mustafa AYHAN
Dr. Ahmet Tuğrul BAŞOKUR
Dr. Turan BATAR
Dr. Oktay BAYAT
Dr. İrfan BAYRAKTAR
Dr. İsmail BENTLİ
Dr. Nuh BİLGİN
Dr. Mustafa BİRİNCİ
Dr. Volkan BOZKURT
Dr. Mehmet CANBAZOĞLU
Dr. M. Emin CANDANSAYAR
Dr. Yakup CEBECİ
Dr. Ahmet Kemal CENGİZ
Ekrem CENGİZ
Dr. Atilla CEYLANOĞLU
Dr. İlknur CÖCEN
İmam ÇELİK
Dr. M. Sabri ÇELİK
Dr. Emin Cafer ÇİLEK
Dr. Alaattin ÇAKIR
Dr. Yaşar ÇİLİNGİR
Dr. Hanifi ÇOPUR
Dr. Dilek ÇUHADAROĞLU
Dr. A. Hamdi DELİORMANLI
Dr. Ahmet DEMİRCİ
Dr. Halim DEMİREL
Dr. Nuray DEMİREL
Hürriyet DEMİRHAN
Dr. Hacı DEVECİ
Dr. Vedat DİDARİ
Dr. Çağatay DİKMEN
Ahmet DİNÇER
Dr. H. Şebnem Başkan DÜZGÜN
Dr. İ. Göktay EDİZ
Dr. Zafir EKMEKÇİ
Dr. Birol ELEVLİ
Zerrin ENTOK
Dr. Selamet Gürbüz ERÇELEBİ
Dr. Bülent ERDEM
Dr. Mustafa ERDOĞAN
Dr. Levent ERGÜN
Dr. Bahri ERSOY
Dr. Metin ERSOY
Mücella ERSOY
Dr. Şinasi ESKİKAYA
Abdulgani EŞİYOK
Dr. Hasan GERÇEK
Dr. İsmail GİRGİN
Dr. Mete GÖKTAN
Dr. M. Cemal GÖNCÜOĞLU
Uğur GÖNÜLALAN
Dr.Kazım GÖRGÜLÜ
Dr. Nilgün GÜLEÇ
Dr. OGUZ GÜNDOĞDU
Dr. Lütfullah GÜNDÜZ
Oğuz GÜNER
Dr. Özcan GÜRSOY
Dr. Tevfik GÜYAGÜLER
Dr. Mehmet Ali HİNDİSTAN
Dr. Çetin HOŞTEN
Dr. Halil İPEK
Dr. Üner İPEKOĞLU
Dr. Ali KAHRİMAN
Dr. Fikri KAHRAMAN
Galip KALAYCIOĞLU
Mehmet KARADENİZ
Dr. Dogan KARAKUŞ
Dr. Nuray KARAPINAR

Dr. Celal KARPUZ
Dr. Cemal KAYA
Dr. Erol KAYA
Mehmet KAYADELEN
Musa KAYNAR
Dr. Mevlüt KEMAL
Dr. Ayhan KESİMAL
Halil İbrahim KIRŞAN
Dr. Yaşar KİBİCİ
Dr. Ahmet Mahmut KILIÇ
Dr. Alaettin KILIÇ
Dr. Sait KIZGUT
Dr. Sabiha KOCA
Dr. Adnan KONUK
Dr. Halil KÖSE
Dr. Seyfi KULAKSIZ
Dr. Haldun KURAMA
Dr. Orhan KURAL
Asım KUTLUATA
Dr. Cengiz KUZU
Şaban KÜÇÜK
Selami LELOĞLU
Dr. Yadigar V. MÜFTÜOĞLU
İlhan ODABAŞI
Dr. Turgay ONARGAN
Dr. Ahmet Hakan ONUR
Dr. Güner ÖNCE
Ali ÖNEMLİ
Dr. Bahri ÖTEYAKA
Dr. Ahmet ÖZARSLAN
Dr. M. Evren ÖZBAYOĞLU
Dr. Gülhan ÖZBAYOĞLU
Dr. Yılmaz ÖZÇELİK
Dr. Hüseyin ÖZDAĞ
Dr. Metin ÖZDOĞAN
Dr. Ümit ÖZER
Mesut ÖZTÜRK
Hakkı Tarık ÖZKAHRAMAN
Dr. Şafak G. ÖZKAN
Dr. Eyüp SABAH
Sabahatdin SAKATOĞLU
Dr. Cem SARAÇ
Dr. M. Saim SARAÇ
Dr. Ömer Lütfi SÜL
Dr. Ender SÖNMEZ
Dr. Cem ŞENSÖĞÜT
Dr. Şakir ŞİMŞEK
Dr. Adem TAŞDEMİR
Dr. Nejat TAMZOK
Dr. Abdullah Erhan TERCAN
Dr. Bülent TOKA
Dr. Selami TOPRAK
Dr. İhsan TOROĞLU
Mehmet TORUN
Mehmet TUĞRAN
Dr. Levent TUTLUOĞLU
Dr. Nuray TOKGÖZ
Halil TÜRKMEN
Dr.İbrahim UĞUR
Dr. İsmail UGUR
Dr. Veli UZ
Sait ULUIŞIK
Dr. Yaşar ÜÇBAŞ
Dr. Ahmet ÜÇER
Dr. Ali UÇAR
Dr. Bekir Zühtü UYSAL
Veli ÜNAL
Dr. Taner ÜNLÜ
Dr. Tuğrul ÜNLÜ
Dr. Bahtiyar ÜNVER
Ömer ÜNVER
Dr. Mahir VARDAR
Berna Fatma VATAN
Dr. Ercüment YALÇIN
Dr. Ahmet YAMIK
Dr. Olgay YARALI
Dr. Hüseyin YAVUZ
Dr. Mahmut YAVUZ
Dr. Meftuni YEKELER
Ömer YENEL
Levent YENER
Liyaddin YEŞİLKAYA
Fehmi YILDIRIM
Dr. Mehmet YILDIRIM
Dr. Ahmet YILDIZ
Necati YILDIZ
Öner YILMAZ
Mustafa YÖRÜKOĞLU
Dr. A. Ekrem YÜCE

Contents

Miscellaneous

Mining Economics

The Economic Crisis and Mining – a Global Trade Union Perspective

Joseph Drexler
International Federation of Chemical, Energy, Mine and General Workers' Unions

The International Federation of Chemical, Energy, Mine and General Workers' Unions (ICEM) is a global trade union federation representing over 400 national trade unions in over 130 countries. The ICEM is the main global federation in the mining industry with over 60 affiliated national mining unions. We are pleased to have several unions in Turkey representing miners and other mine employees officially affiliated with the ICEM.

We exist to organize and build trade union power in the industrial sectors of chemical, energy, mining, rubber, tire, paper, glass and industrial materials. Organizing global trade union power in a world where the economy is increasingly globalized and concentrated is absolutely necessary,. Worker power must be organized globally to confront the immense challenge of providing decent work and ensuring that workers secure a fair share of the wealth created by their labor.

The specific functions of the ICEM are:

- negotiating and monitoring global agreements with multinational companies - mainly on workers' rights, equality at work and the highest standards of health, safety and environmental protection worldwide
- networking of trade union representatives within global corporations
- coordinating solidarity and support for member unions during disputes
- union-building in countries where unions are weak or non-existent
- providing information and expertise on topics ranging from collective bargaining to health and safety standards
- representing workers' interests within the UN, its agencies and other intergovernmental bodies
- skills training and development work with trade union officers and rank-and-file union members.

ICEM and Mining

Mining trade unions have always played a key role in the development of the trade union movement throughout the world. Even in countries where mining has declined, the influence of mining unions is still felt. It is notable that both

the president and general secretary of the ICEM are from national mining unions.

Our key work in mining has consisted mainly of developing global and regional coordination of mining unions through conferences, workshops and networks. We provide direct assistance to mining trade unions experiencing labor disputes by organizing broad networks of support. We encourage mining unions in respective countries to put aside ideological differences and to work together in confronting many challenges set forth by employers. We also help to organize assistance for mining trade unions in developing countries from more established and better financed trade unions. We provide a key global perspective to many of the problems that mining unions face.

Currently, the ICEM is directly engaged in advocating for improved health and safety standards in mining countries through the ratification of International Labour Organization (ILO) Convention 176 on Health and Safety in Mines. On April 28th, which has been designated by the United Nations and ILO as "World Day for Safety and Health at Work", the ICEM announced the start of its global campaign to promote ratification of the convention. So far, only 22 countries have ratified. Turkey has not yet ratified the convention, and we call on trade unions, employers and the government to work together for ratification. Among European Union mining countries, only Bulgaria, Romania and Serbia have not ratified the convention. The ICEM is prepared to work with trade unions, employers and government institutions in Turkey to secure ratification of the convention.

The ICEM works closely with several non-governmental organizations (NGOs) to challenge the unsustainable practices by many multinational companies that exploit workers, damage the environment, and disrupt communities. Consistent efforts have been underway to make mining companies practices transparent and hold them accountable for these practices. We keep open channels of communication with the International Council on Metals and Mining, the main global employers' organization in mining, and with the Responsible Jewellery Council, which seeks to ensure that precious metals and gems are mined in a responsible manner. We routinely challenge these global organizations to demonstrate improved industry practices. The Global Reporting Initiative, in which the ICEM participates directly, requires that mining companies report more honestly and openly on their practices. We believe strongly that improved reporting will lead to positive changes in practices.

Campaigning is central to what the ICEM does. Among these campaigns is a global effort to stop the Mexican government and Grupo Mexico, one of the largest mining companies in the world, from crushing the Mexican miners union known as Los Mineros; establishing a global network for unions representing workers at Xstrata, one of the largest mining companies in the world; challenging both Chinese and multinational corporate investment in mining in Africa to ensure that long-term development occurs; and fighting efforts to privatize mines in countries such as India.

Climate change and controlling greenhouse gas emissions is a critical challenge for the ICEM, since we represent trade unions in sectors which will be profoundly impacted on how climate change is addressed. The ICEM is a key member of a task force created by

the International Trade Union Congress consisting of national trade union centers throughout the world to address the climate change process. We have been a forceful advocate for increased research and funding for clean coal technologies and insisting that these technologies are placed at the forefront of the debate and in finding solutions. The ICEM strongly advocates for the development of Carbon Capture and Storage technology as a way to address both the need for coal as an energy source, particularly in developing countries, and reductions in greenhouse gas emissions. The ICEM also supports real and implementable "just transition" policies to ensure that workers who lose their jobs as result of addressing climate change will receive adequate income, training and jobs. We challenge NGOs, environmental organizations and other global federations to develop concrete implementable "just transition" policies.

Finally, the ICEM plays the leading role among global trade union federations in addressing the adverse effects of contract or agency labor, which undermines trade unions, lowers wages and benefits, and reduces safety practices. Mining companies are increasingly resorting to use of contract labor, condemning those workers and their families to a life of poverty, insecurity, and inadequate health care. Use of inexperienced, ill-trained and itinerant miners can also pose major safety hazards.

Background to The Global Economic Crisis and Mining

The global economic crisis is severely impacting all aspects of mining. However, the crisis in mining cannot be separated from the overall global economic meltdown that was predicated on a variety of factors,

Mining in the last 150 years can be characterized by a gradual global shift from developed countries to developing countries. Although mining has been practiced for millennia, the industrial revolution propelled mining to the forefront of the economies of most industrial nations. However, as sources of nonrenewable raw materials declined, particularly in Western Europe, demand for these products by Western countries

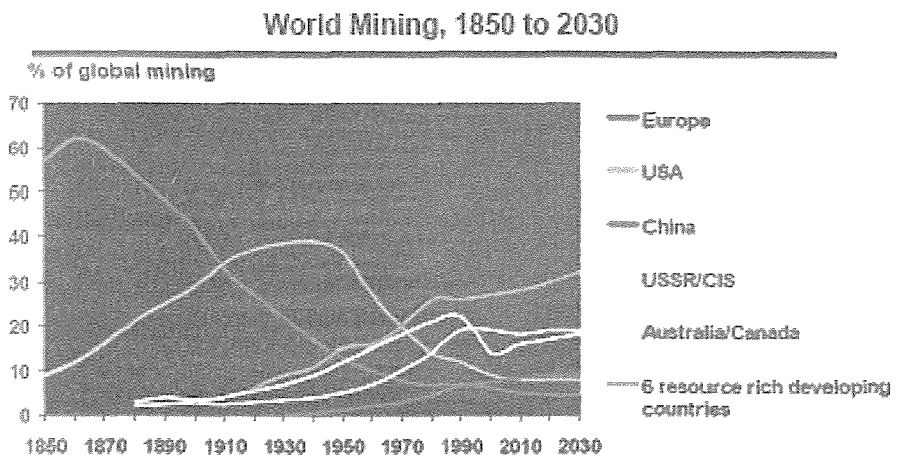

Sources: Raw Materials Data, Stockholm 2004 and Sames.

TNCs IN GLOBAL MINING

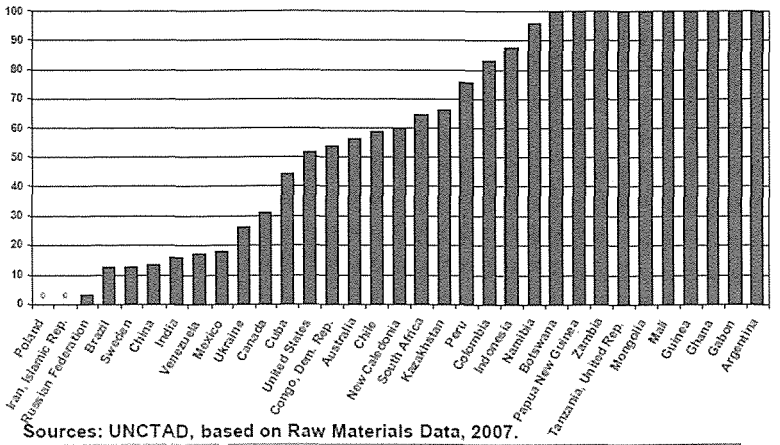

Sources: UNCTAD, based on Raw Materials Data, 2007.

Raw Materials Group

resulted in colonization of many countries and later economic control by multinational enterprises (MNEs) over these raw materials. The graph below illustrates the change in the output of mining over the last 150 years.

The more recent emergence of mining industries in many developing countries was made possible through foreign direct investments (FDI) of western MNEs. Privatization of mines was strongly supported by Western international organizations, such as the IMF, and the MNEs picked up the pieces as state mining industries collapsed, and penetrated the economies of many nations. Most developing countries have a mining industry that is dominated by foreign companies..

Many developing countries are highly dependent on mining as a source of income and foreign exchange.

Beginning in 2002, there was an enormous spike in the prices of all raw materials including coal, metal and precious stones. Most mining companies made unprecedented profits which even rivaled some of the oil companies. As profits rose, the wages and salaries of miners did not rise accordingly. While operating expenditures and income tax increased somewhat, revenue and profit soared.

Net Indexed Growth of the 40 Largest Mining Companies

Profits of the major mining companies were used to acquire smaller companies and new sources of raw materials. Mergers and takeover abounded in the mining industry. Executive salaries and bonuses, which were pegged to acquisitions, further incentivized the increasing concentration of the industry.

Mining Consolidation in 2007

According to the Raw Materials Group, 149 mining companies today control approximately 83% of total global

Dependence on Metal Mining as a Percent of Total Exports by Country

Economy	Ores and metals	Product description
Guinea	89.2	Bauxite, alumina, gold and diamonds
Botswana	87.2	Diamonds, copper, nickel
Suriname	70.0	Alumina (aluminium oxide)
Zambia	61.5	Copper, cobalt
Jamaica	60.8	Alumina, bauxite
Niger	46.1	Uranium and gold
Chile	45.2	Copper
Mozambique	42.3	Aluminium
Papua New Guinea	36.6	Gold, copper
Congo Republic	34.0	Various metals
Ghana	33.3	Gold
Cuba	33.2	Nickel
Peru	32.0	Gold, copper, zinc
Rwanda	32.2	Various metals
Uzbekistan	30.3	Gold
Georgia	24.9	Various metals
South Africa	21.7	Platinum, gold
Bolivia	19.1	Zinc, gold
Kazakhstan	18.0	Various metals
Bahrain	16.2	Aluminium

Source: UNCTD World Investment Report 2007

some larger mining companies attempt to acquire smaller mining companies at cheaper prices in the current economic downturn.

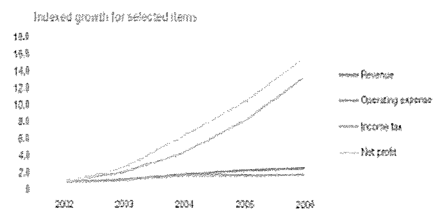

Source: PricewaterhouseCoopers Review of Metal and Mining: Review of Global Trends in the Mining Industry – 2007

Rising demand and commodity prices were in large part fueled by the unparalleled growth of the BRIC (Brazil, Russia, India and China) countries as well as overconsumption in the West based on phantom capital. Equally important in changing the landscape of mining was the emergence of the BRIC countries as not only as consumers of mining raw materials but as the location of major private and state-controlled global mining companies. Valle (formerly CVRD) of Brazil became the fourth largest mining company in the world. Norlisk Nickel of Russia became the world's largest nickel mining company. Vendata of India and China Shenhua became major players in iron ore, coal and copper. This was also accompanied by the emergence of major global steel industry giants such as Arcelor Mittal and and Tata of India.

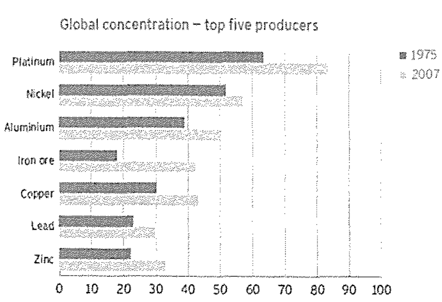

China in particular has emerged as a major global player in the mining industry. Through its $1 trillion (USD) sovereign wealth fund, which has been used as a "carrot" to secure access to metals and other raw materials in other counties, the Chinese government constructs schools, roads, stadiums and opera houses to gain access to mining raw materials, particularly in Africa.. The acquisition of raw materials, not in sufficient supply in China, is necessary to fulfill the Chinese government's ambitious plans for continued growth. Unfettered by transparency, China has been able to out-compete MNEs for raw material access. The CEOs of several global mining companies held a meeting last year with the World Bank and IMF to lobby these institutions to offer aid similar the Chinese government so the MNEs could effectively compete.

Available reports indicate that Chinese mining operations that were established during the boom years of high commodity prices were some of the worst abusers of worker, environmental and human rights. Some Chinese companies imported the entire labor force from China, and there has been little knowledge transfer to indigenous populations. Many Chinese companies which employed local workers have paid wages lower than industry standards and provided no benefits. Safety laws and regulations have been routinely ignored.

Figure 3: Top Ten - mining deals 2007

No.	Value of transaction ($m)	Date announced	Buyers	Sellers	Primary Continent
1	[illegible]	11 Jul 07	Rio Tinto plc	Alcan Inc	North America
2	[illegible]	[illegible]	UC Rusal	[illegible]	Russian Federation
3	[illegible]	[illegible]	Norilsk Nickel OAO	LionOre Mining International Ltd	North America
4	[illegible]	[illegible]	Teck Cominco Ltd	Aur Resources Inc	North America
5	[illegible]	[illegible]	Yamana Gold Inc	Meridian Gold Inc	North America
6	[illegible]	[illegible]	SXR Uranium One Inc	UrAsia Energy Ltd	Asia Pacific
7	[illegible]	[illegible]	Xstrata plc	Jubilee Mines NL	Asia Pacific
8	[illegible]	[illegible]	BHP Billiton Ltd & plc	BHP Billiton Ltd & plc [illegible]	Asia Pacific
9	[illegible]	[illegible]	[illegible]	AngloGold Ashanti Ltd [illegible]	Africa
10	[illegible]	[illegible]	[illegible]	[illegible]	Africa

Source: PricewaterhouseCoopers, Mining Deals Annual Review 2007, based on published transactions from the Dealogic 'M&A Global' database, December 2007

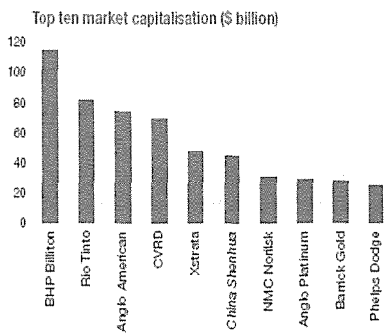

Source: Datastream

The Current Crisis and Mining

Metal prices have fallen dramatically since peaking in 2008. The main exception is gold, due to investors seeking new ways to store assets and convert cash into something tangible. Coal prices have also declined, but they are still far above what they were a decade ago. The biggest drop in coal demand has been in coking coal as steel production has declined with falling manufacturing.

Companies that once stated their largest need was for skilled workers have been laying off miners in droves. Hundreds of thousands have lost their jobs. All major mining countries, developed and developing, have been hit very hard by the crisis. Australia and Canada have been affected by both the decline in metal commodity prices and the decline in the steel industry. Russia has seen steep declines in mining employment, and the Ukraine, a major coal and iron ore producer, hovers on the verge of bankruptcy. Their main mining and steel region in Donetsk has seen 50,000 workers laid off or working reduced hours. Trade unions in Zambia, South Africa, and Namibia are struggling to keep workers on payrolls. Brazil, China and India may generate enough internal demand to keep mines in the country operating at higher levels than in other parts of the world, but they are also experiencing significant recessionary impacts.

It is expected that some companies will not survive the current crisis and a new wave of mergers and acquisitions will occur, leading to even greater concentration than before. In addition, companies in a better cash position, credit ratings and access to lenders will be the long-term beneficiaries of the crisis by being able to gobble up smaller companies at much cheaper prices.

Xstrata is closing mining facilities throughout the globe, not only in response to slacking demand but also due to heavy debt from expensive acquisitions. Rio Tinto, which acquired Alcan Inc., is now so heavily debt that it had to reach out to Chinalco, a Chinese company, for a capital infusion. The Chinalco investment now faces major political hurdles due to concerns by the Construction, Forestry, Mining and Energy Union, Australia's main mining union, and the Australian government. The Chinese government, which previously opposed the BHP takeover of Rio Tinto, is being accused of attempting to corner the iron ore market, a charge the Chinese government made against BHP. Chinese investment in Africa is also experiencing a turn. Some Chinese companies have packed up and left without paying their workforce or

suppliers. China is now driving a harder bargain with African countries where it is still investing. There are reports of Chinese companies abandoning some of their African operations and leaving workers unpaid and communities damaged in the wake of the economic downturn.

How Trade Unions Are Reacting to the Economic Crisis and Downturn in Mining

The current crisis is the most profound since the Great Depression. However, what marks this crisis will not be the staggering impact in industrialized countries but in the less developed countries, where over a billion persons live in abject poverty and regular employment is in many areas almost nonexistent. The United Nations estimates that over 200 million additional people will be thrown into extreme poverty due to the economic crisis, and the number of persons surviving on less than $2 per day will rise to 1.4 billion. Mining communities, isolated, with mining providing the main or sole source of gainful employment, will be impacted greatly. Some mining countries will experience major decreases in foreign exchange and will be not able to purchase enough food for their populations without major increases in foreign aid.

A solution to the mining crisis is linked to a solution to the overall global financial crisis. The ICEM participated in the development of a joint strategy to address the current economic crisis from a trade union perspective. The program calls for an end to the neoliberal policies that have dominated world trade and financial markets for the past several decades. In its place must be a new system of global and national regulations to ensure that the current cause of the crisis is dealt with and will not happen again. The ICEM is demanding major reform of the international institutions that not only contributed to the crisis but who destroyed or prevented the development of social safety nets. However, these changes cannot occur without trade unions and their international representatives having a seat at the table where policies are being negotiated. Getting a seat at the table will require more pronounced actions by trade unions in all countries and higher levels of national and international trade union organization and mobilization.

Each national mining union has dealt with the crisis differently based on the power relations in in each country and the current balance of power between trade unions and employers. There has been no clear pattern that has emerged, and mining trade unions, although holding some contractual power or other rights as afforded under national laws, are struggling to face the crisis.

The most radical approach to mining has emerged in Latin America, where some left-wing governments have been passing laws to nationalize the mining industry and take control away from multinational companies. It is not clear if the trade unions, although generally supporting the effort, have been central to these decisions on nationalization. Mining trade unions in Latin America tend to be highly fragmented based on ideology. Venezuela started its program to nationalize mines in 2007. The effort includes the nationalization of small scale mines in order to integrate them in national enterprises and take control over strategic minerals such as gold, diamonds, bauxite and uranium. Bolivia has begun steps to nationalize mines.

In Africa, there is also growing

sentiment for nationalization of mines, but the main impetus is coming from the trade unions. The Mineworkers Union of Zambia has demanded that mine owners intending to close mines surrender the entire assets of the mines to the government. The union has taken the position that the assets of any mine to be closed should be turned over to the government, and mining companies should not be permitted to select which assets should be taken over, thereby allowing only the best assets to remain in private hands. The union is also supporting the formation of a national task force from various disciplines to look more closely at nationalization and how mining can be utilized more effectively to contribute to the wealth of the country.

The Mineworkers Union of Namibia (MUN) has been openly supporting the nationalization of mines. MUN president Andries Eiseb has stated that "the MUN can no longer allow multinational companies to rape Namibian resources and disappear." The union has proposed full cooperation with the government in determining how nationalization should occur and to develop an educational process that would equip workers and trade unionists with business acumen to operate the mines. This demand came on the heels of an announcement by London-based Weatherly PLC that it would shut down its copper mine and smelter, sacking over 2,000 miners and trade union members. The MUN has maintained a flexible position on the question of nationalization that includes the government and workers having an equity position in the mine.

In South Africa, the National Union of Mineworkers (NUM) has threatened strikes in the face of layoffs. Lonmin, the world's third largest platinum producer, announced in 2008 that it would sack over 5,000 miners at its main platinum mines due to a 50% drop in the price of platinum from slumping global auto sales. However, an agreement was later reached. Currently, the use of strikes to leverage employers over layoffs is on hold.

How mining unions address the economic crisis is clearly a function of their power and relationships with mining employers and respective governments. The ICEM proposes that mining trade unions consider the following in the face of massive layoffs:

1) The mining industry has been enormously profitable prior to the economic downturn, and most mining companies, private or state controlled, have accrued significant revenues and profits. The miners who extracted the minerals, precious stones and metal from the earth provided the source of the profits. Therefore, the first responsibility of employers should be to protect the workers in this economic downturn.

2) Actions should be taken against employers who are using the crisis to extract unfair concessions. Trade unions must demand access to financial data to ensure concessions are justified. If concessions are granted, provisions should be made for recovery of lost wages and benefits once mines return to profitability.

3) When concessions are granted, mining trade unions should use the current situation as an opportunity to extract non-economic concessions from employers such as an agreement to allow contract workers to unionize and become part of the permanent work force once a mine returns to full production, or a commitment to improve health and safety and campaign actively for ratification of ILO 176.

4) Although no one can predict when the current global economic crisis will end, when recovery occurs commodity prices are likely to increase dramatically due to constricted supply since both mine production and exploration have dropped dramatically. Those employers who have skilled workers in place and have kept mining operations viable will be in a unique position to take full advantage of an economic recovery.

5) Mining companies have consistently cited a shortage of skilled workers as a major problem in the mining industry, and sacking skilled workers may be creating a severe disadvantage when the global economy recovers.

6) Capital shortages to keep current mines operating and maintaining employment of skilled workers can be partly due to enormous debt incurred by some companies to fund acquisitions and soaring executive pay which in turn rewarded acquisitions and debt. Miners should not have to pay the price for the unwillingness of mining companies to retain sufficient capital.

7) The current economic crisis may lead to further conglomeration in the mining industry, as larger companies seek to acquire smaller ones at cheaper prices. This will lead to more common global employers among trade unions and increase the need for global solidarity and bargaining.

8) Trade unions should increasingly challenge mining employers about their responsibilities to the communities where they operate and ensure sustainable development.

9) Mining trade unions should work with NGOs to build power in mining communities to address the economic crisis in these communities.

10) Mining trade unions should carefully consider legislation to make mining of non-renewable resources contribute to long-term sustainability.

For further information on the ICEM and mining, see www.icem.org

Sustainable Development In Mining Industry: An Indian Perspective

T. Kumar
Indian School of Mines University, Dhanbad

1 INTRODUCTION

The debate surrounding sustainable development in the mining industry is a drawn-out one, which has long gained considerable attention from a wide range of parties. The Brundtland Commission, in its landmark report *Our Common Future*, defined sustainable development as "meeting the needs of the present without compromising the ability of future generations to meet their own needs" (WCED, 1987). This definition, however, fails to outline an effective sustainability framework for any industry to follow. The Brundtland Report emphasizes that no single blueprint for sustainability exists and that the ways in which countries achieve sustainable development will vary among the different economic and political systems around the world (NRC, 1995), prompting a number of academics, industrialists and government employees to provide personal viewpoints on the applicability of sustainable development to mining. Consequently, the body of literature on this subject now contains a wide-range of interpretations, and increasingly it is becoming unclear as to how exactly mines can contribute to sustainable development.

Since the release of the Brundtland Commission's landmark report *Our Common Future*, 1987, there has been an increased commitment by both government and industry to environmental protection and extended socioeconomic responsibility. The Brundtland Report highlights the need to account for the impact of industrial activities and offers a vision of sustainable development; meeting the needs of the present without jeopardizing the requirements of future generations (WCED, 1987); that can be achieved through improved environmental management practices and socioeconomic performance. In government and corporate policy-making, a commitment to sustainable development, which integrates the needs of the environment, economy, and society, typically produces solutions that represent the 'best fit' for all parties impacted by decisions. Many governments and companies from a wide range of industrial sectors have finally recognized the merits of sustainable development and are now using it as a guiding principle in policy-making activities.

Although many have defined and applied the concept differently,

sustainable development, generally, is the combination of enhanced socioeconomic growth and development, and improved environmental protection and pollution prevention. It first received global endorsement as a management and developmental strategy at the highly popularized United Nations Conference on Environment and Development (UNCED), commonly known as the "Earth Summit", in Rio, 1992, where 116 Heads of State or Government, 8000 delegates from 172 countries, and 3000 accredited individuals from non-governmental organizations (UNCED,1992) gathered to discuss practical strategies for tackling pressing global problems. Sustainable development has since become a key focus of planning, environmental protection, and remediation efforts worldwide, and several academics and industrialists, in an attempt to operationalize the concept, have developed a number of policy frameworks, indicator sets, and management guidelines for use by governments and businesses.

Most of the discussions on mines, minerals, and sustainable development to date are concerned with sustainability at the global and national scales. Some authors (e.g. Brown, 1993; Auty and Warhurst, 1993; Mikesell, 1994; Tilton, 1996; Auty and Mikesell, 1998) provide perspectives on how the benefits of mineral production and use can be sustained from generation to generation. Primary examples include sustained mineral assets (prolonged longevity of reserves) through conservation, and increased minerals and metals recycling.

Others (Carbon, 1997; Miller, 1997) discuss the value of sustainable development as a guiding principle in mining environmental management. They argue that sustainable development has enormous utility when drafting key environmental codes of practice and in target setting, and or generally indicate that by preventing significant environmental problems from the outset, and by adopting proactive environmental standards, the mining industry can contribute to improved sustainability. Another group (e.g. James, 1999; Labonne, 1999; Eggert, 2000) view enhanced socioeconomic relations—more specifically, stakeholder consultation and participation—as an integral component of mine sustainability, or argue that social and cultural issues represent an important dimension of sustainable development.

Again, most of these and the other major mining sustainability pieces are global and national in focus, or are simply broad, holistic perspectives. However, very little attention has been paid to mines themselves and on interpreting the appropriate role of mining corporations. In response to this trend, the mining industry has shown increasing interest in environmental and social sustainability in recent years. This concern is evidenced by initiatives such as the formation of the International Council on Mining and Metals (ICMM); the Mining, Minerals and Sustainable Development (MMSD) report; the Global Reporting Initiative (GRI); the Mining Certification Evaluation Project (MCEP); and an alphabet soup of other acronyms.

The purpose of this paper, therefore, is to describe more clearly how mines can contribute to sustainable development, and to provide guidelines for mining companies seeking to operate more sustainably. The paper begins with an overview of mining industry with special reference to the Indian mining industry.

Then the sustainable development in the corporate mining context by examining the key environmental and socioeconomic issues in the industry is dealt with. Some guidelines are then presented as a performance tool for those mines keen on becoming more active in the arena of sustainable development. The paper concludes by presenting some case studies of Indian mines; the management of whose have been active in improving the sustainability of mine operations — in an attempt to illustrate how selected mining companies are embracing sustainable development at the corporate level.

2 OVERVIEW OF MINING SECTOR IN INDIA

Minerals which India is eminently endowed with are the back-bone of Indian economy. Geological evidence suggests that India is richly endowed with mineral resources. Explorations have found over 20,000 known mineral deposits and recoverable reserves of more than 60 minerals. 11 States account for 90 % of the total number of operational mines (Andhra Pradesh, Orissa, Chhattisgarh, Jharkhand, West Bengal, Maharashtra, Tamil Nadu, Gujarat, Madhya Pradesh, Rajasthan, and Karnataka). India produces 89 minerals including four fuel minerals, 52 non-metallic minerals, 11 metallic minerals and 22 minor minerals. Based on the 1996-97 production statistics, India stood as world's largest producer of mica blocks and mica splitting and ranked second in the production of chromites, third in coal & lignite, and barytes, fifth in iron ore, sixth in bauxite and manganese ore, eleventh in aluminium and twelfth in crude steel in the World (IBM, 1999). Fig1 shows the state wise distribution of the mineral deposits of the nation.

In comparison with many other sectors, the potential social and environmental issues associated with mining and mineral processing operations are both significant and complex to manage. The fixed location of the mineralized zone of interest imposes a constraint on all aspects of mining developments including the method of mining, location of mine facilities, requirements for new infrastructure and services (or conflict with existing infrastructure), and the suitability of waste management or disposal methods. The challenges with environmental assessment of mining projects are twofold. Firstly, environmental, social and health costs should be given adequate consideration while determining the economic viability. Secondly, adequate mitigation measures should be incorporated into the project cycle, including project design, implementation and decommissioning closure plans.

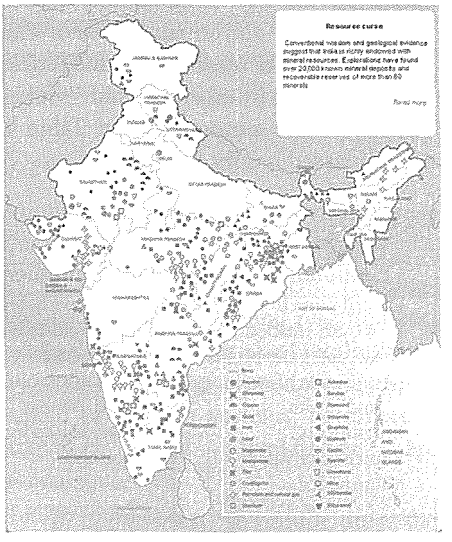

Figure 1: State wise Distribution of the Mineral Deposits of the India.

3 CURRENT THRUST AREAS

Sustainable development indicators translate sustainability issues usually into quantifiable measures of economic, environmental and social performance with the ultimate aim of helping address the key concerns. Identification of relevant issues, that capture the specific characteristics of each type of industry, is therefore crucial in the development of indicators. Addressing sustainable development requires a holistic approach based on life cycle thinking and mining and minerals industry is no exception to this. Thus, identification of sustainability issues must be done by considering all activities in the supply chain from 'cradle to grave'. Yet, without broadening the traditional system boundary and considering sustainability issues along the whole supply chains, the mining and minerals sector will not be able to respond appropriately to the challenge of sustainable development.

Following a widely accepted categorization of sustainability concerns, the key sustainability issues for the mining and minerals sector can be classified into three major categories: economic, environmental and social. The issues are summarized in Table 1 and discussed briefly below:

4 ENVIRONMENTAL AND SOCIAL CHALLENGES FACING THE MINING INDUSTRY

Mining in the country is associated with significant social and environmental impacts, mainly as a result of the large scale of mining activities and the significant expansion and dominance of open-cast mining.

4.1 Environmental Issues

It is important to understand the environmental impacts of mining. The choice of mining method is largely determined by the geology of the mineral deposit.

Some of the key environmental issues related to mining sector are:

4.1.1 Impact of Mining on Air Quality

Air pollution in mines is mainly due to the fugitive emissions of particulate matter and gases including methane, sulphur dioxide, oxides of nitrogen and carbon monooxide. The major operations producing dust are drilling, blasting, hauling, loading, transporting and crushing. Basically, dust sources in mines can be categorized as primary

Table 1: Summary of the Key Sustainability Issues for the Mining and Minerals Sectors

Economic issues	Environmental issues	Social issues
- Contribution to GDP and wealth creation - Costs, sales and profits - Distribution of revenue and health - Investments - Shareholder value - Value added	- Biodiversity loss - Emissions to air - Energy use - Global warming - Land use mgt. And rehabilitation - Nuisance - Product toxicity - Resource use and availability - Solid waste - Water use, effluents & lechates	- Bribery and corruption - Creation of employment - Employee education & skills development - Equal opportunities and non-discrimination - Health & safety - Human rights & business ethics - Labour/Mgt. Relation - Relationship with local community - Stakeholder involvement

(*Source:* Adisa Azapagic, 2003)

sources that generate the dust and secondary sources, which disperse the dust and carry it from place to place called as fugitive dust.

4.1.2 Impact of Mine Fires

A number of mines in the country are affected by fires leading to steady destruction of precious energy resource. The reason for mine fires presumably involves the phenomenon of spontaneous heating through two interrelated processes viz., the oxygen coal interaction or oxidative process and the thermal process. If remains uncontrolled, the fire could spread further through interconnected pathways and fissures in the strata. Mine fires give rise to several environmental problems besides safety hazards and economic losses. The major adverse impacts of mine fires are observed on all the four basic components of the environment viz. air, water, land and population (Singh, 2005).

4.1.3 Impact of Mining on Water regime

Mining and its associated activities not only uses a lot of water but also affects the hydrological regime of the district and often affects the water quality. The major hydrological impact of a large and deep opencast mine, however, is on the ground water regime of the region. The water seeping into the mine and collected in the mine sump is partly used up in the mine and the excess amount is discharged into the surface drainage system.

4.1.4 Impact of Mining on Land

Land is one of the most important resources for the human beings as this is needed for all the activities. Mining activities affect the land in various ways. Topography and land scenario changes due to digging of open pits, dumping of overburden rock mass in the form of the heaps and subsidence. Leachate from overburden dumps and other rock masses and polluted water from the pits affect the characteristics of the top-soil affecting the land-use. Disturbances in the effective land-use due to damage to the surface, sub-surface and underground water bodies.

4.1.5 Impact of Noise and Vibrations from Mining

A cumulative effect of all mining activities produces enormous noise and vibrations in the mining area, which constitutes a source of disturbance. The availability of large diameter, high capacity pneumatic drills, blasting of hundreds of tonnes of explosive etc. are identified as noise prone activities. Inpit crushing system with mobile crusher and large capacity materials handling plants are being installed to facilitate speedy handling of large quantities.

4.2 Social Issues

Mining and associated activities cause the following impacts on the society.

(i) Landlessness: MIDR (mining-induced displacement and resettlement) raises the significant risk of landlessness by removing the foundations upon which productive systems, commercial activities, and livelihoods are articulated.

(ii) Joblessness: In mining areas the land is taken for mining and associated activities the ethnic people loose their livelihood. Post-displacement

unemployment or underemployment is often chronic following the dismantling of the local income-generating resource base.

(iii) Homelessness: Defined as the "loss of house-plots, dwellings and shelter." For many people homelessness may be only temporary, but in poorly executed displacements, it remains chronic.

(iv)Risk of Marginalization: The risk of marginalization threatens displaced individuals and entire communities as they slip into lower socio-economic status relative to their local areas.

(v) Changes in population dynamics: All the manpower required for mining and associated activities comes from outside as such trained manpower is usually not available in ethnic population. Thus, the population dynamics of the area undergoes a major change over the years resulting in dilution of the ethnic population.

(vi)Cost of living: Increased industrial and economic activities generate more money and increase the buying power of the people directly and indirectly associated with these activities. This leads to an increase in the cost of living.

(vii)Health Risks: Recurring problems are reported with resettled populations gaining access to safe potable water and safe sanitation; increased diarrhoea, dysentery and epidemic infections often result.

(viii) Disruption of Formal Educational Activities: Displacement and relocation often cause a significant interruption in the functioning of schools and in child access to education during the year of transfer or for longer periods of time.

(ix) Addictions: Increased economic activities and affluence brings in more addictions in the society. In the tribal areas the ethnic people may also get affected by additional addictions. (Saxena & Pal, 2000)

(x) Economic disparity and frustration: Industrial and economic activities in mining complexes bring about economic disparity among the population living in the complexes.

(xi) Disparity of Women: The general perception is that women suffer from disproportional levels of poverty compared to men as evident from the employment figures for both the sexes. This observation is more pronounced in the mining sector .

5 THEORETICAL INTERPRETATION OF SUSTAINABLE DEVELOPMENT AND MINING

A major weakness of many sustainability interpretations and assessments is that 'sustainable development' is used interchangeably with 'environmental management' or 'environmental protection'. In such cases, there is the propensity to resolve only one type of problem — environmental deterioration — while ignoring the importance of economic and social goals (De Graaf et al., 1996), two equally important pillars of sustainable development. The focus of many mining sustainable development assessments has, too, been environmental protection, with little mentioning of socioeconomic needs. Crowson (1998), however, argues that if a mine is solely viewed from the standpoint of mineral exhaustion, then no operation is sustainable. As Emel et al. (1995) explain, many minerals sector firms have already joined other industries in going green, and some have used the

language of sustainable development in the context of the relationship between industry, environment and community. The sustainable development priority at the corporate level, therefore, is not mineral economics or prolonged mineral wealth for a nation's economy, but simply ensuring that all constituents of the environment and society that are potentially affected by mining operations are not adversely impacted by industrial activities.

5.1 Outlining the sustainable development agenda for mines

Sustainable development, however, extends beyond simply committing to improving environmental performance. Achieving this can be an enormous challenge for firms since most perceive mining activities as being environmentally and ecologically destructive. Being socially active, such as providing locals with employment benefits, contributing to pension funds, and utilizing local services, eases community acceptance of mining operations, and in turn contributes to sustainable development.

6 NEED FOR SUSTAINABLE DEVELOPMENT POLICIES IN INDIAN MINING SECTOR

The greatest need of sustainable development in mining is simply because of its propensity to cause significant environmental damage on numerous fronts. It is therefore imperative for the Indian government and Indian mining companies themselves to have a clear understanding of industry priorities in both the socioeconomic and environmental arenas, to become more rigorous in sustainable development goal setting, and to strive toward continuous industrial improvement. Mining companies and selected governmental groups have set important goals and have undertaken a number of activities in an attempt to operationalize sustainable development. It is clear from their policy-making activities that both groups are now carefully planning for sustainable development. Thus, carrying out of these goals will help achieve a more desirable socioeconomic-environmental balance, hence contributing to improved sustainability in the industry. The sections to follow are devoted to examining more extensively the sustainable development policy-making efforts in the Indian mining industry.

6.1 Key Mining Policies

The management of mineral resources in India is the responsibility of both Central Government and State Governments as per the Constitution of India. The Mines and Minerals Development and Regulation Act, 1957, and the Mines Act, 1952, together with the rules and regulations framed under them, constitute the basic laws governing the mining sector in India. The Mineral Conservation and Development Rules, 1988 lays down guidelines for ensuring mining on a scientific basis, while at the same time, conserving the environment. The minor minerals are separately notified and come under the purview of the State Governments. All mining activities have to comply with the environmental legislation of India as specified in various acts particularly the act Forest Conservation Act (1980) in conjunction with the EIA Notification 2006.

6.2 Environmental Clearance process

As per EIA Notification various projects required environmental clearances are categorized as 'A' & 'B' Categories. Mining projects having more than 50 ha lease area are classified as Category 'A' while less than 50 ha lease area in Category B. Asbestos Mining irrespective of lease area classified as 'A'.

All projects or activities included as Category 'A' in the Schedule, including expansion and modernization of existing projects or activities and change in product mix, shall require prior environmental clearance from the Central Government in the Ministry of Environment and Forests (MoEF) on the recommendations of an Expert Appraisal Committee (EAC) to be constituted by the Central Government for the purposes of this notification,

All projects or activities included as Category 'B' in the Schedule, including expansion and modernization of existing projects *will* require prior environmental clearance from the State/Union territory Environment Impact Assessment Authority (SEIAA). The SEIAA shall base its decision on the recommendations of a State or Union territory level Expert Appraisal Committee (SEAC) as to be constituted for in this notification. In the absence of a duly constituted SEIAA or SEAC, a Category 'B' project shall be treated as a Category 'A' project.

The environmental clearance process for new projects will comprise of a maximum of four stages, all of which may not apply to particular cases as set forth below in this notification. These four stages in sequential order are:-

- Screening (Only for Category 'B' projects and activities)
- Scoping
- Public Consultation
- Appraisal

Screening

In case of Category 'B' projects or activities, this stage will entail the scrutiny of an application seeking prior environmental clearance made in Form 1 by the concerned State level Expert Appraisal Committee (SEAC) for determining whether or not the project or activity requires further environmental studies for preparation of an Environmental Impact Assessment (EIA) for its appraisal prior to the grant of environmental clearance depending up on the nature and location specificity of the project . The projects requiring an Environmental Impact Assessment report shall be termed Category 'B1' and remaining projects shall be termed Category 'B2' and will not require an Environment Impact Assessment report.

Scoping

"Scoping": refers to the process by which the Expert Appraisal Committee in the case of Category 'A' projects or activities, and State level Expert Appraisal Committee in the case of Category 'B1' projects or activities, including applications for expansion and/or modernization and/or change in product mix of existing projects or activities, determine detailed and comprehensive Terms Of Reference (TOR) addressing all relevant environmental concerns for the preparation of an Environment Impact Assessment (EIA) Report in respect of the project or activity for which prior environmental clearance is sought. The Expert Appraisal Committee or State level Expert Appraisal Committee concerned shall determine the Terms of Reference on the basis of the information furnished in the prescribed application Form1/Form 1A including Terns of Reference proposed by the applicant.

The Terms of Reference (TOR) shall be conveyed to the applicant by the Expert Appraisal Committee or State Level Expert Appraisal Committee as concerned within sixty days of the receipt of Form 1. The approved Terms of Reference shall be displayed on the website of the Ministry of Environment and Forests and the concerned State Level Environment Impact Assessment Authority.

Applications for prior environmental clearance may be rejected by the regulatory authority concerned on the recommendation of the EAC or SEAC concerned at this stage itself. In case of such rejection, the decision together with reasons for the same shall be communicated to the applicant in writing within sixty days of the receipt of the application.

Public Consultation

"Public Consultation" refers to the process by which the concerns of local affected persons and others who have plausible stake in the environmental impacts of the project or activity are ascertained with a view to taking into account all the material concerns in the project or activity design as appropriate. All Category 'A' and Category B1 projects or activities shall undertake Public Consultation, except the few listed in EIA notification 2006. following:-

The Public Consultation shall ordinarily have two components comprising of:-

(a) A public hearing at the site or in its close proximity- district wise, to be carried out in the manner prescribed in Appendix IV, for ascertaining concerns of local affected persons;

(b) Obtain responses in writing from other concerned persons having a plausible stake in the environmental aspects of the project or activity.

Appraisal

Appraisal means the detailed scrutiny by the Expert Appraisal Committee or State Level Expert Appraisal Committee of the application and other documents like the Final EIA report, outcome of the public consultations including public hearing proceedings, submitted by the applicant to the regulatory authority concerned for grant of environmental clearance. This appraisal shall be made by Expert Appraisal Committee or State Level Expert Appraisal Committee concerned in a transparent manner in a proceeding to which the applicant shall be invited for furnishing necessary clarifications in person or through an authorized representative. On conclusion of this proceeding, the Expert Appraisal Committee or State Level Expert Appraisal Committee concerned shall make categorical recommendations to the regulatory authority concerned either for grant of prior environmental clearance on stipulated terms and conditions, or rejection of the application for prior environmental clearance, together with reasons for the same.

Grant or Rejection of Prior Environmental Clearance (EC)

The regulatory authority shall consider the recommendations of the EAC or SEAC concerned and convey its decision to the applicant within forty five days of the receipt of the recommendations of the Expert Appraisal Committee or State Level Expert Appraisal Committee concerned or in other words within one hundred and five days of the receipt of the final Environment Impact Assessment Report, and where Environment Impact

Assessment is not required, within one hundred and five days of the receipt of the complete application with requisite documents except few cases listed in EIA Notification 2006.

Validity of Environmental Clearance (EC)

The "Validity of Environmental Clearance" is meant the period from which a prior environmental clearance is granted by the regulatory authority, or may be presumed by the applicant to have been granted to the start of production operations by the project or activity, or completion of all operations, to which the application for prior environmental clearance refers.

Post Environmental Clearance Monitoring

It shall be mandatory for the project management to submit half-yearly compliance reports in respect of the stipulated prior environmental clearance terms and conditions in hard and soft copies to the regulatory authority concerned, on 1st June and 1st December of each calendar year.-

All such compliance reports submitted by the project management shall be public documents. Copies of the same shall be given to any person on application to the concerned regulatory authority. The latest such compliance report shall also be displayed on the web site of the concerned regulatory authority.

7 PROMOTING SUSTAINABLE DEVELOPMENT

The role of mining in sustainable development is one issue that decision makers and resource managers have wrestled with for decades. With the development of their income-accounting tool, it can be attempted to show how mining activities, which have a finite life span, can be integrated with social and environmental concerns in a way that promotes long-term community development. The approach adopted can place a monetary value on the effects of mining, such as air and water pollution, loss of forests, groundwater depletion, mineral resource use, and reduced agricultural productivity. It also takes into account the direct and indirect benefits to society. To ensure the economic viability of communities after the resource has been exhausted, money would be set aside to finance human and community development. This could help offset one of the main problems associated with mine closures: the lack of skills and resources for alternate economic development. Support is directed toward developing an indigenous research capacity to sustain policies and technologies developing countries need to build healthier, more equitable, and more prosperous societies.

8 CASE STUDIES

8.1 Environmental and Social Management by Coal India Limited (CIL)

Mining-induced displacement and resettlement (MIDR) increased substantially since the 1970s as the countries coal production shifted from underground to opencast mining. The issue has gone beyond economics and environment; local NGOs, such as Operations Research Group (ORG), a consultant of Coal India Limited (CIL), reported that MIDR is creating a pattern of "gross violation of human rights," and "enormous trauma in the

country." By the mid-90s, Resettlement and Rehabilitation (R&R) Policy of CIL has been designed to ensure that affected people improve or at least regain their former standard of living and earning capacity after a reasonable transition period. Coal India Limited implemented the Environmental and Social Mitigation Project (ESMP) in 25 selected opencast mines with World Bank funding during 1996 to 2002. Environmental and Social Mitigation Project (ESMP) aimed to mitigate adverse effect of coal mining on environment and people affected by such activities. ESMP consisted of two components:

➢ **Environmental component** - implemented through Environmental Action Plan (EPA).

Environmental Action Plan (EAP) includes Domestic Effluent Treatment Plant, Workshop Effluent Treatment Plant, Mine Water Discharge Sedimentation Plant, Dust Suppression Majors, Tree Plantation, OB Dump Reclamation, Top Soil Storage and Spreading for Bio Reclamation, Environmental Monitoring.

Environmental Measures Adopted

Air Pollution Control Measures

- Water spraying on haul roads by mobile and fixed sprinklers
- Dust extractors in the Coal Handling Plants and drilling equipment
- Black topping of service roads
- Avenue plantation
- Dust masks

Water Pollution Control Measures

- Industrial effluent treatment plants
- Silt arrestors/ Siltation ponds/ Sedimentation ponds
- Sewage Treatment Plants (STPs)

Noise & Ground Vibration Control Measures

- Use of Controlled blasting techniques.
- Green belts around colonies and mine areas.
- Proper maintenance of heavy Earth Moving Machinery.
- Issue of earmuffs to the excavation workmen.

➢ **Social component** - implemented through Rehabilitation Action Plan (RAP) and Indigenous Peoples' Development Plan (IPDP).

Rehabilitation Action Plan (RAP) includes Shifting of villagers affected by mining, Resettlement and rehabilitation of project affected families (PAFs) by giving a plot of land in well developed resettlement sites or a lumpsum package to settle at a place at their choice. The PAPs are also trained in different trades for their economic rehabilitation.

Under **Indigenous People Development Plan (IPDP)** villages falling within one kilometer area from the leasehold of the mines are considered. Activities under IPDP include 1.Development of Community infrastructure like School Building, Community Hall, Dispensary Building, Village Roads, School Furniture, Wells, Tube wells etc.2. Community Activities like Mahila Mandal, Youth Club, Self Help Groups, Sports, Cultural Programmes etc. 3.Training & Capacity Building, Training for self-employment, Non-formal Education etc. (http://www.coalindia.nic.in/)

8.2 Neyveli Lignite Corporation (NLC)

Afforestation: In and Around Mines

- The dreary and parched atmosphere of Neyveli, where mining began has

now given way to lush greenery. The plantation helps control air pollution, acts as a windbreaker and prevents soil erosion. Massive afforestation were carried out in Mine spoil area, Industrial Units and Township.

- Reclamation in Mine Spoil
- Ash Pond Reclamation
- Formation of artificial lakes, ponds and picnic spots :

Water Conservation

- Optimization of ground water pumping in Mines,
- Introduction of dry ash disposal system.
- Artificial recharging of ground water etc., and
- Stoppage of ground water pumping for Township and using mine storm water after treatment for Township.

Air Pollution Control

- Dilution of gases emission through wind sweeping and vertical mixing.
- Green belt development to act as a barrier.
- Water spraying at excavator face, along the conveyors and on haul roads.
- Dust extractors and wet drilling.
- Black topping of service roads.

Social Welfare

- Mine design is mostly oriented towards minimum disturbance of Human Environment.
- NLC had been offering jobs to the land affected to the extent possible, apart from resettling them in the well-developed Resettlement Centers (RCs).
- Further, a Corporate Resettlement and Rehabilitation Policy has also been implemented for the benefit of the various sections of the Project Affected Persons (PAPs).
- The Displaced persons are being resettled smoothly as per the provisions of the Resettlement & Rehabilitation Action Plan (RAP)
- NLC is implementing various welfare activities and need based (Peripheral Development) programmes such as providing drinking water, health care and basic educational facilities.
- The company has been providing surplus water from its Mines for irrigation to around 23000 acres of lands in nearby villages for decades.
- NLC contributes for infrastructure development of neighboring villages such as Schools, Roads, foot-bridges, causeways, Canals, Public toilets etc.

(http://www.nlcindia.co.in/)

8.3 Nuagaon Iron Ore Mines, Keonjhar, Orissa

Air Pollution Control

- Control of fugitive emissions by adopting best environmental management practices like using dust collectors in drill machine, water sprinkling on haul road and dumping areas.
- Avoiding over loading of trucks
- Controlled blasting technique
- Green belt development around the mining area and suitable pollution control equipment in the crushing plant.
- Development of green belt intermixed with dust filtering trees to reduce dust pollution.

Noise & Ground Vibration Control Measures

- Procurement of less noise generating machines/vehicles.
- Maintenance of machines/ requirements/vehicles in good condition.
- Ear muffs or other protecting device or sound proof cabins to employees near noise generating source.
- Adoption of scientific blasting method.

• Development of green belt as noise barriers

Water Pollution Control

• Afforestation of degraded forestlands and construction of check dams across the original course of stream to restrict sediment transport to water bodies.

• Collection of runoff/leachate water from overburden dumps and stockpiles in sedimentation tank before disposal.

• Proper rainwater harvesting methods to supply water to mine lease area.

Social Welfare

• Creation of direct and indirect employment to local people

• Improvement of Infrastructural facilities and improvement in quality of life.

• Improvement in primary and secondary employment opportunities to local people to reduce their dependence on the forest.

• Betterment of Infrastructural facilities and cultural environment to raise the Quality of Life.

(www.ospcboard.org)

9 CONCLUDING REMARKS

The concept of sustainable development has already been advanced in the Indian mining industry through policy-making and related activities. Its implementation helped to initiate a progressive sustainable development movement in the industry itself, where both mining organizations and individual companies have begun using government policies as guidance to craft sustainable development policies of their own. It is concluded that most of the mining sustainable development policies in place thus far on both sides address key mining sustainable development issues, but in selected cases, particularly on the government side, tend not to be too comprehensive and fail to detail suitable measurement criteria for proposed strategies. However, important mining sustainable development policy groundwork has been laid on both the government and corporate sides, and if both parties became more active in promoting environmental management and public consultation, the Indian mining industry will continue along a path of improved sustainable development.

Further improvements can be made in the arena of sustainable development if both the government and the mining industry become more active in promoting environmental management. The Government needs to investigate various incentives for voluntary action, and research and develop practical mining strategies that would lead to improved sustainability. The merits of new environmental benign management tools such as environmental management systems and life-cycle assessment should also be further investigated in the mining context as implementation could serve to benefit both the environment and the mining company. Finally, more mining industry-sustainable development-community workshops should be held, as it would lead to the development of a common knowledge base of what works and what does not work.

These issues need to be addressed in the mining sustainable development policies of both the government and the mining industry. Some specific policy recommendations that could help lead to further improvement include:

• Outlining the procedures and goals of mine abandonment and reclamation.

• Outlining the goals (if any) of NGO involvement.

• To outline more clearly the roles of all stakeholder parties in the mining process.

- To prescribe actions for environmental monitoring and response.
- To suggest mechanisms to curb the harmful impacts of mining activities.
- With growing global expectations for industry to perform at high levels of sustainable development, it makes practical sense for the Indian government and mining companies to increasingly address these and issues of similar scope in mining policies.

REFERENCES

Adisa Azapagic, 2003. Developing a framework for sustainable development indicators for the mining and minerals industry. Journal of Cleaner Production.

Auty, R.M., Mikesell, R.F., 1998. Sustainable Development in Mineral Economies. Clarendon Press, Oxford, UK.

Auty, R.M., Warhurst, A., 1993. Sustainable development in mineral exporting economies. Resources Policy 19 (1), 14–29.

Brown, D.S., 1993. Minerals and the environment in the 21st century. Nonrenewable Resources 2 (3), 181–186.

Carbon, B., 1997. Sustainable Development and the evolving agenda for environmental protection in the mining industry. Industry and Environment 20 (4), 10–13.

Crowson, P., 1998. Mining and sustainable development: measurement and indicators. *Raw Materials Report* 13 1, 27–33.

De Graaf, H.J., Musters, C.J.M. and ter Keurs, W.J., 1996. Sustainable development: looking for new strategies.

Eggert, R., 2000. Sustainable Development and the mineral industry. In: Otto, J.M., Cordes, J. (Eds.), Sustainable Development and the Future of Mineral Investment, Chapter 2. UNEP, France.

Emel, J., Angel, D. and Bridge, G., 1995. New models for exhaustible resource development. *Business Strategy and the Environment* 4, 200–207.

IBM, 1999. Indian Bureau of Mines. Annual Report 1999-2000. Chapter-4

James, P.M., 1999. The miner and sustainable development. Mining Engineering 51 (6), 89–92.

Labonne, B., 1999. The mining industry and the community: joining forces for sustainable social development. Natural Resources Forum 23, 315–322.

Mikesell, R., 1994. Sustainable development and mineral resources. Resources Policy 20, 83–86.

Miller, C.G., 1997. Mining and sustainable development: environmental policies and programmes of mining industry associations. Industry and Environment 20 (4), 14–17.

NRC, 1995. Sustainable Development and Minerals and Metals. Minerals Strategy Branch, Minerals and Metals Sector, Natural Resources Canada, Ottawa.

Saxena, N.C. and Pal, A.K., 2000. Societal cost of environmental pollution, Minetech, 21(1), 51-54.

Singh, Gurdeep 2005. Water sustainability through Augmentation of Underground Pumped Out Water for Potable Purpose from Coal Mines of Eastern India. Environmental Geochemistry, 8(1&2):89-94.

Tilton, J., 1996. Exhaustible resources and sustainable development. *Resources Policy* **23** 1–2, pp. 91–97.

UNCED, 1992. Report of the United Nations Conference on Environment and Development Annex I A/CONF.151/26 (Vol. I) Aug. 12 1992.

WCED, 1987. Our Common Future. World Commission on Environment and Development, Oxford University Press, Oxford, UK.

www.coalindia.nic.in

www.nlcindia.co.in

www.ospcboard.org/download/Nuagaon%20Iron%20Ore%20Mines

The Future Role of Coal In Europe

Bernd Bogalla
Euracoal

INTRODUCTION

The gas crisis in the first half of January 2009 has again shown that lignite and hard coal are important components of the European energy and electricity mix. Lignite, hard coal and also nuclear delivered the electricity needed when gas was not available in many countries of the German example demonstrates that even with its capacity of already 25 GW of solar and wind power, of which only about 2 GW could be used for production during the crisis due to low winds and of course barely no solar power in winter.

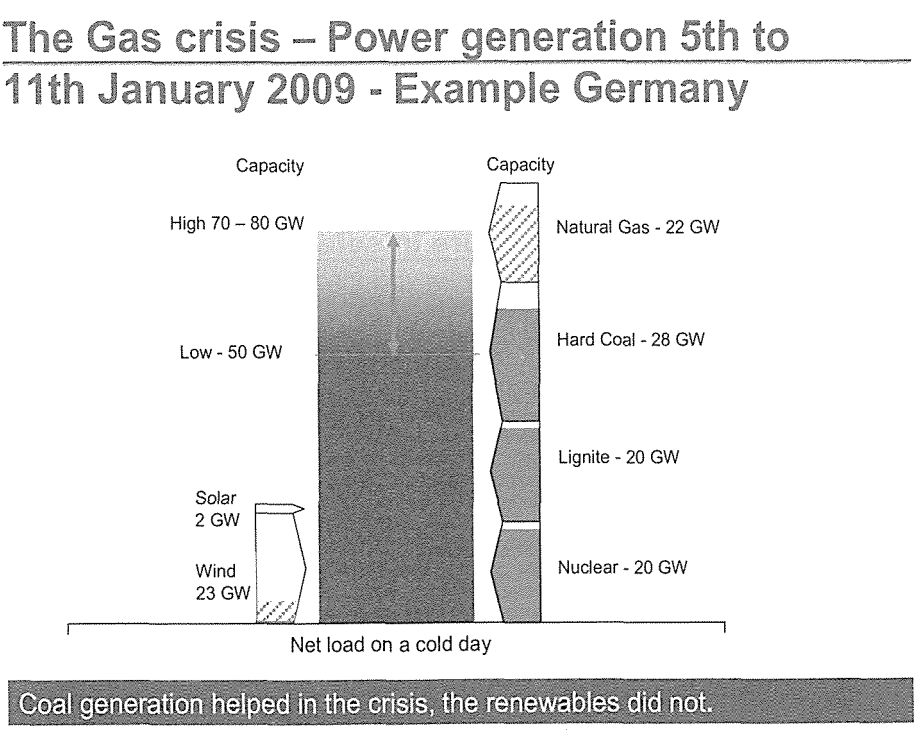

1. THE COMMISSION'S STRATEGIC ENERGY REVIEW II

EU. At that time, renewables were also barely not available. The EURACOAL presentation at the Kemer-Antalya Conference Abstract

In November 2008, the European Commission released its Second Strategic Energy Review. It focussed on the EU's security of energy supply and particularly on the missing interconnections for electricity and gas within Europe. However, the Strategic Energy Review also turned to coal. It made clear that coal will remain an essential component of the EU's and also Europe's domestic energy supply and that a continued substantial use of coal and lignite for power generation in Europe is in the general interest. Looking at the climate protection challenges coal has to face, the Commission emphasised that in the longer term, coal will be compatible with climate change if highly efficient plants predominate and if CCS is widely available. Because some Members of the European Parliament had asked for mandatory CO2 emissions standards, the Commission stressed that these could "be considered only after results of industrial CCS demonstration plants had been evaluated".

2. EU POWER GENERATION STRUCTURES

The Commission is aware that the electricity generation mix differs a lot within the EU -27 Member States. Coal and lignite are particularly important in the power production structures of Poland, whose power generation mix is about 90 % coal, but also of the Czech Republic, Greece, Germany, Bulgaria, Romania and the UK, who all produce more than 40 % of their electricity from coal. There is also a considerable percentage of coal-based power generation in Spain, Hungary, Italy, Slovenia and Slovakia. Outside the current EU Membership, Turkey, the

Ukraine, Serbia and Bosnia also rely on coal and lignite to a considerable extent. EURACOAL considers the difference in power generation structures

Power generation structure in selected EU 27 Member States

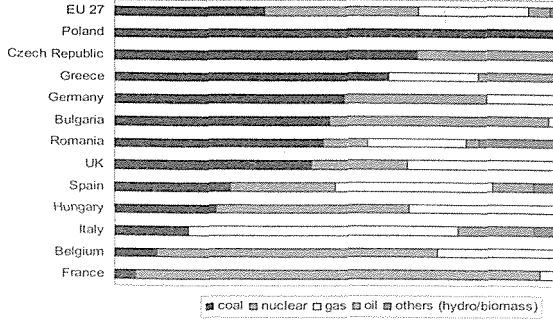

	Gross power generation TWh	Share of coal in %
EU 27	3.357.958	29
Poland	161.743	92
Czech Republic	84.361	59
Greece	60.789	53
Germany	636.600	42
Bulgaria	45.843	41
Romania	62.698	40
UK	398.327	38
Spain	303.007	22
Hungary	35.859	20
Italy	314.122	14
Belgium	85.535	8
France	574.473	4

Source: EUROSTAT – Energy / Yearly Statistics 2006
As at 9/2008

Belchatow 16th May 2009 Figure 6

EURACOAL

throughout the EU Member States as a strength. The gas crisis has shown that different generation structures offer solutions to better react to crises.

3. EURACOAL'S CURRENT VIEWS

With regard to European coal and energy policy issues in general, EURACOAL currently emphasises four issues in order to protect coal mining and coal utilization:

3.1. Access to resources

If Europe wants to make the best use of its fossil fuels, in particular its coal reserves, security of energy supply should be tackled jointly by Member States and industry. This means that Member States and industry should both emphasise that ensuring access to resources is a common task for all involved. It means first of all that mines must not be closed hastily and on the basis of rather short term considerations if they still have appreciable coal reserves. Once abandoned, reserves can only become operational again if at all at substantial additional costs because of the necessary lead times and high investments necessary to re-start operations. Secondly, the legal system in the European Union and at national level must be further developed in such a way that access to coal resources, whether opencast or underground, is also possible in practice. The fact that coal-mining is bound to a location must be kept in mind. This must appropriately extend to all considerations in the context of local / regional planning and approval procedures, e.g. nature protection.

3.2. A list of strategic energy resources

In this context, it may be a good idea to enhance investments in domestic fossil fuel reserves and resources by drawing up a comprehensive list of strategic energy resources for the EU and – if possible – also for Turkey, the Ukraine, Bosnia &

CCS – EURACOAL's overall position

- CCS is a promising technology within climate protection policies
- The demonstration project network proposed by the Commission / the Technology Platform must be set up as soon as possible
  - Project selection - criteria and modalities to be definitely fixed in the Comitology procedure
  - Encourage Member States to co-finance the projects from auctioning revenues
- Decisions on CCS obligations only after results of industrial demonstrations have been evaluated
- Retrofit with CCS after 2020: in some places, top efficiencies may be the best option; any retrofit is subject to proportionality
- Capture-readiness as defined in the CCS Directive is backed

Belchatow 16th May 2009 Figure 13

EURACOAL

Hercegovina as well as Serbia. It would of course show that hard coal and lignite are abundant and that -with improved power plant efficiency and with CCS technologies once the knowledge base has been further developed and they are technically as well as economically feasible on an industrial scale- domestic coal will be able to contribute to less import dependence from geo-politically difficult regions and thus increase the EU's security of energy supply.

Such a list or registry should best be regularly up-dated and published at EU level. It would indirectly favour coal-related investments and positively influence acceptance of coal-fired power generation in Member States and by the public. This could already be achieved in the short term.

3.3. Continuous modernisation of power plants

With coal remaining a permanent and important component of the energy mix in Europe, coal utilisation has to be looked at as well. A continuous renewal of old coal-fired power stations would substantially and relatively quickly contribute to the reduction of CO2 emissions. A state-of-the-art 1 000 MW power station, i.e. with substantially higher efficiency than the old power station it replaced, could alone save nearly 3 million tons CO2 annually. In addition to such a renewal programme, contributing to the EU goals for 2020, CCS demonstration plants would also have to be built and operated. The objective would be to make CCS technically mature and economically viable by 2020 or soon after. New power stations can be built in such a way that they can later be retro-fitted with CO2 separation, depending upon geographical location and size. If policy makers and industry would more often refer to the positive impact of continuous modernisation of coal-fired power stations on climate protection and also on security of supply, the acceptance

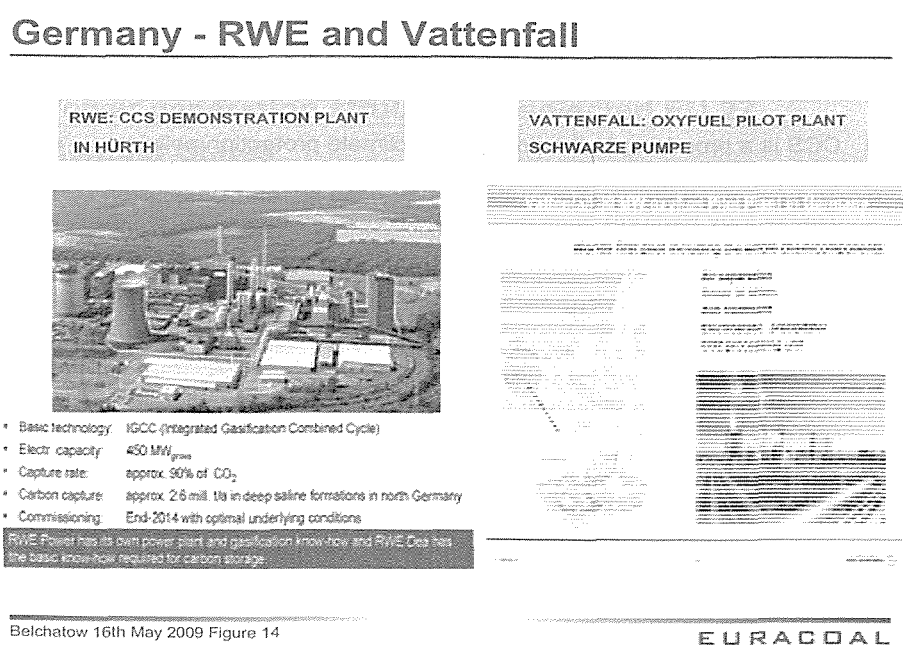

Czech Republic - ČEZ GROUP

NORTH BOHEMIA CLEAN COAL PROJECT

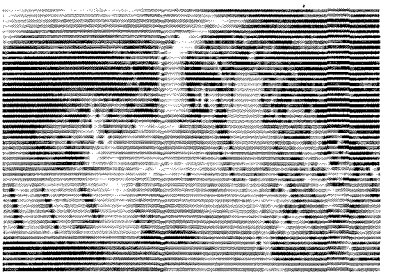

- New power plant
- 660 MWe & supercritical steam parameters
- Lignite
- 2015

HODONIN CO2 SEPARATION PROJECT

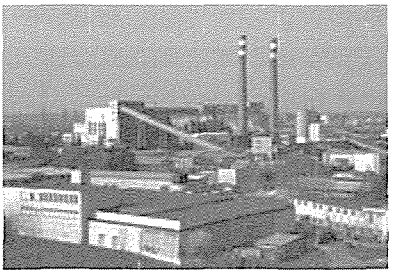

- Existing power plant
- 105 MWe (2 x FBC, 1996-7)
- Lignite + biomass
- 2015

Poland – BOT and PKE/ZAK

BELCHATOV, BOT, PGE and others

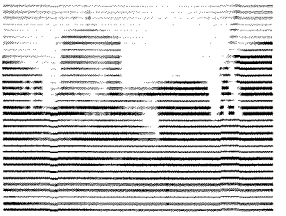

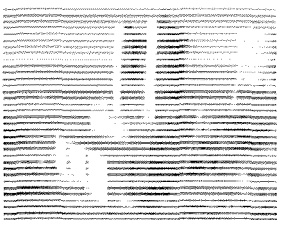

- New 858 MW lignite-based, post-combustion capture, 2015, 1/3 CCS

KEDZIERZYN, Poludniowy Koncern Energetyczny/Zaklady Azotowe Kedzierzyn

- New 500 MW syngas and 250 MWel, polygeneration, 2014

CO_2 transport and storage – CCS depends on approval procedure – RWE example

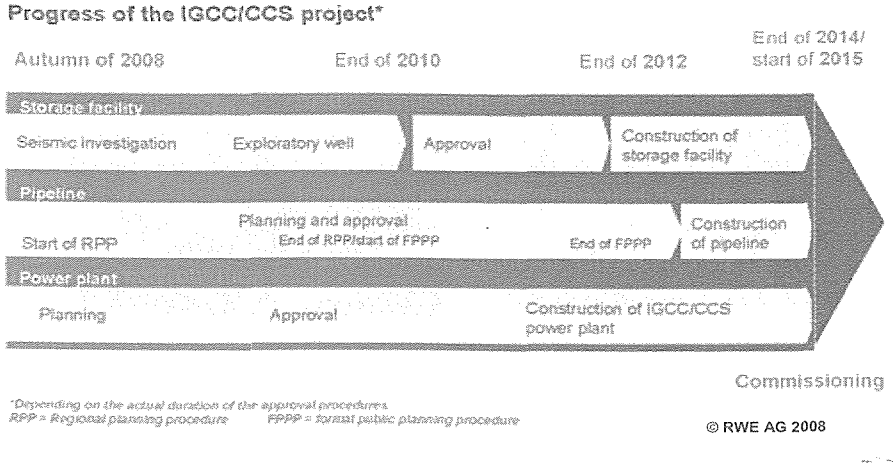

Belchatow 16th May 2009 Figure 19

EURACOAL

of coal not only at EU level but also in the regions and when discussing the approval of plants in Member States could be enhanced.

3.4. Investment in new capture-ready coal-fired power plants

When negotiating the EU ETS as from 2013 at the December 2008 Summit, with a view to medium term investments, the Commission declared that between 2013 and 2016, Member States may use revenues generated from the auctioning of allowances to support the construction of highly efficient new and CCS-ready power plants. The declaration aims at partially compensating disadvantages for new coal-fired power plants and the resulting hindrance to investments by full auctioning of allowances. The concrete implementation of this significant declaration seems to entail some obstacles. Criteria for its implementation have to be determined. For example, the Commission's explanation stipulates that from 2013 to 2016 Member States may use revenue from auctioning to promote investments. However, there will hardly be a power plant project during this period that will obtain permission, start construction, operation and obtain the "Efficiency criterion for long-term operation" label. So that the regulation is not left empty, as much flexibility as possible should be maintained. Also, the explanations must be given as soon as possible, at the latest by 2010, if it is supposed to promote investments in new installations.

4. CARBON CAPTURE AND STORAGE (CCS)

Within EURACOAL, the concept of carbon capture and storage has been discussed since about 2003. EURACOAL Members think that CCS

is a promising technology within climate protection policies. In the laboratory, all steps of the technology function well. First pilot projects have started to operate. However, before the technology can enter the market probably after 2020, the different capture and storage technologies have to be demonstrated. Together with the Technology Platform Zero Emission Fossil Fuel Power Plant (ZEP), the Commission already proposed to set up a demonstration project network by 2015. This initiative that is backed by EURACOAL could lead to CCS plants being on the market after 2020. It can be assumed that the project selection criteria and modalities have to be definitely established as soon as possible, in any case till end of 2010. Decisions on CCS obligations can only be taken after the results of industrial demonstrations have been evaluated. For the moment there is a lack of infrastructure that would be necessary. Furthermore, in some places, top efficiencies of power plants may be the best option. And finally, for any obligation for industry to invest, legislators have to prove their proportionality. The following slides illustrate the variety of demonstration projects planned in the EU:

Vattenfall already operates an oxy-fuel power plant at the Schwarze Pumpe site. First results show that the technology works, also on a 30 MW scale. The separated CO2 is transported by road to storage sites in the Altmark area about 300 km away from Schwarze Pumpe; however, this concept can only serve for a pilot plant. Vattenfall plans a CCS demonstration plant at Jänschwalde about 50 km south east

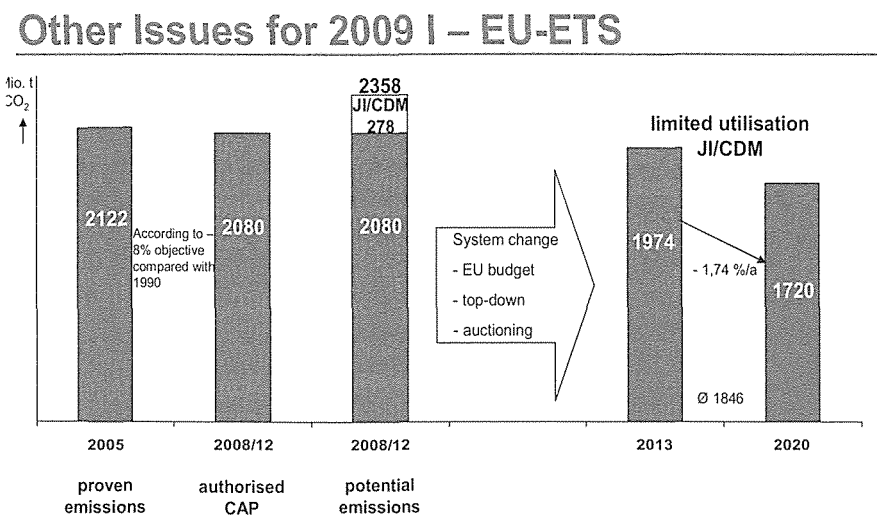

of Berlin for 2015. RWE announced it will build a CCS demonstration plant in Hürth close to Cologne by 2014 / 2015. It is supposed to have an electrical capacity of 450 MW; it is foreseen to capture 90 % of the CO2 and to store about 2.6 million tons per year in deep saline formations in northern Germany. The transport will be done via pipeline. In the UK, a number of demonstration projects are being discussed. Since the beginning of 2008, a tender is open; the British government will decide which of the plants are to be financed by state aid. It has already been decided that the plant that will be supported has to be based on a post-combustion capture technology. A decision on this will be taken in spring or summer 2009.

The CEZ Group plans to build a CCS demonstration plant in the Czech Republic. A decision will have to be made whether to build a new power plant

Other Issues for 2009 II – Industrial Emissions Directive (Draft)

- The rules for coal fired power plants are supposed to be moved from the Large Combustion Plant Directive (LCPD) into the Industrial Emissions Directive
- EURACOAL welcomes Best Available Technologies as the basis for plant operation permits, but will make sure that
  - Domestic coal with relatively high sulphur is not excluded from use
  - Emission Limit Values for SO_2, NO_x and dust do not go beyond BAT – they must be different for existing and new plants
  - There will not be any ELVs for CO_2

Belchatow 16th May 2009 Figure 13 EURACOAL

in northern Bohemia with an output of 660 MW electrical on the basis of lignite by 2015 or to retro-fit an existing power plant in Hodonin with CCS separation. The latter installation has an output of 105 MW electrical; the CCS separation part could work with lignite and / or biomass also by 2015.

Further projects are known in Poland, including the Belchatow CCS demonstration project.

UK – A number of demonstration projects

- Kingsnorth, e.on, 300 MW new post-combustion, 2014
- Ferrybridge, Scottish and Southern Energy, 500 MW retrofit, 2015+
- Tilbury, RWE nPower, 1600 MW new post-combustion, 2016
- Hatfield, Powerfuel Power, 900 MW new pre-combustion, 2012-14
- Teesside, Centrica etc., 800 MW new pre-combustion, 2013
- Killingholme, e.on, 350 MW new pre-combustion, 2016+

KINGSNORTH POST-COMBUSTION

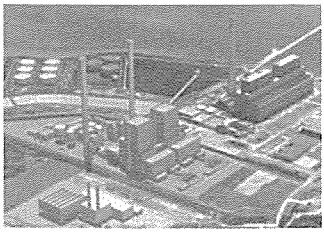

Belchatow 16th May 2009 Figure 15 EURACOAL

The EU's objective to bring Carbon Capture and Storage on the markets by or shortly after 2020 are very ambitious. A brief look at the approval procedure for a demonstration project confirms how tight the timing for the construction will be. The example of the RWE power plant in Hürth shows that even if plant approval is expected by 2010 and would allow the construction of the plant, the pipeline approval may take much longer. All types of regional planning procedures will have to be gone through. In addition, all environmental law has to be respected, in particular the fauna, flora habitat regulation and the water regulation. Of course, the transport and the storage permit can only be granted after the transposition of the CCS Directive into national law.

The European Economic Recovery Plan adopted by the Commission end of January 2009 and then amended and adopted by the European Summit at the March 2009 Summit may to a certain extent help to finance those plants. The Commission proposed to foresee € 1 250 million for five demonstration plants; on the basis of the Council decision € 1 050 million will be given to seven plants. Those plants will have to capture 85 % of the CO2, they will have to have a minimum electrical output of 300 MW; and the operators have to give a binding declaration on a future knowledge transfer. As already indicated, a maximum € 180 million per plant will have to be used already in 2009 and in 2010.

5. OTHER HARD COAL AND LIGNITE ISSUES FOR 2009

5.1. The EU Emissions Trading Scheme

In previous years, the European coal industry has worked a lot on climate protection issues. During the March 2007 European Summit, the EU committed itself to a binding 20 % greenhouse gas reduction objective for 2020 compared with 1990. This objective is already ambitious. However, it was decided to go for a 30 % objective if other developed countries commit themselves to comparable emissions reductions and economically more advanced developed countries contribute adequately. In order to avoid major disadvantages in competitiveness for the EU's industry and also to force other developed countries to contribute, the EU should not go beyond its 20 % objective if the other developed countries do not make comparable commitments close to a 30 % objective themselves. EURACOAL of course closely observes the new measures the Commission and Member States are taking to detail the Emissions Trading Directive. There will for example be a Regulation on how auctioning is supposed to be carried out in Member States, on details about allowances from the new entrants reserve for Carbon Capture and Storage demonstration plants and also for the derogation for the eastern European power plants that have the opportunity not to auction all of their allowances. EURACOAL also looked at the instruments foreseen in the scheme to lower the demand for certificates and to enhance the supply of allowances. Here, the main issue is to enhance Joint Implementation and Clean Development Mechanisms in order to make sure that also in practice, 50 % of the EU-wide reductions can be achieved by those instruments.

5.2. Emission Limit Values for Large Combustion Plants

Another challenge facing the European coal industry in 2009 is the development

of Emission Limit Values for SO2, NOx and dust from coal-fired plants. The Commission has proposed much tighter Emission Limit Values for 2016 and later. The European Parliament backed this approach in general. The proposal even threatens complete mining regions. Both the Commission and the European Parliament deleted an important alternative for sulphur-rich domestic coals; that is to apply a very ambitious desulphurisation rate instead of a stringent ELV. The future

Large Combustion plant regulation, but also other environment-related initiatives of the EU are a good exempla for the need of EURACOAL's work. We, the EU coal industries, need to further join forces to influence national and EU policy makers. We need to find common positions to push these both in Brussels and at national level. We need to make sure that there are voices for lignite and hard coal in the Council negotiation, in the Parliaments and within the authorities. This way, coal will be able to contribute to our security of energy supply in the long term.

Z:\Meetings and Events\...\EURACOALspeechantalyaconf.doc

Mineral's Commodities Boom, Prices and Investment

Mateus Patrice Piermatei Soares, Marco Antônio Tourinho Furtado
Universidade Federal de Ouro Preto, Ouro Preto, Brazil

ABSTRACT Up to the year of 2008, the mining industry was going through an outstanding growth period, due to the high demand for commodities and the following high of their prices. In this context, the investments in the sector increased every year. However, in 2008, the real estate crisis in the US initiated a period of recession that might compromise this growth. This article aims to analyze and establish the relation between the high on prices and the investments. The studied aspects were, among others, the transient difference between the changes in prices and investments and the projects' execution stage. The rise in prices, especially since 2004, led to a wave of new investments in 2006 and 2007, especially for the projects on studies of feasibility and mines reactivation or expansion. Following the prices drop over 2008, we believe that the new data may reveal a new context for investments.

1 INTRODUCTION

A remarkable growth has taken place in the mining industry in the last few years. Among other factors, this growth was conceived through great investments in projects, either for the construction of new mines or the expansion or reactivation of old ones. (brownfield projects).

From the beginning of 2000 until the first half of 2008, the great moment in the world economy and the promising growth of China and India caused the world market to thrive and expand. The high consumption of raw materials caused an increase on prices, what had an impact on the metallic commodities. New investments were emerging and at great numbers every year because of the high prices.

This article attempts to show the current development of investments in the mining industry over recent years, as well as its reasons and consequences.

The study analyzes the relation between the rise in prices and its impact on investments, their temporal disparity; verifies how much of the investments really turned into executed projects; and exposes the real industry growth through the new accomplished projects or the expansion of old mines. Five commodities will be studied, besides the absolute numbers: Iron ore, Copper, Gold, Zinc and Nickel.

At the end of the first half of 2008,

the real estate crisis in the US provoked a period of stock exchange fall and recession that affected the mining industry with the drop on commodity prices. This, combined to the lack of credit for the projects, led to a reduction on investments, which caused standstills, delays and even the abolishment of some projects. This study also presents the variance of prices throughout 2008, highlighting the drop, especially after the middle of the year.

This study will continue, in order to include data from 2008 and 2009, so to evaluate the effects of the recession on mining investments.

2 MATERIALS AND METHODS

This work is based on secondary data.

The information on the prices was acquired from the London Metal Exchange, the COMEX – New York Mercantile Exchange and from data given by Vale, via the EconStats website.

The data on investments were collected from annual reports published on the Engineering and Mining Journal. On this publication, the main projects of the world mining industry are listed and, also, data about investments sorted by country, metal and stage of execution.

The collected data were organized in tables and graphics, and they were analyzed separately, then the prices and investments were analyzed simultaneously.

At first, we will display the prices fluctuation throughout the years, until 2008. Then we will display the data on the investments progression from 2000 to 2008, sorted by kind of metal, project stage and investment value. Following the graphics presentation, the data will be analyzed.

3 RESULTS

3.1 The fluctuation of the prices

The graphics below represent the price fluctuation of commodities, studied throughout the years:

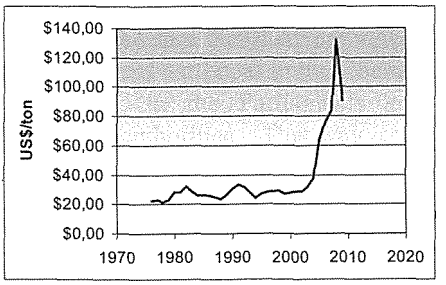

Figure 1. Iron ore prices (Contracts-Fines). Annual average. Created by the author based on data from: EconStats – CVRD.

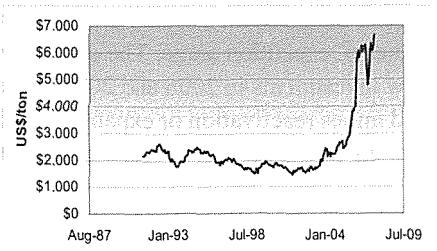

Figure 2. Copper Prices (Futures Exchange). Monthly average. Created by the author based on data from: EconStats – London Metal Exchange.

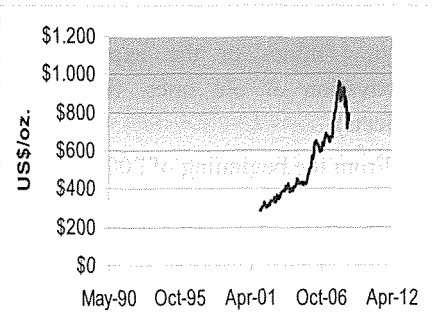

Figure 3. Gold Prices (Futures Exchange). Monthly average. Created by the author based on data from: EconStats – COMEX.

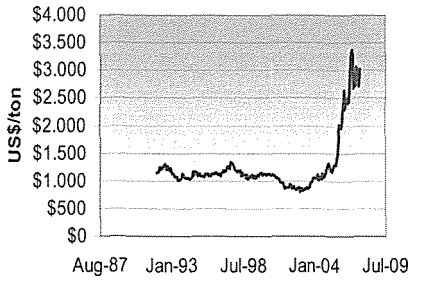

Figure 4. Zinc Prices (Futures Exchange). Monthly average. Created by the author based on data from: EconStats – London Metal Exchange.

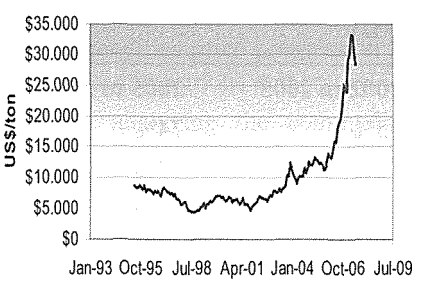

Figure 5. Nickel Prices (Futures Exchange), in US$/ton. Monthly average. Created by the author based on data from: EconStats – London Metal Exchange.

3.2 Fluctuation of the investments

The graphics below are based on the data published every year on the Engineering and Mining Journal. These reports gather information of the main mining projects throughout the years. Data from 2000 to 2008 are presented. The graphics were firstly organized by general numbers and, then, by studied metals.

On the publications, the projects data were classified in three distinct stages:

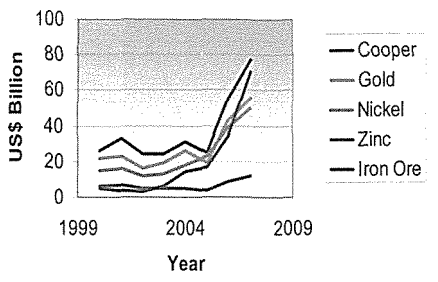

Figure 6. Total of investments according to metal produced. Created by the author based on data available at the Engineering and Mining Journal publications.

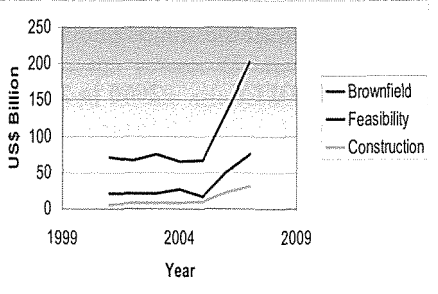

Figure 7. Total of investments according to the project stage. Created by the author based on data available at the Engineering and Mining Journal publications.

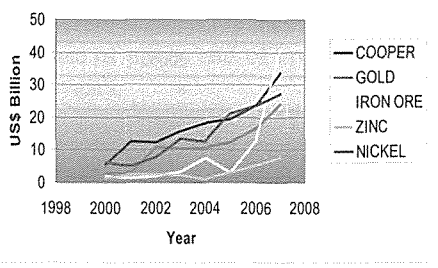

Figure 8. Investments in feasibility studies (numbers on the listed projects). Created by the author based on data available at the Engineering and Mining Journal publications.

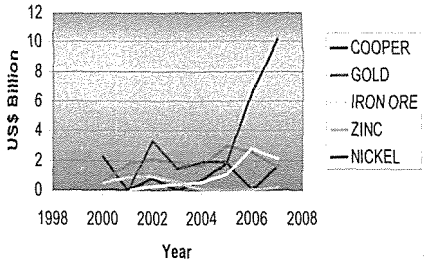

Figure 9. Investments in new projects at the stage of construction (numbers on the listed projects). Created by the author based on data available at the Engineering and Mining Journal publications.

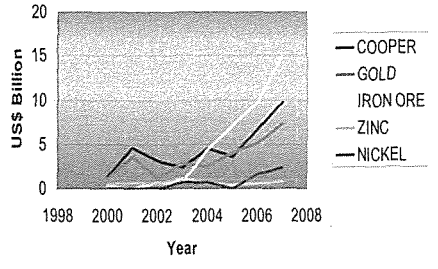

Figure 10. Investments in Brownfield projects (numbers on the main listed projects). Created by the author based on data available at the Engineering and Mining Journal publications.

Table 1. Fluctuation of investments in feasibility studies (according to the main projects, listed on the annual publication by E&MJ).

COMMODITY	2000 to 2002	2002 to 2005	2005 to 2007
COPPER	121%	55%	74%
GOLD	285%	11%	99%
IRON ORE	-2%	75%	1178%
ZINC	95%	21%	145%
NICKEL	27%	170%	29%

Created by the author based on data available at the Engineering and Mining Journal publications.

Table 2. Fluctuation of investments in new projects at the construction stage (according to the listed projects

COMMODITY	2000 to 2007
COPPER	-29%
GOLD	200%
IRON ORE	*
ZINC	-62%
NICKEL	**

*** In 2000, there were no investments in nickel projects under construction, while in 2007, the amount reached US$ 10.15 Bi*

** In 2000, there were no investments in iron ore projects under construction, while in 2007, the amount reached US$ 2.08 Bi.*

Created by the author based on data available at the Engineering and Mining Journal publications.

Feasibility: represents the stage in which studies about the feasibility of the projects are performed. The aspects analyzed are the ore bed, local infrastructure, the market, local political issues, among others.

Construction: represents the projects that are under construction and will be operating afterwards.

Brownfield: represents projects of expansion or reactivation of old mines.

Hence, the following graphics and tables present these three stages and their progression. Their data are discussed in item 4.

Table 3. Fluctuation of investments in projects at the brownfield stage (according to the listed projects).

COMMODITY	2000 a 2004	2004 a 2007
COPPER	231%	114%
GOLD	126%	192%
IRON ORE	1734%	237%
ZINC	11%	38%
NICKEL	*	258%

** In 2000, there were no investments in brownfield projects of nickel, while in 2004, the amount listed was US$ 0.65 Bi.*

Created by the author based on data available at the Engineering and Mining Journal publications.

4 DISCUSSION

4.1 Prices Progression

The commodities price progression has been studied by various authors.

When analyzing the commodities price progression throughout the last few years in relation to Constant Dollars, Radetzki (2006) exposes a general tendency for the depreciation of the metallic and the non-fuel commodities (food and raw materials from the agriculture industry) until the beginning of 2000, when this new tendency turned into a prices increase. Prates (2007) claims that in 2001 the prices reached historic low levels, reducing stocks and production, and in 2002 they started to rise again.

From 2002, the demand for metallic commodities starts to increase remarkably. This is due to the world economy turnaround and, mainly, to the development of countries like India and China. With the rise of demand and the lack of stocks and production, the prices increased substantially at a very short period of time, what is confirmed by the graphics previously presented (Figs. 1-5).

With the world in crises, due to the collapse of the real estate sector in the United States, a recession period has started, causing the consumption to fall, and so the prices. However, the data displayed in this article only shows the first impacts of this crisis. It is necessary to wait for future data in order to analyze this period as a whole; its progression will determine the new ore prices.

4.2 Investments Progression

From the data displayed on Fig. 6, it is possible to assess an increase on the total of investments from 2002, and further more from 2006 and 2007. This could be related to the great rise in prices since 2004, as described in the former section. If so, there is a discrepancy between the increase of prices and of investments in three years.

However, caution is needed when analyzing these absolute numbers. The mining projects were sorted in this article by three stages: feasibility studies, construction and brownfield. The feasibility studies projects do not necessarily represent projects effectively initiated, therefore the valid investments comprehend the stages of construction and brownfield.

When analyzing the Figs. 7-10 and the Tables 1-3, we conclude that the projects still on feasibilities studies display a rise from 2002, increasing further in 2006 and 2007. Nevertheless, when comparing to the absolute numbers of projects under construction, there was not a significant change in the numbers for the metals in question, but nickel. Investments in brownfield projects have increased since 2004 and kept on, reaching maximum values, in 2007.

5 CONCLUSION

When analyzing the graphics on the prices, we can notice a change of the tendency since 2002, when the prices started to increase, due to the positive period experienced by the world economy, especially in China and India. These factors combined created an environment of high demand for metallic commodities.

Prior the year of 2000, the commodities prices achieved historic low levels and therefore the stock and the production were depleted. The low prices did not encourage new investments in minerals.

The high demand caused the prices to increase and the mining companies were forced to intensify the investments to increment the supply, so they could respond the increasing demand.

Hence, it is possible to identify the correlation between the rise in prices and the rise in investments. This is even more evident when we analyze the accentuated tendency of a rise in prices in 2004, causing an increase on investments in 2006 and 2007. So three years was the period of time needed so that the price variation could have an impact on the investments, expressing the worries that the increase of prices and the high demand were perceived as constant and not as a fleeting moment.

It is necessary to pay attention to the data of each of the projects stages. There is a certain regularity of investments in projects under construction, while, for brownfield projects, there is a rise starting in 2003 and intensified in 2004. This is justified once it is faster and cheaper to expand old mines rather than developing new units. Hence, this kind of investment quickly responds to pressures of demand and prices increase. The investments that had effectively intensified are the ones of projects in the feasibility studies stage. But projects on this stage do not necessarily represent the consummation of the investment. We can then conclude, from the data analysis, that little has changed about new projects, remaining at a stable level, even with the rise of prices. On the other hand, the expansions and/or reactivations of existing mines were significant, representing the real growth of the mining industries. But the growth of feasibility studies projects could suggest the advent of new mines soon.

We can highlight the progression of investments in iron ore. Until 2003, among the five studied commodities, iron ore did not receive a significant part of these investments. However, in 2007, this commodity received the majority of the investments in brownfield and feasibility studies projects, reflecting its great ratings since 2004.

With the world crisis caused by the American real estate sector, the resulting prices drop can be noticed on the graphics of prices above, but, since the data from 2008 was not available yet, we can not assess the actual effect on the investments. Each day, new facts make us realize that we are really facing

a period of world recession. However, there is still no information to quantify this as in previous years.

We then conclude that:

a) The real increase of prices of the mining commodities caused a great movement of investments;

b) In a short period of time, since 2003, there has been an expressive increase on the number of expansions and/or reactivation of mines;

c) A great number of new investments stood at the feasibility study stage, and the drop in prices at the end of 2008 may have an effect on those, materializing them.;

d) The investments in iron ore had an outstanding increase comparing to the absolute number of investments in minerals, due to the fast rise of prices between 2004 and 2008.

6 SPECIAL THANKS TO

Professor Marco Antônio Tourinho Furtado for his guidance along this research, to my father, Marcos José Veroneze Soares, for his help with the writing of the article, to Ouro Preto Federal University, for its high quality teaching, and to the Raw Materials Group, from Sweden, for the information given about its publications.

REFERENCES

COMPANHIA VALE DO RIO DOCE. Iron Ore – Annual Contract Prices. Available on: <http://www.econstats.com/rt_ironore.htm> Accessed on: Jan. 08, 2009.

LME. EconStats: Futures Open Metals Exchange London LME Volume. Prices. Available on: < http://www.econstats.com/fut/xlme_ew0.htm> Accessed on: Jan. 08, 2009.

PRIMEDIA INTERTEC. 2000, 2000 Project Survey. Engineering and Mining Journal, 201, n. 1, pp. 25-26.

PRIMEDIA INTERTEC. 2001, 2001 Project Survey. Engineering and Mining Journal, 202, n. 1, pp. 28-37.

PRIMEDIA INTERTEC. 2002, 2002 Project Survey. Engineering and Mining Journal, 203. n. 1, pp. 28-36.

PRIMEDIA BUSINESS MAGAZINES. 2003, Project Investment Survey 2003. Engineering and Mining Journal, 204, n. 1, pp. 28-34.

ERICSSON, M. 2004, Mine Project Survey 2004. Engineering and Mining Journal, 205, n. 1, pp. 24-28.

ERICSSON, M. 2005, Industry Registers Record Investment. Engineering and Mining Journal, 206, n. 1, pp. 34-37.

ERICSSON M.; OLSSON A. 2006, E&MJ's Project Survey 2006. Engineering and Mining Journal, 207, n. 1, pp. 55-59.

ERICSSON M.; OLSSON A. 2007, Project Survey 2007 Another strong year for mining investment. Engineering and Mining Journal, 208, n. 1, pp. 28-32.

ERICSSON M.; LARSSON V. 2008, E&MJ's Annual Survey of Global Mining Investment. Engineering and Mining Journal, 209, n. 1, pp. 31-35.

RADETZKI M. 2006, The anatomy of three commodity booms. Resources Policy, 31, n. 1, pp. 56-64.

PRATES D. M. 2007, A alta recente dos preços das commodities. Revista de Economia Política, 27, n. 3 (107), pp. 323-344.

The Current Debate About The "Brazilian Disease": A Revision

B. G. G. Batista, M. A. T. Furtado
School of Mines Ouro Preto Federal University, Ouro Preto, Brazil

ABSTRACT The "Brazilian disease" could be described as a kind of Dutch disease (DD) observed within national borders, though in the Brazilian economic context: iron instead of natural gas. For some national economists this is what has been occurring to the Brazilian economy nowadays, and its main reasons, as well as with the Dutch disease, might be the over-appreciation of the exchange rate, the deindustrialization of other tradable sectors of the economy and, finally, the low GDP growth rates. This subject has currently been discussed on academic and journalistic fields in Brazil, since the iron ore economic boom provoked by the enormous demand from China. This article aims to promote a literature review, focused on the Brazilian authors, and to contribute by exposing the way Brazilian economists stance on the reasons, effects, neutralization and even the very existence of the market failure called Dutch Disease.

1 INTRODUCTION

One of the main themes currently in debate in Brazil, not only at academic field, but also in the political and journalistic, is the possible "disease" the national economy could be suffering with. The reason is simple: the country, that for a long time experiences a huge success in its balance of trade, through the stout growth of the agribusiness and the mineral extraction activity, shows lower growing rates of the Gross Domestic Product (GDP) if compared to other developing countries.

The current debate that stimulates the production of written works about the performance of the Brazilian economy has actually begun in Europe, more specifically in the Netherlands, almost fifty years ago. It is very tempting to compare the current Brazilian situation to the Dutch in 1967. At that time, many economists "diagnosed" the Dutch disease (DD), and the big issue being raised nowadays is if Brazil is developing or not a similar syndrome.

This article intents to promote a bibliographic revision of works about the Dutch disease, emphasizing the Brazilian authors, as a way of contributing to the organization of ideas and promoting this debate even further.

However, so we can contextualize the reader, we will present, at first, a brief report about the Dutch disease in its original country, also presenting the natural resource curse concept, besides the classic analysis model by Corden and Neary. Then, we will present the orientations and differences, from the perspective of Brazilian authors, on important issues regarding the discussion about the existence of the Dutch disease and, finally, an analysis of the proposals for economic policies to eliminate the possible effects of this "disease".

Unfortunately, even as a matter of space, it will not be possible to present and interpret the Dutch and Brazilian economic data as an empirical analysis, which is being done on an essay, developed simultaneously to this article.

2 THE DUTCH DISEASE

The great negative effect on the economy of a country observed by the intense growth of only one industry, especially of commodities, over the other exporting industries of the same economy, in developed and developing countries, caught the attention of economists around the world. The phenomenon occurred on the Dutch economy in the 60's and 70's, affected by the natural gas extraction and commercialization at the North Sea marginal, is the most famous example, what later originated the term "Dutch disease"[1].

However, even with the great contribution of foreign capital since 1967 (the year in which the commodities exportations were initiated), the country did not achieve the expected growth after many years of resource exploitation and great flow of investments to expand the productive capacity of the sector. (Sachs & Warner, 2001).

It is in this context that the Dutch economy was inserted, allowing for the first academic reflections on this experience with the intense natural gas exploitation and its consequences for this country's economy.

2.1 The Natural Resource Curse

Authors like Graham A. Davis and John E. Tilton believe that the extraction of the natural resources of a country encourages and promotes the expansion of this economy (regardless of being less developed, developing or developed). They ground this conviction quoting the United States, Australia, Canada and Chile, emphasizing the honesty and competence of those governments concerning how and when to exploit such resources. (Graham & Tilton in Lagos, 2005).

However, authors like the Americans Jeffrey D. Sachs and Andrew M. Warner, the Argentinean Raul Prebish, the Chilean Enzo Faletto, the Austrian-Brazilian Paul Singer and the Brazilian sociologist Fernando Henrique Cardoso, for at least 50 years, and based on former studies, have been harshly criticizing the traditional point of view. For these authors, the natural resource curse are the negative effect of the intensive extraction of those resources, despite the economic diversification of the secondary and tertiary sectors of the same economy

1 Term first used by "The Economist" magazine, in na article called "The Dutch Disease", in November 26th, 1977

(Sachs & Warner, in Lagos, 2005).

The reverse relation between the GDP per capita growth rates (Y axis) and exportations of these resources in relation to the GDP (X axis) has been proved since earlier studies by Sachs and Warner (1997), making it clear that the more a countries' economy is based on the exportation of primary products, slower will be the growth of its economy and vice-versa. The graphic below illustrates this relation:

There is also a reverse relation between the growth of manufacture exports and the rate of natural resources exports of the same country. We can then affirm that the most one country's GPD is based on the natural resources export, the frailest its manufactures exports will be, and vice-versa (Sachs & Warner in Lagos, 2005). Thus, we can assume that the economic weakening of the Dutch economy was based on the reduction on the participation of the manufactures' sector. This fact can be

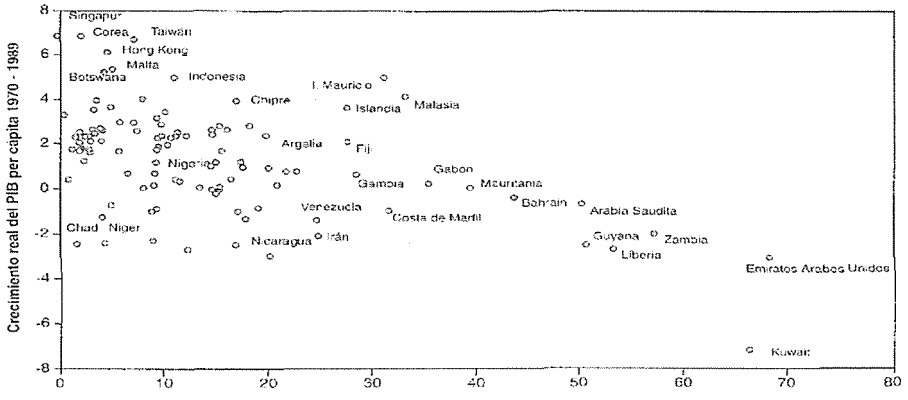

Figure 01: GDP Growth X Natural Resources Exportation, Source: Sachs & Warner apud Lagos, 2005

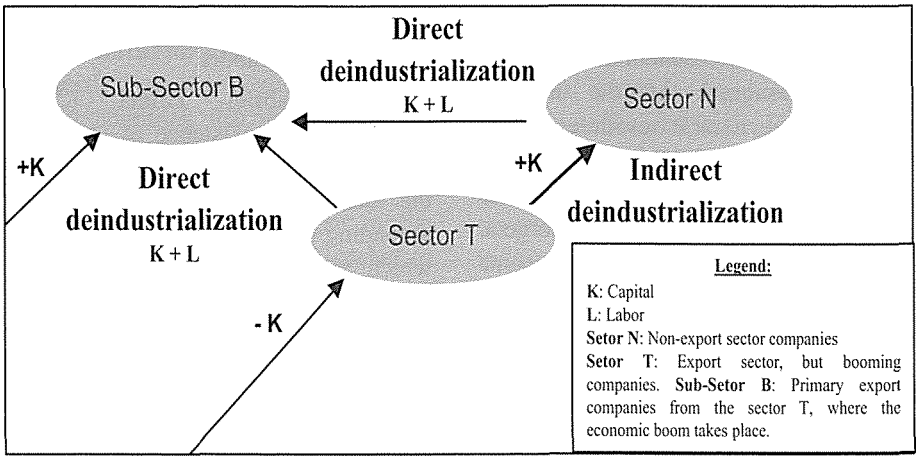

Figure 02: Partial Equilibrium Model, Source: Corden W. M.; Neary, J. P. (1983).

explained by the intensification of the Dutch natural resources exports, leading to a deindustrialization process. This process is displayed by the model below, called the "Partial Equilibrium Model", developed by Corden and Neary (1983):

In this model, direct and indirect deindustrialization takes place, distinctive and asynchronous processes. The direct deindustrialization occurs in an initial moment when sector B attracts capital and labor from sectors T and N, once the indirect deindustrialization occurs at a later stage, when sector N drains resources from sector T compensating the direct process for the indirect, one for the other.

3 THE DISCUSSION IN THE BRAZILIAN ACADEMIC FIELD

The possibility that the Dutch disease could be taking place at the Brazilian economy caught the attention of various national academic authors.

Instigated by this possibility, they began to further study the subject, and, in the heat of discussions, different results and conclusions arose among the authors.

José Alexandre Scheinkman (2006)[2] strongly disagrees of the noxious effects of the natural resources in the economy. Scheinkman states that the majority of the Dutch disease cases refer to countries that export energetic goods and, this way, due to great income gained with the commercialization of these materials, the losses with the deindustrialization of the manufacturing sector would be paid off. This thinking is shared with Rubens Ricupero (2006) on the Brazilian economic conjuncture. Ricupero denies the existence of the Dutch disease in Brazil, though admits the deindustrialization. However, he affirms that the balance of agricultural and mineral commodities can compensate the deficit in manufacturing. Also according to Sheinkman "in economic literature there are lots of examples of candidates to the Dutch disease, but only a few really contracted the "condition" (Folha de São Paulo, 2006). He actually disagrees about the classic case: the Dutch disease itself, in the Netherlands. According to Scheinkman the performance achieved by the Dutch economy in the 70's and 80's would not have been very different from the French and German at the same period of time. (Folha de São Paulo, 2006). We believe Scheinkman's statement to be contradicting, since the difference between France's, Germany's and Netherland's GDP is, in our opinion, a clear symptom of the Dutch disease, once the Dutch economy, at these decades, was going through an astonishing growth of the natural gas exports sector, therefore, it would be logical that the Netherlands have a superior growth if compared to its continental neighbors.

José Gabriel Palma (2005)[3] believes in the existence of two kinds of Dutch diseases: the ascending and the descending *Dutch disease*. The ascending *Dutch disease* is the one in which a mature economy changes its acting focus, simply by redirecting part of its industrial activities to other sectors, specially to tourism, in places

2 Professor of the Economics Department of the Princeton University.
3 Professor of the Faculty of Economics and Politics, Cambridge University, United Kingdom.

like Greece, or financial services, in Switzerland. The ascending *Dutch disease*, also called "normal" by Palma, represents a natural process of development of these economies. The second case, the descending Dutch disease, includes developing and least developed countries economies, as in Latin America, for example, that opt, and are satisfied with, the establishing of a budget surplus caused by the exploitation and exportation of primary goods.

The author searches for other explanations for the deindustrialization of economies. A recent study, based on Kaldor (in Palma, 2005), states that the beginning of the deindustrialization process of developed economies started at the post-war period, in developed countries and with high rates of per capita income, empirically proved using the inverse "U" relation. (Industrial employment X Per capita income) achieved with the Rowthorn's regression. In the specific case of Brazil and the countries of the Southern Cone (Argentina, Chile and Uruguai), the deindustrialization would have occurred in a subsequent moment, with a lower per capita rate, after the crisis of the external debt in 1982 (Mexican government default), being closely related to a drastic change in the economic policy of these countries, that sharply changed from the ISI model (Import Substitution Industrialization) to the neoliberal model (prescribed by Ronald Reagan in the United States and Margaret Thatcher in England) redirecting its economic activity to its Ricardian natural position (Palma 2005). Hence, he rejects the term "natural resource curse", stating that the discovery of new ore beds, the agricultural export potential, the development of the tourism sector or the financial services are not the heart of the matter, actually it would be "an specific kind of excess", some sort of complementary deindustrialization, associated to a main cause: the financial and commercial liberalization provoked by the established neoliberalism (Palma, 2005).

Luiz Carlos Bresser Pereira[4], one of the most active figures on the discussions about the Dutch disease, dissents from, but also agrees with, many of these authors.

He is emphatic to say that the DD is a great obstacle to the development of the economies, concerning the aggregate demand, with effects on the supply.

According to him, the natural resources are important and beneficial when the economy is not developed yet, thus to break the vicious cycle of poverty, huge amounts of resources are needed to exceed the primitive accumulation of capital and to perform the Industrial Revolution. Once this process is completed, in which the natural resources "financed" the emerging industrial sector (as happened in Brazil with the coffee and in the United States with the mining), this economy is ready to prepare for the question of supply, investing on education and work force training, in research and progress to innovate and modernize the machinery, increasing the productivity of the

4 *Professor of the Getúlio Vargas Foundation (FGV/SP), economist and political scientist, former minister on the governments of José Sarney (Finance Minister - 1987) and Fernando Henrique Cardoso (State Administration and Reformation Minister - 1995 to 1998; Science and Technology Minister - 1999).*

industrial state. In this way, he confronts the argumentation of Graham and Tilton that mention countries like the United States, Australia and Canada (all mining and developed countries) to deny the *Dutch disease* (Bresser-Pereira, 2007).

However, for economies such as the Brazilian, that he considers as an "average income economy" and in the process of *catching up*[5], the natural resources start to play a negative role when affecting other competitive exports sectors (with a state-of-the-art technology and productivity) through the exchange rate appreciation.

Bresser-Pereira (2007), agreeing with Palma, mentions the cases of Brazil and Mexico that, according to him, were successful in *catching up* between 1930 and 1980 when unconsciously defeated the Dutch disease[6], but unfortunately, were "forced" to adopt what he calls radical liberalism, due to accusations of protectionism, led to a premature deindustrialization. Hence, the non-neutralization of the DD, associated to the increase of commodity prices exported by them, intensified the gravity of the "illness" of these countries' economies and of the Latin American countries in general.

Another important issue in this author's work is the distinction he makes between the restricted and the enlarged DD. The former is based on the work of the English economist David Ricardo and it is supported by the theory of the Ricardian income, and the latter analyses the amplitude of the industrial "wage range", that is, the difference between the earnings of non-skilled and skilled employees, in distinct sectors of the same economy, when comparing to other economies. Bresser-Pereira shows that the greater the Ricardian incomes obtained with the efficiency differential between the local extractive industry and the less efficient competitor admitted in the international market, the greater the exchange rate appreciation and the intensity of the Dutch disease as a result. In the same way, the greater the wage range is (that in developed countries is of three or fourfold and in developing countries is of more than tenfold), also the greater will be the pressure on an exchange rate that makes viable the sector that uses cheaper labor (and that consequently has a lower per capita aggregated value), causing difficulties to sectors that need a more skilled labor, and inevitably aggregate a greater value per capita. He also believes that China is "ill", but, nevertheless, neutralizes the effects by managing the exchange rate. (Bresser-Pereira, 2007).

Luiz Carlos Mendonça de Barros (2006)[7] states that the Dutch disease phenomenon cannot be denied. He

5 *The catch-up effect, also called the theory of convergence is the process in which economies in development go through to reach developed countries in terms of GDP, Welfare State, etc...*

6 *Unconsciously, because Brazil, for example, adopted multiple exchange rates to different sectors, subsidizing some hindering others, strong protectionism through burdensome importation tariffs and subsidy to some exportation sectors. According to Bresser-Pereira, all these policies neutralized the Dutch disease, because in practice they had the same effect of the exchange rate control, capital control and export tariffs on commodities that cause the Dutch disease (author's suggestions for the neutralization).*

believes it to be a chronic and not a severe "disease", with effects arising slowly and lasting for a long period, making it difficult to be diagnosed. When analyzing the conjuncture of the national productive sector, he notices the symptoms in the manufacturing sector of the Brazilian economy, affected by the extreme loss of competitiveness brought by the appreciated exchange rate. In those export sectors (textiles, for example), the investments to expand the industrial park are being postponed or cancelled or, in some cases, being transferred abroad, to countries like China, therefore displacing the production and the creation of new employment posts (Folha de São Paulo, 2006).

On extensive studies, Sidney Nakao Nakahodo[8] and Marcos Sawaya Jank (2006)[9] analyzed empirical data of Brazil's balance of trade, in which they discuss the existence, or not, of the deindustrialization process, in order to investigate the *Dutch disease* in Brazil. Nakahodo and Jank clash with Palma on the discussion about this fundamental issue as we will see on the next topic.

3.1 Brazilian Economy Deindustrialization

Nakahodo and Jank (2006) deny the existence of a deindustrialization process due to the positive performance of the processed commodities exports in Brazil, and also of industrialized products of medium-high and high technology, based on empirical evidences related to the balance of trade data, the good performance of the national industrial sector and the supposed deindustrialization process; and they also accept that one of the main indicators of industrialization or deindustrialization of a country is the analysis of its industrial employment rate.

In order to measure the industrial employment rate these authors take into account the total number of people working in the industrial sector, contradicting Palma (2005), who considers the number of people working in the industry against the total number of workers in the economy. It is evident that there is a key disagreement point, and it is important to reflect upon the differences of analysis methods of industrial employment rates employed by the authors.

Comparing the number of professionals employed in the industry to the total number of workers in the economy, the Palma's method is able to best evaluate if there is a relative flow of workers between sectors of the country's economy. For example: the stability of the absolute number of industry's workers in an economy makes us think about the stability of industrial employment rate in Nakahodo and Jank's method. But the industrial sector could be reducing its participation if the number of workers of the country is increasing, thus displaying a greater attraction to the agricultural and cattle raising and/or services sectors. However, this phenomenon is recognized

7 *Economist and Engineer, former president of BNDES (Brazilian Development Bank) and former Communications minister in Fernando Henrique Cardoso's government.*

8 *Researcher and collaborator of ICONE (Institute for International Trade Negotiations).*

9 *ICONE's president and professor of FEA-USP (São Paulo University Department of Economics).*

only with the use of Palma's method. Palma also analyses the changes in employment structure in the world's economy, especially in developed countries, initiated by the Agricultural Revolution[10]. Following the liberation of the work force previously used in the fields, at first other sectors, like services and industry, absorb, mostly, but not completely, this labor excess, causing the phenomena of unemployment and informal employment. Afterwards, he states, the services sector keeps growing and absorbing work force, nevertheless the industry, that presents a more modern park and very intensive in capital, stabilizes its labor needs. Finally the deindustrialization process happens, when the rate of formal industrial employment declines, both relatively or absolutely, lasting only the services sector to absorb part of surplus workers, according to figure 3 (Ser = services sector; mf = industrial sector) (Palma, 2005).

Analyzing the graphic we realize how part of this process happened, more specifically at the third moment (deindustrialization) with the analysis of the different evolution rhythms of productivity and production of the industrial and service sectors:

The employment reduction in the industry, according to the figure above, happened due to a strong increase on the productivity accompanying the growth of production, however the former being greater than the latter;

In the services sector the employment growth is derived, reversely, from a great

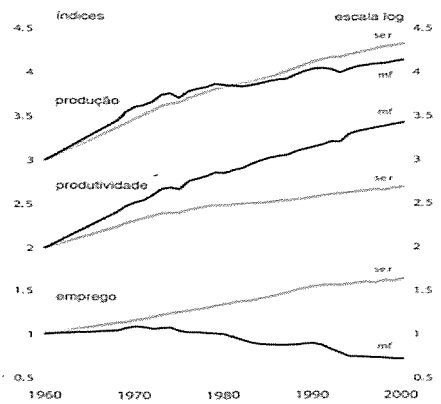

Figure 03: Industry and Service on UE

Source: Rowthorn apud Palma, 2005

expansion of production levels (in part a response to the outsourcing of many activities in the industry itself) followed by a less expressive expansion of the tertiary sector productivity.

The process of intersectorial reallocation of employment posts confirms the inclination of the service sector to absorb, at least in part, the reduction of the industry employment level. Palma (2005) analyses 105 different economies in all continents: Africa, Asia, Oceania, Europe and the Americas. He concludes that this process is shared common[11], though there is a direct relation between the economic development level and the early deindustrialization process, that is, the most developed nations went through this process between 1960 and 1970, on the other hand, the developing countries, between 1980 and 1990. Palma emphasizes that our economy, just

10 *Increase of productivity at the agriculcultural sector, due to the mechanization of activities and the consequent reduction of labor needs to the operations of the sector.*

11 *Countries like Norway, Sweden, Finland, Malaysia, Indonesia and The Philippines would be exceptions.*

like other countries', has been through a reduction of the employment rate contrary to what Nakahodo and Jank claim, using absolute values and supported by data from ICONE[12], concluding that the drop on industrial employment rates in Brazil stabilized from 1999 and is recovering since 2004.

3.2 *Neutralizing the possible Brazilian disease*

The economic policies employed for eliminating the nasty effects of the Dutch disease are harshly criticized by academics, politicians and citizens involved in this issue, despite of being instruments already employed by many countries. And it could not be different, being an issue that lacks consensus, the potential ways of neutralizing DD are also controversial.

To Bresser Pereira (2007), the market failure is so clear that it is impossible to maintain one of the bases of the current economy: the floating exchange rate. The author does not propose to fix it, on the contrary, he just does not accept the opposites of a fixed or a floating exchange rate. As the market presents some failures, and in the case of the Dutch disease, this failure was indentified and acts with externalities through the exchange rate, he suggests a floating but controlled exchange rate. This control can be performed in three ways, as mentioned previously:

1. Purchase of foreign exchange reserves;
2. Tariff on exports goods that create the DD;
3. Control of capital flowing into the country.

Bresser-Pereira (2007) affirms that the purchase of foreign exchange reserves by Brazilian government happens only at times of great exchange rate appreciation, but not to secure the quotation at interesting levels to the exports sectors. However, it is important to remember that the Brazilian government is managing the exchange rate since 2003, so the country could take advantage of the strong international market liquidity (ended with the American crisis) in order to reduce the total foreign debt, adding aggressively to its foreign reserves. So, recently, and for the first time in history, the country became an international creditor. On February 2008, the Brazilian Central Bank estimated that the total net foreign debt (foreign debt minus foreign reserves) became negative in approximately US$ 4 billion. Just as a comparison, in 2002 our foreign exchange reserves achieved US$ 16.3 billion while on February 9th, 2008, it was of US$ 200.115 million (Brazilian Central Bank, 2008).

On the other hand, the export tariff would be a way to secure the quotation in levels that would help the potential exporter of the country without being an onus to the tariffed sector. This tariff would work like this: it would affect only the difference between the market exchange rate (updated and appreciated by the DD) and what he calls industrial exchange rate, the one that makes it feasible to other export sectors with state-of-the-art technology. Hence, the commodities export sector would be punished with the tariff, but only on the differential gain caused by the currency depreciation (Ex.: the rate would go

12 Institute for International Trade Negotiations.

from the current R$ 1.70 – R$ 1.80 to R$ 2.00 and the tariff would be applied to these R$ 0.30 – R$ 0.20) (Bresser-Pereira, 2007). Admitting that the tariff would suffer resistance from the private sector that is going through a *boom*, there would be political opposition to its implementation. The author cites Norway and the countries part of OPEC[13] (petroleum), Chile (copper), to demonstrate that this proposal is achievable, even in a developing country. Another recent example is India, which has already been tariffing its exportations, in this case iron ore, in 10%, and informed, in January, an increase of this percentage to 15% from April, 2008 (China Economic Review –January 9, 2008).

However, Bresser-Pereira remarks on the last two cases: the amount obtained with the tariff should originate an international fund, as done in Norway, and not be returned to the country, as in Chile and the OPEC countries. These resources should not be used, because in this way they do not affect the exchange rate, and correspond only to a simple tax burden.

Ming (2007), on the other hand, does not believe in the efficiency of those proposals, specially the export tariff. When comparing the Brazilian balance of trade, more specifically the national export sectors, to other countries, that in the author's opinion are accused of having the Dutch disease and trying to neutralize it, he states it is not the Brazilian case. He states that in Brazil the primary products exports are less than 40% of the total, therefore needing an enormous "confiscation" of the income from these products so that it could affect the exchange rate. Also, according to the author, even if it was Brazil's case, the tariff is administratively complex due to the great variety of products to be tariffed (different from the cases of Norway, petroleum only, and Chile, copper) and the price variation due to the international quotation of the products.

Ming (2007) states that, in fact, Brazil should idealize some actions to reduce production costs, working on issues such as the tax burden and social benefits paid by the productive sector. This would be a means of gaining competitiveness, especially to sectors affected by the exchange rate appreciation.

Yoshiaki Nakano (2006)[14], despite of not mentioning the DD issue, admits that a control of capital is necessary so the country can overcome the low growth rates, according to him, and besides other factors like the high interest rates, that strongly influences this issue. Bresser-Pereira also shares this opinion, and recommends this measure for extreme cases of DD, when the pressure on the exchange rate is so intense that neither the purchase of foreign exchange reserves, nor the exports tariff takes effect. Both of them also agree about the market resistance to accept this measure. A resistance by intellectuals and liberal politicians that strongly defend a varying exchange rate manipulated by

13 *The Organization of Petroleum Exporting Countries.*

14 *Economist, director and professor of the Getúlio Vargas Foundation (FGV-SP), former secretary of the Finance Ministry during the Mário Covas government (1995-2001).*

the market itself, even if it presents so visible failures.

Oreiro and Lara (2006) emphasize that among the BRICs (the fast growing developing economies: Brazil, Russia, India and China), Brazil is the only that does not control the exchange rate, possibly one of the reasons for the country's inferior growth rate in the last years when compared to the other countries of the group, besides the signs of deindustrialization.

Mentioning specifically China and India, where there is a control of capital, the authors defend the adoption by the Brazilian government of compulsory deposits of 30% on investments in the country of less than a year, that is, the speculative capital. They also proposed, based on the suggestions of Tarapore Committee to the Reserve Bank of India, the adoption of an exchange rate band, monitored by the government, but without being obliged to intervene in case the exchange rate goes out of the band (Oreiro & Lara, 2006).

4 CONCLUSION

This article aimed to review, systematize and analyze the main ideas currently being discussed in Brazil about the existence of a "Brazilian disease". In order to contextualize the reader, we initially presented some arguments by a few authors about the Dutch disease, through models and classic theories on this issue.

Subsequently, we introduced the authors that study the Brazilian context, and the existence of the DD in Brazil.

We believe that the discussion about the existence of a "Brazilian disease" is one of the most important current debates in Brazil's economy, that derives from the "commodification" of our exportations, caused by the increase of prices and the quantity produced of many of those commodities, especially minerals, and by the damaging effects caused by the exchange rate appreciation.

This debate is not over, because these factors continue to influence determinedly the national economy. Further depth on this debate is urgently required, once the diagnosis and future actions in response to this serious market failure should be done, if possible, in a very short term.

REFERENCES

BARROS, L. C. M. de, 2007. A Doença Chama-se Hemocromatose. Folha de São Paulo (Internet Home Page). São Paulo. Accessed on January 20, 2007. Available on: http://www1.folha.uol.com.br/fsp/dinheiro/fi1108200603.htm.

BOLETIM FOCUS, 2008. Indicadores de Sustentabilidade Externa do Brasil – Evolução Recente. Accessed on March 30, 2008. Brazilian Central Bank (Internet Home Page). Available on: http://www4.bcb.gov.br/pec/GCI/PORT/focus/X20080221-Indicadores%20de%20Sustentabilidade%20Externa%20do%20Brasil-Evolução%20Recente.pdf.

BRESSER-PEREIRA, L. C., 2007. Carta de Bresser a Ming: Ganho ao invés de confisco. São Paulo.

BRESSER-PEREIRA, L. C., 2007. Doença Holandesa e sua Neutralização: Uma Abordagem Ricardiana.

BRESSER-PEREIRA, L. C., 2008. A Maldição dos Recursos Naturais Bresser Pereira. Web Site (Internet Home Page). São Paulo. Available on:http://www.

bresserpereira.org.br/ver_file.asp?id=1548&busca=maldicao%20dos%20recursos%20naturais.

CORDEN W. M.; NEARY, J. P., 1983. "Booming Sector and De-industrialisation in a Small Open Economy" in *The Economic Journal*, vol. 92, pp. 825-848. Reprinted in W.M. Corden, "The Exchange Rate, Monetary Policy and North Sea Oil: The Economic Theory of the Squeeze on Tradables", *Oxford Economic Papers*, vol. 33, Supplement, pp. 23-46. Reprinted in W.M. Corden, "International Trade Theory and Policy", Edward Elgar Publishing, 1992.

DAVIS, G. A.; TILTON, J., 2005. E. La Maldición De Los Recursos Naturales In: LAGOS, G. (org.) *Minería Y Desarrollo – Foro en Economia de Minerales vol III.* Santiago: Ediciones Universidad Católica de Chile.

Indian tax could affect steel negotiations, China Economic Review, 2008. Accessed on April 17, 2008. Available on: http://www.chinaeconomicreview.com/dailybriefing/2008_01_09/Indian_tax_could_affect_steel_negotiations.html.

MING, C., 2007. Confisco de exportação. O Estado de São Paulo.

MING, C., 2007. Exportações sem Confisco. O Estado de São Paulo.

NAKAHODO, S. N.; JANK, M. S., 2006. A Falácia da Doença Holandesa no Brasil. ICONE: Instituto de Estudos do Comércio e Negociações Internacionais (Institute for International Trade Negotiations Home Page). São Paulo. Accessed on January 20, 2007. 24p. Available on: http://iepecdg.com/DISK%201/Arquivos/Leiturassugeridas/Doenca%20HOLANDESA%20FINAL%206MAR%20-%20final-27032006.pdf.

NAKANO Y., 2006. Marca de Nakano. Jornal Valor Econômico.

Nam - Bron van Energie Web Site (Internet Home Page). Assen, Holanda. Accessed on March 14, 2007. Available on:http://www.nam.nl/home/Framework?siteId=nam-en&FC2=/nam-en/html/iwgen/algemeen/zzz_lhn.html&FC3=/nam-en/html/iwgen/algemeen/aardgas_nederland.html.

OREIRO, J. L. C., LARA, L., 2006. Uma nova política cambial para o país. Jornal Valor Econômico.

PALMA, J. G. Quatro Fontes de "Desindustrialização" e um Novo Conceito de "Doença Holandesa", 2005. Work to be presented in: Industrialization, deindustrialization and development Conference. FIESP e IEDI, Centro Cultural da FIESP. São Paulo.

Reservas Internacionais – Conceito de Liquidez Internacional (Foreign exchange reserves – Concept of International Liquidity) (Position in February 5, 2009). Brazilian Central Bank. Accessed on February 9, 2008. Available on: http://www4.bcb.gov.br/?RP20090205

SACHS, J. D.; WARNER, A.M., 1997. Natural Resource Abundance and Economic Growth. HIID Working Paper. Cambridge MA.

SACHS, J. D.; WARNER, A.M., 2005. Recursos Naturales Y Desarrollo Econômico In: LAGOS, G. (org.) Minería Y Desarrollo – Foro en Economia de Minerales vol III. Santiago: Ediciones Universidad Católica de Chile.

SANDRONI, P., 2005. Dicionário de Economia do Século XXI. Rio de Janeiro. Editora Record.

SILVA, K. M. O. de., 1994. The Political Economy of Windfalls: The "Dutch Disease" Theory and Evidence. St. Louis.

The Dutch Disease. The Economist. November 26, 1977. pp. 82-83.

The Iron Ore Industry in China

R. F. Ferreira, M.A.T. Furtado,
Universidade Federal de Ouro Preto, Ouro Preto, Brazil

ABSTRACT China is, currently, the greatest raw iron ore producer of the world, but it needs to import millions tons of ore to blend with the domestic iron ore and to provide its steel industry. This is because, despite the high demand, the Chinese iron ore has a low grade, with an average of 35% of Fe, occurring almost always associated with other metals and various types of contaminants, in deposits of often complex geology. However, given the high price charged by foreign mining companies, the investment in local mining, in the mineral exploration and technologies development that enable the expansion of economically exploitable reserves of that country has grown in recent years, stimulated by government policies. This study provides a profile of the Chinese iron ore industry, from the deposits' geology to the market, including the mining aspects, infrastructure, new technologies development for low grade ores beneficiation, guidelines and policies. It also discusses the trade relations, in this commodity, between China and Brazil.

1 INTRODUCTION

The most populous country in the world grows amazingly. It is currently the only country that can surpass the United States in the global economy. With an area of 9.6 million square kilometers, China has 1,330,044,605 people, with 94% of these are concentrated in 40% of its vast territory. The Chinese GDP (Gross Domestic Product) grew 11.4% in 2007, representing the fifth year of growth above 10%. The GDP rose to 24.66 trillion yuan (U.S. $ 3.41 trillion), which keeps the Asian giant in the fourth position worldwide, behind the United States, Japan and Germany.

The Chinese government's current guidelines are the development of the region west of the country (March to the West) and rural area, and intensive urbanization. There is also concern about the environmental impacts caused by the country development. At present, China aims to reduce the growth rate, which is justified by inflation and the energy issue.

China is putting into practice its plan to become a superpower. Investment in light industry, which was prioritized since 1986, requires labor, which causes migration to cities, expected in up to 800 million people in 30 years. The government intends to promote such

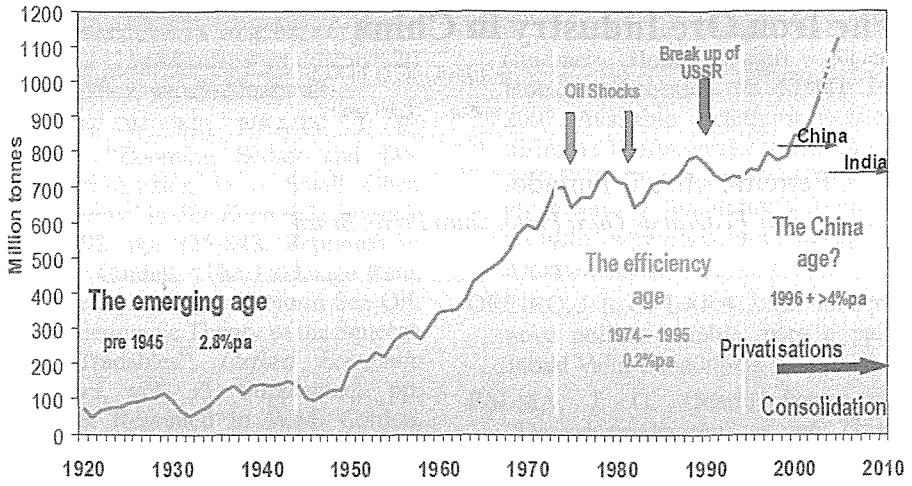

Figure 1: Evolution of global steel production. Source: BHP Billiton (2005).

migration on a highly controlled manner. A peasant could move to a city only if it has jobs and housing available. China therefore needs to modernize the existing cities and build new cities according to a plan aimed at an urban infrastructure capable of absorbing the huge mass migration. For this are necessary inputs for construction, as cement, aggregates and steel. Appears, then, the huge Chinese demand for steel (figure 1), which stimulates the iron ore extractive industry both in its own territory and abroad.

2 GEOLOGY

China has a huge iron ore reserve, up to 68 billion tons (measured reserves, data from Ministry of Land and Resources of China, 2007), and the reserves economically exploitable are of 60.7 billion tons. About 41.5 billion tons of ore have magnetite as the mineral-ore. The country leads the run of mine ore production; however, is also the largest iron ore importer in the world. This is because the Chinese iron ore has low grade, with an average of 35% iron. According Xhun (2006), the Chinese reserves are distributed in 30 provinces, municipalities and autonomous regions (excluding Taiwan), among which Liaoning, Hebei and Sichuan are the main holders of reserves. The North and Northeast regions have the largest reserves, followed by the regions west, east, south-central and northwest. The principal mining districts are: Anshang Benxi (Liaoning Province), East of Hebei, Panzhihua - Xichang (Sichuan Province), Luliang - Wutai - Ningwu (Shanxi Province), Bayan Obo (Inner Mongolia), Shangdong Central, East Hubei and Hanxing (Figure 2).

The iron ore geology in China is complex when compared to Brazilian ore. Various types of deposits occur as to the origin, quality, contaminants, contents, etc. In most of the deposits (more than 90% according Xhun 2006), the iron is associated with other (s) metal (s) (polygenic and polymetallic deposits), this being one of the most important characteristics of Chinese iron ore. As to the genesis, occur in China the following types of ferriferous mineralization, mainly:

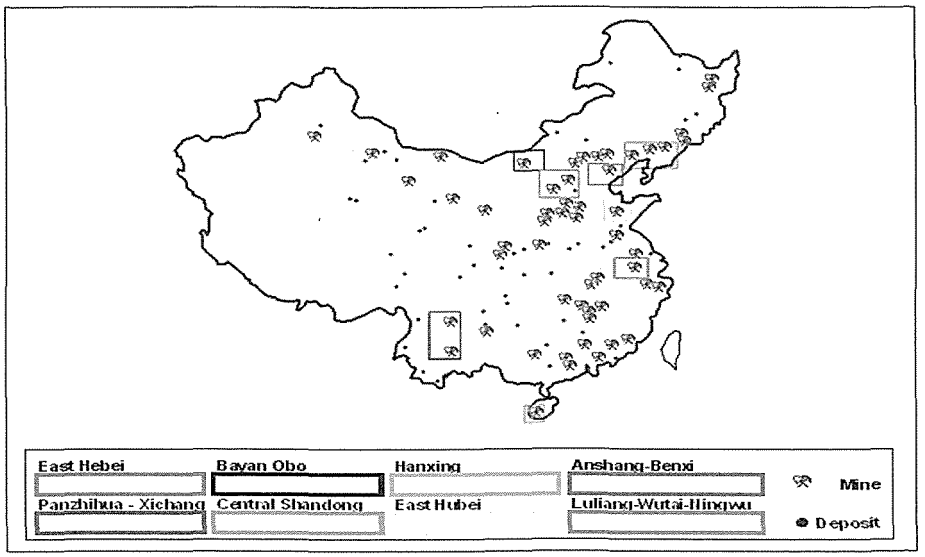

Figure 2: Main iron ore deposits and mining districts of China.

- Banded Iron Formation of the Lake Superior type: occurs, for example, in Daxigou Mine (Longmen Steel Group), open pit, with reserves of 302 Mt at 28.01% Fe.

- Banded Iron Formation of the Algoma type: these are, for example, in Qidashan Mine (Anshan Steel Corporation Limited), open pit, with reserves of 308.12 Mt at 28,79-31,79% Fe.

- Skarn: metamorphic rocks formed by contact metamorphism and that has generally as protolith carbonatic rocks as limestone and dolomite. The ferriferous skarn may be, according to Biondi (2003), calcium-Fe (iron associated with copper, cobalt and gold) or magnesium-Fe (iron associated with copper and zinc). Most iron deposits with other metals in China is of skarn origin. An example of mine whose ore is skarn is Changlongchan in Anhui Province, with reserves of 34.4 Mt at 45.31% Fe.

- Polygenic of rare-earth-Fe-Nb: there is an occurrence of this kind in China, the Bayan Obo Mine (Baotou Iron & Steel), located in the Province of Inner Mongolia. Besides containing iron, is the largest rare-earth deposit known today throughout the world and the largest niobium deposit in China. The ore origin, according to the most accepted hypothesis is epigenetic, hydrothermal and metassomatic (Chao et al. 1997). The mine is exploited by open pit method, and has reserves of 1459 Mt with average content of 33.5% Fe.

- Volcanogenic - sedimentary-hydrothermal polymetallic: occurs, for example, in Dahongshan Mine (Xi'nin Special Steel), Fe and Cu deposit, open pit, with reserves of 458 Mt of ore Fe and 1.35 Mt of Cu, at 25-50% Fe and Cu 0,52-0,60%.

(Ferriferous mineralization subdivisions according to Rodionov et al. 2003).

3 MINING ASPECTS

We can divide the Chinese iron ore extractive sector into three groups:

- Integrated firms: are those with verticalized production from the mine to the steel industry. Few of these mines produce enough and on the quality needed to supply the steel industry. It is necessary, therefore, ore imports for blending. Some are self-sufficient, or because the production level and high quality of the product, or because of distance from ports, which makes anti-economical to purchase imported ore.

- Independent mining companies: are those wich only exploits and processes the iron ore. Many of these companies supply steel industries located away from the coast. The distance to the ports, where the imported ore enters the country, makes it less costly to buy domestic iron ore, despite the lower quality, than buy and transport imported ore. They are usually state enterprises.

- Small and medium mining companies: are private companies, small and medium businesses, responsible for most of the Chinese iron ore production. A major problem faced by the Chinese government is the illegal mining. There are small mines producing in an irregular manner, without control and without technology. Resources are not taken properly. There is also the lack of security, resulting in serious accidents, being many of these mines underground.

China has about 66,000 mines, considering all substances exploited, most of them located in the eastern country. The western region is still poorly explored, showing itself as an area of great potential for future discoveries. Chinese mines are considered the most dangerous in the world.

There are many underground iron mines in China. As there is occurrence of karstic terrain in much of the territory, the problem of subsidence becomes a reality to be faced by miners. The carbonatic rocks from these regions are predominantly Paleozoic and occupy about 3.25 million square kilometers of Chinese territory (Yu, 1994). In 1994 were identified approximately 797 subsidence areas in China, with more than 30,000 subsidences occurred mainly in mining areas in karst and groundwater exploitation.

The mining operations in major Chinese mines follow the international standard, with mechanized exploitation and use of large equipment (table I).

One of the guidelines of Iron & Steel Industrial Development Policy in China, launched by the government in 2005, is the investment in research and process technology development for the domestic iron ore. Many universities and research centers develop projects aiming to improve processes and enable the exploitation of low quality ore huge reserves available, through new technologies development. New equipment was developed, such as vertical ring and pulsating high gradient magnetic separator - Slon (Ganzhou Institute of Nonferrous Metallurgy), widely used in Chinese plants, and the Column Magnetic Separator (University of Science and Technology of Liaoning). Researches have been developed, too, with the objective of improving existing technologies, developing new types of reagents used in flotation, for example.

Mining industry development requires infrastructure. Iron ore, domestic or imported, must be transported from mines or ports to the steel industries, which depends on the rail and ports. Currently in China, 80% of exploited iron ore is transported to the steel industries by rail, and the remaining 20% transported

by road or waterways. However, the transport capacity of the Chinese railway was growing less than 10% a year, unless the industrial production (Qiujun & Qun, 2008). According to The Development and Reform Commission of China the Chinese road system is almost complete, however, the rail is far from complete. This scenario tends to change: China has invested in construction and reform of railways. According to the Department of Development and Planning of the Ministry of Railways of China, 135 projects are under construction or undergoing feasibility studies and involve investments of 1665 trillion yuan. In 2020, China will have more than 120 thousand kilometers of railways in operation and the rail will cover all cities with population exceeding 200,000 inhabitants. According to the Embassy of the Republic of China in Brazil, investment in railways in China rose 37.5% between January and July of 2008. This is a result of the rapid growth of high-speed lines and corresponds to the expectations of connecting distant regions of the country. The investment reached 133.78 billion yuan (U.S. $ 19.6 billion), according to the Ministry of Railways. The country has approximately 75,438 km of railways, occupying the third place in the world ranking, behind the United States (226,612 km) and Russia (87,157 km).

The Chinese railways' relatively low transport capacity also influence the imported ore transport: piles of ore

Table I: Technical parameters of the main Chinese iron ore mines. Prepared according to China Iron Ore Mining Industry Research Report data (2008).

Company	Mine		Production (2006)	Exploitable Resources (Mt)	ROM Grade (%Fe)	Concentrate Grade (%Fe)	Tallings Grade (%Fe)
Benxi Iron&Steel Co., Ltd	Nanfen	OP	6245412	1100	29,12	67,38	8,45
Benxi Iron&Steel Co., Ltd	Waitoushan	OP		2400	29,25	67,01	7,49
Baotou Iron&Steel Co., Ltd	Bayan Obo	OP	4788712	1500	32,81	66,00	-
ShouGang Group	Shuichang	OP	4743299	902	26,55	67,51	7,18
ShouGang Group	Malanzhuang	OP		180			
ShouGang Group	Mengjiagou	OP		260			
ShouGang Group	Miyun	OP		900			
ShouGang Group	Yichang	OP		700			
Panzhihua Iron and Steel Group Corporation	Lanjian	OP	4719002	131	34,35	52,84	16,93
Taiyuan Iron&Steel Co., Ltd	Ekou	OP	3772366	290	28,54	66,37	13,55
Taiyuan Iron&Steel Co., Ltd	Jianshan	OP		600	33,47	69,60	8,41
Wuhan Iron and Steel (Group) Co	Daye	OP	3324293	30	50,67	-	-
Wuhan Iron and Steel (Group) Co	Jingshandian	UND		133	42,96	61,63	8,80
Wuhan Iron and Steel (Group) Co	Chengchao	UND		133	48,30	65,77	8,68
Wuhan Iron and Steel (Group) Co	Enshi	OP		1285	33,00	-	-
Wuhan Iron and Steel (Group) Co	Xuchang	OP		236	39,75	-	-
Tangshan Iron and Steel Group Co., Ltd.	Shirengou	UND	3194332	79	29,12	67,68	4,42
Tangshan Iron and Steel Group Co., Ltd.	Bangmoshan	OP		3	33,20	68,02	5,13
Tangshan Iron and Steel Group Co., Ltd.	Miaogou	OP		19	26,68	63,71	7,42
Tangshan Iron and Steel Group Co., Ltd.	Sijiaying	OP		2000	30,00	-	-
Ma Steel	Aoshan	OP	2956144	30	27,54	64,30	10,01
Ma Steel	Dongshan	OP		11			
Ma Steel	Gaocun	OP		342			
Ma Steel	Heshangqiao	OP		27			
Ma Steel	Gushan	OP		86			
Ma Steel	Baixiangshan	UND		145			
Ma Steel	Luohe	OP		341			
Jiuquan Iron & Steel Company (Group) Limited	Jingtieshan	UND	2743871	463	33,21	51,88	16,41

remains stockpiled in ports for days waiting for transport. In May 2008, for example, imported iron ore stockpiles in Chinese ports reached a record of 79.22 million tonnes, which forced the government to restrict imports in excess. According to the National Development and Reform Comission, congestion has occurred mainly in the northern ports: Qingdao, Tianjin, Rizhao and Lianyungang, the largest iron ore port in China.

With respect to road and waterways transport, China has 1,930,544 km of roads, of which 1,575,571 km are paved, and 124,000 km of navigable waterways.

4 PRODUCTION

China is currently the world's largest raw iron ore producer (figure 3). Among the provinces, the main producers are Hebei, Liaoning and Inner Mongolia, and the production of these provinces corresponds respectively to 43.8%, 15.4% and 7.9% of total production in the country. These data show a relative concentration of the iron ore production.

Small mines are responsible for 79% of production. These mines are private and very influenced by the iron ore price: the high prices makes viable their operation. This shows the small-mining importance on extractive industry in China, and justifies the efforts by the government in to regulate and monitor the activities of such mining companies. There is a strong trend of large companies take control of these small mines, following a policy of protection and appropriate utilization of mineral resources implemented by the government.

Due to the difficulty to compute private and small mining companies output, the production estimates in China are difficult to achieve, and can deviate from reality. China Metallurgical Mines Association estimated a production of 944,000,000 tons of ore in 2009.

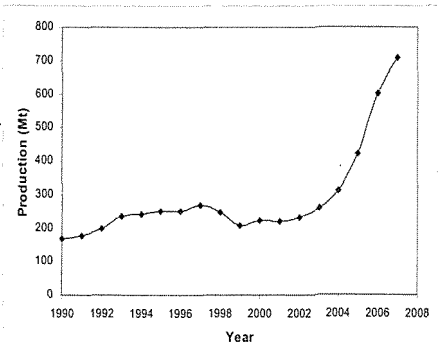

Figure 3: Chinese iron ore production. Prepared according to USGS data (2008).

5 GOVERNMENT POLICIES

In 2005 the Chinese government released a document called "Iron & Steel Industrial Development Policy", containing the guidelines for both the steel industry itself and for the exploitation of raw material applied to the steel production, including iron ore.

According to the document, the steel industry is vital to the national economy, and the sector development depends on several aspects: technology, resources, capital, energy and environment. Given the high steel demand in China, the document states that the technological level and resources management, at the time of this policy launch, were not satisfactory, therefore, the technological and structural upgrading should be the center of steel industry development. This includes the exploitation of raw

materials needed to produce steel. We present below the greatest importance points with respect to iron ore, contained in the document.

- Support from the State for large steel companies to exploration and exploitation of resources such as iron ore. Such activities must be authorized by the State in accordance with applicable law. Mine projects whose reserves exceed 50 million tonnes must be reviewed and ratified by a government agency called National Development and Reform Commission (NDRC).

- Prohibition of uncoordinated exploiting, surveillance intensification and offenders punishment. All the mining project to be established should include mining planning, and plans related to security and environmental preservation. These actions emphasizes the government's concern for the small miners, constant sources of accidents, and to mineral resources management, because of exploitation activities without proper control often involve the use of only the better quality portion of the deposit. The lack of control also leads to poor use of resources due to lack of technology, both in mining and in processing the ore.

- New technologies development for low quality ores beneficiation. The document states that the nation should encourage companies to develop technologies for poor ores treatment in order to make full use of national resources, expanding the country's exploitable reserves and optimizing the iron ore recovery of the processing plants. This premise has been accomplished successfully, with equipment development and existing processes improvement through research developed by companies, universities and government agencies.

- Strengthening the cooperation between Chinese companies and foreign mining companies. The government supports the stable supply establishment bases of iron ore, chromium, manganese, nickel, scrap steel and coke abroad, through companies' investment (purchase of mineral reserves in other countries) or joint ventures. With the high iron ore price practiced today, many Chinese companies have launched programs to search overseas for iron ore.

- Coordination of the sector through the China Iron and Steel Association, aiming to stabilize the domestic and foreign markets for raw materials. In case of competition between domestic enterprises with resources from outside, the State may take administrative actions, as companies unify or choose only one to receive investment in order to avoid this type of competition.

6 CHINA–BRAZIL MINING TRADE

Brazil is currently the second largest iron ore producer and the fifth largest reserves holder. The measured and indicated reserves in Brazil are in the order of 33 billion tons (9.8% of world reserves), with average content of 56.1% iron (source: National Department of Mineral Production of Brazil, DNPM, 2008).

The country's production reached in 2007, 354.7 million tons, with average content of 65.9%. This production is divided between 36 companies operating 53 open pit mines and 54 processing plants, with average recovery of 75%. Only 8 of these companies were responsible for 94% of total production. The main producer is Vale (the world's largest producer), with 308.4 million tonnes (2007).

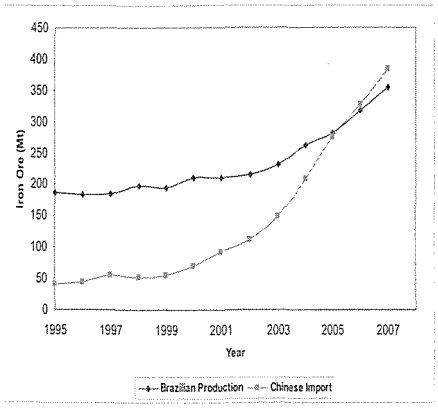

Figure 4: Brazilian Production and Chinese import of iron ore. Prepared according to USGS data (2008).

The high demand from China has stimulated the iron ore mining in Brazil, causing large companies announce plans for expansion and new projects (figure 4). If all these new projects is enforce the country's production will increase by more than 1 / 3 of current production.

The main Brazilian ore importer is China, followed by Japan and Germany. However, Brazil is in second place among the ore exporters to China, behind Australia, which, despite export an inferior quality product, is located in favorable geographical position, which results in logistical advantages (figure 5). The transport of 1 tonne of ore from Brazil to Beilun (Baoshan) in China, costs on average U.S. $ 59,672 (February 2008) and the transport cost per tonne from Australia to China is about two-thirds lower (source: China Iron Ore Mining Industry Research Report 2008). According to the DNPM, Brazil exported in 2007, 264.4 million tons of ore and pellets, of which 33% were imported by China.

In recent years, driven by demand, primarily coming from China, the iron ore price has been increasing. In 2007, the average price of fines amounted to USD 89.21 / t, with an increase of 41% with respect to 2006. The average price of lump was 87.38 USD / t, with a 35% increase relative to 2006. The average price of pellets was USD 112.02 / t, with an increase of 26.87% relative to 2006.

This prices' rise began in 2002, the year in which China joined the World Trade Organization (WTO), increasing

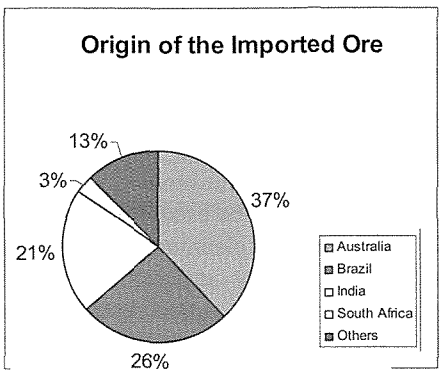

Figure 5: Origin of the imported ore in China. Prepared according to China Iron Ore Mining Industry Research Report data (2008).

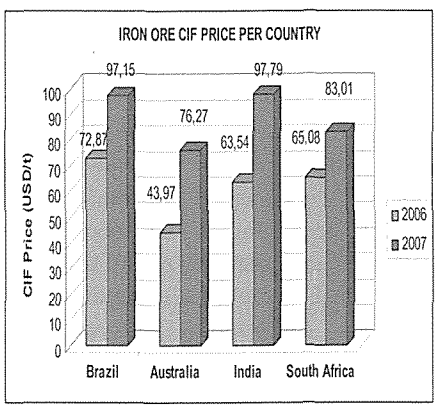

Figure 6: Iron ore price per country. Prepared according to China Iron Ore Mining Industry Research Report data (2008).

their participation in the international market (figure 6). Suppliers began to operate at full capacity and expansion projects were launched.

The power to determine ore prices by leading companies (Vale, BHP Billiton and Rio Tinto) worries the Chinese steel industry, who fear the creation of an "iron ore OPEC". The steel companies are required to accept the high prices to avoid the very expensive spot market, which would be required to use in case of cut raw material.

The Chinese steel industry focus on new options to purchase ore to face the major mining companies, the main one being the domestic ore. However, the evaluation and estimation of trends in iron ore production in China suggests that the domestic mining companies unable to meet the internal demand.

7 CONCLUSIONS

China has large mineral wealth. It is currently the world's largest iron ore producer (707,073 million tons produced in 2007) but also the largest importer. The main features of Chinese iron ore are:

- Scattered deposits, but with three main ore producing provinces;
- Usually low grade (average of 35% Fe content);
- Mineralogically complex, with polymetallic ores occurrence and various types of contaminants;
- Deposits occurrence of several genetic types;

To date, the production structure is characterized by the large number of companies in the sector. Most of these companies are small, and they are responsible for 79% of total production in the country, but their mining and processing operations are inefficient. The government invests in larger groups creation in various mineral sector activities, and implemented various actions to ore extractive industry control and development, as well as steel industry. There is a strong State presence in new partnerships and joint ventures that are happening in all Chinese economy sectors, which must also occur with iron ore.

In the future, a possible growth in domestic iron ore production will accelerate the exhaustion of the Chinese best quality reserves, and will increase the challenges related to technology for processing. It also brings challenges with respect to exploiting and the increasing costs, mainly in underground mining. This may make many mines becomes anti-economic, depending on future demand for ore.

REFERENCES

Xhun, Z., 2006. *Mineral Facts of China*, Geological Publishing House, Beijing.

Biondi, J.C. (ed. 1), 2003. *Processos Metalogenéticos e os Depósitos Minerais Brasileiros*, Oficina de Textos, São Paulo, 528 p.

Chao, E.C.T. et al., 1997. The Sedimentary Carbonate-Hosted Giant Bayan Obo REE-Fe-Nb Ore Deposit of Inner Mongolia, China: A Cornerstone Example for Giant Polymetallic Ore Deposits of Hydrothermal Origin, *USGS Bulletin 2143*.

Rodionov, S.M. et al., 2003. *Preliminary Metallogenic Belt and Mineral Deposit Maps for Northeast Asia*, USGS, United States of America, 104 p.

Yu, P., 1994. Surface Subsidence in the Karst Mining Area in China, *Mine Water and the Environment N.2,* volume 13, pp.21-26.

Qiujun, S., Qun, Z., 2008. Evaluation on Sustainable Development of China's Iron and Steel Industry, *2008 International Symposiums on Information Processing (ISIP)*, pp.700-704.

Metallurgical Council, 2005. *China Metallurgical Newsletter N.14*, volume 7.

Departamento Nacional da Produção Mineral (DNPM), 2008. *Sumário Mineral Brasileiro*, Ministério das Minas e Energia, Brasília.

Beijing HL Consult Co. Ltd, 2008. *China Iron Ore Mining Industry Research Report 2008*, Beijing, 281 p.

Toth, P., 2005. *Chinese Iron ore Demand - "Stronger for Longer" An update on BHP Billiton's Expansion Plans*, BHP Billiton, presentation in Power Point.

United States Geological Survey, USGS, 2008. *Iron Ore: Statistics and Information*, United States of America.

Efficiency Estimation of Mining Organization processes

Vladan Jovičić, Vlada Pavlović
Electric Power Serbia, Lazarevac, Serbia

ABSTRACT In order for mining organization to carry out the evaluation of its efficiency and effectiveness before all it has to establish which method is suitable for evaluation of its performances.

Methods of measuring performances, which are suitable for mining and process oriented organizations, have to include the evaluation of product quality, capability and capacity of production processes, possibility of equipment and human resources exploitation. Also, modern methods of measuring process of performances have to support change of focus of the management to customer and environment.

Based on well defined and balanced key performance index, top management will be able to make the decisions on measures of improvement of efficiency and effectiveness of business processes, i.e., continual growth of mining organization.

INTRODUCTION

Each business organization should allow measuring, analysis and assessment of its business results, capabilities of business processes, customer satisfaction, costs and everything else that comes from requests of interested parties. In other words each organization should enable measuring, analysis and assessment of its efficiency and effectiveness, in order to conduct its improvements continually. Conduct of these requests implies constant collection, grouping and analysis of information necessary for their monitoring. The results of analysis of this information should be the input into the process of reexamining by the management and should be used in whole business organization as support to efficient and effective management and increasing of efficiency and effectiveness of the company for well fare of all interested parties.

In order for organization to carry out the exact evaluation of its efficiency and effectiveness, it must determine which method is suitable for its evaluation. If a business organization uses methods for evaluation of efficiency and effectiveness which are out-of –date or not suitable for its form of business operations, obtained results will not give a real picture of conditions in the business organization. Mining organizations which deal with coal exploitation for needs of energy production have a line of specificities which influence the choice of suitable way of evaluation of its efficiency and

effectiveness. This especially refers to a fact that these business organizations exploit non renewable natural resources where dramatic ecological changes in their near and further surroundings are most often initiated. Because of this, suitable method of measuring of performances of mining business organization, besides standard views, must specially focus on, for example, local community, environment etc.

There is a line of methods which from different aspects measure performances of business organization, but most frequently used method is balanced scorecard – BSC and before due to its rationality, because it follows optimal number of key business characteristics whose choice has come from vision and strategy of the company. Researches have shown that BSC in regard to other methods is most directed towards results and it's the closest to the user and besides that, it is easily connected with other tools for measuring success if they are used in the company.

1 BALANCED SCORECARD METHOD

Balanced scorecard is a new concept established by scientist Robert Kaplan and David Norton at the end of last century as revolutionary new system for measuring organizational performances. Balanced scorecard is a method which tries to balance financial and non financial success which is measured through evaluation of short term and long term reports. By balancing of mixture of financial and non financial measures, balance of results focuses the attention of managers to short term and long term business operations. Balanced scorecard is one type of assistance for creating balance between different factors, which have the same opinion on strategy of business organization for its future development.

Balanced scorecard – BSC transfers the mission and strategy of business organization into understandable group of executive measures which ensure the frame for implementation of business strategy. It is not focused only on achieving financial goals, but especially emphasizes the non financial goals which organization must achieve in the aim of obtaining financial goals. That is why this methodology can in the best way respond to requests of mining company for continual follow up of efficiency and effectiveness of very business processes as well as all other parameters which can influence the business operations. This method is especially well accepted by the management because it is based on transformation of organizational strategic goals into performances indicators. Having in mind its structural approach for using information connected to measuring performances, BSC significantly facilitates setting up the goals, helps with resources allocation, ensures maintenance or change of strategy for managers, enables reporting on progress of accomplishing strategic goals. Also, BSC enables establishment of one integrated management model in organization, because it enables for observed strategic aspects to determine the relevant goals and to include characteristics which will be measured. In its basic form BSC uses four perspectives: financial perspective, buyer's perspective, perspective of internal processes and perspective of learning and innovations.

On the basis of these four perspectives BSC method builds the frame for integration of suitable measuring carried out from the strategy. Real strength of

BSC is when it is transformed from the system of measuring into the business system. It fulfills the void which exists in many management systems, i.e., shortcoming of systematic process to implement and carry out feedback on strategy, because if an organization wants to succeed and survive it has to use measuring systems and management obtained from strategy.

BSC concept with each of the four mentioned perspectives connects elements of strategy, and for each element of the strategy it determines the measurable performances.

Financial perspective focuses financial measures. Some of them can be: operational profit, return of investments, cutting down expenses in key areas etc.

Perspective of a buyer is established on identification of target users and part of the market where they would compete and where the performances would be measured. This perspective includes indicators such as customer's satisfaction, keeping the customers, new customers, spreading their share of the market. The perspective of a buyer tells us what the capability of the organization to deliver high quality product is in optimal time with the lowest possible price, which generally provides general satisfaction of the buyer and for business organization the increase of the profit.

Perspective of internal processes is in charge of identification of critical internal processes in which the organization must be distinguished. This perspective is focused on processes which have the largest influence on buyer's satisfaction and financial goals. These processes enable organization to attract and keep the buyers and to satisfy the expectations of share holders in view of returning invested capital. Perspective of internal processes of mining organization contains three main sub processes:

- Innovation process: Creation of products, services and processes which would satisfy the buyers' needs

- Operational process: Production and delivery of existing products to buyers,

- Post selling service: Rendering services and help to buyers after selling or product delivery.

Perspective of learning and development identifies the infrastructure which organization must build in order to accomplish long term development and progress. Learning and development come from people, business system and surrounding and this perspective implies continual investment into education employed on all levels, improvement of business systems and improvement of organizational procedures.

2 CONSTRUCTION AND IMPLEMENTATION OF BSC MODEL IN MINING ORGANIZATION

Mining organizations in regard to other companies have a line of specificities which during construction and implementation of BSC method have to definitely be taken into consideration. Significant differences of mining organizations in regard to others are that they carry out the exploitation of non renewable natural resources where they significantly influence the ecological changes in environment. Further more, the influence on local community is more significant than of other organizations because the development of local community is mostly connected to development and life expectancy of the mining organization. Due to this fact, the market of mining organizations is

different regarding behavior and extent in regard to markets of other organizations. Due to this fact, during construction and implementation of BSC in mining organization, the analysis should be carried out through four views:

- Human oriented,
- Internal,
- External,
- Process oriented,

The description of perspectives of BSC through four views is shown on the Picture 1.

One completed BSC in mining organization with four mentioned views is necessary to have the following components:

- Identified strategy bases,
- Identified strategy goals
- Measures for executing strategy goals
- Competitive benchmarking,
- Short term and long term goals for identified measures,
- Initiative for directing strategic goals towards execution and evaluation.

When BSC system is established on the highest organizational level, it's then when its implementation on lower levels, business functions, business processes and very business activities begins. For each organizational level it is necessary to define additional measures of performances which adjust single goals with organization goals. In this way built and implemented BSC metrics, enables managers fast and reliable detection of weak spots in organization, i.e. which organizational parts do not function in accordance with business strategy.

Model of construction of BSC in mining organization comprises of the following phases:

- Analysis of organization and its surroundings,
- Establishment of vision and mission of organization,
- Definition of strategy,
- Setting up of the perspective,

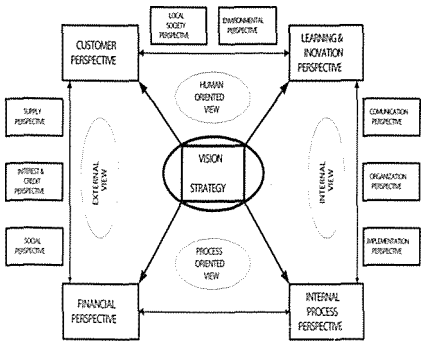

Figure 1. Perspective of BSC through four views

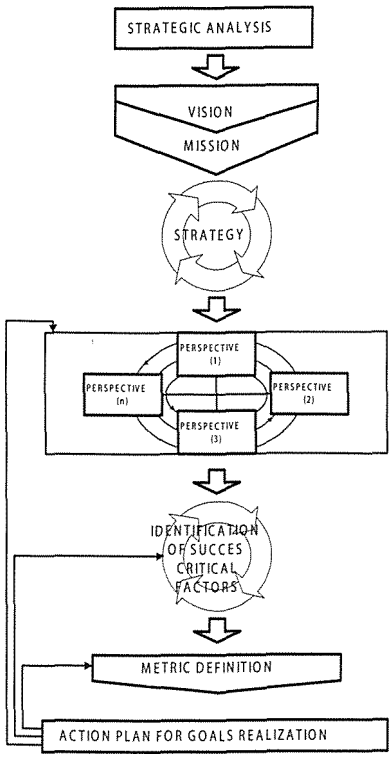

Figure 2. Model of BSC construction in mining organization

- Identification of a critical success factor,
- Metrics definition
- Action plan for accomplishing goals.

Model of BSC construction in mining organization is shown on the Picture 2.

Organization analysis and its surrounding are conducted for clearer definition of current condition of the organization and to determine the factors, positive as well as negative, which have the influence on the organization. For strategic analysis of the organization the SWOT analysis is most often used (S-strengths, W-weaknesses, O- opportunities, T-threats) because it represents the group of analytical methods which enable recognition of positive and negative factors which have an influence on accomplishment of strategic orientation of the company and give possibility to influence them timely. SWOT analysis is conducted in two phases. First phase includes gathering of key parameters of the organization and its surroundings, while the second phase includes classification of gathered parameters per groups: threats, opportunities, strengths and weaknesses. During conduct of SWOT analysis it is necessary to include all specificities which mining organization possesses.

Determination of the vision and mission of the organization is carried out and it is the responsibility of top management, because it represent the most general view of the directions in which the organization intends to develop, and mission defines and further determines the vision of the organization from the aspects of business areas in which it wants to participate, target markets, geographical areas and of business and production services. The purpose of the vision is to lead, control and motivate whole organization towards accomplishment of joint goals in the future, while the vision has to be clear, feasible, challenging, and practical and future oriented and to identify critical factors of the organization's success, to consider the priorities of all interested groups, to be lasting and at the same time flexible. Due to this, on this occasion, it is necessary to include all specificities of the mining organization in order for its vision and mission to define real strategic goals of the mining organization, before all, from the aspect of total sustainability.

Strategy defining is a process which includes definition of strategic goals and measures for its conduct, with planning and securing resources for its conduct. This process is very complex due to existence of numerous specific aspects and variables which with mining organizations must be taken into consideration. The basic idea of the vision gets its full meaning only with operationalization towards strategic goals which should be real, because goals for which it is not possible to define adequate measures through which they will be accomplished, are not real goals.

Setting up of the perspective is carried out by each organization for itself, that is, each mining organization should choose with four basic perspectives, depending on its specific situation, more additional perspectives. It is important for the perspectives to be chosen in such a way to secure balance of quality and quantity, subjective and objective, financial and non financial, historic and future success criterion. Definition of perspectives

is a key phase in the construction of BSC model of the mining organization. Due to importance of this phase it is necessary to analyze in more iteration all possible aspects of mining organization and their importance for definition of perspectives.

Identification of critical factors of the success is very important because the accomplishment of defined strategic goals depends on them. The organization should identify critical success factors in each perspective. This is very demanding and sensitive task, because it is necessary to have a good knowledge of current conditions of the organization, and mistakes in this part of BSC conduct can cause large consequences for accomplishment of the vision and strategy. Also, due to significance, this phase of construction has to be carried out in more iteration, that is, as much iteration as needed to accomplish the compatibility with adopted strategy.

Definition of metrics for each critical factor of the success should be carried out by the organization in a way that each critical factor is defined with at least one measurable characteristic. For defined measurable characteristics it is necessary to give description, measuring frequency and target values which are used for comparison with measured values.

Action plan for the accomplishing goals is conducted after defined metrics of critical success factors, that is, when the action plan of BSC is known. If management wants whole organization to follow the action plan it is necessary to be sure that all employees are familiar with it and to understand it. On the other hand, if all employees do not work as one team, there will be no success in conduct and action of BSC. The essence of understanding the plan by employees is for all of them to understand in which direction the development moves and what their obligations are in order to accomplish determined strategic goals. Practically, the implementation of the action plan is conducted in this way. Complete implementation of the action plan implies that the quality plan of action has been developed with complete understanding by employees with constant feedback of planned and accomplished. In that way the plan for accomplishment of wanted goals has been formulated and implemented.

3 CONCLUSION

In order for mining organization to conduct the strategic plans, it has to continually carry out the evaluation of its efficiency and effectiveness. In this paper BSC method has been shown, as method widely accepted, and which has been modified in regard to standard so all specificities of mining organization must be satisfied. This model is not final and it has to be at all times reexamined in the function of reexamination of business strategy of the organization. By constant reexamining of the strategy and BSC model, mining organizations as well as other business organizations, have a chance to accomplish a continual and sustainable growth of its business possibilities, taking into consideration requests for environment protection and to the satisfaction of employees, owners and wider social community.

REFERENCES

Andersen Henrik, Lawrie Gavin, Shulver Michael, 2000. The Balanced Scorecard vs. the EFQM Business Excellence Model", 2GC Working Paper

Creelman James, 1998. "Building and Implementing a Balanced Scorecard, International Best Practice in Strategy Implementation", Business Intelligence

Kaplan S. Robert, Norton P. David, 1992. "The Balanced Scorecard – Measures that Drive Performance", *Harvard Business Review*, pp. 71-79.

Kaplan S. Robert, Norton P. David, 1996. "The Balanced Scorecard, Translating Strategy into Action", Harvard Business School Press, Boston, Massachusetts,

Kaplan S. Robert, Norton P. David, 2001. "The Strategy focused Organization, how balanced scorecard companies thrive in the new business environment", Harvard Business School Press,

Maltz C. Alan, Shenhar J. Aaron, Reilly R. Richard, 2003. "Beyond the Balanced Scorecard: Refining the Search for Organizational Success Measures", Long Range Planning, pp. 187 - 204

Olve Nils-Göran, Roy Jan, Wetter Magnus, 1999. "Performance Drivers, A Practical

Guide to Using the Balanced Scorecard",

John Wiley & Sons.

The Coal Reality in Energy Production and a Research of the Global-Local Effects on Atmospheric Warming In Turkey

Enerji Üretimindeki Kömür Gerçeği ve Türkiye'nin Küresel - Bölgesel Ölçekli Atmosferik Isınmadaki Etkileri Üzerine Bir Araştırma

N. Tokgöz

İ.Ü. Mühendislik Fakültesi, Maden Mühendisliği Bölümü, İstanbul

ÖZET Türkiye'nin enerji üretimindeki kömür gerçeğinin, 1995 yılından bugüne gerek çevre yaptırımlarına sığınılarak, gerekse yanlış ve yabancılaşmış enerji politikalarıyla göz ardı edilmek istemi-çabalarının artarak süregelmesi, bu konunun bilimsel ve teknik boyutuyla titizlikle irdelenmesi gerektiğini ortaya koymuştur.

Süregelen kömür odaklı bu düşüncelerden hareketle; öncelikle, fosil yakıtların tüketiminden kaynaklanan CO_2'in küresel ve bölgesel bazda atmosferik ısınma sürecine katkısını sayısal olarak analiz edilerek la bir durum değerlendirilmesi yapılmıştır. Bunun için, 2005 yılında toplam 136 ülkenin "toplam birincil enerji miktarları (TPES)"- "CO_2 emisyonu" yanında "TPES /fert"- "ton CO_2 / fert" gibi temel göstergeler birbirleriyle ilişkilendirilerek, özellikle küresel ölçekte sayısal bir değerlendirme verilmiştir.

Ayrıca, incelenen konunun bütünselliğini sağlamak amacıyla; Türkiye'de fosil yakıtla çalışan termik santralların coğrafya bölgelerine göre dağılımı ve bu bölgelerdeki orman varlığı (F) ile 1970-1992 /1993-2006 dönemleri arasındaki yıllık ortalama sıcaklık artışlarının (ΔT) ilişkisi, toplam 133 makro-klima meteoroloji istasyon verilerine göre yine bu çalışma kapsamında irdelenmiştir.

Sonuç olarak; Türkiye'deki sıcaklık artışlarının coğrafya bölgelerine göre farklı olduğu ve 0.5C° - 0.9C° arasında değişen değerler aldığı belirlenmiştir. Ancak bu artışların, Türkiye'nin yerli kaynağı kömürün termik santrallerinde tüketiminden kaynaklanan CO_2'in etkisi altında değil, büyük oranda kuzey yarım kürede dolaşan yaklaşık 25 milyar ton CO_2'in sebep olduğu ilgili sayısal değerlendirmeler sonucu ortaya koyulmuştur.

ABSTRACT The fact that the increasing ignorance of the coal reality in energy production of Turkey, via exploiting not only the environmental sanctions but also

improper and estranged energy policies, has still been persisted since 1995 makes this problem to be scrutinized, in terms of scientific and technical methods.

Due to continual coal - focused views; a numerical evaluation has been constructed primarily by analyzing the regional and global impact of CO_2 resulting from fossil fuel consumption on global warming process. In particular, the evaluation on a global scale utilizes the "total primary energy supply (TPES)"-"CO_2 emission" from 136 countries in 2005 together with such basic indicators as "TPES/capita" and "ton CO_2/ capita".

Moreover, to maintain the integrity of the subject under study, the distribution of thermal power plants based-fossil fuels among the differing geographical regions of Turkey, additionally, the relationship between forests (F) in these regions, and the average annual increase in temperature (ΔT) between 1975-92 and 1993-2006 have been examined according to the data obtained from 133 macro-climatic meteorological stations within the scope of this study.

In conclusion, it is determined that the event of warming varies in the seven geographical regions in Turkey and that the atmospheric warming based on the increase in temperature changes between 0.5°C and 0.9°C. However, the numeric evaluations have shown that Turkey has come under a process of atmospheric warming not due to the impact of CO_2 resulting from thermal power plants based-fossil fuels by itself, but mostly due to the global effects released into the atmosphere and 25 billion tons CO_2 moving around the Northern Hemisphere.

1 INTRODUCTION

The climate system of the earth, globally and locally, obviously has been changed from pre- industrial period to present. Some of the changes are due to human activities where the vital role has been played by the emission. In particularly, fossil fuels are still dominant energy source of the world, even though usage is limited due to the green house gas. However, besides the fact that development cannot be sustained if the environmental problems are ignored, it should be born in mind that economically weak countries do not have sufficient sources to bear the expenses of environmental protection.

CO_2 accounted for the largest share of green house gas with 80-82%. The emission is mainly caused by the usage of fossil fuels (oil, natural gas, and coal) which are used in every sector of industry and economy (IPCC, 2005; IEA, 2005; UNFCC, 2006). Therefore, energy policies directly affect the emissions of CO_2.

According to the data from IPCC, within the last century the global surface temperature has increased by 0.6 °C on average. According to the data from World Meteorological Organization, the hottest two years of the last 150 years are 1998 and 2002 (IPCC, 2005). It is envisaged that from 1990 to 2100 the average increase in the global surface temperature will be 1.4-5.8 °C. Atmospheric CO_2 reaching from 280 ppm to 360 ppm causes a 1.4°C increase in temperature (IPCC, 2005). Knowledge of past CO_2 levels and associated paleo-environmental and pale-ecological changes is useful for prediction future consequences of the current increase in atmospheric CO_2 (Ghosh, et.all, 2005).

It is also well known that temperature variation in the Atlantic/European sector

of the Arctic partly is accounted for by the North Atlantic Oscillation (NAO) (Hurrell 1995) or the Arctic Oscillation (AO) (Thomson & Wallace 1998). Natural climate phenomena, such as the North Atlantic Oscillation (NAO) and the Arctic Oscillation (AO) also have strong regional (particularly in Europe) and global impacts on weather and climate. The dominant mode of atmospheric and climate variability in the North Atlantic region is the NAO, which is a dipole meridional oscillation in atmospheric pressure between the Iceland Low and Azores High (Hurrell, 1995). The atmospheric pressures follow a path toward Turkey (Erinç, 1969; Kantarcı, 2006; Türkeş and Erlat 2008).

As a result of this climate change, it is suggested that in the forthcoming years excessive droughts will occur in some regions of the world whereas flood disasters will occur in others. Disasters such as hurricanes, floods or excessive droughts that will occur as a result of the climate change also threaten both biological diversity and the future of animal species.

2 GENERAL OUTLOOK WORLD WIDE CO_2 EMISSION TRENDS BASED ON FOSSIL FUELS

To provide a numerical information on CO_2 emission based - fossil fuels, the number of 136 world countries were analyzed according to main energy indicators named as "reserves and its dynamic life", "Total Primary Energy Supply (TPES)", "ton CO_2/capita", efficiency of power plants, electricity generation trends (Figure 1 and 2). Data were analyzed according to 1971-2005 period in order to determine past and future trends of the world CO_2 emission. When the Figure-1 and 2 together are carefully examined, some important evaluations can be produced;

- World CO_2 emission caused by fossil fuel combustion grew from 26.58 Gt in 2004 to 27.136 Gt in 2005, an increase of 2.09% (0.556 Gt). The world CO_2 emission increase in 2004 is 27.3% compared to 1990.
- It is reported that total 7887 industrial CO_2 sources have produced 13 466 Mt CO_2 in a year. (IPCC, 2005; IEA, 2006). Globally, emissions of CO_2 from fossil fuel use in the year 2004 totaled about 26.58 Gt. Of this, close to 51% was attributed to large (0.1 - 1 Mt CO_2/year, stationary emission sources (see in Figure 1).
- Fossil fuel based-industrial source of CO_2 emission was produced by power sector as 10539 Mt/year (63 %, 4942) (IPCC, 2005). It is followed by cement production 15% (1175), refineries 8.1% (638), petrochemical industry % 6 (478), Biomass 3.9 % (330), Iron and steel industry 3.4 % (270), and other sources 0.6 % (90). It clearly seems that large amount of CO_2 have been emitted by power sector. If the sources evaluate according to distributed throughout the world, the database shows four main clusters of emissions: North America (Midwest and eastern USA), Europe (northwest region), East Asia (eastern coast of China and Japan) and South Asia (Indian subcontinent) (Figure 1).
- It is clearly seen that among all fossil fuels, coal is distributed more "equally" in ratio than oil and natural gas reserves and that it is gradually gaining importance for the countries which do not have energy resources or which have limited ones or have resources on the verge of exhaustion [(Figure 1(a)].
- World proven coal reserves are 907 billion ton and total coal production of the world is 4.9 billion tones (IEA,

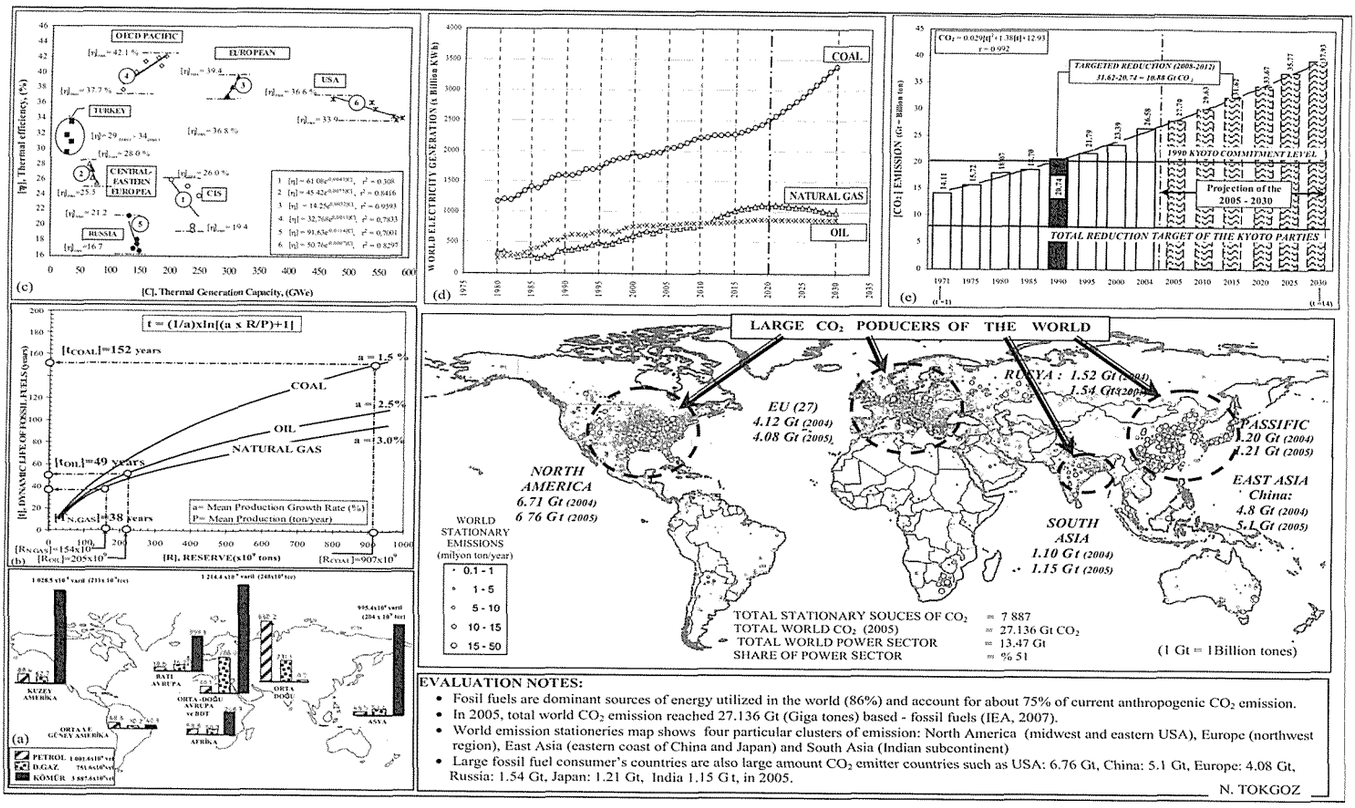

Figure 1. General Outlook to World Fossil Fuels and Its CO_2 Emissions

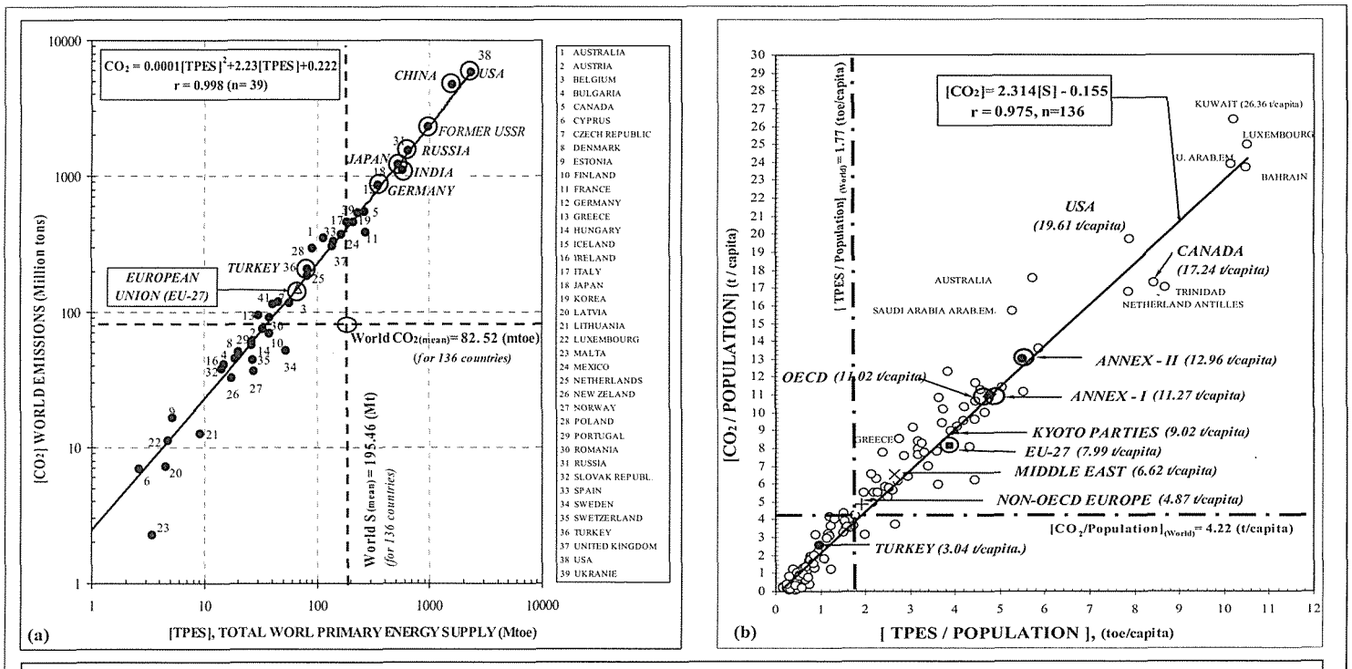

ASSESSMENT NOTES:

- The USA, which is the greatest CO_2 emission producer in the world, had a per capita CO_2 emission of 19.61 tones in 2005
- CO_2 emission, 2.29 tones per capita in Turkey in 1990 is even below the level of 3.04, which is the world average (4.22 t/capita). This means that Turkey's per capita responsibility concerning the production of CO_2 emission which causes global warming is less than the other countries. The average values of OECD and the EU member states are approximately three-fold higher than those of Turkey.

N. TOKGOZ

Figure 2. World Total Primary Energy Supply (TPES) and "ton CO_2/capita" values in 2004

2004). Numerical evaluation shows that coal will be available for a couple of hundred years if there were no growth in the rate of production (static case) in future generating electricity in all regions around the world [(Figure 1(b)].

- China is ranked first in the world in coal production with the 1.55 % ratio of reserve usage in coal, and it is also ranked second after USA with CO_2 emission of 5.10 billion ton capacity it produces. The ratio of increase in the value of CO_2 emission in China from 1990 to 2005 has been estimated as 119% (1.19 fold). India is also a coal-producing country which is ranked second in the world after China. The ratio of coal reserve usage in India is 0.45 % [(Figure 1(a) and (b)]. India is also a coal-producing country which is ranked second in the world after China. The ratio of coal reserve usage in India is 0.45 % [(Figure 1(a) and (b)].
- When the power plants working with fossil fuels in the world are examined according to their efficiencies (η); it is seen that they are operated with extremely low efficiency as in Russia: 16.7-21.2 %, CIS: 19.4-26.0 %, Central and Eastern Europe: 25.5-28.0 %. It is also known that this low efficiency results from the old combustion technologies in the power plants not rehabilitated and increases CO_2 emission together with SO_2 and NO_2 emissions [(Figure 1(c)] (Tokgöz, 2001 and 2005).
- In the electric energy trends of the world between the years of 1980 and 2030, it is clearly seen that notably coal takes the most important place among the primary energy supplies. As to natural gas, it is seen that this increase will go on till 2020 and in this mentioned year it will decline after a breaking point as a result of the exhaustion based on its dynamic existence in its existent reserves [(Figure 1(d)].
- To estimate the world CO_2 emission trends for 2005 - 2030, CO_2 emissions are analyzed in Figure 1(e) according to 1971- 2004 years (in 5 years periods). Regression analysis method was used in the emission estimation. The highest correlation coefficient (r = 0.992) was obtained from polynomial regression type which is given below:

$$CO_2 = 0.029[t]^2 + 1.38[t] + 12.93$$

"t" is defined as time (year). In calculations, "t" value is taken into consideration as $t_{1971}=1$ and $t_{2030}=14$. CO_2 emission of the world in 2030 has been predicted as approximately 37.93 billion tones from the regressional equation. The reduction in emission aimed between the years of 2008-2012 has been estimated as 10.88 billion tones of CO_2 [Figure 1(e)].

- The USA, which is the greatest CO_2 emission producer in the world, had a percapita CO_2 emission of 19.61 tones in 2005 [Figure 2(b)](*).
- CO_2 emission, 3.04 tones per capita in Turkey in 1990 is even below the level of 2.92 in 2005, which is the world average (4.22 t/capita) [Figure 2(b)]. This means that Turkey's per capita responsibility concerning the production of CO_2 emission, which causes global warming, is less than the other countries. The emission figures of Turkey, who was included in the group of countries in Annex - I in compliance with UNFCCC, becomes more striking when compared to those

(*) Raw data were taken from the "IEA, 2006 and IEA, 2007" references.

of OECD countries and the EU. The average values of OECD and the EU member states are approximately three-fold higher than those of Turkey.

3 RESEARCH ON THE EFFECTS OF CO_2 ON ATMOSPHERIC WARMING IN TURKEY

3. 1 Short Outlook Power Plants and Electricity Generation of Turkey based on Fossil Fuels

Although Turkey's oil and natural gas reserves are limited, coal reserves are more abundant than natural gas. The main lignite consuming sector is power sector. Turkey has 9.2 billion ton lignite and 1.4 billion ton hard coal reserves. The Afsin-Elbistan region holds 3.3 billion tons of lignite reserves and this covers 40% of the Turkey's total coal reserve. The construction and operation of power plants in Turkey had started in 1950s (Arıoğlu-Tokgöz, 1993; Arıoglu, 1996; Tokgöz, 2005).

The electricity generation of Turkey has undergone a rapid grow. Installed capacity was 16.318 TW in 1990 and it reached 36.824 TW by the end of the 2004. The capacity of power plants has been improved over the period 1990-2004. Thermal resources increased from 9.554 TW in 1990 to 24.179 TW in 2004. Ratios of coal, oil, and natural gas, which take the most important place in Turkey's total electricity generation and ratios of CO_2 emissions caused by these fossil fuels are shown in the Table 1.

After 1985 in Turkey, share of the lignite power plants in electricity generation was gradually decreased (34 %) due to rapid increasing in the share of natural gas plants (52.1 %) in 2004. This increase in natural gas depends on the fact that Turkish Energy Policy increased its dependency on foreign sources with "take" or "pay" agreements and leaned its energy production on natural gas it imports with high prices. As the required fuel for the thermal power plants fueled by coal is provided by most abundant domestic resources, the energy supply is more reliable and cheaper. What is more important is that the payments affected for the cost of coal remain within the country and create added value. On the contrary, in natural gas, there is dependency on foreign resources, which is highly risky and may create pressure in regional relations. Energy planning is of great importance, especially in developing countries such as Turkey for preventing extravagance in investments. Furthermore, electricity cannot be stored and should be produced in "neither insufficient, nor too large amounts" (i.e., in the event of a demand and in demanded amounts), and this makes planning in issues of energy even more crucial.

Total electricity production of Turkey based-fossil fuels combustion in 2005 was 122.27 TWh; the natural gas holds the largest share in the total of 58 % which is 71 TWh, while coal represents 35 % of the total with 43 TWh, and fuel oil represents 7 % with 8 TWh.

3. 2 Research on the effects of CO_2 on Atmospheric Warming in Turkey

3.2.1. Methodology of Meteorological Data Analyses

Atmospheric warming has led to significant effects in Turkey especially after 1993. In Turkey, a significant warming phenomenon draws attention in the comparison of the annual average temperature values of total 133 macro-climate meteorology stations. The statistical data(*) was analyzed according

(*) Statistical raw data was taken from Turkish State of Meteorological Service (TSMS, 2006).

Table 1. General Outlook to Turkey's Electricity Production in 1971-2004 period and Fossil Fuels based - CO_2 Emission

YEARS	ELECTRICITY PRODUCTION (TWh)	CO_2 EMISSIONS FROM FOSSIL FUEL COMBUSTION (Million tonnes)					CO_2 EMISSIONS PER KILOWATT HOUR
		COAL (1)	OIL (2)	GAS (3)	TOTAL(*) (1+2+3)	TOTAL(**)	(grammes CO_2 / KWh)
1971	57.5	16.0	25.7	-	41.7	-	588
1975	78.3	20.7	39.0	-	59.6	-	583
1980	86.2	27.1	44.6	-	71.6	-	535
1985	94.9	45.2	50.0	0.10	95.3	-	538
1990	***103.3***	***58.9***	***63.3***	***6.50***	***128.8***	***132.13***	***550***
1995	111.0	62.4	80.0	13.0	155.4	160.79	558
1999	116.4	77.6	79.3	24.3	181.3	190.61	577
2000	124.9	90.9	83.9	28.9	203.7	212.55	600
2001	122.7	75.8	78.2	31.1	185.2	196.02	619
2002	129.4	77.7	81.8	34.1	193.6	204.02	537
2003	140.6	81.4	80.3	41.1	202.9	218.00	496
2004	***151.1***	-	-	-	***209.5***	***227.43***	-
2005	162.0	-	-	-	-	-	-

(*) Internal Energy Agency (IEA)- 2005 and 2006
(**) Turkish Statistics Institute (TURKSTAT), 2006.

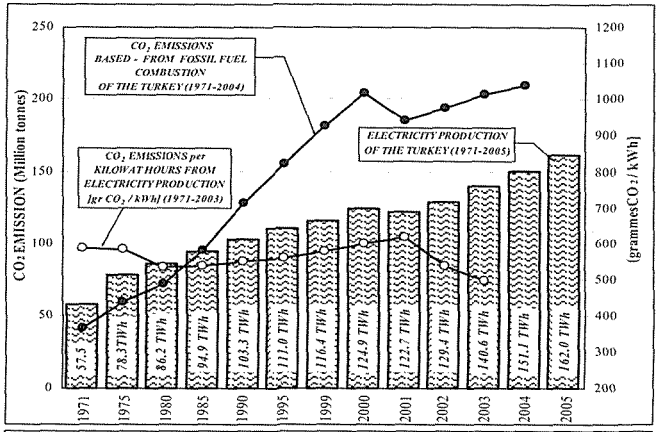

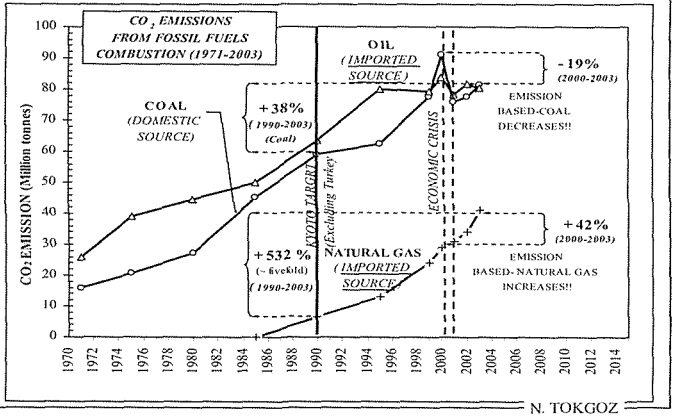

ASSESSMENT NOTE:

• Analyzing the fossil fuels on base of sectors, Turkey's CO_2 emission was 209.45 million tons in the year of 2004. However, when this emission value is considered on fuels base, CO_2 emission growing out of coal consumption declined to 81.4 million tons in 2003 from 90.9 million tons in 2000 with a share of 12%. Similar decline was obtained in petroleum with a rate of 4.5%. In contrast to the decline, there was an increase of 45% in natural gas after the year of 2000 and it reached 41.1 million tons. This increase in natural gas depends on the fact that Turkish Energy Policy increased its dependency on foreign sources with "take" or "pay" agreements and leaned its energy production on natural gas it imports with high prices. As a matter of fact, the total electricity production of Turkey in 2005 was 122.27 TWh based-fossil fuels combustion; the natural gas holds the largest share in the total of 58% which is 71 TWh, while coal represents 35% of the total with 43 TWh, and fuel oil represents 6% with 6 TWh.

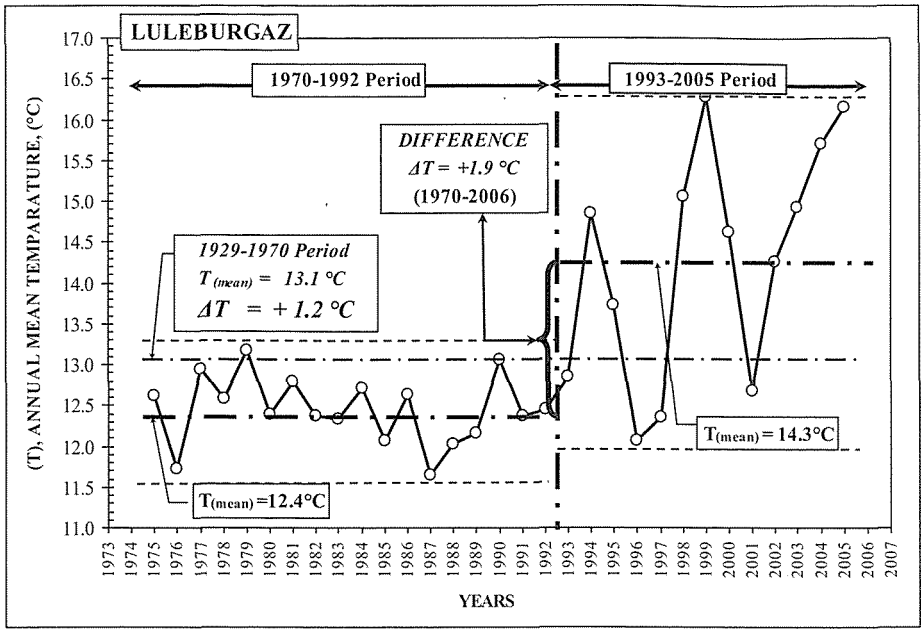

Figure 3. Statistical Data Analyses of the Annual Mean Temperature Measurements during 1929-1970 and 1970-1992 and 1993-2006 periods.

to local scale time series (last 30 years) for different two periods (1975-1992 and 1993-2006). The analysis methodology was given in Figure 3 as a local scale region (Lüleburgaz) example. The same methodology was used for remain 132 meteorological stations.

When the distribution of the thermal power plants working with fossil fuels among geographical regions in Turkey and the relationship between the existence of forests (F) in these regions and average annual increase in temperature (ΔT) between the periods of 1975-1992 and 1993-2006 are examined according to the data from total 133 macro-climatic meteorological stations; warming based on the increase in temperature changing between 0.5 °C and 0.9 °C calls attention (Figure 4). However, it is understood that the event of warming differs among the 7 geographical regions in Turkey. When the Figure 3 and 4 together are carefully examined, some important results can be listed as follows;

- In the regions, which are under the effect of the sea in the Mediterranean Region, the Black Sea Region, the Marmara Region, and the Aegean Region, the average annual increase in temperature differs between 0.4 - 0.7°C, whereas in the Middle Anatolian and the Southeastern Anatolia Regions, and in rest of the Mediterranean Region, which are not under the effect of the sea, the average annual increase in temperature differs between 0.5°C and 1.2 °C.
- The Black Sea Region, the Marmara Region, the Aegean Region and parts of the Mediterranean Region, which are influenced by the sea, are under the effect of temperate and rainy climate types. Middle Anatolia, Eastern Anatolia, Southeastern Anatolia and

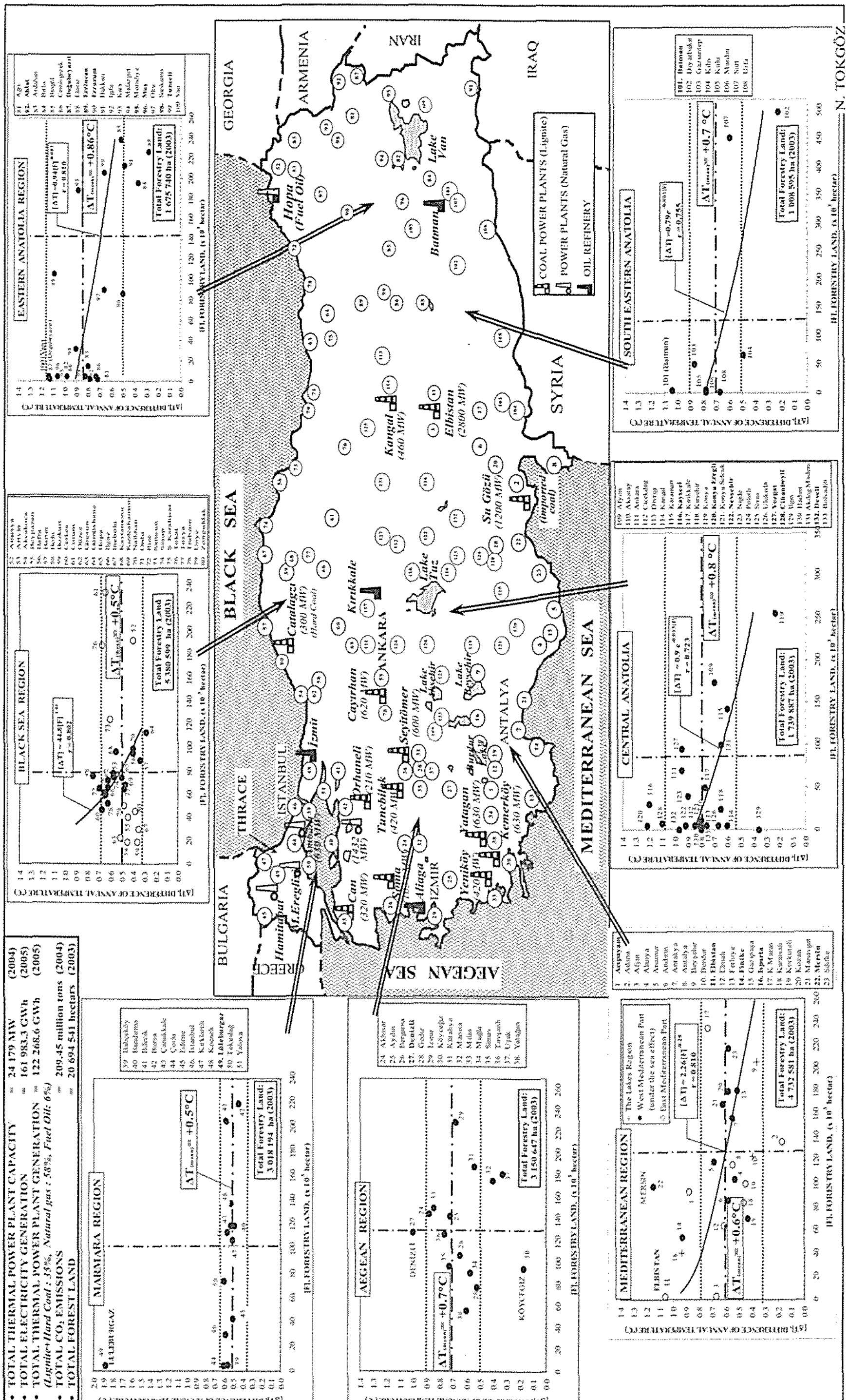

Figure 4. General Outlook to Turkish Power Stationeries Based - Fossil Fuels and Relationships between Forestry Lands (F) and Differences of the Annual Mean Temperature (ΔT) (1975-2004)

parts of the Mediterranean Region, which are behind the Mediterranean are under the influence of terrestrial climate type, which is hot and dry in summers and cold in winters. It may be assumed that the precipitations wash the CO_2 in the air as H_2CO_3 (carbonic acid) and take it down to earth. However, the regions having dry climate don't get much precipitation.

- The Black Sea Region, the Marmara Region, the Aegean region and parts of the Mediterranean Region, which are under the influence of the sea, are rich in forests. In the regions having temperate climate, the amount of CO_2 fixed by the forests (forest ecosystems) by photosynthesis is high. The CO_2 fixed by the forest ecosystems reduces the amount of CO_2 in the atmosphere and the amount of warming. On the other hand, in the Middle Anatolia, Eastern Anatolia, Southeastern Anatolia and the rest of the Mediterranean Region, which are behind the Mediterranean, there are very few forest areas. Moreover, there is no thermal power plant unit in these regions. The amount of CO_2 absorbed by photosynthesis in these regions depends merely on the existence of agricultural and grassland plants. In the regions without forests, the temperature increase is more noticeable.
- In hollow valley regions, which are between the mountains such as the Middle Anatolia, it is considered that the CO_2, which is heavier than the subsiding cold air (44 gr/mol) concentrates and causes increase in temperature (e.g. Konya-Eregli).
- It is understood that the CO_2 produced by thermal power plants fueled by coal or natural gas causes temperature increase in the environment. A typical example for increasing of temperature exists in Mersin. The chimney gases of Su Gözü Thermal Power Plant, which is fueled by imported coal, gather in front of the Bolkar Mountains, and in and around Mersin. On the other hand, in Adana, which lies in an open field, winds prevent the CO_2 concentration. Another striking example is seen in Elbistan (Afşin - Elbistan Thermal
- Power Plant), whereas Lüleburgaz (Inner Thrace) is also an example. The Hamitabat Thermal Power Plant in Lüleburgaz is fueled by natural gas. In the Eastern Black Sea Region, the effects of Hopa Thermal Power Plant can be seen, which is fueled by fuel oil. In the Aegean Region, the influence of some Thermal Power Plant draws attention in Akhisar. Influences of oil refining plant exist in Batman.
- In residential and industrial areas, which are heated by coal and natural gas and which exist in hollow valley lands, the temperature increase draws attention. The most typical examples of these areas are provincial centers s
- increase draws more attention in areas of high mountains.
- The total of the lands of destroyed and highly destroyed forests and the lands that should be included in forests is 16 million hectares, and these areas should immediately be afforested and the soil protection measures should be taken (Kantarcı, 2005).
- Turkey's total GHG emissions excluding LUCF (Land Use Change and Forestry) of rose from 170.1 Mt to 296.6 Mt between 1990- 2004 period. In 2004, net GHG emission was reported as 222.53 Mt (TMOEF, 2007). CO_2 makes up the largest share of Turkey's total emissions, account for 81.6 % (Figure 5). The figure clearly shows that approximately coal based

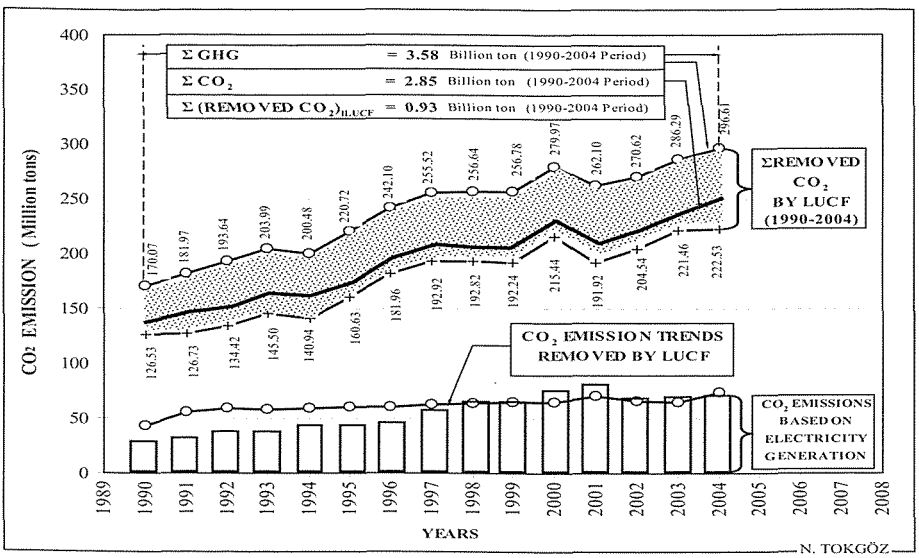

Figure 5. GHG and CO2 Emissions Based on Electricity Generation of Turkey and Removals between 1990 and 2004

- 70 Mt CO_2 emissions removed by sinks (74.1 Mt) in 2004. The amount of the removed CO_2 fixed by the forests is approximately 90 % (74.1x 0.90 = 67 Mt). In the CO_2 emission resulting from electricity generation; the parallel between the values of "produced CO_2 and fixed CO_2" particularly after 1997 or close relationship with the scale is extremely striking. 0.93 billion tones out of the total 2.85 billion tones of CO_2 emission released between the years of 1990-2004 in Turkey has been fixed by its own forests (sink).

5 SIGNIFICANT EFFECTS OF ATMOSPHERIC WARMING IN TURKEY

Atmospheric warming has led to significant effects in Turkey especially after 1993. In 2005, 25.54 giga tones of CO_2 released into atmosphere moved around of the Northern Hemisphere. Turkey also has come under a process of warming/drought such as other countries due to the impact of this high CO_2 (Table 2). The impacts can be summarized as follows:

- The obvious results of the warming could be seen in glaciers in high mountains and lakes at low lands (especially in shallow lakes).
- Shallow lakes located in low altitudes either dried (e.g. Lake Aksehir, Lake Eber, and small lakes in closed Konya basin) or shrank (e.g. Lake Tuz, Lake Burdur) (Kantarcı, 2006).
- Another important issue to consider within these lines is the increased frequency of heavy rains and their damaging effects in recent years. Deforestation in mountains and erosion also contribute to the destruction.
- Two significant result need to be emphasized. On the one hand, the warming/drought period resulted in the mass reproduction of Thaumetopoeae pityocampa larvas. On the other hand, dry habitat provided caterpillars with more desirable volatile resin

Table 2. A Short Outlook to Atmospheric Movements of Turkey and Circulating of CO_2 around of the Northern Hemisphere.

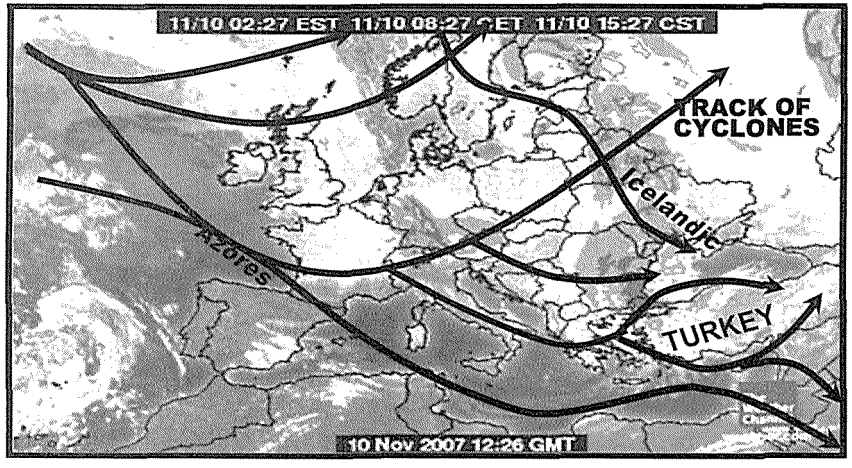

ASSESSMENT NOTES:

- The North Atlantic Oscillation (NAO) consists of opposing variations of barometric pressure near Iceland and near the Azores. On average, a westerly current, between the *Icelandic* low pressure area and the *Azores* high pressure area, carries cyclones with their associated frontal systems towards Europe.
- The atmospheric pressures follow a path toward Turkey (over the northwestern and western Mediterranean).
- In winter, velocities of the cyclones have changed between 50 and 65 km/h, whereas they have changed between 25 and 50 km/h in summer. Due to the fact that their motions have become much slower in summer, CO_2 has become more effective on warming of Turkey (Erinc, 1969).
- In 2005, 25.54 Giga tones of CO_2 (including LULUCF) released into the atmosphere and moved around of the Northern Hemisphere. Turkey is affected by the CO_2 production of countries to the north and northwest and the CO_2 emission (from the Mediterranean Sea and the Aegean Sea)
- Turkey has come under a process of warming/drought due to the impact of this high CO_2 emission.

components which have already become obvious on the Pinus nigra needles (Kantarcı, 2009).

6 CONCLUSIONS

Whole of the study, some of the important results can be summarized as follows:

- World CO_2 emission caused by fossil fuel combustion grew from 26.58 Gt in 2004 to 27.136 Gt in 2005, an increase of 2.09% (0.556 Gt). The world CO_2 increase in 2005 is 27.3% compared to 1990.
- The warming and the climate change

period that the world is experiencing are having serious impacts and implications on Turkey. CO_2 emission released by Turkey into atmosphere is close 1% of the CO_2 emission in Northern Hemisphere. An annual average temperature increase of 1.4 C° is calculated by the increase which is from 280 ppmv to 370 ppmv in the CO_2 amount (27.136 billion tones in 2005) that is released from the Northern hemisphere. Turkey has stepped into a warming process under the focusing of the high amount of CO_2 circulating from west to east. The annual average increases in temperature, especially of the lands facing south and west is between 0.7 - 0.9 °C. The annual average temperature increases in particular, the low and hollow lands between 1.2 - 1.9 °C. However, the average temperature increase during summer months is around 1- 2 °C.

- Although coal usage is limited by the CO_2 emission in the world, it still continues to be dominant energy source. In 2006, coal has a share of % 41 in generation of electricity in the world.
- Recently, coal-based power generation have focused on advanced technologies such as pulverized coal-based systems, fluidized-bed combustion systems, and integrated gasification-based systems. The advanced power systems have not only produced significantly lower emissions than current coal-fired plants but also have competed economically with other future options.
- Electricity generation of Turkey based on natural gas policy of such great amounts (50-60%) formed by completely foreign agreements with take-or-pay obligation. Instead of maximum use of abundant coal and hydraulic potential, the tendency to import natural gas can be led to serious problems. Therefore, strict plannings taking geo-strategic and geo-politic facts into consideration and edging towards its domestic resources with the understanding of "*energy-economy-ecology*" are required in determining the main features of national energy policies. Energy planning is of great importance especially in developing countries such as Turkey for preventing extravagance in investments.
- Capture and storage are the most important techniques in order to mitigate of CO_2 emission. Depleted oil and gas reservoirs, possibly coal formations and particularly saline formations can be used for storage of it. Turkey must urgently prepare for geological storage inventory of CO_2. Especially, coal mining companies and electricity - generation companies should start to investigate geological storage as a mitigation option of relevance to their industry.

ACKNOWLEDGMENT

The author would like to sincerely thank Prof. Dr. M. Doğan KANTARCI for his valuable comments on the research.

REFERENCES

Arıoğlu, E., 1996. General Outlook for Worldwide Hard Coal Mining and the Evaluation of the Zonguldak Coal Enterprise/Turkey. *Privatization in the UK and Turkey with particular reference to the Coal Sector*, Dartan, M. (Ed.), University of Marmara Publication No: 578, European Community Institute, ISBN 975-400-142-2, (205-248), Istanbul.

Arıoğlu, E., Tokgöz, N. 1993. Turkish Lignite Deposits and Researches of the Geometrical Technological Characteristics Based on the Drilling Data. *Mining Engineering Department of Istanbul Technical University*, (42p). Scientific Report, Istanbul (in Turkish).

Erinç, S, 1969. Climatology and Methods. *Istanbul University Press* No: 994, Geography Institute no:35, Tas publisher), 538 p, (in Turkish).

Ghosh, P., Phattacharya, S.K., Ghosh, P.R. 2005. A History of Atmospheric CO_2 and Its Effects on Plants, Animals, and Ecosystems. *Ecological Studies* 177, (Edits: Ehleringer, J.R., Cerking, T.F, Dearing M.D.), ISBN:0-387-22069-0, (8-34). Springer Science.

Hurrel, J.W., 1995. Decadal Trends in the North Atlantic Oscillation: Regional Temperatures and
Precipitation. *Science*, 269, (676-679).

IEA, 2004. Coal Statistics, *IEA Press*, Part I, II and III, France. (http://www.iea.org/statistics/)

IEA, 2005. Key World Energy Statistics, *IEA Press,* 82 p. (http://www.iea.org/statistics/).

IEA, 2006. Key World Energy Statistics, *IEA Press,* 76 p. (http://www.iea.org/statistics/).

IEA, 2007. CO_2 Emissions From Fuel Combustion
1971-2004, *IEA Press*, 559 p. France. (http://www.iea.org/statistics/)

IPCC, 2005. Carbon Dioxide Capture and Storage., Special Report, (Edits: Mertz, b., Davidson, O.,
Coninck, H., Loas, M., Meyer, L). *Cambridge University Press*, ISBN: 0-521-68551-6 431 p.

Kantarcı, M. D., 2005. Regional Site Slassification of Turkey and Importance of Forest Potential and Continuity in This Unit. *Istanbul University* published book no: 4558, Forest Faculty published no: 484, ISBN: 975-404 752 9 (XXVI+ 321 pp.) Istanbul (in Turkish).

Kantarcı, M. D., 2006. Effects Of Climate Change And Aridity On Ergene River Basin Water Productivity, *Proceedings of International Conference on Climate Change and the Middle East Past, Present and Future,* (Edits: Unal, Y., Kahya, C., Barı, D.D.), 20-23 November 2006, 246-258. Turkey,

Kantarcı, M. D., 2009. Researches into the Relationship Between the Damage of the Thaumetopoeae Pityocampa on the Forests of Izmit Enterprise with the Temperature Increase in Catalca and Kocaeli Peninsulas in the Climate Change Period (*in publish*)

Thompson, D.W.J., J.M. Wallace, 1998. The Arctic Oscillation signature in the wintertime geopotential height and temperature fields. *Geophys. Res. Letters* 25, 9, (1297-1300).

TMOEF, 2007. First National Communication of Turkey on Climate Change, *Turkish Ministry of Environmental and Forestry Report*, (Edits: Apak, G., Ubay, B), 265 p.

TSMS, 2006. Statistical data of 1975-2006 periods. *Turkish State of*

Meteorological Service, Ankara.

Tokgöz, N., 2005. "General Outlook of World Main Energy Resources and Numerical Approach for Prediction of SO_2 Emission Value". *Energy Sources*, 27 (7): 641-649.

Tokgöz, N., 2001. "A Conception Model of Thermal Power Plant and General Evaluation Based on the Energy Production - Air Pollution Parameters". *Proceedings of Second International Symposium on Air Quality Management at Urban, Regional and Global Scales,* 25-28 September 2001 ISBN 975 561 193 2 (134-140), Istanbul-Turkey.

Türkes M., Erlat E., 2008. Influence of the Arctic Oscillation on Variability of Winter Mean Temperatures in Turkey. *Theoretical and Applied Climatology* 92 (75-85).

UNFCCC, 2006. National Greenhouse Gas Inventory Data for Period 1990-2004 and Status of reporting, *Frame work Convention on Climate Change,* 6-14 November 2006, Nairobi, 23 p.

Production Methods and Mining Technologies

Selecting the Suitable Loading-Haulage Equipment in Open Pit Mines by Fuzzy AHP method

A.Aghajani Bazzazi,
Faculty of Mining Engineering, Islamic Azad University, Savadkooh Branch, Iran.

M.Osanloo,
Department of Mining and Metallurgy Engineering, Amirkabir University of technology, Tehran, Iran.

B.Karimi
Department of industrial Engineering, Amirkabir University of technology, Tehran, Iran.

ABSTRACT Equipment selection in mining engineering is one of the most important decision that is affected the mine design, production planning and economic parameters in open pit mining. Mine planning engineers generally use of their intuition and experiences in decision making even though equipment selection is a complex multi criteria decision problem. In real-world situation, because of incomplete or non-obtainable information, the data (attributes) are often not so deterministic, there for they usually are fuzzy-imprecise. The conventional AHP method is incapable of handling the uncertainty and vagueness involving the mapping of one's preference to an exact number or ratio. This paper presents a fuzzy AHP model to overcome this problem. A case study is presented to illustrate the use of the model and to demonstrate the capability of the model. The result of this study show significant reduction of time consumption of calculation and good accuracy compared to existence methods.

1 INTRODUCTION

Equipment selection is one of the most important factors in open-pit design (pit slopes, bench height, block sizes and geometries, ramp layout as well as excavation sequences and open-pit layout) and production planning. Further, equipment selection also affects economic considerations in open-pit design, specifically overburden, waste rock and ore mining costs and cost escalation parameters as a function of plan location and depth. The purpose of equipment selection is to select the most optimal equipment with minimum cost.

Mine planning engineers often use their intuition and experiences in decision making. Linguistic variables (the weather is raining, soil is wet, etc.) are ambiguous and decision-makers may not know how these variables are computed. Since the advent of the fuzzy set theory, these uncertainties are easily evaluated in decision making process (Bascetin & Kesimal 1999).

The selection of equipment for mining applications is not a well-defined process and because it involves the interaction of several subjective factors or criteria, decisions are often complicated and may even embody contradictions. Traditionally, procurement costs become elevated through a system of public tendering to appear as the primary criterion and the major costs of looking after the equipment during its useful life are not taken into account (samanta et.al 2002).

Various models have been proposed for application to the selection of mining equipment. General guidelines and a survey related to the selection of surface mining equipment were discussed by Martin et al (1982). Expert system as decision aid in surface mine equipment selection was applied by Bandopadhyay & Venkatasubramanian (1987) and Denby & Schofield (1990).

Hrebar (1990) and Sevim & Sharma (1991) used net present value analysis for selection of a dragline and surface transportation system. Chanda reviewed the fundamental concepts of equipment selection (1995).

Use of a linear breakeven model has been proposed by Cebesory (1997). Models for equipment selection and evaluation described by Celebi (1998) were aimed at selection of the equipment fleet on the basis of minimizing the unit stripping cost and maximizing production.

Hall et.al (2003) illustrated how reliability analysis can provide mine management with quantitative information of value for decision making about surface mining equipment. Analytical hierarchy process has proposed for application to selection of equipment by some researchers (Samanta et al. 2002; Bascetin 2004).

EQuipment Selection (EQS) is computer software that used fuzzy logic for equipment selection in surface mines and proposed by bascetin et al (2006). Application of AHP-TOPSIS method for loading- haulage equipment selection in open pit mines was used by Aghajani & Osanloo (2007). Aghajani et.al (2008) illustrated how Fuzzy TOPSIS method can applied for Optimal open pit mining equipment selection.

Most of these decision-making tools either rely on objective input data, with little or no subjective judgment, or spotlight on a single parameter. Also, because of incomplete or non-obtainable information, the data (attributes) are often not so deterministic; there for they usually are fuzzy-imprecise and application of fuzzy logic (Zadeh 1965) for surface mine equipment selection is exigent. Fuzzy multi-criteria decision-making (Fuzzy-MCDM) techniques can be very useful in encompassing several subjective criteria with conflicting objectives to arrive at an eclectic decision. Combination of fuzzy set theory and Analytic Hierarchy Process (AHP) is developed to solve open pit mining equipment multi-attribute selection problem.

2 MULTIPLE ATTRIBUTE DECISION MAKING (MADM) METHOD

MADM methods are developed to handle concept selection problems. In this class of problems, the "best" solution is determined from a finite and usually small set of alternatives. The selection is performed based on the evaluation of the attributes and their preference information.

In the decision making process, many MADM techniques use decision matrix (or goal achievement matrix) D to describe the states of the attributes of each alternative. In decision matrix format, columns indicate attributes considered in

a given problem; and in which rows list the competing alternatives. Specifically, a MADM problem with m alternatives (A_1, A_2 ... A_m) that are evaluated by n attributes (C_1, C_2... C_n) can be viewed as a geometric system with m points in n-dimensional space. An element x_{ij} of the matrix indicates the performance rating of the i^{th} alternative, A_i, with respect to the j^{th} attribute, C_j, as shown in following equation (Hwang & Yoon 1981):

$$D = \begin{array}{c} \\ A_1 \\ A_2 \\ A_3 \\ \vdots \\ A_m \end{array} \begin{array}{c} \begin{array}{ccccc} C_1 & C_2 & C_3 & \cdots & C_n \end{array} \\ \begin{bmatrix} x_{11} & x_{12} & x_{13} & \cdots & x_{1n} \\ x_{21} & x_{22} & x_{23} & \cdots & x_{2n} \\ x_{31} & x_{32} & x_{33} & \cdots & x_{3n} \\ \vdots & \vdots & \vdots & \ddots & \vdots \\ x_{m1} & x_{m22} & x_{m3} & \cdots & x_{mn} \end{bmatrix} \end{array} \quad (1)$$

Generally, MADM methods can be classified into compensatory and non-compensatory methods based on the treatment of the attribute information. The compensatory methods allow trade-offs between criteria, assigning a number to each multidimensional representation of an alternative. The non-compensatory methods do not permit the trade-off between criteria, i.e. one unfavorable criterion value cannot be offset by reducing a favorable value of another criterion (Hwang & Yoon 1981).

open pit mining equipment is multi attribute decision making problem that decision makers want to choice best alternative, large number of attribute and small number of alternative, pairwise comparison, model don't using thresholds and giving complete order and finally, all the performance values are qualitative and quantitative. Consequently, Fuzzy AHP method is most appropriate method for solving open pit mining equipment selection problems.

3 METHODOLOGY

The proposed approach is developed within the AHP framework consisting of (1) hierarchy developments, (2) fuzzy pairwise comparisons and (3) relative weight calculations with regard to group decisions. These systematic procedures of the proposed method are similar to the process of human thinking and capable of turning the complex decision-making process into simple comparisons and rankings.

3.1 Analytical hierarchy process

Hierarchy is the structural frame in AHP (Saaty 1990), which is used to determine the influence of all the decision criteria. The AHP structures the decision problem in levels which correspond to one understands of the situation: goals, criterion, sub-criterion, and alternatives. At the highest level is the overall goal of the problem, and the alternatives are at the lowest level. Between them are criteria and sub-criteria. By breaking the problem into levels, the decision-maker can focus on smaller sets of decisions.

3.2 Fuzzy pairwise comparison

Once the hierarchy is established, the pairwise comparison evaluation takes place. All the criteria on the same level of the hierarchy are compared to each of the criterion of the preceding (upper) level. A pairwise comparison is performed by using linguistic terms.

Based on the Chen's definition (Chen 2000), seven linguistic terms, "Very Low Important" (VLI), "Low Important" (LI), "Medium Low Important" (MLI), "Medium Important" (MI), "Medium High Important" (MHI), "High Important" (HI) and "Very High Important" (VHI) ranging 0–10 are used

to develop fuzzy comparison matrices. These seven linguistic variables are described by fuzzy numbers as denoted in Table 1 or by membership functions as illustrated in Figure 1. It can be found in the figure levels are characterized by symmetric triangular membership functions. Fuzzy comparison matrix, $\tilde{A}$, is given by:

$$D = \begin{bmatrix} 1 & \tilde{r}_{12} & \tilde{r}_{13} & \cdots & \tilde{r}_{1n} \\ \tilde{r}_{21} & 1 & \tilde{r}_{23} & \cdots & \tilde{r}_{2n} \\ \vdots & \vdots & \vdots & \ddots & \vdots \\ \tilde{r}_{n1} & \tilde{r}_{n2} & \tilde{r}_{n3} & \cdots & 1 \end{bmatrix} \quad (2)$$

In Chang method (Chang 1996), the element of the negative judgment is treated as an inverse and reversed order of the fuzzy number of the corresponding positive judgment. For example, suppose that criterion A compared to criterion B is "high important" denoted by fuzzy number (7, 9, 10), so that the negative judgment, "less important", is described by (1/10, 1/9, 1/7). Thus, it requires careful checks to avoid errors arising from such tedious manipulations while constructing a reciprocal matrix. To overcome this difficulty, each negative reciprocal element is characterized by its own representative fuzzy number as defined in Table 1.

To reflect particular degrees of uncertainty regarding the decision making process, the α-cut concept is applied. This is another enhancement of the proposed method made to Chang model. The value of α is between 0 and 1. α=0 and α=1, signify the degree of uncertainty is greatest and least, respectively.

In practical applications, α=0, α=0.5, and α=1 are used to indicate the decision-making condition that has pessimistic, moderate, and optimistic view, respectively.

In practical applications, α=0, α=0.5, and α=1 are used to indicate the decision-making condition that has pessimistic, moderate, and optimistic view, respectively. Fig. 2 shows that a triangular fuzzy number regarding a given value can be denoted by (Xα,L, Xα,M, Xα,R). Xα,M, Xα,L, and Xα,R represents the most-likely value, minimum value, and maximum value of the fuzzy number, respectively.

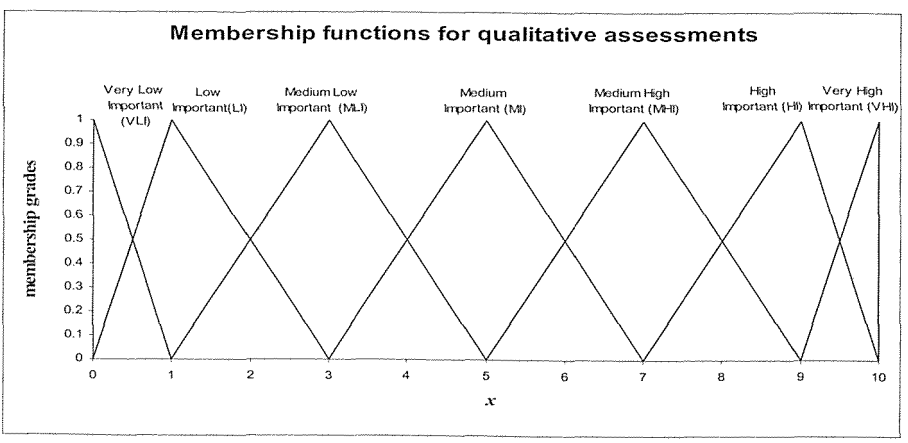

Figure 1. Membership functions for linguistic values

Table 1. Fuzzy importance scale

Table 1. Fuzzy importance scale

Verbal judgment	Explanation	Fuzzy number
Very Low Important (VLI)	A criterion is very strongly inferior to another	(0,0,1)
Low Important (LI)	A criterion is strongly inferior to another	(0, 1, 3)
Medium Low Important (MLI)	A criterion is slightly inferior to another	(1, 3, 5)
Medium Important (MI)	Two criteria contribute equally to the object	(3, 5, 7)
Medium High Important (MHI)	Judgment slightly favor one criterion over another	(5, 7, 9)
High Important (HI)	Judgment strongly favor one criterion over another	(7, 9, 10)
Very High Important (VHI)	Judgment very strongly favor criterion over another	(9, 10, 10)

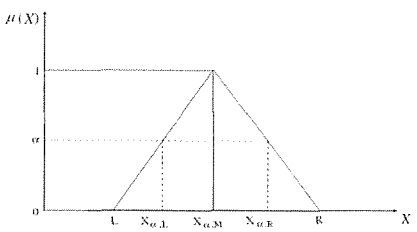

Figure 2. Triangular fuzzy intervals under α-cut

The five membership functions shown in Fig. 1 can also be mathematically expressed through Equations 3– 9.

$$x_\alpha(\text{Very Low Important}) = \begin{cases} X_{\alpha,L} = 0 \\ X_{\alpha,M} = 0 \\ X_{\alpha,R} = 1-\alpha \end{cases} \quad (3)$$

$$x_\alpha(\text{Low Important}) = \begin{cases} X_{\alpha,L} = \alpha \\ X_{\alpha,M} = 1 \\ X_{\alpha,R} = 3-2\alpha \end{cases} \quad (4)$$

$$x_\alpha(\text{Medium Low Important}) = \begin{cases} X_{\alpha,L} = 1+2\alpha \\ X_{\alpha,M} = 3 \\ X_{\alpha,R} = 5-2\alpha \end{cases} \quad (5)$$

$$x_\alpha(\text{Medium Important}) = \begin{cases} X_{\alpha,L} = 3+2\alpha \\ X_{\alpha,M} = 5 \\ X_{\alpha,R} = 7-2\alpha \end{cases} \quad (6)$$

$$x_\alpha(\text{Medium High Important}) = \begin{cases} X_{\alpha,L} = 5+2\alpha \\ X_{\alpha,M} = 7 \\ X_{\alpha,R} = 9-2\alpha \end{cases} \quad (7)$$

$$x_\alpha(\text{High Important}) = \begin{cases} X_{\alpha,L} = 7+2\alpha \\ X_{\alpha,M} = 9 \\ X_{\alpha,R} = 10-\alpha \end{cases} \quad (8)$$

$$x_\alpha(\text{Very High Important}) = \begin{cases} X_{\alpha,L} = 9+\alpha \\ X_{\alpha,M} = 10 \\ X_{\alpha,R} = 10 \end{cases} \quad (9)$$

A fuzzy comparison matrix is given by:

$$\tilde{A} = \begin{bmatrix} 1 & (x_{12,L}, x_{12,M}, x_{12,U}) & \cdots & (x_{1n,L}, x_{1n,M}, x_{1n,U}) \\ (x_{21,L}, x_{21,M}, x_{21,U}) & 1 & \cdots & (x_{2n,L}, x_{2n,M}, x_{2n,U}) \\ \vdots & \vdots & \ddots & \vdots \\ (x_{n1,L}, x_{n1,M}, x_{n1,U}) & (x_{n2,L}, x_{n2,M}, x_{n2,U}) & \cdots & 1 \end{bmatrix} \quad (10)$$

For instance, $(x_{12,L}, x_{12,M}, x_{12,U})$ in Equation (10) shows the lower, middle and upper value of the 1st element compared with the 2nd element at the higher level, respectively. To facilitate fuzzy weight computations, matrix $\tilde{A}$ is further decomposed into three crisp matrices: the lower bound matrix (A_L), most-likely matrix, (A_M), and upper-bound matrix (A_U). Concerning A_L as an example, A_L is defined by:

$$A_L = \begin{bmatrix} 1 & x_{12,L} & \cdots & x_{1n,L} \\ x_{21,L} & 1 & \cdots & x_{2n,L} \\ \vdots & \vdots & \ddots & \vdots \\ x_{n1,L} & x_{n2,L} & \cdots & 1 \end{bmatrix} \quad (11)$$

3.3 Relative weight calculations with regard to group decisions

Several methods were used for element weight calculation such as normalization of geometric mean, eigenvalue, etc. In this research, normalization of arithmetic mean (NAM) is applied to compute local weights and given by

$$w_i = \frac{g_i}{\sum_{i=1}^{n} g_i} \qquad (12)$$

Where

$$g_i = \frac{\sum_{j=1}^{n} r_{ij}}{n} \qquad (13)$$

In the above equations, g_i is geometric mean of criterion i. r_{ij} is the comparison value of criterion i to criterion j. w_i is the i^{th} criterion's weight, where $w_i>0$ and $\Sigma w_i=1$, $1\leq i\leq n$.

Group decision making was applied for weight calculation. For group evaluation, because the assessment of alternative weights is usually made by multiple evaluators whose preference may vary based on individual's perception, experience, and knowledge, it is required to aggregate different evaluators' opinions into one. To achieve this task, the pooled assessments of multiple evaluators represented by membership functions need to be defuzzified. Defuzzification plays an important role when a conversion of a fuzzy number to a single representative value is required. In the proposed method, at first minimum and maximum value between evaluators eliminated when one criterion compared with another one. This procedure was done because in real situation each elevator may interest one main criteria such as economic, environment and price so he/she consider this interest in decision questionnaire used to asses criteria. The proposed model employs the Center of Sum (COS) techniques because the COS approach involves the simplified algebraic sum of individual fuzzy sets, which is much faster than most related methods and easy to implement. This method is given by:

$$Z^{*} = \frac{\int z \sum_{k=1}^{n} \mu_k(z)dz}{\int \sum_{k=1}^{n} \mu_k(z)dz} \qquad (14)$$

Where Z* is the deffuzified value or weighted average; $\mu(z)$ is the membership value of the element z in the subset.

Accordingly, the synthetic weight of the k^{th} sub- criterion (s_k) can be determined as follows:

$$S_k = w_j \times s_{kj} \qquad (15)$$

By the same manner, the weight of the ith alternative (i=1,2,. . .,m) with respect to the kth sub-criterion (eik) can be obtained.

Consequently, the overall weight of the ith alternative (ri) is given by:

$$r_i = s_k \times e_{ik} \qquad (16)$$

Finally, the overall weight of the ith alternative regarding all sub-criteria, Ri, can be found by the following:

$$R_i = \sum_{k=1}^{K} s_k \times e_{ik} \qquad (17)$$

4 CASE STUDY

Sungun mine is one of the largest copper deposits of Iran which is located in the north-west of the country close to Azerbaijan, Armenia and Turkey borders (fig.3).

Technical and economical studies were shown that the most appropriate of mining method for this deposit is open pit mining method. By this method 384

million tons of ore with 0.665 percentage of copper grade can be mined. Total mine's life estimated to be 31 years with annual production of 7 million tons in first 5 years and 14 million tons for remaining years. During this period 680 million tons of waste must be removed. So, the waste to ore ratio in this mine is 1.8:1(Hoseinie et al 2006).

Three potential transportation system alternatives have been evaluated for ore transportation. These are loader- truck (A1), shovel-truck (A2) and shovel-truck-belt conveyor (A3) systems.

The basic hierarchy of the decision problem was constructed based on the experts' suggestions. Each expert was asked to identify possible factors that could somehow affect the final decision through several surveys, questionnaires and discussions. Also, the criteria used in the hierarchy were based on the suggestions from the references in (Samanta et al. 2002; Bascetin 2004; Bandopadhyay & Venkatasubramanian 1987).

Figure 3. Geographical location of Sungun copper mine

As shown in Figure 4, the top level and the lowest level of the hierarchy denote the overall objective (selecting the suitable loading-haulage equipment in open pit mine) and the candidates, respectively. The five main criteria, namely Financial Consideration (FC), Operating condition, Safety and Environment (OSE), Mine Parameter (MP), Reliability & Maintainability

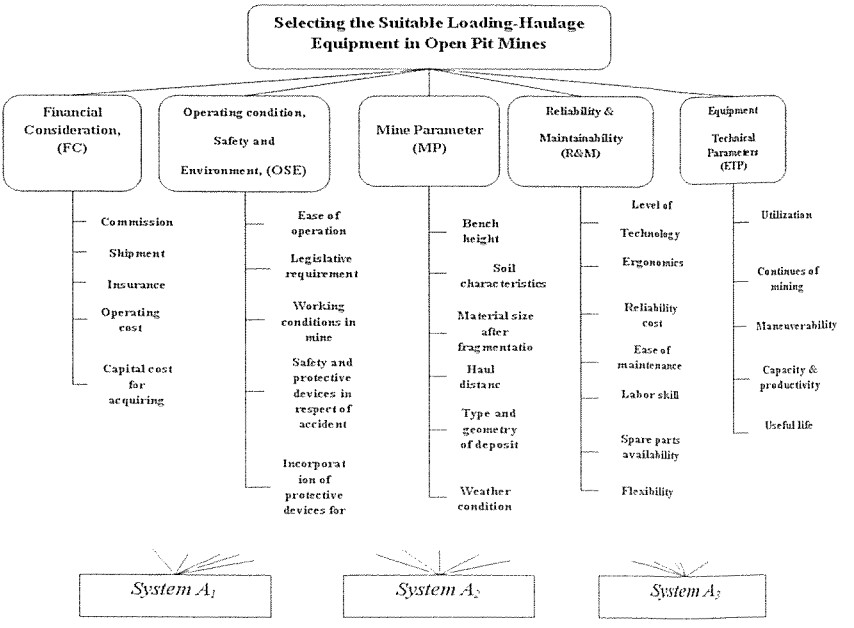

Figure 4. The hierarchy for selecting the suitable loading-haulage equipment in open pits mine

(R&M) and Equipment Technical Parameters (ETP) were included at the second level.

The main criteria were further broken down into sub-criteria. Financial consideration was characterized by commission, shipment, insurance, operating cost and capital cost for acquiring equipment.

Operating condition, safety and environment was divided into ease of operation, legislative requirement, working conditions in mine, safety and protective devices in respect of accident and finally incorporation of protective devices for environment pollution.

Mine parameters was associated with bench height, soil characteristics, material size after fragmentation, haul distance, type and geometry of deposit and weather conditions.

Reliability & maintainability criterion was broken down into level of technology, ergonomics, ease of maintenance, reliability cost, labor skill, spare parts availability and flexibility.

Equipment technical Parameters was divided into utilization, continues of mining, Capacity & productivity, maneuverability and useful life.

Once the hierarchy was established, experts' knowledge was elicited through interviews and questionnaires. A series of questionnaires were designed and used to direct pairwise comparison judgments.

As an example, table 2 depicts a particular questionnaire for evaluating main criteria with respect to the overall goal.

By the use of Table 2, each expert performed a pairwise comparison to indicate his or her preference for each criterion. The assessment result can be found in Table 3.

As mentioned before, minimum and maximum value in each pairwise compression eliminated so the results were illustrated in table 4 after eliminated. In this table, 1st and 2nd replaced with 1st exp and 2nd exp. To better illustrate the use of the proposed model, only the first and the second column assessment in Table 5 is exemplified.

Table 2. Questionnaire used to assess main criteria

Q1. How important is FC when it is compared to OSE?
Q2. How important is FC when it is compared to MP?
Q3. How important is FC when it is compared to R&M?
Q4. How important is FC when it is compared to ETP?
Q5. How important is OSE when it is compared to MP?
Q6. How important is OSE when it is compared to R&M?
Q7. How important is OSE when it is compared to ETP?
Q8. How important is MP when it is compared to R&M?
Q9. How important is MP when it is compared to ETP?
Q10. How important is R&M when it is compared to ETP?

First, the fuzzy comparison matrix based on the first column judgment in table 5 is given by:

$$\tilde{A} = \begin{bmatrix} 1 & (7,9,10) & (7,9,10) & (3,5,7) & (7,9,10) \\ (0,1,3) & 1 & (0,0,1) & (0,0,1) & (3,5,7) \\ (0,1,3) & (9,10,10) & 1 & (1,3,5) & (3,5,7) \\ (3,5,7) & (9,10,10) & (5,7,9) & 1 & (9,10,10) \\ (0,1,3) & (3,5,7) & (3,5,7) & (0,0,1) & 1 \end{bmatrix} \quad (18)$$

$$\tilde{A}_1^L = \begin{bmatrix} 1 & 7 & 7 & 3 & 7 \\ 0 & 1 & 0 & 0 & 3 \\ 0 & 9 & 1 & 1 & 3 \\ 3 & 9 & 5 & 1 & 9 \\ 0 & 3 & 3 & 0 & 1 \end{bmatrix} \quad \tilde{A}_1^M = \begin{bmatrix} 1 & 9 & 9 & 5 & 9 \\ 1 & 1 & 9 & 0 & 5 \\ 1 & 10 & 1 & 3 & 5 \\ 5 & 10 & 7 & 1 & 10 \\ 1 & 5 & 5 & 0 & 1 \end{bmatrix} \quad \tilde{A}_1^U = \begin{bmatrix} 1 & 10 & 10 & 7 & 10 \\ 3 & 1 & 1 & 1 & 7 \\ 3 & 10 & 1 & 5 & 7 \\ 7 & 10 & 9 & 1 & 10 \\ 3 & 7 & 7 & 1 & 1 \end{bmatrix} \quad (19)$$

Next, the arithmetic mean of FC with regard to OSE, MP, R&M and ETP can be calculated by using Equation 14 to produce the following:

$$g_1^L = (1+7+7+3+7)/5 = 5 \quad (20)$$

By the same manner, the arithmetic mean (gL) for OSE, MP, R&M and ETP yields 0.8, 2.8, 5.4, and 1.4, respectively. Hence, the relative weight of FC can be estimated by using Equation 13 to the produce following:

$$w_1^L = \frac{5}{5+0.8+2.8+5.4+1.4} = 0.324 \quad (21)$$

$$Z^* = \left\{ \begin{array}{l} \int_{0.286}^{0.314} \frac{1-0}{0.314-0.286}(x-0.286)xdx + \\ \int_{0.314}^{0.325} (\frac{0-1}{0.325-0.314}(x-0.314)+1)xdx \end{array} \right\} + \left\{ \begin{array}{l} \int_{0.245}^{0.267} \frac{1-0}{0.267-0.245}(x-0.245)xdx + \\ \int_{0.267}^{0296} (\frac{0-1}{0.296-0.267}(x-0.267)+1)xdx \end{array} \right\} + \left\{ \begin{array}{l} \int_{0.232}^{0238} \frac{1-0}{0238-0.232}(x-0.232)xdx + \\ \int_{0.238}^{0250} (\frac{0-1}{0.250-0.238}(x-0.238)+1)xdx \end{array} \right\} \quad (22)$$

$$+ \left\{ \begin{array}{l} \int_{0.252}^{0.269} \frac{1-0}{0.269-0.252}(x-0.252)xdx + \\ \int_{0.269}^{0.313} (\frac{0-1}{0.313-0.269}(x-0.269)+1)xdx \end{array} \right\} + \left\{ \begin{array}{l} \int_{0.286}^{0.314} \frac{1-0}{0.314-0.286}(x-0.286)dx + \\ \int_{0.314}^{0.325} (\frac{0-1}{0.325-0.314}(x-0.314)+1)dx \end{array} \right\} + \left\{ \begin{array}{l} \int_{0.245}^{0.267} \frac{1-0}{0.267-0.245}(x-0.245)dx + \\ \int_{0.267}^{0296} (\frac{0-1}{0.296-0.267}(x-0.267)+1)dx \end{array} \right\} +$$

$$\left\{ \begin{array}{l} \int_{0.232}^{0238} \frac{1-0}{0238-0.232}(x-0.232)dx + \\ \int_{0.238}^{0250} (\frac{0-1}{0.250-0.238}(x-0.238)+1)dx \end{array} \right\} + \left\{ \begin{array}{l} \int_{0.252}^{0.269} \frac{1-0}{0.269-0.252}(x-0.252)dx + \\ \int_{0.269}^{0.313} (\frac{0-1}{0.313-0.269}(x-0.269)+1)dx \end{array} \right\} = 0.2783$$

Table 3. Evaluation results of the main criteria with respect to the overall goal

Pairwise criteria	1st exp	2nd exp	3rd exp.	4th exp.	5 th exp.	6 th exp.
FC vs. OSE	VHI	HI	VHI	MHI	HI	MI
FC vs. MP	VHI	HI	MI	MHI	MLI	MHI
FC vs. R&M	MI	MHI	MLI	MI	VHI	MI
FC vs. ETP	VHI	HI	MI	MI	MI	MHI
OSE vs. MP	VLI	LI	MLI	VLI	MLI	LI
OSE vs. R&M	VLI	VLI	LI	MI	MVI	LI
OSE vs. ETP	MI	MI	MHI	MI	LI	MLI
MP vs. R&M	MLI	MI	MLI	MI	LI	MI
MP vs. ETP	MI	MLI	MLI	MI	LI	MI
R&M vs. ETP	VHI	HI	HI	MI	HI	VHI

Similarly, the weights for OSE, MP, R&M and ETP yield 0.051, 0.181, 0.350 and 0.090, respectively. Also, regarding A1M and A1U, the weights for FC, OSE, MP, R&M and ETP result in (0.314, 0.067, 0.190, 0.314, 0.114) and (0.286, 0.098, 0.195, 0.278, 0.143), respectively. Consequently, the minimum, mean, and maximum weight of FC yields (0.286, 0.314, 0.324). It is notable that these values didn't correspond to wL, wM and wU respectively. By the same manner, the weight of FC deriving from the second, third and forth expert's judgment yields (0.245, 0.267, 0.296), (0.232, 0.238, 250 and (0.252, 0.269, 0.313) respectively.

The aggregate of the four experts' evaluations can be obtained as shown in Figure 5.

Table 4. Max &min eliminated from table 3

Pairwise criteria	1st	2nd	3rd	4th
FC vs. OSE	HI	VHI	MHI	HI
FC vs. MP	HI	MI	MHI	MHI
FC vs. R&M	MI	MHI	MI	MI
FC vs. ETP	HI	MI	MI	MHI
OSE vs. MP	VLI	LI	LI	MLI
OSE vs. R&M	VLI	LI	LI	MLI
OSE vs. ETP	MI	MI	MLI	MI
MP vs. R&M	MLI	MI	MLI	MI
MP vs. ETP	MI	MLI	MLI	MI
R&M vs. ETP	VHI	HI	HI	HI

The representative weight of quality FC, z*, can be found by using Equation 14 to produce the following:

By using the foregoing procedures and the whole experts' evaluations (Table 5), the weights for OSE, MP, R&M and ETP yield (0.0892, 0.1948, 0.2890, 0.1412) regarding α=0. main criteria weight yield (0.279, 0.091, 0.201, 0.289, 0.140) and (0.274, 0.088, 0.198, 0.281, 0.160) regarding α=0.5 and α=1.0 respectively. The results indicate that FC and R&M are the two most important main criteria for selecting the suitable loading-haulage equipment in open pit mine in this case study; whereas OSE is least important.

Based on the main criteria weights, the overall weights of sub-criteria can be estimated by using Equation 15 (table 5).

Applying equation 16, the alternative weights relating to each sub-criterion can be obtained as shown in table 6.

Due to space limitations, just results for α=0 are illustrated in tables 6 and results for α=0.5 and α=1 are not shown.

Table 5. Overall sub-criteria weights under α=0, 0.5, and 1

	α=0	α=0.5	α=1
commission	0.016	0.016	0.014
shipment	0.037	0.037	0.038
insurance	0.052	0.059	0.058
operating cost	0.088	0.087	0.086
capital cost	0.085	0.082	0.082
ease of operation	0.016	0.014	0.017
legislative requirement	0.015	0.015	0.015
working conditions in mine	0.030	0.029	0.028
safety and protective devices	0.015	0.016	0.016
incorporation of protective devices…	0.013	0.016	0.013
bench height	0.037	0.038	0.036
soil characteristics	0.018	0.019	0.019
material size after fragmentation	0.030	0.031	0.031
haul distance	0.057	0.057	0.057
type & geometry of deposit	0.034	0.033	0.033
Weather conditions	0.020	0.019	0.019
level of technology	0.056	0.056	0.054
ergonomics	0.029	0.030	0.031
ease of maintenance	0.032	0.033	0.033
reliability cost	0.069	0.069	0.068
labor skill	0.022	0.024	0.023
spare parts availability	0.048	0.045	0.046
flexibility	0.033	0.035	0.034
utilization	0.013	0.011	0.012
continues of mining	0.042	0.039	0.043
Capacity & productivity	0.039	0.038	0.040
maneuverability	0.019	0.023	0.021
useful life	0.028	0.030	0.025

The final alternative weight can be obtained by summing all the weights up using Equation 17. It can be found in the bottom row of table 6, the weights for Loader-truck, shovel-truck and shovel-truck-conveyor belt regarding α=0 yield (0.327, 0.349, 0.323).

the weights for Loader-truck, shovel-truck and shovel-truck-conveyor belt regarding α=0.5 and α=1 yield (0.325, 0.353, 0.321) and (0.326, 0.352, 0.320), respectively.

The results suggest that shovel-truck is the most desirable alternative; whereas shovel-truck-conveyor belt is the last one that will be considered to select.

5 DISCUSSIONS

This paper presents a fuzzy AHP model to tackle the open pit equipment selection problem. The proposed model characterizes each negative reciprocal fuzzy number as its own representative membership value, rather than an inverse and reversed order of its corresponding positive fuzzy number in Buckley's method that requires tedious manipulations. Additionally, the proposed approach is easier to implement and faster than Buckley's (Buckly 1985) and chang's (chang 1996) methods.

The model enables to tackle the difficulty in using Saaty's AHP method while transforming the imprecise judgment into an exact number. It should be noted that in proposed model, minimum and maximum value between evaluators eliminated when one criterion compared with another one, so, caused to better attribute weighting.

Other advantage of proposed model is normalizing score when ranking

Table 6. Overall weights of the alternatives estimated by the proposed model

	System A1		System A2		System A3	
commission	e_{ik}	r_i	e_{ik}	r_i	e_{ik}	r_i
	0.334	0.005	0.355	0.006	0.311	0.005
shipment	0.578	0.021	0.261	0.005	0.578	0.021
insurance	0.568	0.030	0.163	0.021	0.261	0.010
operating cost	0.424	0.037	0.568	0.010	0.163	0.006
capital cost	0.370	0.031	0.252	0.006	0.568	0.030
ease of operation	0.422	0.007	0.182	0.030	0.252	0.013
legislative requirement	0.301	0.005	0.424	0.013	0.182	0.009
working conditions in mine	0.329	0.010	0.380	0.009	0.424	0.037
safety and protective devices	0.108	0.002	0.188	0.037	0.380	0.033
incorporation of protective devices for environment pollution	0.179	0.002	0.370	0.033	0.188	0.017
bench height	0.098	0.004	0.316	0.017	0.370	0.031
soil characteristics	0.562	0.010	0.311	0.031	0.316	0.027
material size after fragmentation	0.093	0.003	0.422	0.027	0.311	0.026
haul distance	0.218	0.012	0.445	0.026	0.422	0.007
type & geometry of deposit	0.146	0.005	0.137	0.007	0.445	0.007
Weather conditions	0.078	0.002	0.301	0.007	0.137	0.002
level of technology	0.130	0.007	0.399	0.002	0.301	0.005
ergonomics	0.593	0.017	0.309	0.005	0.399	0.006
ease of maintenance	0.593	0.019	0.329	0.006	0.309	0.005
reliability cost	0.324	0.022	0.525	0.005	0.329	0.010
labor skill	0.556	0.012	0.124	0.010	0.525	0.016
spare parts availability	0.401	0.019	0.108	0.016	0.124	0.004
flexibility	0.486	0.016	0.323	0.004	0.108	0.002
utilization	0.154	0.002	0.551	0.002	0.323	0.005
continues of mining	0.120	0.005	0.179	0.005	0.551	0.008
Capacity & productivity	0.082	0.003	0.379	0.008	0.179	0.002
maneuverability	0.565	0.011	0.439	0.002	0.379	0.005
useful life	0.166	0.005	0.098	0.005	0.439	0.006
overall weight of the alternative regarding all sub-criteria (Ri)		0.327		0.349		0.323

alternative so sum of overall weight of the alternative regarding all sub-criteria is equal to one. As can be shown in table 5 and table 6 the weight of the alternative regarding to sub criteria is very close together when α change from 0 to one because in this model minimum and maximum value eliminated when we calculate weight of the alternative regarding to sub criteria.

5 CONCLUSION

Nowadays, capital cost of open pit mining equipment is very high so any mistake in selection of quantity, type and capacity of equipment were caused irreparable impact on mining project. The open pit equipment selection problem is a strategic issue and has significant impacts to the open-pit design and production planning.

The outputs produced by the model are the weights of sub-criteria, main criteria, and alternatives. The input requirements include the hierarchy of the decision problem, and the pairwise comparison judgments.

A suitable level of experience on the part of the expert is crucial because the expert usually relies heavily on experiences and knowledge while evaluating alternatives. Likewise, a judgment of the quality of information regarding design and construction, and sufficient knowledge of the expertise is also significant for the assessments.

The results deriving by using the model depend on the expert's pairwise assessments; thus, a suitable level of experience on the part of the expert and adequate knowledge of the expertise is essential. The proposed method may be applied in different area of mining engineering and other alternative selection problems such as mining method selection, waste dump selection and selection of underground equipment.

REFERENCES

Aghajani Bazzazi, A. Osanloo,M. Karimi,B, 2008. Optimal open pit mining equipment selection using fuzzy multiple attribute decision making approach. *Seventeenth international symposium on mine planning and equipment selection*, China, pp. 253-268.

Aghajani, A. Osanloo, M. Akbarpour, M, 2007. Optimizing loading system of Gol-e-Gohar iron ore mine of Iran by genetic algorithm. *Iron ore conference*, Australia, pp. 211-217.

Bandopadhyay, S. Venkatasubramanian, P, 1987. Expert systems as decision aid in surface mine equipment selection. *International Journal of Mining, Reclamation and Environment*, 1, pp. 59–165.

Bascetin, A, 2004. An application of the analytic hierarchy process in equipment selection at Orhaneli open pit coal mine. *Mining Technology (Trans. Inst. Min. Metall. A)*, 113, pp. 192-199.

Bascetin, A. Kesimal, A, 1999. The study of a fuzzy set theory for the selection of an optimum coal transportation system from pit to the power plant. *International Journal of Mining, Reclamation and Environment*, 13, pp. 97-101.

Bascetin, A. Oztas, A. Kanli, A, 2006. EQS: computer software using fuzzy logic for equipment selection in mining engineering". *The Journal of the South African Institute of Mining and Metallurgy*, 106, pp. 63-70.

Buckley, J.J, 1985. Fuzzy hierarchical analysis, *Fuzzy Sets and Systems,* 17, pp. 233-247.

Cebesory, T, 1997. Surface mining equipment cost analysis with a developed linear break even model. *International Journal of Mining, Reclamation and Environment,* 11, pp.53-58.

Celebi, N, 1998. An equipment selection and cost analysis system for open pit coal mines. *International Journal of Mining, Reclamation and Environment*, 12, pp.181-187.

Chanda, M.W, 1995. Equipment selection for small scale mining. *International conference on mine planning and equipment selection*, Canada, pp. 379-384.

Chang, D. Y, 1996. Applications of the extent analysis method on fuzzy AHP. *European Journal of Operational Research*, 95, pp. 649–655.

Chen, C. T, 2000. Extension of the TOPSIS for group decision-making under fuzzy environment. *Fuzzy Sets and Systems*, 114, pp. 1–9.

Denby, B. Schofield, D, 1990. Application of expert systems in equipment selection for surface design. *International Journal of Mining, Reclamation and Environment*, 4, pp. 165–171.

Hall, R. Daneshmand, K, 2003. Reliability Modeling of Surface Mining Equipment: Data Gathering and Analysis Methodologies. *International Journal of Mining, Reclamation and Environment*, 17, pp. 139-155.

Hoseinie, S.H., Pourrahimian,Y.,and Aghababae,H, 2006. Application of rock mass index (RMi) to determine of blasting index (BI) - A case study Sungun copper mine – Iran. *International conference on mine planning and equipment selection*, Italy, pp. 1013-1018.

Hrebar, M. J, 1990. Preliminary dragline selection for surface coal mining operation. *2nd International conference on mine planning and equipment selection*, Canada, pp. 133–43.

Hwang, C. L. Yoon, K, 1981. *Multiple Attribute Decision Making Methods and Applications: A State of the Art Survey*, New York: Springer-Verlag.

Martin, J.W. et al, 1982. *Surface mining equipment* (Colorado: Martin Consultants, Inc.), pp. 6–52.

Saaty, T.L, 1990. *The Analytic Hierarchy Process*, McGraw Hill. New York.

Samanta, B. Sarkar,B. Mukherjee,S, 2002. Selection of opencast mining equipment by a multi-criteria decision-making process. *Mining Technology (Trans. Inst. Min. Metall. A)*, 111, pp.136-142.

Sevim, H. Sharma, G, 1991. Comparative economic analysis of transportation systems in surface coal mines. *International Journal of Mining, Reclamation and Environment*, 5, pp. 17-23.

Zadeh, L.A, 1965. Fuzzy sets. *Information and Control*, 8, pp. 338–353.

Slice Thickness and Height Ratio Effects on Excavation Resistance in Open Pit Mine Drmno

Ivica Jakovljević,
Electric power industry of Serbia, Carice Milice 2, Belgrade, Serbia
Vladimir Pavlović
University of Belgrade, Faculty of Mining and Geology, Belgrade, Serbia

ABSTRACT This paper presents a research methodology for the bucket wheel excavator excavation resistance as a function of slice parameters variation. The researches were conducted on the open coal mine Drmno in Kostolac coal basin. The engaged power on the motor for the excavator bucket wheel drive is measured using modern measurement instruments and the specific excavation resistance and specific power consumption were calculated. The slice parameter values and the achieved capacity of the bucket wheel excavator were measured applying the GPS system.

Special attention was dedicated to the analysis of the effect the slice thickness to the slice width ratio had on the excavation resistance. The dependence of specific resistance variation as the function of slice thickness to width ratio is established and graphically presented in order to increase the operating efficiency of the bucket wheel excavator in the specific working environment.

1 INTRODUCTION

The efficiency indexes of the process depend on many various factors. The physical and mechanical characteristics of the excavated material, operation regime of an bucket wheel excavator, selection of the technological parameters of an excavated block, sublevel and slice, geometry and condition of cutting elements, should be specially noted.

One of the basic preconditions for the efficient operation and realization of satisfactory bucket wheel excavator efficiency, along with the efficiency of the whole technological system in open pits, is in the right selection of power for the excavator bucket wheel drive, meaning the coordination of excavation force with the expected excavation resistance. In other hand, it lies also in the right selection of the excavation block, sublevel and slice optimal parameters for the particular environmental conditions.

2 METHODOLOGY FOR EXCAVATING RESISTANCE CALCULATION

The rim force (1) on the excavator bucket wheel can be defined with:

$$Pt = Prez + Ppod + Ppunj + Ptr + Pkin \quad (1)$$

where:

- *Prez* - cutting resistance of the material cut from the massive block, including friction resistance of the cutting elements and working block front,
- *Ppod* - resistance on the material elevation in buckets to the unloading height in the bucket wheel unloading sector,
- *Ppunj* - resistance on the material loading into buckets,
- *Ptr* - friction resistance between material in buckets and circular slides of excavator bucket wheel in the process of material elevation to the buckets unloading height,
- *Pkin* - resistance on kinetic energy transfer to the material in a bucket, i.e. acceleration of the material to the bucket velocity.

All the world`s major producers of bucket wheel excavators use the following way to determine the rim force (2) on a excavator bucket wheel:

$$Pt = Pk + Ppod \quad (2)$$

in which excavation force is (3):

$$Pk = Prez + Ppunj + Ptr + Pkin \quad (3)$$

For the field measurements on a bucket wheel excavator of SRs 2000.28/3 + VR type, operating in overburden excavation in Drmno open pit mine, the Wattmeter method was used. In this method, the measurement of motor power engaged for the excavator bucket wheel drive is used to determine excavation specific resistance.

Electro motors for the excavator bucket wheel drive are exposed to variable loads, varying from neutral to maximal. It occurs due to anisotropy of the excavated material and discontinuous arrangement of buckets along the bucket wheel rim. This can be regarded as the most frequent occurrence. This variability requires a special regime for the measurement of power used in the excavation process. It is a continuous measurement regime using an electric current recorder. This recorder registers torque current used to calculate the total power spent in the excavating process, i.e. the effective power. With this effective power, we determine the engaged power. The recorder can be double-channel or multi-channel recorder, so that it can be used not only to measure the current of the motor for the excavator bucket wheel drive and motor for turning the upper frame, but also to measure other values. The average torque current is estimated with planimetry, while maximum and minimum values are read from the recorder paper. Effective current can be calculated by:

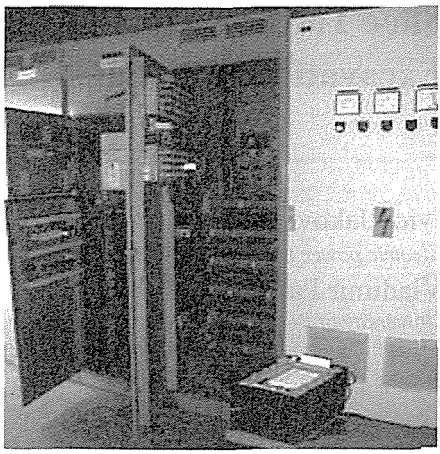

Figure 1. Electric recorder

$$Ief = \frac{I\,mom}{\sqrt{2}} \quad (4)$$

where:

Imom - torque current (A).

The power spent in the excavating process is estimated by the following relation (5):

$$Ns = \sqrt{3}\, U\, Ief \cos\varphi 10^{-3} \quad (5)$$

where:
Ief - effective current (A);
Imom - torque current (A);
Ns - engaged power (kW);
U - rated voltage (V);
cosφ - power factor.

Power consumed by the motor (6) is calculated as:

$$Np = Ns\, \eta \quad (6)$$

where:
η – is efficiency of the motor.

Power used for excavation (7) is estimated when a power needed for lifting the excavated material to the unload height is subtracted from the total transferred power:

$$Nk = Np - Npod \quad (7)$$

Power required for elevating the material (8) to the unload height is calculated as:

$$Npod = \frac{Q\,\gamma\, g\, hd}{3600} \quad (8)$$

where:
Q - is capacity of excavator (m³/h);
γ - is mass of the material (t/m³);
g - gravity acceleration (m/s²).
hd - material unload height (m).

Force required for the material excavation is calculated through power needed for the excavation:

$$Pk = \frac{Nk}{V} \quad (9)$$

where:
V - is bucket wheel rim velocity (m/s).

On the basis of the known excavating force and calculated length of all cutting edges, i.e. total cross sections of the slices, all buckets which are in the contact with the material at the same time, the specific excavation resistance is calculated as:

$$Kl = \frac{Pk}{\sum_{i=1}^{i=m} Li} \quad (10)$$

or:

$$Kl = \frac{Pk}{\sum_{i=1}^{i=m} Fi} \quad (11)$$

where:
Kl - excavating specific resistance of material along the bucket cutting edges (N/cm);
Kf - excavating specific resistance of material on the cross section (N/cm²);
Pk - excavating force (N);
Li - total length of all bucket cutting edges which are in the contact with material at the same time (cm);
Lf - total area of slice cross-section of all buckets which are in contact with the material at the same time (cm²);
i,m - number of buckets which are in contact with material at the same time.

Specific energy consumption (12), required for the excavation of 1 m³ of material, can be estimated when a difference between spent and neutral power is divided by the realized capacity:

$$E = \frac{Np - Npr}{Qt} \quad (12)$$

where:
E-specific energy consumption (kWh/m³);
Np - consumed power (kW);
Npr - neutral power (kW);
Qt-capacity of bucket wheel excavator (m³/h).

3 FIELD INVESTIGATION

Measurements of excavation resistance in Kostolac coal basin were performed in Drmno open pit mine on November 09, 2006. The measurements were performed on system 1 on overburden excavation, on SRs 2000 28/3+VR bucket wheel excavator with technical parameters presented in table 1..

Table 1. Technical characteristics of SRs 2000 28/3+VR bucket wheel excavator

Escavator type SRs 2000 28/3	
Manufacturer	TAKRAF
Power of excavator bucket wheel drive motor (kW)	2x500
Volume of bucket with ring-shaped space (lit)	1300
Number of buckets (com)	18
Number of bucket unloads (min^{-1})	90
Diameter of excavator bucket wheel (m)	11
Length of excavator bucket wheel mast (m)	41
Cutting speed (m/s)	2,92
Specific cutting force (N/cm)	900
Theoretical capacity (m^3/h)	6000
Mass of excavator framework (t)	2658
Total installed power (kW)	3000
Excavation height (m)	28
Excavation depth (m)	3
Speed of lifting and lowering the excavator bucket wheel mast (m/min)	5
Speed of circular movement – turning: from-to (m/min)	8-40

The weather was fair, with sunny periods, without wind, and the air temperature was 17 to 20°C. There were no special preparations of the system or excavator. After the installation of equipment and measuring instruments, the measurements were carried out in real operating conditions of the bucket wheel excavator. The excavation was in vertical cuts with the given parameters of a slice. The measurements were performed with partially worn out angle teeth. A very sophisticated way of measurement with GPS system was used in order to achieve high accuracy of slice parameters and excavator capacity, as well as to improve the monitoring of the measurement process, creating the possibility of on-line monitoring of the realized capacity in Drmno open pit mine.

Individual measurements are related to the limited length of a turning process of the excavator for at least 28° and maximum of 45° from the excavator longitudinal axe towards the left or right side. Four sets of measurements

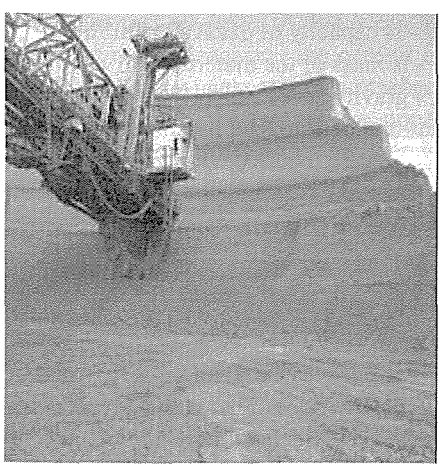

Figure 2. Operation environment in which the measurements of excavation resistance were conducted in open pit mine Drmno

of specific excavation resistance of k_L and k_F, excavator capacity and specific energy consumption were performed, with total of 128 measurements. The measurements were carried out at the excavation of the fourth and fifth cut along the block height on the first overburden bench.

Slice parameters variation was done in the manual regime of excavator operation, in the following way:

- for the constant slice height of h_1=4,65 m and constant rotation speed of upper excavator frame, V_1=18 m/min. Due to permanent excavator unload of constant slice width of b_1=0,20 m in a time unit, the fourfold variation of slice thickness is performed s_1=0,24 m, s_2=0,30 m, s_3=0,50 m and s_4=0,75 m (measurement set no.I);
- for the constant slice height of h_1 and new value of constant rotation speed of upper excavator frame, V_2=26 m/min, and constant slice width of b_2=0,29, the fourfold variation of slice thickness was performed again s_1, s_2, s_3 and s_4 (measurement set no.II);
- for a new value of slice height, h_2=2,9 m, and constant rotation speed of upper excavator frame V_1, and constant slice width of b_1, the fourfold variation of slice thickness were performed s_1, s_2, s_3 and s_4 (measurement set no.III);
- for the constant slice height, h_2, and constant rotational speed of upper excavator frame V_2, i.e. constant slice width b_2, the fourfold variation of slice thickness was performed s_1, s_2, s_3 and s_4 (measurement set no.IV).

Table 2. Review of average values of physical and mechanical characteristics of litho logical members of Kostolac coal basin

Lithological members Complex	Humidity W (%)	Volumetric weight γ (kN/m^3)	Angle of inner friction φ (°)	Cohesion C (kN/m^2)
Peat	29,0	20,00	26 ± 2	15 ± 5
Send gravel	14,5	20,50	33 ± 2	3 ± 1
Fine sand	24,0	20,00	29 ± 1	5 ± 1
Clay	36,0	19,50	21 ± 3	28 ± 4
Coal	/	11,80	38 ± 4	39 ± 1
Foothill clays	39,0	18,00	22 ± 3	28 ± 3
Foothill sands	16,5	20,00	30 ± 3	5 ± 3

4 INVESTIGATION RESULTS

The obtained results of four measurements series in the working environment of the open pit mine Drmno, for the values of excavation specific resistance along the total excavation length (K_L) and along total slice cross-section (K_F) as a function of a slice thickness to width ratio are graphically shown on figure 3,4,5 and 6.

Graphical presentation for the slice height of 4,65 m is given on Figures 3 and 5, and for the slice height of 2,9 m on Figures 4 and 6.

Qualitative course of the specific excavation resistance along the total length of bucket cutting edges (k_L) as the function of slice thickness and width ratio (s/b), at constant slice height of 4,65 m (Fig. 3), shows that the increase of s/b values reduces the k_L value. The k_L curve decreases when the s/b value increases, converging to the approximate constant course. Maximal value of k_L occurs when ratio s/b=1,2 (k_L=314,2 N/cm).

The qualitative course of k_L graph also shows the decreasing trend with the increase of s/b ratio, at the constant level

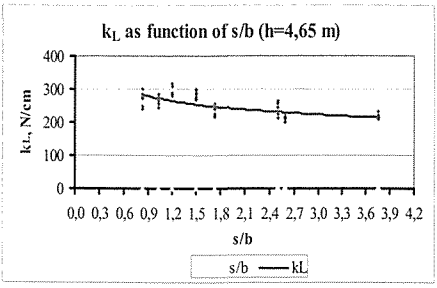

Figure 3. Graphical presentation of k_F as function of s/b (SRs 2000 28/3)

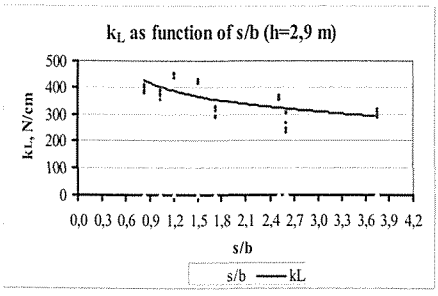

Figure 4. Graphical presentation of k_L as function of s/b (SRs 2000 28/3)

height of h=2,9 m (Fig. 4). Maximal value of k_L is again at the ratio value of s/b = 1,2 (k_L=449,7 N/cm). The lowest k_L values are, in this case also, in the range of the highest values of s/b ratio. The k_L values are significantly at smaller slice heights than at optimal slice heights.

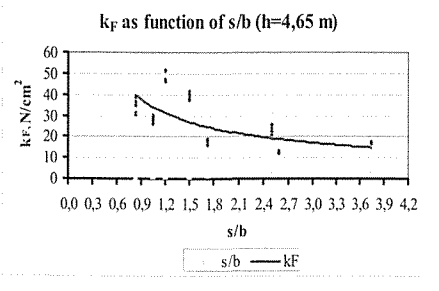

Figure 5. Graphical presentation of k_F as function of s/b (SRs 2000 28/3)

Qualitative course of specific excavation resistance, along the total slice cross-section area (k_F), as the function of slice thickness and width ratio (s/b), at constant slice height of h=4,65 m (Fig. 5), shows that the k_F value decreases when value of s/b ratio increases. The k_F graph decreases and converges to the approximate constant course with the increase of s/b value. Maximal value of k_F is when s/b=1,2 (k_F=51,8 N/cm²).

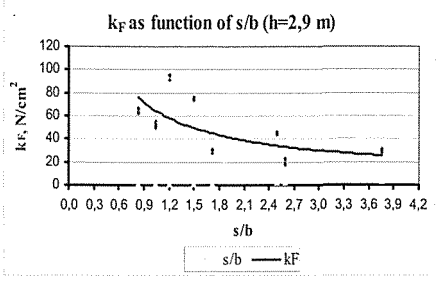

Figure 6. Graphical presentation of k_L as function of s/b (SRs 2000 28/3)

Qualitative course of k_F graph also shows decreasing trend with the increase of s/b ratio, at a constant level height of h=2,9 m (Fig. 6). Maximal value of k_F is again at s/b=1,2 (k_F=95,6 N/cm²). The lowest k_F values are, again, in the range of the highest values of s/b ratio. The k_F values are significantly higher at lower than at optimal slice heights.

5 CONCLUSIONS

The following may be concluded for the effect of slice thickness and width on specific excavation resistance on the basis of the measurements:

- According to the measurement results at open mine pit Drmno, the specific excavation resistance increases at first and then slightly decreases with the increase of s/b ratio. The highest value for the specific excavation resistances, k_L and k_F, is at the ratio value of s/b = 1,2.

6 REFERENCES

Drebenstedt C., Paessler S., 2006, Output calculation model of bucket wheel excavator, supported by virtual reality with regard to the slewing velocity at the turning points, *ISCSM Aachen*.

Himel W., 1963, Der specifische Grabwiderstand in Abhangigket von der Spanflache und der Spanform bei verschidenen, Bodenarten.

Kressner M., Drebenstedt C., Balke D., 2006, Cutting resistance and cutting tool design on Bucket Wheel Excavators, *ISCSM Aachen*.

Ignjatović, D., 1993., Izbor metode za određivanje otpora na kopanje rotornim bagerima u uslovima površinskih kopova lignita Kolubare, Magistarski rad, Rudarsko geološki fakultet, Beograd,

Jakovljević, I., 2008., Određivanje optimalnih parametara odreska rotornog bagera u funkciji otpora na kopanje, Doktorska disertacija, Rudarsko geološki fakultet, Beograd.

Jakovljević, I., Pavlović V., Šubaranović T., 2007., Slice parameters variation effect on excavation resistance at bucket wheel excavator SRs 2000 28/3 in open pit mine Drmno , *7-th European coal conference Lviv*.

Tehnička dokumentacija PD TE-KO Kostolac i Elektroprivrede Srbije, Beograd.

The Revolution in Continuous Mining

Peter F Moden, Darron W Dixon-Hardy
Energy and Resources Research Institute, University of Leeds, Leeds, LS2 9JT, United Kingdom
I Göktay Ediz
Department of Mining Engineering, Dumlupinar University, Kütahya, Turkey

ABSTRACT In this paper the concept of a Flexible Conveyor Train (FCT) for use in continuous mining is introduced. A comparison as an alternative to shuttle cars as a means of transporting ore or coal from the Continuous Miner (CM) in a mining circuit to the main conveyor belt is made. This specialist piece of equipment enables a Continuous Miner (CM) to become truly continuous whereas before, with the use of shuttle cars, there was a period of time where the CM was not cutting owing to waiting time for an empty shuttle car to arrive. This revolutionary piece of equipment is set to improve.

1 INTRODUCTION

Underground mining methods have developed rapidly over recent years with continued research into new technologies. Many mines use continuous miners (CM) that are capable of continuously cutting into rock/mineral and then propel themselves to other working areas within the mine, often by remote control. The material cut by the continuous miner is ultimately discharged onto some form of conveyor. The current problem faced by development is that the continuous miners can move whereas the main conveyor can only be laid out in straight lines and cannot be attached to the continuous miner. Therefore there is a gap in the mining circuit between the cutter and the transport out of the mine.

From the continuous miner the cut material is transported to the main conveyor using shuttle cars or battery haulers or similar types of equipment. These vehicles create a waiting period in the mining cycle as the vehicle has to reach the continuous miner and then travel to the conveyor and back. This is where the Flexible Conveyor Train (FCT) becomes a large step towards the making of a completely continuous underground mining cycle. The FCT attaches to the rear end of the CM and then feeds the material cut directly in to the main conveyor. This paper describes the use of an FCT developed by Joy Mining Machinery (Joy, 2004).

2 CHARCTERISTICS OF AN FCT

The main components of an FCT are a feed bin, the conveyor and a discharge point (refer to Figure 1). Simply put the continuous miner feeds into the

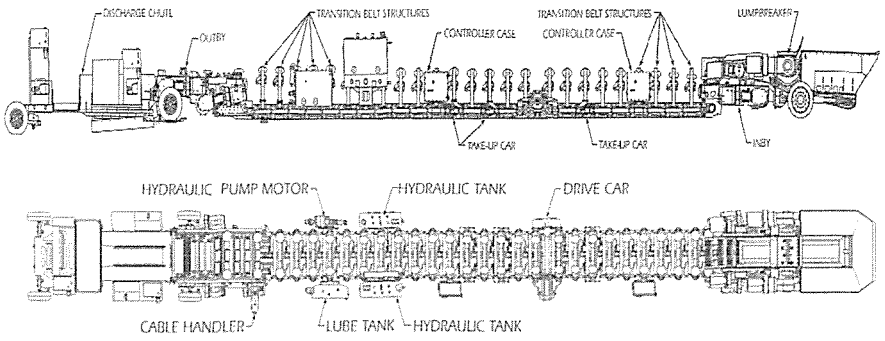

Figure 1. Showing the plan and cross sectional view of a joy FCT403.

bin at the front end, the material then passes through a lump breaker then the conveyor transports the material to the discharge chute from which the material is discharged either sideways onto the main conveyor or it sits on top of the conveyor and drops the material directly onto it by over the top discharge. The FCT is moved by tracks and trams at a maximum speed of 0.38m/s. The length of the FCT ranges from 38m to 152m. Similar to most machinery used underground the FCT is controlled by a remote which means the driver can be located at a safe distance from the machine while it is working. The FCT is also programmed using cards so that it has a "memory" of its route. When moving it snakes along the path chosen by the driver and then returns along the same path when reversed. How the FCT discharges material is important as over the top discharging variants require a Dynamic Movement Unit (DMU) roadway mounted on the main conveyor shown in Figures 2 and 3. This machine

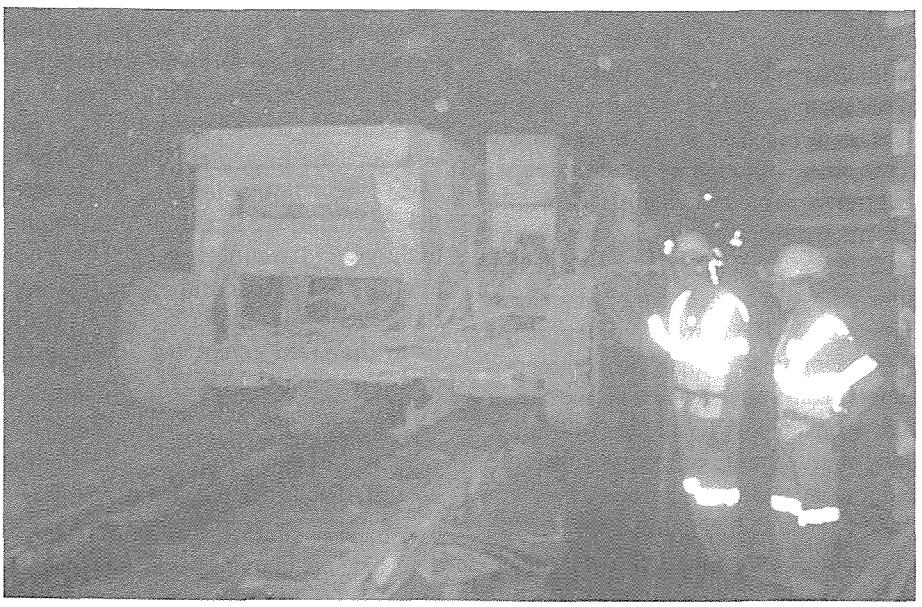

Figure 2. Showing the rear end of the FCT sitting on the DMU roadway.

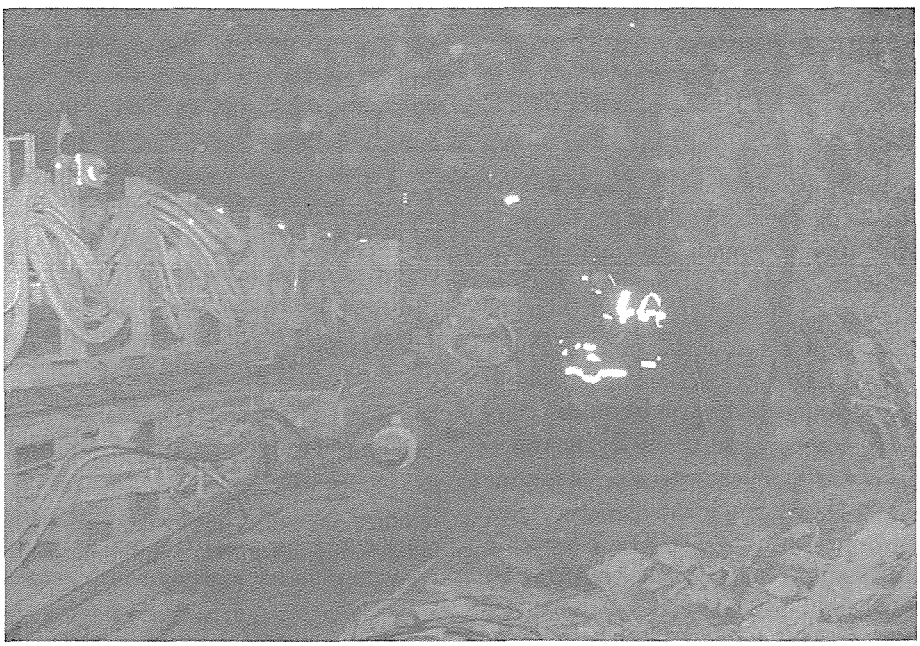

Figure 3. Showing the DMU propulsion cylinders and roadway which the FCT sits on.

uses 15' stroke propulsion rams to lock on to the FCT and propel it. This is done by first driving the rear end of the FCT on the DMU roadway then when cutting proceeds and when the FCT is required to move forward the DMU rams push in the direction of advance and then retracts to the rest position, owing to the 200 tonne weight of the FCT it slides off the DMU by the length of the ram push.

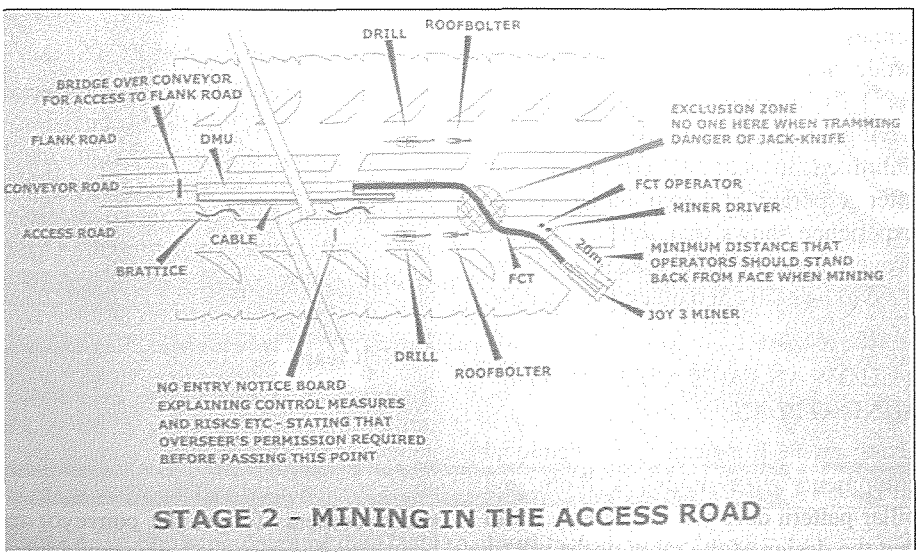

Figure 4. Part of the mine design

3 FCT CONVENTIONAL HAULAGE COMPARISON

FCTs are an alternative to the haulage systems currently used in any underground development, but the decision to choose the FCT over proven shuttle cars or battery haulers can be a difficult one. Shuttle cars and similar vehicles provide a mobile, flexible element to the excavation. These vehicles are fast and can operate on steep gradients as well as being able to be pulled out from one area of the mine to be put in to another quickly. So if one panel was cutting quicker than another or the CM working in that district had just broken down the shuttle cars working with that CM could be pulled out to move to where they could be used elsewhere. With an FCT this cannot be done as it takes several shifts to move and set up the FCT for production to commence. However, shuttle cars only carry a small amount of material in comparison to the 27m^3 a minute of material an FCT can transport. In successful trials at Boulby mine production went from 3000 tonnes of material in a 9 ½ hour shift to 5500 tonnes of material. The increase in production was achieved even allowing for FCT downtime. The benefits of having an FCT over shuttle cars are unlimited in suitable conditions and after a period of conditioning current experience shows that shuttle cars can prove advantageous when problems need to be easily and quickly overcome.

4 HOW AN FACT AFFECTS THE MINING PLAN

Using an FCT instead of conventional equipment when mining a room and pillar pattern does not necessarily mean that the design of the room or the pillars has to be changed. At Boulby mine (CPL, 2008) the adopted the use of herringbone room and pillar extraction and it required little alteration to adopt the use of the FCT within the mine design, as shown in Figure 4. The only considerations that need to be taken when looking at the mine design when using an FCT is the roof support and length of development before movement of the FCT. The FCT advances at the rate at which the CM cuts into the rock. Experience at Boulby found that the FCT could only advance up to a distance where its weight can still hold it on to the DMU. The maximum distance of advance was found to be 32m before the FCT had to be moved, any advance more than this distance resulted in the weight of the FCT dragging itself off the DMU.

The other consideration of the rapid advance while using an FCT is that the roof will need on hand immediate support should there be problems arising from weaknesses in the route. When looking at Figure 4 it can be seen that roof bolters are on hand to bolt when advance of the extraction comes across a weaker area of roof.

5 OPERATIONAL ASPECTS

Although the FCT is a revolutionary piece of equipment its relative complexity and the mass of technology involved means there are several problems that may prevent FCT's taking over from shuttle cars completely at present. These include:

5.1 Belt tear

Although the frame of the FCT has a turning radius of 9.4m the conveyor that rides the frame is put under variable stress as material is conveyed upon it round corners. To get the conveyor to bend round corners the belt is made from a combination of nylon weave covering

a rubber compound with the centreline strengthened with Kevlar. This means that the edges of the belt are susceptible to tearing owing to side tensions and can be punctured by scrap and other debris. Also where the belt is joint the act of conveying round corners means that the pins holding the joint together pull apart or pull the belting apart.

5.2 Working on uneven ground

The FCT used at Boulby mine is a 64m variant of a Joy FCT403 and this machine weighs around 200 tonnes. The sheer weight of the FCT can cause difficulty when cutting a ramp or extracting a dipping seam when the weight of the FCT can result in slip and it may move down slope when stationary and there is a danger it may fall off the main conveyor. This is a problem where the working conditions are uneven as no seam is completely flat and will have dips in it. In Boulby mine the gradient of the roadway that was being mined was 1 in 8 and the conveyor was slipping off the DMU. To solve this problem "fingers" were welded onto the roadway above the conveyor the FCT sits on, this provided some friction to stop the FCT from slipping, shown in Figure 5. This method of arresting the movement of the FCT on the conveyor was a bespoke solution that highlighted how use of the FCT must be adapted to the mining circumstances.

5.3 Costs and future development

Cost is a significant reason why FCTs are not being used more widely at this point in time in the underground mining industry. A unit such as the one used at Boulby mine would cost several million pounds to buy new. This does not compare favourably against the cost of shuttle cars though after this initial investment the cost per tonne produced is far better, in an ideal world, than the cost per tonne produced with the aid of shuttle cars.

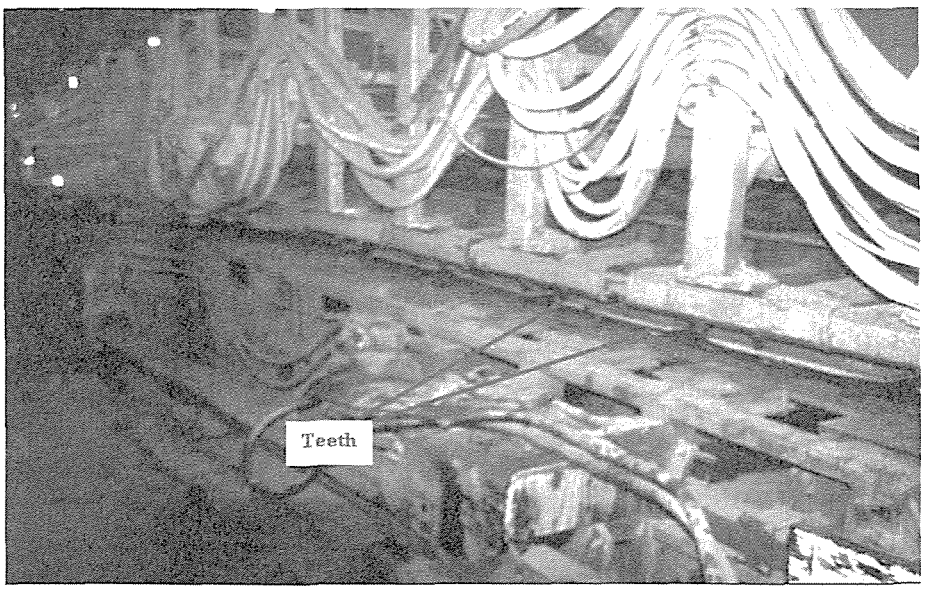

Figure 5. Showing detail of the DMU roadway including the 'teeth' welded on to prevent slipping.

The problems of belt tearing is a focus of development. This problem of having a frame which can turn back on itself while having a belt that tears when turning means that currently the FCT has limited use. Specialist technology such as the programming that enables the FCT to "snake" back along its tram route needs to be developed further and a new composition for the belting is being made so that the edges of the belt are strengthened and that the joint pins lessen the likelihood of the belt tearing itself apart.

6 CONCLUSION

The use of Flexible Conveyor Trains will, in the future, be more common place in underground mining as they offer a real alternative to shuttle cars. The development of the FCT is truly making continuous mining a possibility and is a real revolutionary idea but has several problems at present that hinder it from a more wide spread and effective machine. Belting problems and testing will eventually solve the problem of extensive down time and when this occurs FCTs will be essential in underground development.

REFERENCES

www.joy.com. haulage brochure,, 2004, http://www.joy.com/jmm/products/pdf/Haulage_Brochure_Joy.pdf.

Cleveland Potash Ltd, 2008. www.clevelandpostash.co.uk.

ACKNOWLEDGEMENTS

Special thanks to Boulby Potash for their time and consideration and for their help in gathering information for this paper.

The views and opinions contained in this paper are those of the authors themselves and in no way reflect those of the University of Leeds, Dumlupinar University, Cleveland Potash Ltd or Joy Mining Machinery.

High Production, Low Cost, Flexible Alternate to Lignite Mine Bucket Wheel.

Adam Wood
P&H Mining Equipment (UK) Ltd, Wigan, United Kingdom

ABSTRACT Miners focusing on Bucket Wheel systems may be missing out on significant operational cost savings, which are available through alternative technologies. This article describes and illustrates Equipment, Methods and Examples of High Production, Low cost alternatives to bucket wheel technology, specific to large European lignite mines.

Alternative production methods for greater than six thousand tonne per hour, per extraction line have been available for decades and comprise of proven reliable machinery. Operational costs to extract convey and spread material, of less than €0.70 per BCM can be realized. Applying the concepts to European lignite mines could improve efficiency and profitability.

1 INTRODUCTION

Lignite is a major energy resource, and will continue to be part of many nations energy mix for power for many years to come.

Larger volume European lignite mines are predominantly dependant on Bucket Wheel technology for excavation of overburden and lignite. They have been so for many decades, whereas, other high production mines outside of Europe predominantly utilize alternative technologies.

When contemplating new excavating lines, mine sites may process calculations and studies internally, or obtain the services of external consultants to plan their mine site for them.

If the people involved in the study do not know enough about the alternatives available, the alternatives will be discounted without fair consideration. Bucket Wheel mines may only use Bucket Wheel consultants, or Consultants who are stronger in Bucket Wheel philosophy than other technologies.

2 APPLICATION ALTERNATIVES

2.1 Walking Draglines

Draglines in one guise or another have been utilized by high production surface miners since the early 1900's.

The main advantage of draglines is that they are direct spoil excavating systems. They do not require any other ancillaries to transport the excavated

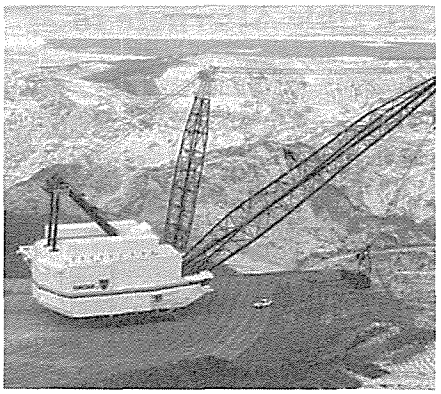

Figure 1. Large walking dragline.

material to its final resting spot. What this means is simple planning, logistics, and lower cost of operations.

Other benefits include ability to excavate harder materials and materials with rock inclusions.

Draglines are a lowest cost mining tool due to direct spoil capability, in the correct application. The correct application includes having material that is able to be directly spoiled, coal/lignite that is bedded over a large area which allows long strips, and excavation with few major repositioning / relocations (long walks) and long mine life

2.2 In Pit Crushing And Conveying IPCC

The concept of mobile and fully mobile Crushing solutions, attached to conveyor systems is by no means new. Krupp made its first mobile crusher in 1955, (Moore, 2008).

The in-pit-crushing systems are not only economical in solid rock but also in seam deposits, (Schroeder, 1998).

Shovel - Truck operations offer the most flexible systems for excavating, transporting and dumping material. With the greater flexibility comes lower

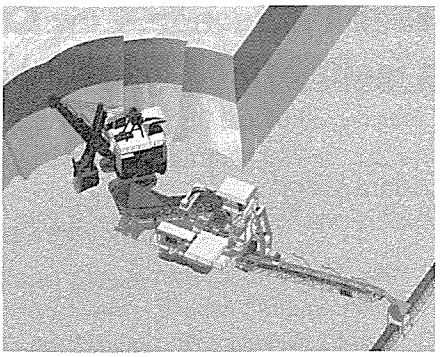

Figure 2. Shovel feeding mobile mining crusher (MCC).

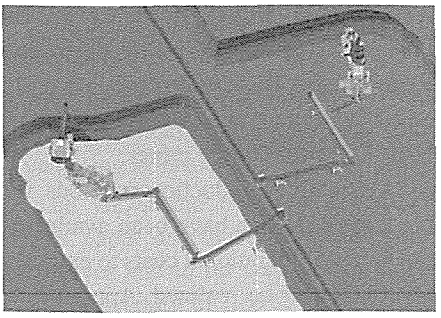

Figure 3. Shovels feeding mobile mining crushers (MCC).

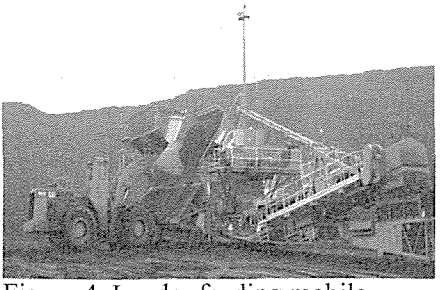

Figure 4. Loader feeding mobile mining crusher (MCC).

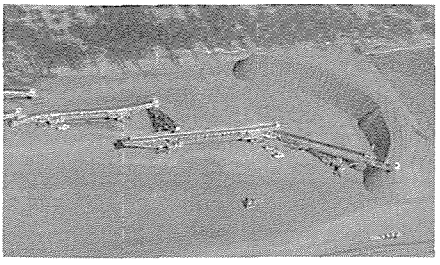

Figure 5. Specialty spreader stackers.

production and higher operating costs.

Still, Shovel - Truck operations form the majority of surface mining activities around the world, especially in rock applications.

Eliminating the truck and replacing with a continuous haulage system, is a method that is, and has been available, since conveyors were first introduced.

The main challenge is how mine operators load the materials onto the conveyors, in a manner which does not damage the conveying line.

In Pit Crushing and Conveying (IPCC) Systems are completely integrated, continuous material handling and processing systems, consisting of Face Shovel, Mobile Mining Crusher (MCC), Conveyor Networks and Material Spreaders.

There is a definite trend toward mobile primary crushing plants, (Casteel, 2008).

3 DRAGLINES

3.1 Method

Typically draglines are used where long strips can be taken to remove overburden, and when overburden can be dumped near by.

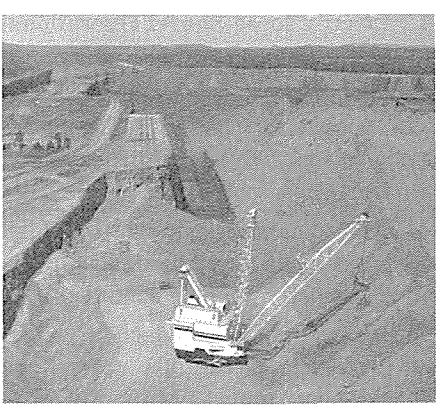

Figure 6. Strip mining with dragline.

Where overburden requires blasting, production can be assisted by cast blasting, where the explosive moves a significant amount of overburden to its final resting place, without the need of excavating equipment.

3.2 Production

General reference for annual productivity of draglines can reasonably be assessed as (Backus, 2009) :-

Production = 250,000 BCM*Bc (1)

Where;

BCM = Bank Cubic Meter

Bc = Bucket Capacity in m^3

If a dragline has a $100m^3$ Bucket, it should move 25 Million BCM per year. Efficient operations can raise this value to 29 Million BCM per year. Modern draglines can have buckets up to $125m^3$ capacity.

These productive capacity numbers are only bettered by Large Bucket Wheel excavators.

3.3 Dragline Operational Costs

Large high production draglines have total "All In" operating costs of €0.42 to €0.50 per BCM, (Backus, 2009).

This is increased if the material needs to be re-handled.

3.4 Maintenance, Availability and Planning

Draglines are relatively simple machines to operate and maintain.

There are no maintenance people "assigned" to a dragline, but the mine utilizes general maintenance personnel that also look after any facilities, the dozers and other mobile equipment. For maintenance days two electricians, a mechanic, and two welders. The

mechanics and welders are often on the bucket more than the machine.

Availability of draglines is, like all other machines, subject to the quality of maintenance practices, but is typically 90-95% excluding scheduled down time, (Backus, 2009).

Continuous excavating systems are complex and require high levels of planning to accomplish the target production requirements. Conversely, Draglines as a complete excavating system, are much simpler to plan and manage due to the lack of reliant subsequent processes.

3.5 Equipment Life

As with other massive excavating equipment, draglines are designed for decades of use. 150,000 - 200,000 operational hours is not uncommon, (Backus, 2009).

4 IN PIT CRUSHING AND CONVEYING SYSTEMS (IPCC

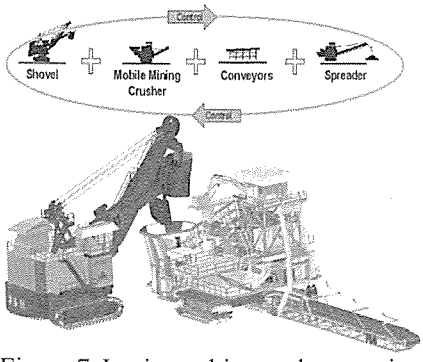

Figure 7. In pit crushing and conveying. Control of complete system from the shovel.

4.1 High Production Face Shovel

Electric Mining Shovels have been operating in all materials, in all the worlds major deposits since the early 1900's. Hydraulic shovels and backhoes have also contributed to mine production since being up-rated from small construction project machines over the past few decades.

It is important that miners acknowledge the productive capacities of the modern range of High Production Shovels, versus the small machines that miners use for menial duties.

Large Electric Rope Shovels have achievable peak productive capacities of 13,000 tonne per hour, with dippers sizes of 76m³, material dependant.

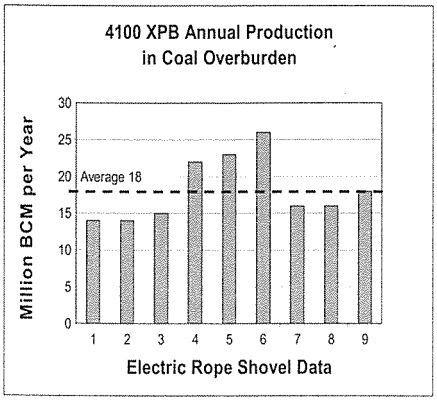

Figure 8. Factual production data from monitored mine sites, (Paterson, Williams, 2005).

4.2 Electric Rope Shovel Operational Data

The largest Electric Rope Shovels achieve total operational costs of US$0.10 per tonne, (Anon, 2009). (US$0.20 per BCM at a bank density of 2).

Such equipment is designed for high production, hard rock digging conditions, in the harshest of mining conditions.

Average yearly production values for the largest classes of Electric Rope Shovel, range from 12 Million BCM to 26 Million BCM per year, depending

on mine efficiencies and Truck availabilities.

Availability of Electric Rope Shovels is greater than 90% for most of the working life with good maintenance practices.

180,000 operational hours is achievable and planned, on this type of equipment, in hard rock digging conditions, with good maintenance, (Anon, 2008).

Soft ground conditions found in European lignite mines, results in easier digging and extended component life.

High production Shovel Truck operations can run at less than €1.00 per BCM, and offer greater flexibility over bucket wheels.

4.3 Conveying Systems

The use of overland conveyors is widely accepted as the most efficient method of moving material from location to location, and has significant cost savings over transportation by trucks.

Savings made from use of electrical power versus diesel, and the reduced manpower to operate and maintain conveying systems, are significant when compared to truck operations.

Availability of tires has been a critical issue for truck operators, and has led to down time and significant cost increases to maintain trucks.

Conveyors, and stacking systems, are utilized in both bucket wheel and IPCC systems and their continuous transportation benefits are accepted over trucks.

In world wide efforts to make large open pit mining more economic, the adoption of belt conveying is progressing, (Schroder, Schwier, 1996).

4.4 Transfers System – Fully Mobile Mining Crushers

Where Bucket Wheel systems use band wagons to transfer material from the bucket wheel to the conveying lines, Shovel systems use Mobile Mining Crushers (MCC), to receive material, and if necessary, crush to size before discharging on to conveyors.

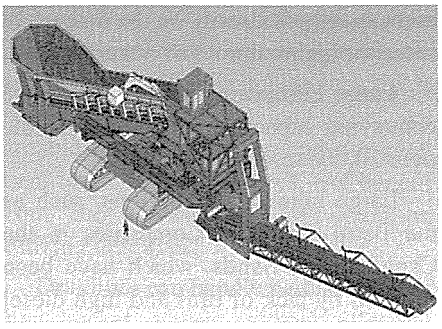

Figure 9. Mobile mining crusher (MMC).

Mobile Mining Crushing systems are, and have been utilized in various industries for many years. Most leading manufacturers have some form of mobile crushing technology available, in varying sizes, capacities and crushing method.

Not all mine sites require material to be crushed, in which case a mobile hopper, based on the MCC can be utilized, to transfer loose material from shovel to conveyor.

When considering high production sites such as European Lignite mines, Fully Mobile Crushing and Conveying systems coupled with Large Face Shovels, can be assessed as viable alternative solutions to Bucket Wheel technology.

4.5 IPCC Production

Modern IPCC systems are designed so that the bottle neck is the productive capacity

of the Loading Unit. Recent performance trials, using the latest technology in mineral sizers, and the increasing maturity of large-scale materials handling systems, has seen the emergence of competitive and credible suppliers of continuous materials handling machines for all kinds of open-cut mining operations, (Morrison, 2008).

Conveying and spreading technology and capacity is already on the market, to cater for high volumes of material.

Large European Lignite mines have conveying capacities which can handle over 20,000 tonnes per hour.

Large mining corporations, such as the Petro Chemical Companies in the Canadian Oil Sands, which have been affected by lack of tires and high diesel costs, have specifically asked for high production alternatives to Trucks.

Fully Mobile Crusher Conveying systems are available today with peak production of 13,000 tonnes per hour. Nominal 10,000 tonnes per hour.

4.6 IPCC Operational Costs

IPCC systems have total operating costs of less than €0.70 per BCM, (Zelenovskiy, 2008) for 3,000 BCM per hour, (12 Million BCM per year), and significantly less for larger systems of 6,000 BCM per hour, as Economies of Scale allow.

4.7 Maintenance, Availability and Planning

As with bucket wheel systems, maintenance of an IPCC system is of key importance.

The scale and requirements of Bucket Wheel and IPCC systems are comparable, in terms physical attributes and of maintenance manpower.

Similarly, as with Bucket Wheel systems, planning is also of high priority, to ensure consistent production, and availability.

4.8 Equipment Life

Again, in easy digging conditions as found in European lignite mines, equipment lives of over 150,000 operational hours can be expected with good maintenance practices.

4.9 MMC manufacturers

- P&H Mining Equipment.
- Thyssen Krupp
- MMD
- Sandvik.
- FLSmidth
- Terex,
- Metso.

5 HIGH PRODUCTION SHOVEL TRUCK WITH SEMI MOBILE CRUSHING AND CONVEYING

5.1 Method

Shovel Truck operations offer the greatest flexibility. Production is not reliant on a continuous system, and individual components of the production line can be down, without significantly affecting production.

Trucks are dependant on diesel costs and tire availabilities, but European miners need to understand the Economies of Scale of this method of mining.

The main Equipment Manufacturers offer trucks with capacities up to 360 Tonnes. Needless to say, that these mighty movers are significantly less expensive to run than a large fleet of 80 tonne trucks.

A 360 tonne capacity truck can deliver what 4.5 x 80 tonne trucks can. Significant savings are made on operators, maintenance and running costs.

Similarly, one large Electric Rope Shovel with a dipper capacity of 76 m^3, can move more than seven times the capacity of a 10m^3 shovel. Significant savings are made on operators, maintenance and running costs.

The key to this method of production is to minimize the distance a truck needs to travel.

Once more, transferring the material to a conveying line as soon as practical will cut down on the expense of operating trucks.

Short Haul trucking to Semi Mobile Skid Mounted Mining Crushers / Hoppers, which feed directly on to conveying lines can be a solution for many mines looking for a cost effective solution for some applications.

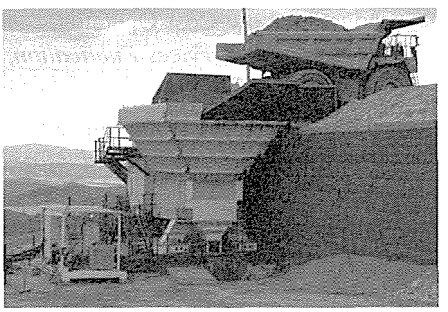

Figure 10. Skid mounted semi mobile mining crusher

Reclaim feeders can be fitted with crushing systems to size material before it gets to the conveyor.

6 CONCLUSIONS

Alternative technologies are walking draglines and Electrical Rope Shovels operating in conjunction with in pit crushing and conveying systems, or large scale trucks.

Continuous excavating systems are complex and require high levels of planning to accomplish the target production requirements.

Draglines

Large sedimentary deposits such as lignite, coal fields, phosphate rock fields and borax deposits, with long mine lives suitable for strip mining, and dumping local to the excavation area, can benefit from the lowest cost of operation utilizing draglines.

Draglines can handle harder material than bucket wheels without affecting production.

Walking draglines may be considered a good alternative to BWE for excavating overburden and lignite. It involves no transportation means, such as off-highway trucks and crushing and conveying systems.

In an appropriate application, no system can compete with draglines on cost per ton basis.

Equipment Manufacturers have draglines products to suit capacities of most European Lignite Mines.

IPCC Systems

Suitable for any size deposits from 3 to 30 Million BCM per year per production line.

In appropriate applications, IPCC systems can be considered attractive alternatives to bucket wheel systems.

Allow for excavation of harder materials, and handling large fragments without damage to subsequent processes.

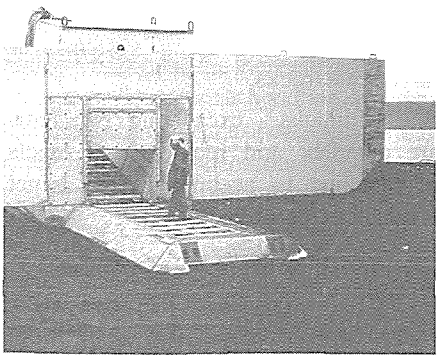

Figure 11. Flat back reclaim feeder.

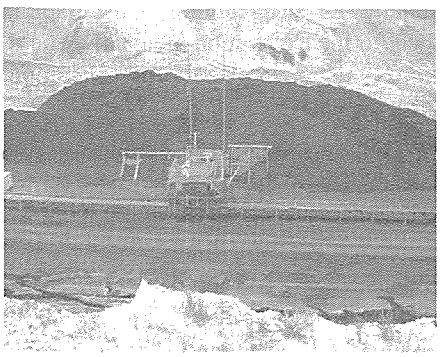

Figure 12. Reclaim feeder / breaker.

Can excavate significant castles or islands of materials left behind by bucket wheels. Offers attractive production and operational costs.

High Production Shovel truck

Offers complete flexibility and lower levels of planning to achieve production goals.

Shovel truck operations have realized 56 Million Tonnes per year from one shovel and its associated fleet of trucks.

The magnitude of scale savings in this system can be considered as a flexible alternative to bucket wheel lines.

Coupling this system with short haul dumping and semi mobile crushing stations or hoppers, to feed conveying lines, can make this system even more financially attractive. On lignite extraction, the crushing /sizing can be done before material reaches stock piles.

Financial Comparison

Draglines €0.42 to €0.50 per BCM. Low Flexibility – Excellent Operational Cost Upto 29 Million BCM per year

IPCC Systems €0.50 to €0.70 per BCM Upto 25 Million BCM per year

Shovel Truck €0.70 to €1.00 per BCM With Semi Mobile Crushing Up to 25 Million BCM per year

Shovel Truck €1.00 per BCM High Flexibility - Higher Operational Cost Up to 25 Million BCM per year

All systems based on high production in European Lignite Mines

REFERENCES

Anon. 2002, Peak Performance Practices-Excavator Selection for High production Low Cost Operations. *A P&H MinePro Services Publication, Milwaukee, U.S.A.*

Anon. 2008. Personal Communication, *Maintenance manager, Gold Mine, U.S.A.*

Anon. 2009. Personal Communication,, *P&H Mining Equipment, Milwaukee, U.S.A.*

Backus, T., 2009. Personal Communication, *P&H Mining Equipment, Milwaukee, U.S.A.*

Casteel, K., 2008. New Focus on In-Pit Crushing Systems, *E&MJ European Editor. Volume 5, Story 24.*

Ozdogan, M., 2009. Personal Communication, *Ideal Machinery and Consultancy Ltd. Co., Ankara, Turkey.*

Moore, P., 2008. In Pit Crushing and Conveying, *Mining Magazine. March 2008, Pages 36-42.*

Morrison, D.,2008. Materials Handling Options to Reduce Costs, Achieve Article, 2008, *Sinclair Knight Mertz Consulting., Australia.*

Paterson, L.B. and Ozdogan, M., 2001. Performance of the Bigger, Faster and Smarter New Generation Electric Mining Shovels, *The 17th International Mining Congress and Exhibition of Turkey, IMCET 2001, Ankara, Turkey pp.237-242*

Paterson, L.B. and Williams, A.J. 2005. Larger Shovels-The Reality, *The 19th International Mining Congress and Fair of Turkey, IMCET 2005, Izmir, Turkey pp.121-124*

Schröder, D. Dipl-Ing, and Schwier, U. Dipl-Ing, 1996. Selection of Mining Systems for Large Open Pits, *Braunkohle Surface Mining,48 (1996) September/October.*

Schröder, D., Dipl-Ing, 1998. Economic and technologic aspects of Bucketwheel Excavator – and Crusher / Conveyor-Systems, *Krupp Fördertechnik GmbH, Essen, Germany.*

Szalanski, S., 2009. Personal Communication, *P&H Mining Equipment, Milwaukee, U.S.A.*

Zelenovskiy, I., 2008. Personal Communication, *P&H Mining Equipment, Milwaukee, U.S.A.*

Optimisation of Open Cast Mining Production Process in Serbian Lignite Mines

Darko Danicic,
Kolubara Metal d.o.o, Vreoci, Serbia
Slobodan Mitrovic,
Elektroprivreda Srbije, Belgrade, Serbia
Dragan Ignjatovic,
Faculty of Mining and Geology, Belgrade, Serbia
Sava Kovacev,
Kolubara Metal d.o.o, Vreoci, Serbia

ABSTRACT Energy sector represents a key industrial branch for national, environmental and economic success. With its exclusive access to domestic deposits, lignite industry represents a guarantor of reliable raw materials, offering long-term supply security based on verified reserves.

Currently operated coal mines in Serbia (Kolubara and Kostolac) have production around 36 million tons of lignite, and over 108 million m^3 of overburden.

Consequently, sustainability of lignite production requires cost reduction and environmental protection, as well as capacity increase.

In order to rationalise, and increase efficiency of Serbian lignite mines, it is necessary to focus the activities on major issues shown within the triangle of energy policy objectives (security of supply, competitive prices and environmental protection).

Production process optimisation singled out several special programs, where the following are most important:

Equipment revitalisation and modernisation. Life of currently operated machinery is up to 25 years. In the forthcoming period, changes of deposit conditions are also expected.

Production process automation. Equipment modernisation, introduces partial or full automation possibility, what enables high level of technical operation in the field of open cast mines management.

Lack of coal quality uniformity. Lack of coal quality uniformity represents a great problem in lignite production optimisation, improving the problem of the lack of homogenisation since great amounts of coal reserves are used uneconomically.

Planning and training. Efficiency increase also requires selective planning with

transparent positioning of machines which is constantly updated, as a regular activity on the planning of the sequence of operations.

Cooperative software for business procedures. Finally, it is necessary to implement cooperative software for business procedures and work order management.

All these measures represent a key precondition for maintaining competitive position of lignite production on an international level.

1. INTRODUCTION

In the end of the last and the beginning of this millennium, energy sector, together with the natural environment preservation with which it has an unbreakable bond, is presented as an essential question for global sustainable development. Within this context, certain strategically important questions arise, such as: sustainable coal mining, sustainable coal utilisation, whether this is a different issue in developed countries and developing, i.e. transition countries, etc. By following the efforts oriented towards the settlement of these problems, one reaches individual, specific questions both on the regional and narrower national plan.

Proved amount in place (total coal, million tonnes) - 21 176, proved recoverable reserves (total coal, million tonnes) - 13 885

Serbia has Europe's largest proven deposits of lignite. The Serbian WEC Member Committee reports that the proved amount of coal in place is over 21 billion tonnes, of which by far the greater part (97%) is lignite. Within the other ranks, 6 million out of the 27 million tonnes of bituminous coal in place (22%) is deemed to be recoverable. The recovery factor attributed to the lignite reserves is also approximately 66%. The pattern of Serbia's coal reserves is replicated in current production levels: lignite (all of which surface-mined) accounted for more than 98% of total output in 2005. Most of the lignite is used for electricity generation, with minor quantities being briquetted or directly consumed in the industrial and residential sectors.

In any case, energy sector represents a key challenge for the national, environmental and economic progress. With its exclusive access to domestic deposits, lignite industry represents a guarantor of reliable raw materials, offering long-term supply security based on verified reserves.

Coal is the most significant energy potential, with the share of 84% in the structure of energy reserves. Lignite-fired power plants at this moment supply over 60% of electricity in Serbia.

Coal production in Serbia is based on two mining basins: MB 'Kolubara' and MB 'Kostolac'. Current capacity of these open cast mines is over 36 million tons of lignite, with over 108 million cubic meters of overburden. On the other hand, European integration in the field of energy requires permanent adaptation of technological and corporate structures in lignite mining, which specially goes for costs and competitiveness of generation energy prices. In addition to this, environmental requirements have been imposed in the past several years as a special condition.

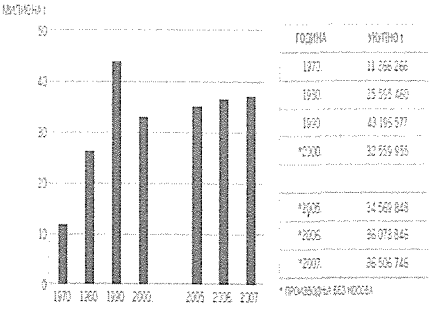

Figure 1: Coal Production in Serbia

From 2004 electricity market has undergone liberalisation and private energy traders have emerged. One specific quality of coal production in Serbia is that it has so far never been in rough competition with other energy sources and that there is also coal demand tendency in future.

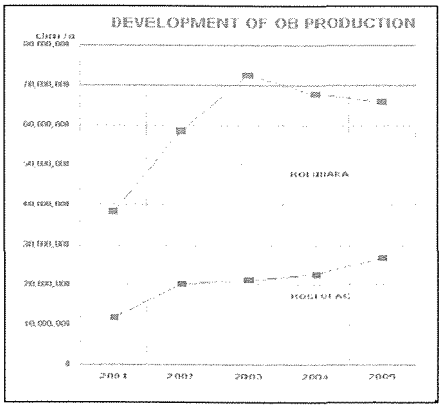

Figure 2: Overburden Removal

According to expert predictions of the World Bank from the study developed in 2004 (The European Union's CARDS Programme for the Balkan Region), with annual electricity consumption increase of up to 1.1% to maximum 1.6%, Serbia will in 2012 become a permanent electricity importer.

Table 1: SEE Electricity demand forcasts CAGR 2003-2020

Compound annual growth value in gross electricity demand 2003-2020			
	Case 1 (%)	Case 2 (%)	Case 3 (%)
Albania	2.0	4.0	4.9
BiH	2.3	3.0	3.4
Bulgaria	0.8	1.6	2.5
Croatia	2.5	3.2	3.9
UNMIK	1.7	3.2	4.3
FYR Macedonia	1.5	2.5	3.0
Montenegro	-1.3	0.7	1.2
Romania	1.2	2.6	3.6
Serbia (excl. UNMIK)	1.1	1.1	1.6
SEE	1.3	2.3	3.1

However, according to the latest indicators increase rate is higher than the anticipated one, showing that Serbia will be faced with electricity shortage earlier than predictions made several years ago. This requires urgent construction of new capacities for electricity generation, inevitably leading to the modernisation and restructuring of mining capacities with production increase.

2. COAL MINING PROCESS OPTIMISATION PROGRAMME RETROSPECTIVE

Impact of energy and environmental policies on coal mining in Serbia may be divided in several phases. During the seventies, after oil crises, supply security was placed in the focus of energy policy. In the course of this period, there was forceful modernisation of Serbian open cast mines, purchase of, at that time, modern mining machinery, as well as looking up to the countries with the traditionally developed open cast mines and equipment manufacturing for the latter.

In the second half of the eighties, environment protection started to play an increasingly higher role in the energy policy and investments. However, at that moment ex-Yugoslavia disintegrated

causing a serious standstill in the following of European and international trends on all levels, lasting until 2000. Coal mine rehabilitation and coal production increase was designated by the Government of Serbia as the top priority after 2000, while the Development Strategy of Serbia confirms that the relying of energy sector on the increase of domestic lignite production, together with the measures for production optimisation, revitalisation of existing and procurement of new equipment and rehabilitation of existing electricity generation capacities is the only proper path towards the sustainable development of the society.

3. PROBLEMS AND PROGRAMMS FOR COAL MINING PROCESS OPTIMISATION

3.1 Problems Identified in Lignite Production in Serbia

- The issue of secure provision of necessary lignite amounts and quality within the short, mid and long term periods;
- The issue of providing economic lignite supply to power plants, aimed at the lowest prices and production costs.
- The issue of environmentally sustainable development.

3.2 Lignite Production Optimisation Programmes in Serbia

The following activities have been recognised with regard to the lignite production optimisation.

3.2.1 Equipment Revitalisation and *Modernisation*

Equipment, this especially goes for bucket-wheel excavators, has been supplied, depending of commercial conditions, in the period of several decades, which has conditioned its high variety, making maintenance especially difficult. In addition to this, the mining concept created at the time of procurement of the first continuous systems was made according to the 100% system efficiency, which has given rise to a lot of efforts in the latter years related to maintenance, since there have been frequent unexpected system outages, as well as certain number of emergency situations, thus reducing the mine efficiency. This has also caused faster devastation of the machinery in addition to its objectively long operation life. This programme has several important aspects.

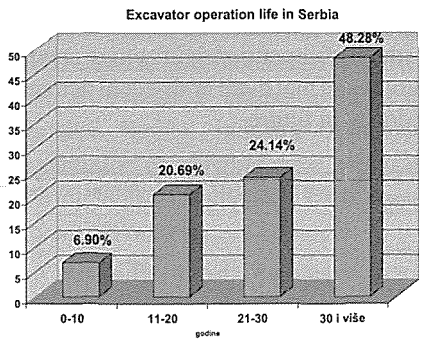

Figure 3: Excavator operation life in Serbia

The basic one is the provision of reliable equipment operation on open cast mines, capacity increase, productivity increase, consequently labour reduction due to equipment modernisation. In order to accomplish the revitalisation process in an adequate manner, the concept of structure state establishment was developed in cooperation with expert institutions and firms, as well as measures to be taken, e.g. for bucket wheel excavators:

- Balancing – determination of barycentre position projection of the rotating superstructure;

- Radial-axial ball bearing control;
- Geometrical – structural control of the support structure;
- Testing of steel wires;
- Rotating elements state control through the method of vibro-diagnostics;
- Ultrasound and magnetic flux control of liable welds and structural segments;
- Control of liable screw connections.

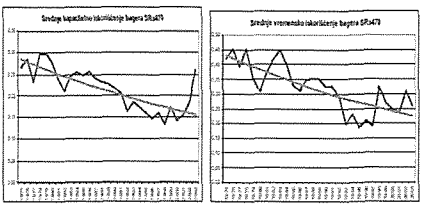

Figure 4: Change of capacity (left) and time (right) coefficient during operation of excavator № 311103 (purchased 1974)

Several revitalisations have been done since 2000, executed by original equipment manufacturers or by experts coming from Serbian companies. In this manner, the following revitalisations have been carried out:

SchRs 630	capacity 4.100 t/h (Kolubara)
SRs 1200	3.400 m³/h (Kolubara)
C 700	3.100 t/h (Kolubara)
SRs 1300	3.400 t/h (Kolubara)
SRs 1300	3.400 t/h (Kostolac)

Revitalisation of several machines at Kostolac Mining Basin is in progress (SRs 400 and SRs 470), as well as several spreaders and belt wagons.

Monitoring project of online state of steel structures and equipment of vital importance for the excavator SRs 1300 at Kolubara has also been performed.

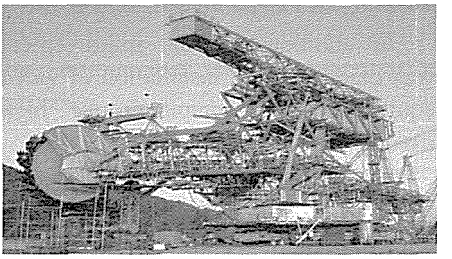

Figure 5: Revitalised excavator SRs 1301 with measuring points

Throughout this period, several studies have been developed having direct or indirect task to plan and develop this field, both in terms of technology and costs.

During 2006, a new transport (dumping) system at Kolubara (Tamnava West Field) was commissioned, with the capacity of about 7.000t/h, while the delivery of two more complete transport systems together with excavators and spreaders of the same capacity is in progress – one for MB Kolubara (Tamnava West Field) and one for MB Kostolac (Drmno).

3.2.2 Production Automation Process

Programme objective is efficiency increase of technical processes through the wide spectre of optimisation, with subsequent reduction of lignite mining costs and energy generation for about 25%.

Computer equipment application, hardware and software, trained personnel performing the supervision are the basic premises of automation. One example of the technical improvement measure is partial or complete control automation of bucket wheel excavators, spreaders

and equipment enabling the reduction in the number of employees, even up to 30%.

In addition to this, improvement was made through installation of video equipment and equipment for high capacity signal transmission.

Among four open cast mines at Kolubara Mining Basin, automation with the control centre was introduced on one of them, serving for the control of production parameters.

Application of higher excavation and transport capacities, longer conveyers has additionally enabled optimal application of frequency regulation in transport system control, in addition to higher efficiency. This has directly reduced starting impacts and necessary engaged power, contributing to lower energy and spare parts costs in the course of mining.

3.2.3 Lack of Coal Quality Uniformity

Having in mind an expressed lack of coal quality uniformity at Kolubara and Kostolac Mining Basins, homogenisation advantages are manifold. We can differentiate benefits related to open cast mines and thermal power plants. Benefits related to open cast mines include limitation of high quality variation and maximum utilisation of the deposit, while the thermal power plant benefits include more efficient and regular operation, increase of boiler plant efficiency, reduction of mazout usage, used for the 'improvement' of the calorific value of coal, reduction of auxiliary consumption, due to the reduction in usage of various stand-by systems, reduction of failures and cheaper and more efficient maintenance of transport, dozing, grinding and

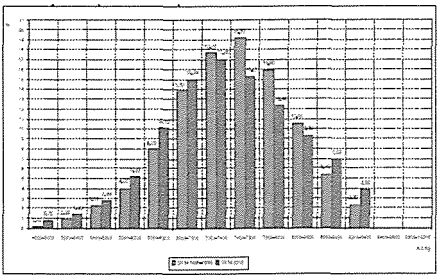

Figure 6: Distribution histogram of lower calorific value of coal supplied to TPPs Nikola Tesla at Obrenovac

Finally, the one to benefit the most is the environment (natural environment), since optimal emission and imission allocation is achieved through quality control and homogenisation.

The basic problem occurring at our coal mines is high quality variation, both along the excavation block vertical and along the benches. Coal quality at the open cast mine 'Tamnava' for example varies from 1.000kJ/kg to 9.700 KJ/kg. The substance whose lower calorific effect (LCE) is above 5.320 KJ/kg falls under the category of 'balance coal'. In accordance with that, relative coal price was developed and contracted. According to that document, it does not 'pay off' for the coal mine to deliver coal to the thermal power plant having LCE lower than 5.230 kJ/kg (not paid!), i.e. above 8.000 KJ/kg (no premium!). With quality control through coal homogenisation it is possible to shift the limit defining balance reserves of coal within the deposit, and extend the operation life of active open cast mines, together with the increase of economic effects. By applying the coal quality control system, i.e. by mixing of poorer quality coal with the coal of better quality, the boundary between balance and off-balance coal is shifted. If taken into account that coal on open cast mine 'Tamnava' at Kolubara

Mining Basin is excavated with three excavators on different positions along working benches (currently with very different qualities), it is necessary to synchronise their operation (through capacity and excavation point variation), in order to obtain coal of necessary quality as a result.

For the purpose of avoiding high variations in quality on open cast mines, coal sections with the quality below 5000 kJ/kg are currently transported to the excavated area (as in the case of the first-sub-bench on open cast mines 'Tamnava') or they remain unexcavated.

During 2004, about 100.000 m^3 of mass from the first sub-bench was dumped besides regular dirt bands on the open cast mine 'Tamnava – East Field'. Within these masses, about 50% goes to coal of average quality, ca. 4.000 kJ/kg. Approximately 70.000 m^3 of coal with the quality similar to the one at 'Tamnava East Field' was dumped on the open cast mine 'Tamnava West Field'. If this coal were to be homogenised with the coal of very good quality, mixture of quality could be obtained, about 6.700kJ/kg. Diagram shown in Figure 1 indicates that it is realistically possible to obtain the coal of contracted quality by means of mixing. According to the data provided on this diagram, 40-42% of coal was delivered under LCE range between 6.200 and 7.400kJ/kg (which would practically be the homogenisation objective). There was 9% of coal with the quality below 6.200kJ/kg, while almost 50% of coal with LCE above 7.400kJ/kg was delivered. Therefore, if coal homogenisation was applied, coal neither below 6.200kJ/kg nor above 7.400kJ/kg would not have been delivered to the thermal power plant, enabling the mine to excavate and deliver dumped dirt bands as coal, without disturbing thermal power plant operation.

It is essential for open cast mines to reduce the need for selective operation by introducing the homogenisation process.

Naturally, quality management in certain intervals requires capacity reduction of certain excavators, however, this loss is compensated by the reduction of the need for selective operation.

3.2.3.1 Environment Protection Contribution

Environmental impact of coal mining and processing is not only present in the excavation and transport phases on open cast mines, but also in the dumping phase, both at the mine and at the thermal power plant, combustion phase and dumping of combustion by-products. Under all these phases the impact is negative and the parameter implicating these problems changes depending on the processing phases.

In terms of environment, optimal allocation of emissions and imissions is achieved by homogenisation and quality management. This unified and uniform emission may have a positive effect on population living in the surrounding area, since it contributes to environmentally more favourable situation and it enables the fulfilment of legally prescribed and permitted pollution norms. This especially goes for more uniform share of sulphur in coal which is combusted.

One of the effects whose significance may not be disregarded emerges from better organisation and necessity to establish better control, which in themselves carry positive effects on some pollution parameters. This is especially related to coal self-combustion issues on dumps and dust dispersion from dumps.

Based on the experience from open cast mines in neighbouring countries and our open cast mines, it is possible to implement a coal quality system starting at the deposit, subsequently continued during excavation, transport, dumping and taking of coal from dumping areas. By establishing such a complex system, it is possible to meet thermal power plant requirements in terms of continuous coal provision of contracted and guaranteed parameters.

This procedure would, from the mining aspect, enable considerable benefits in higher efficiency of available coal reserves at the deposit and technically more favourable mining conditions. From the aspect of thermal power plant engineers, supply of coal possessing a permanent and previously know quality would significantly contribute to the regularity and stability of the combustion process, together with the reduction of auxiliary consumption of units, equipment wear and maintenance costs, while from the wider social aspect, positive effects would be felt in the reduction and re-allocation of pollution around the thermal power plant. Especially important environmental and financial effects would be achieved by the suspension of liquid fuel utilisation serving for the support to thermal power combustion. Viewed from the wider aspect, the state itself has the greatest interest from coal homogenisation process introduction on open cast mines, since it provides more efficient energy usage of available mineral potential.

3.2.4 Planning and Training

Optimization of production of the open pit mines inevitably starts from the requirements for sustainable planning that goes into more levels of spatial planning and regulation, through the strategic plan of meeting supply and demand in the scheduled period, the global planning of building capacity and utilization of resources, and to the detailed planning and positioning of each machine separately.

The question is whether the market environment requires strong planning sector or activities should be left to market mechanisms. Some examples from the recent past, such as the California example from 2001 speak to the planning necessity and can not be left to market activities. This is especially pointed out by the fact that the commissioning of new thermal capacity and the opening of the corresponding open pit mine requires at least 5 years. Electric Power of Serbia (EPS) continued practice of making both short-term and long-term plans and prognosis, as were Estimates of sustainable development, Strategy of sustainable development, Carbon sector to 2015, etc..

After a decade of lagging, in 2001. EPS made a summary of existing conditions and observed delay in the professional skills and knowledge at all levels, from the top and middle management to the training in new technological knowledge and skills. In all related companies, a permanent training is launched for the use of computers in the broadest sense, to postgraduate training for the use of professional software.

With the help of English consultants the following training was managed: Development Programme for Managers of the Future including energy industry, strategic thinking, competetive environment, accounting, finance planning & control, investment appraisal, organization & managers, leadership & teamwork, decision making & communications, change management,

human resource management.

3.2.5 Cooperative Software for Business Procedures

One of the essential elements of efficient functioning is implementation of software for business procedures, as well as application of individual technical software.

Having in mind the original organisational separation of Kolubara and Kostolac Mining Basins, business procedures created within them developed independently from one another.

Currently, there is a pilot project aimed at integration of business procedures at the level of Electric Power Industry of Serbia.

3.2.5.1 MB Kostolac - Current Status

After the merger of power plants in the Kostolac into "Power Plants and Mines Kostolac Ltd.", the IT systems of both of the previously independent companies are also being merged into one IT department. At the time of the **merger of the mines,** the Kostolac mines had an IT department which operated on an old VAX platform with applications for H&R (employees listing) and payrolls, while in power plants since 2003 the development and implementation of ERP software, source code developed by the Serbian company DIGIT, had started. The software is organized through several highly integrated subsystems:

- Marking of working factors

Subsystem for management of unique ID-s for every object processed in system

- Administration subsystem
- Enables alterations in application design, and defining of user rights
- Employees

Full H&R record and organizational chart are covered in this subsystem and relations between users is also defined (i.e. superior – subordinate relation which is lately used in other subsystems for approval of actions)

- Payrolls subsystem - calculation
- Procurement, demand for procurement according to unique ID of product with approval of superior officer
- Stocks management, acceptance of goods delivered from suppliers only after announcement from procurement and issuance on approved list of need
- Sales and purchases
- Financial analysis, Suppliers, Accounting subsystems fully automated
- General ledger, fully automated, all necessary data generated during input

The documentation workflow is completely covered; therefore relations in between applications are highly integrated.

In September of last year, the implementation procedure for maintenance subsystem was initiated in power plants, but due to the merger it was postponed. Classification of plants was completed and it was organized through work orders.

Implementation of this system in mines is ongoing and the only problem represents the unique ID system, which is currently in procedure and education of relevant personnel is also ongoing, and upon completion these employees will get computers and start the work.

3.2.5.2 MB Kolubara Applications

Applications being used in Kolubara today are mainly for financial and commercial purposes. There are 18

existing applications, which are all "domestic products", designed and developed in Kolubara (table 17). All of those applications are multi user applications except Payrolls, Employees and Coal quality, which are being operated centrally, in the Automated Data Processing sector (AOP sector) of Kolubara. All applications are developed internally by permanently employed designers in COBOL. Central database do not exist, every application works with files. All of the applications work on one ALPHA server under HP UNIX. Applications are highly reliable and have fast response over large amount of data.

Due to ongoing transition to SAP following applications will be transferred to modules that will be implemented:

MM module will cover: Material accounting, Investments, Warehousing; Procurement, which was not covered with any of the existing applications, and possibly sales

FI module will cover: Buyers and suppliers, Fixed assets, General ledger and Cash and Bank which has been processed with single home made application written in Visual Basic, working on four isolated computers connected directly to the banks with data transfer by removable media to computers connected to system and manual input of data into existing applications CO module will cover: Controlling (which did not exist so far), and Plant accounting General ledger.

4. CONCLUSION

There is still a remarkable discord between the image existing about coal and actual coal performance and potential. It is of utmost importance for coal industry to send the message that coal could provide a sustainable bridge towards the future, by parallel activity in terms of more efficient operation, better organisation and environmental impact.

Based on all of the above, it may be said that optimal and sustainable coal production in Serbia is within an arm's reach. Lack of investments into this field lasting for a number of years, has left on one hand very big 'thirst' for investments, and on the other hand direct reversion to objectives and solutions within the favourable international environment which have already passed several years long testing under realistic conditions. Thereby, Serbian industry could avoid possible wanderings, and contribute in the most efficient manner to the sustainable development of community.

For this to happen, good management principles need to be applied, implying proper planning on all sectors and level (mining, mechanical, electrical and corporative), training, protection and safety, participation in the development of society and community, environment protection. In addition to this, usage of modern tools for management and maintenance, hardware and software standardisation, as well as cost control, should enable competitive prices. One more specific quality of Serbian coal mines is that equipment revitalisation should be planned together with mine development, and the introduction of new technologies. Cooperation with scientific institutions should be continued in the field the development and more efficient access to the resources.

REFERENCES

Brendow, K., (2004), World coal perspectives to 2030, World Energy Council, Geneva/London

Danicic D., (2004), MSC thesis:

"Methodology for examination of excavator's structure for condition determination for revitalization" (BSc, Faculty of Mining and Geology, Belgrade).

Danicic D., Mitrovic, S., Ignjatovic, D., Maneski, T. (2005): The Testing of Bucket Wheel Excavators for The Testing of Bucket Wheel Excavators, 20th World Mining Congress, Teheran.

Ignjatovic, D., Maneski, T., Lakovic, D., Polovina, D., Danicic, D.(2003): Capital Mine equipment revitalisation on opencast mines in Serbia, Mineral material complex of Serbia and Montenegro, Monograph.

Kolonja, B., Ignjatovic, D., Knezevic, D. (2006): Coal Homogenization Benefits – Example on Open Pit Mine Tamnava – TPP Nikola Tesla B System, International Meeting „Energetika 2006"

PwC Consortium (2004): The Europian Union's CARDS programme for the Balkan region-Contract No. 52276

Resources and Logistics (2006): Technical Assistance in the Preparation of Study for improvement of EPS's maintenance and operational performance

Determination of the Identicalness of the Trucks Working in Open Pit Coal Mine and Using in Availability Analysis

Açık Ocak Kömür Madeninde Çalışan Kamyonların Özdeşliklerinin Belirlenmesi ve Kullanılabilirlik Analizinde kullanımı

H. Ankara
Eskisehir Osmangazi University, Department of Mining Engineering, Eskisehir, Turkey.
S. Yerel
Bilecik University, Bozuyuk Vocational School, Bilecik, Turkey.
M. Taksuk
Turkish Coal Enterprise GLI, Tavsanlı/Kutahya, Turkey

ABSTRACT The equipment of open pit coal mines are generally categorized as loading equipment and hauling equipment. Trucks are usually used as hauling equipment in open pit coal mines. Thus, determining the identicalness of the same model trucks working in open pit coal mine has a key role for the surface mining systems. In this study, whether a group of three trucks picked randomly from the same model trucks working in open pit coal mine was identical or not was examined through a non-parametric statistical test for two independent samples. Then, in order to determine whether the trucks proven to be identical at the end of this test displayed the same performances or not, an availability analysis for the identical trucks was carried out. As a result of the availability analysis, it was observed that the randomly picked trucks displayed the same performances. It was also determined that non-parametric statistical test for two independent samples could be employed together with availability analysis.

ÖZET Açık ocak kömür madenlerinde kullanılan ekipmanlar genellikle yükleme ve nakliye ekipmanları olarak sınıflandırılırlar. Kamyonlar çoğunlukla açık ocak kömür madenlerinde nakliye ekipmanları olarak kullanılır. Açık ocak kömür madenlerinde çalışan benzer kamyonların özdeşliklerinin belirlenmesi açık ocak sistemlerinde oldukça önemlidir. Bu çalışmada açık ocak kömür madeninde çalışan aynı

model kamyonlardan rassal olarak seçilen üç kamyonun özdeş olup olmadıkları iki örneklemli parametrik olmayan istatistiksel test tekniği kullanılarak sınanmıştır. Bu test tekniği sonunda özdeş olduğu kanıtlanan kamyonların, benzer performansı gösterip göstermediğini belirlemek için özdeş kamyonların kullanılabilirlik analizi yapılmıştır. Kullanılabilirlik analizi sonucunda rassal olarak seçilen kamyonların aynı performansı gösterdiği gözlenmiştir. İki bağımsız örneklemli parametrik olmayan test tekniklerin kullanılabilirlik analizleri ile birlikte kullanımının uygun olacağı belirlenmiştir.

1 INTRODUCTION

A mine production system consists of many subsystems. The optimization of each subsystem in relation to one another is imperative to make the system profitable and viable for operation. Effectiveness of the mining equipment is mainly influenced by the availability, reliability and maintainability of the system, and its capability to perform as expected (Barabady and Kumar, 2008).

Availability appears to be a more appropriate measure than reliability for measuring the effectiveness of repairable machines because it also takes into consideration maintainability, another important aspect of a system's performance (Kumar, 1989). To determine the long term performance of a system that alternates between two capability states, up and down states according to some random process, one is often primarily concerned with the long run availability of the system (Ananda, 1999).

Although availability analysis is a common tool used other industries but this analysis is not so common in the mining industry. Some studies conducted in the mining industry using availability analysis are as follows:

Kumar et al., (1989), a comprehensive estimate of the operational reliability of load haul dump machines, located items or assemblies which needed an improved design to enhance the reliability.

Hosseini (1999) discussed the equipment reliability issue and addressed the need for the analysis of various performance measures through "what-if" examination of various business conditions and operation scenarios.

Samanta et al. (2004), presented the reliability, availability and maintainability of a load haul dumper machine with failure and repair data.

In this paper, the identicalness of three trucks belonging to time to failure (TTF) and time to repair (TTR) are examined using the Kolmogorov-Smirnov nonparametric test. Finally, the availabilities of three trucks are determined.

2 THE KOLMOGOROV-SMIRNOV TEST FOR TWO INDEPENDENT SAMPLES

The Kolmogorov-Smirnov test for two independent samples compares the cumulative probability distributions of two independent samples. If the two independent samples are derived from the same population, the two cumulative probability distributions would be expected to be identical. If there is a significant difference at

any point along the two cumulative probability distributions, the two independent samples would be expected to derive from different populations (Sheskin, 2000).

Sheskin (2000) showed that, for determination of relationship between the two independent samples, the Kolmogorov-Smirnov test for two independent samples should be sequentially followed as;

a. A cumulative probability distribution should be constructed for each of the two independent samples,
b. The test statistic (D_{max}) is defined by the point that presents the greatest vertical distance at any point between the two cumulative probability distributions.
c. The null (H_0) and alternative (H_1) hypotheses are derived.
d. The test statistic (D_{max}) is compared with critical value (D_α) in the Kolmogorov-Smirnov test for two independent samples table.
e. The test result is interpreted and decision making is realized.

The Kolmogorov-Smirnov test for two independent samples is used to determine whether two cumulative probability distributions are different or not. The first cumulative probability distribution for n_1 observations is defined as $F_1(x)$. The second cumulative probability distribution for n_2 observations is defined as $F_2(x)$. The test statistic of two cumulative probability distributions for any one of signs of positive or negative directions is given by (Ankara et. al., 2007; Yerel et. al., 2007);

$$D^{+}_{max} = \max(F_1(x) - F_2(x))$$

or

$$D^{-}_{max} = \max(F_2(x) - F_1(x))$$

The test statistic is obtained from the point that presents the greatest vertical distance at any point between two cumulative probability distributions. The test statistic based on the H_0 hypothesis claims that equality of two cumulative probability distributions is true. According to this assumption, the H_0 and H_1 hypotheses are established;

H_0: $F_1(x) = F_2(x)$

H_1: $F_1(x) \neq F_2(x)$

respectively. H_0 hypothesis claims that the two independent samples are almost the same because of equality of two cumulative probability distributions. H_1 hypothesis claims that two independent samples are quite different because of inequality of two cumulative probability distributions.

D_{max} is compared with D_α in the Kolmogorov-Smirnov test for two independent samples table. If D_{max} is less than D_α, H_0 hypothesis is accepted. In addition, D_{max} is equal or greater than D_α, H_0 hypothesis is rejected and H_1 hypothesis is accepted.

3 AVAILABILITY ANALYSIS

Failure rate and repair rate are the two significant parameters in availability analysis. Failure rate is represented by λ and repair rate by μ. These rates are defined as the number of the failures and the repairs per unit time.

λ is computed by dividing the mean time to failure (MTTF) by the unit time involved. Similarly, μ is computed by dividing the mean time to repair

(MTTR) by the unit time involved. In short, λ and μ are the reciprocals of MTTF and MTTR in the unit time, respectively (Ankara, 1997).

Availability of single equipment is given by Eq. 1.

$$A(t) = \frac{\mu}{\lambda+\mu} + \frac{\lambda}{\lambda+\mu} \times e^{-(\lambda+\mu)\times t} \quad (1)$$

4 CASE STUDY

In this paper, three 170-short-tonne trucks of the 10 trucks working overburden stripping in open pit coal mine were picked out randomly for the identicalness levels of trucks using in availability analysis. TTF and TTR data of these three trucks were monitored through computer system over one-year period. The data was first used for Kolmogorov-Smirnov nonparametric test and then for availability analysis.

Table 1. Failure rates and Repair rates for the trucks

Truck No	MTTF (mins.)	MTTR (mins.)	Failure rates (λ)	Repair rates (μ)
T1	6,745.28	1,037.64	0.000148	0.000964
T2	5,875.63	981.56	0.000170	0.001019
T3	5,129.74	1,261.41	0.000195	0.000793

Time To Failures (TTFs) and Time To Repairs (TTRs) were firstly tested with Kolmogorov-Smirnov test for two samples. By using Kolmogorov-Smirnov test, the identicalness levels of the trucks were examined in pairs. In order to determine the identicalness levels of T_1-T_2, T_1-T_3 and T_2-T_3 truck pairs, the following hypotheses were established.

The hypotheses for the TTFs of T_1-T_2, T_1-T_3 and T_2-T_3 truck pairs are;

H_0: Truck pair is identical in terms of the time to failures.

H_1: Truck pair is not identical in terms of the time to failures.

The hypotheses for the TTRs of T_1-T_2, T_1-T_3 and T_2-T_3 truck pairs are;

H_0: Truck pair is identical in terms of the time to repairs.

H_1: Truck pair is not identical in terms of the time to repairs.

As a result, it was determined in statistical terms that those three trucks were identical in terms of both TTFs and TTRs. Because those three trucks were identical according to Kolmogorov-Smirnov nonparametric test, the availability of the trucks should be identical as well.

The parameters needed for the availability analysis, TTF and TTR values, were calculated in MTTF and MTTR respectively. By using MTTF and MTTR, failure rates and repair rates for each truck were calculated and presented in Table 1.

When the availabilities of these trucks are calculated through Eq.1., the availability curves of the trucks were plotted as a function of the time. The availabilities of three trucks are very close and high, as seen in Figure 1.

It is clearly seen that the availabilities of these trucks are identical and efficiently support Kolmogorov-Smirnov non-

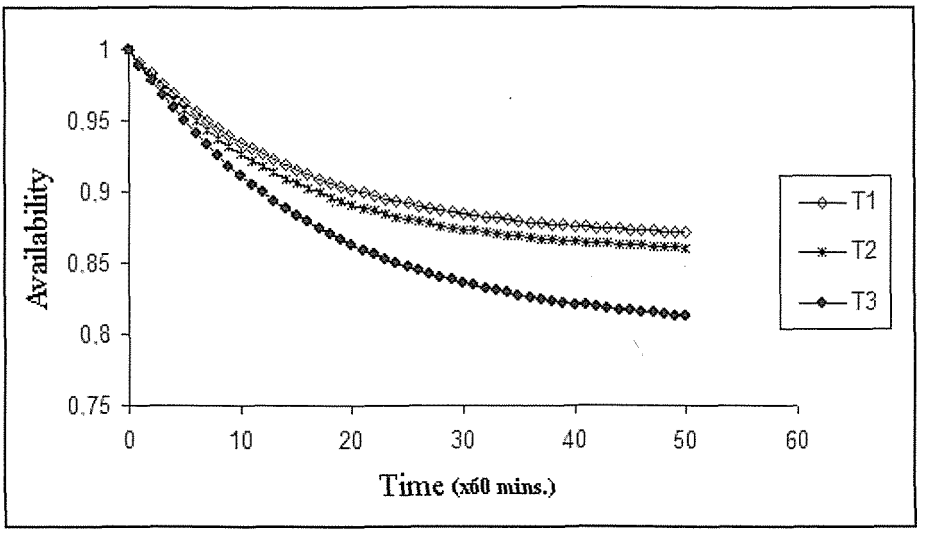

Figure 1. Curves of availabilities versus time.

parametric test. In order to put that more clearly, these trucks' steady state availabilities, that is their availabilities when t goes to infinity, were calculated as $T1 = 0.867$ (or 86.7%), $T2 = 0.857$ (or 85.7%) and $T3 = 0.803$ (or 80.3%) respectively.

4 CONCLUSIONS

In this paper, it was presented the identicalness levels of the same model three trucks working in open pit mines could be determined by using the Kolmogorov - Smirnov non-parametric test. After, these three trucks were applied availability analysis.

As a result of the availability analysis of the trucks determined to be performance was very high. In conclusion, it was determined that the Kolmogorov - Smirnov nonparametric test and availability analysis could be used as an efficient analysis technique for determining the identicalness levels of the same model equipments in open pit mines.

REFERENCES

Ananda, M.M.A., 1999. Estimation and testing of availability of a parallel system with exponential and repair times, *Journal of Statistical Planning and Inference*. 77, s. 237-246.

Ankara, H., 1997. *Availability Analysis for Truck-Shovel System in Surface Mining*, Ph. D. Thesis, Middle East Technical University, Turkey.

Ankara, H., Yerel, S ve Konuk, A., 2007, Açık Ocak Madenindeki Kamyonların Özdeşliklerinin İki Örnek Kolmogorov-Smirnov (K-S) Testi ile Belirlenmesi, *Fırat Üniv. Fen ve Müh. Bil. Dergisi*, 19(1), s. 105-108.

Barabady, J. And Kumar, U., 2008. Reliability analysis of mining equipment: A case study of a crushing plant at Jajarm Bauxite Mine in Iran, *Reliability Engineering & System Safety*, 93, s. 647-653.

Hosseini, M., 1999. Reliability revolution is a new shift in paradigm occurring?, *Canadian Mining Journal*. 120, s. 33-35.

Kumar, U., Klefsjö, B. and Granholm, S., 1989. Reliability investigation for a fleet of load haul dump machines in a Swedish Mine. *Reliability Engineering and System Safely*. 26, s. 341-361

Kumar, U., 1989. Availability studies of Load-Haul-Dump machines, P*roceedings of the 21st International Symposium on the Application of Computers and Operations Research in the Mineral Industry*, s. 323-335 , Las Vegas, USA.

Samanta, B., Sarkar, B. and Mukherjee, S.K., 2004. Reliability modeling and performance analyses of an LHD system in mining, *The Journal of the South African Institute of Mining and Metallurgy*. 104, s. 1-8.

Sheskin, D.J., 2000, *Handbook of Parametric and Nonparametric Statistical Procedures*, Second Edition, Chapmand and Hall/CRC, USA.

Yerel, S., Ankara, H., Konuk, A. and Ozdag, H., 2007. Preventive Maintenance Policy Supported by a Quality Control Chart and Kolmogorov-Smirnov Tests: Emet Colemanite Mineral Processing Plant, Turkey, *Minerals & Metallurgical Processing*, 24, s. 152-156.

Rock Mechanics

Estimation of Equivalent Permeability In Amirkabir Tunnel Alignment With Neural Network

A.Aalianvari, H.Katibeh,
Amirkabir University of Technology, Iran
H.Mahmoudabadi
Iran Mineral Production and Supply Co. (IMPASCO), Iran

ABSTRACT Groundwater flow into tunnels has always been a major technical problem in tunnel constructions, so it is very important to estimation of groundwater inflow into tunnel. There are a lot of parameters that relating to groundwater flow into tunnel such as permeability, RQD, joint frequency, joint aperture, porosity, head of water above tunnel and radius of tunnel. Permeability is very variable in tunnel alignment because of variation in geological conditions. Therefore, estimation of equivalent permeability is very necessary.

In this research with use of artificial neural network, equivalent permeability of Amirkabir tunnel is estimated. A number of boreholes was drilled, cored and hydraulically tested in the investigation stage. Records at the boreholes have been considered as the main source of facts for seepage calculations. The general variation of analytical and RBF neural network results along tunnel path line is alike, Average of permeability into tunnel is calculated around 1.3*10-7 to 1*10-5 m/Sec according to analytical and RBF neural network results respectively. Regarding results and general geologic considerations, seepage is concentrated at fault zones and crashed zones, and other geological conditions have not major problems.

1 INTRODUCTON

Groundwater control is a significant issue in most underground construction. An estimate of the inflow rate is required to size the pumping system, and treatment plant facilities for construction planning and cost assessment. An estimate of the excavation-induced drawdown of the initial groundwater level is required to evaluate potential environmental impacts. The groundwater inflow during excavation can cause serious instability of tunnel roof and walls as well as ground settlement due to ground losses or consolidation of soft overburden deposits. It can also cause flooding inside the tunnel, construction difficult, and ultimately abandonment of tunnel. It is not possible to accurately predict water flow into rock tunnels during construction, because all of the relevant factors cannot be accurately determined

ahead of time. There currently is no simple, generally accepted method of estimating inflow. Although there is no generally accepted solution for estimating the rate of inflow into a tunnel in a jointed rock mass, current practice relies mostly on analytical solutions, which assume a homogeneous, isotropic porous medium around the tunnel. Generally, results from field packer tests are used to provide representative hydraulic conductivity values for the analytical model. Table 1 contains a listing of analytical equations of the water inflow.

Table 1 Analytical equation for groundwater inflow into tunnel

Equation	Method	ID
$Q = 2\pi K \frac{h}{\ln(\frac{2z}{r})}$	**Goodman(1965)**	1
$Q = 2\pi K \frac{h}{\ln(\frac{2h}{r} - 1)}$	**Karlsruod(2001)**	2
$Q = 2\pi K \frac{h}{\ln(\frac{h}{r} + \sqrt{(\frac{h}{r})^2 - 1})}$	**Lei (1999)**	3
$Q = 2\pi K \frac{1 - 3(\frac{r}{2h})^2}{[1 - (\frac{r}{2h})^2]\ln(\frac{2h}{r} - (\frac{r}{2h})^2}$	**El Tani-1(1999)**	4
$Q = 2\pi K \frac{\lambda^2 - 1}{\lambda^2 + 1} \frac{h}{\ln \lambda}$ & $\lambda = \frac{h}{r} - \sqrt{\frac{h^2}{r^2} - 1}$	**El Tani-2(2001)**	5

Where Q is the groundwater flow, h is the head of water above the tunnel, z is the overburden thickness, K is the equivalent permeability and r is the radius of tunnel. Fig 1 shows the parameter regulation in these equations.

As discussed above, the most important factor influencing water inflow is rock mass permeability, since its potential variability is so much greater than that the other factors. Permeability of a rock mass fracture system can vary widely between different rock

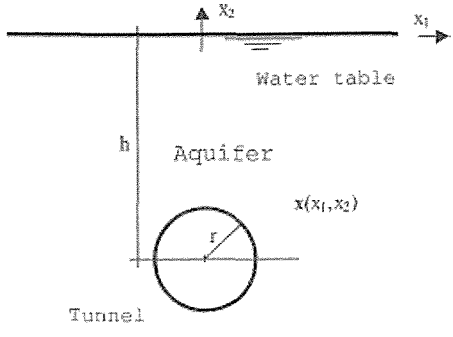

Figure 1: Circular tunnel in a semi-infinite aquifer with a horizontal water table.

formations, and even from place to place within a given formation along a tunnel line. Possibly the most accurate way to measure, the mass permeability at a specific location is a full-scale pump test. This may be done with a central, pumped deep well, surrounded by an array of piezometers. It may be done by isolating portions of an individual well, making detailed measure of head decrease versus time during pumping. Pump tests are of limited use for rock tunnels because they are expensive, and are meaningful only at the specific test site, the most common method is a double packer water pressure test conducted in a normal exploratory core boring. Geological features have very important roles in location of packer test in site. The actual water inflow into tunnel in a jointed rock mass is often significantly lower than the predicted water inflow using equivalent permeability from packer tests.

Water inflow can be often dominated by distinct geological features (i.e. shear, fault, or shatter zone) which might not be intersected by conventional packer intervals. The presence of distinct geological features with high hydraulic conductivity in the vicinity of the tunnel can result in large water inflows and the anisotropic, large hydraulic conductivity resulting from these features would not be included in analytical solution. Therefore, it is very important that to estimate the actual rock permeability to estimate groundwater inflow into tunnels. In this research groundwater, flow into Amirkabir tunnel has been estimated with neural network.

The 30 Km water conveying tunnel, named Amirkabir is supposed to be drilled in Alborz mountain range in Iran. The area under study is located in Karaj formation consisting of complex sedimentary and volcanic rocks such as monzodiorite, gabro, tuff, sandstone and conglomerate limestone. In the geological point of view, the tunnel crosses three geologic units as GTA1, (monzodiorite, gabro), GTA2, (sandstone, tuff) and GTA3, (massive conglomerate, green tuff, massive limestone). Attention to geological condition of tunnel alignment, design 12 lugeon test borhole in different distance. It is judged not useful to attempt to calculate an average equivalent permeability of the rock mass. To do so mask the significance of the rock mass variability, and the variability of inflow, which can be expected from place to place in the tunnel, Instead, the equivalent permeability results are presented in a histogram. The histogram would not be restricted only to tests near tunnel level, unless there is reason to believe tests at different elevations are not representative of what the tunnel might encounter. For example, if the boring test results show occasional high permeability values close to top of rock in an apparent zone of near surface weathering effects, those occasional high values should not be counted unless the tunnel is shallow and may encounter such zones. Otherwise, all tests for the entire boring depth below the natural ground water level in the formation of interest are considered.

If the entire tunnel is in one rock formation, or in formations of similar nature,

All test data from the entire tunnel length would be plotted on one histogram. The variation in test results is assumed to represent a random, statistical sampling of mass permeability at various points in the mass. It is assumed that a tunnel driven through this mass will experience the same percentages of its length in different ranges of permeability, as did the exploratory borings.

Most research on the application of neural networks aims to improve estimation for problems that are not clearly understood using physically based methods. The physical relations among input and output variables are not considered after spatial modeling. In contrast, sensitivity analysis on neural networks specifies the factors that characterize spatial distributions of geologic values such as joint aperture, joint roughness, etc. The analysis quantifies influence magnitudes of geologic factors, which include lithology, lugeon value , and discontinuities, on the spatial patterns identified by the neural network.

Because of special geometry of the place and limited data, we are not able to predict actual groundwater inflow into tunnel with general equitions (table 1). Therefore, in this study neural network method is used to estimate the equivalent permeability to predict groundwater inflow into Amirkabir tunnel. A redial basis function neural networks with one input layer, one hidden layer and one output layer are employed for this goal. Coordination of each sample is considered as input data set while their corresponding lugeon tests are used as output data set. Number of hidden layer neurons is obtained using trial and error technique. Finally, the results of these methods were compared.

1.1 Research procedure

In this research work, according to an exact study of the geological and hydrogeologic features of Amirkabir tunnel, used results of packer test to estimate equivalent permeability with neural networks. According to packer test along tunnel alignment, assumed that study area is 2-D that X axis is along tunnel and location of packer tests(local coordinate), and vertical axis is the elevation of hole from sea. We use Eq.1 to estimate lugen value for any point of tunnel alignment.

$$h = \frac{u - l}{2} \qquad (1)$$

Where u is distance of upper packer from hole and l is the lower packer from hole, after that coordinate of points that lugeon is estimated, calculated from Eq.2:

Z=Zi-h

Where Zi is borehole elevation from free sea.

1.2 Radial Basis Function Neural Network (RBF)

Radial basis functions (RBF) are designed to find a surface in a multidimensional space that provides a best fit to the training data

They have found to be very attractive for many engineering problems because: (1) they are universal approximators, (2) they have a very compact topology, (3) their learning speed is very high because of their locally tuned neurons. The RBF neural network has a feed forward architecture with an input layer, a hidden layer and an output layer.

The first layer consists of n inputs. They are fully connected to the neurons in the second layer. Radial basis networks perform non-linear mapping from the input space to the hidden layer (radial basis layer), in most kind of these networks applications, and the hidden space is multidimensional. The output layer is linear mapping from the hidden layer to the output space (linear layer), providing the network's response to the presented vectors at the input layer. Since the output is a linear function of

unknown weights, they can be computed easily by simply a matrix inversion. Hence, it largely reduces the computation time during training phase.

In this structure, hidden nodes are named RBF units. These in turn are fully connected to the output layer units.

The activation function of the RBF units is expressed as following:

$$R_i(X) = R_i(-d_i^2(X) \quad , \quad i = 1,2,...,s \qquad (10)$$

$$d_i(X) = \frac{\|X - C_i\|}{s_i} \qquad (11)$$

Where $d_i(X)$ is called the distance function of the i-th RBF unit, $X=(x_1,x_2,\ldots,x_n)^T$ is an n-dimensional input feature vector, C_i is an n-dimensional vector called the center of the i-th RBF unit, σ_i is the width of i-th RBF unit and s is the number of the RBF units. Typically, the activation of the RBF units is chosen as a Gaussian function:

$$R_i(X) = \exp[-d_i^2(X)]$$

The output units are linear and therefore the response of the j-th output unit for input X is given as:

$$y_j(X) = b(j) + \sum_{i=1}^{s} R_i(X) W_2(j,i)$$

Where $W_2(j,i)$ is

the connection weight of the i-th RBF unit to the j-th output node and $b(j)$ is the bias of the j-th output .

The bias is omitted in this network in order to reduce network complexity. Therefore:

$$y_j(X) = \sum_{i=1}^{s} R_i(X) W_2(j,i) \qquad (14)$$

The general equations which describe this network are

$$a(1) = f(1)(||W(1) - p||b(1))$$

$$a(2) = f(2)(W(2)a(1) + b(2))$$

where $f(1)(n) = e-n2$ and $f(2)(n) = n$. The bias $b1$ determines the width of the area in the input space to which each neuron responds by using a constant called spread

$$b^1 = \frac{(-\log(0.5))^{0.5}}{spread}$$

Too large a spread means a lot of neurons will be required to fit a fast changing function. Too small a spread means many neurons will be required to fit a smooth function, and the network may not generalize well. It is important to make sure that the spread is large enough such that the network can generalize well. The lager the spread is, the smoother the network will be. In the radial basis functions (*RBF*), the number of neurons is determined according to the value of the sum squared error of the training set. The input layer connects the RBF network to the input vector space.

The nature and the magnitude of the output emerging from the basis functions usually depends upon two factors (i) the type of basis function used, and (ii) the relative distance between the input data space to radial basis function centers.

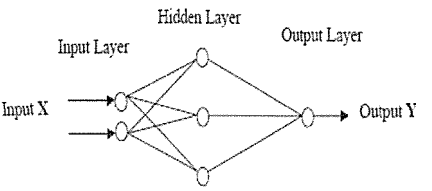

Figure 2. RBF neural network structure [21]

The last estimation of connection weights is to determine the strength of a network. Usually the connection weights are adjusted through a process termed training by introducing a set of known input-output patterns to the network such that final weights produce outputs, which are close to actual outputs. Through the process of training, a network learns general properties of the input-

output relationship of a system, and thus generalizes beyond training data points (training data set). Performance evaluation of the models was carried out on the test data set. The generalization of a model might be guaranteed by comparing predicted values with the actual values at some known locations. Therefore, it is a typical practice to keep aside some data for model testing, while using the rest for model training. In preparing training and test data sets, sample members usually are selected at random and put into one of the data subsets. Detailed discussions of neural network are given in the literature [22].

For this purpose, the entire data set is divided into training and test data sets. Here, 75% of samples are considered for training, and the remaining 25% are considered as test data set. Before presenting the data to the network, all the input and the output variables were normalized in two ways. At first all coordinates and lugeon test results, equivalent permeability input values were normalized within the range of 0–1 by their minima and maxima. In the other way input values were normalized within the range of [-1 1]. Two databases were made from these normalized ways.

This paper proposes a sensitivity analysis method of a trained neural network by selecting spatial distributions of the groundwater inflow into tunnel(Q) in the Amirkabir tunnel in Iran, as a case study.

Sensitivity analysis of the neural network was carried out to identify factors influencing spatial distributions of the groundwater inflow into tunnel(Q).

Let a function y D f (x1, x2, : : : , xn) be an output from a system for inputs (x1, x2, : : : , xn). Coordinates, equivalent permeability, lugeon test results, joint parameters such as aperture, roughness, persistence and specific lithology were determined to be influencing factors. Sensitivity analysis is aimed at detecting the influence factors that affect the distributions of Q. In general, sensitivity means the relative change on the output with a small change of xi. It is useful to clarify the significance of the input variable on output.

Throw the all parameters, sensitivity analysis show that X, Z and lugeon value are more influencing factors. Different networks created with various values of spread and number of neurons of the hidden layer. These networks train for all categories and results are shown in tables 2, 3. and figures 3,4,5,6.

2 CONCLUSION

As shown in Table 2 and Figure 3, the results are presented for all networks in

Table 2, The results of the networks with database between 0 to 1

ID	Number of hidden layer's neurons	Spread	MSE of training data set	MSE of test data set
RBF1	38	0.1	0.014	5.252
RBF2	37	0.3	0.059	0.480
RBF3	37	0.8	0.147	0.307
RBF4	40	0.08	0.0117	2.345
RBF5	10	0.01	0.08	1.524
RBF6	5	0.05	0.145	1.503
RBF7	12	0.5	0.128	0.467

Table 3, The results of the networks with database between -1 to 1

ID	Number of hidden layer's neurons	Spread	MSE of training data set	MSE of test data set
RBF11	38	0.1	0.23	2.426
RBF22	37	0.3	0.102	7.693
RBF33	37	0.8	0.365	3.217
RBF44	40	0.08	0.23	1.451
RBF55	30	0.2	0.129	5.917
RBF66	37	0.02	0.34	0.144

case of database between 0 to 1. Although the MSE error of the training set is decreased by increasing the number of neurons, the MSE error of the test data is increased. Results shown that networks RBF3 and RBF7 have the maximum MSE of training data set. In addition, RBF1 and RBF3 have minimum MSE of training set and the maximum MSE of test data set, therefore it maybe happen overtraining.

According to the results the performance of RBF2 is more than the other networks in database between 0 to 1.

As shown in Table 3 and Figure 4, with the increase of the spread, the error of the test set is improved for the networks and then decrease, Viceversa with the increase of the spread the error of the test set is decrease and then increase. Table 2, 3 show that networks with database between -1 to 1 performance better than other database. The results show that the network with spread value 12 performs better than other RBF networks too. Therefore, it is preferred to use RBF66 network for estimation of equivalent permeability of Amirkabir tunnel.

According to RBF66 network results variation of permeability along Amirkabir tunnel alignment has been estimated. Results shown that range of permeability along tunnel variated from 7-10*3/1 to 5-10*1m/sec. So it is not dangerous for tunnel construction, but according to geological maps, there are main faults in tunnel alignment that make a wide crashed zone, therefore these zones are very dangerous, results

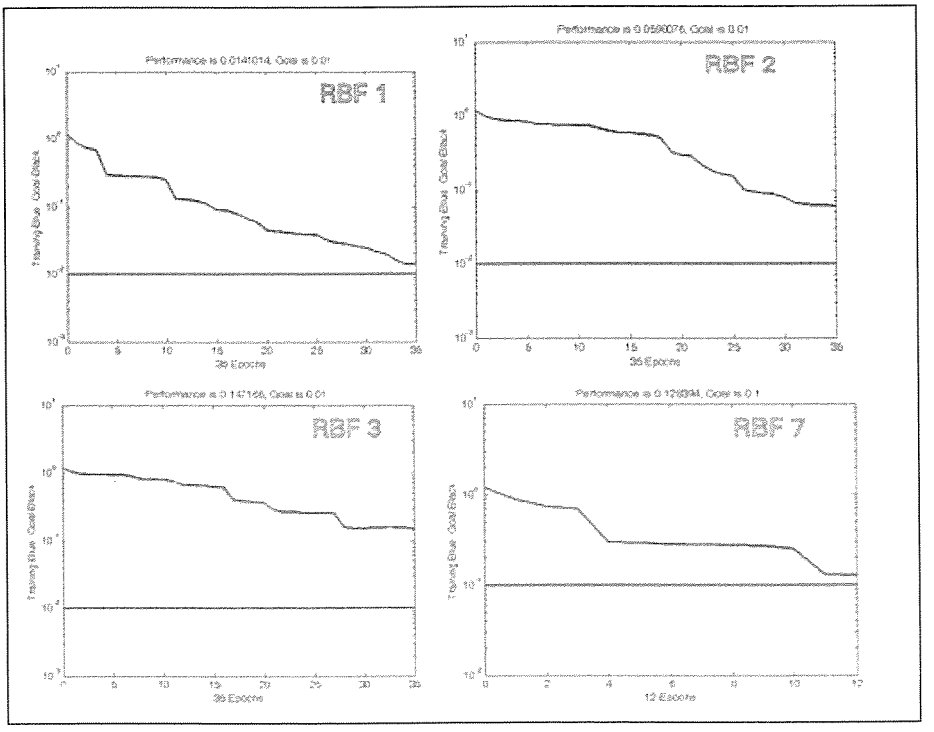

Figure 3. Diagrams of training the networks (a) RBF1, (b) RBF2, (c) RBF3, (d) RBF5, (e) RBF6 and (f) RBF7 for database between 0 to 1

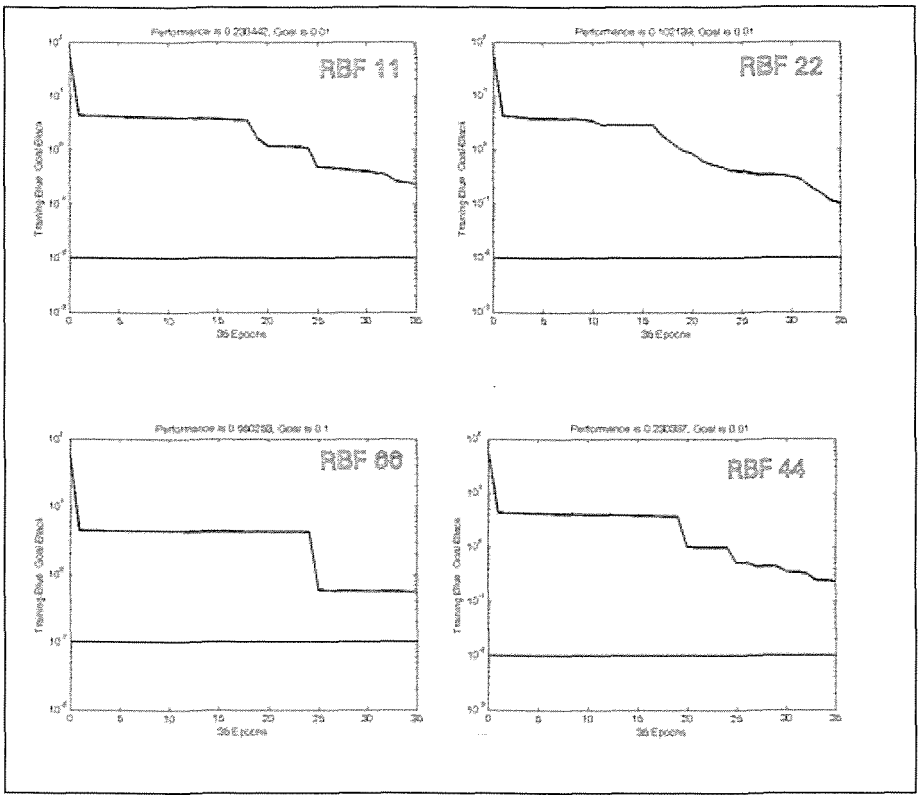

Figure 4. Diagrams of training the networks (a) RBF11, (b) RBF22, (c) RBF33, (d) RBF44, (e) RBF55 and (f) RBF66 for database between -1 to 1

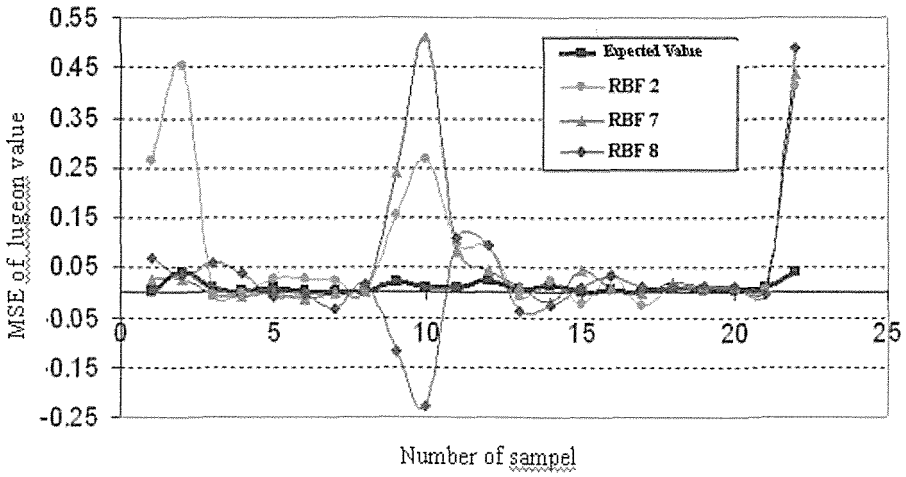

Figure 5. MSE of lugeon value number on samples for database between 0 to 1

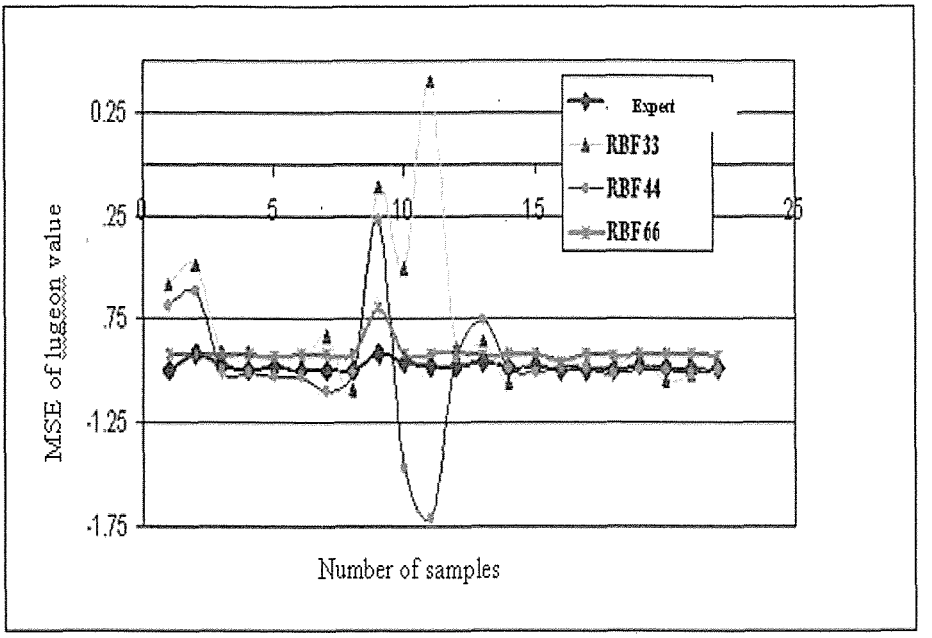

Figure 6. MSE of lugeon value number on samples for database between -1 to 1

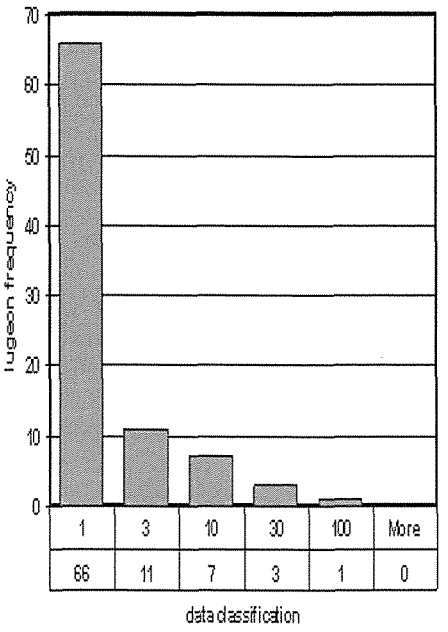

Figure 7. lugeon results along Amirkabir tunnel

of permeability variation from analytical equations are shown in fig 5.

3 SUMMARY

In this paper, neural networks and analytical equations were investigated for estimation of groundwater inflow into Amirkabir tunnel.

The modeling of tunnel alignment was complicated because of the geological condition of area. Two neural network models: RBF1 and RBF2 were trained separately using training data. Training was stopped when a model reached the minimum mean squared error in the validation data. The performance evaluation of the models was done on the test data.

The results indicated that the neural network (RBF) have acceptable predictions for equivalent permeability.

Results show that permeability variated from $1.3*10^{-7}$ to $1*10^{-5}$ m/sec, Regarding results and general geologic considerations, seepage is concentrated at fault zones and crashed zones, and other geological conditions have not major problems

REFERENCES

Bandis, S.C., Lumsden,A.C. and Barton, N.R., 1983. Experimental studies of scale effects on the shear behavior of rock joints. Int. J. of Rock Mechanics & Min. Sci., Abstracts, Vol. 18, 1-21.

Barton, N. 1997 Joint aperture and roughness in the prediction of flow and groutability of rock masses. Int. J. of Rock Mechanics & Min. Sci., Vol. 34.

El Tani, Mohamed., 2003. Circular tunnel in a semi-infinite aquifer. Tunneling and Underground Space Technology, 18 , 49–55.

El Tani, M., 1999. Water inflow into tunnels. Proceedings of the World Tunnel Congress ITA-AITES 1999, Oslo, pp. 61–70, Balkema.

Goodman, R.E., Moye, D.G., Van Schalkwyk, A., Javandel, I., 1965. Ground water inflows during tunnel driving. Bull. Ass. Eng. Geologists 2, 35–56.

Karlsrud, K., 2001. Water control when tunnelling under urban areas in the Olso region. NFF publication No. 12, 4, 27–33, NFF.

Lei, S., 1999. An analytical solution for steady flow into a tunnel. Ground Water 37, 23–26.

Priest, S., 1993. Discontinuity analysis for rock engineering", Published by Chapman& Hall, first edition.

Zhang, L. and Franklin, J.A. 1993. Prediction of Water Flow into Rock Tunnels: an Analytical Solution Assuming a Hydraulic Conductivity Gradient, Int. J. of Rock Mechanics & Min. Sci., Abstract, Vol. 30, 37-46.

S.Haykin, "Neural Networks:A Comprehensive Foundation" ,Mcmillan College Publishing Company , Canada,1994.

Bishop, C. M., 1995, Neural networks for pattern recognition: Clarendon Press, Oxford, 482 p

Hagan, M. T., Demuth, H. B., and Beale, M., 1996, Neural network design: PWS Publishing Company, Boston, 19 chapters.

H. Mahmoudabadi, M. Izadi, M.B. Menhaj, "A new hybrid method for grade estimation using genetic algorithm and neural networks", computational geoscience, in press.

Ultrasonic Evaluation of Igneous and Metamorphic rocks under Compressive Loading

Murat Karakus
The University of Adelaide, School of Civil, Environmental & Mining Engineering, Adelaide, SA, Australia
Bülent Tütmez
Inonu University, School of Engineering, Mining Engineering Department, Malatya, Turkey
Devkan Kaleci
Inonu University, Faculty of Science and Art, Department of Physics, Malatya, Turkey
Corresponding author: murat.karakus@adelaide.edu.au

ABSTRACT This research aims to assess deformability characteristics of extrusive volcanic and metamorphic rocks under compressive loading using ultrasonic wave propagation technique. An experimental methodology developed in house was used to measure applied load, resultant strain, P and S wave velocities along with maximum amplitudes simultaneously. Wave velocities were measured perpendicular to the compressional axis using pairs of receivers' lead-zirconate piezoceramic transducers (PZT) which are specifically designed for use in geological testing. PUNDIT instrument was used to generate low frequency ultrasonic pulses. According to the results, a non-linear relationship between velocities and stress level that rock specimens have undergone were found. Increase in velocities is closely related to closure of void spaces in the specimens. Rate of velocity increments was also found to be greatest at the early stress level. As a result, ultrasonic velocities can be used to detect high stress concentrations and to monitor stress level in the underground structures.

1 INTRODUCTION

Ultrasonic velocity techniques have been widely used in rock mechanics due to its overwhelming advantages over conventional testing. The mechanical and physical properties of rocks can be determined with ultrasonic techniques. Ultrasonic waves can penetrate solid materials. Because of the fact that ultrasonic velocities are much slower than electromagnetic waves, more information can be obtained about

materials in time. In the field of rock mechanics, the ultrasonic pulse velocity has also been suggested as a useful method for estimation of the elastic and the strength properties of rocks (Vasconcelo, 2008).

Recently there have been a large number of non destructive researches carried out to determine mechanical and physical properties of materials. Shkolnik et al. (2003) and Akkaya et al. (2003) used non destructive testing to evaluate strength of concretes. Balcı et al. (1998) carried out ultrasonic velocity tests to calculate the static (E_{st}) and the dynamic (E_d) elastic properties of some rocks and they concluded that there is no apparent correlation between static and dynamic elastic properties of rocks. Contrary to this result, Karakus et al. (2008) suggested that there is a good relation between dynamic and elastic properties. Starzec (1999) studied dynamic elastic properties of 300 crystalline rocks and pointed out that there is a strong relationship in between P-wave velocity and density as long as in between static and dynamic elastic properties of rocks which supports findings of Karakus et al. (2008). Mashinskii (2002) examined effects micro cracks and micro plasticity of rocks on dynamic and elastic properties. He observed that there are effects of visco-elasticity and micro-plasticity on static and dynamic elastic constants. Couvreur et al. (2001) studied crack initiation in limestone using ultrasonic wave propagation and reported that P&S-wave signals improve the understanding of the damage process and objectively define the successive steps of the deformational behaviour up to failure. A combination of various ultrasonic parameters (velocity, energy and quality factor of both P&S-waves) is therefore required. Strain, velocity and quality factor of P- as well as S-waves indicate the end of the crack closure phase, which is probably related to the original in situ state of stress. Ciccotti and Mulargia (2004) investigated a compact homogeneous mudstone-limestone in Italian Alpenian. They showed that P-wave velocity is increasing approximately from 1000 to 4500 m/s second with depth, which is significantly lower than the laboratory measurement of 6200 m/s concluding a severe state of cracking and damage of Calcare Massiccio near the surface of the quarry.

Dodds et al (2007) performed a series of experimental and theoretical rock physics on sandstones, shale and artificial sandstones under a range of controlled stress conditions. They reported that velocity and elastic constants increase as a function of mean effective stress in Muderong Shale as a result of porosity loss and crack closure. In addition, they reported that the v_P/v_S ratio is pressure history dependant.

Meglis et al. (2005) studied damage induced during excavation of a test tunnel in granite using ultrasonic wave velocity and amplitude. Sixteen 1-m deep boreholes drilled into the tunnel wall and transducers were installed inside the boreholes. It was reported that velocities are generally lowest in the sidewall in which tensile stresses are large whereas velocities are highest at the tunnel crown where compressive stresses induced.

Fortin et al. (2005) investigated ultrasonic velocity properties of

Bleurswiller sandstone under triaxial stresses. They reported that P&S wave velocities increase up to the onset of cataclastic dilatancy. After this point there is a drastic decrease in velocities pointing out the damage effects.

In this study, basalt and marble specimens were subjected to ultrasonic test while axially loaded. In section 2, experimental work and methodology adopted were explained in details. In section 3, results were presented and relations amongst the velocities, amplitudes and stress-strain were discussed. Conclusions and recommendations for the future works were included in section 4.

2 EXPERIMENTAL SETUP

NX (54 mm) sized core specimens drilled from the same rock blocks, which were collected in Malatya region, were used in all tests. Specimens were trimmed and their both ends flattened according to ISRM suggested methods. Physical properties of rocks such as dry and saturated densities, effective porosity were determined and are summarised in Table 1 (ISRM, 1977).

Testing methodology developed in house at the Mining Engineering Department, Inonu University is shown in Figures 1 and 2 where deformabilities, ultrasonic velocities and amplitudes of rocks were measured simultaneously. FLA-10-11 product of TML strain gauges with 120±0.3Ω gauge resistance attached to the surface of rock specimens were used to measure lateral and axial strain. P&S wave velocities were measured perpendicular to the compressional axis using pairs of source receivers lead-zirconate piezoceramic transducers (PZT). They are specifically designed for use in geological testing and compression rigs in particular. The housing is of stainless steel and can withstand a load of 220kN (22 tons) maximum.

Transducers have 1 MHz resonance frequency and are specifically designed for testing sedimentary, metamorphic and igneous rocks. However, it should be noted that igneous rocks may exhibit dynamic brittle failure and thus compressive load should not exceed the 60 % of the expected ultimate failure load.

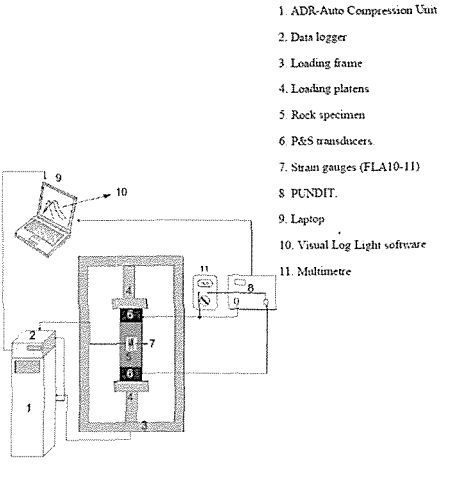

Figure 1. Schematic view of testing method

Strain gauges attached to the surface of the specimens were connected with Wheatstone full bridge. Axial strain and lateral strain were measured and visualised with Visual Log Light® software using RS232C connection between data logger and laptop. Therefore, sample reactions to compressive loading were

observed simultaneously and failure point were traced before specimens were fully broken. This enabled us to stop loading as to prevent any damages to transducers. Travel time of Pulse and Shear waves were measured with PUNDIT and amplitudes were measured with multimeter attached to the PUNDIT instrument.

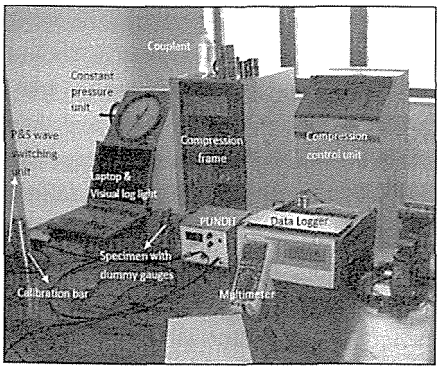

Figure 2. A view from the experimental setup

P-waves can travel through gases, liquids and elastic solids. On the other hand S-waves travel only in solids as the liquids does not support shear waves. Polarisation of P-waves in isotropic and homogeneous solids is always longitudinal. Velocity of P-waves can be calculated using the Equation 1.

$$v_P = \sqrt{\frac{K + \frac{4}{3}G}{\rho}} \text{ (km/s)} \qquad (1)$$

Where K is bulk modulus, G is the modulus of rigidity and ρ (g/cm^3) is the density of materials.

Velocity of S-waves can be calculated as:

$$v_S = \sqrt{\frac{G}{\rho}} \text{ (km/s)} \qquad (2)$$

3 RESULTS AND DISCUSSION

Excitation voltage and pulse repetition frequency (PRF) were set to 500 V and 100 pulse per second (pps) respectively in all the tests. Physical and ultrasonic properties along with the static and dynamic elastic properties of the rocks are given in Table 1. The dynamic elastic properties of rocks were calculated according to the Equation 3.

$$E_d = \rho v_S^2 \left(\frac{3v_P^2 - 4v_S^2}{v_P^2 - v_S^2} \right) \qquad (3)$$

Where;

v_P: P-wave velocity - km/s

v_S: S-wave velocity - km/s

ρ : Density - g/cm^3

E_d: Dynamic elasticity modulus – GPa

As the velocities of the rocks can change during loading, initial velocities were used to calculate the dynamic properties of the rocks. The static elasticity properties of the rocks based on the uniaxial deformability test suggested by ISRM (1978) were determined for each rock specimens for the comparison purposes. The ratios for E_d/E_{st} varied between 4.2 to 4.9 for basalts. On the other hand, the ratios of E_d/E_{st} were found to be in between 3.1 ile 4.5 for marbles.

Ultrasonic waves cannot travel through large air gaps and thus closure of void spaces led to increase in velocities for both marbles and basalts.

Table 1. Physical, elastic and ultrasonic properties of rocks.

	Rock ID	ρ_{sat}, g/cm^3	ρ_{dry}, g/cm^3	Porosity (n), %	V_P, km/s	V_S, km/s	E_s, GPa	ν	E_d, GPa	E_d/E_s
BASALT	B1	2.72	2.72	0.27	6.39	4.80	25.2	0.27	106.8	4.2
	B2	2.72	2.71	0.31	6.37	4.79	21.5	0.25	105.9	4.9
	B3	2.71	2.71	0.35	6.36	4.76	25.3	0.27	106.1	4.2
	B4	2.72	2.72	0.40	6.31	4.73	24.6	0.27	104.5	4.2
	B5	2.71	2.71	0.26	6.38	4.81	23.7	0.27	105.4	4.4
	B6	2.71	2.71	0.22	6.39	4.84	24.5	0.29	104.8	4.3
	B7	2.72	2.71	0.30	6.38	4.55	24.6	0.26	110.1	4.5
	B8	2.71	2.71	0.29	6.37	4.68	25.5	0.28	108.4	4.3
MARBLE	L1	2.74	2.71	3.48	5.79	4.50	20.2	0.23	81.2	4.0
	L2	2.72	2.68	4.26	5.68	4.41	20.1	0.24	77.5	3.9
	L3	2.73	2.69	4.32	5.61	4.42	19.1	0.24	72.2	3.8
	L4	2.71	2.66	4.28	5.70	4.25	18.6	0.2	83.9	4.5
	L5	2.74	2.71	3.49	5.79	4.53	23.3	0.26	79.1	3.4
	L6	2.72	2.67	4.81	5.60	3.92	18.8	0.2	83.7	4.5
	L7	2.70	2.65	4.61	5.61	4.37	19.5	0.24	73.9	3.8
	L8	2.74	2.71	3.74	5.65	4.12	21.4	0.23	85.7	4.0
	L9	2.74	2.70	3.55	5.85	4.61	25	0.25	78.1	3.1

Approximately 0.5-1% increase in the P-wave velocities was detected for basalts due to the low porosity content. Nevertheless, marble specimens reflected a non-linear increase in the P-wave velocities which were ranged from 6.1 to 9.9 per cent. For the basalt specimens 1.6-3.3 % increase detected

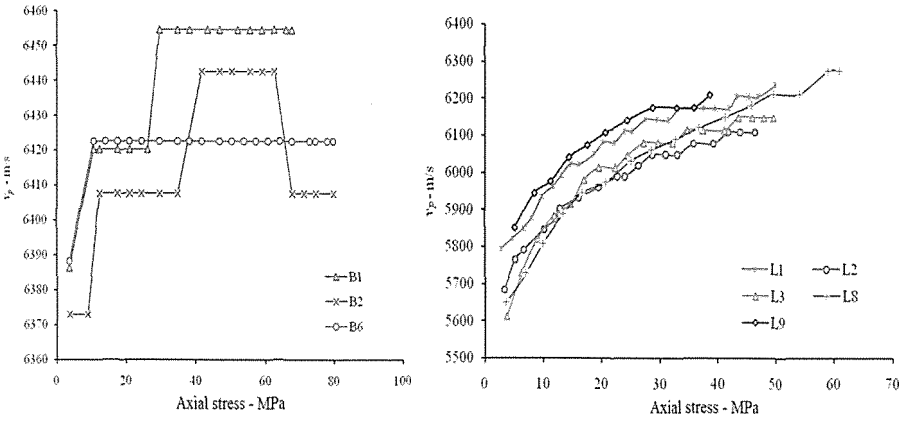

Figure 4. P-wave velocities and axial stress relations for basalts and marbles

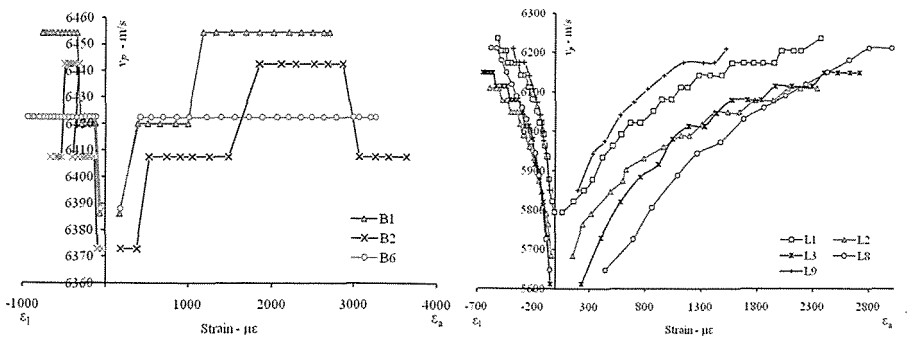

Figure 5. P wave velocities and strain relations for basalts and marbles

in S-wave velocities whereas 8.5-26.5% increase were observed for marbles.

According to the results maximum and minimum v_P/v_S ratios are found to be approximately 1.3-1.4 for basalts and 1.25-1.43 for marbles. A_P/A_S ratios for basalts and marbles are 1.5-1.9 and 1.1-1.4 respectively.

As can bee seen from Figures 4 and 5, P-wave velocities increase non-linearly for marbles as stress increases. However, basalts did not show any significant increase in P-wave velocities. Similar observations were found for strain for basalts. Figure 6 and 7 illustrates the S-wave velocities in relation to stress and strain. A logarithmic relation between S-wave velocities and stress can be seen clearly for marbles in Figures 6 and 7. Hence, both P and S wave velocities would be used to indentify the deformations and damages in the rock materials.

In terms of the amplitudes, A_P increased sharply reaching to a peak value at the early stress level and then decreased to the initial level until failure for basalts as shown in Figure

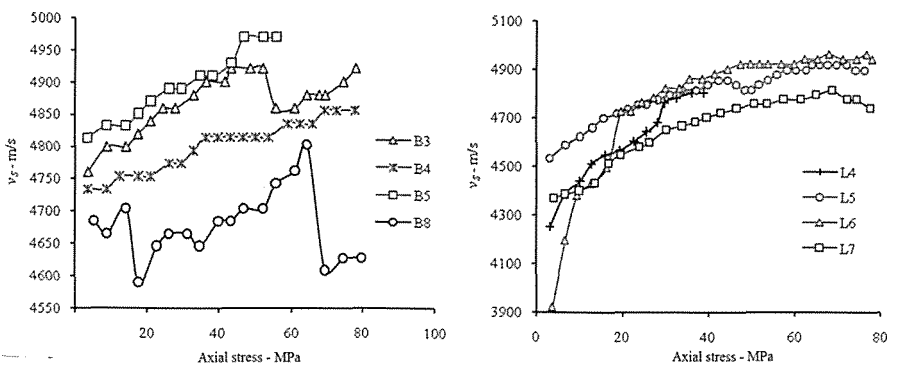

Figure 6. S-wave velocities and axial stress relations for basalts and marbles

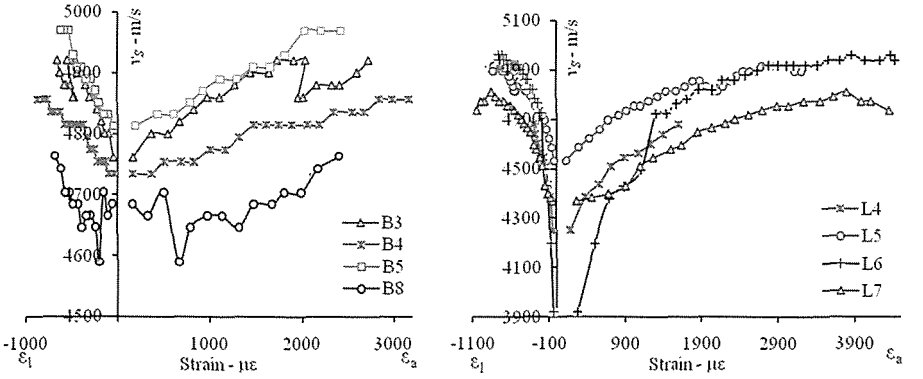

Figure 7. S-wave velocities and strain relations for basalt and marbles

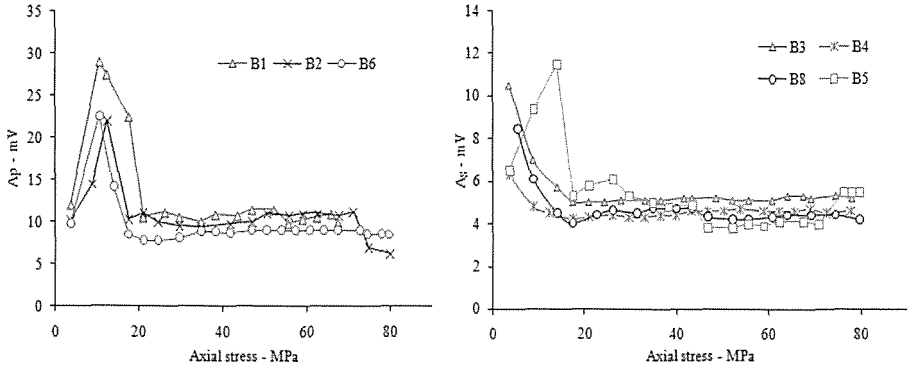

Figure 8. P and S wave amplitudes for basalts

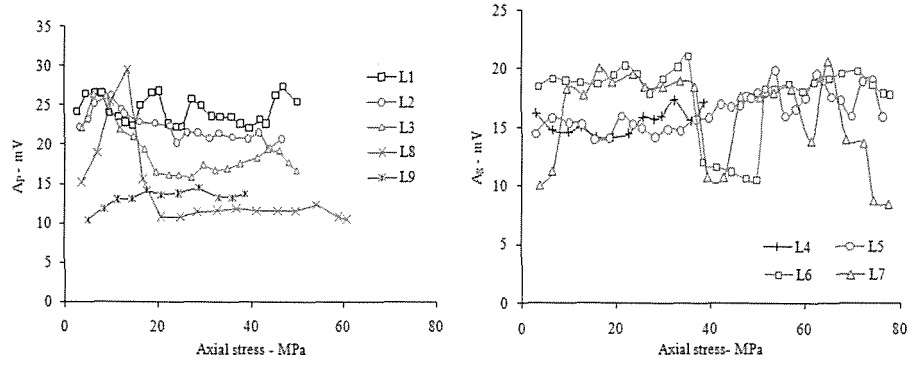

Figure 9. P and S wave amplitudes for marbles

8. On the other hand, A_P and A_S values were fluctuating for marbles. It is believed that the closure of the voids due to the stress increments caused reduction in reflections, ratio of energy sent back from a surface to the total energy striking the surface and thus this led to sudden boost in amplitudes for basalts.

4 CONCLUSIONS AND RECOMMENDATIONS

Following conclusions and suggestions summarize the present research:

P and S velocities are found to be strongly related to the stress and strain level that rock specimens were subjected. S wave velocity was found to be much more sensitive to the loading. Therefore it is recommended that use of S velocities along with P velocities can be more efficient for detecting stresses and damages in the rocks.

A strong logarithmic relation between velocities and stresses for marbles were observed. However, similar relation was not detected for the basalts as they contained low porosity. Bearing this point in mind, rocks with high void contents can exhibit this type of logarithmic correlation. However, further researches need to be carried out to verify this postulate.

As a future study, it is suggested that an integrated system containing ultrasonic waves, acoustic emission and electromagnetic waves can be developed to identify crack damages and stress level during mining operations. Hence, excavation damaged zones and critical regions around underground openings can be determined directly.

ACKNOWLEDGEMENT

Technological and Research Council of Turkey (TUBITAK) is gratefully acknowledged for the financial support during this project (107M413).

REFERENCES

Akkaya Y, Voight T, Subramaniam KV, Shah SP. 2003. Nondestructive measurement of concrete strength gain by ultrasonic wave reflection method. Materials and Structures. 36(8): 1-10.

Balcı C, Avşar S, Özbakır O, 1998. Bazı kayaçların dinamik ve elastik modüllerinin karşılaştırılması, 4. Ulusal Kaya Mekaniği Sempozyumu, 22-23 Ekim, Zonguldak, s.13-22.

Bieniawski ZT, 1967. Mechanism of brittle fracture of rock, Part II. Experimental studies. Int. J. Rock Mech. Min. Sci. Geomech. Abstr. 4 : 407–423.

Ciccotti M, Mulargia F, 2004. Differences between static and dynamic elastic moduli of a typical seismogenic rock. Geophys. J. Int. 157: 474-477.

Couvreur JF, Vervoort A, King MS, Lousberg E, Thimus JF. 2001. Successive cracking steps of a limestone highlighted by ultrasonic wave propagation. Geophysical Prospecting. 49: 71-78.

Dodds KJ, Dewhurst DN, Siggins AF, Ciz R, Urosevic M, Gurevich B, Sherlock DH, 2007. Experimental and theoretical rock physics research with application to reservoirs, seals

and fluid processes, Journal of Petroleum Science and Engineering. 57: 16–36.

Fortin J, Schubnel A, Gueguen G, 2005. Elastic wave velocities and permeability evolution during compaction of Bleurswiller sandstone, International Journal of Rock Mechanics & Mining Sciences. 42: 873–889.

ISRM, 1977. Suggested Methods for Determining Water Content, Porosity, Density, Absorption and Related Properties and Swelling and Slake-Durability Index Properties. Pp 143-151.

ISRM, 1978. Suggested methods for determining sound velocity, Int. J. Rock Mech. Min. Sci. & Geomech. Abstr. 15: 53-58

Karakus M, Tutmez B, Kaleci D, 2008. Symbolic Regression Analysis for the Relationship between Static and Dynamic Elasticity Moduli of Some Intact Rocks via Genetic Programming. The IX. th Regional Rock Mechanics Symposium, İzmir, October 30-31.

Mashinskii EI, 2002. Influence of microplasticity on the static and dynamic elastic moduli of rocks. Journal of Mining Science. 38(3): 213-219.

Meglis IL, Chow T, Martin CD and Young RP, 2005. Assessing In Situ Microcrack Damage Using Ultrasonic Velocity Tomography, International Journal of Rock Mechanics and Mining Sciences, 42 (1), 25-34.

Shkolnik I, Aktan H, Birgul R, 2003. Nonlinear non-destructive methods for evaluating strength of concrete. International Symposium; Non-Destructive Testing in Civil Engineering, September 16-19, Berlin, Germany.

Starzec P, 1999. Dynamic elastic properties of crystalline rocks from south-west Sweden. Int. J. Rock Mech. Mining Sci. 36: 265-272.

Vaconcelos G, Lourenço PB, Alves CAS, Pamplona J, 2008. Ultrasonic evaluation of the physical and mechanical properties of granites. Ultrasonics. 48: 453-466.

Empirical Estimation of Intact Rock Elastic Modulus

Kaya Malzemesi Elastik Modülünün Ampirik Tahmini

İbrahim Ocak
İstanbul Metropolitan Municipality, İETT General Directorate, İstanbul

ABSTRACT The modulus of elasticity of intact rock (E_i) is an important rock property which is used as input parameter in the design stage of engineering projects such as slopes, tunnel and mining excavations. However, it is difficult to obtain the modulus of elasticity directly from laboratory test and high-quality cores are necessary for the laboratory experiments. For this reason, empirical methods for predicting of the elastic modulus of intact rock have been one of the popular research topics in the literature. In this study, the relations between the uniaxial compressive strength (UCS) and elastic modulus of different types of rock were analyzed by using 381 data obtained from laboratory test performed on the cores collected from the drill holes within the corresponding area of Kadıköy-Kartal Metro Project, Marmaray Project and İstanbul Metro Project. In addition, some empirical equations proposed in the literature and this study was also considered to evaluate their prediction performance on the collected data in this study. As a result, a good relationship between the modulus of elasticity and the uniaxial compressive strength is found and modulus of elasticity may be estimated via these relationships.

ÖZET Elastisite modülü (Ei) tünel kazıları, madencilik kazıları, şevler gibi pek çok mühendislik projesinin dizaynında kullanılan önemli bir parametredir. Ancak elastisite modülünün doğrudan belirlenebilmesi zordur ve deney için yüksek kalitede karotlar gerekmektedir. Bu nedenle elastisite modülünün ampirik yollarla tahmini literatürde popüler araştırma konularından biridir. Bu çalışmada Kadıköy-Kartal Metrosu, Marmaray Projesi ve İstanbul Metrosu metro kazıları kapsamında yapılan sondajlardan alınan karotlardan elde edilen 381 adet veri kullanılarak değişik litolojilerdeki kayaçların serbest basınç dayanımları (UCS) ile elastisite modülü arasındaki ilişki araştırılmıştır. Ayrıca, literatürde önerilen bazı ampirik yöntemler ve bu çalışmanın tahmin performansı çalışmadaki datalarla değerlendirilmiştir. Sonuçta, basınç dayanımı ile elastisite modülü arasında kuvvetli bir ilişki olduğu ve bu ilişkiye dayanılarak elastisite modülünün yaklaşık olarak tahmin edilebileceği görülmüştür.

1 INTRODUCTION

The modulus of elasticity is used as input parameter together with the poisson's ratio unit weight, cohesion, and internal frictional angle in design stages of the projects of mining engineering and construction engineering fields. However, high-quality core samples are needed to obtain this parameter from laboratory test. Due to the weak, thinly bedded and heavily jointed pattern of the rock mass, it is not possible to obtain high-quality cores from these types of the rock masses. To overcome this limitation, the estimation of the modulus of elasticity in rock engineering problems have been widely used in the recent literature of the rock mechanics.

While in some of the studies such as Deere and Miller, 1996; Aufmuth, 1973; Sachpazis, 1990; and Xu et al., 1990; the Schmidt hammer has been used. Several researchers such as Wuerker, 1959; Dhir and Sangha, 1972; Lama and Vutukuri, 1978; Wilson, 1978; Dennis et al., 1982; Bell, 1983; Sachpazis, 1990; Rohde and Feng, 1990; Arıoğlu and Tokgöz 1992; Tugrul and Zarif, 1999; Palchik, 1999; Lashkaripour and Nakhaei, 2001 and Ocak, 2006 used uniaxial compressive strength for the estimation elastic modulus. Another team of researchers (Sonmez et al., 2004a; Sonmez et al., 2004b; Ocak, 2007; Ocak 2008) used both unit weight and UCS for the estimation of the modulus of elasticity. And another team of researcher (Sonmez et al., 2006) used both modulus ratio of intact rock and UCS for the estimation of the modulus of elasticity.

The practical value of the empirical approaches depends upon not only the number of data but also the number of types of intact rock considered in the relations. However, in most of the studies given above, the limited number of data is considered. One of the other deficiencies of these studies was to obtain statistical relationships from different lithologic units together and the second one is ignoring the sample sizes.

Table 1. Test results of the rock samples (İBB, 2005; STFA, 2003).

Lithology	Number of data	Uniaxial compressive strength, UCS (MPa)		Modulus of elasticity, E_i (GPa)	
		Mean	Std. dev.	Mean	Std. dev.
Mudstone	47	36.69	23.20	8.29	5.80
Diabase	13	54.35	34.07	11.48	6.68
Claystone	40	39.30	33.26	10.09	10.35
Limestone	76	41.01	28.16	10.54	7.12
Conglomerate	13	49.09	17.68	10.62	3.11
Sandstone	180	54.13	36.19	11.83	8.90
Siltstone	12	60.78	25.21	16.99	10.72

In this study, 381 data sets including UCS and E_i have been established from different types of rock. These data have been obtained from the 381 drilling holes during the works of the Kadıköy-

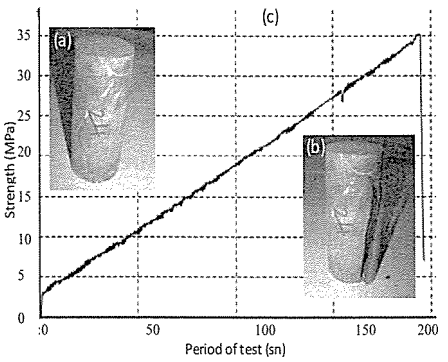

Figure 1. (a) Test specimen before UCS test (b) Test specimen after UCS test (c) a typical strength–period of test curve obtained from the UCS tests (Ocak, 2008).

Kartal Metro line project, Marmaray Project and İstanbul Metro Project. The data sets including UCS and E_i were obtained from laboratory test employed on the cores according to the suggested methods of ISRM, 1981 (Figure 1). Length/diameter ratio is about 2. The average UCS value is 47.8 MPa. The average modulus of elasticity value is 11.6 GPa. The mean values of UCS and E_i of the rocks collected from the tunnel routes are given in Table 1.

2 GENERAL INFORMATION ABOUT THE STUDY REGION

The study region covered three projects which are under construction. These are Kadıköy-Kartal Metro Project, Marmaray Project and İstanbul Metro Project. The project of the Kadıköy-Kartal rail transport system starts from Kadıköy and passes through the districts of Üsküdar, Maltepe and Kartal. The length of the rail transport system is 21.6 km and the constructions of 16 stations are planned. The project of the

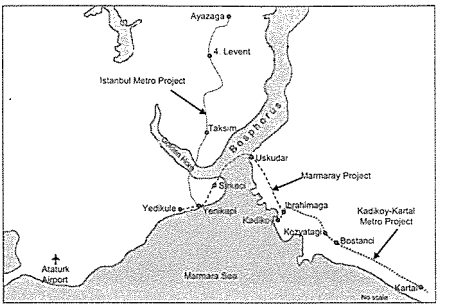

Figure 2. General view of study area.

Marmaray starts from Ibrahimaga and passes through the districts of Üsküdar, Sirkeci and Yenikapi. The length of the rail transport system is about 13.6 km. Kadıköy-Kartal rail transport system is integrated with the Marmaray undersea rail tunnel project which will join the European and Asian halves of İstanbul in the İbrahimağa Station with an immersed tunnel under the sea. Both passenger transportation and the connection with the European side of İstanbul with the Marmaray Project will be provided with the integration with the Marmaray Project. The project of the İstanbul Metro starts from Ayazaga and passes through the districts of 4. Levent, Taksim and Yenikapi. The length of the rail transport system is about 20 km. General view of study area is given Figure 2.

3 PROPERTIES OF DATABASE

The database composed of uniaxial compressive strength and elastic modulus represents the rock formations found in Kadıköy-Kartal Metro System route, Marmaray Metro System route and İstanbul Metro System route. The database established from the laboratory experiments carried out on the drillings cores were obtained from the Directorate

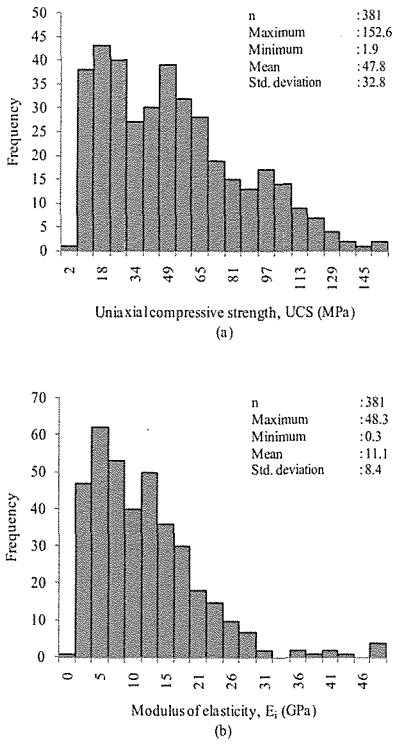

Figure 3. The histograms and statistical evaluations of the data used to predict E_i.

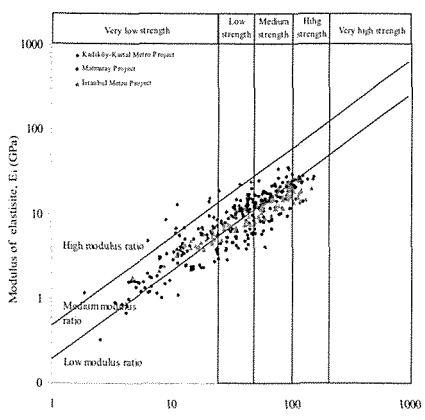

Figure 4. The distribution of the data base on the modulus rate graphic by Deere&Miller 1966.

General of İETT, İstanbul Metropolitan Municipality and General Directorate of Railways, Harbours and Airports Construction. While the values of uniaxial compressive strength vary between 1.9 MPa to 152.6 MPa, the modulus of elasticity change from 0.3 GPa to 48.3 GPa. The variations of geomechanical data are given in Figure 3. The distribution of the data on the modulus ratio graph suggested by Deere & Miller (1966) is shown in Figure 4.

The statigrafic zone of the İstanbul consists of İstanbul Palaezoic Zone, which is mostly known as "İstanbul Group", and sediments of Trias and Terciary, which are located upon İstanbul Palaezoic. Alluvial deposits within the river beds and clastic sediments are the youngest geological units. The İstanbul Group includes the Ordovisien and Carbonifer aged sediments. The lower parts of the group which is covered with Trias and younger units above are situated in the eastern side of the Bosphorus and the younger parts are in the western side.

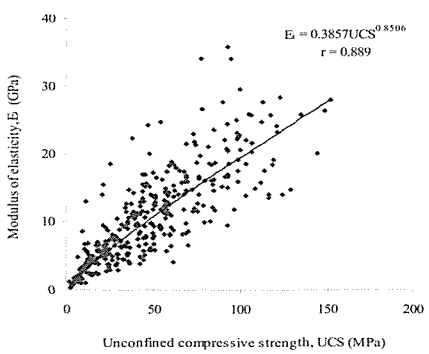

Figure 5. Correlation between UCS and modulus of elasticity for all formation.

Table 2. List of the obtained equations.

Formation	Number of data	Equations*		r
Mudstone	47	$E_i = 0.3436UCS^{0.8721}$	(Eq. 1)	0.884
Diabase	13	$E_i = 0.1627UCS^{1.0588}$	(Eq. 2)	0.942
Claystone	40	$E_i = 0.3485UCS^{0.8866}$	(Eq. 3)	0.837
Limestone	76	$E_i = 0.4153UCS^{0.8692}$	(Eq. 4)	0.935
Conglomerate	13	$E_i = 1.1329UCS^{0.5761}$	(Eq. 5)	0.849
Sandstone	180	$E_i = 0.3341UCS^{0.8818}$	(Eq. 6)	0.893
Siltstone	12	$E_i = 6.7152e^{0.0131UCS}$	(Eq. 7)	0.639

* E_i : GPa, UCS : MPa

4 THERELATIONSHIPBETWEEN THE UNIAXIAL COMPRESSIVE STRENGTH AND THE MODULUS OF ELASTICITY

The relationships between the uniaxial compressive strength and the modulus of elasticity for intact rocks of the rock formations representing the Kadıköy–Kartal Metro System Route, Marmaray Metro System Route and İstanbul Metro System Route have been investigated separately for each formation and for all the formations together in the tunnel routes. Correlation coefficients have been changed from 0.639 to 0.942 for various formations (Tab. 2). Correlation coefficients has been found as 0.889 for all formations (Fig. 5).

The relationships between the predicted modulus of elasticity (E_{ip}) obtained by using the equations 1-7, obtained by using E_i=0.3857$UCS^{0.8506}$ and the measured modulus of elasticity (E_{im}) have also been searched. Cross-control graphics have been also drawn for each formation individually and for all formations (Fig. 6a, 6b). The

$$VAF = \left(1 - \frac{var(y - y')}{var(y)}\right) \cdot 100 \quad (8a)$$

$$RMSE = \sqrt{\frac{1}{N}\sum_{i=1}^{n}(y - y')^2} \quad (8b)$$

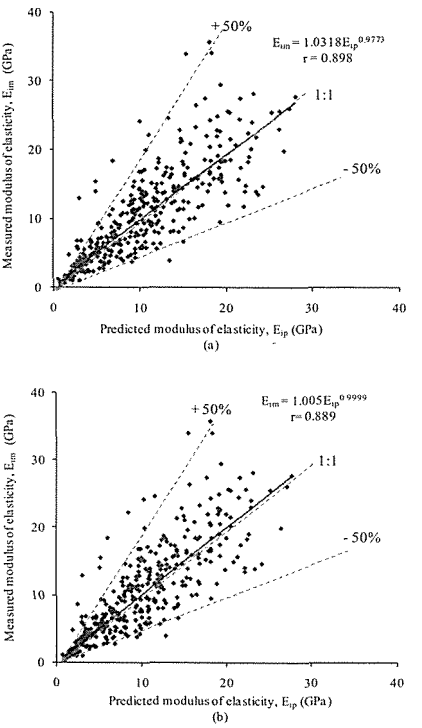

Figure 6. Cross-correlation between predicted and measured values of E_i, (a) separately for each formation and (b) all formation.

predicted and measured values for separately each formation (Fig. 6a) and all the formations (Fig. 6b) give very significant correlation coefficients along

1:1 line. In short, it has been seen that the equations obtained from the statistical analysis show that elasticity modulus of rock samples representing different geological formations can be predicted from compressive strength for practical purposes.

5 THE PREDICTION PERFORMANCE OF SOME EMPIRICAL RELATIONS USED UCS

The first empirical equation, which considers UCS as an input parameter, was proposed by Wuerker in 1959. The equation suggested by Wuerker was derived based on only 6 data which included UCS. After Wuerker, a lot of researchers developed various empirical equations to estimate the elastic modulus of the intact rock by using the UCS.

The prediction performances of some empirical relations are given in Table 3. Prediction performances of these models were evaluated by employing variance account for (VAF) and root mean square error (RMSE) given in Eqs. (8a) and (8b) respectively.

Where y and y' are the measured and the predicted values, respectively, and N is the number of data. If the model has excellent prediction capacity the VAF and RMSE will be 100% and zero, respectively.

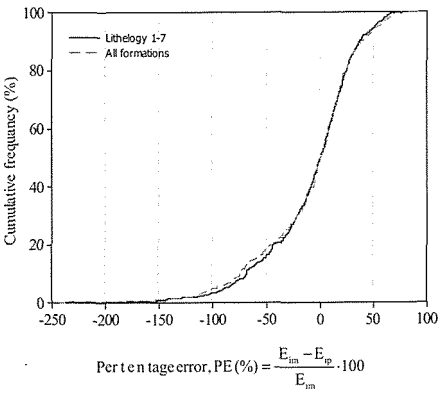

Figure 7. The relation between percentage error and cumulative frequency.

In addition, by using 381 datasets collected from various lithologic types of rock, percentage errors are drawn (Fig. 7). Percentage errors for approximately 90% of the data are between -100% and +50%. Therefore, the proposed empirical equations have a sufficient prediction capacity and can be used to estimate the modulus of elasticity of intact rock for practical purposes.

Table 3. List of some empirical equations used UCS for estimating the modulus of elasticity and their performances.

Originator(s) of empirical equations	Equation	VAF	RMSE
This study	Eqs. 1-7	68.6	4.2
This study	$E_i = 0.3857UCS^{0.8506}$	68.4	4.2
Arıoğlu et al. (1992)	$E_i = 1.03UCS^{0.73}$	53.3	7.6
Sönmez (2004a)	$E_i = 0.3031UCS^{1.0157}$	20.3	7.9
Sönmez (2004b)	$E_i = 0.4385UCS^{0.6759}$	47.0	7.6
Ocak (2006)	$E_i = 0.7071UCS^{0.7076}$	68.2	4.3

It can seen from Table 3 and Figure 7 that, the performance of the proposed empirical equations are sufficient for practical uses.

6 CONCLUSIONS

Determination of modulus of elasticity of rocks requires high quality core samples and therefore it is sometimes difficult to determine elasticity modulus using direct methods applied to core samples obtained in difficult ground conditions such as stratified (thinly bedded), highly fractured and block-in-matrix rock. In this study, to overcome these problems, several basic equations were prepared by using an extensive database including elastic modulus and uniaxial compressive strength of intact rock.

The significant relationships in the statistical analysis were evaluated by using a wide range of data base from different rocks of different formations whose mechanical and deformational characteristics change in a wide range. The data base used is of great importance for the current engineering applications since it is obtained from the data of the 381 drillings carried out in three metro projects of İstanbul. The empirical equation presented has a strong prediction capacity and can be used to estimate the modulus of elasticity of intact rock for practical purposes.

Assessments of some recent existing empirical equations given in the literature for estimating the modulus of elasticity using UCS of intact rock discussed. The performance of the proposed empirical equations is better than other discussed equations.

As a result of this study, it has been shown that the modulus of elasticity can be estimated significantly from the uniaxial compressive strength of the rock. Therefore, especially the nine ongoing metro projects under the construction in İstanbul pass through these formations to a great extend the correlations obtained from this study can be utilized for estimating the modulus of elasticity.

REFERENCES

Arıoğlu E., and Tokgöz N., 1992, Relationship between Modulus of elasticity and uniaxial compressive strength in sedimentary rocks, *Rock Mechanic Journal*, Turkish Rock Mechanic Association, Vol . 7, pp. 5-15. (in Turkish)

Aufmuth, R. E., 1973, A systematic determination of engineering 20 criteria for rock: *Bulletin of Association of Engineering Geology*, Vol. 11, pp. 235-245.

Bell, F. G., 1983, Engineering properties of soil and rocks, London

Deere, D. V., Miller. R. L., 1966, Engineering classification and index properties of intact rock: *Department of Civil Engineering University of Illinois*, Urbana. pp. 90-101.

Dennis, R. D., Horing, F.G., Hooker, E. V., 1982, Mechanical properties of oil shale and overlying strata: Naval Oil Shale Reserve, Anvil Points, Colo. pp. 1-43.

Dhir, R. K., Sangha, C.M., 1972, Rock strength, *Colliery Guardian.*, pp. 525-256.

İETT, 2005, The Project of the İstanbul Kadıköy–Kartal Rail Transport System, *Engineering Geology Report.*

ISRM, 1981, *International Society for Rock Mechanics Suggested Methods*: *Rock characterization, testing*

and monitoring. E.T. Brown (ed.). Permagon presss. London, 211 pp.

İBB, 2005, İstanbul Metropolitan Municipality, İETT General Directorate, *Kadıköy-Kartal Metro Project Geotechnical Report.*

Lama, R. D., Vutukuri, V. S., 1978, *Handbook and mechanical properties of rock, Trans. Tech. Publ.:* Switzerland. Vol. 2, pp. 481

Lashkaripour, G. R., Nakhaei M., 2001, A statistical investigation on mudrocks characteristics: *Rock Mechanics*, pp. 131-136.

Ocak, I., 2006, Correlation compressive strength and of modulus of elasticity in Kadıköy-Kartal Metro line's rocks: *İstanbul University Engineering Faculty's Earth Sciences Review*, Vol. 19. İstanbul

Ocak, I., 2007, The study of relationship between the modulus of elasticity and compressive strength for rocks, *Proceedings of the 20th International Mining Congress of Turkey,* Ankara.

Ocak, I., 2008, Estimating the modulus of elasticity of the rock material from compressive strength and unit weight, *The Journal of The Southern African Institute of Mining and Metallurgy,* Vol 108, pp. 621-626.

Palchik, V., 1999, Influence of porosity and elastic modulus on uniaxial compressive strength in soft brittle porous sandstones: *Rock Mechanic and Rock Engineering,* Vol. 32 (4), pp. 303-309.

Rohde, J., Feng, H., 1990, Analysis of the variability of unconfined compression tests of rock, *Rock Mechanic and Rock Engineering,* Vol. 23, pp. 231 -236.

Sachpazis, C. I., 1990, Correlating Schmidt hardness with compressive strength and Young's modulus of carbonate rocks, *Bulletin International Association Engineering Geoogyl*, Vol. 42, pp. 75-83.

Sonmez, H., Gökçeoğlu, C., Kasapoğlu, K. E., Tuncay, E., Zorlu, K., 2004a, An empirical equation for estimating elasticity modulus of intack rock, *ROCKMEC'2004-VIIth Regional Rock Mechanics Symposium*, Sivas-Turkey

Sonmez, H., Tuncay, E., Gökçeoğlu, C., 2004b, Models to predict the uniaxial compressive strength and the modulus of elasticity for Ankara agglomerate: *International Journal of Rock Mechanics & Mining Sciences,*

An Analytical Approach for Natural Rock Blocks Bounding Two Discontinuities and Free Surfaces in Engineering Structures

Mühendislik Yapılarında İki Süreksizlik ve Serbest Yüzeylerle Sınırlanmış Doğal Kaya Bloklarının Tanımlanması İçin Analitik Bir Yaklaşım

A.Turanboy
Selçuk Üniversitesi, Seydişehir Meslek Yüksekokulu, 42360, Konya, Turkey,

ABSTRACT The spatial positions of the discontinuities and the shapes of rock blocks that are bounded into rock masses are important features that should be taken into consideration, especially to further comprehend the sliding mechanisms in rock media. Therefore, explicit representation of in situ rock mass structures is strongly required in many areas of mining and construction engineering.
In this paper, a new classification of two discontinuities as a construction method is developed according to their spatial orientations and their location relative to each other. In addition, in the developed method, discontinuities were geometrically analyzed in a rectangular prism. Thus, the geometries of the possible sliding blocks in engineering structures, such as road cuts, open slopes, or dam walls founded on rock media, were produced. Several basic mathematical equations, and approaches derived from them, were used. In addition, the isometric perspective method was used to for illustrations. The results obtained from two experiment fields show the effectiveness of the proposed modeling method.

ÖZET Kaya kütlesi içindeki süreksizliklerin ve onların oluşturduğu kaya bloklarının uzaysal pozisyonlarının açık bir biçimde ortaya konulması özellikle, kaya ortamında kazılan mühendislik yapılarının duraylılığı açısından oldukça önemlidir. Bu çalışmada, İki süreksizliğin uzaysal konumları hem bireysel hem de birbirine göre durumu incelenerek yeni bir sınıflama sistemi geliştirilmiştir. Model çalışması ile kaya kütlesi temsili bir dörtgen prizma içinde değerlendirilip, iki süreksizlik ve serbest yüzeylerle sınırlı olası doğal kaya blokları üretilmiştir. Çeşitli lineer ifadelerden üretilen yaklaşımlar kullanılarak açık ocak ve karayolu şevleri, baraj duvarları gibi kaya kütlesinde açılan mühendislik yapılarında olası kayma blokları analitik olarak incelenmiştir. Teklif edilen model ve arazi verileri göz önüne alındığında etkili sonuçların alındığı görülmektedir.

1 INTRODUCTION

Slope engineering is perhaps the geotechnical subject most dominated by uncertainty since slopes are composed of natural materials (El-Ramly et al., 2002). Slope stability analysis requires kinematic and kinetic evaluation. In kinematic analysis, the question is whether slope failure of a rock mass is possible based on the geometry of discontinuities and slope orientation (Park et al., 2005).

On the other hand, explicit rock slope analysis can provide valuable information for the design of engineering structures in rock media, and one of the principle tasks for these analyses may be geometrically identifying the discontinuities and natural blocks that respond to several sliding modes, such as planar, wedge, toppling, and buckling.

A basic assumption in many former studies is that the possible failure block behaves like a rigid body, either sliding along a discontinuity plane or along the intersection line segment between two planes. In addition, evaluations of the sliding mechanism were often realized by linear approaches. One of the first research projects associated with the subject was a three-dimensional wedge failure analysis presented by Coates (1967). The Key Block analysis (Goodman and Shi, 1981, 1985) is a means of determining the most critical or "key" blocks of rock formed by an excavation in jointed, competent rock. Block Theory (Goodman and Shi, 1985) is a means of analyzing the stability rock blocks around tunnels. A relatively simple method, it uses only the orientation and friction angle of each joint set as input parameters. In addition, vectorial technique of the key-block was also presented by Warburton, 1981. Wedge analysis (Hoek and Bray, 1974) is a means of explaining a solution to the wedge failure problems in which both planes of sliding possess different cohesions and angles of friction. Various discontinuity properties were assessed comprehensively in finite, distinct elements in classical stereographic and kinematic analyses, limit equilibrium, and with many commercially available codes (such as DIPS, ROCFALL, SWEDGE, SLIDE, SLOPE/W by Rocscience, 2004 and FLAG2D/3D, UDEC, 3DEC, PFC2D/3D by Itasca, 2001). These tools are successfully applied in many rock engineering applications. In many geometrical and numerical analyses, discontinuities and blocks of them are classified according to the spatial positions of the discontinuities and whether or not there are finite or infinite numbers of them. For example, potential block failure modes are identified as key blocks or critical blocks that present particular risk to the stability of an excavation boundary. The blocks are classified around the excavation boundaries as infinite, finite and tapered, or finite and non-tapered. When these analyses are realized, scales, shapes and boundaries of the engineering structures and the orientation of the discontinuities are regarded together. However, quick and simple description and classification systems are still needed for practical and basic applications. Especially when directly recording data from an appropriate survey technique, a simple and quick analysis for simple results is needed. For these reasons, discontinuity geometry is analyzed, and a new classification system and a model based on this classification are proposed

based on two district discontinuities onto a surface. In the developed method, several mathematical approaches are developed and the isometric perspective method was used for illustrations. The developed model enables 2D and 3D diagrams of rock mass.

The rock block boundaries are defined by discontinuity traces in three source directions (X, Y and Z) in the developed model. Therefore, the model may be evaluated as the orthogonal. The assumption of orthogonality has been widely used in several formerly studies (Childs (1957), Snow (1965), LaPointe et al. (1997), Peaker (1990), Maerz and Germain (1996), Hadjigeorgiou et al. (1998) and Jern (2004). Two other principal assumptions in the model are listed below:

1. All the discontinuity traces and intersection line segments are perfectly linear and

2. All the discontinuity planes extend entirely through the rock mass. Due to this assumption, all rock blocks created are convex.

2 USED MATHEMATICAL COMPONENTS

The model is evaluated in a 3D Cartesian coordinate system, which is used not only to describe the (linear) position of points, but also to describe the angular position of axes, planes, and rigid bodies. In this section, the basic components used, which are points, lines, and planes, are described briefly based on the developed methodology. In addition, mathematical tools and derived relations are also explained.

2.1 Point

A spatial point describes a specific point within a given space that consists of neither volume, area, length, nor any other higher dimensional analogue. A given point (P) (Fig. 1(a)) in a 3D coordinate system is described as P(x, y, z). In the model, it is equivalent to intersection points that are between discontinuity trace- discontinuity trace, discontinuity trace- prism edge and prism edge- prism edge.

2.2 Line and line segment

A line can be described as an ideal, zero-width, infinitely long, perfectly straight curve containing an infinite number of points. In Euclidean geometry, exactly one line can be found that passes through any two points. On the other hand, a line segment provides the shortest connection between two points ($P_1(x_1, y_1, z_1)$, $P_2(x_1, y_1, z_1)$) (Fig. 1(a)). In the model, a line segment is equivalent to prism edges, discontinuity traces, and intersection line segments between two discontinuity surfaces.

2.3 Plane or surface

A plane is a two-dimensional manifold or surface that is perfectly flat. It is described with the plane passing through three points, $A_1(x_1, y_1, z_1)$, $A_2(x_2, y_2, z_2)$ and $A_3(x_3, y_3, z_3)$ (Fig. 1(b)). In the model, a plane is equivalent to a discontinuity plane and a prism surface. To prevent confusion, discontinuity planes and prism surfaces were both used in the model. In addition, without using detailed determinant equations for the plane descriptions, the classification system and isometric presentation are applied

only using points and line segments?

2.4 Angle

An angle is the figure formed by two rays sharing a common endpoint, called the vertex of the angle. It can be measured by considering the length of the circular arc swept between the two rays. In the model, an angle is equivalent to a dip (β), a search angle (φ), the dip direction of a discontinuity (α), or the dip direction of outcrop (γ).

3 INTERSECTION POINT OF TWO LINES

Fundamentally, the model is based on calculating the intersection points of two lines from their parametric form in a 3D Cartesian coordinate system and connecting these points systematically.

Given points L1 = (x_1, y_1, z_1) and L2 = (x_2, y_2, z_2), the parametric forms for the two lines are:

$$\text{For L1} \quad \begin{aligned} X &= x_1 + \lambda \text{Cos}\ \delta_1 \\ Y &= y_1 + \lambda \text{Cos}\ \beta_1 \\ Z &= z_1 + \lambda \text{Cos}\ \varepsilon_1 \end{aligned} \qquad (1)$$

and

$$\text{For L2} \quad \begin{aligned} X &= x_2 + t\text{Cos}\ \delta_2 \\ Y &= y_2 + t\text{Cos}\ \beta_2 \\ Z &= z_2 + t\text{Cos}\ \varepsilon_1 \end{aligned} \qquad (2)$$

In these equations, λ and t are linear coefficients ($0 \leq \lambda \leq 1$ and $0 \leq t \leq 1$), and δ, β and ε are clockwise angles to the x, y and z axes, respectively. In the model, β is the dip angle, δ is equal to 90° and ε is equal to β+270° on the YZ surface. On the other hand, for the XY surface (the upper surface of the prism) angle φ is used similarly.

Finding the intersection of two lines can be solved by using a simultaneous equations method as:

$$\begin{aligned} x_1 + \lambda \text{Cos}\ \delta_1 &= x_2 + t\text{Cos}\ \delta_2 = x_3 \\ y_1 + \lambda \text{Cos}\ \beta_1 &= y_2 + t\text{Cos}\ \beta_2 = y_3 \\ z_2 + \lambda \text{Cos}\ \varepsilon_1 &= z1 + t\text{Cos}\ \varepsilon_2 = z_3 \end{aligned} \qquad (3)$$

Here, (x_3, y_3, z_3) is solved as the intersection point (I) between lines L1 and L2 (Fig. 1 (a)).

4 DESCRIPTION OF METHOD

In this research, the main objective is to reveal the geometry of rock blocks that responds to sliding.

The main parts of the methodology are presented as follows;

1. Description of several geometrical features with one and two distinct discontinuities in a representative prism;

2. Construction of a geometrical classification system taking into account spatial positions of discontinuities on both perpendicular and horizontal surfaces as the visible surfaces;

3. Combination along the intersection line segments these perpendicular and horizontal surfaces, thus completing the classification;

4. To realize a fully 3D description, projection of the visible surfaces onto hidden surfaces; and

5. 3D visualization using isometric transformation.

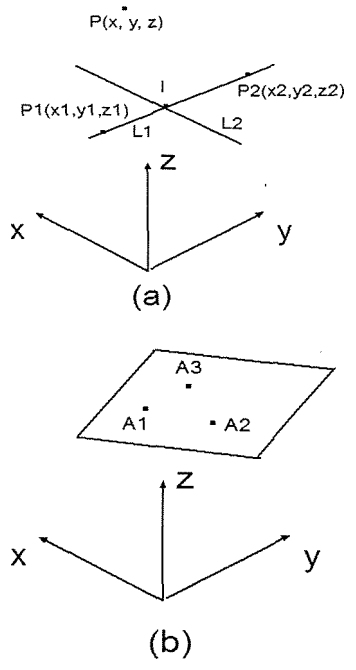

Figure 1. Several mathematical components: (a) points, lines, line segments and (b) a surface, or plane, in 3D.

In geometric models, first, geometrical components of an object, along with specifications and relations with each other that will be basis of the model, should be identified.

In this study, the zone of a rock mass of interest is defined as a rectangular prism [ABCDEFGH] in the developed model (Fig. 2). According to this structure, which also consists of a single discontinuity plane, geometrical components can be given as follows.

Rock mass dimensions: (hx x hy x hz); A: origin point; D1: any discontinuity; C1: cumulative spacing belonging to D1 (all records are taken throughout the Y axis); β: apparent dip; φ: search angle that will be explained later; hx: width of the rock mass; hz: height of the rock mass; hx/tg(90°-φ) and hy/tgβ: sizes of the discontinuity onto the surface of interest that that are used to obtain the intersection or non-intersection conditions on surfaces, which will be explained later.

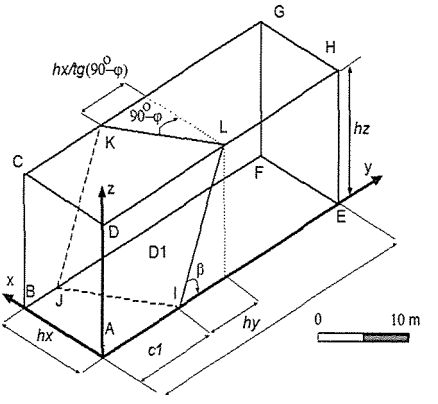

Figure 2. The zone of a rock mass of interest that includes one discontinuity and its geometrical components.

4.1 Possible Orientations of Discontinuities

In this paper, a classification system is developed for only one discontinuity or two discontinuity traces on a 2D surface according to their possible spatial positions and their relation to each other if two discontinuities on a surface are considered. Discontinuities perpendicular and parallel to coordinate axes are ignored in this system. Only visible traces on free surfaces are regarded.

4.1.1 Situations of only one discontinuity trace

For a discontinuity trace on the YZ surface, two possible conditions should be regarded according to dip angles (β), which are clockwise from the discontinuity trace to the Y axis. These

are (β_1>90°) and (β_2<90°) (Fig. 1(a)), and they are called type YZ_1 and type YZ_2, respectively.

4.1.2 *Situations of two distinct discontinuity traces*

Dip angles, cumulative spacing, height of the rock mass, and intersection points that are between discontinuity traces and the upper edges of the sample rock mass (Fig. 2) and conditions derived from them are regarded for these situations. For example, intersection points that are between discontinuity traces and the upper edges of the sample rock mass can be indicated for type YZ_1 as *C1-hz*/tg (β1–90°) and for type YZ_2 as ($C2+hz/\text{tg}(90°-\beta_2)$. Here *C*, *hz* and β are cumulative spacing, height of the rock mass and dip angle (Fig. 3(a)). If [YZ_1] and [YZ_2] are regarded on the YZ surface, three situations can be derived. These are type [YZ_{1-2}], type [YZ_{2-1}] and type [YZ_{2-1}^{*}] (Fig. 3(b)). In here (*) indicates the intersection between two discontinuity traces. The intersection situation is realized with only the $C2+hz/\text{tg}(90°-\beta_2) > C1-hz/\text{tg}(\beta1–90°)$ condition (Fig. 4). In addition, the two types YZ_1 can be projected onto the YZ surface, but their dip angles are different. Thus, three situations can be derived (Fig. 3(c)). The same relation can be derived if the two YZ_2 situations are projected onto the YZ surface (Fig. 3(d)). Thus, nine situations are obtained for two discontinuity traces on the YZ surface. According to the derived conditions, different situations are given in Table 1 and 2.

The same relations can be similarly used projecting onto the XY surface. In this study, the search angle (φ) concept was used except for the dip angle (β). The search angle (φ) cannot be measured with a compass-clinometer and is derived from the dip direction angle (α) and the dip direction of outcrop (γ) (Fig. 5). The search angle (φ) concept was described in Turanboy and Ülker, 2008 in detail. In addition, *hx* (width of the rock mass) is valid for XY surface calculations.

Table 1 Situations and conditions for the single trace.

	1	Alone onto a plane	
Situations	2	type1	type2
Conditions (according to)	itself	$\beta1>90°$	$\beta2<90°$
	each other	$\beta2>\beta1$	

	1	Alone onto a plane	
Situations	2	type1a	type1b
Conditions (according to)	itself	$\beta1a>90°$	$\beta1b>90°$
	each other	$\beta1b>\beta1a$	

	1	Alone onto a plane	
Situations	2	type2a	type2b
Conditions (according to)	itself	$\beta2a<90°$	$\beta2a<90°$
	each other	$\beta2a>\beta2b$	

Table 2 Situations, conditions and results for the two traces.

	1	both onto a plane		
Situations	2	type1-2	type2-1	type2-1
Conditions (according to)	cumulative spacing	*c2>c1*	*c1>c2*	*c2>c1*
	height of rock mass	non-relation	*C1-hz/tg(β1-90°) > C2+hz/tg(90°-β2)*	*C2+hz/tg(90°-β2)> C1-hz/tg(β1-90°)*
Results	intersection or non-intersection	non-intersection	non-intersection	intersection

	1	both onto a plane		
Situations	2	type1a-1b	type1b-1a	type1b-1a
Conditions (according to)	cumulative spacing	*c1b>c1a*	*c1a>c1b*	*c1b>c1a*
	height of rock mass	*C1b-hz/tg(β1b-90°)> C1a-hz/tg(β1a-90°)*	non-relation	*C1a-hz/tg(β1a-90°)> C1b-hz/tg(β1b-90°)*
Results	intersection or non-intersection	non-intersection	non-intersection	intersection

	1	both onto a plane		
Situations	2	type2a-2b	type2b-2a	type2b-2a
Conditions (according to)	cumulative spacing	*c2b>c2a*	*c2a>c2b*	*c2a>c2b*
	height of rock mass	non-relation	*C2a+hz/tg(90°-β2a)> C2b+hz/tg(90°-β2b)*	*C2b+hz/tg(90°-β2b)> C2a+hz/tg(90°-β2a)*
Results	intersection or non-intersection	non-intersection	non-intersection	intersection

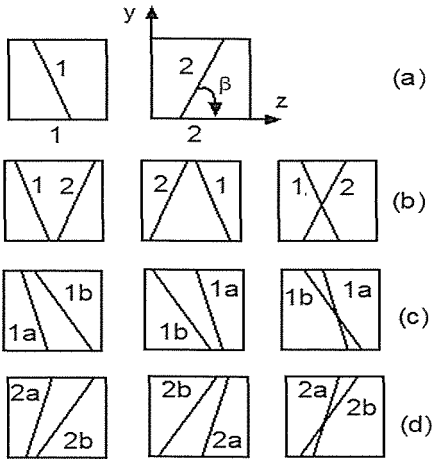

Figure 3. Different situations for discontinuity traces on the YZ plane; a) for only one discontinuity trace (the first one is > 90°, the other one's dip angle (β) is < 90°); b) for two discontinuity traces (dip angle (β) of the first one is > 90°, the other one's dip angle (β) is < 90°) and cumulative spacing values are different in each situations; c) both of their dip angles (β) are > 90° but different, and cumulative spacing values are different in each situations; d) both of their dip angles (β) are > 90° but different, and cumulative spacing values are different in each situations.

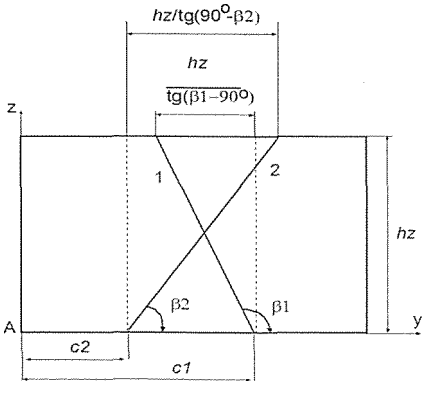

Figgure 4. Two discontinuity traces onto the YZ surface and their dimensions.

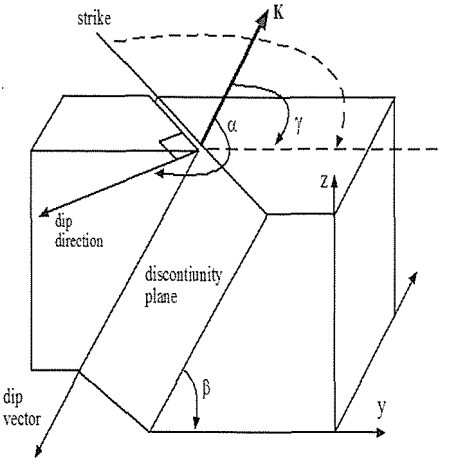

Figure 5. For a discontinuity surface on the XY surface, the search angle (φ) (shown with a dashed line) and the parameters from which it is derived: the dip direction of the discontinuity (α) and the dip direction of outcrop (γ).

4.2 Two surfaces combined

Discontinuity representations in 3D can be achieved by integrating descriptions onto the YZ and XY surfaces. In this study, these surfaces, which are perpendicular to each other, are combined along the [DH] line segment. Thus, if the 9 different 2D situations in Fig. 1(a) are taken into account, (9X9) =81 different 3D situations can be obtained (Fig. 6).

Furthermore, every situation was indexed to describe the 81 different situations in the model. For example, the situations in Fig. 4 (a, b, c, d, e, and f) were indexed as $[YZ_{1\text{-}2}XY_{1\text{-}2}]$, $[YZ_{1\text{-}2}XY_{2\text{-}1}]$, $[YZ_{1\text{-}2}XY_{2b\text{-}2a}]$, $[YZ_{2\text{-}1}XY_{1\text{-}2}]$, $[YZ_{2a\text{-}2b}, XY_{1\text{-}2}]$, and $[YZ_{2b\text{-}2a}\ XY_{2b\text{-}2a}]$, respectively.

One of the critical results from this approach is that finite or infinite blocks that are between the two discontinuities can be defined according to the 0X,-0X,

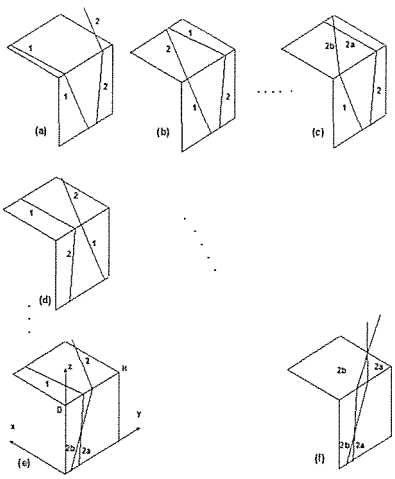

Figure 6. 81 different 3D situations for combined YZ and XY surfaces.

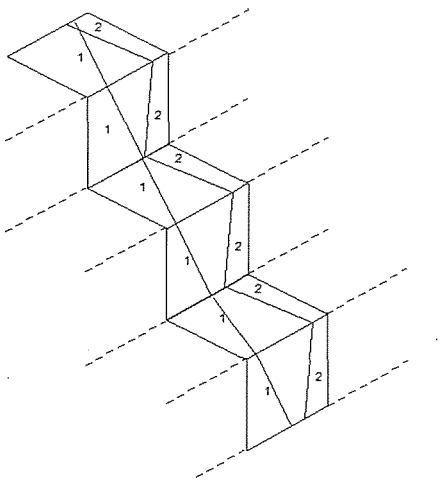

Figure 7. Adaptation of the situation [YZ1-2XY1-2] to part of an open pit.

0Y,-0Y, 0Z and -0Z axes. For example, the first situation in Fig. 6(a) shows that the block of interest (visible surfaces of it are shown with grey tone) can be defined in 3D along the 0X,-0X, 0Y,-0Y, 0Z and -0Z axes as infinite, finite, finite, finite, infinite and finite, respectively. These definitions can be obtained simply for the other situations, as well. In addition, this visual approach enables directly showing which in-situ blocks are bounded by discontinuity planes and free surfaces. For example, in the last situation shown in Fig. 6(f), if the two intersection points on the XY and ZY surfaces are combined with a line segment using basic computational geometry, a tetrahedron (wedge) structure (visible surfaces of it are shown with grey tone) can be reached simply.

In addition, the in situ rock blocks will acquire significance in several analyses, such as sliding or stability analyses, when

Table 3. The intersection points for the sample in Fig. 2.

Coordinates/ points	A	B	C
X	0.000	10.000	10.000
Y	0.000	0.000	0.000
Z	0.000	0.000	13.000
Coordinate points	D	E	F
X	0.000	0.000	10.000
Y	0.000	30.000	30.000
Z	13.000	0.000	0.000
Coordinates/ points	G	H	I
X	10.000	0.000	0.000
Y	30.000	30.000	9.533
Z	13.000	13.000	0.000
Coordinate points	J	K	L
X	10.000	10.000	0.000
Y	3.455	9.810	15.587
Z	0.000	13.000	13.000

Table 4. Isometric coordinates for the sample in Fig. 2.

Coordinatetes/ points	A	B	C
Y"	0.000	(-)7.071	-7.071
Z	0.000	4.082	14.695
Coordinate points	D	E	F
Y"	21.213	21.213	14.142
Z"	10.613	12.246	16.328
Coordinatetes/ points	G	H	I
Y"	14.142	21.213	6.740
Z	26.941	22.859	3.891
Coordinate points	J	K	L
Y"	-4.628	2.121	11.021
Z"	1.410	18.699	16.976

the engineering structures are regarded together. The rock mass of interest can be assumed to be an engineering structure such as a slope in open pits, a highway or a dam wall. In this paper, each of the 81 situations are regarded as engineering structures, such as a rock cut, with only one step or element that is part of a larger engineering structure, such as slopes belonging to an open pit. However, only one situation of the 81 situations should be valid for repeated structures such as in an open pit. For example, adaptation of the situation [$YZ_{1\text{-}2}XY_{1\text{-}2}$] to part of an open pit can be followed in Fig. 7.

It is possible to calculate where the coordinates of the intersection points are located, if they exist. For such structures, except for the coordinates of the intersection point between two traces, the axis the intersection point lies on (horizontal or perpendicular) can be calculated by dividing the height and width of the intersection point by the slope height and width, respectively. Eq. 3 can be used to calculate the intersection point in both the YZ and XY planes, and the coordinates obtained combine to be a final coordinate (x=0 on the perpendicular surface and z = 0 on the horizontal plane). A sample will be explained in field applications.

For a numerical example, the imaginary situation in Fig. 2 is regarded. Let the representative prism dimensions be (10 x 30 x 13 m); c_1 = 10 m, β =65° and φ=120°. The intersection point of the two lines can be solved as (x_3, y_3, z_3) using Eq. 3. For this sample, Table 3 is given.

4.3 Isometric Transformation

In the model, the isometric perspective method was used as the visualization tool. In the isometric perspective method, a sample object is first rotated 45° through the 0Z axis and then 35° 26' through the 0X axis. in an isometric scale are 2/3 times the true length or approximately 80 percent of true size. The derived formula consists of the first and the final transform points of the sample object edges (Eq. 4).

$$P(y'',z'')=\left[0.7071(-x+y),\ 0.40820(x+y+2z)\right]$$

Here, P (y ", z ") is the final isometric point, and P(x, y, z) gives the real coordinates of the point.

For the sample in Fig. 2, isometric coordinates (y ",z ") for the real point coordinates (x, y, z) can be calculated using Eq. 4 as follows in Table 4. In addition, the scale is the isometric scale in Fig. 2.

In this model study, 3D visualizations of the discontinuity planes have been obtained that use two discontinuity traces on the XY and YZ surfaces, which are project to hidden surfaces.

5 FIELD APPLICATIONS

Two fields were selected for the field application. The first one is in the south sector of the Doğankuzu North Block Bauxite Open pit (Fig. 8(a)). The open pit is located in the Central Taurus 3 km southeast of Madenli Village, 25 km south of Seydişehir, and connected with the Konya-Antalya main road at km 28. The main formation in this field is bedded crystalline and dolomitic limestone. Two types of joint sets were investigated, and one of them is approximately perpendicular to the bedding. The two joint traces selected on the excavated surfaces are approximately shown as red

lines in Fig. 8(b). Measurements were taken from initial point (A) (Fig. 2) along the 0Y axis with scan line surveying.

The second and third applications were realized on two road cuts near the province of the first application (Fig. 9 (a) and 10(a)). The main formations are also bedded limestone, and two distinct joint traces on the excavated surfaces are approximately shown with red lines in Fig. 9(b) and Fig. 10(b).

In the first application, if the two joints are considered individually on the YZ surface, the first one that intersects the scan line ($\beta_2 = 65^o < 90^o$) is referred to as [YZ_2] and the second one that intersects the scan line ($\beta_1 = 105^o > 90^o$) is referred to as [YZ_1]. In addition, if the two joints are considered together on the YZ surface (C2= 1 m and C1= 29 m), the [$YZ_{2\text{-}1}$] situation is valid for the excavated surface on which data was taken. Furthermore, if the situation on the YZ surface were combined with the XY surface ($\varphi_1 = 115^o$ and $\varphi_2 = 74^o$), the situation [$YZ_{2\text{-}1}$ $XY_{2b\text{-}2a}$] is reached. The coordinate points of the intersection point can be calculated using Eq. 3, resulting in (0, 18.73, 37.5) on the YZ surface. Similarly, the (28.3, 0, 37.5) coordinate points can be reached on the XY surface. From here, final coordinate is obtained as (28.3, 18.73, 37.5). This

(a)

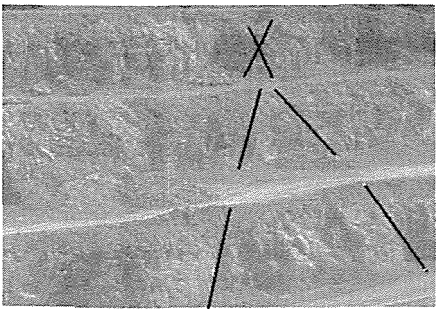

(b)

Figure 8. First application field; (a) modeled sector of the open pit; (b) the two joints selected on the excavated surfaces (shown with the red lines).

(a)

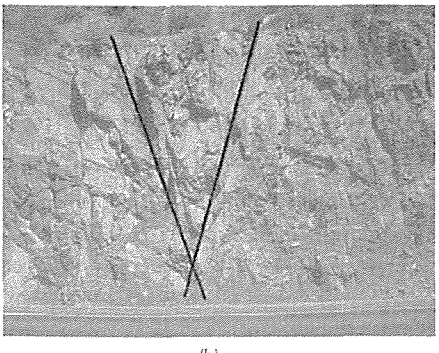

(b)

Figure 9. Second application field; (a) modeled road cut; (b) the two joints selected on the horizontal surface (shown with the red lines).

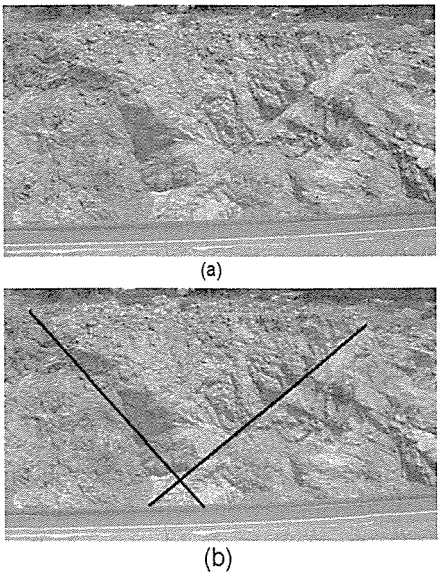

Fig. 10. Third application field; (a) modeled road cut; (b) the two joints selected on the horizontal surface (shown with the red lines).

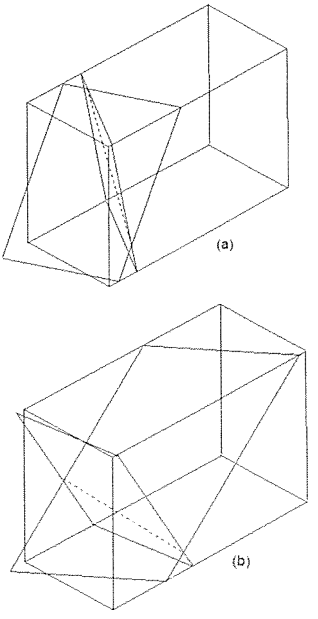

Fig. 11. Isometric representations; (a) for the second and (b) for the third applications.

coordinate point is on the horizontal surface of the third step, regarding the approximately 13 m slope bench and 6.5 m slope width.

For the second and third applications, the same calculation can be realized. The [$YZ_{2\text{-}1}$ $XY_{2\text{-}1}$] and [$YZ_{2\text{-}1}$ $XY_{1a\text{-}1b}$] classifications can be obtained for the second and third application, respectively. Here, the obtained intersection points (discontinuity trace-discontinuity trace, discontinuity trace-prism edge and prism edge-prism edge) were used in LIP-RM (Linear Isometric Projection of Rock Mass) code (Turanboy and Ülker, 2008) and isometric representations are given in Fig. 11 (a) and (b). For this analysis, discontinuity planes, intersection points and lines are illustrated. In Fig. 11(a), the tetrahedron (wedge) formed can be seen clearly.

In the last two applications, the height of the rock cut is used directly.

6 CONCLUSIONS

First, because the developed classification is evaluated in an engineering structure, more effective and meaningful results are reached.

In this study, a rock structure was taken as a sample rectangular prism. Discontinuities were analyzed as linear features within this prism. In the field, simple measurement instruments, including a tape measure and a compass-clinometer, were adequate to collect the data from the exposure of rock masses.

It is well known that natural blocks slide on a planar surface or a wedge of two planes with a down slope-oriented intersection. Based on the results, the rock blocks were adequately modeled in 3D as finite or infinite for many practical engineering and pre-evaluation applications. By developing the present

model, it is possible to analyze rock masses for detailed slope stability engineering applications.

The proposed method is a quick and simple analysis tool for evaluating the geometry of in situ rock blocks that are visible on a surface of rock slopes.

In this study, even using the basic mathematical rules and an appropriate visualization method, it is provided that the geometries of possible sliding rock blocks can be acquired.

REFERENCES

El-Ramly H, Morgenstern NR, Cruden DM (2002) Probabilistic slope stability analysis for practice. Can. Geotech. J. 39: 665– 683.

Park HJ, West TR , Woo I (2005) Probabilistic analysis of rock slope stability and random properties of discontinuity parameters, Interstate Highway 40, Western North Carolina, USA, Engineering Geology 79: 230-250.

Coates DF (1967) Rock mechanics principles. Canadian Department of Energy, Mines and Resources, Monograph, 874.

Goodman RE, Shi GH (1981) Geology and rock slope stability—application of a "keyblock" concept for rock slopes," Proceedings 3rd International Conference on Stability in Open Pit Mining, Vancouver.

Goodman RE, Shi GH (1985) Block theory and its application to rock engineering. London: Prentice-Hall.

Warburton PM. (1981) Vector stability analysis of an arbitrary polyhedral rock block with any number of free faces. International Journal of Rock Mechanics and Mining Sciences & Geomechanics Abstract 1981; 18: 415-427.

Hoek E, Bray JW(1974) Rock Slope Engineering, The Institution of Mining and Metallurgy, London, England.

Rocscience (2004) Rocscience Software Products, DIPS, SLIDE, ROCFALL, SWEDGE, Toronto, Rocscience Inc.

Itasca (2001) Itasca Software Products, FLAC2D/3D, UDEC, 3DEC, PFC2D/3D, Minneapolis. Itasca Consulting Group.

Childs EC (1957) The anisotropic hydraulic conductivity of soil. J. Soil Sci. 8(1): 42–47.

Snow DT (1965) A parallel plate model of fractured permeable media. Ph.D. dissertation. University of California, Berkley.

LaPointe PR, Dershowitz WS, Foxford T (1997) Reservoir compartmentalization, fractured reservoir discrete feature network technologies. Research report, Golder Associates, Redmond, Washington, 26 pp.

Peaker SM (1990) Development of a simple block size distribution model for the classification of rock masses. M.Sc. thesis, University of Toronto.

Maerz NH, Germain P (1996) Block size determination around underground openings using simulations. In: Franklin, J., Katsabanis, T. (eds.), Measurement of blast fragmentation. Balkema, Rotterdam, 215-223.

Hadjigeorgiou J, Grenon M, Lessard JF (1998) Defining in-situ block size. CIM Bull. 91(1020): 72–75.

Jern M (2004) Determination of the in situ block size distribution in fractured rock, an approach for comparing in-situ rock with rock sieve analysis. Rock Mech.Rock Eng. 37(5):391-401.

Turanboy A, Ülker E (2008) LIP-RM: an attempt at 3D visualization of in situ rock mass structures, Computational Geosciences, 12(2): 181-192.

A Landslide Analysis for the Post Coal Mining Sites Developed in the Course of the Reclamation and Forestation

Üretimi Sona Ermiş Kömür Sahalarının Yeniden Düzenleme Ve Ağaçlandırma Faaliyetleri Sırasında Gelişen Bir Heyelan Analizi

N. Tokgöz

İ.Ü. Mühendislik Fakültesi, Maden Mühendisliği Bölümü, İstanbul

ABSTRACT In this study, to determine the effects of water erosion on the stability of a landslide which occurs during the reclamation and forestation processes located in the northern coastal part of the Agaclı / Istanbul. Due to this reason, the study was focused on the runoff waters and the stock watering ponds. The continual water flow, which is observed in the summer months, made this problem to be scrutinized. In order to research place of the water, the vertical electrical sound method was used. It has been determined that this water comes from the water storage ponds that have been formed so as to store uncontrolled run-off waters. In conclusion, insitu observations and measurements indicate that water erosion and the development of gullies in the afforested area have stopped. However, gullies have been constantly enlarging and deepening in the bare material area, due to uncontrolled run off waters.

ÖZET Bu çalışma, İstanbul'un kuzeyindeki Ağaçlı Yöresinde üretimi sona ermiş bir kömür ocağının, yeniden düzenleme ve ağaçlandırma faaliyetleri sırasında karşılaşılan bir heyelanın oluşma ve gelişme sürecinde, su erozyonun etkisini belirlemeye yöneliktir. Bunun için özellikle kontrol edilemeyerek yüzeysel akışa geçen sular ile bunları önlemek için kullanılan depolama havuzlarına odaklanılmıştır. Yerinde gözlem ve ölçmelere dayanarak, yaz aylarında heyelan tabanındaki yarıntılarda saptanan sürekli su geliri, bu konunun daha ayrıntılı araştırılmasını gerektirmiş ve bu suyun yerini belirleyebilmek için "düşey elektrik sondaj yöntemi" kullanılmıştır. Sonuç olarak; ilgili gözlem ve ölçmeler, bu suyun heyelanın doğusunda yüzeysel akışa geçen suların toplandığı bir su depolama havuzundan geldiğini ve heyelanı tetikleyerek genişlettiğini göstermiştir. Ayrıca, ağaçlandırılmış alanda su erozyonu ve buna bağlı yarıntıların gelişiminin durduğu, çıplak alanlarda ise sürekli genişleyerek derinleştiği gözlenmiştir.

1 INTRODUCTION

Successful mining reclamation requires geological and ecological data, in addition to engineering data, to ensure the selection of a land use compatible with the environment. In particular, topsoil replacement is a key component of land reclamation at post-coal-mining sites. In particular, reclamation strategies for landslide-prone slopes usually involve a reduction in water infiltration by the construction of drains at the head of the slope, drainage of water from the toe of the slope, and the use of chemical additives to stabilize clays. It is well known that the infiltration of water is a common trigger for landsliding. Water acts to increase the weight of the material upon the slope until the downward force exceeds the resisting force, resulting in failure. Water also acts as a lubricant, reducing frictional resistance to sliding. Finally, many clay minerals expand when exposed to water, and some saturated clays are prone to flowing and sliding behavior (Murray 1972).

To understand the processes leading to the initial development and subsequent growth of rills and gullies, we must first consider the specific hydrologic and topographic conditions of the area of interest. Previous laboratory- and field-based studies have investigated gully erosion and sought to predict the amount of soil loss upon hill slopes (Heede 1976, Rickson and Morgan 1988, Morgan and Rickson 1995).

For many geomorphologic structures (both natural and man-made), shallow landsliding is one of the most important components of hillslope denudation, thereby playing an important role in determining the magnitude of sediment transport (Burton and Bathurst 1998). Because the triggering of shallow landslides by rainfall events and consequent erosion and deposition are highly sensitive to changes in land use and land cover, there exists the need for methodologies for evaluating the effect of such changes on landslide occurrence. A major obstacle in terms of assessing rates of landsliding is the difficulty involved in obtaining data over medium to long time scales.

The long-term magnitude–frequency distribution of landslides is usually estimated from rates calculated over decadal time-scales, based on analyses of aerial photographs (Hovius et al., 1997; Martin et al., 2002). Analytic expressions such as power-law models are then fitted using probability density functions for empirically derived landslide properties such as area or volume (Hunter, 2003). Previous studies have sought to link climate data with landslide inventory data and to identify, for example, the magnitude of storms that trigger landslides (Glade 2003). Heede (1976) and Istanbulluoglu et al. (2004) investigated the effects of forest vegetation and disturbance to the vegetation on total sediment production by several erosion processes (e.g., runoff, creep, gully erosion, and landsliding).

Shallow landslides result in the rapid downslope movement of slope material in the case that failure occurs along a well-defined shear plane. Such movements are commonly triggered when intense rainfall results in high pore pressure at the contact between the soil mantle and an underlying impermeable layer, thereby leading to saturation of the soil and a reduction in the factor of safety (Montgomery and Dietrich 1994). Shallow landslides generally evolve into debris flows due to water infiltration

(Borga et al. 2002).

The electrical resistivity method, herein referred to as vertical electrical sounding (VES), is used to detect vertical or lateral variations in the electrical properties of geologic material. In the fields of engineering and hydrogeology, seismic refraction (using sound waves) is also employed in many applications. This method involves accurate measurement of the travel time of the sound wave from the source to refracting layers, along the layers, and finally back to detectors (geophones) at the surface.

The present paper examines the factors and process responsible for triggering a landslide–gully complex in response to changes in land use. The landslide gully-complex events correlated with some geological - geophysical researches are presented which could be assessed the possibility of slope instabilities in the regions investigated.

2 STUDY AREA

2.1 A Post-Coal Mining Site and Its Production-Reclamation-Forestation History

Coal was found in the Agaclı Region prior to 1908, leading to widespread mining by various methods by 1914. A topographic map of the area compiled in 1908 shows the locations of coal mines, thereby indicating that mining operations began prior to 1908. Today, coal is still extracted by surface mining at recently established mines located on the coast between Kilyos and Karaburun (Tokgöz and Izibelli 1995; Tokgöz 2003).

In total, 19527 ha of land is subjected to an operation certificate for mining, with 4991 ha already under excavation. The land-use pattern, surface topography, and coastline in this area have experienced constant change since 1908 because of ongoing surface mining (Figure 1). Eighteen small-scale coal mines have operated in the area. Between 1995 and 2006, around 100 million m^3 of overburden was removed each year to extract 4.5 million tons of coal, corresponding to a stripping ratio of 22 m^3 of overburden per ton of coal.

Coal seams extend beneath the Black Sea in some regions. In order to extract this coal (-40 m), overburden material is used to fill in these regions a lagoon forms over the coal mine, and the water is drained away. The next step is to reach the depth of the coal by removing the dumped overburden (Tokgöz and Izibelli 1995; Tokgöz 2003, 2004, 2005). Coal production has currently reached the –40 m level.

Topsoil replacement is a crucial component of land reclamation at abandoned mine sites. In particular, topsoil must be removed and stored prior to mining to enable its use in later remediation works. In the present case, large amounts of Pliocene and Miocene overburden were removed and transported to nearby valleys in order to reach the coal beds, which are located at depths below the surface of up to 100 m or more. These works changed the topography of the area, resulting in new landforms such as hills and ponds, and changes to the coastline.

In the autumn of 1988 and spring of 1989, a forestation program (67.5 ha planted in Maritima Pine, Stone Pine, and Pseudoacacia) was initiated at a site in the Agaclı Region covered in residual soil material. The aim of this program was afforestation of an abandoned opencast coal mine within non-calcareous Pliocene-I sediments (sandy loam, loam, and clay) (Kantarcı 1989; Tokgöz 2003).

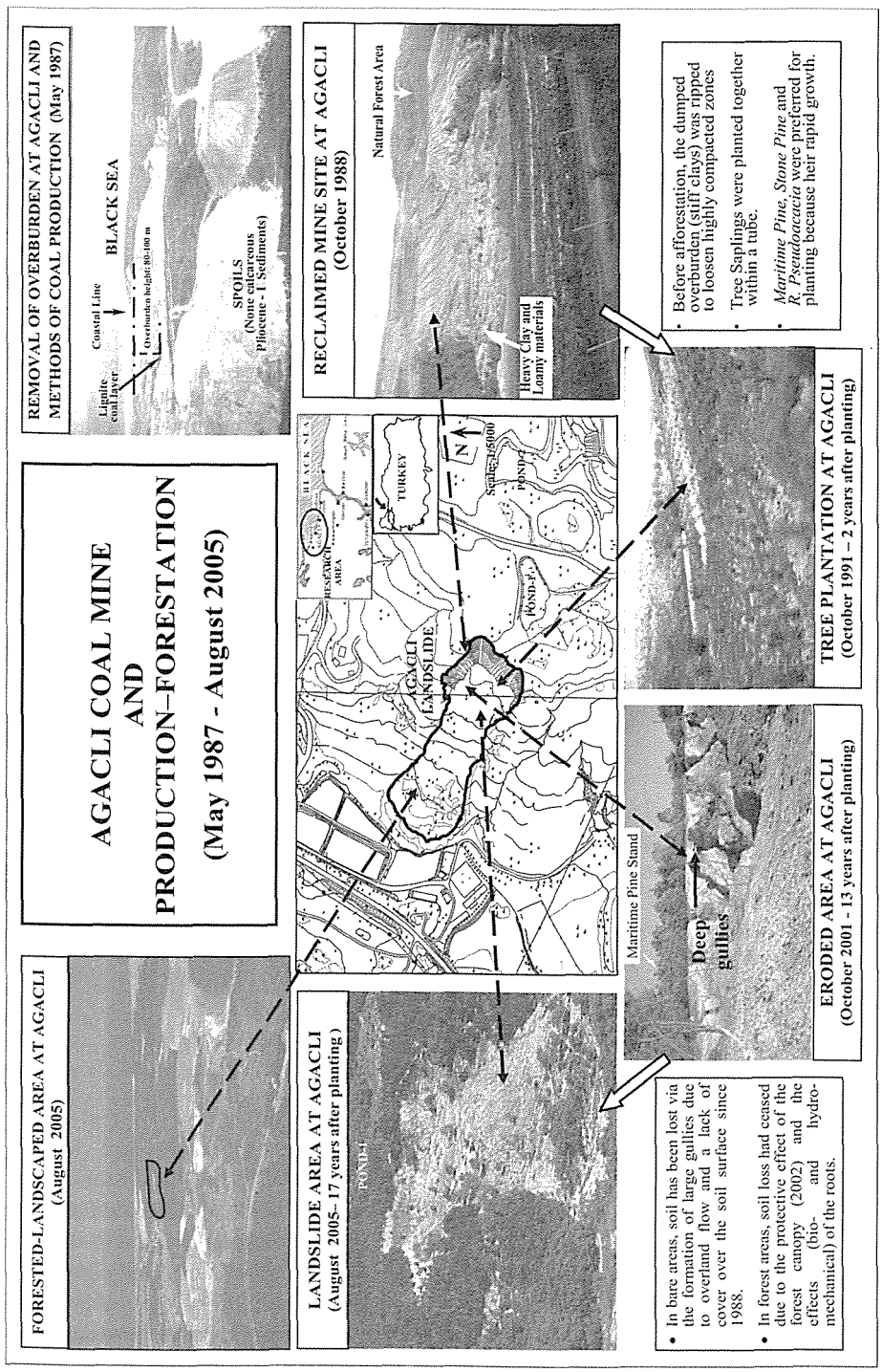

Figure 1. Production-Reclamation-Forestation History of a Coal Mine (Tokgoz 2007)

Several years after planting, when the trees were only saplings, a landslide developed at the site, extending over 470 m in length, 118 m in width and ranging in elevation from +11.80 m to +70.00 m above the bed of Agaclı Stream [Figure 2 (b) and (c)]. Deep gullies have since developed across the landslide (both on the flanks and central portion) in areas of bare soil, and are currently 100–120 m in length and 45-110 cm in width and 80-220 cm in height (Figure 1).

Minor gullies have also formed upon the landslide in response to heavy rainfall. Tension cracks develop in areas with steep (sometimes vertical) slopes, in low- strength soil. During rainy periods, water infiltrates the cracks and, because drainage is usually much slower than infiltration, high hydrostatic pressure (pore water pressure) develops, leading to block failure (Figure 3).

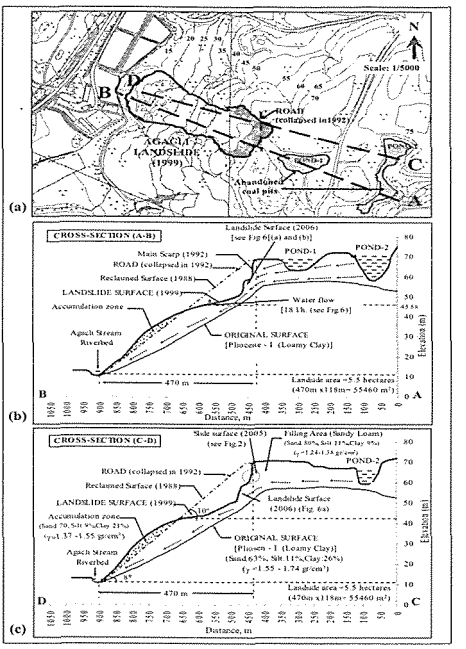

Figure 2. Map (a) and Cross Section (b and c) of the Agaclı Landslide.

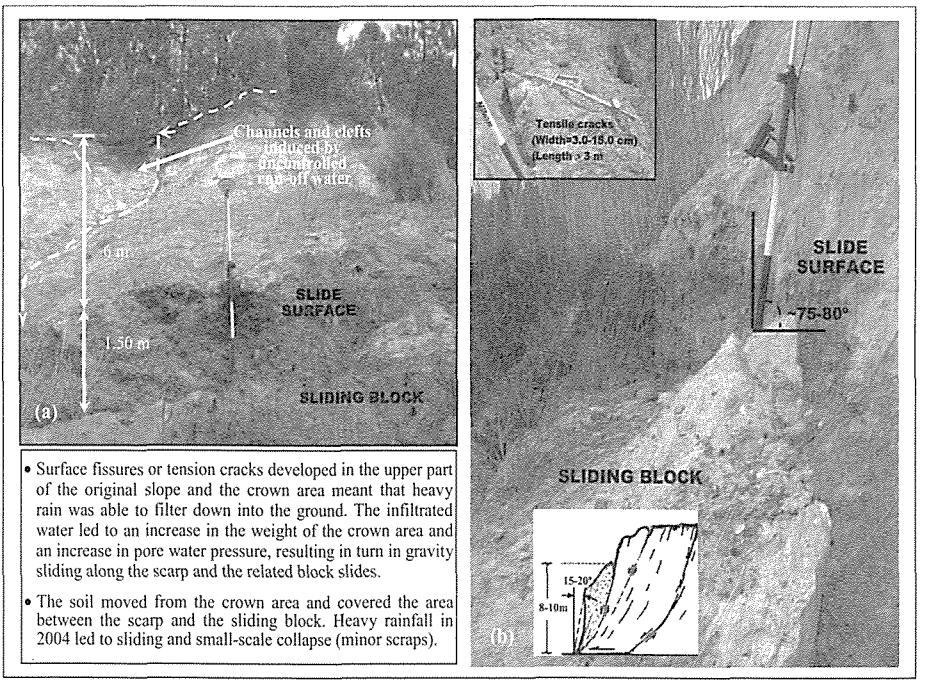

- Surface fissures or tension cracks developed in the upper part of the original slope and the crown area meant that heavy rain was able to filter down into the ground. The infiltrated water led to an increase in the weight of the crown area and an increase in pore water pressure, resulting in turn in gravity sliding along the scarp and the related block slides.
- The soil moved from the crown area and covered the area between the scarp and the sliding block. Heavy rainfall in 2004 led to sliding and small-scale collapse (minor scraps).

Figure 3. Progression of block-type failure [(a)- front view and (b)- side view in the field)] (Tokgoz 2007).

3 INVESTIGATION METHODS AND FINDINGS

3.1 Analysis of Rainfall Data

Many landslides are triggered by the infiltration of rainfall. To investigate the possibility that rainfall triggered the development of the landslide considered in the present study, we reviewed annual precipitation data recorded at the Kumköy meteorological station over the past 35 years (Figure 4).

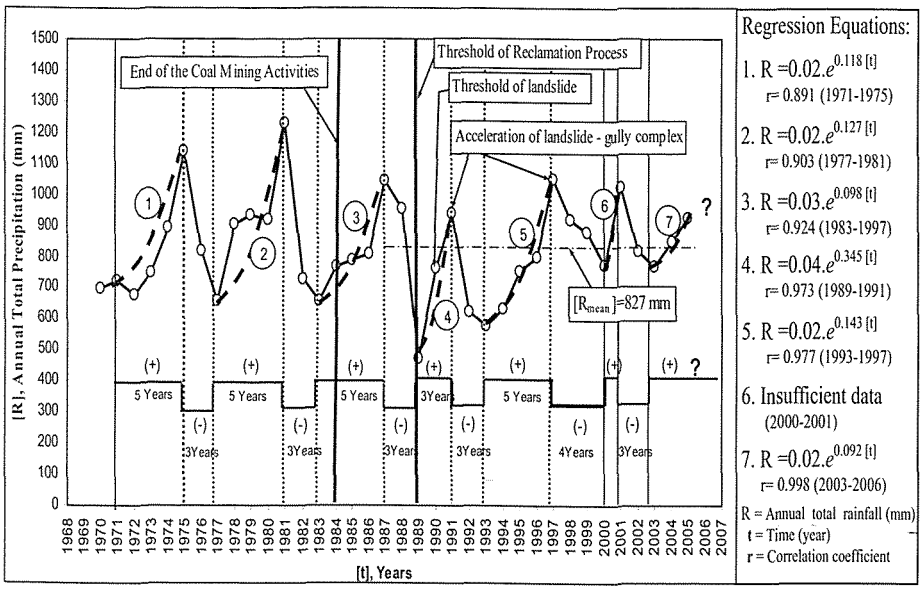

Figure 4. Analysis of annual total precipitation during 1970-2005 period.

Periods of increasing precipitation were analyzed using a regression technique with an exponential form. The analysis revealed the following points:

- Between 1970 and 1997, precipitation was strongly periodic, characterized by 5 years of increasing precipitation followed by 3 years of decreasing precipitation. The constants obtained for the regression equations support the occurrence of a periodic rainfall pattern (see the right-hand side of Figure 4).
- A rainfall intensity of about 60 mm/hour is estimated to be the threshold value at which the 1991 landslide would have been initiated. Because the infiltration of water led to an increase in the weight of the crown area and an increase in pore water pressure, the soil moved from the crown area, covering the area between the scarp and the sliding block. It is clear that local high-intensity/short-duration rainfall events influence landslide development.
- During the period 1993–1997, movement of the landslide accelerated when the total annual precipitation reached a maximum value of 1084 mm. The mean annual precipitation was 827 mm during 1988-2006.
- The years with greatest precipitation (and therefore the critical periods in

which landslide might have occurred) were 1989–1991 and 1993–1997.

3.2 GPS Surveys

To determine the extent of the landslide and gullies, site data were collected in 2006 using Ashtech Promark 2 single-frequency (L1) GPS receivers [Figures 5 and 6 (b)].

Both static and stop-and-go kinematic survey methods were employed. The latter method makes use of an antenna and receiver attached to a rover rod; consequently, after an initialization period, locations are determined by collecting GPS data for a short period (30 seconds in this study) before moving on to the next point, hence the term "stop-and-go." For such surveys, the accuracy is 12 mm + 2.5 ppm baseline length (horizontal) and 15 mm + 2.5 ppm baseline length (vertical). All of the GPS data were processed using the manufacturer's proprietary Ashtech Solutions software (V2.6), yielding 6832 data points (Figure 5) (Tokgöz 2007).

Figure 5. Determination of gullies and landslide limits with GPS (Promark-2) Surveys (Tokgoz 2007).

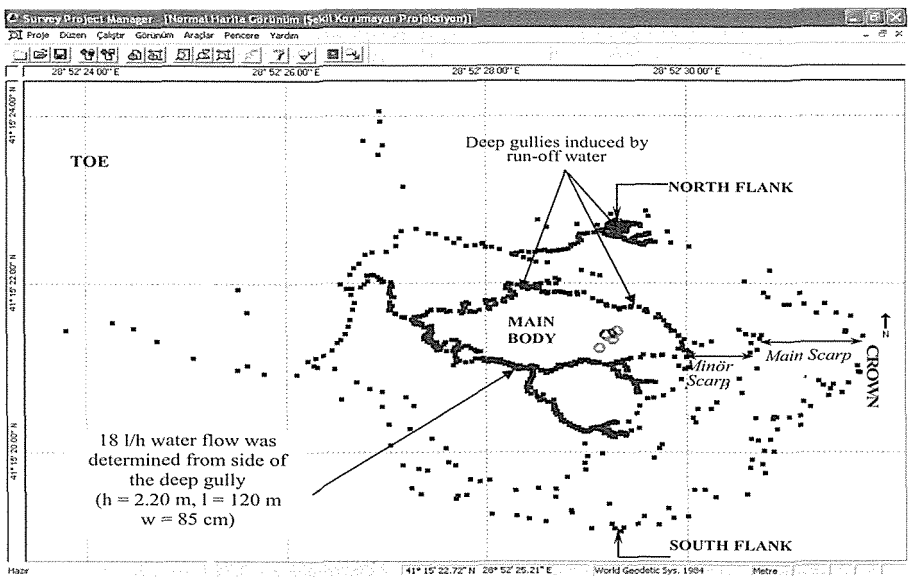

Geophysical Investigation: Method and Results

Geophysical surveys are effective upon unstable, landslide-prone slopes to characterize their internal structure and material dynamics with respect to factors that might contribute to failure. In the present study, VES and seismic refraction methods were used to determine subsurface variations in resistivity and dynamic elastic parameters (Figure 6 and Table 1).

Since 2002, water flowed through the main body of the landslide (i.e., the landslide floor) at a rate of approximately 18 l/h, across an altitude difference of 24.12 m (between 70.00 and 45.88 m); this flow has negatively affected the stability of the landslide. When the water flow was measured on the gully floor, it

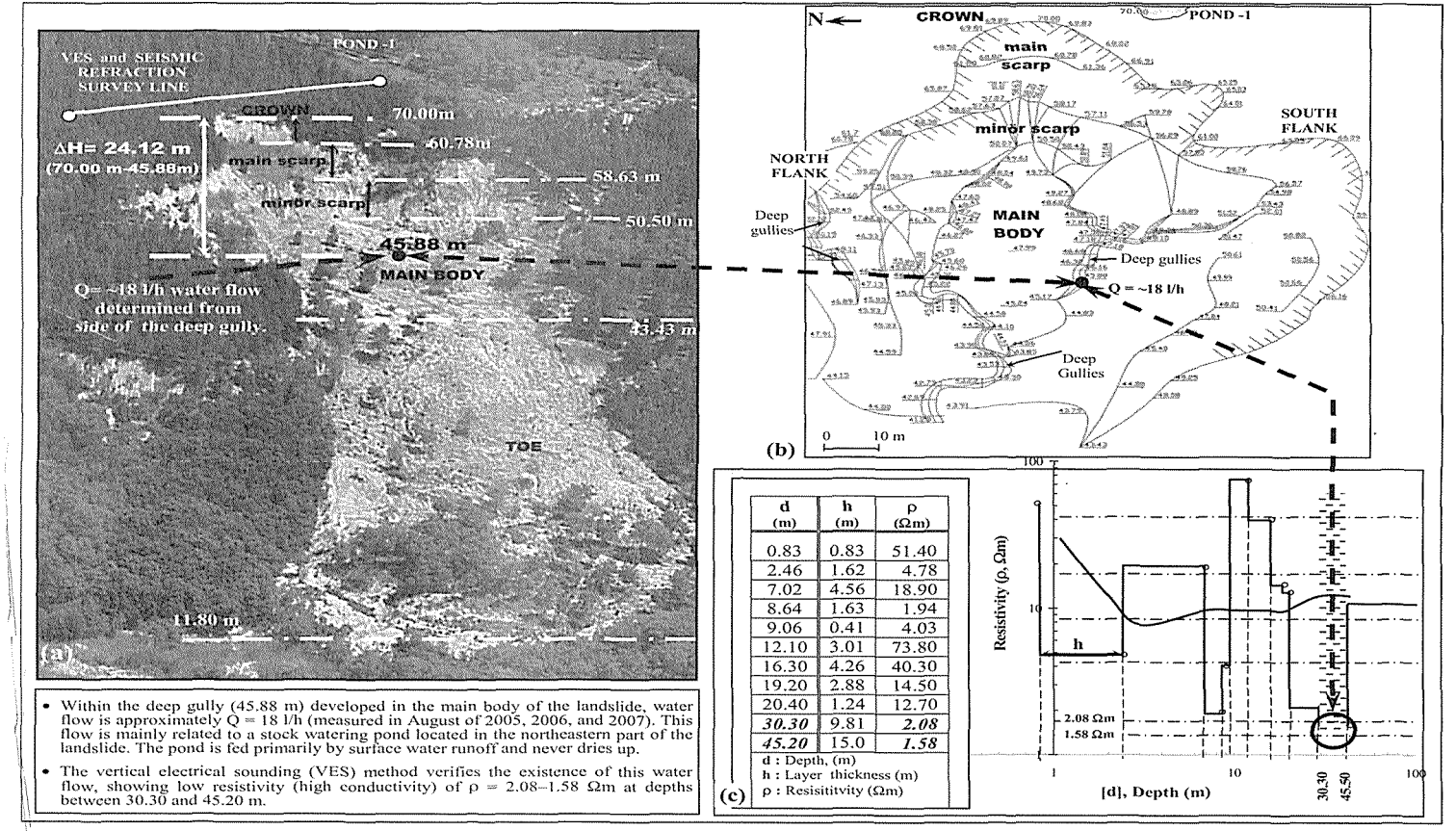

Figure 6. Determination of water flow that triggered development of the Agacli landslide, based on geophysical data (Tokgoz, 2007)

was surrounded by small concrete walls (50×50 cm^2) to enable collection of the water. A steel pipe was sealed within the wall as a water outlet. A 1 liter measuring box was chosen as a scale, with a filling time of about 200 sec., equating to a flow rate of 18 l/h. Of note, the same flow rate was measured in August 2006, highlighting the need to investigate the flow. To this end, a VES survey was performed to investigate the water flow (Figure 6 and Table 1).

The VES data reveal two main subsurface layers: a surface layer with high resistivity and low conductivity (51.40 Ωm; thickness, 0.83 m), a layer with similar resistivity (73.80–40.30 Ωm; thickness, 3.0–4.0 m) consisting of loose sandy material, and finally a layer of very low resistivity and high conductivity (2.08–1.58 Ωm; thickness, 9.81–15.00 m) consisting of saturated, porous sediment. The VES data raise the possibility of water flow between 30.30 m

Table 1 shows seismic refraction data along five transects overlaid on resistivity. Two main layers are detected in all five profiles. The first layer extends from the surface to an average depth of 16 m, and has an average V_p value of about 337 m/s, typical of loose material such as coarse sand. The second layer, which has a maximum average V_p of 1974 m/s, is found at depths of 16–30 m, with an average thickness of 14 m. The V_p value indicates the existence of water or porous material in this layer.

4. RESULTS AND DISCUSSION

During reclamation and forestation, dumped overburden material, especially relatively heavy material such as loamy clay, is compacted, stiffened, and hardened beneath overlying pallets and the paths of heavy vehicles. This results in turn in a reduction in pore size, meaning that the roots of saplings cannot take in sufficient air or water, thereby blocking the spread and development of roots. Furthermore, the stiffened material can no longer absorb rainwater, meaning that clay minerals become saturated and swollen by rain and snow during autumn and winter. Spring rains, especially high-intensity rains, result in the development of gully erosion over the dumped overburden material. Swelling of the mineral grains results in an increase in bulk weight and slippery surfaces which in turn leads to a reduction in gully stability. To overcome these problems, a ripper is used to loosen compacted zones to a depth of 80 cm.

Slope slides that arise from factors such as erosion of the surface of a filled slope by surface rain water, a lack of preventive measures against drainage, and a lack of vegetation on slope surfaces may in fact be more hazardous in terms of degradation that occur in incised slope slides. In fact, land reclamation and plowing (ripping) to a depth of 80 cm and length of 1.0 m encourages rain water to penetrate deep into the ground, thereby reducing surface flow; however, in some areas "gullies" have begun to develop as a result of water erosion, 2 years after afforestation was begun in 1988. Although these gullies are sparsely distributed, they rapidly deepened and enlarged, changing into minor scarps. In the second year of afforestation, these gullies were stabilized by fences (wooden piles) made from the branches of oak trees and strawberry plants. These fences have

largely prevented the development of gullies and the removal of material, as the trees covered the land and lessened

Table 1. Landslide Location and Dynamic Elastic Parameters of the Soil Layer

Location of Landslide

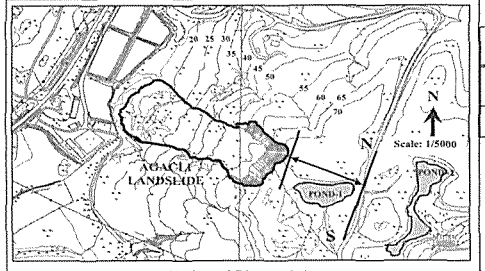

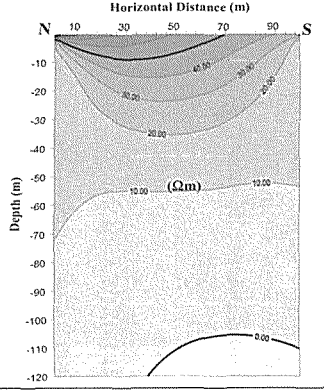

Dynamic Elastic Parameters

Layer	Dynamic Elastic Parameters								
	d	ρ	V_p	V_s	ν	E	k	q_u	q_s
1	16	1.67	337	125	0.42	755	1577	2.08	0.77
2	14	1.99	1974	212	0.49	2733	78066	4.21	0.91

Explanations:

- **d** : Layer thickness (m)
- **ρ** : Unite weight, (g/cm³)
- **V_p** : P wave velocity, (m/sn)
- **V_s** : S wave velocity, (m/sn)
- **ν** : Poisson ratio
- **E** : Elasticity modulus, (kg/m²)
- **k** : Bulk modulus, (kg/m²)
- **q_u** : Ultimate bearing capacity, (kg/m²)
- **q_s** : Safety soil bearing capacity, (kg/m²)

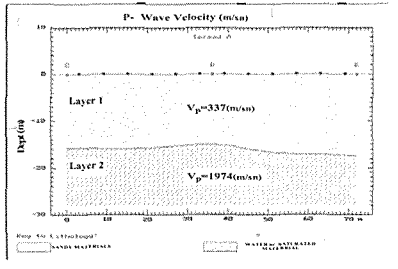

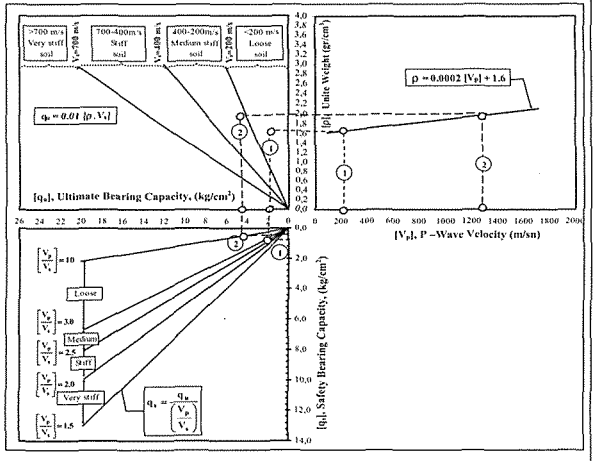

- The north–south directional geo-electrical (vertical electrical sound; VES) ground section was transected along the road, approximately 120 m from the landslide crown. The landslide is located in the western part of this section, whereas the eastern part of the section heads toward the pond. The distance between VES-1 and VES-2 is approximately 90 m.
- Conductivity increases with depth. At depths below 35–40 m, a marked decrease is observed in the resistivity, indicating the presence of ground water. The uppermost 10 m is resistive, indicating porous materials (0.40 <u <0.45) with high conductivity, such as sand, sandy material, or sandy clay. In fact, the development of root systems requires 80 cm of sandy material to be laid down and ripped to increase porosity, upon the existing clay material.

the impact of heavy rains on the surface material, thereby preventing surface flow.

Fine material is transported by rainfall runoff. Field observations at the study site reveal that surface erosion and gully development have ceased in the afforested area; in contrast, gullies continue to grow and deepen in the area without ground cover. During the past 16 years, remarkable differences have arisen between soil material at depths of 0–5 and 20–25 cm. Surface erosion at the site has principally involved the transport of fine material (silt and clay) (Kantarci and Oztürk, 2005).

Our measurements and observations reveal the following findings:

- Geophysical surveys reveal that the uppermost 10 m exhibits high resistivity (low conductivity), indicating porous materials with low conductivity, such as sand and sandy gravel [see Figure 6 (c)]. In fact, the development of tree root systems requires 80 cm of sandy material to be laid down (and ripped) upon the clay material during remediation to increase porosity [see Figure 2 (a) and (b), Table 1].
- The second layer shows decreasing resistivity (increasing conductivity) with depth. This trend is especially marked at depths below 35–40 m, where a remarkable decrease in resistivity is observed due to the presence of groundwater.
- A deep gully (45.88 m) developed within the main body of the landslide records a water flow of approximately 18 l/h (measured in August 2005 and 2006). High resistivity (low conductivity) in this area confirms the existence of this water, which moves across an altitude difference of approximately 24.12 m (Figures 2 and 6). This water is mainly derived from stock watering ponds located in the northeastern part of the landslide. The ponds are primarily fed by surface runoff, and never dry up.

4. CONCLUSIONS

Assessment of the stability of landslides in abandoned mining areas is important for sustainable development. The effects of afforestation of abandoned coal mines in the Agaclı region and the opening up of these areas for forestry have been evaluated within the framework of the basic disciplines of mining, the environment, and ecology. The results of this study led to the following conclusions.

- The observed erosion forms suggest that gully development is associated with landsliding, which developed due to a change in land use following the cessation of coal mining.
- The afforestation of mine overburden was initiated in 1988–1989. The removal of overburden by strong northerly winds and intense rain has been prevented in afforested areas, whereas surface erosion has continued in non-forested areas, resulting in the development of rills and gullies.
- Areas of bare land have formed within the reforestation site. In such areas, rills and gully systems have developed and deepened as a result of uncontrolled surface-water flow.
- Trees were planted in 1988–1989 upon overburden material dumped in an abandoned open- pit coal mine in the Agaclı region. Our study undertaken in 2007 revealed that the material had stabilized following the rapid growth of roots within 16 years of planting. The raw material was bound by tree

roots to a depth of 1.80–2.60 m, as observed within landslide scarps.

- Multiple slides have developed in response to the over-saturation of overburden material following high-intensity rainfall, leading to a reduction in shear strength. The contributions of tension cracks, steep slopes, local high-intensity rainfall, and stock watering ponds have triggered block-type wall failures on the face and flanks of the landslide. These findings are verified by dynamic elastic parameters calculated for the fill layers.
- The studied landslide, which developed within afforestation (*Maritima Pine, Stone Pine, and R. Pseudoacacia*), was triggered by water sourced from two ponds that formed in a deep coal pit in the northeastern part of the larger landslide. Water flow was measured at about 18 l/h during August of 2005, 2006, and 2007. A remarkable decrease in resistivity (increase in conductivity; ρ = 2.08–1.58 Ωm between 30.30 and 45.20 m depth) indicates the existence of groundwater. Loamy clays that previously existed at the ground surface were fed by ground-water sourced from the ponds which have yet to be removed. Since 1991, uncontrolled surface water has triggered gully erosion and rapid sedimentation, resulting in over-steepening. In particular, field observations indicate that the landslide has become enlarged on both flanks as a result of gully erosion. For future control of the landslide–gully complex, planned mitigation measures include pre-saturation of the slope and flanks of the landslide, and the construction of drainage systems to adequately channel surface water away from the landslide. In particular, it is planned to dry the ponds via deflection pits and the use of geosynthetic barrier layers to prevent the infiltration of water into the landslide–gully complex.

ACKNOWLEDGMENT

This work was supported by the research Fund of University of Istanbul. Project number :191/15012004 and UDP-271/06042004. The author would like to sincerely thank to Assist. Prof. Dr. F. Ahmet YUKSEL for geophysical surveys during the field studies.

REFERENCES

Borga, M., Fontana, G. D., Gregoretti C., Marchi, L., 2002. Assessment of shallow landsliding by using a physically based model of hillslope stability, *Hydrological Processes* 16: 2833–2851.

Brand, E.W.,1989. Correlation between rainfall and landslide. *Proceedings 12th International Conference on Soil Mechanics and Foundation Engineering*, 5: 3091-3093, Rio, 1989.

Burton, A., Bathurst, J.C., 1998. Physically based modelling of shallow landslide sediment yield at a catchment scale, *Environmental Geology* 35:89–99.

Glade, T., 2003. Landslide occurrence as a response to land use change: a review of evidence from New Zealand, Catena 51:297–314.

Heede, BH., 1976. Gully development and control: the status of our knowledge. *USDA Forest Service. Res. Paper* No. RM 169, Rocky Mountain Forest and Range Experimental Station, Forth Collins, Colorado.

Hovius,. N., Stark, C.P., Allen, P.A., 1997. Sediment flux from a mountain belt derived by landslide mapping, *Geology* 25:231-234.

Hunter, G. C., 2003. The pre and post failure deformation behavior of soil slopes. *PhD Thesis*, The University of South Wales (www.geotechlinks.com/download/GL2076)

Istanbulluoglu, E., Tarboton, D.G., Pack, R.T., Luce, C.H., 2004. Modeling of the interactions between forest vegetation, disturbances, and sediment yields. *JGR - Earth Surface* 109(F1): F01009, DOI:10.1029/2003JF000041.

Kanlı, A.I., Tildy, P., Pronay, Z., Pınar, A., Hermann, L., 2006. Vs^{30} Mapping and soil classification for seismic site effect evaluation in Dinar region, SW Turkey. *Geophys. J.Int.*, 65: 223-235.

Kantarcı, M.D., 1989. Land use and main ecological research and assessment of open pit coal mining area for forestation at the northern part of Catalca Peninsula (Agaclı/Istanbul Region). *Istanbul University, Faculty of Forestry Press.* Series: A. 38: 60-90, (in Turkish).

Kantarcı, M.D., Oztürk, M., 2005. Surface erosion induced by rainfall on the Agaclı Reclaimed Site and Preventing Effects of the Reforestation. *3rd Atmosphere Science Symposium.* ITU Meteorological Department. In: Sen O, Saylan L, Kocak K, Toros H (eds), Ayasaga / İstanbul,107–130, (in Turkish).

Martin, Y., Rood, K., Schwab, J.W., Church, M., 2002. Sediment transfer by shallow landsliding in the Queen Charlotte Islands, British Columbia, *Canadian Journal of Earth Sciences* 39:189–205.

Morgan, R.P.C., Rickson, R.C., 1995. Water erosion control. In: Morgan RPC, Rickson R (Eds) *Slope stabilization and erosion control: A Biotechnical Approach.* Chapman & Hall 133-190.

Montgomery, D.R., Dietrich, W.E., 1994. A physically based model for the topographic control on shallow landsliding. *Water Resources Research* 30:1153–1171.

Murray, R.M.C., 1972. Geology and land reclamation. *The Ohio Journal of Science*,72:65-74.

Neidell, N.S., 1981. Stratigraphic modeling and interpretation: *Geophysical Principles and Techniques*, 141 p.

Rickson, R.C., Morgan, R.P.C., 1988. Approach to modeling the effect of vegetation soil erosion by water. *Commission of the European Communities Report*, No. EUR 10860 EN., 237-253.

Sidle, R. C., Pearce, A. J., O'Loughlin, C. L., 1985. Hillslope stability and land use, *Water Resources* Monograph 11 Edition, American Geophysical Union,140p.

Tatham, R.H.,1982. V_p/V_s and Litology. *Geophysics* 47:336-344.

Tokgöz, N., Izibelli, U. 1995. Coal deposit and technical characteristics of Istanbul / Agaclı Coastal Line. *Air pollution and coal reality,* Section: III, Arıoglu E. (Ed.). Chamber of Mines - Istanbul Branch, ISBN- 975 - 395 -149 -3, May, 76-90, Istanbul, (in Turkish).

Tokgöz, N., 2003. Research on the effect of the tree roots on the forested land over the open coal mine

residual materials, amelioration and stabilization the land. *PhD Thesis*, Istanbul University, 250 p. (in Turkish).

Tokgöz, N., 2004. Research on the effect of the tree roots on the forested land over the open coal mine residual materials; rehabilitation and stabilization of the land. Proceedings of the Eight *International Symposium on Environmental Issues and Waste Management in Energy and Mineral Production - SWEMP 2004*, In: Pasamehmetoglu G, Ozgenoglu A, Yesilay AY (eds), 17-20 May 2004, Antalya-Turkey, 305-311.

Tokgöz, N,. 2005. A study on the bio - hydro mechanical effects of the tree roots on the Agaclı coal reclaimed-forested land. *Geotechnical and Geological Engineering*, Springer Science (Former Kluwer), 23 (5), September, 519-535 (17).

Tokgöz, N., 2007. Investigation of for post production of coal reclamation-forestation sites based on bio-engineering characteristics. *Research Fund of Istanbul University* (Project no: 191 / 15 01 2004), (in Turkish).

A New Methodology to Suppress Blasting Induced Ground Vibrations: Modelling of Surface Waves

G.G.U. Aldas, B. Ecevitoğlu

Ankara Üniversitesi Mühendislik Fakültesi Jeofizik Mühendisliği Bölümü, Ankara

ABSTRACT This paper is related to the surface waves generated from blasting operations in mines and quarries. To mitigate the blast-induced ground vibrations, we proposed a new methodology quite different from conventional methods which does not take in account the mechanics of seismic waves. The methodology aims to employ most suitable time-delays among blast-hole groupings to render destructive interference of surface waves at the location where the blast-induced vibrations are to be minimized. The crucial point of the proposed methodology is the use of pilot-signal which takes account of the seismic properties of all complex geology between the blast and target locations. Therefore, the methodology does not require any geological model and assumption. The methodology has been implemented on substantial amount of field studies and satisfactory results are obtained.

1 INTRODUCTION

Blast-induced ground vibrations and their mitigation have been discussed by several researchers (Bollinger, 1971, Siskind et al., 1980, Anderson et al., 1982, Anderson et al., 1993, Dowding, 1985, Siskind et al., 1989, Persson et al., 1994, Muller, 1997, Muller and Hohlfeld, 1997, Hoshino et al., 2000, Siskind et.al., 2000, Chen and Huang, 2001, Tripathy and Gupta, 2002, Adhikari et. al. 2004, and many others). They have proposed various approaches to reduce blast vibrations, those includes: use of delay-times between holes, decrease the number of holes sharing the same delay-time, use of deck-charges with or without delay times between decks, ignite at the borehole bottom, and the like. They conducted exhaustive empirical studies to account for the frequency, charge weight, and distance effects of blast vibrations on structural response and damage. Most of the research comprises a database of ground vibration, which contains PPV (Peak-particle-velocity), frequency information, and other vibration-related and blast-design parameters. Regression analysis of the data is carried out to derive site-constants for individual quarries. Evaluation of the whole data yields to a generalized predictor equation to assess and control ground vibration.

$$PPV=k\,(SD)^{-\beta} \quad (1)$$

Where,

PPV: peak particle velocity, mm/s,

k and β are site constants,

SD: scaled distance $SD=R/Q^{1/2}$, R: distance between source-target, Q: explosive amount per delay, kg.

The researchers have also investigated the effect of time-delays among blast-holes, and properties of traversed-medium on dominant frequencies of ground vibrations.

Most studies reported in the blasting literature are merely based on amplitude measurements around some dominant frequencies and on some statistical parameters. However, full waveform studies provide complete information to blast vibration analysis. Those includes: (1) PPV, (2) Blast-frequencies stimulating soil resonance frequencies (wave interferences), (3) Duration of the blast vibrations. Two notable exceptions were the studies of Yamamoto and Noda et al. (1999) and Crenwelge and Peterson (1988). The study of Yamamoto and Noda et al. (1999) depends on prediction of far-field-signal with the help of near-field signal by using stochastic methods (statistical, random, Wiener-Levinson Least Square Algorithms) and applying the appropriate delay-elements to mitigate blast-induced vibrations. We believe that, modeling of dispersive and absorptive surface waves from one station to the other by stochastic methods is not a proper approach. The predictive deconvolution is based on the randomness (normal distribution) of the reflection coefficient series so that the input wavelet can be extracted from the time series to design a deconvolution filter. However, randomness of the reflection coefficients is seldom in practice resulting in the generation of the artificial events which mislead the interpreter. Crenwelge and Peterson's study (1988) depends on: evaluations of two seismic records belong to seismic stations near the blast-area in Frequency domain; determination of impulse-response function belongs to geological structure; prediction of the function belongs to Group-blast by using impulse-response function; optimization of the function belongs to Group-blast to mitigate blast-induced vibration. The researchers determined impulse-response function by using Pilot-blast signal. However, they can easily use Pilot-blast signal directly to model Group-blast signal. The researcher's approach is not wrong but leads to complex calculation. This case brings unnecessary numeric-roll in the calculations.

This paper introduces a new methodology in minimizing blast-induced ground vibrations at the target location, different from the classical approach, which do not take in account the mechanics of seismic waves. The methodology aims to employ most suitable time-delays among blast-hole groupings to render destructive interference of surface waves at the target location (where the blast-induced vibrations are to be minimized).

2 THEORIES AND APPLICATION OF THE METHODOLOGY

The crucial point of the methodology is to use pilot-blast signal. Pilot-blast is constituted of a single or few neighboring blasts in the vicinity of the Group-blast. Pilot-blast signal embraces the seismic properties of all complex geology between the blast and target locations. Therefore, the methodology does not require any geological model and assumption. It is based on two seismic records related to: (1) Pilot-blast, (2) Group-blast. Group-blast is made of Pilot-blasts, i.e. gather of Pilot-blasts representing the Group-blast. The seismic records obtained from pilot and

group blasts share the same blast-design properties, such as explosive types and amount, hole-diameter and depth, etc. We assume that seismic waves initiated from pilot and group blasts should travel the same geological structures, such as lithology, stratigraphy and tectonics. Since Pilot-blast carries whole information related to above sited factors, there is no need to take in account all the details of a complex geology. The data analysis technique used in this work is based on Linear System Theory (Oppenheim and Schafer, 1975, Karu 2002), and its immediate result: the Superposition Principle. Although the blasting event is non-linear in its nature, still linear behavior may be acceptable for practical reasons.

2.1 Data Acquisition

Blast-induced vibrations were recorded by two seismographs. Differing from classical approach, these two seismographs were used in combination with radio-telecommunication units. The details of the system are given below:

The system is composed of one-magneto and three-radio telecommunication units. While one exit of the magneto performs firing, the other exit transfers the firing time to the transmitter radio-station (Magneto and transmitter radio-station are in the same box and form control station). Transmitter radio-station conducts the signal to the Near and Far field receiver radio-stations. Near and Far-field receiver radio-stations transfer the firing time to the "External Trigger" of the seismographs connected to the receiver radio-station units. By this way (external triggering), seismographs start to record.

The aim of using external triggering (by radio signal) is to make the two seismographs start to record at the same time. In classical data acquisition (geophone triggering), first part of the seismic signals cannot be recorded due to delay in recordings. This situation causes error in seismic wave velocity calculation. In order to avoid this case, we used seismographs with radio-telecommunication units. For this way, we can calculate healthy seismic wave velocities which should be considered in determining the locational time-delays (in addition to time-delays given by delay elements). The new methodology requires at least two 3-component seismometers placed on a profile in-line with the source

2.2 Data analysis using newly developed software

Data obtained from Near and Far stations are analyzed with the newly developed software. The analysis software consists of three programs: (1)FILTER, (2) VELOCITY, (3)DELAY

Band-pass filtering is useful in removing the mean (DC) from seismic data at very low frequencies, and suppressing the high frequency noise which becomes dominant for long-travel distances, where S/N (signal to noise) ratio decreases. FILTER program applies the mentioned band-pass filter to the seismic data.

VELOCITY program provides seismic phase velocities, especially approximate velocities of the surface waves. Seismic surface waves are the main source of blast-induced vibrations. In order to compute seismic phase velocities, data from Near and Far Stations are required. To compute the contribution of blast-hole location-

delays to the travel-time, the blast-hole coordinates and approximate surface wave velocities are needed. Surface waves are dispersive in nature, resulting in continuous wave form changes as they travel, causing difficulties in time-break readings. We advise picking the first or the second cycles of the surface waves on Near and Far station seismic records.

DELAY is the main program in the developed software. FILTER and VELOCITY programs prepare seismic data to DELAY program. DELAY program displays the geometry of the individual blast-holes, let the user group the blast-holes and assign appropriate time-delays to each group. If the Pilot-blast is made of more than one blast-hole (due to signal-strength concerns), then each group should be constituted from integer-multiples of Pilot-blast. In practice, more than two groups (each group may have different number of blast-holes determined by the data analysis) should be designed to suppress various wavelengths of the surface waves. However, the prime objective of mining is to properly fragment the rocks. Therefore, when designing the shot-holes with the vibration minimization problem in mind, user should also consider proper fragmentation of the rocks to serve the mining purposes.

To test the developed methodology, an experiment was carried out at Turkish Coal Mine Company's Eskihisar Lignit Mine. Figure 1 shows the topographic map of Eskihisar Coal Mine . P, Y and U illustrate Pilot blast, near-field record station and far-field record station, respectively. The dispersive effects of surface waves are seen clearly (vibration process is longer at far-field with respect to near-field). The amplitudes of particle velocities and frequency contents are higher at near-field record station and they

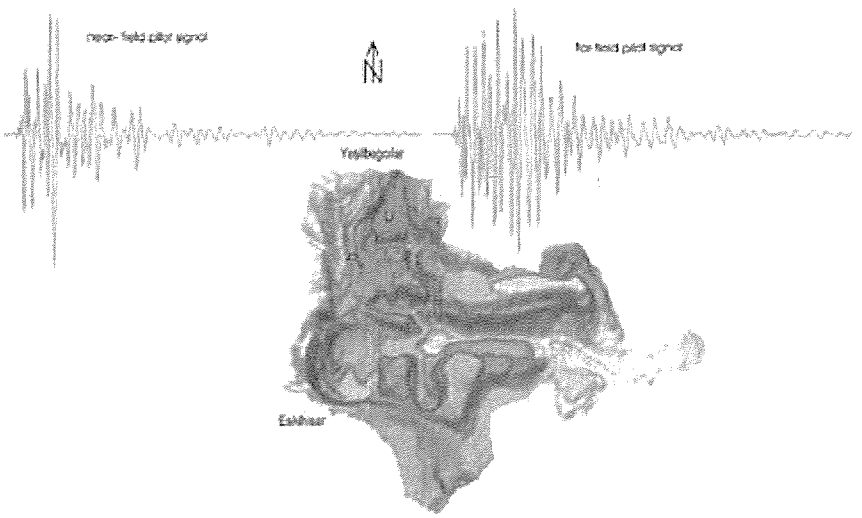

Figure 1. Eskihisar Lignite mine: topographic map.

are decreased at far-field. Decreasing of amplitudes with distance does not mean that vibration-damage risk decreases. With traveled distances, seismic waves loose their high-frequencies. Therefore, wave-lengths extend and this situation causes mechanical resonance between seismic waves and travelled media or structure.

Since the base of the methodology is using pilot-signal, a pilot-hole was prepared for blasting. The pilot-blast parameters were: 20m hole-depth, 100kg ANFO, 0.5 kg primer dynamite. Beside the pilot-blast, 8 blast-holes constituting a group–blast were prepared with the same blast-parameters. Blast-hole diameters were 165mm. Spacing between blast-holes were 10m. Different from classical methods, this methodology deals with only seismic wave. Therefore, we did not interfere to choose the group-blast design parameters (explosive type, amount, hole depths..etc). The engineers who are responsible from blasting in the mine prepared the group-blast as their usual blast-design. Firstly, the pilot-blast was fired to get the signature of the seismic wave-forms between source-target locations. Then, three programs (FILTER, VELOCITY and DELAY) were applied to the pilot-signal in the field to determine blast-hole groupings and time-delays between each group. Band-pass filter parameters applied to pilot signal were f1=0.0, f2=1.7, f3=10.6 and f4=15.1 Hz. By using VELOCITY program, surface wave velocity was determined as 850m/s. This information was given to DELAY program as an input to calculate locational time-delays. Because, for especially low surface wave velocities, locational time delays become important and they must be added to the time delays given by delay-elements.

Upper left quadrant of Figure 2 displays the blast-hole configuration at DELAY program. Blast-holes are shown with various colored circles with hole-numbers in them. Blast-holes sharing the same color are blasted simultaneously. The green arrow points the target location (The Far station) which is out of the figure's scope. The NE-SW oriented blue-line segment represents the free surface of the blast-bench which should be taken in account while designing the group-blast.

The right corner of Fig. 2 shows: First row: "VerZ" denotes the original seismic amplitudes of the Pilot-blast at the time "Time" (third row). Second row: "VerD" denotes the seismic amplitudes after the implementation of the appropriate time-delays to mitigate the vibrations. "Ver" denotes the Vertical seismic component. In the middle of Fig.2, Transversal (light-blue), Vertical (red), and Longitudinal seismic components (blue) obtained from the superposition of (according to Linear System Theory) the zero-delay Pilot-signals are shown.

Bottom half of Fig. 2 shows: Blast-hole numbers at far left; next, the individual delays corresponding to each grouping in milliseconds (in this case, "000" denotes no-delay); next, the left and right-oriented arrow-heads control the shifts toward early and later times of the Pilot-signal, respectively; colors assigned to Pilot-signals match the colors of the groupings. Blast-holes 01 and 07 constitute one grouping (blue), other holes with different colors (06, 05, 02, 04, 03, 08) constitute their individual groupings, each represented with different row in the bottom half of the Fig.2.

Figure 3 illustrates the DELAY analysis subsequent to the application of appropriate time-delays. In this example, the applied delays are 0ms, 50ms, 150

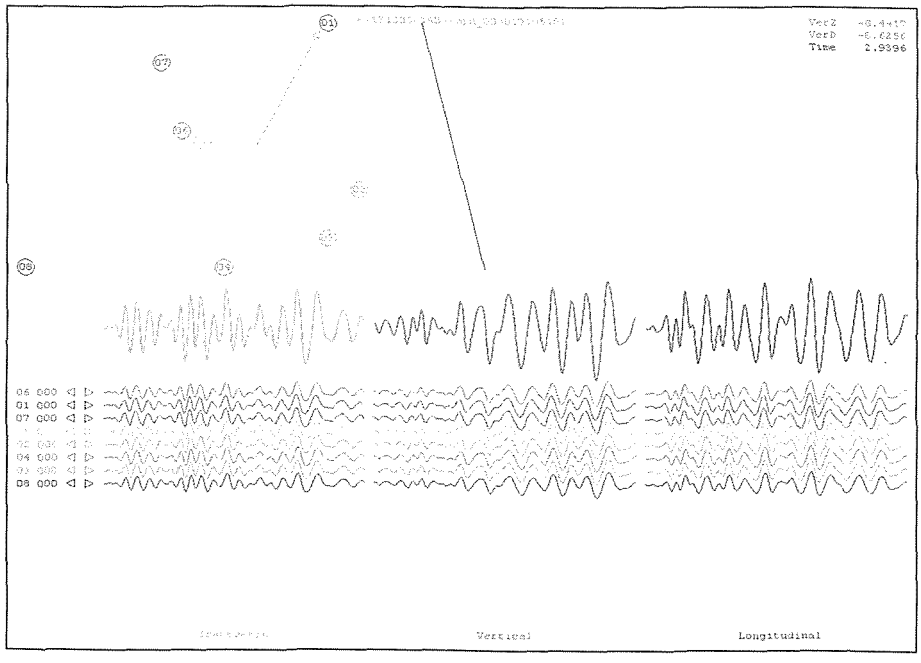

Figure 2. DELAY analysis with zero-delay.

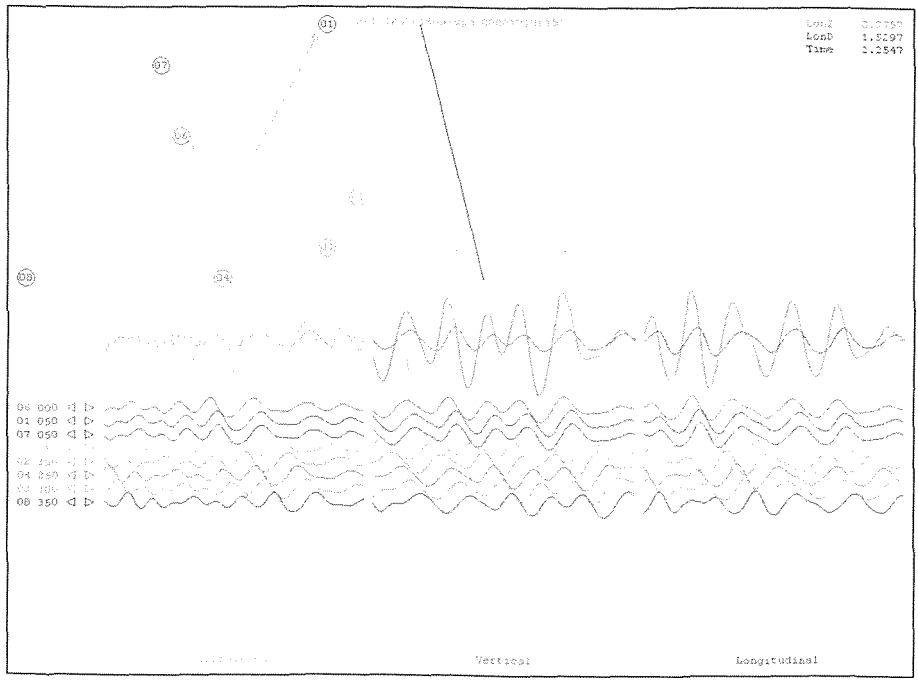

Figure 3: DELAY analysis with delays applied.

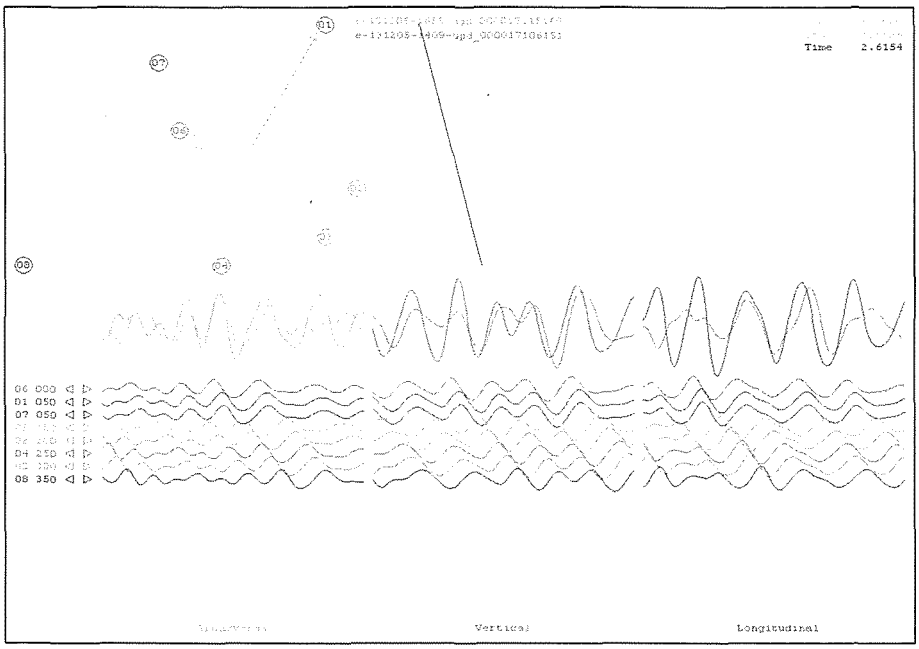

Figure 4. Comparison screen of DELAY analysis.

ms, 200ms, 250ms, 300ms and 350ms corresponding to the blast-holes (6), (1, 7), (5), (2), (4), (3) and (8), respectively. The purpose of this specific blast-design is: Following the collapse of the center of the blast-area upon itself, appropriate time-delays are given to the individual blast-holes to minimize the remaining seismic amplitudes step-by step.

Inspection of the Longitudinal component reveals destructive interference of the seismic signal. For instance, at the time 2.2547s, the modeled amplitude based on the Superposition Principle (Linear System Theory) with zero-delay is 8.3757 units, with appropriate delays applied is 1.5297.

After investigating the pilot signal and determining the blast-hole groupings and their respective time-delays by using three software packages, real group-blast was carried out.

Modelled group blast signal (each blast holes in the group were modelled from pilot signal and optimum time-delays to perform destructive interference of surface waves were applied to each blast-holes in the model group) was compared with real group blast signal. Figure 4 shows the comparison. In the middle of Fig.4, dark-colors denote the modeled-seismic signal, light-colors denote the actual signal (real data). The resemblance of two data should be noted. At the time 2.6154s, the modeled data amplitude is 1.5526 units, the actual data amplitude is 1.3968 units. Comparison of the model and the actual seismic signals reveals that linear system theory works in this experiment.

5 DISCUSSION AND CONCLUSIONS

The theory of the proposed methodology is based on Linear System Theory where

the superposition principle holds. We assume that, there exists minimum amount of interaction among the blast-holes. It is obvious that earlier blasts modify the conditions of the later blasts in a group-blast sequence. This fact causes some discrepancy during the model and real data comparisons (Fig.4).

Advantages of the new methodology with respect to the conventional methods are: (1) Data evaluation is not solely based on PPVs, as it is the case for conventional methods. Seismic wave-forms, their frequency content, and their time-duration are also taken in account, (2) The proposed methodology does not impose any restriction on the amount and type of explosives to be used, and blast-design, (3) The new methodology requires fewer seismic stations than the conventional methods to analyze blast-induced vibrations. Actually, one seismic station located at the target location is sufficient for data analysis, if approximate surface wave velocity is known. Conversely, in case of conventional methods based on empirical models, at least 30 seismic records are needed to make a reliable data analysis.

Although one example data is given in this paper, results obtained from dozens of field studies prove the validity of the methodology proposed.

6 ACKNOWLEDGEMENTS

We are grateful to Turkish Coal Company (TKI) for their continuous support to this project during two full years. We would like to thank to Asli Can, Betul Unucok and Ozgur Sagol for their generous assistance throughout the study.

REFERENCES

Adhikari G.R., Theresraj A.I., Venkatesh S., Balachander R., Gupta R.N., 2004. Ground Vibration due to Blasting in Limestone Quarries. FRAGBLAST – International Journal of Blasting and Fragmentation, 8 (2) 85–94.

Anderson D.A., Winzer, S.R. and Ritter, A.P., 1982. Blast Design for Optimising Fragmentation While Controlling Frequency of Ground Vibration. In: Proceedings of the 8th Conference on Explosives and Blasting Technique, New Orleans, 69–89.

Anderson, D.A., 1993. Blast Monitoring: Regulations, Methods and Control Techniques. In: J.A. Hudson (ed.): Comprehensive Rock Engineering, (4), Pergamon Press, 95–110.

Bollinger G.A., 1971. Blast Vibration Analysis. Southern Illinois University Press, 132 pages.

Bullen K.E., 1963. Introduction to the Theory of Seismology. Cambridge University Press, 381 pages.

Chen G. and Huang S., 2001. Analysis of Ground Vibrations Caused by Open Pit Production Blasts: A Case Study. FRAGBLAST – International Journal of Blasting and Fragmentation 5(1), 1-2, 91-107.

Crenwelge JR O. and Peterson T., 1988. Method for controlling blasting operation. Patent number: US4725991.

Dowding, C.H., 1985. Blast Vibration Monitoring and Control. Prentice-Hall, Inc., Englewood Cliffs, NJ.

Hoshino T., Mogi G. and Shaoquan K., 2000. Optimum delay interval design in delay blasting. FRAGBLAST – International Journal of Blasting and Fragmentation 4: 139–148.

Karu Z. Z., 2002. Signals and Systems Made Ridiculously Simple. ISBN 0-9633752-1-4, ZiZi Press, 124 pages.

Kearey P. and Brooks M., 1991. An Introduction to Geophysical Exploration. Blackwell Scientific Publications, 254 pages.

Muller, B., 1997. Adapting blasting technologies to the characteristics of rock masses in order to improve blasting results and reduce blasting vibrations. FRAGBLAST 1: 361-378.

Muller, B. and Hohlfeld, Th., 1997. New possibility of reducing blasting vibrations with an improved prognosi. FRAGBLAST 1: 379-392.

Oppenheim A.V. and Schafer R.W.,1975. Digital Signal Processing. Prentice Hall, 585 pages.

Persson, P.A., Holmberg, R., Lee, J., 1994. Rock Blasting and Explosives Engineering. CRC Press, Inc.: 365-367.

Shearer, P.M., 1999. Introduction to Seismology. Cambridge University Press, 260 pages.

Siskind, D.E. , Stagg, M.S., Kopp, J.W., Dowding, C.H., 1980. Structure response and damage produced by ground vibrations from surface mine blasting. USBM RI 8507, 77 pages.

Siskind, D.E., Crum, S.V., Otterness, R.E., Kopp, J.W., 1989. Comparative study of blasting vibrations from Indiana surface coal mine. USBM RI 9226, 41 pages.

Siskind, D.E., 2000. Vibrations from blasting, International Society of Explosives Engineers. 120 pages.

Tripathy G. and Gupta I. D., 2002. Prediction of Ground Vibrations due to

Construction Blasts in Different Types of Rock, Rock Mech. Rock Eng, 35 (3), 195–204.

Yamamoto M. and Noda H., 1999. Excavation method by blasting. Patent number: EP0939291A1.

- This paper is a part of the study called "Waveform analysis in mitigation of blast-induced ground vibrations" which was published at a Journal of Geophysics 66 (2008), 25-30.

Mine Heatlth and Safety

The Effect of Historical Workings on Spontaneous Combustion of Coal in Opencast Operations

Peter F Moden, Darron W Dixon-Hardy
*Energy and Resources Research Institute, University of Leeds, Leeds, LS2 9JT, United Kingdom
I Göktay Ediz
Department of Mining Engineering, Dumlupinar University, Kütahya, Turkey

ABSTRACT Spontaneous combustion is a serious problem in coaling operations as it poses a potential serious of production and can lead to problems with mine restoration. This paper looks at how previous underground mining operations interact with new operations, specifically looking at how historical underground operations that are being worked out by opencast methods create spontaneous combustion problems. After describing the geological and physical factors that cause spontaneous combustion and how underground workings promote these problems, methods of combating spontaneous combustion are then presented.

1 INTRODUCTION

Owing to the ever increasing demand for coal in the modern market there are many coal mines that, having become uneconomic to work, have been reopened as they have once again become a workable mineral body. Or in some cases uneconomic methods of working a coal seam have become feasible. The reopening of mines and the working out of previously worked seams poses several different problems, one of those problems that is particularly important when considering the production from of a coal mine is whether there is a significant spontaneous combustion problem created when reopening or starting work on a coal seam.

Spontaneous combustion (sponcom) of coal is not entirely predictable (McPherson, 1992) and many factors can lead to sponcom occurring; coal can catch fire at any point within the mining operation from when it is initially exposed to when it is put on to the stockpile. The result of sponcom can be a loss of production, damage to equipment, problems with restoration as well as several other problems. These can lead to a possible economic resource becoming uneconomic or can lead to land use restrictions on the site of the mine after it has been restored or for restoration measures to fail.

2 CAUSES OF SPONTANEOUS COMBUSTION

Spontaneous combustion of coal is such a significant problem in coal production from mines, stockpiling coal and waste from coal operations because there are several factors that lead to the occurrence of sponcom and it is not fully understood how they interact (MVSSA, 1982). There are several factors that are inherent in the content of the coal that, when they react with certain conditions in the environment that the coal is in, can lead to combustion. Therefore when considering the causes of sponcom the factors listed in Table 1 must be considered (Kaymakçi et al, 2000).

Generally recent and ongoing research indicates that the process of sponcom involves the exposure of coal to the environment, either underground or on the surface. After being exposed the coal then undergoes a degree of low temperature (ambient conditions) exothermic oxidization (Hargraves, 1981). The oxidation rate increases over the initial hours of exposure and then decreases under natural conditions, during this period the oxidisation process creates a heating of the environment. If sufficient oxygen is available this heating will increase, the heating draws out the moisture within the coal, moisture is important in preventing the oxidisation of coal as it produces a gas-liquid interface which diffuses oxygen on the surface of the coal (Blazek, 2001). After the moisture has been drawn out of the coal and the gas-liquid interface (peroxy-complexes) decomposes at around 70-85^{0}C rapid reaction takes place and with sufficient air supply the coal can catch alight.

Past research into this field came up with the "Pyrite theory" which indicated that only coal that contained pyrite would be liable to sponcom, whereas continued research has shown that this is not the case and that coals that do not contain pyrite do spontaneously combust but the presence of pyrite only accelerates the process.

Another important factor that is shown in Table 1 is the affect of the mining method. If the method is an underground operation that leaves coal behind in the form of goaf or pillars in situ after working then this may increase the likelihood of sponcom. This is because this waste material has more surface area exposed, certainly in the case of goaf and this can lead to an increase of air that can

Table 1. Factors that affect the spontaneous combustion of coal

Properties of coal	Environmental Factors
Pyrites	Temperature
Moisture	Moisture
Particle size and surface area	Barometric pressure
Rank and petrographic constituents	Oxygen concentration
Chemical constituents	Bacteria
Mineral matter	Coal seam and surrounding strata
	Method of working
	Ventilation system and air flow rate
	Timbering
	Roadways
	Exposure

circulate over the coal. The amount of air is critical in either propagating sponcom or reducing it. A lot of air moving past the coal will carry off the heat produced by the exothermic oxidisation whereas too little air, as can be the case with most underground ventilation, will lead to an increase in the likelihood of sponcom. This is important when considering the exposure of coal in open pit and opencast operations, the material on the high wall will be relatively sheltered unless the wind direction blows straight across the face of the high wall leading to high probability of the face catching fire owing to sponcom.

3 EFFECTS OF SPONTANEOUS COMBUSTION

There are several problems caused by the sponcom of coal both within the pit, in stockpiles and when being processed. Any burning in these three areas can also lead to problems in different areas within a mine, an incident within the pit can affect the stockpile and a problem within the stockpile can then cause a problem within the processing plant. There are also problems with rehabilitation caused by burning of coal that can mean that the rehabilitation steps used at a mine can fail.

When working within the pit the action of extracting the coal can lead to ignition of the seam upon the highwall as it becomes exposed, as well as the seam that is being worked. The coal seam upon the highwall is exposed for an extended period of time as each cut is completed, therefore leaving a period of time where exothermic oxidation can occur. This is then propagated by air flowing down the working face that increases the rate that oxidisation occurs and then leads to combustion. If sponcom occurs during this period while the coal is being extracted from the current cut it means that the coal poses a threat to the rest of the seam though combustion is left in as a "frozen" portion, this makes sure that large coal fires do not occur but leads to a loss in production. Removing the seam would lead to further exposure of the coal and then a higher probability of the coal catching fire. This means that time has to be spent keeping the portion intact and also the immediate production loss; although the problem portion should naturally correct itself there is the risk that this portion of risk coal could lead to problems in future cuts.

When extracting the coal from the working face there is also the chance of it spontaneously combusting. As the working face exposes a large surface area to the air, good fragmentation of the coal at this point through use of explosives leaves many lines of weakness and channels through which air can flow creating the right conditions for sponcom to occur. Coal that catches fire at this point poses several problems. The first problem is that the coal that is on fire heats up the cutting teeth on the machinery extracting it, which then leads to an increase in wear, more teeth are replaced increasing the cost of coal production per tonne. After the burning coal has been removed it then creates a risk where ever it is moved to, if the material is put into a dump truck then all the coal within the dump truck can catch fire leading to a loss of the entire load. If the coal is then deposited in the stockpile then the fire can spread through the stockpile.

The stockpile for the coal product is a high risk area when considering those areas that are most prone to sponcom. When the material is dumped onto the stockpile the action of dropping the

material exposes the surface area of each particle to the air and therefore means that there is a high potential for the coal to set fire if oxidisation was already in progress or for heating to start. This can lead to the loss of part of, or the entire, stockpile of coal if left unchecked.

Coal susceptible to sponcom can cause problems within the processing plant. When coal is dumped into the crusher the same effect as dumping material onto the stockpile takes place and fires can occur. This leads to the crusher catching fire and therefore processing has to come to a stop, even if the coal does not catch fire the heating of the coal causes higher levels of wear on the machinery within the plant especially the conveyors. Conveyors can catch fire or burn through in places if the coal temperature is not properly controlled.

Waste material on top of the coal seam, high ash content shale, that is moved on to the spoil heap can contain low grade coal, usually lignite. Low grade coals and high ash content shale are more susceptible to sponcom than coals of higher rank, this is not fully understood but this means that material used as spoil and therefore used to fill in worked out areas in rehabilitation are likely to catch fire. The burning of rehabilitated ground leads to the destruction of the soil and therefore any measures taken to grow vegetation on this ground will not take as the nitrates and oxygen within the soil fuel the combustion and are burnt out (AusIMM, 1995).

4 CASE STUDY: KLEINKOPJE COLLIERY, SOUTH AFRICA

Historical underground workings have an impact on the affect of sponcom of coal when opencast operations are the used to extract the same coal. A good case study showing these effects is Kleinkopje colliery, from looking at the situation at Kleinkopje, in relation to sponcom, it can be seen that coal fires are a considerable problem that can be enhanced by working through historical workings.

The colliery is owned by Anglo Coal and is located 10 miles south of Witbank within the Mpumalanga province in the North East of the Republic of South Africa. The Colliery consists of 4 large opencast pits using walking draglines. Historically the mine was exploited using room and pillar methods prior to opencast operations. The operation now exploits 2 of 5 seams including the seam previously worked out by underground methods (seam 2) and now extracting the old pillars. (Figure 1 and Figure 2)

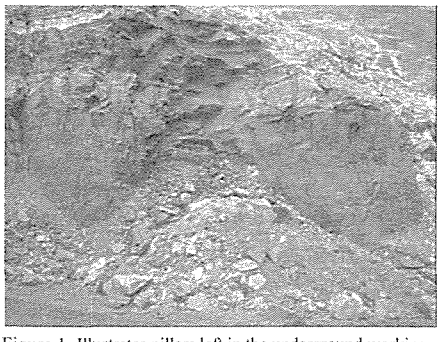

Figure 1. Illustrates pillars left in the underground workings that are now being extracted by opencast methods.

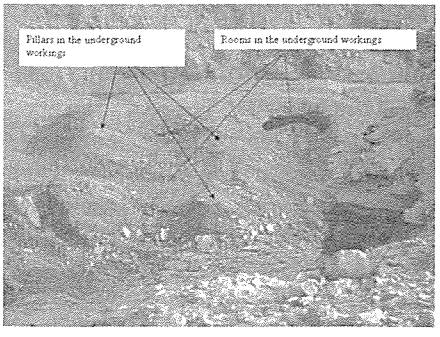

Figure 2. Pillars and rooms from former workings.

The underground operation that extracted the seam (seam 2) now being exploited by Kleinkopje began before the Coalbrook disaster occurred, as such in some areas of the mine there is significant risk of pillar collapse. With the working of the seam above seam 2 this propagates the collapse of ground into the "rooms" in the old workings. This collapse of ground creates channels through which air can pass through creating the right conditions for exothermic oxidisation of coal as there is sufficient oxygen for oxidisation but restricts the flow enough for the area to heat up so that the process does not naturally decrease. This heating can be seen from smoke rising from the collapsed areas, seen in Figure 3.

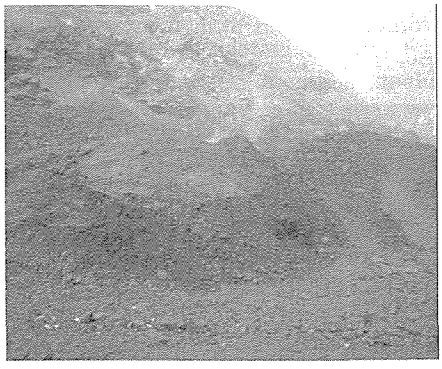

Figure 3. Showing smoke rising from coal heatings

The heating of the underlying seam makes drilling operations more difficult. The mining method used in the Kleinkopje mine requires that the overburden is blasted so that the material becomes fragmented enough for the dragline to dig through and then the coal is drilled and blasted so that it can be loaded by front end loaders. Drilling into the underlying worked seam, 2 seam, presents several problems. The first is the wear and tear on the drill machinery, not only does the heat from the coal mean that there is more drilling wear on the drill bits but after the drill hole has been completed they sometimes cannot be used as the hole is too hot to put explosives down. "Hot Holes" are a serious problem and can disrupt the production of a cut severely. Figures 4 and 5 shows "Hot Holes" on the drilling area. When "Hot Holes" occur they must be filled in and then another location for the drill hole must be found, alternatively the hole can be left to burn out and then be blasted out, and the last option is to leave that area as a frozen portion as it cannot be blasted.

Owing to the heating of the coal seam prior to be extracted as seen in Figures 1 and 2 areas are often found on fire when the Front End Loader (FEL) loads the coal from the working face. This can be seen in Figure 6 where the FEL loading the trucks is circled. This

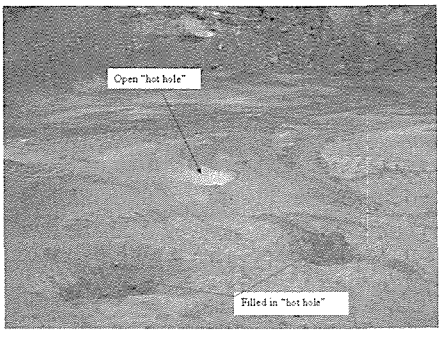

Figure 4. Showing open and closed 'Hot Holes'

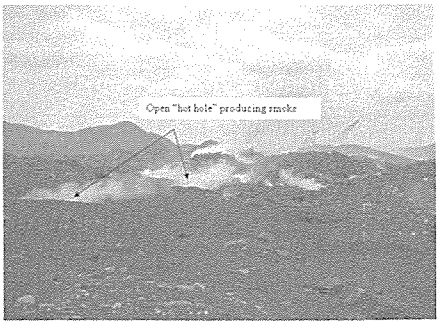

Figure 5. Showing smoke rising from open 'Hot Holes'

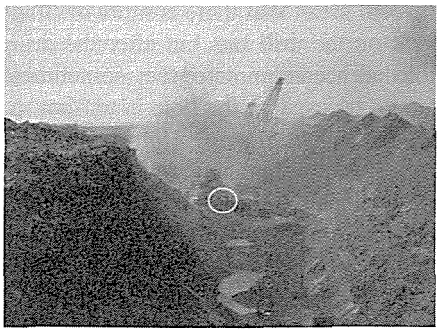

Figure 6. Front end loader opening and then loading a burning area of coal.

material that is burning was then taken to the stockpile or to another area left to burn depending on the severity of the burning. This presented further problems as the operator of the FEL would often be more concerned with coal sent to the plant rather than keeping the coal within the stockpile from burning as coal sent to the processing plant counts towards to a financial bonus. Therefore it was not uncommon to see trucks being loaded with burning coal and then seeing them take it to the stockpile. This led to a number of large stockpile fires on site as can be seen in Figure 7. Large numbers of complaints are received from the local population as this also creates a large smoke plume and also creates a high sulphurous odour.

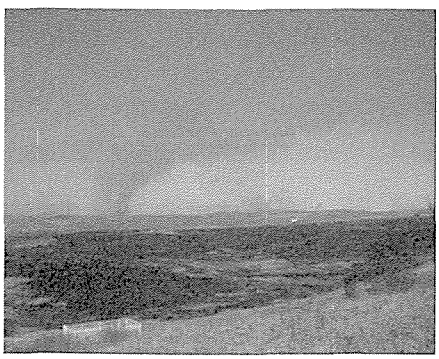

Figure 7. Coal fires seen from a distance of 2 miles.

The material above the coal seams, high ash content shale and low grade coal, that was dumped onto the spoil heaps was also subject to heating and fires. As can be seen in Figure 8 where haze and smoke can be seen coming from the slope of the spoil heap. The restoration plan used by the mine meant that these spoil heaps were then shaped and covered with topsoil for final vegetation and rehabilitation as grassland. The coal was allowed to burn out and then a final capping was put on and then topsoil on top of this. If the coal had not stopped burning then this would mean that the soil would burn through and then leave the ground unable to support vegetation. There have been several occurrences of this in South Africa and it has become known that it is very difficult to return worked out areas to their previous land use.

Figure 8. Spoil heaps with zones of heating identified by smoke & haze.

5 MEASURES TAKEN TO REDUCE SPONTANEOUS COMBUSTION

Managing sponcom is done in three stages; prevention, detection and control. The first focuses on good practise and recognising areas which are likely to cause problems, the second looks at early warning of fires occurring through physical signs of heating and the last

stage looks at sealing to deal with the problem of fires when they occur.

Areas that are likely to suffer from heating include tailings, spoil heaps, open cut coal faces, coarse waste material and stockpiles. Looking at where historically at the site there have been problems is also important because of the way that heating occurs means that there are areas that generally do not induce heating whereas others do. For instance at Kleinkopje heating occurs in the seam below the working seam in some places leading to "Hot Holes" when drilling. Generally speaking in these areas where there is a history of heating there are two methods to use; layering and covering. When stockpiling material within the tailings or waste material and spoil, the material is best layered and then compressed by roller so that there can be no air circulating through the carbonaceous material, then this should be covered with an inert material so that it is closed off from the air. If it is stockpiled coal or run of the mine then it should be stockpiled in layers and compressed and only kept stockpiled for a shorter period of time than the time taken for heating to occur, this time can be found out through testing the coal. At Kleinkopje the open cut coal face was buttressed with inert material, spoil was pushed over the high wall onto the seam so that air could not get to the face. Also in the stockpiling area material was compacted by bulldozer in layers. Water was also used by way of water monitors on the coal faces and on the stockpile in order to cool the material and stop heating from occurring. Hot holes were filled in with inert material and then left.

Detecting an area while it is heating is essential in order to stop fires from breaking out, there are several signs that can be seen on casual inspection that will indicate when heating is taking place and as such means that combustion can be prevented. Visually the temperature change that heating produces gives off a haze or steam that can be seen, Figure 9 shows this steam affect. This picture also shows

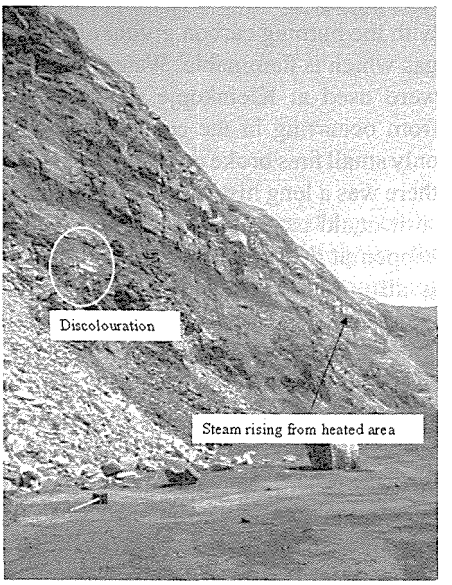

Showing the effects of heating, white discolouration caused by the oxidization of pyrite & steam rising from heated areas.

the discolouration caused by the decomposition of pyrite because of oxidisation which is another indication of heating. As well as being seen by eye more in depth observation can be made using an infrared scanner. In opencast mining the affects of heating are readily visible as can be seen from the pictures from Kleinkopje. Another indication of heating that is easily recognisable is the odour that heating gives off. Sulphur dioxide, oxidised nitrogen, carbon monoxide, methane and hydrogen are a few. The coal at Kleinkopje had a high sulphur content and therefore the heating of

coal there meant that there was a heavy sulphurous odour.

When fires do occur the fire should be starved of oxygen by flooding the material with water or burying it, or allowed to burn out. In large fires burying or flooding cannot effectively stop the fire but can buy time in which to control the burning. In small fires water can react with the burning carbon giving off water gas which is flammable. Water monitors were used at Kleinkopje to stop fires from occurring in the coal stockpile as only small fires broke out in this area, and there was a long history of this occurring so it could be predicted that fire would happen at this location. Liquid nitrogen is also used in underground workings in order to inert carbonaceous material which is likely to combust, this method could be used to inert the seams in the old underground workings at Kleinkopje but would be very expensive and gains from doing such a drastic measure would be minimal in relation to the cost.

6 CONCLUSION

Although surface operations exploiting coal do produce risk from sponcom it can be seen that if surface operations exploit historical underground workings then the risk of sponcom increases significantly. In order to reduce this increased risk careful monitoring and good housekeeping needs to take place. Problem areas need to be monitored and regular pit inspections need to take place and when heating occurs then there must be contingencies in place in order to stop the heating in time before combustion occurs. Therefore the time from exposure to combustion must be known so site specific testing should take place in order to predict the time frame of exposure to heating of a working coal seam. This way measures can be brought into place which will stop heating from occurring. When old workings are exposed then these areas should be covered by inert materials or flooded until they are to be worked in order to stop the oxidisation process.

REFERENCES

McPherson M.J. *Subsurface Ventilation and Environmental Engineering.* Chapman and Hall, 1992.

The Mine Ventilation Society of South Africa. *Environmental Engineering in South African Mines.* Cape and Transvaal Printers, 1982.

Erdoğan Kaymakçi, Vedat Didari, 2000 *Relations between Coal Properties and Spontaneous Combustion Parameters*, Department of Mining Engineering, Zonguldak Karaelmas University, Zonguldak Turkey.

Hargraves, A.J. (ed). (1981). *Symposium on Ignitions, Explosions, and Fires in Coal Mines, AusIMM, Melbourne.*

Christopher Blazek, 2001, *The Influence of Moisture on the Spontaneous Combustion of Coal*, Benetech report (http://www.benetechusa.com/pdf/article/SpontaneousCombOfPRBCoal.pdf), 14p.

Department of Minerals and Energy, Queensland Government, 1995, *The Technical Guidelines for the Environmental Management of Exploration and Mining in Queensland, Part D: Rehabilitation of spontaneous combustion areas.* ISBN 0 7242 5260 6.

ACKNOWLEDGEMENTS

The views and opinions contained in this paper are those of the authors themselves and in no way reflect those of the University of Leeds, Dumlupinar University, or Anglo American.

Simulations of the Ventilation Network at Vulcan Mining Unit

D. Cioclea, C. Lupu, L. Jurca, I.Toth, I. Gherghe, C. Boantă

National Institute for Research and Development in Mine Safety and Protection to Explosion, Petroşani, Romania

ABSTRACT Healthy and safe working conditions in the underground especially in those areas with hazard of potential atmospheres, shall depend mainly on the production implementation and the management of the ventilation system. Improving the management of the ventilation system involves thorough and complex analyses of the ventilation network, i.e. a huge amount of data to be processed only by IT. This paper shows an analysis of the ventilation network at Vulcan Mining Unit, with the use of the IT to simulate certain situations that may come up in the ventilation system (1, 3).

1 INTRODUCTION

The best management of the ventilation network used by a mine involves the use of the IT with the view to performing relevant analyses and to successfully preventing the occurrence of hazardous situations. Expert software can simulate the occurrence of the alterations that may come up in the ventilation system considering certain possible hypotheses.

2 GENERALS

For getting the best possible working conditions in underground, it is necessary to provide the primary protection, i.e. a suitable ventilation. The purpose of this ventilation is to:

- provide the concentration in oxygen necessary for the personnel currently working in underground;
- dilute the explosive and/or toxic gases existing in the mine network;
- diminish the heat emitted inside mine workings, both due to human activities and to thermal gradient.

A good ventilation of each mine working involves the best possible repartition of air flows along each branch of the ventilation network. In this spirit it is necessary to settle the ventilation network of each mine. An example of complex ventilation network is the one belonging to Vulcan mine.

3 DESCRIPTION OF THE VENTILATION NETWORK OF VULCAN MINE

The ventilation network of Vulcan mine was quite complex. At present it has diminished because of some accidents (such as explosions) and due to the depletion of the useful mineral deposits. Therefore, the ventilation network includes four ventilation shafts: Chorin Shaft, Puţul cu Schip, Prokop Shaft and X Shaft - Valea Arsului. It also includes three ventilation raises with the related ventilation stations (B'Allomas Raise, Karollus Raise and Ionaşcu Raise) and underground mine workings located on four levels (level 315; level 360; level 420; level 480). These mine workings are made of main cross sectional galleries, directional galleries, diagonal galleries, plain cross sectional galleries, inclines, working faces, connection raises.

The whole ventilation network includes 251 junctions (knots) and 300 branches (2).

4 PROVIDING THE SOLUTION FOR THE VENTILATION NETWORK OF THE MINE

For providing the best solution available for such a complex ventilation network, we have used the Hardy-Cross method for successive approximation. This method represents the grounds of an expert software CANVENT designed in Canada (4). This software helped us to provide the solution for the ventilation network as well an optimization of the air flow distribution within the ventilation branches.

The settlement of the ventilation network related to Vulcan mine made necessary to run several stages:

a) Marking the junctions of the ventilation network on the spatial diagram;
b) Determining the geodesic coordinates of the identified junctions;
c) Inputting the geodesic coordinates of junctions and the existing branches into the database of the software;
d) The carrying out of measurements in situ; these measurements include:
    1. measurements of the aerodynamic parameters of mine workings;
    2. measurements of the geometrical parameters of mine workings;
    3. measurements of the physical parameters of the air;
e) Calculation of aerodynamic strength specific to each branch;
f) Inputting the values of parameters specific to the ventilation network into the expert software CANVENT;
g) The 2D or 3D drawing of the ventilation network;
h) Balancing the ventilation network;
i) Settling the ventilation network. Both the direction and the optimum distribution of the air flows along each branch are being identified in this stage;
j) Getting the results.

This final stage provides the data on electronic support or paper regarding the graphic settlement of the ventilation network.

5 SIMULATIONS IN THE VENTILATION NETWORK

CANVENT software allows to simulate

certain changes that may come up in the ventilation network. Hence, the following situations have been simulated out the ventilation network of Vulcan Mine:

a) removal of the air outlet circuit from no. 4 / 3 / VI towards Terezia raise (360 - 420);

Simulation no. 1 - removal of the air outlet circuit from no. 4 / 3 / VI towards Terezia raise (360 - 420).

This simulation involves the placing of sealing structures on the connectivity gallery with the raise no. 3 bl. VI, branch 100-101 and on the raise no. 4 floor, branch 92-93.

The placing of these sealing structures removed the following branches from the ventilation system: 92-93; 93-94; 94-95; 95-96; 96-97; 97-98; 98-99; 99-100 and 100-101.

As a result of this removal and to maintain the specified flow rate at the longwall no. 2, bed 3, bl. VI, the regulating door on the transverse gallery, level 420 (branch 75-101) was eliminated.

The alteration carried out for this simulation are shown in Figure no. 1.

We have got the following results that can be compared to the present situation:

- The air flow rate along the fresh air intake at the level 360, branches 22-23; 15-24; 30- 31; 193-194 increased from 33.91 m^3/s to 34.54 m^3/s (from 2035 m^3/min to 2073 m^3/min);
- The air flow rate at the face working with undermined coal layer no. 2 bed 3 bl. VI
  didn't change significantly;
- The air flow rate along the ventilation incline 360-315 increased from 16.03 m^3/s to 16.98 m^3/s (from 962 m^3/min to 1019 m^3/min);
- The air flow rate at the face working with undermined coal layer no. 4 bed 3 bl. VI changed from 2.1 m^3/s to 2.8 m^3/s;
- The air flow rate at the longwall no. 0, bed 3, bl. VIII, level 376 m and at the longwall no. 0, bed 3, bl. VIII, level 386, didn't change significantly;
- The air flow rate increased from 8.19 m^3/s to 8.76 m^3/s (approx. 34 m^3/min) along the air outtake related to longwall no. 2 bed 3 bl. VI (branch 181-183) level 480;
- The air flow rate diminished from 5.18 m^3/s to 4.01 m^3/s (approx. 70 m^3/min) along the air outtake related to longwall no. 4 bed 3 bl. VI (branch 90-89) level 360;
- The air flow rates didn't change significantly along the air outtake of longwalls no. 0 bed 3 bl. VIII, level 376 m and no. 0 bed 3 bl. VIII, level 386 m (branches 249-208 ; 152-153);
- Virtually, the air flow rates stayed the same in the mine (branches 240-242, 235-237).

b) the tank from the skip is empty and the door in the gallery that connects the tank with the skip (the upper part of the tank) is open and the collecting tank, level 360, is full;

Simulation no. 2 - the tank from the skip is empty and the door in the gallery that connects the tank with the skip (the upper part of the tank) is open and the collecting tank, level 360, is full.

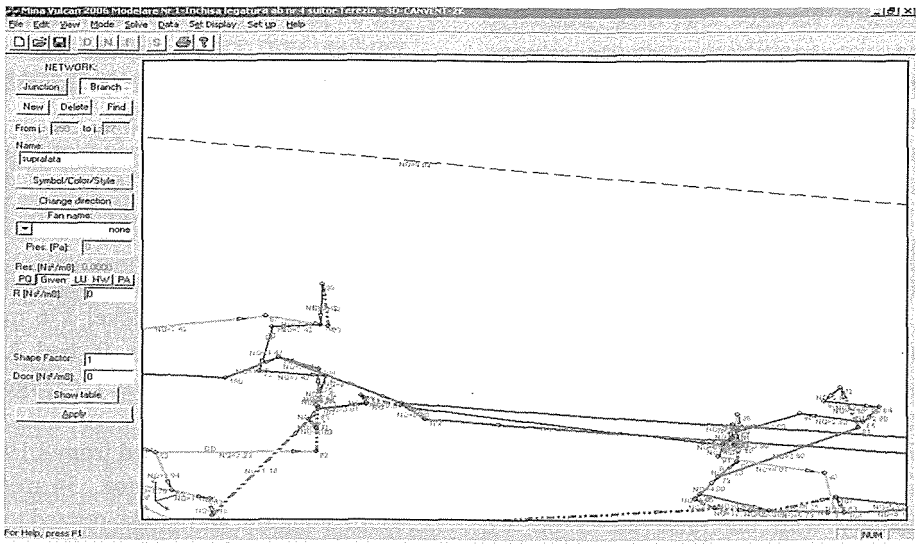

Figure 1

To carry out this simulation, we take as closed the circuit between the outtake of longwall no. 4 bed 3 bl. VI, level 360 m and the transverse gallery Terezia raise level 420 m, i.e. simulation no. 2 relies on simulation no. 1.

The removal of the door on the gallery that connects the skip to the upper part of the tank level 387 m (branch 8-15) removed the initial strength of 5 Ns^2/m^8 on the connecting tank, branch 14-15; thus we simulated the empty tank. Also, we increased strength on the collecting tank, level 360 m (branch 46-48) and simulated the full silo.

The alteration carried out for this simulation are shown in Figure no. 2.

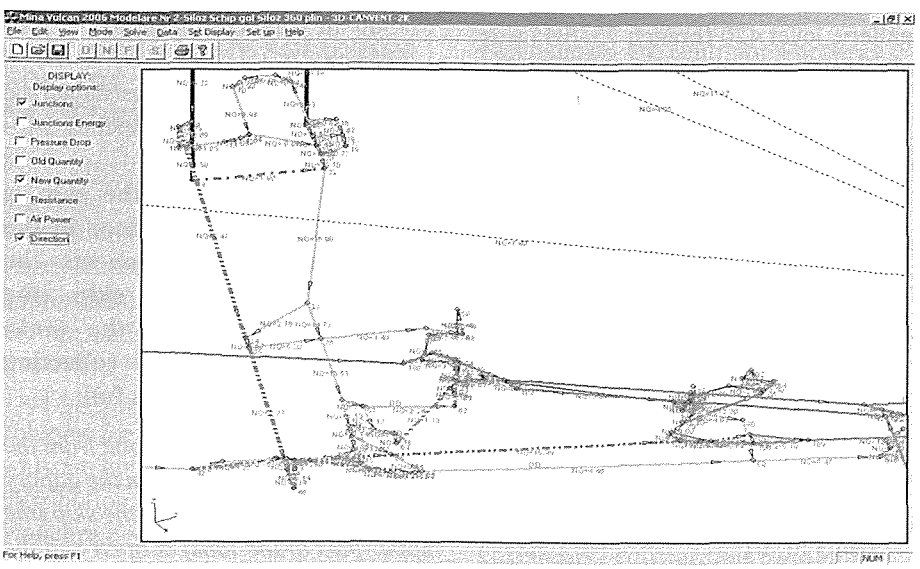

Figure 2

We have got the following results that can be compared to the present situation:

- The air flow rate along the fresh air intake at the level 360, branches 22-23 ; 15-24 ; 30-31 ; 193-194 increased from 33.91 m^3/s to 34,65m^3/s;
- The air flow rate at the face working with undermined coal layer no. 2 bed 3 bl. VI didn't change significantly;
- The air flow rate along the ventilation incline 360-315 increased from 16.03 m^3/s to 17 m^3/s;
- The air flow rate at the face working with undermined coal layer no. 4 bed 3 bl. VI changed from 2.1 m^3/s to 2.8 m^3/s;
- The air flow rate at the longwall no. 0, bed 3, bl. VIII, level 376 m and at the longwall no. 0, bed 3, bl. VIII, level 386 m, didn't change significantly;
- The air flow rate increased from 8.19 m^3/s to 8.80 m^3/s along the air outtake related to longwall no. 2 bed 3 bl. VI (branch 181-183) level 480 m;
- The air flow rate diminished from 5.18 m^3/s to 4.03 m^3/s along the air outtake related to longwall no. 4 bed 3 bl. VI (branch 90-89) level 360;
- The air flow rates didn't change significantly along the air outtake of longwalls no. 0 bed 3 bl. VIII, level 376 m and no. 0 bed 3 bl. VIII, level 386 m (branches 249-208 ; 152-153);
- Virtually, the air flow rates stayed the same in the mine (branches 240-242, 235-237).

c) the tank from the skip is full and the door in the gallery that connects the tank with the skip (at the upper part of the tank) is closed and the collecting tank, level 360, is empty;

Simulation no. 3 - the tank from the skip is full and the door in the gallery that connects the tank with the skip (at the upper part of the tank) is closed and the collecting tank, level 360, is empty.

To carry out this simulation, we take as closed the circuit between the outtake no. 4 bed 3 bl. VI, level 360 m

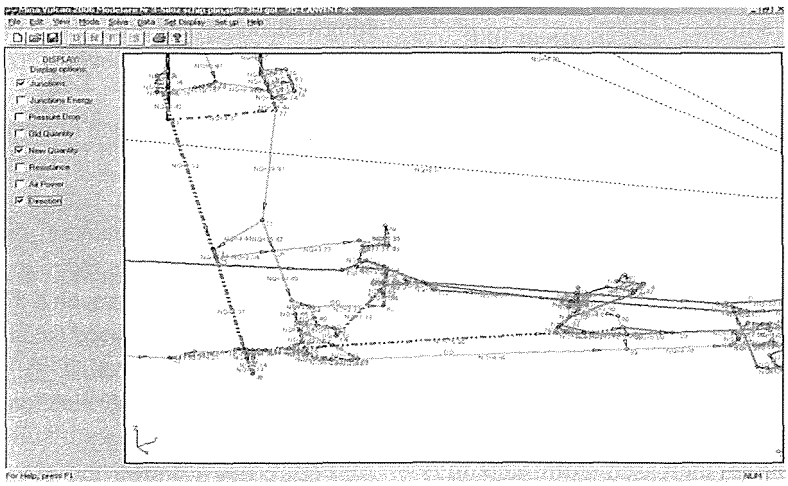

Figure 3

and the transverse gallery Terezia raise level 420 m, i.e. simulation no. 3 relies on simulation no. 1.

We reduced the strength of the collecting tank level 360 m and thus we simulated the situation when the tank is empty. Also, we increased strength on the tank from the skip to simulate the case when the tank is full.

Figure no. 3 shows the alterations made for this simulation.

We have got the following results that can be compared to the present situation:

- The air flow rate along the fresh air intake at the level 360 m, branches 22-23; 15-24; 30-31; 193-194 increased from 33.91 m^3/s to 34,46 m^3/s;
- The air flow rate along the connecting raise (branch 25-44) increased from 1.8 m^3/s to 4.31 m^3/s;
- The air flow rate at the face working with undermined coal layer no. 2 bed 3 bl. VI didn't change significantly;
- The air flow rate along the ventilation incline 360 - 315 increased from 16.03 m^3/s to 16.97 m^3/s;
- The air flow rate at the face working with undermined coal layer no. 4 bed 3 bl. VI increased from 2.1 m^3/s to 2.8 m^3/s;
- The air flow rate at the longwall no. 0 bed 3 bl. VIII, level 376 m, ant at the longwall no. 0 bed 3 bl. VIII, level 386 m, didn't change significantly;
- The air flow rate along the air outtake of longwall no. 2 bed 3 bl. VI (branch 181-183) at the level 480 m, increased from 8.19 m^3/s to 8.72 m^3/s;
- The air flow rate along the air outtake of longwall no. 4 bed 3 bl. VI (branch 90-89) at the level 360 m, diminished from 5.18 m^3/s to 4.02 m^3/s;
- The air flow rate along the air outtake of longwall no. 0 bed 3 bl. VIII, level 376 m and of longwall no. 0 bed 3 bl. VIII, level 386 m (branches 249-208 ; 152-153) didn't change significantly;
- Virtually, the air flow rates stayed the same in the mine (branches 240-242 and 235-237).

d) the tanks from the skip is empty and the door in the gallery that connects the tank with the skip is open and the connecting tank, level 360, is empty;

Simulation no. 4 - the tanks from the skip is empty and the door in the gallery that connects the tank with the skip is open and the connecting tank, level 360, is empty.

To carry out this simulation, we considered the simulation no. 1 where the connection between the outtake of longwall no. 4 bed 3 bl. VI, level 360 m and Terezia raise, level 420 m, is closed.

We reduced the strength from the raise of the skip (branch 14-15) and simulated the situation when the tank from the skip is empty. The ventilation door on the gallery that connects the skip to the upper side of the raise (branch 8-15) was eliminated. We also reduced the strength of the collecting tank level 360 m (branch 46-48) and simulated the situation when the collecting tank is empty.

Figure no. 4 shows the alterations made for this simulation.

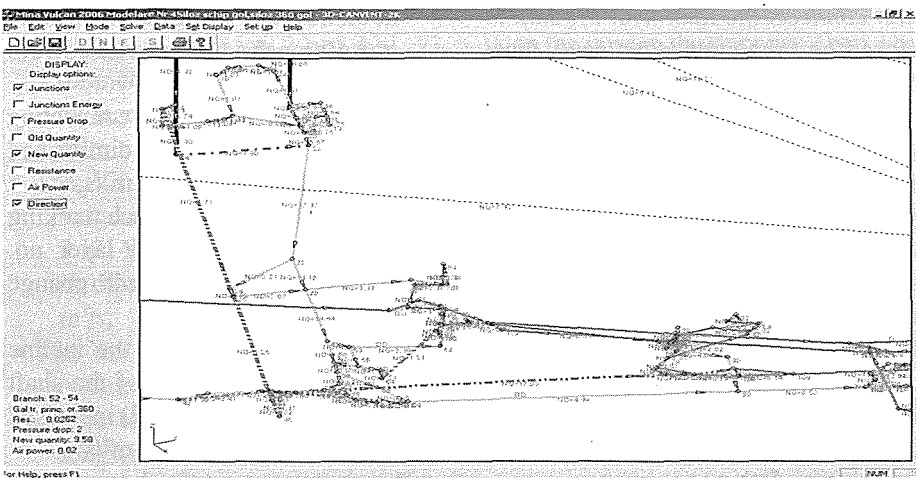

Figure 4

We have got the following results that can be compared to the present situation:

- The air flow rate along the fresh air intake at the level 360 m, branches 22-23 ; 15-24 ; 30-31 ; 193-194, increased from 33.91 m^3/s to 34.85 m^3/s;
- The air flow rate along the connecting raise (branch 44-45) diminished from 1.8 m^3/s to 0.92 m^3/s;
- The air flow rate on the connecting gallery (branch 8-15) increased from 2.18 m^3/s to 3.68 m^3/s;
- The air flow rate at the face working with undermined coal layer no. 2 bed 3 bl. VI didn't change significantly;
- The air flow rate along the ventilation incline 360 - 315 increased from 16.03 m^3/s to 17.09 m^3/s;
- The air flow rate at the face working with undermined coal layer no. 4 bed 3 bl. VI increased from 2.1 m^3/s to 2.8 m^3/s;
- The air flow rate at the longwall no. 2 bed 3 bl. VIII, level 376 m and at the longwall no. 0 bed 3 bl. VIII, level 386 m, didn't change significantly;
- The air flow rate along the air outtake of the longwall no. 2 bed 3 bl. VI (branch 181-183) at the level 480, increased from 8.19 m^3/s to 8.79 m^3/s;
- The air flow rate along the air outtake of the longwall no. 4 bed 3 bl. VI (branch 90-89) level 360 m, diminished from 5.18 m^3/s to 4.05 m^3/s;
- The air flow rates along the air outtake of the longwall no. 0 bed 3 bl. VIII, level 376 m, and of the longwall no. 0 bed 3 bl. VIII, level 386 m (branches 249-208 ; 152-153) didn't change significantly;
- Virtually, the air flow rates stayed the same in the mine (branches 240-242 and 235-237).

e) the tank from the skip is full and the door in the gallery that connects the tank with the skip is closed and the connecting tank, level 360, is full;

Simulation no. 5 - the tank from the skip is full and the door in the gallery

that connects the tank with the skip is closed and the connecting tank, level 360, is full

To carry out this simulation, we take simulation no. 1 as the starting point.

We also increased the strength: on the tank of this skip (branch 8-15) to simulate the situation when the tank of the skip is full and on the collecting tank level 360 m (branch 46-48) to simulate the situation when the collecting tank is full.

Figure 5 shows the alterations made for this simulation.

We have got the following results that can be compared to the present situation:

- The air flow rate along the fresh air intake at the level 360 m, branches 22-23; 15-24; 30-31; 193-194, increased from 33.91 m^3/s to 34.33 m^3/s;
- The air flow rate along the connecting raise (branch 44-45) increased from 1.8 m^3/s to 2.03 m^3/s;
- The air flow rate on the connecting gallery (branch 8-15) diminished from 2.18 m^3/s to 1.98 m^3/s;
- The air flow rate at the face working with undermined coal layer no. 2 bed 3 bl. VI didn't change significantly;
- The air flow rate along the incline for acces to the base of the shaft with skip (branch 34-22) increased from 3.19 m^3/s to 4.34 m^3/s;
- The air flow rate at the face working with undermined coal layer no. 4 bed 3 bl. VI increased from 2.1 m^3/s to 2.79 m^3/s;
- The air flow rate at the longwall no. 0 bed 3 bl. VIII, level 376 m and at the longwall no. 0 bed 3 bl. VIII, level 386 m, didn't change significantly;

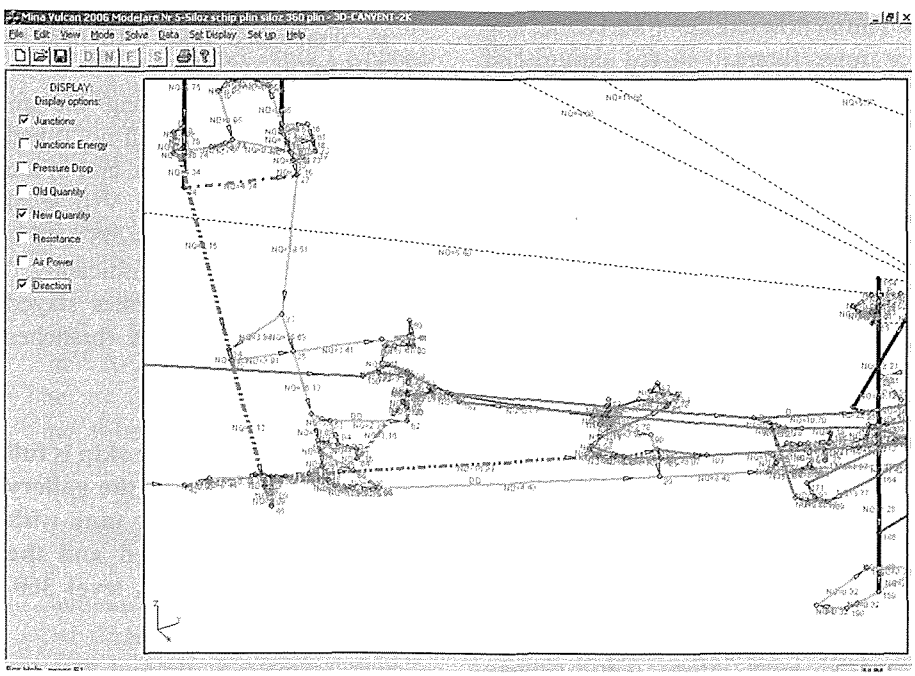

Figure 5

- The air flow rate along the air outtake of the longwall no. 2 bed 3 bl. VI (branch 181-183) at the level 480 m, increased from 8.19 m^3/s to 8.73 m^3/s;
- The air flow rate along the air outtake of the longwall no. 4 bed 3 bl. VI (branch 90-89) level 360 m, diminished from 5.18 m^3/s to 4.0 m^3/s;
- The air flow rates along the air outtake of the longwall no. 0 bed 3 bl. VIII, level 376 m, and of the longwall no. 0 bed 3 bl. VIII, level 386 m (branches 249-208 ; 152-153) didn't change significantly;
- Virtually, the air flow rates stayed the same in the mine (branches 240-242 and 235-237).

f) case when the working face no. 1 / 3 / VIII level 366, is put to operation.

Simulation no. 6 - case when the working face no. 1 / 3 / VIII level 366, is put to operation.

To carry out this simulation, we have taken into consideration the simulation no. 1.

We have also introduced new knots: 21, 26, 49, 139, 140, 168, 175, 177, 228, 230, 241, based on the topographic coordinates got from the topo department of Vulcan Mining Unit. We have also introduced new branches: 12-21, 21-26, 26-49, 49-139, 139-140, 140-168, 168-175, 175-177, 177-228, 228-230, 230-241, 114-241, 241-215.

Consequently we have simulated the existence of a new longwall (no. 1 bed 3 bl. VII, level 366 m) in the current network of the mine, with the air intake on level 315 m on the transverse gallery no. 1 (branch 12-21) and the air outtake is on the raise in the floor no. 2 bed 3 bl. VIII (branch 241-115).

The presence of this new longwall unbalanced the distribution of air flow rates on the circuits related to the ventilation network of Vulcan Mine. Consequently, it was necessary to:

- remove the ventilation door in the transverse gallery no. 2 bed no. 3 bl. BII, level 360 m (branch 115-125);
- place a regulating door in the access gallery to raise no. 2 bed no. 3 bl. VII, roof of level 315 m (branch 110-114);
- place a regulating door in the directional gallery bl. VII-VIII, level 315 m (branch 113-126);
- place a sealing door in the raise no. 1 bl. VIII, level 315-360 m (branch 130-181) for balancing the ventilation network and getting a normal distribution of air flow rates, especially at longwalls.

Figure no. 6 shows the alterations made for this simulation.

We have got the following results that can be compared to the current situation:

- The air flow rate along the fresh air intake at the level 360 m, branches 22-23; 15-24 ; 30-31 ; 193-194 increased from 33.91 m^3/s to 34.39 m^3/s;
- The air flow rate at the face working with undermined coal layer no. 2 bed 3 bl. VI didn't change significantly;
- The air flow rate along the ventilation incline 360 - 315 increased from 16.03 m^3/s to 16.77 m^3/s;

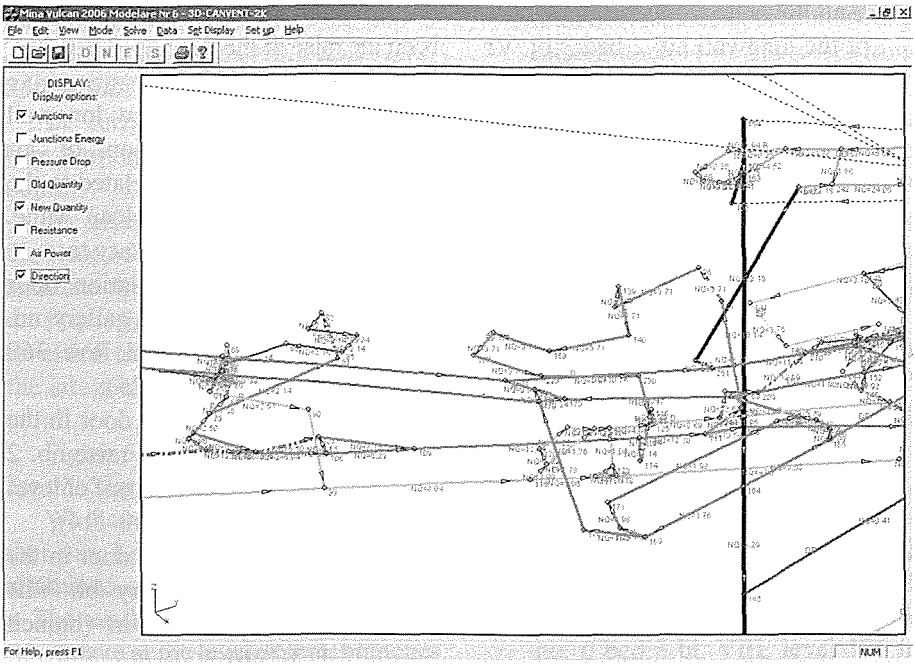

Figure 6

- The air flow rate at the face working with undermined coal layer no. 4 bed 3 bl. VI didn't change significantly;
- The air flow rate at the longwall no. 1 bed 3 bl. VII reached 3.67 m^3/s, i.e. the value stated in the ventilation project for this longwall;
- The air flow rate at the longwall no. 0 bed 3 bl. VIII, level 376 m and at the longwall no. 0 bed 3 bl. VIII, level 386 m, reduced insignificantly;
- The air flow rate along the air outtake of the longwall no. 2 bed no. 3 bl. VI (branch 181-183), level 480 m, increased from 8.19 m^3/s to 8.79 m^3/s;
- The air flow rate along the air outtake of the longwall no. 4 bed no. 3 bl. VI (branch 90-89), level 360 m, diminished from 5.18 m^3/s to 3.46 m^3/s;
- The air flow rate along the air outtake of the longwall no. 1 bed no. 3 bl. VI (branch 125-249), level 360 m, increased from 7.18 m^3/s to 8.80 m^3/s;
- The air flow rate along the air outtake of the longwall no. 0 bed 3 bl. VIII, level 376 m and of the longwall no. 0 bed 3 bl. VIII, level 386 m (branches 249-208 ; 152-153), didn't change significantly;
- Virtually, the air flow rates stayed approx. the same in the mine (branches 240-242 and 235-237);
- The air flow rate along the directional gallery bl. VII - VIII (branch 113-126) diminished from 10.95 m^3/s to 8.52 m^3/s;
- The air flow rate along the raise no. 1 bed no. 3 bl. VIII (branch 130 - 131) diminished from 2.75 m^3/s to 1.18 m^3/s.

6 CONCLUSIONS

- Giving solutions for the ventilation networks with the help of the it is a huge step forward that allows an optimum ventilation and a visualisation of the changes made on the network in real time.
- The ventilation network given as example belongs to Vulcan mine and includes 4 shafts, 3 ventilation raises, 4 levels and several underground workings (cross-sectional galleries, directional galleries, diagonal galleries, inclines, connection raises and working faces).
- The best solutions available for the ventilation network of Vulcan mine have been obtained with the help of the Canadian software called CANVENT. It includes the run of 10 main steps.
- We have been able to perform 6 simulations on this software that involved certain changes which might come up in the ventilation network.
- Giving solutions for the ventilation network with the help of IT allows the best possible solutions irrespective of its complexity.

REFERENCES

Bălţăreţu R., Teodorescu C., *Aeraj şi protecţia muncii în mină*, E.D.P. Bucureşti 1971

Cioclea D., ş.a., *Rezolvarea reţelei de aeraj în baza măsurătorilor depresiometrice în vederea stabilirii debitelor de aer, a depresiunilor, a rezistenţelor aerodinamice, pe locuri de muncă din cadrul E.M. Vulcan*, INSEMEX Study, 2006

Todorescu C., Gontean Z., Neag I., *Aeraj minier*, E.T. Bucureşti 1971

CANVENT – *Mining and Minerals Sciences Laboratories Underground Mine Environment and Ventilation, Manual de utilizare – 3D program – CANVENT – 2K*

Mineral Processing

Estimation of the Bond's Grindability from Sink-Float Test Data for Two Different Pumices

Vedat Deniz
Amiroğlu Companies Group, Amiroğlu Mining Co., Denizli, Turkey
Yakup Umucu
Department of Mining Engineering, Süleyman Demirel University, Isparta, Turkey
Serkan Çayırlı
Department of Mining Engineering, Niğde University, Niğde, Turkey

ABSTRACT In this study, a method for calculating the Bond's grindability by the sink–float test data of pumice was studied. Primarily, the cumulative weight and porosity content of the floating fraction have been determined for two different pumice samples in all relative densities tested. Then, grindability of the pumice samples is determined for its constituent specific gravity fractions. Though the grindability of the constituent specific gravity fractions of both the pumices varies in a systematic manner, certain differences, however, can be observed in the variation pattern between the two pumices which are easy washability and moderate difficult washability characteristic pumices. The relationships between the Bond's grindability and relative densities and between the Bond's grindability and porosity have been stated as simple equations and the calculated values from equations have been compared with the experimental results. Finally, the float–sink test results can be stated by simple equations relating to the Bond's grindability value. The Bond grindability (G_{bg}) is easily measured by carrying out sink–float separation, and by measuring the constituent relative density fractions and porosity content.

1 INTRODUCTION

Pumice is a natural volcanic material that is used many areas such as in construction industry and wastewater treatment because of its high porosity, as well as in a wide rage of industries such as agriculture, dental, cosmetic, pigment, textile, chemical, abrasives, cement, ceramic and glass (Deniz and Onur, 2002; Deniz, 2005).

Italy is the biggest pumice producer in the world (% 44 in total) and Turkey is the second (9% in total). Pumice is being produced in various regions of Turkey, mainly in Nevşehir Cappudocia and Isparta Gölcük regions. Nevşehir pumice is produced mostly by SOYLU Co. and Isparta pumice is produced mostly by ISBAŞ Co. (Deniz and Umucu, 2005).

As an industrial mineral, pumice has a low specific gravity because of its porosity. This feature makes the pumice important for using areas. Gravity of pumice (dry unit volume weight) is

approximately 0.8-1.2 g/cm^3. The most important gang minerals of pumice are andesite, travertine, serpentine and basalt. Gravity of these gang minerals are approximately between 2.09 - 2.46 g/cm^3. This huge difference between pumice and its gang minerals show us that gravity processing can be very useful for this mineral. However, the results might be different in practice (Deniz and Umucu, 2004; Deniz, et al., 2007; Deniz and Umucu, 2008).

The separation of mineral mixture into fractions of varying specific gravities is one of the most useful laboratory techniques, which is testing for gravity concentration amenability. In this technique the samples are subjected to a single sink-float separation and the two products are weighed and analysed. For lower-gravity minerals, sink-float separation could be conducted in water solutions of metal salts such as zinc chloride (Burt, 1984).

Sink-float test is a routine exercise, especially in coal preparation and mineral processing plants to evaluate and cross-check the washability characteristics of the coal and minerals treated and the washer performance of equipments. Data obtained from the float–sink tests are used to form a set of washability curves, which are then used to assess the degree of difficulty of gravity separation of raw minerals and to provide qualitative or quantitative data for the products of the separation at a selected relative density (Leonard, 1979; Burt, 1984; Osborne, 1985).

Comminution is known to be a large consumer of the energy, which consumes 3–4% of the electricity generated world-wide and comprises up to 70% of all energy required in a typical mineral processing plant, and is one of the most important unit operations in mineral processing. The grinding process has many variables, some of which are difficult to understand (Deniz, 2004)

Grindability data, based on various techniques to measure comminution characteristics, are used to evaluate the crushing and grinding efficiency in mineral processing operations. The importance of achieving improved comminution efficiency, in terms of energy consumption, has been emphasized increasing in the cost of electricity, recently (Horst and Bassarear, 1976).

Many expressions of grindability have been proposed over the years, but of these two of them have come into prominence because they have become the recognized basis for design of certain types of mill. One of them is the Hardgrove index, associated mainly with vertical spindle mills and the other is Bond's grindability, associated with tumbling mills (Prasher, 1987).

In the design of grinding circuits in mineral processing plant, the Bond method is widely used to evaluate the performance and determine the powder required and mill size for a material. This method is very long time and complex. In additional, it is very sensitive to procedural errors.

Way back in the thirties, it was reported that grindability decreased with the increase in specific gravity of the fraction with the constant weight sample for the coals studied (Yancey and Geer, 1936). It was also shown that for the coal tested, the grindability of a sample composed of a mixture of different specific gravity fractions could be calculated from the grindabilities of the individual fractions (Yancey et al., 1934). Fitton et al. (1957) observed a high HGI value for fractions floating at a

specific gravity of less than 1.4, and that a grindability of specific gravity fractions of more than about 1.4, reporting to the middling and tailing, could vary to a large extent. Ghosal et al. (1958) observed that with higher specific gravity fractions, there was a gradual decrease in the HGI with the exception of the highest gravity fraction which generally recorded a higher index value than the values for intermediate fractions. In the large number of coals, mostly coking, studied by Sinha et al. (1969) the grindability of clean coal was highest followed by the middlings and it again rose in the case of sinks. Bhattacharya et al. (1986) showed that a coking and a non-coking coal and to explore the possibility of estimation of grindability from sink-float data obtained from routine plant sampling. However, they also noted an exception to this trend. Cebeci and Aslan (2002) investigated the interpretation of float–sink test data by simple equations on coals of different origins with respect to sulphur content. They results reveal that the float–sink test results can be stated by simple equations relating to the sulphur content.

In the subsequent years, however, little work has been reported in the literature on the variation of grindability with specific gravity and on the relationship between the two.

Some work has already been carded out on the variation of grindability with specific gravity, in particular for some selected specific gravity fractions or for some simulated washing products. Little work has so far been reported on the variation of grindability with all the constituent specific gravity fractions of any coal and on the estimation of grindability from sink-float data. But, there are not any works between the Bond's grindability and sink-float data. Additionally, one work has not reported on grindability with sink-float data on an ore studied such as pumice. Objectives of this investigation have, therefore, been to study the variation of the Bond's grindability, if any, with constituent specific gravity fractions of an easy washability and a moderate-difficulty pumice samples and to explore the possibility of estimation of grindability from sink-float data obtained from routine plant sampling.

2 MATERIALS AND METHOD

2.1 Materials

Pumice samples taken from deposits belong to ISBAŞ Co. in Isparta (Turkey) and SOYLU Co. in Nevşehir (Turkey), which are called the Isparta and the Nevşehir were used as the experimental materials. The characterization of the raw material included chemical analysis with an XRF spectrometer to determine its chemical composition. Chemical properties of pumice samples used experimentally are presented in Table 1.

Table 1. Chemical composites of pumice samples using in experiments

Oxides (%)	Isparta	Nevşehir
SiO_2	57.37	71.22
Al_2O_3	18.74	13.47
Fe_2O_3	5.93	1.18
MgO	2.95	0.63
Na_2O	4.25	6.07
K_2O	3.66	3.32
CaO	2.16	0.96
SO_3	1.23	---
TiO_2	0.45	0.67
Loos of ignition	1.75	1.22

2.2. Mineralogical analysis

In mineralogical analysis of Isparta pumice, mafic minerals (pyroxene, biotite, sanidine, feldspar and plagioclase) were observed in thin sections of the samples having density fractionation between 1.0 g/cm^3–1.7 g/cm^3. While the samples having glassy groundmass with thin sections have lower density, porphyritic samples have higher density. It has been observed that the density is proportional to the alteration degree, amount and size of the mafic minerals. In general, micro crystals occurred in the high-density thin section samples with intersertal texture. On other hand, low-density thin section samples include grains with higher hardness. Some of thin sections in the low-density samples have been filled with secondary minerals such as clay and kaolin.

In mineralogical analysis of Nevşehir pumice, oxidised biotite and hornblende minerals can be recognised. Any compositional change weren't observed in the Nevşehir pumice in all thin section. But porosity decreases with increasing density in thin section. Plagioclase minerals in Nevşehir pumice are coarser than Isparta pumice.

In additional, it can be seen that there is not an important difference depending on particle size for pumice-gangue liberation for Nevşehir. However, there is a significant difference depending on particle size for Isparta pumices. Sanidine, pyroxene and feldspar minerals, which are abrasive minerals in Nevşehir pumice, are much less than in Isparta pumice.

2.3 Bond Grindability Test

The standard Bond grindability test is a closed-cycle dry grinding and screening process, which is carried out until steady state condition is obtained. This test was described as follow: (Bond and Maxson, 1943; Yap et al., 1982; Austin and Brame, 1983; Magdalinovic, 1989; Deniz and Özdağ, 2003).

The material is packed to 700 cc volume using a vibrating table. This is the volumetric weight of the material to be used for grinding tests. For the first grinding cycle, the mill is started with an arbitrarily chosen number of mill revolutions. At the end of each grinding cycle, the entire product is discharged from the mill and is screened on a test sieve (P_i). Typical choices for P_i are 212, 150, 106 and 75 microns. The oversize fraction is returned to the mill for the second run together with fresh feed to make up the original weight corresponding to 700 cc. The weight of product per unit of mill revolution, called the ore grindability of the cycle, is then calculated and used to estimate the number of revolutions required for the second run to be equivalent to a circulating load of 250%. The process is continued until a constant value of the grindability is achieved, which is the equilibrium condition. This equilibrium condition may be reached in 6 to 12 grinding cycles. After reaching equilibrium, the grindabilities for the last three cycles are averaged. The average value is taken as the standard Bond grindability (G_{bg}).

2.4 Sink-Float Test

Gravity concentration is the most important unit operation in coal or mineral washing circuit. Normally, sink-float analyses of the representative coal or mineral samples to be washed is carried out in a laboratory to predict the theoretical yield and contents of

clean product obtainable in an ideal gravity concentrator at different specific gravities. It is a common practice to plot a series of washability curves, from the sink-float data of a mineral sample in order to generate much useful information relating to its amenability for producing clean product of desired quality.

To ensure accuracy in the sink-float tests, original samples were separately subjected to size analysis, maintaining a top to bottom ratio of about 1.0-1.7. A small head sample was collected from each size fraction for porosity analysis to cross-check the accuracy of subsequent sink-float tests. Each one pumice was subjected to sink-float tests with seven specific gravity cuts. Zinc chloride was used as the medium. Each size-specific gravity fraction thus obtained was then subjected to porosity percents determination. In addition, the average specific gravity was determined for the final sink product of both pumices, by using specific gravity buckets. The porosity percent of pumices were used to derive the equation.

In general, the porosity content is determined using the main method called specific gravity (ASTM C-127).

3. EXPERIMENTAL STUDIES

3.1 Sink-Float Experiments

Two pumices obtained from two different sources, Nevşehir and Isparta, have been used for this investigation. Each sample weighed about 250 kg. Sink-float curves for particle sizes of 50-30 mm of Nevşehir and Isparta pumices were given in Figure 1 and Figure 2, respectively. It can be seen in Figures that Isparta pumice appears to be moderate and difficult to wash while Nevşehir pumice is easy to wash.

Each specific gravity fraction thus obtained was then subjected to porosity analysis and Bond's grindability determination.

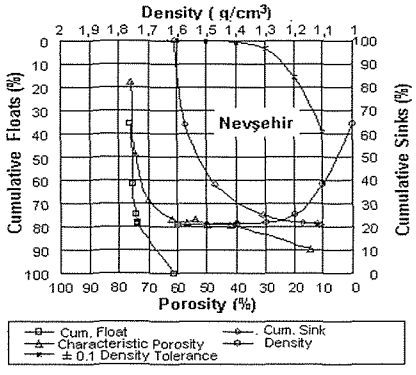

Figure 1. Sink-float curves of Nevşehir pı

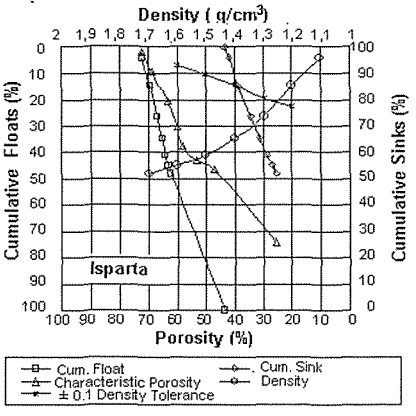

Figure 2. Sink-float curves for Isparta pumices

3.2. Variation of the Bond's grindability with relative density and porosity

Table 2 shows the grindability and weight percentage distribution obtained for the constituent specific gravity fractions for the two pumice samples. It can be argued that grindability values obtained for the relative density of the Isparta pumice

are quite close to each other except for the lightest fraction constituting less of the whole mass of pumice. In the case of the Nevşehir pumice, however, substantial differences can be observed in the Bond' grindability values obtained for the relative density, each of which constitutes more of the whole mass of pumice.

A definite trend can be observed in the variation of grindability with specific gravity for Nevşehir pumice sample. Bond's grindability values power decrease with the increase in relative density for the lighter. Variation of the Bond's grindability with specific gravity for the Isparta pumice follows the different pattern that Bond's grindability values power increase with the increase in relative density for the heaviest fraction.

Relation of G_{bg} with relative density for the Nevşehir and Isparta pumice samples, on as determined basis, are shown in Fig. 3 and Fig. 4, respectively. The Bond's grindability determined by experimental for both pumices are found to be in good agreement with the relative densities, which are shown Eqs. (1) and (2).

Nevşehir;

$$G_{bg} = 3.277(D)^{-1.797} \qquad r^2=0.974 \qquad (1)$$

Isparta;

$$G_{bg} = -3.16(D)^2 + 10.82(D) - 5.65 \quad r^2=0.956 \qquad (2)$$

Eqs. (3) and (4) have been obtained from Fig. 3 and Fig.4 for the Bond's grindability determined by experimental for both pumices, which are found to be in good agreement with porosity. Coefficient r^2 of Nevşehir and Isparta pumice samples can be found to be 0.952 and 0.951 for Eqs. (3) and (4), respectively.

Nevşehir;

$$G_{bg} = 0.3916\ e^{0.0279P} \qquad r^2=0.952 \qquad (3)$$

Isparta;

$$G_{bg} = -0.006P^2 + 0.646P - 14.85 \quad r^2=0.951 \qquad (4)$$

Table 2. Bond grindability indices of Nevşehir and Isparta pumices—porosity and relative density wise variation

Specific Gravity g/cm^3	Nevşehir Pumice			Isparta Pumice		
	Weight (%)	Porosity (%)	G_{bg} (g/dv)	Weight (%)	Porosity (%)	G_{bg} (g/dv)
< 1.0	30.88	76.84	3.54	0.58	74.03	1.90
1.0 - 1.1	27.04	73.08	3.22	0.49	73.67	2.15
1.1 - 1.2	17.68	68.73	2.37	3.30	70.92	2.35
1.2 - 1.3	7.74	61.12	2.11	8.45	68.81	3.11
1.3 - 1.4	1.80	57.71	1.95	9.57	65.28	3.28
1.4 - 1.5	0.37	54.15	1.84	5.20	61.01	3.42
1.5 - 1.6	0.22	50.79	1.45	2.72	55.78	3.51
1.6 - 1.7	0.09	40.08	1.30	0.86	52.36	3.57
> 1.7	14.18	10.78	---	68.83	24.55	---

3.3 Estimation of the Bond's Grindability

Estimation of the Bond' grindability index for the two pumices studied by the statistical relationship described above has the following advantages. As it appears, any change in the relative density distribution of the pumices may lead to changes in grindability of the same, and the routine sink-float data can, therefore, be monitored closely to detect any possible change in G_{bg}.

It is evident, therefore, that the Bond's grindability of the relative density fractions of Nevşehir pumice power decreases with the increase in specific gravity for most of the relative density fractions followed by a nominal increase in G_{bg} values for the heaviest fractions (Table 2). The relationship obtained for the Isparta pumice is more consistent as the G_{bg} of relative density fractions steadily decreases with the increase in specific gravity.

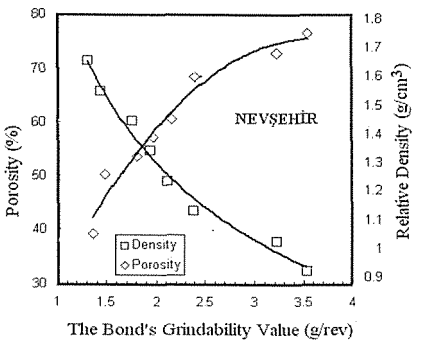

Figure 3. Relationship between Bond's grindability value with porosity and relative density of Nevşehir Pumice

Examination of Figs. 3 and Fig. 4 indicate that the equations proposed have accurately interpolated the grindability value using relative density or porosity values. In other words, the equations proposed are useful for interpolation of the Bond's grindability index from the float–sink data. It can be also seen from these figures that in spite of a small deviation in some relative densities, interpolated values of Bond's grindability are in good agreement with the actual values. Furthermore, more harmonious results can be obtained using the average relative densities and porosity.

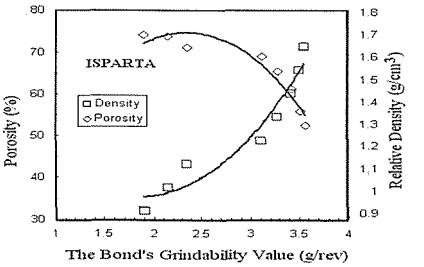

Figure 4. Relationship between Bond's grindability value with porosity and relative density of Isparta Pumice

In Fig. 5, predicted G_{bg} values derived from Eq. (1) was plotted against the experimental G_{bg} values. It can be concluded that porosity relative density of pumices can be used for the estimation of G_{bg} with a higher correlation coefficient ($r^2 = 0.985$). As a result of this, the time needed for tests, and numbers of Bond' grindability test are reduced.

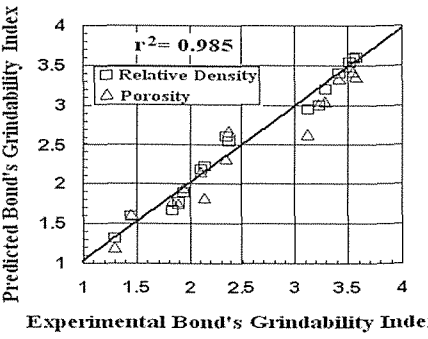

Figure 5. Correlation between experimental and predicted values of Bond's grindability

4. CONCLUSIONS

In the results of the tests, it can be concluded that, the washability of Nevşehir pumice is easier than that of Isparta pumice

The values of cumulative weight and the porosity percent of float material can easily be estimated by describing the float–sink data, in the form of equations in all relative density levels.

Mineralogical analysis of Isparta pumice contained decomposed feldspar minerals and pyroxene minerals. Abrasive minerals such as feldspar, sanidine, pyroxene and amphibole are rather more. Matrix has considerable porosity. Additionally, there is a significant difference depending on particle size for Isparta pumices. Sanidine, pyroxene and feldspar minerals, which are abrasive minerals in Nevşehir pumice, are much less than in Isparta pumice.

The Bond's grindability values of Nevşehir and Isparta pumices appear to be entirely determined by the Bond's grindability of constituent specific gravity fractions of these pumices and the porosity percentage distributions of the same fractions. Two distinct trends can be observed in the variation of the Bond's grindability (G_{bg}) with relative gravity and porosity percentage. Nevşehir easy washability pumice though, shows the grindability to be power decreasing with the increase in specific gravity, with the smallest the Bond's grindability for the heaviest fraction. Isparta moderate-difficult washability pumice shows the different broad trend and does not record the smallest the Bond's grindability value for the heaviest fractions. A different relationship, however, appears to exist for both pumices between the specific gravity and the Bond's grindability of the same float products.

Since sink-float tests are routine exercises in washing plants to evaluate and cross-check the washability characteristics, data generated from the same tests can be used to estimate the grindability without actually determining it, thereby saving considerable time and labour. Since changes in grindability affect the grinder performance, such a quick estimation would enable the operator to quickly intervene in the process to get the desired process performance.

As a result, it appears to be possible to accurately estimate through empirical relationship the Bond's grindability of both pumices from the routine sink-float data. Such estimation offers a number of practical advantages. Moreover, there are have not been publications on the use of washability values to predict the G_{bg} of minerals.

In this study, it has been appeared that, these experimental values for every sample must be seen in order to lower the energy costs in grinding process.

REFERENCES

Armstrong, D.G., 1986. An alternative grindability test: An improvement of the Bond procedure, *Int. J. of Mineral Processing*, Vol. 16, 197-208.

ASTM C-127: Specific Gravity and Absorption of Coarse Aggregate (1959a).

Austin, L.G. and Brame, K., 1983. A comparison of the Bond method for sizing wet tumbling ball mills with a size-mass balance simulation model. *Powder Technology,* Vol. 34, 261-274.

Bhattacharya, S., Anand, V. and Banerjee, P., 1998. Estimation of grindability from sink-float test data

for two different coals. *Minerals Engineering*, Elsevier Science, Vol. 53, 99-106.

Bond, F.C. and Maxson, W.L., 1943, Standard grindability tests and calculations, *Trans. Soc. Min. Eng., AIME*, Vol. 153, 362-372.

Burt, R.O, 1984, *Gravity Concentration Technology*, Elsevier, Amsterdam, Netherlands, 33-51.

Cebeci, Y. and Aslan, N., 2002, Using float–sink data in simple equations to predict sulfur contents, *Fuel Processing Technology*, Vol.76, 231–239.

Deniz, V and Onur, T, 2002. Investigation of the breakage kinetics of pumice samples as dependent on powder filling in a ball mill. *Int. Journal of Mineral Processing,* Elsevier Science, Vol. 67, 71-78.

Deniz, V. and Özdağ, H., 2003. A new approach to Bond grindability and work index: dynamic elastic parameters. *Minerals Engineering,* Elsevier Science, Vol. 16, 211-217.

Deniz, V., 2004. Investigation of breakage behaviour of two different pumice in respect to their mineralogical composition. *European Journal of Mineral Processing and Environmental Protection,* Vol.4, No=2, 154-159 pp.

Deniz, V. and Umucu, Y., 2004. Comparison of the washability characteristics of Nevşehir and Isparta pumices. *Proceedings of The Xth International Mineral Processing Symposium,* Çeşme, Turkey, 191-197.

Deniz, V., 2005. Pomzanın ufalanma özelliği ve çok ince pomzanın kullanımı. *Türkiye Pomza Sempozyumu ve Sergisi 2005.* BSB ve SDU-POMZAMER, Türkiye, 51-60.

Deniz, V. and Umucu, Y., 2005. Interpretation of using sin-float dates by simple recovery equations of two different pumices. *Transactions Section C: Mineral Processing & Extractive Metallurgy*, Vol.114, No:2, C109-C114(6).

Deniz, V., Yazıcı, D.E., Durmaz, H ve Umucu Y., 2007. ISBAŞ A.Ş.'nin Pomza Zenginleştirme Tesisindeki Jig Performansının Zamana Bağlı Olarak Ölçülmesi. *6. Uluslararası Endüstriyel Hammaddeler Sempozyumu*, İzmir, 123-128.

Deniz, V. and Umucu, Y., 2008. Investigation of Gravity Beneficiation Possibilities by Simulation of Kars Region Pumice Using Sink-Float Results of Two Different Jigs Plant, *Proceedings of The XIth International Mineral Processing Symposium*, Antalya, Turkey, 235-241 pp.

Fitton, A., Hughes, T.H. and Hurtley, T.F., 1957. Grindability of British coals-a laboratory examination. *J. Inst. Fuels*, Vol.30, 54-65.

Ghosal, A., Roy, L.C., Bose, R.N. and Lahiri, A., 1958. A study on grindability of coal. *J. Inst. Fuels.* Vol. 31, 34-43.

Horst, W.E. and Bassarear, J.H., 1976. Use of simplified ore grindability technique to evaluate plant performance, *Trans. SME- AIME*, Vol.260, 348-351.

Leonard, J.W., 1979, *Coal Preparation*, AIME, 4th edition. New York.

Magdalinovic, N., 1989. A procedure for rapid determination of the Bond Work Index. *Int. J. of Min. Processing.* Vol. 27, 125-132.

Osborne, D.G., 1988, *Coal Preparation*

Technology, Graham & Trotman, Vol. 1, Chapter 5, London, 179–188.

Prasher, C.L. 1987. *Crushing and Grinding Process Handbook.* John Wiley & Sons, Chichester, England.

Sinha, N.C., Nair, C.P.P. and Bagchi, S., 1969. Studies on the Hardgrove grindability of coals. *J. Min. Met. Fuels.* Vol.18, 265-273.

Yancey, H.F. and Geer, M.R., 1936. Further investigation of methods for estimating the grindability of coal. *Trans. AIME,* Vol.119, 353-357.

Yancey, H.F., Furse, O.L. and Blackburn, R.A., 1934. Estimation of the grindability of coal. *Trans. AIME* , Vol.108, 267-275.

Yap, R.F., Sepulude, J.L. and Jauregui, R., 1982. Determination of the Bond Work Index using an ordinary laboratory batch ball mill, Desing and Installation of comminution circuits. *Soc. Min. Eng., AIME*, New York, 176 -203.

Numerical Simulation Of Coal/Air Flow In A Bowl-Mill Coal Pulverizer

Nuray Kayakol, Bernd Epple
EST- Energy Systems and Technology, Technische Universität Darmstadt Petersenstr
Jan Ericson
VattenFall A/S
Mogens Berg
VattenFall UTVECKLING AB

ABSTRACT Coal pulverizers as a fuel preparation equipment play an essential role in maximizing the consistency of fuel delivered to boilers or steam generators. The study describes development of 3D numerical modeling to simulate complex flow structure of coal pulverizers. The internal geometry of this equipment is very complicated and has not been investigated in detail. The flow field inside a bowl-mill coal pulverizer is investigated by using FLUENT. The CFD model takes full account of the internal geometrical features. Strong swirling flow structure of the pulverizer is examined numerically using a higher level turbulence model, namely Reynolds Stress Model. Eulerian-Eulerian multiphase approach with six phases, one phase for air flow and five more for coal particles having size distribution is used for simulation of two-way couling of mutliphase flow regime which takes into account fluid-particle interaction. The coal/air mixture flow pattern at the pulverizer is captured successfully.

1. INTRODUCTION

The demand for energy is growing worldwide. Coal is the most abundant and affordable of the fossil fuels. It is expected to further on play an important role in the energy mix as the electricity demand is anticipated to continue to grow in both industrialized and developing countries. Pulverized coal combustion is still the current standard technology for electricity generation from coal (Epple et al, 2008). In case of ban or limited use of nuclear power there is considerable need for power plants.

Coal pulverizers play an essential role in maximizing the consistency of fuel delivered to boilers or steam generators. Optimization of a pulverizer performance can contribute to a reduction in a coal-fired boiler's NOx emissions (Storm et al, 2006). Coarse particles of coal don't burn as quickly, easily, or cleanly as finer particles. Because they take longer to burn, coarse coal particles raise a boiler's average NOx emissions. They also foster agglomeration and deposition of slag, making boilers and heat-recovery boilers more vulnerable

to fouling. Amount of unburnt carbon in flyash may increase. Making coal particles smaller increases the overall fuel surface area. Poor fineness traps fuel-bound nitrogen within the carbon char particles. Fuel balance usually improves with better fuel fineness. Fine coal particles mixed in the transport air become more uniformly distributed than coarsely ground coal particles at a similar air/fuel ratio. The better the mixing of the combustion products in the available residence time reduce required excess air levels. By reducing the total airflow and reducing the excess air, thermal NOx production is reduced.

The bowl-mill coal pulverizer is illustrated in principles in Figure 1. Raw coal is fed through a central coal pipe at the top of coal mill and falls by gravity to rotating grinding table where it is pulverized between grinding rollers. Hot primary air, for drying and coal transport, enters from the primary air inlet, flows upward through a ring section having multiple sloped nozzles fixed to surrounding grinding table. The developed swirl air flow induces larger particles to return to the grinding table. During this first stage of classification, fine particles are carried upward from grinding zone into classifier zone in the stream of air and coarser particles fall back to the table for regrinding. In the next stage of classification, the velocity in the classifier zone decreases and larger particles are dropped out. Fine particles are carried to the classifiers. Oversized coarse coal particles return for regrinding.

The last stage of classification takes places in the rotating and stationary classifiers located at top of the pulverizer. An arrangement of circumferentially angled vanes spins the air stream so that the coarser particles are thrown out and return to the grinding zone, while the finer particles pass on with the air stream. The classification is dependent on the velocity of the primary air, rotation speed of classifier, position of blades and the cyclonic action of the primary air/coal mixture. Fine pulverized coal exits the outlet section through typically four discharge coal pipes leading to the burners.

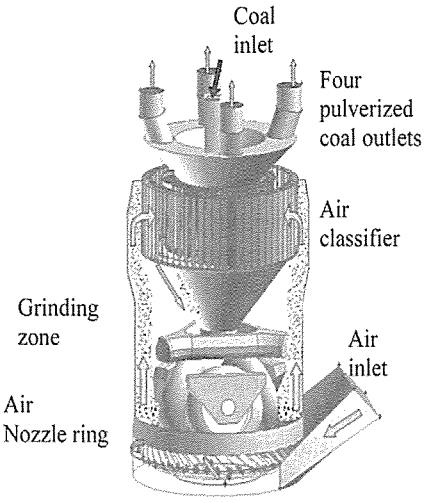

Figure 1. Flow patterns in the pulverizer.

Coal pulverizers rely on a uniform air flow distribution to entrain the varying sizes of pulverized coal particles. If the primary air flow is poorly distributed excess air in some regions of the pulverizer carries large coal particles that are not properly pulverized. This can lead to blocking of the pulverizer at the classifier, reducing the total pulverizer output. If air flow through the pulverizer is too low, pulverized coal can stagnate in ducts or irregular sections inside the pulverizer, therefore giving rise to fire or explosion risk. Thus, it is important to ensure proper air distribution in the pulverizer.

CFD has a great potential to predict the flow field characteristics and particle trajectories through the coal pulverizer as well as the pressure drop. The complicated swirling turbulent flow in coal pulverizer places great demands on the numerical techniques and turbulence models employed in the CFD codes. Generally, CFD predicts turbulent flows through three approaches: direct numerical simulation (DNS), large-eddy simulation (LES), and Reynolds-averaged Navier-Stokes (RANS) equation simulation with turbulence models (Versteeg, and Malalasekera, 2007). DNS and LES provide detailed information on instantaneous airflow and turbulence with the cost of still considerable computing time. For the design and study of air distributions in enclosed environments, the mean air parameters are more useful than instantaneous turbulent-flow parameters. Thus, the interest is stronger in solving the RANS equations with turbulence models that can quickly predict air distributions. The RANS approach calculates statistically averaged (Reynolds-averaged) variables for both steady-state and dynamic flows and simulates the turbulence fluctuation effect on the mean airflow by using different turbulence models, namely standard k-ε, RNG (Renormalization Group Method) k-ε and Reynolds Stress Model (RSM).

In recent years there are several studies published for the prediction of two phase (air/coal) flow in cyclones and coal pulverizers which have swirl flows. The results show that the quality of the numerical solutions depends on the type of turbulence model used for the continuous phase flow.

Vuthaluru et al. (2004) carried out multiphase flow simulation of a simplified pulverizer using a granular Eulerian-Eulerian approach. Turbulence was modeled using standard k-ε model for individual phases. The study can be a good basis for the development of complex coal pulverizer model which includes stationary and rotating classifiers and air inlet duct.

Slack et al. (2000) performed simulation of flow fields in a cyclone in three dimensions, using both the RSM and LES turbulence models. Although both methods have shown good agreement with experimental data, RSM was found as computationally inexpensive method.

Karunakumari et al. (2005) investigated rotating wheel air classifiers experimentally and numerically. RNG k-ε was used as turbulence model. It is stated that RSM did not converge due to geometrical complexity of classifiers.

Benim and Epple (2005) investigated the particle-laden flow in the separator of a labroatory beater wheel mill computationally and experimentally. The standard k-ε model is applied as turbulence model. It is found that the computations under predict the measurements by about 20% on average.

Bilirgen (2005) focused on balancing of pulverized coal flows from verticle spindle mill to burners in boilers. An experimental study were performed for a cyclone in order to use for coal mill since both the mill and cyclone have strong swirling flow and particle separation within the geometry. Based on the comparisons between the experimental data and the CFD model, the RSM was found to be the most suitable turbulence model in predicting the flow domain in strong swirling flow. The CFD model

was used to understand the complex three-dimensional flow structures in the upper half of the coal mill and to help design the flow control mechanism.

The aim of this study is to understand the flow structures within the coal pulverizer. CFD analysis of the pulverizer is carried out only for a 3D single-phase flow (cold clean air) employing FLUENT v6.3 (2008). Clean air flow structure analysis is important to understand possible imbalances in the coal air flow (Vijiapurapu, and Munukutla, 2006). Multiphase-phase swirling turbulent flow in the pulverizer has been simulated using Reynold Stress turbulence Model (RSM) and Eulerian-Eulerian multiphase approach with six phases, one phase for air flow and five more for coal particles having size distribution.

2. MATHEMATICAL MODELING

Reynolds-averaged equations of continuity and momentum for single phase can be written as follows:

$$\frac{\partial \rho}{\partial t} + \frac{\partial (\rho U_i)}{\partial x_i} = 0 \qquad (1)$$

$$\frac{\partial (\rho U_i)}{\partial t} + \frac{\partial (\rho U_i U_j)}{\partial x_j} = \frac{\partial p}{\partial x_i} + \frac{\partial}{\partial x_j}\left[\mu\left(\frac{\partial U_i}{\partial x_j} + \frac{\partial U_j}{\partial x_i}\right)\right] + \frac{\partial}{\partial x_i}\left(-\rho\overline{u_i u_j}\right) + \rho g_i \qquad (2)$$

where ρ and μ are the density and viscosity of the fluid, U_i and u_i are x_i components of the mean and the fluctuating fluid velocities, p is pressure and g is gravity acceleration and

r $\overline{u_i u_j}$ are the components of turbulent moment flux, known as "Reynolds stress".

Particle-laden flow can be simulated using Eulerian-Eulerian approach which assumes all the phases as interpenetrating continua. Conservation equations are solved for each of the phase. A single-phase model is modified with the introduction of the volume fractions $\alpha_1, \alpha_2 \ldots \alpha_n$ for the n multiple phases, as well as the mechanism for the exchange of momentum between the phases.

2.1 Turbulence Model

The Reynolds Stress Model, RSM, is a higher level turbulence model than the standard k-ε family of models. The standard k-ε model assumes isotropic turbulence and does not have any correction for swirl flow. RSM incorporates anisotropy arising from swirling. It involves solving the transport equations for the individual stresses of appearing in Eqn. (2) together with an equation for turbulence energy dissipation rate. This means that seven equations are required for three-dimentional flows. Therefore, it is computationally more expensive than the standard k-ε model, which is known as two-equation model. The equations of RSM can be written as:

$$\frac{\partial}{\partial x_k}(\rho U_k \overline{u_i u_j}) = D_{ij}^T + P_{ij} + \Phi_{ij} - \varepsilon_{ij} \qquad (3)$$

with D_{ij}^T being turbulent diffusion, Φ_{ij} the pressure-strain term, ε_{ij} the dissipation term, and P_{ij} the production term. These quantities are given by Eqns. (4)-(7).

$$D_{ij}^T = \frac{\partial}{\partial x_k}(\overline{\rho u_i u_j u_k}) + \overline{p(\delta_{kj} u_i + \delta u_j)} \qquad (4)$$

$$P_{ij} = -\rho(\overline{u_i u_k}\frac{\partial U_j}{\partial x_k} + \overline{u_j u_k}\frac{\partial U_i}{\partial x_k}) \qquad (5)$$

$$\Phi_{ij} = -p(\frac{\partial u_i}{\partial x_j} + \frac{\partial u_j}{\partial x_i}) \qquad (6)$$

$$\varepsilon_{ij} = 2\mu(\frac{\partial u_i}{\partial x_k} + \frac{\partial u_j}{\partial x_k}) \qquad (7)$$

2.2 Meshing and Solution Procedure.

Governing equations are solved numerically employing finite volume based code, FLUENT. Due to difficulty in reaching convergence in simulations first order upwind scheme was applied for discretization of Reynold stresses and other flow variables.

The three-dimensional model was set up in GAMBIT using an unstructured grid with tetrahedral cells. The geometry was created considering the actual dimensions and thus no scaling was involved. All the geometric details of the equipment, such as air inlet duct, blades of air nozzle ring, grinding rollers, loading frame holding rollers, stationary and the rotating blades of the mill and pulverized coal outlets, are considered. The number of cells, 1.56 millions, is sufficient to obtain grid-independent solution. Meshed geometry of the coal pulverizer without cylindrical housing is given in Fig.3.

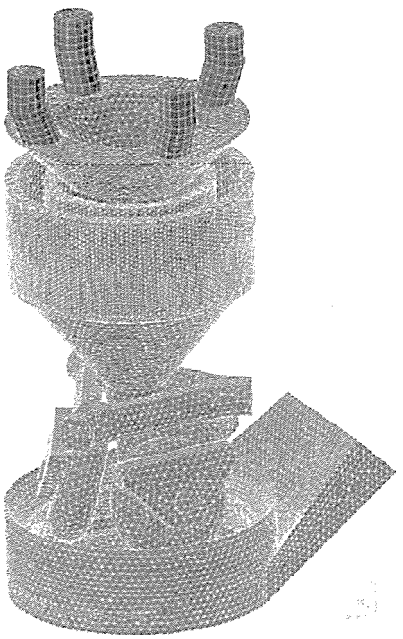

Figure 3. meshing of the pulverizer.

3. RESULTS AND DISCUSSION

Contours of velocity magnitude in the vertical mid-plane of the pulverizer is given in Figure 4. It can be seen that fully developed flow profile in the air inlet duct is obtained. The primary air exits from the nozzle ring as highly swirling air stream that moves upward through the pulverizer. The high speed air jet flow that comes from air nozzle ring is then reduced in the main pulverizer housing.

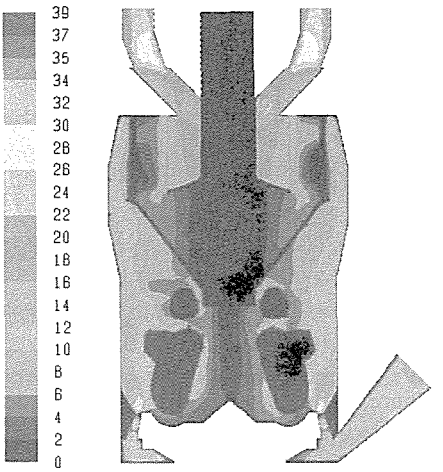

Figure 4. Contours of velocity magnitude (m/s) in the pulverizer.

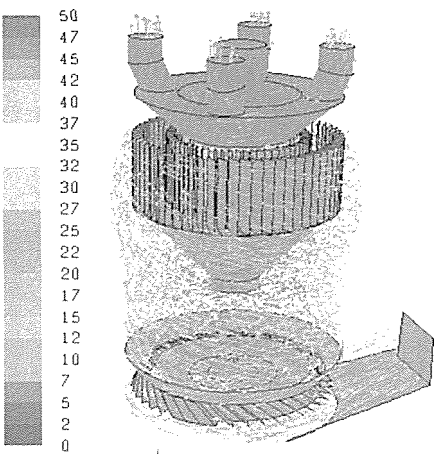

Figure 5. Velocity vectors (m/s) in the pulverizer.

The highly advanced turbulence model, namely RSM is captured swirling flow successfully, as shown in Figure 5.

Figure 6 gives contours of velocity magnitude (m/s) on a horizantal plane in the iddle of the air classifier having static and moving blades, which are located at the upper part of the pulverizer. As can be seen from Figure 7 the classfiers rotate in clockwise direction.

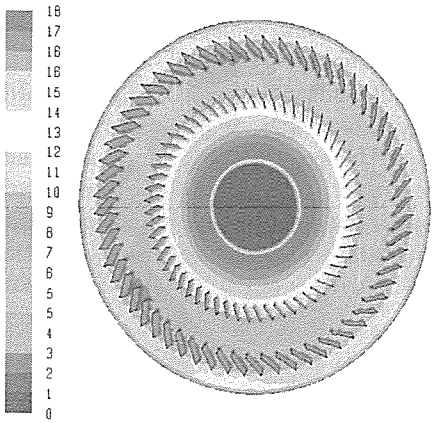

Figure 6. Contours of velocity magnitude (m/s) in the air classfier having stationary and moving blades.

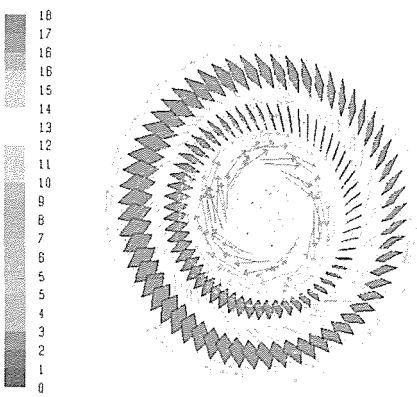

Figure 7. Velocity vectors (m/s) in the air classfier having stationary and moving blades.

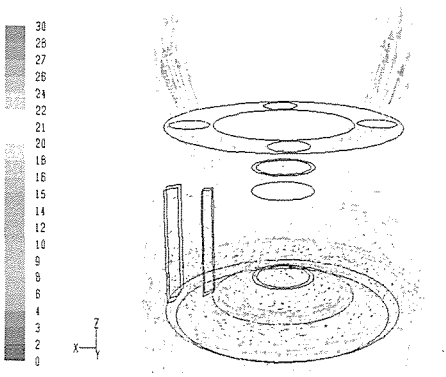

Figure 8. Velocity vectors (m/s) in upper part of the coal pulverizer.

Figure 8 shows contours of velocity vectors in the upper part of the coal oulverizer. Swirling air stream flows through stationary classifier. Due to presence of rotating classifier air circulation pattern in the clockwise direction is created. Internal recirculation regions occur between the stationary and rotating classifiers.

Figure 9 shows contours of velocity vectors at air nozzle ring at the lower part of the coal pulverizer. Primary air is non symmetrically fed at the bottom

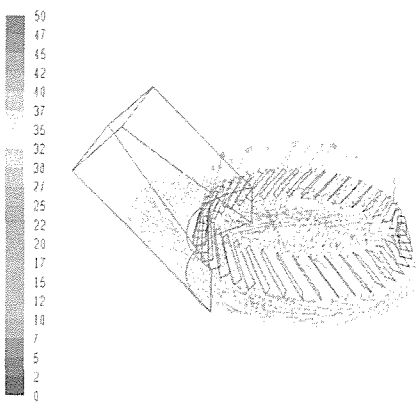

Figure 9. Contours of velocity vectors (m/s) at air nozzle ring.

of the coal pulverizer. The air stream goes down through the inclined air inlet duct and then enters the bottom part of the pulverizer. Then it splits into two streams in front of the cylindrical obstacle, which is at the bottom part of the grinding table. The velocity in these two streams increases due to lower flow area while turning over the cylindrical solid object. Then, the splitted flow streams come together at the back of the cylinder. Inclined blades accelerate and orient the flow through air nozzle ring.

The required air jet velocity in a pulverizer has a lower limit, because a minimum air velocity is needed to entrain the coal upwardly from the rotary table and prevent it from falling back down through the air port openings into the air plenum. This minimum air jet velocity is a function of the coal particle size and weight. For a coal particle size of about 40 mm the minimum required jet velocity is approximately 40 m/s for which velocity prevents the coal particles from falling back down through the air ports. The minimum jet velocity is the terminal velocity which can be calculated as

$$1.75\sqrt{\frac{gD_p(\rho_p-\rho)}{\rho}}=1.75\sqrt{\frac{9.81\times0.04*(1100-1.2)}{1.2}}$$

=33 m/s for coal particles having density of 1100 kg/m^3. As can be seen from Figure 9 maximum air jet velocity calculated from CFD model is 50 m/s which is larger than the minimum required jet velocity.

Figure 10 indicates a smooth uniform distribution of flow to each nozzle on the ring. The air flow patterns are visualized using flow path lines.

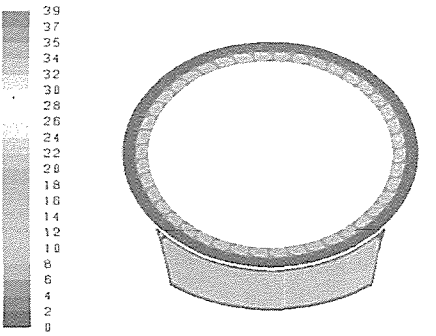

Figure 10. Contours of velocity magnitude (m/s) on the horizontal plane at air nozzle ring.

Figure 11 gives the flow path lines between blades of air nozzle ring. The path lines show that air stream flows between the blades and change directions to induce swirling flow.

Figure 12 displays for a case with no separating blades on the air nozzle ring flow inside the mill. It shows that higher upward velocities in the "back" half of the pulverizer. This indicates that the primary air non-uniformly distributed in the pulverizing house, but not in the air nozzle ring. Figure 13 indicates that swirling affect of air nozzle ring is diminished in the pulverizer.

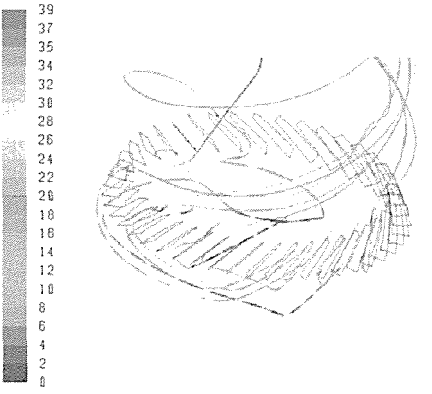

Figure 11. Flow path lines on the horizontal plane at air nozzle ring.

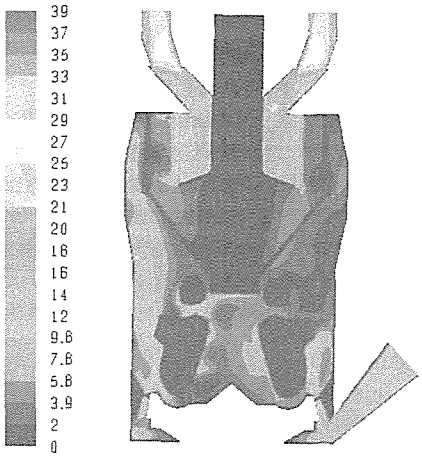

Figure 12. Contours of velocity magnitude (m/s) in the pulverizer having no separating blades on air nozzle ring.

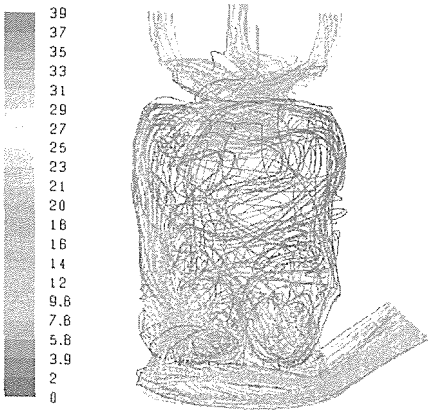

Figure 13. Flow path lines in the pulverizer having no separating blades on air nozzle ring.

Comparison of results shown in Fig. 4 and Fig. 12 and 13 shows that separating blades on air nozzle ring give swirling affect in the mill and affect uniformity of flow distribution in the pulverizer.

Multiphase-phase swirling turbulent flow in the pulverizer has been simulated using Reynold Stress turbulence Model and Eulerian-Eulerian multiphase approach with six phases, one phase for air flow and five more for coal particles having size distribution. The mixture model, which is the computationally less expensive multiphase model, fails due to presence of heavier particles. Therefore, Eulerian model of Eulerian-Eulerian approach, which is the most complex of the multiphase models available in FLUENT was selected in this study. Due to high CPU and RAM requirements of six-phase simulations a transient solution is computed using less number of cells, which is lowered from 1.5 million to 600 thousand. Two-way couling of mutliphase flow regime which takes into account fluid-particle interaction captures coal/air mixture flow pattern successfully.

Figure 14-18 show contours of volume fraction of 45 μm, 75 μm, 90 μm, 125 μm and 250 μm coal particles having mass fractions of 4.59, 26.18, 32.49, 18.88 and 9.25, respectively. All particles follow a circumferential motion near the walls due to swirling air flow. Particles of small and intermediate sizes are carried up from grinding to classifier zone. Largest particles of coal, 250 μm, stay more closer at the grinding zone and has difficulty in reaching classifier zone.

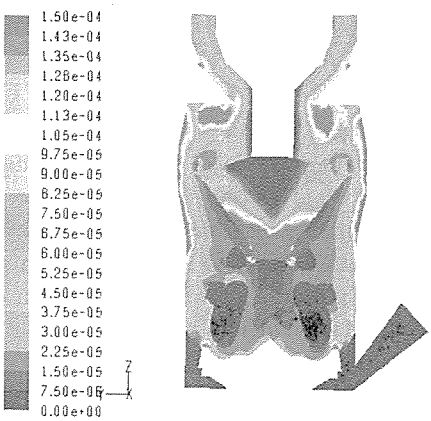

Figure 14. Contours of volume fraction of 45 μm coal particles

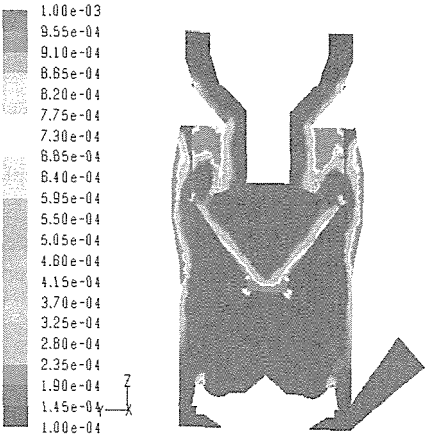

Figure 15. Contours of volume fraction for 75 μm coal particles .

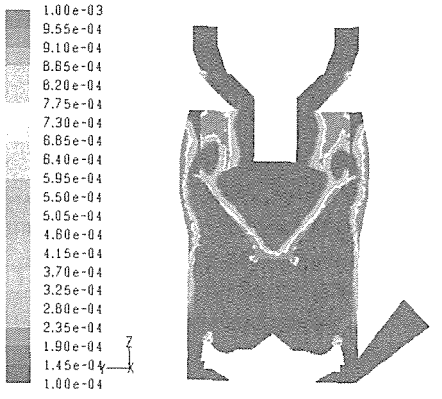

Figure 16. Contours of volume fraction for 90 μm coal particles

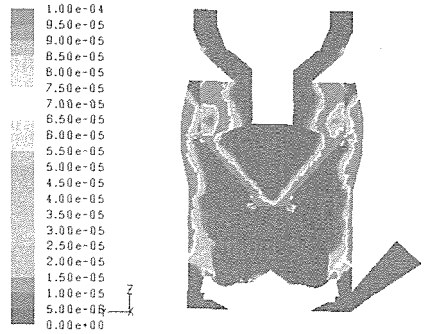

Figure 17. Contours of volume fraction of 125 μm coal particles.

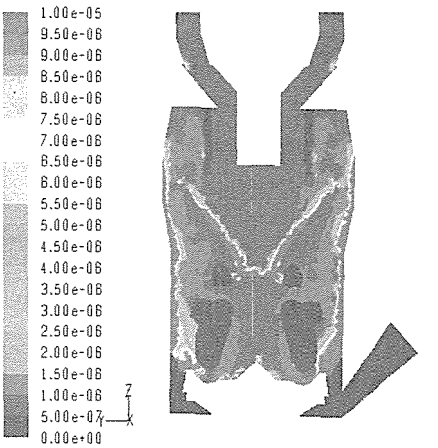

Figure 18. Contours of volume fraction of 250 μm coal particles.

4. CONCLUSION

The 3D swirling turbulent flow field inside a bowl-mill coal pulverizer is calculated using FLUENT, taking full account of the internal geometrical features. High level turbulence model Reynolds Stress Model, which deals with high swirl effects is used.

First, clean air flow without coal particles in the coal pulverizer is simulated to examine a range of geometry and flow options and increase the performance of the pulverizer. This study also contributes to a better understanding of the operation of the stationary and rotating classifiers often used in many process industry applications. Then, multiphase-phase swirling turbulent flow in the pulverizer has been simulated using Eulerian-Eulerian multiphase approach with six phases, one phase for air flow and five more for coal particles having size distribution. Two-way couling of mutliphase flow regime which takes into account fluid-particle interaction captures coal/air mixture flow pattern successfully.

REFERENCES

Benim, A.C., Stegelitz, P. and Epple, B., 2005, Simulation of the Two-Phase Flow in a Laboratory Coal Pulverize, Forsch Ingenieurwes, Vol. 69, pp. 197-204.

Bilirgen, H., 2005, Balancing of Pulverized Coal Flows to Burners in Boilers With Pressurized Vertical Spindle Mills, DEO Report DE-FC26-03NT41867, Bethlehem, PA.

Epple,B., Leithner, R. Linzer, W. L., 2009, Numerical simulation of power plants and energy systems, Springer Press, Germany.

FLUENT v6.3 Users Guide, Lebanon, USA, 2008.

Karunakumari, I., Eswaraiah, C., Jayanti, S. and Narayanan, S.S., 2005, Experimental and Numerical Study of a Rotating Wheel Air Classifier, AIChE Journal, Vol. 51, No.3, pp.776-790.

Slack, M.D., Prasad, R.O., Bakker, A. and Boysan, F., 2000, Advances in Cyclone Modeling Using Unstructured Grids", Trans IChemE, Vol. 78, part A, pp. 1098-1104.

Storm, S. K., Storm, R. F., Storm D. S., Tuzenew, S., McClellan, A., 2006, A case study of how vertical spindle pulverizer performance is related to overall plant performance ASME International Electric Power Conference, Atlanta, Georgia.

Versteeg, H.K. and Malalasekera, W., 2007, An Introduction to Computational Fluid Dynamics, The Finite Volume Method, Prentice Hall, Second Edition, England.

Vijiapurapu, S., Cui, J. and Munukutla, S., 2006, CFD Application for Coal/ Air Balancing in Power Plants. Applied Mathematical Modeling, Vol.30, pp. 854-866.

Vuthaluru, H.B., Pareek, V.K. and Vuthaluru, R., 2004, Multiphase Flow Simulation of a Simplified Coal Pulverizer, Fuel Processing Technology, Vol. 86, pp.1195-1205.

The Solvent Extraction of $HAu(Cl)_4$ from Chloride Solutions by Diethylene glycol dibutyl ether (DBC)

M. Abdollahy and S. Javanshir
Mining Engineering Department, Tarbiat Modares University, Tehran, Iran

ABSTRACT The solvent extraction of $HAu(Cl)_4$ from Chloride solutions by using Diethylene glycol Dibutyl ether (DBC) as extractant has been investigated. The influence of several variables such as agitation time, pH, temperature, agitation speed, volume percentage of diluents, gold concentration and volume ratio of aqueous phase to organic phase were investigated. The results indicated that the organic phase had a high extraction capacity. Almost all of the $AuCl_4^-$ (>98%) was transferred from the aqueous phase into the organic phase. Most of the impurity in the organic phase can be scrubbed with dilute hydrochloride acid (1N) then elemental gold could potentially be recovered by the addition of reducing agents, such as oxalic acid.

1 INTRODUCTION

Gold has attracted humans of all cultures and civilizations since time immemorial. Its beautiful color, excellent corrosion and oxidation resistance, superior malleability, ease of fabrication and limited availability are collectively responsible for the unique place gold has in the family of metals.

With the development of modern industry and high technology, various rare elements and other matters with high purity were required. Solvent extraction method has some advantages, such as large capacity, simple equipment, easy auto control, quick and safe operation and low cost, and has therefore become widely employed for the recovery of precious metals from chloride solutions or neutral solution, and many extractants for gold have been reported, which include oxygenated extractants dibutylcarbitol (DBC), thio extractants Zolotov & Petrukhin (1978), ammonium extract-ants Liu &Wan (2004), phosphorus extractants such as tributyl phosphate (TBP) Wang (1997), 2-ethylhexyl phosphonic acid mono-2-ethylhexyl ester (PC-88A) Bandekar & Dhadke (1998), tributyl phosphine oxide (TBPO) Shen & xue (2007) as well as methyl isobutyl ketone (MIBK) Cox (1992), monoamid compounds Narita & Tanaka (2006) and amine extractants Shillington & Tait (1991), Hasegawa &Kobayashi (1991).

In addition, extraction of Au (III) from chloride media by using thio-

caprolactam as extractant was studied by Nunez (2006). Whereas gold extraction by DBC could follow by direct reduction with a chemical reductant to granular metallic gold (>99.9%), at present work, DBC as an extractant was used.

The Purpose of this study is to elucidate the effective parameters on gold (III) extraction and to determine the optimal conditions for this process.

2 EXPERIMENTAL

2.1 Reagents

The samples of copper anode slimes were kindly provided from the Sarcheshmeh Copper Mine, KERMAN IRAN. All reagents used were of analytical reagent grade and Merck. Standard stock solutions (100 ppm) of Au were prepared from dissolving of pure gold powder (>99%). Diethylene glycol dibutyl ether (DBC) was obtained from Shuyang Hengrun Fine Chemical Co, China. Dibutyl carbitol physical constants: density (20°C) 0.8853 g/cm^{-3}, boiling point 254.6°C, flash point 118°C, and solubility in water 0.3%. Commercial kerosene was obtained from Merck. Distilled water was used in this work. Gold (III) in aqueous phase was analyzed by atomic absorption spectrometry and then concentration of gold in organic phase is obtained by mass balances.

3 RESULTS AND DISCUSSION

3.1 Effect of Stirring Speed on the Extraction

The extraction rate increases by increasing the stirring speed up to 300 rpm that was illustrative of diffusion controlled processes (Fig 1). When the stirring speed is more than 300 rpm, the extraction rate appears constant. So other experiments were done at 300 rpm. All conditions and various parameters are shown in Table 1.

3.2 Effect of Agitation Time on the Extraction

The extraction percentage was measured after different agitation time. In all cases, the equilibrium was reached within 2 min of contact.

Prolonging agitation when stirring speed was more than 300rpm, could not further increased extraction per-centage. Therefore, in the subsequent extraction experiments, the agitation time was exclusively fixed to 5 min (Fig.2).

Table 1. Effect of stirring speed and time on the extraction

RPM	$[Au]_{raff.}$ (ppm)					E%				
	1 min	2 min	5 min	10 min	20 min	1 min	2 min	5 min	10 min	20 min
100	69.1	50	22	16.1	0.78	33.3	51.8	78.8	84.5	99.2
150	56	40.3	15.4	3.04	0.69	46	61.1	85.1	97.1	99.3
200	32.6	7.21	5.26	1.46	0.53	69.52	93.26	95.08	98.63	99.50
300	0.89	0.55	0.39	0.43	0.5	99.16	99.48	99.63	99.59	99.53
450	0.51	0.24	0.33	0.34	0.36	99.52	99.77	99.69	99.68	99.66
600	0.21	0.25	0.31	0.3	0.22	99.80	99.76	99.71	99.71	99.79

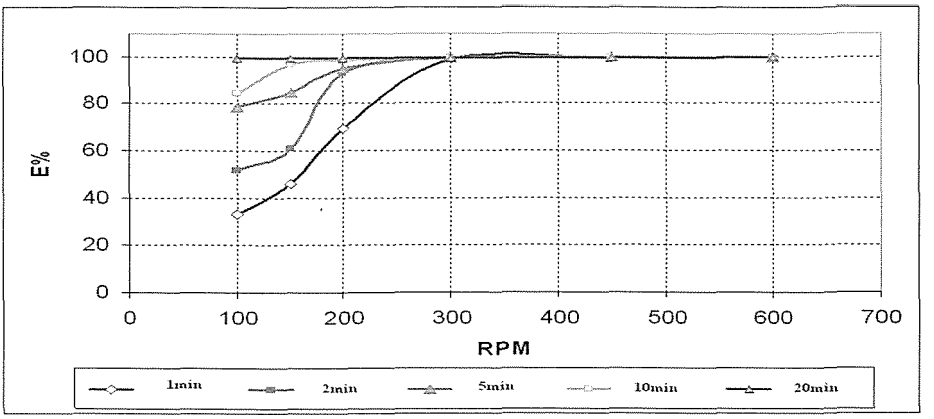

Figure 1. Effect of Stirring Speed on the Extraction (V_o=V_a= 25ml, T=25°C)

3.3 Effect of Gold Concentration in the Aqueous Phase

Because of low grade ore, a leaching process usually produces a very dilute gold chloride solution. Table 2 presents the extraction percentage of gold from solutions with different gold concentrations. The results demonstrate that the influence of the gold concentration in the range of 100 ppm to 400 ppm on its extraction percentage is negligible. More than 99% of gold is extracted into the organic phase in all cases. The reason is high extractable and loading capacity of gold by DBC (Fig. 3).

3.4 Effect of Diluent Content on the Extraction

The extraction percentage of gold as a function of the Kerosene content (in volume fraction) is shown in Figure.4. It can be seen that the diluent plays an important role during the extraction. Without kerosene, all gold entered into the organic phase. An increase in kerosene concentration leads to a decrease in the gold extraction percentage. Therefore further experiments were done without diluents.

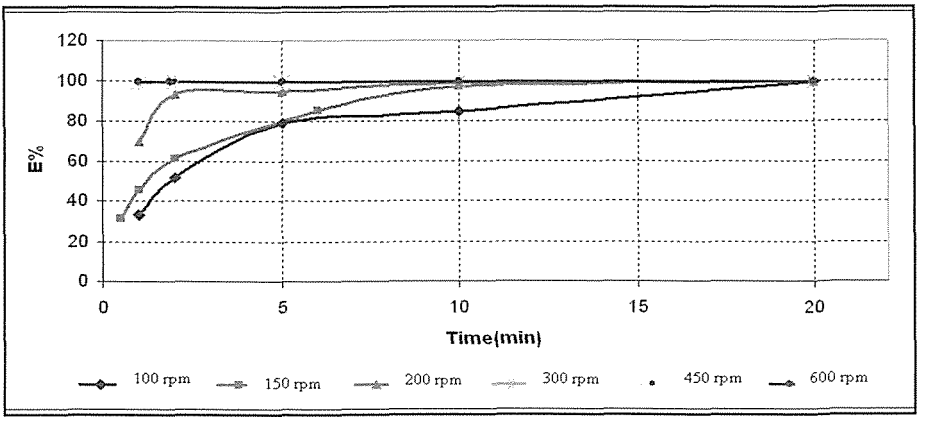

Figure 2. Effect of agitation time and stirring speed on extraction (V_o=V_a= 25ml, T=25°C)

Table 2. Effect of gold concentration in the aqueous phase on the extraction

[Au] ppm	$[Au]_{raff.}$ (ppm)					E%				
	1 min	2 min	5 min	10 min	20 min	1 min	2 min	5 min	10 min	20 min
100	0.51	0.24	0.33	0.34	0.36	99.52	99.77	99.69	99.68	99.66
200	0.46	0.52	0.51	0.57	0.65	99.80	99.77	99.78	99.75	99.72
300	0.8	0.67	0.64	0.3	0.56	99.68	99.73	99.74	99.88	99.77
400	0.64	0.74	0.58	0.48	0.81	99.83	99.80	99.84	99.87	99.78

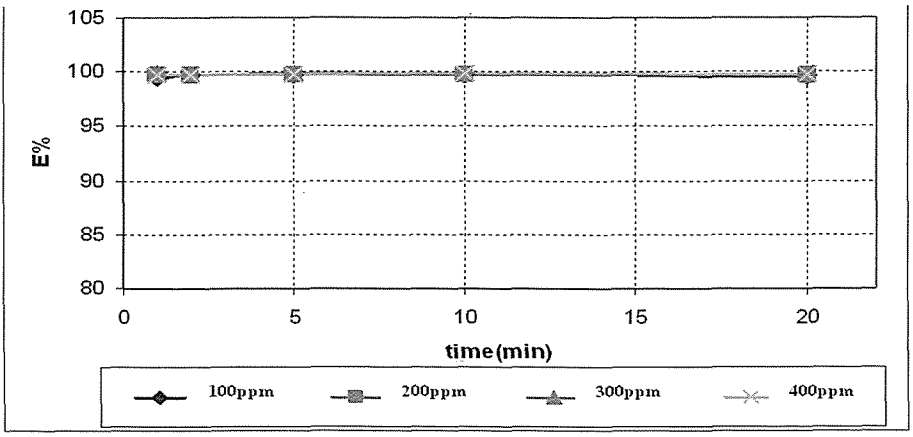

Figure 3. Effect of gold concentration in the aqueous phase and agitation time on the extraction (V_o=V_a= 25ml, T=25°C)

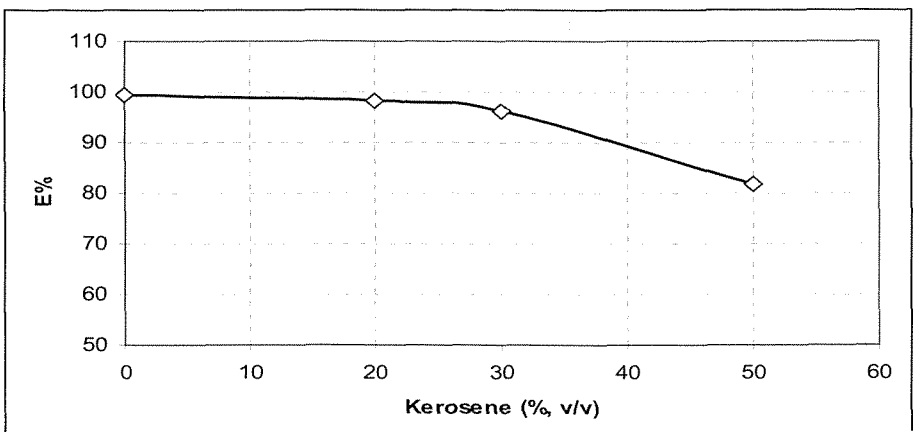

Figure 4. Effect of diluent content on extraction ($V_{o=}V_a$= 20ml, T=20°C, 480 Rpm, t: 15 min)

3.5 Effect of the Volume Ratio (V_{aq}/V_{org})

Since the gold solution usually needs to be further concentrated, an excellent extraction system must possess not only high extraction ability, but also high extraction capacity. So the influence of the volume ratio of the aqueous phase to the organic phase on the extraction percentage was studied. V_{aq}/V_{org} ranged from 2 to 30. The results suggested that the system had a high capacity for extraction of gold (Tab.3) McCabe-Thiele diagram was demonstrated in Figures 5-6 in two different gold concentrate in aqueous phase. It was found DBC was able to extract all gold in these concentration ranges.

3.6 Effect of Solution pH

An interesting result was obtained in the study of the effect of solution pH. In this series of experiments, the solution pH was varied over the range of -0.5 to 2. The DBC and gold concentrations were kept constant at 100% (v/v) and 100 ppm, respectively. The experiments were carried out at the temperatures of

Table 3. Effect of the volume ratio (V_{aq} / V_{org}) on the extraction percentage

[Au]a, ppm	V_{aq}/V_{org}	$[Au]_{(org)}$ ppm	E (%)	[Au]a, ppm	V_{aq}/V_{org}	$[Au]_{(org)}$ ppm	E (%)
103	2	197.22	95.7	480	15	1347.5	99.86
103	4	383.4	93.1	480	20	4598.7	99.13
103	6	557.94	90.3	480	25	5407.3	98.69
103	8	715.64	84.3	480	30	5575.1	98.64

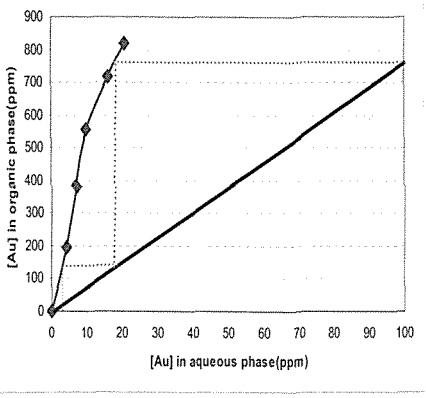

Figure 5 .McCabe-Thiele diagram ($V_{o=}V_a$= 25ml, T=20°C, 480 rpm, t: 10 min, $[Au]_a$:103ppm)

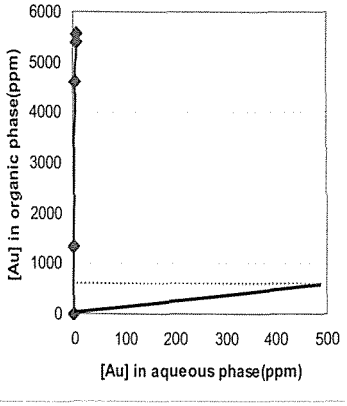

Figure 6. McCabe-Thiele diagram ($V_{o=}V_a$= 25ml, T=20°C, 480 rpm, t: 10 min, $[Au]_a$:480ppm)

19.5°C. The obtained gold extraction percentage is shown as a function of solution pH in Figure 7. It was found that all experiments conducted in acidic solutions providing a high percentage of at pH of -0.5. It is known that the gold (III) ion exists in hydrochloric acid as tetrachloro auric at a low pH, while at a high pH gold (III) hydroxide forms Marsden (1992) that doesn't extract by DBC.

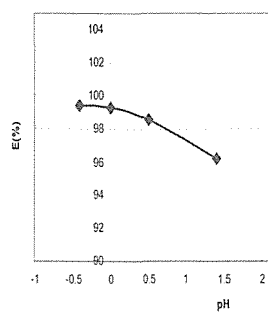

Figure 7. Gold extraction Percentage as a function of solution pH ($V_{o=}V_a$= 25ml, T=25°C, 480 rpm, t: 10 min)

3.7 Effect of Temperature

To study this variable, aqueous solutions of 568 ppm of gold containing HCl (2M), and organic solutions containing DBC (100% (v/v)) were shaken at temperatures from 20°C to 50°C, for 5 min. The results obtained are shown in Figure 8. It may be noted that as temperature increases, gold extraction decreases. ΔH value of -66.43 kJ /mol was obtained from the slope of this diagram (Fig.8) which indicates the exothermic nature of the extraction reaction.

4 CONCLUSIONS

Diethylene glycol dibutyl ether (DBC)

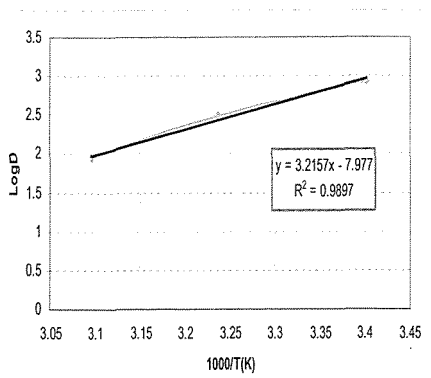

Figure 8. Effect of temperature on distribution coefficient

($V_{o=}V_a$= 25ml, 480 Rpm, t: 10 min)

was used in order to investigate its extraction capability for Au (III) from HCl solutions. Au (III) immediately reaches the extraction equilibrium in 5 min. The extraction of gold into DBC was optimized. Various parameters were studied and optimum conditions for gold extraction were obtained. The result was demonstrated that the extraction rate increases by increasing of the stirring speed up to 300 rpm and then it was not changed by ultra stirring speed. The equilibrium was reached within 2 minute of contact. Also the effect of gold concentration in the range of 100 ppm to 400 ppm on extraction percentage was negligible. Diluent (Kerosene) had negative effect on extraction. So tests were done without kerosene.

It was found that the percentage of extraction in acidic solutions was high (at a pH: -0.5). The volume ratio of the aqueous phase to the organic phase on the extraction percentage was studied. The results suggest that the system has a high capacity for extraction of gold.

Temperature effect also was studied. From the slope of Log D versus 1000/T,

ΔH value was equal to -66.43 kJ/mol, which indicates the exothermic nature of the extraction reaction.

ACKNOWLEDGMENT

The authors would like to express their gratitude to SAR-CHESHMEH for supplying financial support and Tarbiat Modares University for preparing facility for this study.

REFERENCES

Bandekar S.V., Dhadke P.M.(1998), Solvent extraction separation of platinum(IV) and palladium(II) by 2-ethylhexyl phosphonic acid mono-2-ethylhexyl ester (PC-88A), J.Separ. Purif. Technol. 13 ,pp129.

Cox.M(1992),Solvent extraction in hydro- metallurgy, in: J. Rydberg, C. Musikas,G.R.

Choppin (Eds.), Principles and Practices of Solvent Extraction, Marcel Dekker, Inc.,New York, pp. 357–412.

Feather A., Sole K.C., Bryson I.J.(1997a), Gold refining by solvent extraction the Minataur™ process in: Proceedings of the Randol Gold Forum 97, Monterey, CA, 18–21.

Feather A., Sole K.C., Bryson I.J.(1997b). Afr. Inst. Min. Metall. 97 (4), p.169, 1997. Goia D.V., Matijevic E. (1999), Tailoring the particle size of monodispersed colloidal gold, A: Physicochemical and Engineering Aspects, 146, pp 139–152.

Hasegawa.Y, Kobayashi .I, Yoshimoto S.(1991), Extraction of palladium (II) and platinum (IV) as chlorocomplex acids into basic organic solvents, Solvent Extract. Ion Exch. 9 (5) 759-768.

Krzysztof. P, Krzysztof. F. (2006), Kinetics of Reduction of Gold (III) Complexes Using H_2O_2, metallurgical and materials transaction B, vol 37B, p.713.

Liu K.J., Wan T.Y., Shibayama A., Miyazaki T., Fujita T. c. (2004), Gold extraction from thiosulfate solution using trioctylmethyl- ammonium chloride, Hydrometallurgy 73, pp41–53.

Marsden, J.; House, L.(1992) The Chemistry of Gold Extraction; Ltd: New York, pp 144- 158.

Narita H., Tanaka M., Morisaku K., Abe T. (2006), Extraction of gold(III) in hydro-chloric acid solution using monoamide compounds, Hydrometallurgy 81, pp153–158.

Nical M.J., Adams M.D. (1997), Afr. Inst. Min. Metall. 97 (6),p. 281.

Nunez,M.E., Rodríguez de San Miguel. F(2006) Selective ω-hiocaprolactam based recovery of Au(III) from chloride media in solvent extraction and polymer inclusion membrane systems, Separation and Purification Technology, Volume 51, Issue 1, pp 57-63.

Sánchez.L ,Cabrera A., Grote M.(2002), Preparation of gold powders by means of redox-active extractive systems M.G., Materials Chemistry and Physics 76 pp 279–284.

Shen, Y.F., Xue,W.Y., (2007) Recovery of palladium, gold and platinum from hydrochloric acid solution using 2-hydroxy-4-sec-octanoyl diphenyl ketoxime. Separation and Purification Technology 56, 278–283.

Shillington D.P., Tait B.K.(1991), Diamine extractants in metal separation. An illustration of the potential of the chelate extraction

mode in the platinum (IV)–palladium (II) base metal system, Solvent Extract. Ion Exch. 9 (5) ,7499758.

Wang B.Y., Wang Q., Wang X.D.(1997), Study on the synergistic extraction of gold (III) with amine and neutral phosphorus-based extractants, J. Shandong Sci. China 10 (2),pp 10–15, (in Chinese).

Zolotov Y.A., Petrukhin O.A., Shevchenko V.N., Dunina V.V.(1978), E.G. Rukhadze, Solvent extraction of noble metals with derivatives of thiourea, Anal. Chim. Acta 100 pp 613–618.

Zhu. P, Guobang.G (2006), Kinetics of stripping of gold loaded in DBC organic phase by sodium sulfite, J. RARE METALS, Vol. 25, No. 1, pp 1-6.

Eh Effect on a Lead-Zinc Sulfide Ore Flotation

Junia Soares Alexandrino, Geriane Macedo Rocha, Diogo Prata Bussular, Carlos Alberto Pereira
Universidade Federal de Ouro Preto, Ouro Preto, MG, Brazil
Antonio Eduardo Clark Peres
Univerdidade Federal de Minas Gerais, Belo Horizonte, MG, Brazil

ABSTRACT The effect of pulp potential on a lead-zinc sulfide ore flotation is presented. The influence of the reagents sodium sulfide and sodium sulfite and of the use of nitrogen substituting for air as the flotation gas phase on lead and zinc recoveries was investigated with the aid of statistically planned experiments. Values of Eh, pH, and dissolved oxygen were measured during the full flotation sequence. Sodium sulfite did not affect significantly neither the pulp potential nor the lead and zinc recoveries. The interaction between sodium sulfite and the presence of nitrogen decreased the pulp potential in the lead circuit and resulted in enhanced lead recovery. The reagent sodium sulfide individually did not change the pulp potential and increased the lead recovery. Its interaction with the use of nitrogen decreased the pulp potential and impaired the lead recovery. The presence of nitrogen reduced the dissolved oxygen content in the pulp, increasing the zinc recovery and decreasing the lead recovery.

1 INTRODUCTION

Sulfide minerals are prone to surface oxidation under oxidizing environment, such as air. This oxidation impairs the flotation performance, increasing the reagents consumption resulting in higher process costs.

The surface properties study plays a relevant role on the floatability and the minerals separation efficiency. The sulfides surface chemistry is more complex than that of metals and oxides. During grinding, galvanic contact occurs between sulfide minerals and grinding media, resulting in a current that causes redox reactions on the mineral surfaces, due to differences between pulp potentials (Gonçalves, 2003).

Sulfide minerals oxidation has been investigated for decades (Woods, 2003). The reaction products strongly affect the surface mineral hydrophobicity. Dissolved oxygen promotes gangue oxidation, reducing collector adsorption onto these species.

Electrochemical phenomena relevance towards sulfide minerals flotation was pointed out in the last century thirties

decade, but deserved little attention until the sixties. At present, it is essential to correlate the flotation reagents performance with the electrochemical pulp conditions. Ralston (1991) reported Eh influence on minerals recovery with the aid of studies correlating thermodynamic data for species identification.

Reeken et al. (1989) investigated some factors affecting lead and zinc flotation, reporting that selectivity is one of the least serious problems in zinc flotation, when other sulfides are also floated. The characteristics and responses to sphalerite flotation conditions changes are complex and widely different from those prevailing in other systems.

High $ZnSO_4$ dosages may be required for sphalerite depression. This action is based on the following chemical equilibrium:

$$ZnS_2 + 2/n\,M^{n+} \rightarrow M_{2/n}S_s + Zn^{2+} \quad (1)$$

Equation 1 represents chemisorption and desorption of metallic íons such as Pb^{2+}, Ag^{+}, and Cu^{2+} onto sphalerite. Increasing and maintaining the zinc ion concentration shifts the equilibrium of equation (1) to the left.

Plante and Sutherland (1984), apud Ralston (1991), investigated galena, pyrite, chalcopyrite, and sphalerite oxidation products in neutral and alkaline solutions. In the case of sphalerite, sulfur salts were the major detected oxidation products at pH 6, sulfate being a minor component. The species contents increase at pH 10. The main galena oxidation product depends on the pH and also on the exposure time to oxygen. After several hours of oxygen exposure, the surface reaches a maximum oxidation degree. The major sulfur oxidation products are elemental sulfur, under acidic conditions, sulfates in neutral solutions, and thiosulfate, under alkaline conditions. The oxidation products depend on the mineral characteristics. The sulfides oxidation kinetics deserves considerable attention. The reactions dimension depends on the available area, the oxygen partial pressure, the mineralogy, the solution pH, and the temperature. These authors also investigated high purity galena oxidation under controlled oxygen atmosphere between 20 and 76 cmHg, observing that the use of nitrogen enhances the floatability. The PbS surface oxidation, after many hours exposure to oxigen, may be saturated with sulfur, due to the interaction between chemisorbed oxygen atoms and PbS, according to the reaction:

$$PbS + O_{surface} + H_2O \Leftrightarrow Pb^{2+}_{(aq)} + S_{(PbS)} + 2OH_{aq} \quad (2)$$

Ralston (1991) suggested that the pulp potential may vary depending on the source of the mineral. The potential (Eh) is a relevant parameter to be considered, for it may report the nature of surface species. Sulfide minerals processing is usually dominated by oxidation, reduction, and adsorption reactions. Understanding these reactions and controlling and manipulating the Eh provide the flotation processes optimization and enhances selectivity. Pulp potentials may be measured at different confidence levels. Eh values are referred to the standard hydrogen electrode (SHE) and are ruled by oxidation, reduction, and adsorption at the solid-liquid interface.

The sulfides flotation systems present several chemical interactions, leading to changes in the pulp potential

and affecting flotation results. Among the sulfide minerals, pyrite presents the highest pulp potential. In galvanic contact with other sulfides, pyrite increases the medium potential, enhances the oxidation rates of other species, reducing the dissolved oxygen content. In mixed sulfide minerals systems, the reaction products affect the flotation results (Guy e Trahar 1985).

The target of the present study was to monitor the pulp potential in a lead-zinc sulfide ore flotation, aiming at understanding the interference of the reagents sodium sulfide and sodium sulfite, and the use of nitrogen as flotation gas phase.

2 METHODOLOGY

The lead-zinc sulfide ore sample came from an underground mine (Morro Agudo, Votorantim Metais Zinco), collected at the concentrator, after primary crushing. In the laboratory the sample was reground, homogenized and stored under nitrogen atmosphere.

Grinding was performed in a ball mill, previously cleaned with quartz to prevent oxidation and contamination. Each flotation experiment used 1,200 g, ground, immediately prior to the test, to $d_{80} < 44$ μm.

2.1 Experiments Based on Factorial Design

The variables and levels selected for the experiments factorial design, based on exploratory experiments, are illustrated in table 1. Considering three variables and replicate experiments, the number of tests reached 16.

Table 1. Variables and levels

Variables	Levels -	Levels +
a- sodium sulfide (g/t)	0	50
b- nitrogen gas (8NL/min)	no	yes
c- sodium sulfide (g/t)	0	400

The experiments planning is presented in table 2. The sequence of tests was randomly drawn.

Table 2. Factorial design development

Var*	a	b	c	R_{Pb}	R_{Zn}
t	-	-	-	89,40	80,16
a	+	-	-	90,79	80,26
b	-	+	-	84,93	84,93
ab	+	+	-	84,24	82,89
c	-	-	+	86,42	81,75
ac	+	-	+	87,23	80,92
bc	-	+	+	86,00	81,56
abc	+	+	+	90,48	82,47

*Variables

The pulp potential was measured with platinum electrode during the flotation sequence consisting of galena flotation followed by sphalerite flotation.

The steps of the bench scale flotation experiments were:

i) conditioning the pulp for 1 min ;

ii) starting to monitor the pulp potential (Eh), the dissolved oxygen content, and the pH;

iii) collecting a 50 mL fraction;

iv) modulating the pH at 9.8 with hydrated lime (100%);

v) adding collector (20 g/t potassium isopropyl xanthate, 1% w/v) and frother (12 drops methyl amyl alcohol), conditioning for 1 min;

vi) floating galena for 5 min;

vii) adding collector (20 g/t potassium isopropyl xanthate);

viii) floating galena for 5 min;

ix) removing the galena concentrate and collecting a 50 mL pulp sample;

x) using the galena flotation tailings, starting sphalerite flotation;

xi) modulating the pH at 10.5 with hydrated lime (100%);

xii) adding activator (200 g/t copper sulfate 10% w/v), conditioning for 5 min;

xiii) adding collector (50 g/t potassium amyl xanthate, 1% w/v) and frother (12 drops methyl amyl alcohol), conditioning for 1 min;

xiv) floating sphalerite for 5 min;

xv) adding collector (50 g/t potassium amyl xanthate);

xvi) floating sphalerite for 5 min;

xvii) removing the galena concentrate and collecting a 50 mL pulp sample.

The rotor speed was kept at 1,500 in all experiments.

The pulp potential, Eh, the pH, and the dissolved oxygen values were monitored at each minute and after any reagent addition.

The addition of the reagents sodium sulfide and sodium sulfide was performed following the steps:

i) adding 50 g/t sodium sulfide (5% w/v) prior to collector addition in the lead circuit, conditioning for 5 min;

ii) adding 400 g/t sodium sulfite (5% w/v) to the grinding mill.

The same procedure was followed in the tests with nitrogen as gas phase.

3 RESULTS AND DISCUSSION

3.1 Factorial Design Planning

The software MINITAB was used for the statistical analysis of the recovery results of the experiments planned with the aid of the factorial design technique.

Figure 1 illustrates a Pareto's chart for lead recovery. All the effects that surpass the line at 2.31 are significant. At 95% confidence level, the interaction between the presence of nitrogen and sodium sulfite at the high level was significant.

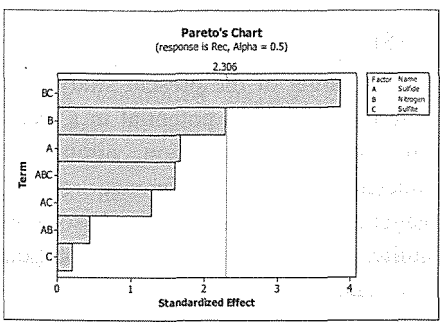

Figure 1. Pareto's chart (lead recovery).

The lead recovery in the lead concentrate as a function of each variable and their main effects is shown in figure 2. It was observed that:

i) the addition of sodium sulfide enhanced lead recovery, in agreement with Toka and Atalay (1996), who reported that sodium sulfide dosages below 64 g/t enhance galena recovery;

ii) the individual effect of the variable nitrogen gas presence was to reduce the variable lead recovery;

iii)the presence of sodium sulfite provided a mild increase in lead recovery.

Figure 3 illustrates the effect of variables interaction (two by two) on lead recovery. It was observed that:

i) the presence of nitrogen gas decreased the lead recovery irrespectively of the presence or absence sodium sulfide;

ii) sodium sulfite at its high level and

sodium sulfide at its low level reduced the lead recovery, the response being increased for both variables at their high levels;

iii) sodium sulfite at the high level and nitrogen presence increased lead recovery, while sodium sulfite at the high level and nitrogen absence reduced the same response. The high slope of the straight lines related to this interaction explains the significance of the factor bc observed at the Pareto's chart.

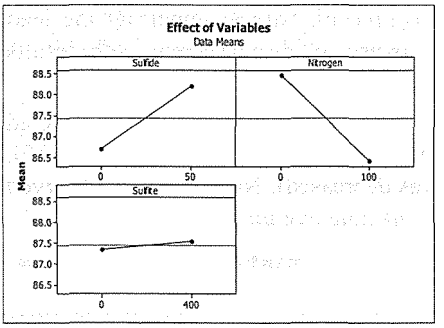

Figure 2. Effect of variables on lead recovery.

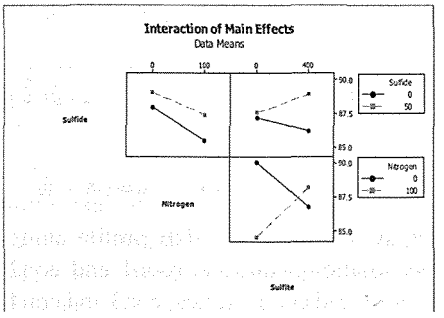

Figure 3. Interaction of main effects (two by two) on lead recovery.

Figure 4 presents the Pareto's chart referring to zinc recovery. All the effects surpassing the line at 2.31 are significant. Factor "b" (presence of nitrogen) was the most significant regarding zinc recovery, followed by the factor "bc", interaction between presences of nitrogen and sodium sulfide.

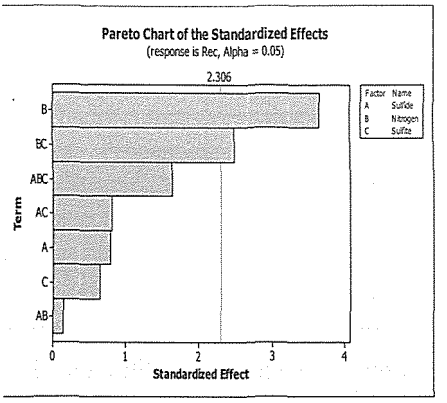

Figure 4. Pareto's chart (Zn recovery).

The zinc recovery in the zinc concentrate as a function of each variable and their main effects is shown in figure 5. It was observed that:

i) sodium sulfide at its high level decreased the response;

ii) the use of nitrogen gas significantly increased the zinc recovery (steep slope of the straight line);

iii)the presence of both, sodium sulfite and sodium sulfide, reduced the response.

Figure 6 illustrates the effect of variables interaction (two by two) on zinc recovery. It was observed that:

i) the presence of nitrogen gas enhanced zinc recovery irrespectively of the use of sodium sulfide;

ii) the interaction of sodium sulfide at the low level with sodium sulfite at the high level increased zinc recovery;

iii) zinc recovery decreased in the presence of nitrogen, even for sodium sulfite at the high level, while sodium sulfite at the high level and absence of nitrogen increased the recovery.

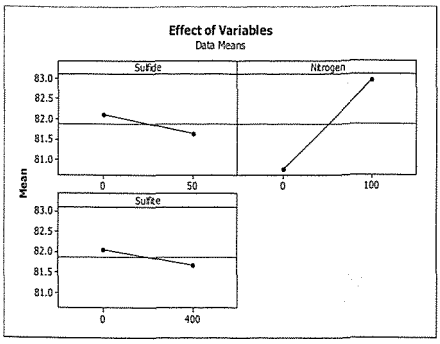

Figure 5. Effect of variables on zinc recovery.

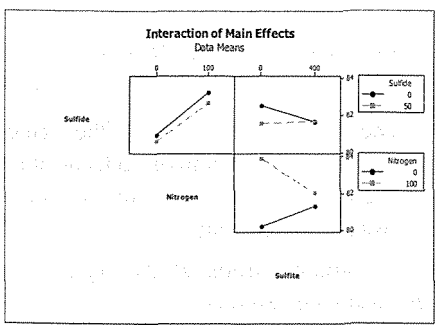

Figure 6. Interaction of main effects (two by two) on zinc recovery.

3.2 Pulp Potential Monitoring

Continuously monitoring the pulp potential during flotation provided an analysis of Eh variation for different pulp conditions caused by reagents addition flotation gas phase change. The Eh variations are illustrated in figures 7 and 8. Figure 8 shows the results of tests in the presence of sodium sulfide.

The use of sodium sulfite alone in flotation tests did not change significantly the pulp potential values, so this reagent did not affect significantly lead and zinc recoveries, as discussed in the former series of results.

The interaction between sodium sulfite and nitrogen lead to more negative values of pulp potential. This effect was stronger in the lead circuit, enhancing the recovery.

The addition of sodium sulfide alone did not change the pulp potential in both circuits, as expected based on results achieved by Bulatovic (1991). It is possible that the addition level practiced in the present investigation (50 g/t) was too low to affect the Eh.

The interaction between the variables sodium sulfide and nitrogen lead to more negative Eh values, impairing the lead recovery, in disagreement with results reported by Kocabag (1994).

The use of nitrogen alone affected the pulp potential in the lead circuit (Eh was decreased). No effect was observed in the zinc circuit.

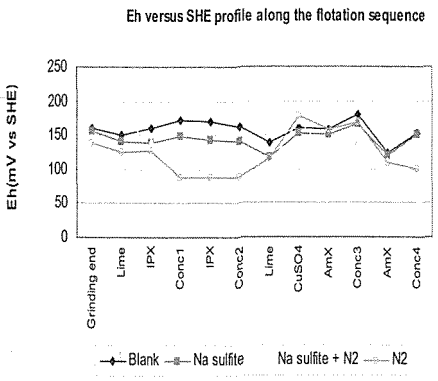

Figure 7. Eh versus SHE profile along the flotation sequence. (con1 and con2 refer to lead concentrates; con3 and con4 refer to zinc concentrates.

Hecker et al. (1985) stressed that the dissolved oxygen in the pulp strongly affects sulfide minerals flotation. These minerals, in the presence of oxygen, catalyze the xanthate oxidation. Depending on the oxidation product, the flotation performance may be enhanced or impaired. Thus dissolved oxygen content was also measured in parallel

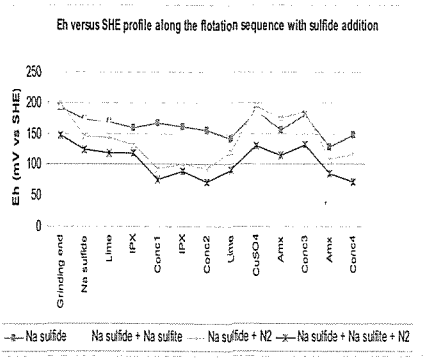

Figure 8. Eh versus SHE profile along the flotation sequence with sulfide addition. (con1 and con2 refer to lead concentrates; con3 and con4 refer to zinc concentrates

to Eh determinations. In the presence of air dissolved oxygen contents around 6.5 mg/L were assessed, the figure dropping to 0.5 mg/L in the presence of nitrogen.

4 CONCLUSIONS

The reagent sodium sulfite did not affect significantly neither the pulp potential nor the lead and zinc recoveries.

The interaction between sodium sulfite and the presence of nitrogen decreased the pulp potential in the lead circuit and resulted in enhanced lead recovery.

The reagent sodium sulfide individually did not change the pulp potential and increased the lead recovery. Its interaction with the presence of nitrogen decreased the pulp potential and impaired the lead recovery.

The presence of nitrogen reduced the dissolved oxygen content in the pulp, increasing the zinc recovery and decreasing the lead recovery.

REFERENCES

Bulatovic, S., Solter, R.S., (1991). Process development of the refractory massive sulphide copper ores. Proceedings of the Copper 91-Mineral Processing and Process Control, p.117-131.

Gonçalves, K.L.C (2003). Surface oxidation effect on Salobo's copper and gold ore. M.Sc. thesis, Curso de Pós-Graduação em Engenharia Metalúrgica e de Minas. Escola de Engenharia da UFMG, Belo Horizonte. 136 p. (in Portuguese)

Guy, P. J, Trahar, W. J., (1985). The effect of oxidation and mineral interaction on sulphide flotation. In: Developments in Mineral Processing, Flotation of Sulphide Minerals, ed. K.E.S. Forssberg, Elsevier Science Publishers B. V.6 , p. 91-110

Hecker, C.H., Castro, S.H., Sepulveda, J.(1985) The Kinetic Of Oxygen Reduction in Aquens Na_2S solutions. Its importance in mineral flotation. Developments in Mineral Processing and 2nd Latin-American Congress on Froth Flotation, 19-23, August.1985, Concepcion, Chile, v.9, Froth Flotation, ed. Castro, S. and Alvarez, J., p.19-23.

Kocabag, D., (1994) Redox effect on the flotation of sulphide minerals , Progress in Mineral Processing Technology, ed. Halim Demierel Salih Ersayn p.105-111.

Ralston, J. (1991), Eh and its Consequences in Sulphide Mineral Flotation, Minerals Engineering, v.4, 7-11, pp.859-878.

Reeken, F.J.M., Lange, J., Steensma, J.J.S., Duyvesteyn, P.C.,(1989) Factors affecting the lead-zinc

separation at the Grund concentrator. Int. J. Miner. Process., v.27,1-2, p.21-37.

Toka, B., Atalay, U.,(1996) Flotation behavior of galena and pyrite, Changing Scopes in Mineral Processingeds. Kemal, Arslan, Akar e Canbazoglu, p. 229-235.

Woods, R. (2003). Electrochemical potential controlling flotation. Int. J. Miner. Process., v.72, p.151-162.

Hydrochemical Processing Of Nepheline Syenites

Erbolat A. Tastanov, Lyazat A. Myltykbayeva, Bakhyt Kh. Edilova, Kulzhaik O. Beisembekova, Saniya S. Temirova

Affiliation: The Center of the Earth Sciences, Metallurgy and Ore Benefication

ABSTRACT Nowadays we can observe increased demand for aluminum in the world market as a result of increase of aluminum consumption in different industrial productions. Since the reserves of high-grade alumina-containing slurrys are limited utilization of the low-grade slurrys, especially nepheline syenites, for producing aluminum is becoming more actual.

In this paper we propose a new process flow scheme of high-silica alumina-containing raw material processing, i.e., nepheline syenites, and their chemical treatment product, i.e., nepheline concentrate. The optimal processing conditions of initial nepheline syenites and nepheline concentrate hydrochemical leaching have been identified.

The proposed process flow scheme of nepheline ores hydrochemical processing includes high-temperature leaching assisted with calcium oxide additions; desiliconizing operation; evaporation, crystallization, decomposition and calcination processes.

The research results demonstrated the proposed process flowchart of nepheline ore processing is promising for industrial implementation.

1 STUDY OF EFFECT OF BASIC PROCESS VARIABLES ON ALUMINA RECOVERY FROM NEPHELINE ORE

1.1 Study of effect Na_2O concentration effect on alumina recovery from nephelyne ore

The effect of basic process variables on the alumina recovery from nephelyne ore has been studied at 200, 220, 240, 260, and 280°C temperatures, 25-180 min leaching time, 341.0, 418.5, and 478.0 g/dm^3 concentration of stock solution, and calcium oxide proportioning at different molar ratios, $CaO:SiO_2$ (1.3÷2.0) : 1.0.

The chemical composition of averaged samples of source ore is as follows, %: Al_2O_3 – 26.0; SiO_2 – 46.5; Fe_2O_3 – 2.5; CaO – 1.37; Na_2O – 6.3;

K_2O – 7.7; MgO – 0.27; Cl – 0.27; S – 0.21.

Figure 1 illustrates the results of investigating the effect of Na_2O concentration on Al_2O_3 recovery for the nephelyne ore leaching.

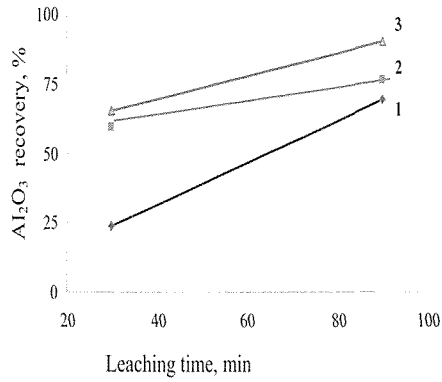

Figure 1. The effect of Na_2O concentration on the alumina recovery: 1 – Na_2O - 341,0 г/дм^3; 2 – Na_2O – 418.5 g/dm^3; 3 – Na_2O – 478.0 g/dm^3.

Linear dependence of alumina recovery on the stock solution concentration has been recorded: on a gradual increase in the alkaline solution concentration at a similar leaching time (90 min) the alumina recovery is respectively 69.13, 76.1, and 93.0 %. The most optimal concentration of alkaline solution corresponds to 478.0 g/dm^3.

1.2 Investigation of $CaO:SiO_2$ ratio effect

The effect of $CaO:SiO_2$ ratio has been investigated at a constant temperature of 280°C, 90 min process time, 478.0 g/dm^3 stock solution concentration, and different content of calcium oxide, $CaO:SiO_2$ = (1.3÷2.0) : 1.0 (Fig. 2).

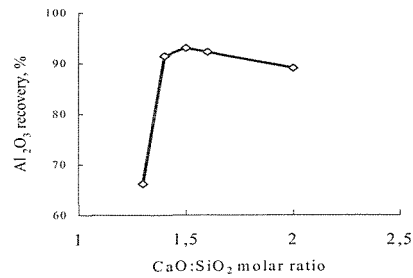

Figure 2. The effect of calcium oxide content on the alumina recovery

It has been found that on increasing the calcium oxide content from 1.3 to 1.5, i.e. at $CaO:SiO_2$ = 1.5:1.0 ratio, the alumina recovery during 90 min nephelyne ore leaching reaches 93.0 %. A further increase in the calcium oxide content in the leaching scheme from 1.6 to 2.0 causes a decrease in the alumina recovery because the excess calcium impairs the leaching conditions.

1.3 Investigation of effect of temperature and leaching time

The effect of temperature (200, 220, 240, 260, 280°C) on the alumina recovery at C_{Na2O} – 478.0 g/dm^3 concentration and 90 min leaching time has been studied.

It has been shown that on an increase in the temperature the alumina recovery to the liquid phase increases, however, the graphic chart is nonlinear (Fig. 3).

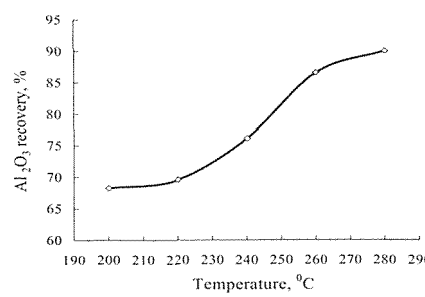

Figure 3. The effect of leaching temperature on the alumina recovery

Thus at 200, 220, 240, and 260 °C temperatures there has been recorded a transition to the liquid phase of respectively 40.33, 53.30, 67.60, and 70.03 g/dm³ aluminum that corresponds to the recovery of 68.26, 69.57, 76.09, and 86.52 % alumina. On an increase in the leaching temperature from 280 °C during the same time interval the aluminum content in the liquid phase reaches a maximum value of 73.32 g/dm³ that is equal to 93.04 % alumina recovery. A further increase in the temperature does not change significantly this value.

The effect of leaching time on the alumina recovery rate is complicated (Fig. 4).

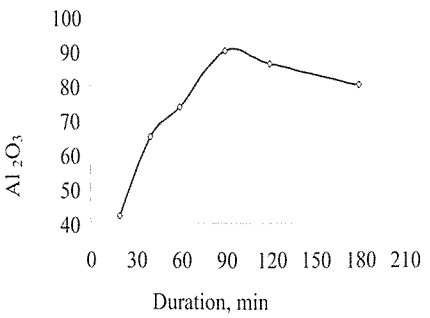

Figure 4. The dependence of alumina recovery on process duration

The highest alumina recovery has been observed at 90min leaching time; a further increase in the process time causes a decrease in the aluminum transition to the liquid phase. After 120min leaching of nephelyne ore the alumina recovery decreases to 86.20%, and in 180min to 80%.

It has been found that the optimal conditions for the nephelyne syenite processing are as follows: 280°C temperature, 478.0 g/dm³ alkaline solution concentration, $CaO:SiO_2$ = 1.5:1.0 ratio, and 90min duration. The found process variables provide a maximum value of aluminum transition, 73.32 g/dm³ that corresponds to 93.04 % alumina recovery.

Phase transformations during processing of nephelyne raw material have been identified.

Figure 5 presents the IR spectrum of slurry after hydrochemical processing of nephelyne ore. In the high-frequency spectrum region, presence of pronounced band of hydroxide ion [OH^-] v OH - 3640 cm^{-1} and [CO_3^{2-}] - 1391, 873, 714cm^{-1} group has been found.

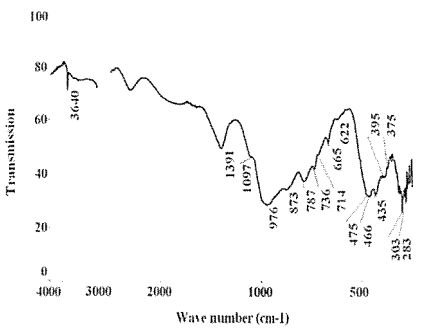

Figure 5. IR spectrum of spent slurry after leaching

The shoulder in 1097 cm^{-1} wave number can be due to M–O–H deformation vibrations. In the long-wave spectrum region one observes valence vibrations: Fe^{2+}–O - 375 cm^{-1}; Ca–O, Mg–O - 303, 283 cm^{-1} and calcium hydrosilicate $CaO \cdot SiO_2 \cdot nH_2O$ - 1097, 787, 665, 622 cm^{-1} [1]. Presence of ferruginous hydrogarnet, $3CaO \cdot Fe_2O_3 \cdot nSiO_2 \cdot mH_2O$, and [$FeO_4$] tetrahedrons is possible.

Figure 6 presents the diffraction patterns of nephelyne raw material and slurry after leaching.

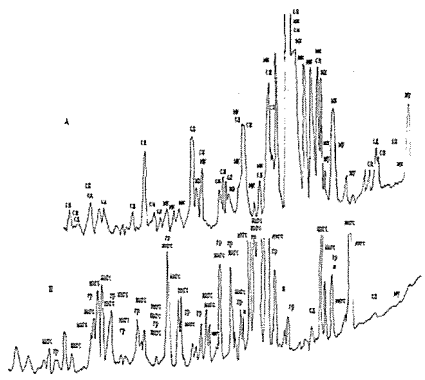

Figure 6. The diffraction patterns of raw material and spent slurry after leaching: A – nephelyne raw material; B – spent slurry after leaching.

The diffraction pattern of raw material shows phases corresponding to $NaAlSiO_4$ nephelyne, (Na,K) $AlSi_3O_8$ sanidine, $KAlSi_3O_8$ microcline, $Na_4Ca_3Al_3Si_3O_{12}Cl$ sodalite, and $KAl_2[AlSi_3O_{10}](OH)_2$ muscovite.

As seen in the diffraction pattern (B), the basic phases of slurry after leaching are sanidine, microcline, and nepheline. At a high content of alkali in the system the crystallization of ($NaCaHSiO_4$) sodium-calcium hydrosilicate and ($Ca_3Al_2[SiO_4]^3$) grossular occurs enabling a substantial transition of aluminum to solution. The forming phases are to some extent a source of losing alkalis and a slight amount of aluminum that has been confirmed by chemical analyses. Traces of ($KAl_2[AlSi_3O_{10}](OH)_2$) muscovite and ($Na_4Ca_3Al_3Si_3O_{12}Cl$) sodalite [2] phases are also presented.

The spent slurry after leaching contains newly-formed phases of $NaCaHSiO_4$ sodium-calcium hydrocilicate, $Ca_3Al_2[SiO_4]^3$ grossular, traces of $KAl_2[AlSi_3O_{10}](OH)_2$ muscovite and $Na_4Ca_3Al_3Si_3O_{12}Cl$ sodalite phases.

The chemical composition of resulting slurry is as follows, %: Al_2O_3 -1.6; Na_2O – 15.8; SiO_2 – 27.1; Fe_2O_3 – 2.1; CaO – 26.5; calcination loss - 9.4. The aluminate solution composition after hydrochemical processing, g/dm^3: Al_2O_3 – 73.32; Na_2O – 409.20; SiO_2 – 5.00; $\alpha_к$ – 9.2.

2 INVESTIGATION OF EFFECT OF BASIC PROCESS VARIABLES ON ALUMINA RECOVERY FROM ALUMINOUS CONCENTRATE

During leaching of aluminous concentrate obtained by chemical processing of nephelyne ore the following has been studied: effect of alkaline solution concentration (341, 418.5, 478.0 g/dm^3); $CaO:SiO_2$ (1,0÷1,5):1,0 proportioning of calcium oxide; and temperature (200, 220, 240, 260, 280 °C) at 90min process time.

The composition of chemically processed concentrate is as follows, %: Al_2O_3 – 31.40; Na_2O – 15.50; SiO_2 – 35.00; Fe_2O_3 – 3.70.

2.1 Study of f Na_2O concentration effect

The dependence of alumina recovery on the stock solution concentration has been ascertained: on a gradual increase in the c Na_2O concentration: 341.0; 418.5; 478.0 g/dm^3 the aluminum content in the liquid phase increases to respectively 54.86; 66.80 and 71.11 g/dm^3 that is equal to the alumina recovery of 78.18, 92.14, and 98.86 %.

It has been found that the optimal conditions of aluminous concentrate processing are: C_{Na2O} – 478.0 g/dm^3, temperature - 280 °C, process time – 1.5h and $CaO:SiO_2$ = 1.1:1.0 ratio.

2.2 Effect of CaO : SiO_2 ratio

The effect of CaO:SiO_2 = (1.0÷1.5):1.0 ratio at a constant temperature of 280 °C, 478.0 g/dm³ concentration of Na_2O stock solution, and 90min leaching time. (Fig. 7) has been studied.

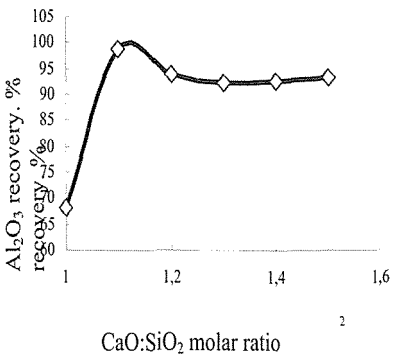

Figure 7. The dependence of Al_2O_3 recovery on calcium oxide proportion

The calcium oxide proportion at CaO:SiO_2 = 1.1:1.0 is the most optimal providing the transition of alumina to solution at 71.11 g/dm³, or 98.86 % alumina recovery.

2.3 Investigation of effect of temperature and leaching time

The effect of temperature on the leaching process has been investigated at 200, 220, 240, and 260 °C. The aluminum content in the liquid phase is respectively 39.0, 53.69, 60.3, and 70.32 g/dm³ that is equal to 38.08, 56.39, 89.67, and 91.25 % alumina recovery. On an increase in the temperature to 280 °C the aluminum content in solution reaches a maximum of 71.11 g/dm³ that corresponds to 98.86 % alumina recovery.

The effect of leaching process time (90, 120, 180 min) on the alumina recovery at a constant temperature of 280 °C, 478.0 g/dm³ stock solution concentration, and CaO:SiO_2 = 1.1 : 1.0 ratio has been investigated.

At 90min time of aluminous concentrate leaching the alumina yield is 71.11 g/dm³ that is equal to 98.86 % alumina recovery.

On increasing the leaching time from 120 and 180min the aluminum transition to the liquid phase gradually decreases and is respectively 64.36 and 53.32 g/dm³, which is equal to 85.33 and 63.33 % alumina recovery.

The optimal process conditions for the aluminous concentrate processing are as follows: concentration of stock solution – 478.0 g/dm³ Na_2O, CaO:SiO_2 = 1.1:1.0 ratio, temperature - 280 °C, and leaching time – 90min.

Phase transformations during concentrate processing have been identified.

The comparative diffraction patterns of samples (Fig.8) show the aluminous concentrate during hydrochemical processing to undergo a number of transformations.

The diffraction pattern (A) of aluminous concentrate shows presence of $NaAlSiO_4$ nepheline, $Na_4Ca_3Al_3Si_3O_{12}Cl$ sodalite, $KAl_2[AlSi_3O_{10}](OH)_2$ muscovite, and sodium hydroaluminosilicate phases.

The diffraction pattern of waste final slurry (B) indicates that the parent phases of aluminous concentrate change to $NaCaHSiO_4$ sodium-calcium hydrosilicate phases, $Ca_3Al_2[SiO_4]^3$ grossular, and $Ca_2Al(AlSi)_2O_7$ calcium aluminosilicate that fosters the transition of aluminum to solution. The formation of new phases involves slight losses of alkali and aluminum that has been confirmed by the chemical analysis of solid phase.

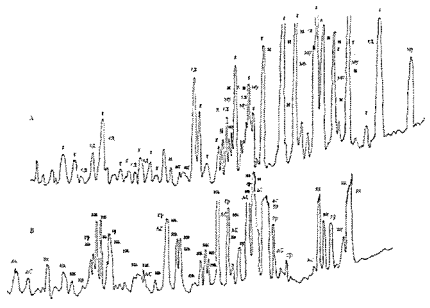

Figure 8. The diffraction pattern of concentrate and slurry.

The chemical composition of slurry is as follows, %: Al_2O_3 – 0.26; Na_2O – 15.8; SiO_2 – 34.0; Fe_2O_3 – 3.2; -CaO – 19.1; calcination loss - 7,1.

The composition of aluminate solution, g/dm^3: Al_2O_3 – 71.11; Na_2O – 443.3; SiO_2 – 8.5; $\alpha_к$ – 10.3.

The hydrochemical leaching products, aluminate-rich solution and calcium-silicate slurry are promising materials for further processing [3, 4].

3 ELABORATION OF PROCESS FLOWSHEET OF NEPHELYNE SYENITE PROCESSING

A process flow sheet of high-temperature autoclave stripping of nephelyne ore by high-modulus alkaline solutions is proposed.

The nepheline concentrate is mixed with quick lime and leached in autoclaves at 280°C temperature, 478.0 g/dm^3 concentration of alkaline solution, $CaO:SiO_2$ = 1.5:1.0, and 90 min time.

The pulp cooled to a certain temperature in a vacuum plant separates to filtrate and slurry.

The obtained composition of aluminate solution is as follows, g/dm^3: Al_2O_3 – 73.32, Na_2O – 409.20, SiO_2 – 5.0, and $\alpha_к$ – 9.2. The solution is directed for the subsequent alumina production.

The slurry, sodium-calcium hydrosilicate, after separation from the aluminate solution are washed with water using an advanced technology and then directed for alkali regeneration.

3.1 Determination of optimal conditions of pulp filtration and slurry washing processes

It has been ascertained that that the level of Al_2O_3 and Na_2O recovery is affected significantly by the number of slurry washing stages. The washing rate depends on slurry fineness and solution flow velocity.

The slurry has been washed up to 40-fold water volume and C_{Na2O} – 22.44 g/dm^3 residual alkali content. Then the second and third stages of 40-fold washing of slurry have been executed as a result of which the final content of Na_2O in the solution is respectively 0.38 and 0.124 g/dm^3.

The precipitate after washing from alkali and drying (105 °C) has been subjected to full chemical analysis. The content of components, % is as follows: Na_2O -15.8, Al_2O_3 -1.6, SiO_2 – 27.1, Fe_2O_3 – 2.1, calcination loss -9.4, and μ_{Si} – 0.06. The aluminum recovery to solution is 93.04 %.

The washed slurry can be used as a raw material for cement production.

3.2 Determination of optimal conditions for aluminate solution desiliconizing process.

After hydro-alkali stripping of concentrate the obtained aluminate solution, g/dm^3: Al_2O_3 – 72.5; Na_2O – 424.7; SiO_2 – 10.5; $\alpha_к$ - 9,7; and μ_{si} – 6.9 was subjected to the autoclave desiliconizing. The desiliconizing was

carried out by diluting the solution to C_{Na2O} – 245.0 g/dm^3 then adding calcium oxide in various proportion.

The basic parameters of desiliconizing process are as follows: time (60, 90, 120, 150, 180 min), ratio CaO : SiO_2 = (3÷10):1), temperature - 150–200 °C.

The composition of solution to be desiliconized is as follows: Al_2O_3 – 46.1; Na_2O – 244.9; SiO_2 – 5.1; $\alpha_к$ – 8.8; and μ_{si} – 9.04.

It has been found that at 150 °C and CaO : SiO_2 = 3.0 : 1.0 calcium oxide proportion during 180 min the aluminate solution is desiliconized to 0.6 g/dm^3 SiO_2 content in the solution. On increasing the temperature to 200 °C the process is slightly slowed down, and the silica content in solution increases to 1.6 g/dm^3. Hence it is most practical to carry out desiliconizing at 150 °C temperature. The optimal proportion activating the desiliconizing process is CaO:SiO_2 = 5:1.

The effect of process duration (60; 90; 120; 150, and180 min) on the stock solution desiliconizing has been studied at 150 °C constant temperature and CaO:SiO_2 = 5:1 calcium oxide proportion.

After 60min desiliconizing process the silicon content in solution decreases to 0.08 g/dm^3, and the silicon modulus is 474.0. On a further increase in the desiliconizing process time to 90, 120, 150, and 180 the modulus characterizing the level of aluminate solution desiliconizing gradually decreases to respectively 432.0, 353.0, 300.0, and 281.0.

Thus the desiliconizing time should be limited to 60min.

The solid phase obtained after desiliconizing (white slurry) has been studied by X-ray phase analysis (Fig.9).

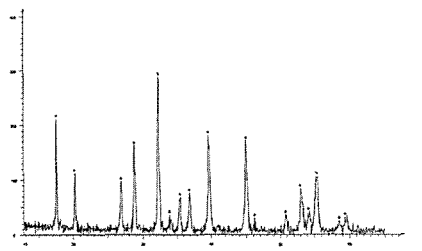

- $Ca_3AlFe(SiO_4)(OH)_8$

Figure 9. The diffraction pattern of slurry after desiliconizing

The diffraction pattern of white slurry shows the formation of ($Ca_3AlFe(SiO_4)(OH)_8$) calcium hydrogarnet phase containing silica, aluminum, and iron compounds, the silica amount prevailing compared to the content of other components. Hence, the addition of calcium oxide promotes the formation of compound characterized by a high content of silicate species in it on hydrochemical processing of nephelyne raw material [5].

Hence the optimal conditions of aluminate solution desiliconizing process are: 150°C temperature, CaO:SiO_2 = 5:1 calcium oxide proportion, and 60min time.

3.3 Determination of optimal conditions for aluminate solution evaporation and sodium aluminate crystallization processes

The aluminate solution composition, g/dm^3 : SiO_2 – 0.27; Al_2O_3 – 40.96; Na_2O – 269.7; $\alpha_к$ – 10.9; and μ_{Si} – 151.7 has been worked out for subsequent technological conversions. The obtained aluminate solution has been subjected to evaporation.

The effect of process duration (60; 120 min) on the evaporation of initial aluminate solution has been investigated.

The required alkaline solution concentration (Na_2O – 563.6 g/dm^3) was achieved after 120min evaporation procedure.

The evaporated solution has been cooled to 40–42 °C temperatures at which the crystallization is carried out.

The freshly settled sodium aluminate seed accelerating the crystallization process has been prepared. The optimal seed amount taken for conducting the crystallization process is 2.5 % of solution weight.

Mixing of solution with the seed was carried out at mixer rotation ~ 60 – 70 rev/min rate of mixer rotation at which the precipitate is in the suspension state.

The parameters of sodium hydroaluminate crystallization (SHA) process are: temperature – 40-42 °C; seed -2.5 % of solution weight; duration – 50 hours.

The crystallization has resulted in the solid phase, sodium hydroaluminate of the following composition, %: 22.3 Al_2O_3; 42.0 Na_2O; 3.6 SiO_2, and 32.1 calcination loss and the mother solution of the following composition, g/dm^3: Al_2O_3 – 16.1; Na_2O - 490; SiO_2 – 0.12; K_2O -16.0.

It has been found that on an increase in the leaching time the level of sodium aluminate supersaturation of solution decreases that accounts for the high rate of crystallization process and an increase in the silica transition to the solid phase. The composition of sodium hydroaluminate formed has been determined. Sodium monoaluminate, $Na_2O \cdot Al_2O_3 \cdot 6H_2O$ forms within the concentration under study.

The formation of sodium hydroaluminate, $Na_2O \cdot Al_2O_3 \cdot 6H_2O$ has been ascertained by X-ray phase analysis.

3.4 Determination of optimal conditions for decomposition process

A plant of our own design has been manufactured to investigate the decomposition of aluminate solution. The processing plant was connected to an automatic timing unit by which an hourly decrease in the temperature was recorded.

The sodium hydroaluminate (SHA) obtained after crystallization, %: 22.3 Al_2O_3; 42.0 Na_2O; 3.6 SiO_2, and 32.1 calcination loss was dissolved in water to obtain the aluminate solution for investigating and carrying out the decomposition process.

The aluminate solution, g/dm^3: Na_2O – 96.1; Al_2O_3 – 98.9; $\alpha_к$ – 1.6 underwent decomposition on introduction of $Al(OH)_3$ seed.

The decomposition process parameters are: 48h duration, ~ 70 rev/min rate of pulp stirring; 62 °C initial temperature with a gradual decrease to 44 °C.

The aluminate hydroxide seed at different seeding ratios (0,1; 0,3) has been introduced into solutions to investigate the decomposition process.

The hydrate pulp samples were taken with a sampler every 24 and 48 hours. The decomposition of alkali-aluminate solution was investigated as a function of the amount of seed introduced. It has been found that the decomposition level of aluminate solution with 0.1 aluminum hydroxide seeding ratio in 24 hours is 23.1%, and in 48 hours it has reached 52.9% (Fig.10). An increase in the seeding ratio to 0.3 causes an increase in the silica transition to the solid phase. Thus the decomposition rate in 24 hours is 39.6 %, and in 48 hours 57.9 %. Hence the depth of solution decomposition on increasing the seed amount has increased.

In this case, the decomposition rate in 48 hours has increased by 5 % .

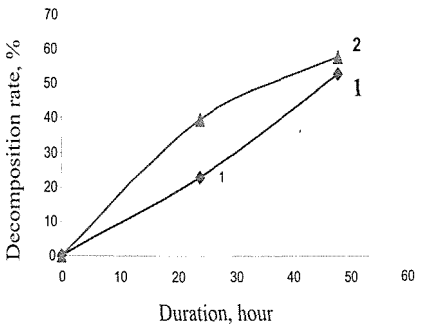

1) 3:O - 0,1; 2) 3:O - 0,3

Figure 10. Decomposition of aluminate solution

3.5 Determination of optimal conditions for aluminum hydroxide filtration and washing processes

The separation of aluminum hydroxide and mother solution has been carried out in a vacuum plant. 6-fold washing by 100ml of water for each step has been carried out (pH of solution varied from ~ 12 to 7.

The chemical composition of obtained aluminum hydroxide at 0.1 seeding ratio is as follows, %: Al_2O_3 – 56.10; Na_2O – 0.30; and calcination loss – 34.40 and at 0.3 seeding ratio, %: Al_2O_3 – 60.30; Na_2O – 0.25; and calcination loss – 33.75.

X-ray phase analysis of obtained aluminum hydroxide precipitates has shown them to be identical: the basic phase is represented by gibbsite.

Thus it has been found that the precipitated aluminum hydroxide is a gibbsite monophase with fine grain sizes from 20 to 50 microns. 600ml of water has been used for washing the obtained aluminum hydroxide; 6-fold washing of hydroxide has been carried put.

3.6 Determination of optimal conditions for calcination process

A laboratory rotating pipe furnace was used for aluminum hydroxide calcination. Aluminum hydroxide was calcined at 1050 °C temperature and 1 hour calcination time, i.e. to obtain the end product, silica [6].

Due to the calcination, silica conforming to Г-00 (GOST–30558-98) grade has been obtained.

X-ray phase analysis has shown the identity of silica phases having similar composition: $\delta\ Al_2O_3$; $\chi \bullet Al_2O_3$; Al_2O_3; $\theta\ Al_2O_3$; $\kappa\ Al_2O_3$; βAl_2O_3 (Fig. 11).

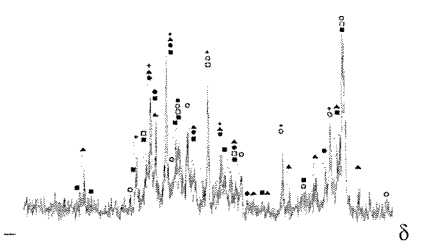

– δ ■ Al_2O_3; □- $\chi \bullet Al_2O_3$; ○ - Al_2O_3; ● – $\theta\ Al_2O_3$; ▲ - $\kappa\ Al_2O_3$; + - βAl_2O_3

Figure 11. The diffraction pattern of silica

Due to the conducted laboratory tests a flowsheet of nephelyne ore processing in autoclave by hydrochemical method has been worked out and presented (Figure 12).

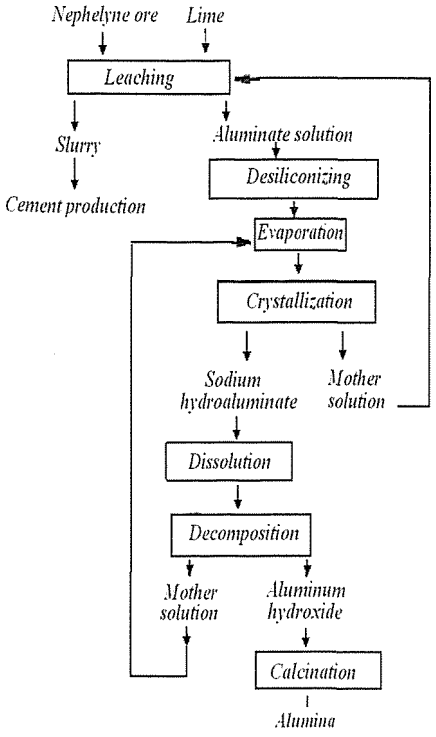

Figure 12. The flowsheet of nephelyne syenite processing

REFERENCES

1 Ni L.P., Khalyapina O.B. Physico-chemical characteristics of raw materials and silica products. – Alma-Ata: Nauka, 1978. - 250 p.

2 Arlyuk B.P., Improvement of procedures of aluminate-alkali nephelyne cake processing Series: Production of light metals and electrode products. Moscow. 1978. 48 p.

3 Abramov V.Y., Alekseyev A.I., Badaliants K.A. Integrated processing of nephelyne- apatite raw material. Moscow. «Metallurgiya» 1990. 391 p.

4 Petrov V.P. The USSR Academy of Sciences. Nephelyne raw material Moscow. «Nauka» 1978. 190 p.

5 Pevzner I.Z., Makarov N.A. Desiliconizing of aluminate solutions. Moscow. «Metallurgiya» 1974. 112 p.

6 Korneyev V.I. Integrated processing of nephelyne slurry. Moscow. «Metallurgiya» 1974. 197 p.

The Effect of Various Parameters on Recovery of Hyred Gold Refractory by Cyanidation Process

Shameli Leila, Shafei Seyed Ziaodin
Technical University Of Shahrood, Shahrood, IRAN

ABSTRACT Gold recovery from low grade ore that is located in south of khorasan province was investigated. Gold is in carbonaceous-siliceous zone with clay. Various parameters were effective on this process such as cyanide content, pH and size particle. Best conditions for high recovery was cyanide consumption 2000 g/t (feed), pH =10.5, d_{85} = 53μm. In this condition gold recovery was 92.2%.
In this paper experimental design was done by DESIGN EXPERT 7 software in two steps. In first step full factorial method was used. Then optimum parameters studied by Response surface, Historical method.

1 INTRODUCTION

The cyanidation process has been successfully practiced for the extraction of gold from their ores for more than 100 years. The well-known Elsner (1846) equation describes the stoichiometry of the leaching reactions:

$$4Au + 8CN^- + O_2 + 2H_2O = 4Au(CN)_2^- + 4OH^-$$

Studies on the leaching of gold in aerated cyanide solution have shown that cyanide, pH rate and grinding play important roles.

Leaching by cyanide solutions in aerated alkaline pulp is the main process for gold extraction from ores. In a large number of plants the reactant addition is made in the grinding section, but the effect of this procedure on the plant performance has not been systematically analyzed. The understanding of the gold leaching in the grinding section of conventional gold extraction plants might help to significantly improve the process profitability.

Gold cyanidation is an electrochemical process,where gold is oxidized and then complexed to the stable complex ion [Au(CN)2]−,oxygen is reduced, and hydrogen peroxide decomposed (Habashi, 1987; Yannopoulos, 1991; Marsden and House, 1992). A typical gold ore processing plant comprises comminution, size classification, gravity concentration, and dewatering operations, followed by gold leaching and gold recovery by adsorption onto activated carbon or by zinc precipitation.

Sodium hydroxide and lime are also used for pH control and, in some plants

.Marsden and House (1992) stated that in the grinding section of a typical counter-current decantation- carbon- in- pulp plant, the gold recovery, in spite of the short residence time of the pulp, could be as high as 60%, while the gold recovery in the leaching section, in spite of the larger residence time, could be of only about 10%.an assumptions are proposed, can recover gold ore from siliceous-carbonaceous zone as case study, these question were the main motivation to collect data around a grinding and leaching circuit for analyzing the result of gold recovery. Main operating variables and concentrations are measured in two campaigns of data acquisition. Then the data are filtered using data reconciliation and used to analyze the gold behavior and recovery in several parts of the plant.

Mineral processing circuit audit is a classical approach to assess metallurgical performances (Green, 1984; Yingling, 1990; Roland-Villasana and Williamqs, 1991; Schena et al., 1997; Williams and Meloy, 2000; Cisternas et al., 2004). Gold ore processing plant audits are challenging since it is difficult to perform reliable analyses due to the low content of the target element, the heterogeneity of the ore, and the difficulty to obtain steady-state operating conditions. In this case study, a gold leaching at Khorasan south province, Iran is analyzed; the results and approach presented can be useful to understand other grinding–leaching plants.

This paper is organized as follows. Section 2 experimental presents plant description geology and mineralogy study. Section 3 presents more detailed study of the grinding–dewatering–primary leaching section of the gold leaching plant and discussion, and Section 4 conclusion of this paper.

Sampling was provided from systematically trenches in December 2007.

The samples were filtered under pressure and the liquid phases analyzed for gold by atomic absorption spectroscopy. The solid phases were rinsed and analyzed for gold by fire assays. The ore feed rate in the plant, the solid concentrations in the slurry, and the free cyanide concentrations during the period of the sampling campaign were provided by the plant operators.

The Hyred anomaly is located southern part of Khorasan province of Iran Figure 1. Sampling was from trenches. In Hyred cyanidation plant, ore is first crushed and then wet ground in mills to liberate gold particles.

Once ground to 53 micron, degree of liberation hence recovery of gold from the ore is achieved.

2 EXPERIMENTAL

2.1 Geology

The Hyred gold deposit is located in Hyred deposit region 9 10 00 -59 15 00 with longitude 59° 10'00"-59°15'00" and latitude 31° 55'00"-32° 00'00"(SE Khorasan, Iran).

Area is covered with Jurassic oldest stone such as shale-sandstone ,there are periodic stones (shale, conglomerate, sandstone ,limy marn, sandy limestone) with Paleocene base conglomerate reach to tertiary magmatic sequence (volcanic and plutonic stones).there are Eocene stones such as conglomerate, sandstone, tuffite sandstone and volcanic stone such as andesit, altered andesit, amygdaloidal andesit, crystallized tuff, pyroxene andesit, quartz andesit. Furtheremore, in-

trusive granitic mass, diorite quartz, granodiorite covered most of the northern parts of area and outcrop in some parts.

Gold mineralization have shown in 2 main veins, trend of one of them is north-south direction (N10E), another is with eastern north-western south trend in pyroclastic sequence .2 veins interact together in northern part of area.

Concentrations of gold here range from 2.2 to 2.6 g/t.

Figure 1.Systematically trenches of Hyred Anomaly

2.2 Mineralogy

Sampling were provided from systematically trenches in southeren khorasan (Iran) in December 2007 from Hyred anomaly is located in southern khorasan (Iran) . 700 kg of them send to processing department for gold recovery. The ore was labeled and was identical to the plant cyanidation feed. Coarse gold had already been crushed at the first by jaw crusher to 3mm ,7 kg of crushed sample was screening for microscopic study in 10 fraction 10, 20, 35, 50, 70, 100, 120, 170, 230, 325 mesh ,100 gr of any fraction send to microscopic analysis also head of the screening analyzed by chemical analyze table1, 57.02 % of ore composed of SiO_2 and Al_2O_3, CaO is 10.65% and Fe_2O_3 is 6.54% and determined grade of gold ore nearly 2.4 gr/t. Also XRF and XRD had been done result are coming in table2 and figure2, respectively.A wet particle-size analysis of the sample indicated that 80% of the sample is 1600 microns. The gold content of the head, obtained by fire assay, is 2.2-2.6 g/t (duplicate). The calculated gold content of the original sample (obtained from all the reported tests) is 2.4 g/t with a variance of 0.2.

The ore consists largely of gangue (94.3%) quartz, calcite, gypsum and dolomite (XRD result). The cyanidation tests performed on finely-ground material (80,85and 90%) 75 microns) indicated that 80-92 % of the gold is leachable (0.2-0.3 g/t Au in the tails).Full factorial design used in first step and for optimizing result used from Historical method.

2.3 Sampling

Sampling was provided from systematically trenches in southern Khorasan (Iran) in December 2007 from Hyred anomaly is located in southern Khorasan (Iran). After mining, the ore was grinding by jaw crusher till 3 mm then sent to a secondary grinding–classification stage composed of two ball mills till 75 μm. We need three levels for grinding size for leaching process therefore; needed remaining time in ball mill was calculated. The ore leaving this section would be in 3 range of grinding 80%, 85%, 90% finer than 75 μm. Then the slurry is dewatered to about 40% of solids and pumped to the primary leaching circuit. Range of the pH in the leaching section is set from 9.5 to 11 by adding lime and sulfuric acid in the bottle leaching. Sodium cyanide; are added to the leaching bottle and other points of the

grinding circuit to promote the dissolution of the gold particles in the early processing stages, a practice which improves the leaching efficiency and reduces the overall plant dissolution time. In the primary leaching stage, sodium cyanide is also added to the pulp, and the concentration of free cyanide ion (CN−) is adjusted from 500 to 1000 ppm .The objective of the first sampling campaign was to produce an overview of the gold leaching profile through the plant, and point at the sections that should be more deeply analyzed. The second campaign objective was to optimum data for a better leaching of the gold ore by cyanide solution. The collected data was modeled by DX7 software.

The results of the sampling campaigns are presented and discussed in Section 3.

The samples were filtered under pressure and the liquid phases analyzed for gold by atomic absorption spectroscopy. The solid phases were rinsed and analyzed for gold by fire assays. The ore feed rate in the plant, the solid concentrations in the slurry, and the free cyanide concentrations during the period of the sampling campaign were provided by the plant operators.

Table1. Chemical Analysis of Hyred Ore

No.	Composition	Content (%)
1	SiO_2	45.95
2	$Al2O_3$	11.07
3	Fe_2O_3	6.54
4	CaO	10.65
5	MgO	4.05
6	TiO_2	0.37
7	P_2O_5	0.12
8	MnO	0.34
9	SO_3	0.87
10	Na_2O	0.46
11	K_2O	2.70
12	L.O.I	16.19

Table2. XRF

No.	Composition	Content (%)
1	SiO_2	38.8
2	Al_2O_3	13.12
3	Fe_2O_3	6.16
4	CaO	16.38
5	MgO	1.93
6	TiO_2	0.44
7	Cl	0.18
8	MnO	0.45
9	SO_3	2.73
10	Na_2O	0.28
11	K_2O	3.05
12	L.O.I	15.66
13	As_2O_3	0.47

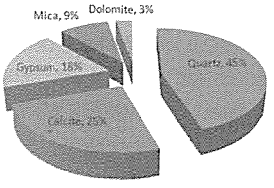

2.4 Test Procedures

2.4.1 General Factorial Design

The general factorial design allows us to have factors that each them have a different number of levels. It will create an experiment that includes all possible combinations of factor's levels.

Cyanide content, pH rate and grinding size were selected as variable factors with three levels Table 4, Andrade Lima (2006).For determining levels of DOE, a series of controlling tests have been done, according to legal free cyanide (500-1000 ppm), three levels of cyanide (NaCN) consumption for a 24-h leaching 1500, 2500 and 4000 gr/ton feed were selected, pH sufficient range in cyanide leaching is changed from 9.5 to 11 that

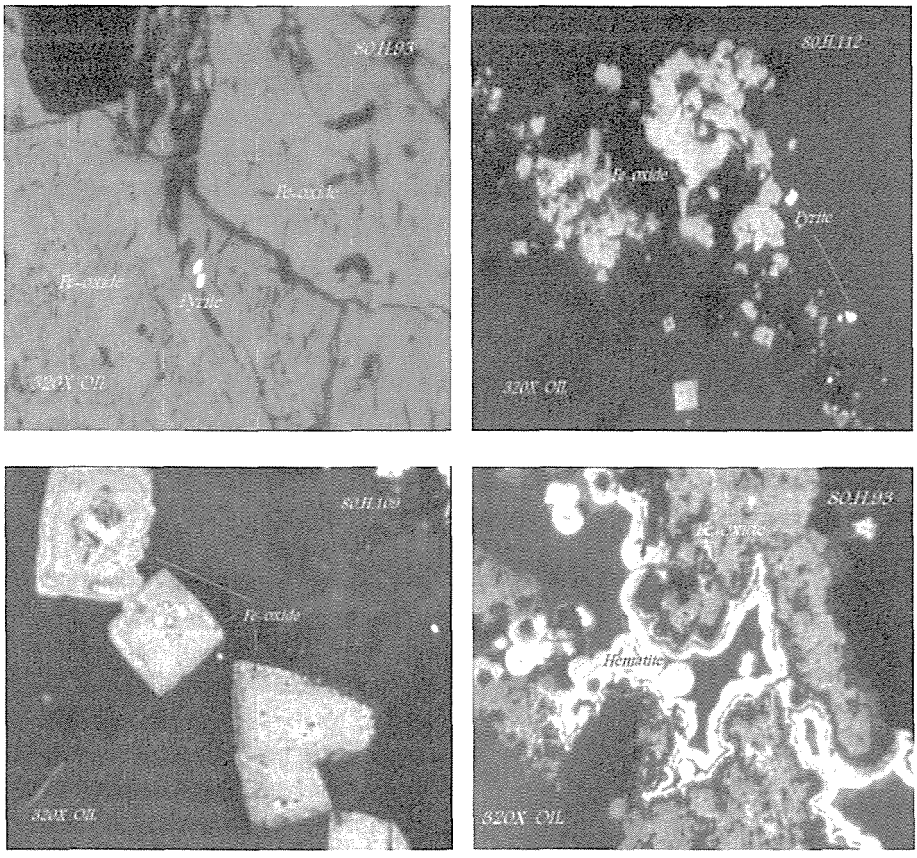

Figure 2.XRF chart of Hyred anomaly

in these series of tests three levels of pH 9.5, 10.5 and 11 were selected.

The short pre-leach duration required means that such a pre-leach could be performed in the grinding circuit.

Three levels of grinding size, 3th factor for leaching, 80%, 85% and 90% finer than 75 μm was selected.

The limes, sodium cyanide, sulfuric acid used were all certified reagent grade chemicals. The gold-leaching cell was plastic, with a capacity of 5lit. The cells uncover which allows for the entrance air and insertion of pH.

A Chemcadet pH monitor provided pH readings. Mixing was conducted by an agitator with 2.5 cm stainless steel paddles powered by a variable-speed electric motor that was kept at a constant rate of 400 rpm. The tests were performed on a pulp of 40% solids (1000 gr of ore with 1500 ml water). Tests were designed with full factorial method according to table 4. The ore was introduced into the leaching cell and pulped for a few minutes .according to control test the cyanidation tests were either 24 hour duration. The calculation of the cyanide consumption as based on the fact that the leach solution is not recycled.

In this paper we cannot describe details of the experimental procedure, Analysis and calculations.

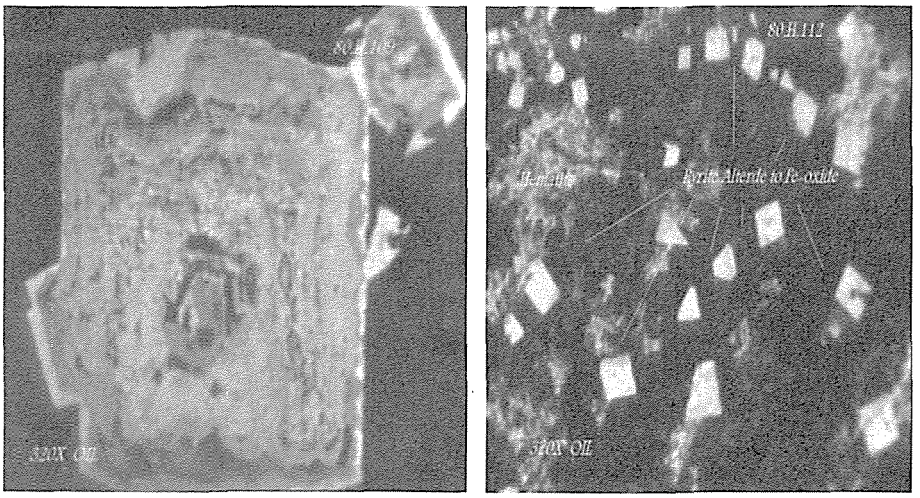

Figure 3.Mineralogical sections of Hyred anomaly

3 RESULTS AND DISCUSSION

3.1 Gold Dissolution

According to the Figure 3, most of the section surface is covered with Fe-Oxide and Hydro oxide such as hematite, Lepidocrosit, goethite in spite of Pyrite and S-oxide and a few S-oxides remain in rock sections, result of the chemical analysis confirmed them, too.

3.2 Discussion

After doing tests, Recovery (%) and Free Cyanide (ppm), are selected as responses. Analyses of variance for general factorial of gold recovery are coming in table 5. For data interpreting in DX7 software, model 2FI fitted effect with order 2FI that would put all main effects and two-factor interactions into the model use as model.

There were six terms; A-Cyanide, B-pH, C-grinding, AB, BC and BC. Values of "Prob > F" less than 0.05 indicate model terms are significant.

The normal probability plot indicates whether the residuals follow a normal distribution, in which case the points will follow a straight line Figure 4

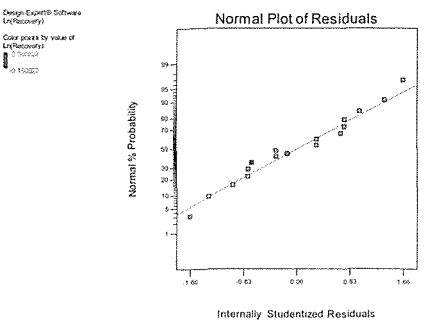

Figure 4.Normal plot of residuals

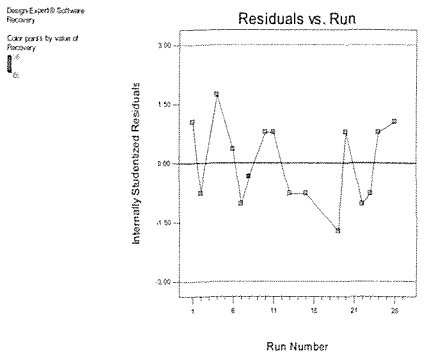

Figure 5.Residuals vs. Run

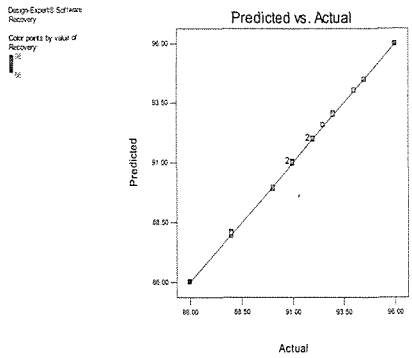

Figure 6.Predicted vs. Actual

Residuals vs.Run plot This is a plot of the residuals versus the experimental run order. It allows you to check for lurking variables that may have influenced the response during the experiment. The plot should show a random scatter. Trends indicate a time-related variable lurking in the background. Blocking and randomization provide insurance against trends ruining the analysis.is a plot of the residuals versus the experimental run order .it allows us to check for lurking variables that may have influenced the response during the experiment. The plot should show a random scatter .Trends indicates a time-related variable lurking in the background .Blocking and randomizations provide insurance against trends ruining the anaResiduals vs Runlysis. This is a plot of the residuals versus the experimental run order. It allows you to check for lurking variables that may have influenced the response during the experiment. The plot should show a random scatter. Trends indicate a time-related variable lurking in the background. Blocking and randomization provide insurance against trends ruining the analysis.

Predicted vs. Actual graph of the actual response values versus the predicted response values. It helps you detect a value, or group of values, that are not easily predicted by the model. The data points should be split evenly by the 45 degree line.

Residuals vs. predicted plot of the residuals versus the ascending predicted response values. It tests the assumption of constant variance. The plot should be a random scatter.

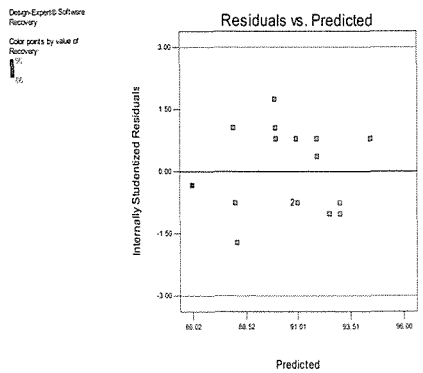

Figure 7. Residuals vs. Predicted

An interaction occurs when the response is different depending on the settings of two factors. Plots make it easy to interpret two factor interactions. They will appear with two non-parallel lines, indicating that the effect of one factor depends on the level of the other. The "I beam" range symbols on the interaction plots are the result of least significant difference (LSD) calculations. If the plotted points fall outside the range, the differences are unlikely to be caused by error alone and can be attributed to the factor effects. If the I beam overlap there is not a significant difference (95% confidence is default) between the two points. You can then

Table4.Tests design with full factorial method

Std	Run	Block 1	Cyanide contents (gr/ton)	PH range	Grinding (μm)	Gold Recovery (%)	Free Cyanide (ppm)	Cyanide solve in solution (ppm)
27	1	Block 1	4000	11	37	89	530	3470
24	2	Block 1	4000	10.5	37	96	550	3450
11	3	Block 1	2500	9.5	53	88	410	2090
15	4	Block 1	4000	10.5	53	91	480	3520
17	5	Block 1	2500	11	53	90	590	1910
21	6	Block 1	4000	9.5	37	93	400	3600
18	7	Block 1	4000	11	53	92.5	620	3380
5	8	Block 1	2500	10.5	75	85	510	1990
1	9	Block 1	1500	9.5	75	88	480	1020
6	10	Block 1	4000	10.5	75	91	610	3390
26	11	Block 1	2500	11	37	91	450	2050
3	12	Block 1	4000	9.5	75	88	570	3430
20	13	Block 1	2500	9.5	37	90	570	1930
23	14	Block 1	2500	10.5	37	92	520	1980
19	15	Block 1	1500	9.5	37	82	490	1010
14	16	Block 1	2500	10.5	53	94	420	2080
12	17	Block 1	4000	9.5	53	90	480	3520
16	18	Block 1	1500	11	53	92	450	1050
2	19	Block 1	2500	9.5	75	92	600	1900
25	20	Block 1	1500	11	37	84	450	1050
4	21	Block 1	1500	10.5	75	91	300	1200
7	22	Block 1	1500	11	75	86	420	1080
8	23	Block 1	2500	11	75	93	420	2080
9	24	Block 1	4000	11	75	90	650	3350
22	25	Block 1	1500	10.5	37	92	510	990
13	26	Block 1	1500	10.5	53	94.5	480	1020
10	27	Block 1	1500	9.5	53	93	450	1050

choose the most economical or convenient level for that factor.

Above interaction plots shows that three factors; grinding size, pH and cyanide consumption were dependent together. Therefore,changing in one of the factors effect on other factor and on recovery.This is a plot of the residuals versus the experimental run order. It allows you to check for lurking variables that may have influenced the response during the experiment. The plot should show a random scatter. Trends indicate a time-related variable lurking in the background. Blocking and randomization provide insurance against trends ruining the analysis.

This is a plot of the residuals versus the experimental run order. It allows you to check for lurking variables that may have influenced the response during the experiment. The plot should show a random scatter. Trends indicate a time-related variable lurking in the background. Blocking and randomization provide insurance against trends ruining the analysis.This is a plot of the residuals versus the experimental run order. It allows you to check for lurking variables that may have influenced the response during the experiment. The plot should show a random scatter. Trends indicate a time-related variable lurking in the background. Blocking and randomization provide insurance against trends ruining the analysis.

There is final equation in terms of coded factors:

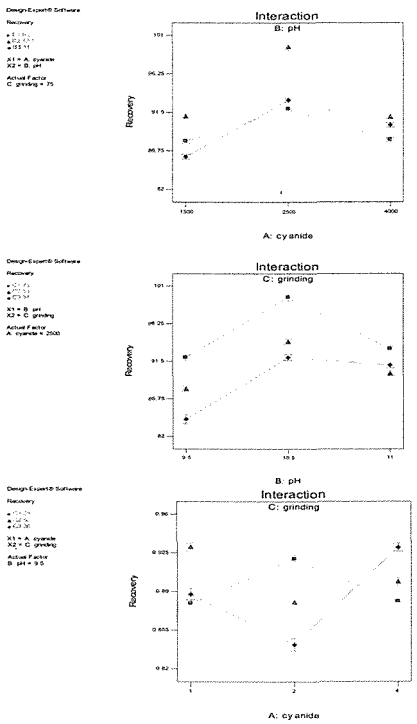

Figure 8. Interaction between 3 factors; pH, Cyanide consumption and grinding size

Table 5. ANOVA for general factorial on gold recovery

Source	Sum Of Squares	df	Mean Square	F Value	p-Value Prob > F
Model	117.8116	18	7	376.997	0.0002
Acyanide	0.9802	2	0	28.229	0.0113
BpH	27.7692	2	14	799.754	< 0.0001
Cgrinding	16.8421	2	8	485.054	0.0002
AB	18.4479	4	5	265.650	0.0004
AC	59.1354	4	15	851.550	< 0.0001
BC	6.6813	4	1.6703	96.210	0.0017
Residual	0.0521	3	0.0174		
Cor Total	117.8636	21			

Std. Dev.	0.131	R-Squared	0.9996
Mean	91.272	Adj R-Squared	0.9969
C.V. %	0.1444	Adeq Precision	81.497

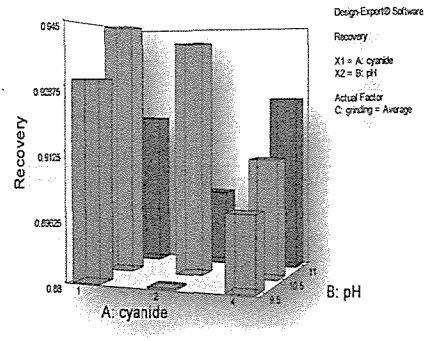

Figure 9. 3D chart; cyanide, pH vs. recovery, average of grinding size is considered with Full Factorial design.

Finally, according to above 3D surface and other plots,the best points was selected,Response surface, Historical data method, was selected for final optimizing gold leaching condition ,two factors pH and cyanid content were investigated in range of the best condition of last step .

Table 6.Tests design with Historical Data (Response surface)

Std	Run	Block 1	Cyanide Contents (ppm)	pH range	Gold Recovery (%)
1	1	Block 1	1	10	86.0
2	2	Block 1	1.5	10.25	89.0
3	3	Block 1	2	10	87.0
4	4	Block 1	1	10.5	87.0
5	5	Block 1	1.5	10.25	88.1
6	6	Block 1	2	10.5	92.2

Interaction plot displayed dependent factors that with increasing in cyanide consumption from 1 ppm to 2 ppm in pH equal with 10.5, recovery increased from 87 % to 92.2%.

Table 7. ANOVA for Historical data method for optimizing gold recovery

Source	Sum Of Squares	df	Mean Square	F Value	p-Value Prob > F
Model	23.63	3	8	21.3363	0.0451
Acyanide	9.610	1	10	26.0316	0.0363
BpH	9.610	1	10	26.0316	0.0363
AB	4.410	1	4	11.9458	0.0745
Residual	0.738	2	0		
Lack of Fit	0.333	1	0	0.8230	0.5309
Pure Error	0.405	1	0		
Cor Total	24.368 3	5			

Std. Dev.	0.60759	R-Squared	0.9697
Mean	88.2167	Adj R-Squared	0.9242
C.V. %	0.6887	Pred R-Squared	0.3063
PRESS	16.9032	Adeq Precision	12.498

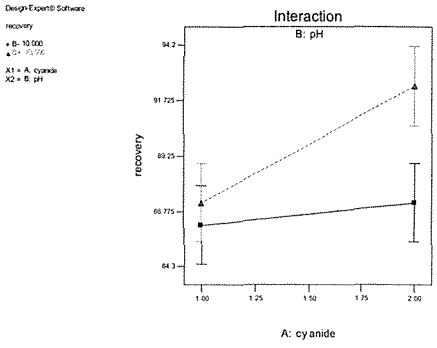

Figure 10. Interaction 2 factors; pH and cyanide

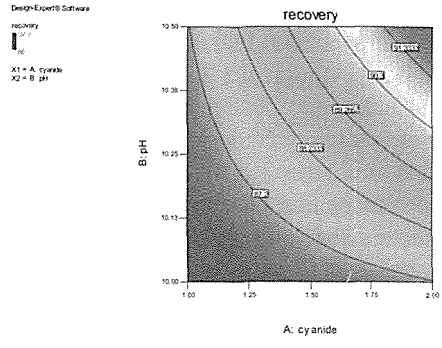

Figure 11.Countor cyanide vs. pH

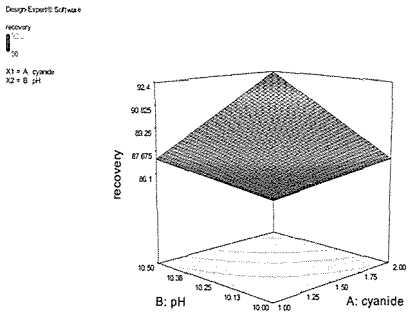

Figure12.3DSurface;cyanide,pHvs. recovery,constant grinding size is considered in Historical design cyanide, pH vs. recovery, average of grinding size is considered.

According to figure11-12, optimum point cyanide consumption 2 ppm and pH rate 10.5 with high recovery 92.2 % were achieved.

4 CONCLUSIONS

When the gold value is high, it is economically important to improve the low grade gold recovery condition.

There are variant effective parameters on gold cyanide leaching circuit that in this paper, we considered three main factors; cyanide content, pH and grinding size as variable parameters and fixing the other parameters such as agitator speed, oxidant rate, light...

This area was nearly unknown area and need to know what condition is good for testing and recovery gold from carbonacious -siliceous zone that seems to use high cyanide content for existing clay to recovery gold from its gunges. Therefore we need to consider all of effective parameters to know which range of parameters would be optimum.

For determining and finding the best condition for cyanide leaching, full fac-

torial design is used to can investigate all of existing conditions. This study shows that there is relationship between factors and changing in one of them affect on the other factors and also on recovery. With analyzing of full factorial testing result the best points had been signified that recovery percentage is upper than the other points, Also ,with considering this matter that low cyanide consumption can help to healthy environment, good rang of cyanide content is selected from 1-2 ppm , pH 10-10.5 and grinding size equal with 53 micron.

Therefore, with full factorial design we achieve the best range of factors and then for optimizing, a series of test was designed and done with response surface, Historical design.

Finally, we achieved optimum condition for high recovery 92.2% from Hyred low grade gold.

ACKNOWLEDGEMENTS

The authors wish to thank the Geological and exploration organization of Iran (Tehran,Iran) and Technological University of Shahrood (Shahrood,Iran)

REFERENCES

Andrade Limba, L.R.P., 2006., Analysis of the gold recovery profile through a cyanidation plant, Int.J.Miner process 80(2006), p.p.15-26.

Cisternas, L.A., 1999. On the synthesis of inorganic chemical and metallurgical processes. Review and extension. Minerals Engineering 12 (1), 15–41.

Cisternas, L.A., Galvez, E.D., Zavala, M.F., Magna, J., 2004. A MILP model for the design of mineral flotation circuits. International Journal of Mineral Processing 74 (1–4), 121–131.

Habashi, F., 1987. One hundred years of cyanidation. CIM Bulletin 80, 108–114.

Marsden, J., House, I., 1992. The Chemistry of Gold Extraction. Ellis Horwood.

Roland-Villasana, E.J., Williams, R.A., 1991. Calculation of a steadystate mass balance for complex hydrocyclone networks. Minerals Engineering 4 (3–4), 289–310.

Schena, G., Zanin, M., Chiarandini, A., 1997. Procedures for the automatic design of flotation networks. International Journal of

Mineral Processing 52 (2–3), 137–160.

Williams, M.C., Meloy, T.P., 1983. Dynamic-model of flotation cell banks-circuit analysis. International Journal of Mineral Processing 10 (2), 141–160.

Williams, M.C., Meloy, T.P., 2000. Grid representation of separation networks. International Journal of Mineral Processing 58 (1–4), 179–186.

Xie,Feng.,2008,The novel application of ferricyanide as an oxidant in the cyanidation of gold and silver., department of material Engineering (2008).

Yingling, J.C., 1990. Circuit analysis —optimizing mineral processing flowsheet layouts and steady-state control specifications. International Journal of Mineral Processing 29 (3–4), 149–174.

Yannopoulos, J.C., 1991. The Extractive Metallurgy of Gold. Van Nostrand Reinhold.

Green, J.C.A., 1984. The optimization of flotation networks.International Journal of Mineral Processing 13 (2), 83–103.

Determining Erratic Results of Boric Acid Grain Size with Clustering Analysis

Kümeleme Analizi ile Borik Asit Tane Boyutuna ait Uyumsuz Verilerin Belirlenmesi

S. Yerel
Bilecik Üniversitesi, Bozüyük Meslek Yüksekokulu, Bozüyük/Bilecik
H. Ankara
Eskişehir Osmangazi Üniversitesi, Maden Mühendisliği Bölümü, Eskişehir
M. Savaş
Emet Bor İşletme Müdürlüğü, Kütahya

ABSTRACT Control charts are commonly used to measure the variation occurring within the processes. In this study, Range (R) control chart was established in order to determine whether the results from the sieve analysis conducted in consecutive days in boric acid manufacture plant were under control or not. When the R control chart was examined, it was observed that some points were incompatible with other points. It is significant for the process to determine whether these incompatible points are erratic results or not. Therefore in this study, single linkage method, one of Agglomerative hierarchical clustering methods, was used to determine whether the incompatible points identified in improper locations were erratic results or not. As a result of this method, erratic results were determined and eliminated from the process. After R control chart was drawn again and it was determined that the re-drawn R control chart displayed the process characteristic. It was suggested in conclusion that it was a necessity to establish R control charts only after determining erratic results and eliminating them from the process by using single linkage method.

ÖZET Kontrol grafikleri, süreçteki değişikliklerin belirlenmesi için yaygın olarak kullanılmaktadır. Bu çalışmada, Range (R) kontrol grafiği borik asit tesisindeki elek analizi sonuçlarının kontrol altında olup olmadığının belirlenmesi için kullanılmıştır. R kontrol grafiği incelendiğinde bazı noktaların diğer noktalardan çok farklı ve uygunsuz yerlerde olduğu görülmüştür. Bu noktaların örnekleme hatası olup olmadıklarının belirlenmesi süreç açısından çok önemlidir. Bundan dolayı, bu çalışmada hiyerarşik kümeleme yöntemlerinden tek bağlantı kümeleme metodu kullanılarak uygunsuz

noktaların örnekleme hatalarından kaynaklandığı belirlenmiştir. Daha sonra örnekleme hatalarından kaynaklanan noktalar süreçten atılmış ve R kontrol grafiği tekrar kurulmuş ve yeni çizilen kontrol grafiğinin süreç karakteristiğini daha iyi temsil ettiği belirlenmiştir. Sonuç olarak R kontrol grafikleri kurulmadan önce örnekleme hatalarından kaynaklanan noktaların Agglomerative hiyerarşik kümeleme yöntemlerinden single linkage metodu kullanılarak belirlenip süreçten atılması ve daha sonra R kontrol grafiğinin kurulması önerilmektedir.

1 INTRODUCTION

The scope of Statistical Process Control (SPC), some statistical methods and techniques such as flow chart, histogram, cause-effect diagram and control charts are utilized to determine and deal with the variation caused in processes by various reasons. Control charts, which are among statistical method and techniques defined as problem determining and solving tools in SPC, are used both to identify the presence of any undesired or unexpected situation and to decrease systematically the variation caused by that condition (Anagun, 1997).

Those control charts applied most commonly in SPC as well as in this study are called Shewhart control charts. Shewhart control charts were developed in 1924 by Shewhart to examine the variations in manufacturing process. One aim of Shewhart control charts is to observe process variability limits through statistical control and determine process continuation ability (Burnak, 1997). The control chart used widely in determining the variability limits of a process characteristic and to be employed in this study as well is Range (R) control chart, a type of Shewhart control charts.

It is crucial that the variability limits of the data obtained from mineral processing and metallurgical processes be determined and this process be observed by means of SPC methods. Sometimes, however, some data are observed to be quite dissimilar and incompatible while employing statistical control methods to monitor the process. Determining whether this incompatibility is erratic data or not and eliminating them if they are erratic data has a great significance for establishing control charts.

In this study, R control charts were formed in order to monitor the variation of the boric acid obtained from + 0.25 mm grain size during 24 days in boric acid processing plant. When the R control chart was examined, it was observed that some of the points were quite different from others and incompatible Single Linkage method – one of the Agglomerative hierarchical clustering methods – was used in order to examine if those data were erratic or not. As a result of this method, the values determined to be erratic data were sorted out from the process and R control chart was established again. When the R control chart formed again was examined, it was determined that this chart yielded more accurate results.

2 STATISTICAL ANALYSIS

2.1 Range (R) Control Chart

Grant and Leavenworth (1985) showed that, The R control chart should be prepared as follows:

- Statistical parameters related to characteristics are computed for each subgroup.
- The averages of ranges of the subgroups

are computed as the parameters of a group.

- The three parameters for R control chart are calculated as Central Line (CL_R), Upper Control Limit (UCL_R) and Lower Control Limit (LCL_R).
- The R control chart is drawn.

2.1.1. Calculation of Range for Subgroups

The range of a subgroup (R_j) is calculated as the subtraction of the minimum measurement value (X_{min}) from the maximum measurement value (X_{max}) in a subgroup (Grant and Leavenworth, 1985; Elevli, 2006). R_j is equal to Eq (1).

$$R_j = X_{max} - X_m, j=1, 2, 3,\ldots,m \quad (1)$$

2.1.2. Calculation of Parameters of R Control Chart

After the calculation of the ranges of subgroups, the average of ranges ($\bar{R}$) is found as the parameters of the group, which consist of the statistical parameters of subgroups (Grant and Leavenworth, 1985).

$\bar{R}$ is the sum of ranges of subgroups divided by the number of subgroups in the group (m).

Three parameters (UCL_R, CL_R and LCL_R) for an R control chart are computed from Eqs. (2), (3) and (4) (Montgomery, 1991; Yerel et al., 2007).

$$UCL_R = D_4\bar{R} \quad (2)$$
$$CL_R = \bar{R} \quad (3)$$
$$LCL_R = D_3\bar{R} \quad (4)$$

Where,

Where,

D_3 and D_4 : The factors taken from table of factors for the control charts

2.2. Agglomerative Hierarchical Clustering Methods

Hierarchical clustering techniques proceed by either a series of successive mergers or a series of successive divisions. Agglomerative Hierarchical Clustering Methods start with the individual objects. Thus, there are initially as many clusters as objects. The most similar objects are first grouped, and these initial groups are merged according to their similarities. Eventually, as the similarity decreases, all subgroups are fused into a single cluster (Johnson and Wichern, 2002; Singh et al., 2005).

The following steps in the Agglomerative Hierarchical Clustering algorithm for grouping N variables.

- Start with N clusters, each containing a single entity and an N X N symmetric matrix of similarities $D = \{d_{ik}\}$.
- Search the distance matrix for the most similar pair of clusters. Let the distance between "most similar" clusters U and V be d_{UV}.
- Merge clusters U and V. Label the newly formed cluster (UV). Update the entries in the distance matrix by (a) deleting the rows and columns corresponding to clusters U and V and (b) adding a row and column giving the distances between cluster (UV) and the remaining clusters.
- Repeat Steps b and c a total of N-1 times. Record the identity of clusters that are merged and the similarities at which the mergers take place.

2.2.1. Single linkage method

The inputs to a single linkage algorithm can be similarities between pairs of variables. Groups are formed from the individual entities by merging nearest neighbours. Initially, we must find the smallest distance in $D = \{d_{ik}\}$ and merge the corresponding objects, say, U and V, to get the cluster (UV). For Step c of the general algorithm of record the identity of clusters that are merged and the similarities at which the mergers take place. The distance between (UV) and any cluster W are computed by

$$d_{(UV)W} = \min\{d_{UW}, d_{VW}\} \quad (5)$$

Here the quantities d_{UW} and d_{VW} are the distances between the nearest neighbours of clusters U and W and clusters V and W, respectively.

The results of single linkage clustering method can be graphically displayed in the form of a dendrogram. The branches in the dendrogram represent clusters. The branches come together at nodes whose positions along a similarity axis indicate the level at which the fusions occur (Johnson and Wichern, 2002; Shrestha and Kazama, 2007).

3 CASE STUDY

In this study, R control chart was established in order to determine whether the results from sieve analysis in +0.25 mm grain size of boric acid in boric acid processing plant were under control or not. Grain size of boric acid is very important for re-crystallization process. A daily total of 7 random samples were collected during consecutive 24 days and the sieve analysis was conducted so that R control chart for +0.25 mm grain size boric acid could be formed. By using these sieve analysis results, the parameters needed to establish R control charts were calculated and presented in Table 1.

Table 1. R control chart parameters.

Parameters	Computation (mm)
$\overline{R}$	5.58
UCL_R	10.74
CL_R	5.58
LCL_R	0.42
D_3	0.076
D_4	1.924

R control charts drawn by using the values in Table 1 are presented in Figure 1. When R control charts in Figure 1 was examined, it was found out that some of the points displayed quite a high level of dissimilarity and incompatibility when compared with the others. Determining whether or not these points are erratic data is extremely significant for statistical process control. Single linkage method among Agglomerative hierarchical clustering methods was utilized to be able to determine the compatibility of these points. The principal objective meant by this method is to measure the similarity among the sieve analysis results during 24 consecutive days and to identify and eliminate erratic data from the process.

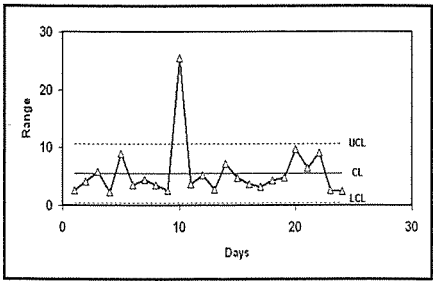

Figure 1. R control chart.

Distance matrix was formed so that the similarity among the days by using single linkage method. For the distance matrix, the number of observations and the number of variables for the samples were taken as 24 (the number of days) and 7 (the number of samples taken per day) respectively. Then, dendrogram was drawn by using distance matrix (Figure 2).

When the dendrogram in Figure 2 is examined, it is seen that the 10^{th} point merges by 33.75%, the 6^{th} point by 55.34% and the 5^{th} point by 67.03%. Due to the fact that the similarity percentage

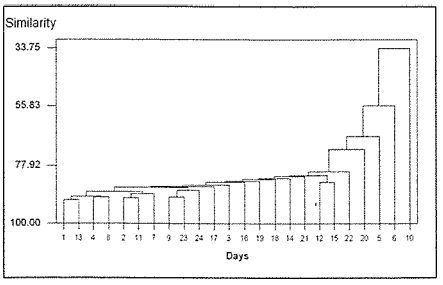

Figure 2. Dendrogram for boric acid values

of the 10th point is lower in comparison with the others, this point was taken as erratic result and eliminated from the process. After this value was sorted out from the process, the parameters required to establish R control chart were calculated again and presented in Table 2.

Table 2. R control chart parameters re-calculated after clustering analysis.

Parameters	Computation (mm)
$\overline{R}$	4.72
UCL_R	9.2
CL	4.72
LCL_R	0.36
D_3	0.076
D_4	1.924

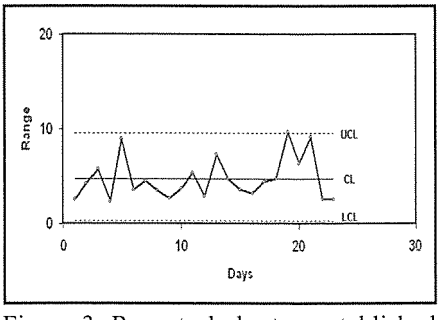

Figure 3. R control chart re-established after clustering analysis

R control chart was established again by using the values in Table 2. It was observed that the revised R control chart provided more accurate results in monitoring the process (Figure 3).

4. CONCLUSION

In this study, sieve analyses were conducted on a daily total of 7 boric acid samples picked from boric acid processing plant during 24 consecutive days. Then, R control chart was established in order to determine if the sieve analysis results of +0.25 mm grain size was under control or not. When the R control chart was examined, it was found out that some of the points were quite different and incompatible compared with the others. In this study, single linkage method among Agglomerative hierarchical clustering methods was utilized to determine if those points were erratic results or not. The erratic result identified by means of this method was eliminated from the process. R control chart was drawn again after this elimination. When the revised R control chart was examined, it was observed that this graphics yielded more accurate results in monitoring the process. For the future studies, therefore, it was suggested that determining and eliminating erratic results first before establishing R control charts by using single linkage method – an Agglomerative hierarchical clustering method – and then establishing R control charts would be advisable.

REFERENCES

Anagun, A. S., 1997. Dusuk Hacimli Uretimde Istatistiksel Proses Kontrolu: Kontrol Grafikleri, *III. Ulusal Ekonometri ve Istatistik Sempozyumu Bildirileri*, s. 271-281, Bursa.

Burnak, N., 1997. *Toplam Kalite Yonetimi Istatistiksel Surec Kontrolu*, Eskisehir Osmangazi University, Faculty of Engineering and Architecture TEKAM Publ. No: TS-97-008-NB.

Elevli, S., 2006. Coal Quality Control with Control Charts, *International Journal of Coal Preparation and Utilization*, 26, 181-199.

Grant, E. L. and Leavenworth, R. S., 1985. Statistical Quality Control, Fong and Sons Ltd.

Johnson, R.A. and Wichern, D.W., 2002. *Applied Multivariate Statistical Analysis*, 5th Edition, Pearson Education International.

Montgomery, D. C., 1991. *Introduction to Statistical Quality Control*, John Wiley & Sons Inc., New York.

Shrestha, S. and Kazama, F., 2007. Assessment of surface water quality using multivariate statistical techniques: A case study of the Fuji river basin, Japan. *Environmental Modelling & Software*, 22, s. 464-475.

Singh, K.P., Malik, A. and Sinha, S., 2005. Water quality assessment and apportionment of pollution sources of Gomti river (India) using multivariate statistical techniques- a case study. *Analytica Chimica ACTA*, 538, s. 355-374.

Yerel, S., Ankara, H., Konuk, A. and Ozdag, H., 2007. Preventive Maintenance Policy Supported by a Quality Control Chart and Kolmogorov Smirnov Tests: Emet Colemanite Mineral Processing Plant, Turkey. *Minerals & Metallurgical Processing*. 24, s. 152-156.

Evaluation of Leachability of Potentially Toxic Elements from Fly Ash Bricks

Uçucu Küllü Tuğlalardan Potansiyel Toksik Elementlerin Liç Değerlendirmesi

H. Cengizler

Celal Bayar University, TMYO, Turgutlu

ÖZET Uçucu küllü tuğlaların içerdiği bazı toksik elementlerin liç durumunu araştırmak için liç deneyleri yapılmıştır. Asit yağmuru ve doğal yağmur koşullarını canlandıran deneyler, bu atmosfer koşullarında elementlerin davranışı hakkında bilgi edinmek ve zehirlilik seviyelerini tespit etmek amacıyla yapılmıştır. TCLP metodunun kullanıldığı deneylerde parça tuğladan elde edilen liç çözeltisinde Fe, Zn ve Mn'in çözünürlük seviyeleri içme suyu standartlarına uygundur. ASTM metodunun kullanıldığı deneylerde ise hem parça hemde öğütülmüş tuğladan elde edilen liç çözeltilerinde hiçbir toksik element tespit edilmemiştir. TCLP metodunun kullanıldığı deneylerde, öğütülmüş tuğladan elde edilen liç çözeltisinde Fe, Zn, Cu, Cr, Ni ve Mn gibi elementlerin çözünürlük konsantrasyonları parça tuğla liç çözeltisinden daha yüksek değerlerdedir. Bununla beraber, sadece Fe, Ni ve Mn konsantrasyonları içme suyu standartlarından daha yüksek olarak tespit edilmiştir.

ABSTRACT Batch leach tests were carried out to investigate the leachability of some toxic elements from fly ash bricks. The tests simulating the acid rain environment and natural rain water were conducted to gain insight regarding the behavior of the elements during weathering and to determine their toxicity characteristics. In the tests using TCLP method, the solubility levels of Fe, Zn and Mn detected in the leachate of the whole brick pieces were in agreement with the drinking water standards. In the tests using ASTM method, no detectable level of any element was found in the leachates of the whole brick pieces and of ground brick. In the tests using TCLP method, the solubility concentrations of the elements such as Fe, Zn, Cu, Cr, Ni, and Mn from the leachate of the ground brick were higher than those of the whole brick pieces. However, only Fe, Ni and Mn concentrations were determined to be higher than those allowed in the drinking water standards.

1 INTRODUCTION

Fly ash is a by-product of coal combustion process generated by thermal power plants. The total amount of fly ash produced in Turkey was about 15 million tonnes in 2000 and expected to reach 50 million tonnes by the year of 2020 (Tütünlü and Atalay 2001). Most of the fly ash is sent to the ponds or landfills near power plants. The disposal is a costly operation causing environmental concerns. In Turkey, only about 3 % of the total amount of fly ash produced is mainly used in cement and concrete production

(Tütünlü and Atalay 2001). This low amount of usage compared with countries such as UK and USA can be attributed to the variations in quality of fly ashes produced and to a limited number of research and development studies aiming at the utilization of fly ash in other industrial areas (Çiçek and Tanrıverdi 2007).

Distributions of the elements within the ash structure are different. The elements such as Ti, Na, K, Mg, Hf, Th, and Fe are mostly bounded in the aluminosilicate matrix of fly ash whereas As, Se, Mo, Zn, Cd, W, V and U concentrate on the surface of the fly ash particles. The elements such as Mn, Be, Cr, Cu, Co, Ga, Ba, and Pb are intermediately distributed between the matrix and non matrix structure (Hansen and Fisher 1980, Cohen et al. 2004a, Cohen et al. 2003b, Güler et al. 2004, Tuzcu 2004)

The leachability of the toxic elements can be kept at low levels when fly ash is incorporated as an additive into cement and concrete due to its chemical fixation (Zhang et al. 2001a, Zhang et al. 2001b). It has been also reported that highly alkaline fly ash assists to retain metals and thus reduces the mobilization of toxic elements (Sear et al. 2003). However, quite high concentrations of the toxic elements were reported through the leachability tests performed with high CaO fly ash (Güler et al. 2004). Due to the conflicting results mentioned above, it seems to be necessary to investigate the leaching potential of such toxic elements in assessing the possible environmental impacts associated with fly ash usage in construction industry. Therefore, in this laboratory study, batch leach tests were carried out to investigate the leachability of toxic elements from light weight fly ash bricks.

2 EXPERIMENTAL

The fly ash bricks produced from the mixture of the Seyitömer fly ash (Turkey) and the Turgutlu brick clay (turkey) were used for tests. In a previous study, it was found that the bricks with 40 wt% fly ash fired at 1050 °C meet the required specifications for vertically perforated

Table 1. Properties of light weight fly ash bricks produced under optimum conditions

Unit volume weight (g/cm^3)	1.2
Compressive strength (MPa)	4.42
Heat conductivity (W/mK)	0.46
Water absorption (%)	25

Table 2. Chemical properties of fly ash bricks

	%		ppm
SiO_2	63.52	Cd	2.4
Al_2O_3	15.02	Pb	90
Fe_2O_3	8.24	Zn	145
CaO	5.80	Cu	72
MgO	3.50	Cr	430
Na_2O	0.80	Ni	1010
K_2O	1.98	Mo	ND
TiO_2	0.45	Co	50
MnO	0.10	Sb	ND
SO_3	0.09	Mn	580
Loss on ignition	0.29		

ND: Not detectable

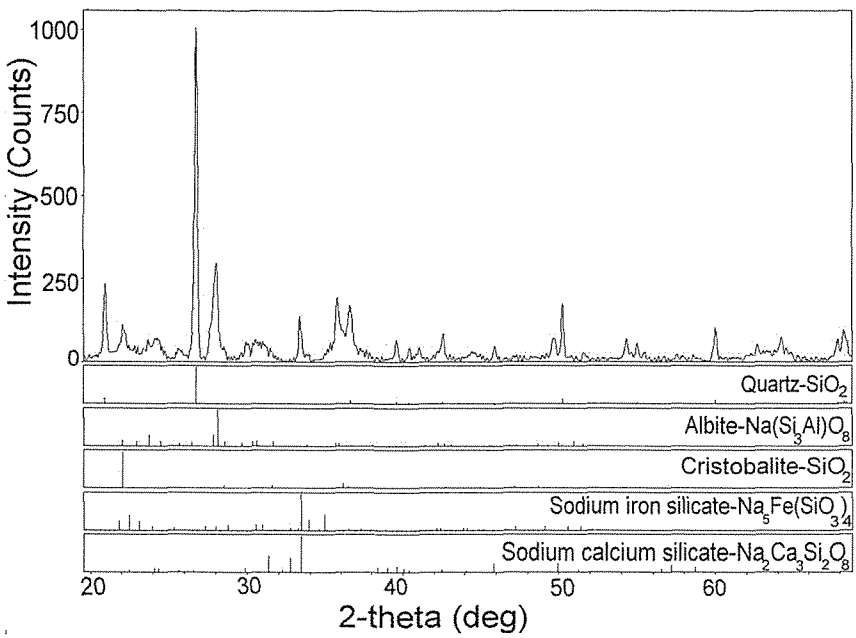

Figure 1. XRD analysis of fly ash brick sample.

bricks (Cengizler et al. 2008). In the present study, the same brick samples made up of 40% fly ash and 60% brick clay were thus used for the leachability tests. The brick firing temperature and the dwelling time were 1050 °C and 1 h respectively (Cengizler et al. 2008). The bricks were formed as cylindrical logs in 45 mm diameter and 100 mm height.

Some physical properties and the chemical analysis of the fly ash bricks are given in Table 1 and Table 2 respectively. The fly ash bricks contain toxic elements such as Ni, Cr, Zn, Pb, Cu, and Cd (Table 2).

X-Ray diffraction (XRD) analyses were also performed on the brick sample using a Rigaku D-max-2200/pc model powder diffractometer. As seen from the XRD pattern of the fly ash brick illustrated in Figure 1, the main phases were quartz (SiO_2), albite [$Na(Si_3Al)O_8$], cristobalite (SiO_2), sodium iron silicate [$Na_5Fe(SiO_3)_4$] and sodium calcium silicate ($Na_2Ca_3Si_2O_8$).

Whole brick pieces and ground brick sample (−100 μm) were used separately for the batch leach tests. The primary aim was to determine the leachability of toxic elements in neutral and acidic water. The leach test procedures applied were as follows:

- TCLP (Toxicity Characteristic Leaching Procedure) [Improved Method 1311]
- ASTM (American Society of Testing and Materials) Method A extraction procedure.

2.1 TCLP Leaching Procedure

This method is used to check the leaching hazards of the solid wastes (it is especially suitable for the acidic wastes). The method predicts the leaching behavior of the trace elements in the disposed waste during weathering (EPRI Report 1987).

A piece of brick (100g) or ground brick (100g) sample was weighed and put it into a bottle. Distilled water for a liquid/solid ratio of L/S = 20 and 11.4 ml of glacial CH_3COOH (pH 2.88) was added. The mixture was put in a capped bottle and placed in an agitation device for 18±2 h with a shaker (at 30±2 rpm) at room temperature (22±3 °C). The eluate was filtered through 0.6-0.8 μm membrane and the concentrations of the leached elements were measured.

2.2 ASTM Leaching Procedure

This method is applied to predict the leaching behavior of the trace elements for long-term weathering conditions. The determination of the leaching behavior of the trace elements in long term stored wastes can be done using this method based on extended extraction with distilled water.

A piece of brick (100 g) or ground brick (100g) sample was weighed and put it into a bottle. Distilled water for a liquid/solid ratio of L/S = 20 was added. The mixture was put in a capped bottle and placed in an agitation device for 24±0.5 h with a shaker (at 30±2 rpm) at room temperature (19-25 °C). The eluate was filtered through 0.6-0.8 μm membrane and the concentrations of the leached elements were measured.

In terms of simulating long-term leaching behaviour of the elements in natural circumstances, TCLP is considered to be too aggressive; whereas, water extraction, as in the case of the Method A extraction procedure seems to be more adequate (U.S. EPA 1987). An Analytikjena AG novaAA 300 flame atomic absorption spectrometer (AAS) was used for measuring the concentrations of the leached elements.

3. RESULTS AND DISCUSSION

3.1 Information on pH of the solutions

As mentioned earlier, two different toxicity test methods were employed. The first one was the TCLP method simulating the solubility of the elements contained in the fly ash brick samples under a weak acid rain water environment. The second one was similar to water leaching.

In the TCLP test, the ground brick sample exhibited a higher acid neutralization power compared with the whole brick piece due to its higher surface area (Table 3). In ASTM Method A extraction test, the pH of the ground brick sample was 9.49 at the beginning of the test indicating the alkaline nature of the bricks (Table 4). The same property was not initially observed for the whole brick pieces. However, at the end of the test, pH value rose up to 9.15 for the whole brick because of its porous structure.

Table 3. Information on the pH of the solution in TCLP tests

Sample	Added acid (mL)	pH after adding acid	Final pH
Brick	11.4	2.78	3.29
Ground brick	11.4	3.79	3.82

Table 4. Information on the pH of the solution in ASTM method A extraction tests

Sample	Initial pH	Added acid (mL)	Final pH
Brick	5.78	-	9.15
Ground brick	9.49	-	9.85

Table 5. Concentration of the elements leached from the light weight fly ash brick samples

Elements	TCLP(Toxicity characteristic leaching procedure) improved method 1311 (mg/L)		ASTM (American Society of Testing and Materials) method A extraction procedure (mg/L)		Drinking water standards (mg/L)	
	Ground brick	Brick piece	Ground brick	Brick piece	WHO	TSE
Fe	**15**	0.2	ND	ND	0.330	0.200
Cd	ND	ND	ND	ND	0.003	0.005
Pb	ND	ND	ND	ND	0.010	0.050
Zn	0.75	0.05	ND	ND	3	5
Cu	0.03	ND	ND	ND	2	3
Cr	0.05	ND	ND	ND	0.050	0.050
Ni	**0.1**	ND	ND	ND	0.020	0.050
Co	ND	ND	ND	ND	0.010	**
Sb	ND	ND	ND	ND	**	0.010
Mn	**0.55**	**0.1**	ND	ND	0.4(C)	0.050

ND: Not detectable
**: Not available in TSE266
C: Concentrations of the substance at or below the health based guideline value may affect the appearance, taste or odour of the water, leading to consumer complaints

3.2 Leachability of Elements

The concentration of the elements leached from the fly ash brick samples are given in Table 5 showing the solubility of the elements determined by the two different test procedures presented for comparison. In the last two columns of Table 5, the drinking water standards according to WHO (World Health Organization) (WHO 2004) and TSE (Turkish Standards Institute) (TSE 2005) are given. No detectable, element concentrations were found in the leachates obtained from the tests carried out with brick pieces and ground brick using the ASTM method (Table 5). This indicates that the leachability of the trace elements from the fly ash bricks is very unlikely under the long term weathering conditions, e.g. natural rain water. In a previous study (Tanrıverdi, 2006) investigating the leachability of the soluble toxic elements contained in lime based steam autoclaved fly ash bricks produced from 88 % fly ash and 12 % $Ca(OH)_2$, no detectable element concentrations were found in the leachates from the both tests conducted with brick pieces. The same results were also obtained in the present study for the whole brick sample using the ASTM method except the detectable concentrations of Fe, Zn and Mn in the leach solutions obtained from the test conducted with the whole brick using TCLP method. Nevertheless, their concentrations were within the required limits of WHO standards of drinking water except the Mn concentration being higher than that specified in the TSE standards of drinking water. On the other hand, Fe, Zn, Cu, Cr, Ni and Mn were found in the leach solution obtained from the test carried out with ground brick using TCLP method. Adding weak acid (acetic acid) with the TCLP method changed the pH of the solutions substantially, thus increasing the solubility values of some elements mentioned above to detectable levels compared with the tests performed with ASTM method using only distilled water. As seen from Table 5, only the dark colored and underlined values are higher than those of the drinking water standards.

4 CONCLUSIONS

Physical and chemical characterizations were performed on the light weight fly ash bricks produced in laboratory scale. Two different toxicity tests were conducted on the whole fly ash brick pieces and ground brick material to determine the solubility values of the elements in their matrix. The results are as follows:

- Although Fe, Zn and Mn were detected in the leachate obtained from the test run with the whole brick pieces using TCLP method, their levels in leachates are in compliance with the regulation levels of the drinking water standards (U.S. EPA 1987, WHO 2004). But the Mn concentration is higher compared with TSE (TSE 2005). Furthermore, no detectable levels of elements were found in the leachates obtained from the test runs performed with the whole brick pieces and ground brick using ASTM method. Therefore, it can be concluded that the light weight fly ash bricks can be safely used in buildings exposed to weathering conditions.

- The leachability of the elements from the ground brick was higher than those from the whole brick pieces in TCLP tests. This result reflects the effect of grinding which promotes the leaching of these elements due

to the increased contact surface area with the leach solution. Therefore, if the large surface areas of the bricks are somehow exposed to weathering conditions acidic in nature, the leaching of above mentioned elements might be expected. However, only Fe, Ni and Mn concentrations were determined to be higher than those allowed in the drinking water standards of WHO and TSE.

REFERENCES

Cengizler, H., Çiçek, T. and Tanrıverdi, M., 2008. Production of light weight bricks containing class F fly ash, *Proceedings of the 11th International Mineral Processing Symposium,* p.995-1002, Belek-Antalya, Turkey.

Çiçek, T. and Tanrıverdi, M., 2007. Lime based steam autoclaved fly ash bricks, *Construction and Building Materials*, 21, pp.1295–1300.

Cohen, H., Lederman, E., Pelly, I., Werner, M. and Polat, M. 2004a. Fly ash as an excellent chemical scrubber to acidic wastes of the phosphate industry in Israel, *Proceedings of the Xth International Mineral Processing Symposium,* pp. 699-706, Çeşme, Turkey.

Cohen, H., Lederman, E., Pelly, I., Werner, M. and Polat, M. 2003b. Synergetic effect of coal fly ash as a scrubber to acidic wastes of the phosphate fertilizers industry, *International Ash Utilization Symposium, Center for Applied Energy Research*, University of Kentucky, Paper #50, Kentucky, USA.

EPRI Report CS-5355, 1987. Evaluation of the Toxicity Characteristic Leaching Procedure (TCLP) on Utility Wastes.

Güler, G., Güler, E., Ipekoglu, U., Seyrankaya, A., Mordogan, H. and Polat, M., 2004. Leachability of elements contained in coal ash samples from coal-fired power plants in western Turkey, *Challenges and Opportunities in Mineral Processing, Proceedings of Xth International Mineral Processing Symposium*, p.717-723, Çeşme, Turkey.

Hansen, L.D. and Fisher, G.L., 1980. Elemental distribution in coal fly ash particles, E*nvironmental Science and Technology*, 14, 9, pp.1111-1117.

Sear, L.K.A., Weatherly, A.J. and Dawson, A. 2003, *International Ash Utilization Symposium, Center for Applied Energy Research*, University of Kentucky, Paper #20, Kentucky, USA.

Tanrıverdi, M., 2006. Toxic elements leachability tests on autoclaved fly ash-lime bricks, *Asian Journal of Chemistry.*18, 3, pp.2310-2314.

TSE 266, 2005. Water intended for human consumption, Turkish Standards Institute, ICS 13.060.20: Drinking Water (in Turkish).

Tuzcu, E. T., 2004. Removal of heavy metals from industrial waste waters with fly ash, *Challenges and Opportunities in Mineral Processing, Proceedings of Xth International Mineral Processing Sympsium*, pp.795-801, Çeşme, Turkey.

Tütünlü, F. and Atalay, Ü., 2001. Utilization of fly ash in manufacturing of building bricks, *Proceeding of International Ash Utilization Symposium,* Center for Applied Energy Research, University of Kentucky, Lexington, Paper # 13, Kentucky, USA.

U.S. EPA, 1987. United States Environmental Protection Agency ()

Characterization of municipal waste combustor ashes and leachates from municipal solid waste landfills and co-disposal sites. I–VII, 530-SW-87-028A-E. Washington, DC, U.S.A., U.S. Environmental Protection Agency.

WHO, 2004. World Health Organization, Drinking-Water Quality, Guidelines for Drinking-Water Quality, Vol. 1:3, ISBN 92 4 154638 7, Geneva, p.491-493.

Zhang, M. H., Blanchette, M.and Malhotra, V. M., 2001a. Leachability of trace metal elements from fly ashes and from concrete incorporating fly ashes, *ACI Special Publication,199*, p.1-28.

Zhang, M. H., Blanchette, M. and Malhotra, V. M.,2001b. Leachability of Trace Metal Elements from Fly Ash Concrete: Results from Column-Leaching and Batch-Leaching Tests, *ACI Materials Journal*, 98, 2, p.126-136.

Enrichment of a Low Grade Chromite Ore

Düşük Tenörlü Kromit Cevherinin Zenginleştirilmesi

T. Çiçek, & İ. Cöcen
Dokuz Eylül University, Mining Engineering Department, İzmir
H. Cengizler,
Celal Bayar University, TMYO, Turgutlu

ÖZET Santrifüj etkili Mozley separatörünün (MGS) düşük tenörlü (9.3 % Cr_2O_3) kromit cevherinin ince fraksiyonuna (−0.1 mm) uygulanabilirliği araştırılmıştır. Elek-metal analizleri deneyler için 1 mm altına öğütülen cevherin % 83.9'unun +0.106 mm boyutunda ve % 8 Cr_2O_3 tenörlü, %16.1'inin de −0.106 mm boyutunda ve %16.12 Cr_2O_3 tenörlü olduğunu göstermiştir. +0.1 and the −0.1 mm fraksiyonları sırasıyla sallantılı masa ve MGS için besleme malzemesi olarak kullanılmıştır. Sallantılı masa deneylerinde düşük kromit veriminde satılabilir kaba bir konsantre elde edilmiştir. Ancak, masa ara ürünlerinin bir kısmı – 100 mikron altına öğütüldükten ve MGS ile zenginleştirildikten sonra sallantılı masa ve MGS kombinasyonu ile % 46.22 Cr_2O_3 tenörlü bir konsantre % 66.1 verimle elde edilebilmiştir. MGS'nin düşük tenörlü bir kromit cevherinin zenginleştirilmesinde ince tane boyutlarında kullanılabilecek bir zenginleştirme yöntemi olduğu görülmüştür. Zenginleştirme tesisi için prensip akım şeması önerilmiştir.

ABSTRACT The applicability of Mozley centrifugal force gravity separator (MGS) to fine fractions (−0.1 mm) of a low grade chromite ore (9.3 % Cr_2O_3) was investigated. The metal-screen analysis revealed that 83.9 % of the material ground under 1 mm for tests was in the +0.106 mm fraction containing 8 % Cr_2O_3. On the other hand, 16.1 % was in the −0.106 mm size fraction containing 16.12 % Cr_2O_3. The +0.1 and −0.1 mm fractions were used as feed for shaking table and MGS tests respectively. A saleable shaking table concentrate with low chromite recovery was obtained by shaking table tests. However, after some of the shaking table products were ground under −100 μm and concentrated with MGS, a chromite concentrate with 46.22 % Cr_2O_3 grade and 66.1 % Cr_2O_3 wt. recovery was obtained by the combination of shaking table and MGS. It was seen that MGS was an applicable beneficiation method at fine fractions for concentration of a low grade chromite ore. A principal flowsheet for the concentration plant was proposed.

1 INTRODUCTION

Turkey is among the countries producing chromite ore, chromite concentrate and ferrochromium. The chromite and chromite concentrate exports have totally reached over 2.7 million tons in 1995. Turkey is the second largest chromite ore producer in the world after South Africa (DPT Report 2001). In terms of chromite ore reserves, Turkey is among the leading countries such as South Africa, Zimbabwe, India, Finland and Commonwealth of Independent States (CIS)

(Gül and et al. 1995). The chromite ore reserve of Turkey is around 300 million tons which is approximately 4 % of the total world reserve (Gül and et al., 1995). The high grade ore reserve assaying 30-48 % Cr_2O_3 is around 31 million tons (Sarıiz 1997). Approximately 200 million tons of the total chromite reserve of the country is a low grade ore deposit (DPT Report 2001, Gül and et al. 1995) situated in Adana-Karsantı region with average 5 % Cr_2O_3 content. The high grade world reserves have been continuously depleted. Therefore the low grade deposits became the focus of attention due to the strategic importance of chromite (DPT Report 2001).

Gravity separation, magnetic separation and flotation are traditionally employed to get rid of the gangue minerals such as serpentine and olivine. They all depend on the liberation particle size of the ore and a saleable chromite concentrate with at least 44 % Cr_2O_3 must be obtained. However, these separation methods lead to significant amounts of fine chromite losses to tailings (Kurşun and et al. 1994, Boci and et al. 1996, Veglio and et al. 1996a, Çiçek and et al. 1998a, Veglio and Gelardi, 2000b). Positive results were reported by flotation and high intensity magnetic separation studies (Gül and et al. 1995, Güney and Önal 2000a, Güney and et al. 2001b). But, flotation of fine chromite is very difficult, costly and not applicable. Because, the gangue minerals such as olivine and serpentine show electrochemical surface properties similar to chromite (Atalay 1986). Flotation also raises environmental concerns due to use of chemical reagents. On the other hand, magnetic separation is a costly process because of expensive electrical energy. Besides, conventional gravimetric equipment such as Humphrey spirals, Reichert cones and shaking tables widely used for chromite beneficiation in Turkey are of low efficiencies below 100 μm particle sizes especially at the plants where the process conditions are not optimized and/or the liberation size of the ore is very fine. Therefore remarkably high value of fine chromite in tailings has been reported by many researchers (Kurşun and et al. 1994, Boci and et al. 1996, Veglio and et al. 1996a, Çiçek and et al. 1998a). MGS is a gravimetric concentrator and uses centrifugal forces to enhance the separation. It is very effective for the beneficiation of very fine materials and appears to be a useful equipment used successfully for upgrading fine cassiterite (Chan and et al. 1991a). It was also used for scavenging of precious metals or valuable minerals from fine tailings and for pre-concentrating heavy mineral sands, coal, etc. (Chan and et al. 1991a, Özdağ and et al. 1994). A number of promising research work have been carried out to study the recovery of chromite fines from chromite beneficiation plants by MGS (Çiçek and et al. 1998a, Güney and Önal 2000a, Özdağ and et al. 1994, Uçbaş and Özdağ 1994, Chan and et al. 1991b, Chan and et al. 1992c, Belardi and et al. 1995, Çiçek and et al. 2000b, Bayat and et al. 1999, Çiçek and Cöcen 2002c, Çiçek et al. 2008d). But they only tackled

the problem pertaining to fine chromite reporting to tailings. Research was also conducted on the recovery of chromite from high grade Turkish chromite ores (Gence 1999). But the investigations on low grade ores which are the biggest part of the total indigenous reserves are only a few. They used rather expensive, difficult and environmentally unfriendly methods mentioned earlier (Gül and et al. 1995).

In this laboratory research work, the applicability of Mozley MGS in combination with shaking table to concentrate a low grade Turkish chromite ore with remarkably high reserves was investigated. The main purpose of the study was to develop a technically feasible beneficiation procedure. The most important aims of the process to be developed were as follows:

- To obtain a chromite concentrate with at least 60 % Cr_2O_3 recovery.
- To obtain a marketable concentrate with at least 44 % Cr_2O_3 content.
- To ensure a positive contribution to the environment by adopting an environmentally friendly beneficiation procedure.

2 EXPERIMENTAL WORK

2.1 Sample Preparation

50 kg of the head sample (−10 mm) representing the ore deposit was ground down to −1 mm using a laboratory rod mill in closed circuit with a 1 mm laboratory screen. A sample of −1mm material was subjected to metal-screen analysis employing 0.106, 0.212, 0.5 and 1 mm screens. The whole sample was screened with 0.1 mm screen using a laboratory/ pilot scale screen machine. The +0.1 mm fraction was used for shaking table test and the −0.1 mm fraction for MGS tests as feed. The screening results showed that 83.9 and 16.1 % of the material was in the +0.1 mm and −0.1 mm size fractions respectively.

2.2 Metal Screen Analyses of the Head Sample

The results of the metal/screen analysis of the head sample assaying 9.3 % Cr_2O_3 are given in Table 1. The wet screening procedure was adopted. The chemical analyses were carried out to determine the Cr_2O_3 content of each particle size fraction (Tab. 1).

It was found that 83.92 wt. % of the material was in the +0.106 mm size fraction containing 8 % Cr_2O_3 and 16.08 wt. % was in the −0.106 mm size fraction containing 16.12 % Cr_2O_3. The cumulative undersize and oversize curves are given in Figure 1. As seen from Table 1, there is clear chromite enrichment towards the finer particle sizes. This can be attributed to different grindability of chromite and gangue minerals.

2.3 Shaking Table Test

The shaking table test on the +0.1 mm fraction of the head sample was carried out using a laboratory size shaking table. The discharge of the table was split into 5 sectors (concentrate, middlings 1-3 and tailings) and separate samples were taken from these sectors during the test. The samples were weighted and analyzed

Table 1. Metal/screen analyses of the head sample.

Size fraction	Weight	Grade	Recovery	Cumulative undersize		Recovery	Cumulative oversize		Recovery
(mm)	(%)	Cr_2O_3 (%)	(%)	Weight (%)	Cr_2O_3 (%)	(%)	Weight (%)	Cr_2O_3 (%)	(%)
−1+0.5	40.32	3.94	17.08	100.00	9.30	100.00	40.32	3.94	17.08
−0.5+0.212	26.67	7.33	21.02	59.68	12.92	82.92	66.99	5.29	38.10
−0.212+0.106	16.93	18.70	34.04	33.01	17.44	61.90	83.92	8.00	72.14
−0.106	16.08	16.12	27.86	16.08	16.12	27.86	100.00	9.30	100.00
Total	100.00	9.30	100.00						

to establish the upgrading performance of the table. The test conditions were as follows:

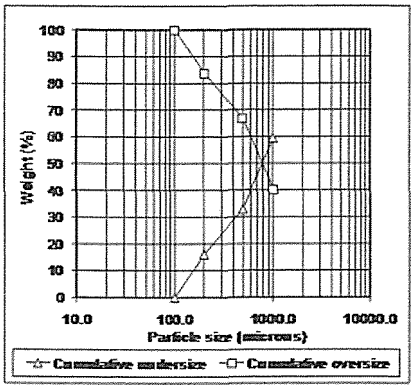

Figure1. The graphical representation of the metal/screen analysis.

Table type: Wilfley lab. Scale; Size: 1270 x480 mm; Stroke: 10 mm;
Tilt angle: 2 degrees; Water: 13 l/min; Speed: 450 rpm; Feed rate: 60 kg/h.

2.4 MGS tests

2.4.1 *Multi Gravity Separator*

A laboratory/pilot size Mozley Multi Gravity Separator (MGS) of type C900 (Figure 2) with a nominal capacity of 150 kg/h was used for the tests. The MGS had an open ended conical drum 500 mm in diameter and 600 mm in length. The drum rapidly rotated in a clockwise direction between 100-280 rpm and was shaken sinusoidally in the axial direction. The scraper assembly of the drum rotated in the same direction but at a slightly higher speed. The feed in slurry form was introduced continuously onto the internal surface of the drum via a perforated ring. Wash water was added via a similar ring positioned near the open end of the drum. The drum could be tilted between 0-8 degrees. During operation the dense particles migrated by means of the high centrifugal forces and the sheering effect of the sinusoidal shakes against the wall of the drum forming a semi solid layer. The scrapers conveyed this dense layer towards the concentrate launder located at the open end of the drum. The light particles were carried by the flow of wash water into the tailing launder at the rear end of the drum. The parameters affecting the separation efficiency of the MGS are the drum speed (100-280 rpm), drum slope (0-8 degrees), shaking amplitude (10-15-20 mm), shaking frequency (4-4.8-5.7 cycles/second), the amount of washwater (0 -10 liters per minute) and feed pulp density (10-50 % solids by weight) (Çiçek and et al. 1998a, Chan and et al. 1991a).

2.4.2. *Test procedure and experimental conditions*

The operation of MGS is very simple because all operational parameters can be adjusted precisely and no middlings are taken. The MGS feed was prepared by mixing the solid material (25 % solid ratio) with water in a container. The pulp was agitated very slowly to prevent the solid particles from further breakage. The pulp was fed with the aid of a peristaltic pump into the MGS drum with constant feeding rate of 3 l/min. 1 minute after the beginning of the concentrate output, the small quantities were taken from the concentrate and tailings launder in 10 seconds intervals until the end of the test. They were mixed together to form the base for the final samples. These samples were analyzed for their Cr_2O_3 content. The experimental conditions of MGS tests are given in Table 2.

3 EXPERIMENTAL RESULTS AND DISCUSSIONS

3.1 Results of shaking table test

The results of the shaking table test are summarized in Table 3. The Cr_2O_3

grade of the concentrate produced from +0.1 mm feed by the shaking table test was 45.03 % with 3.13 % wt. (2.63 wt. % based on the head sample). The Cr_2O_3 grade is sufficient for a saleable product, but 17.7 % Cr_2O_3 recovery is low. However, if the concentrate and the middling 1 are combined, a concentrate with 40.31 % Cr_2O_3 and 33 % Cr_2O_3 recovery can be obtained. The middling 2 with 24.19 % Cr_2O_3 content which is quite high was dried and ground down to −0.1 mm by a vibrating ball mill in a closed circuit with a 0.1 mm screen. The ground middling 2 and the −0.1 mm fraction of the head sample was combined to be used as MGS feed. The middling 3 and the tailings were combined to make up the final tailings of tabling stage due to their low Cr_2O_3 contents.

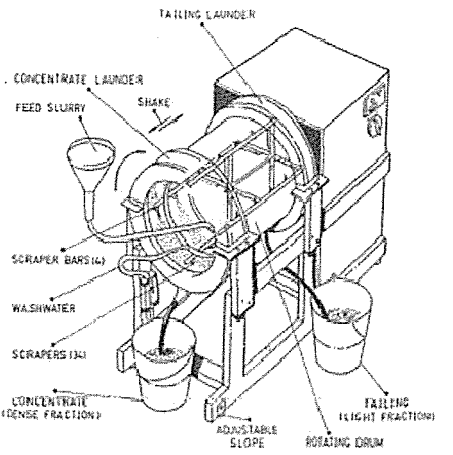

Figure 2. Mozley Multi Gravity separator (MGS).

3.2 The results of MGS tests

The ground middling 2 from the shaking

Table 2. The experimental conditions of MGS tests.

Drum slope	6^0
Drum speed	150, 155, 160, 170, 180, 190 rpm
Amount of wash water	5 l/min
Solid/liquid ratio	25 % solid
Flow rate of feed	3 l/min,
Particle size fraction of feed	100 % under −0.1mm
Shaking frequency	4.4 cycle/sec
Shaking amplitude	15 mm

Table 3. The results of shaking table test.

Products	Weight based on + 0.1 mm feed (%)	Weight based on head sample (%)	Grade Cr_2O_3 (%)	Cr_2O_3 recovery (%)
Concentrate	3.13	2.63	45.03	17.7
Middling 1	3.40	2.85	35.95	15.3
Concentrate+Middling 1	6.53	5.48	40.31	33.0
Middling 2	10.03	8.42	24.19	30.4
Middling 3	13.23	11.10	5.63	9.3
Tailings	70.21	58.92	3.09	27.2
Middling 3 + Tailings	83.44	70.02	3.49	36.5
Total	100.00	83.92	7.97	100.0

table tests containing 24.19 % Cr_2O_3 with 10.03 wt. % (8.4 wt. % based on the head sample) and the −0.1 mm fraction of the head sample with 16.1 wt. % based on the head sample were combined to make up the feed for MGS. The MGS feed contained 18.8 % Cr_2O_3 with 24.5 wt. %. As seen from the results of MGS tests (Tab. 4, Fig. 3), the highest chromite grade (55.00 %) was obtained at the drum speed of 150 rpm with the lowest (70.2 %) Cr_2O_3 recovery among the MGS tests. A concentrate containing 50.4 % Cr_2O_3 with 84.7% Cr_2O_3 recovery was possible by employing a drum speed of 155 rpm. At 160 rpm, despite the high Cr_2O_3 recovery (90.9 %), the concentrate grade was lower (43.46 %) than those at 150 and 155 rpm. At 170 rpm, the highest Cr_2O_3 recovery was obtained.

The optimum operation parameters determined for the concentration of low grade Adana-Karsantı chromite ore by MGS can be given as follows:

Tilt angle (Drum slope): 6 ^{0}
Shaking frequency: 4.4 cycle/sec
Shaking amplitude: 15 mm
Washwater flowrate: 5 l/min
Drum speed: 155 rpm

As seen from Figure 4 showing the laboratory test results given on a mass/metal balance flowsheet, the combination of the shaking table and the MGS concentrate made up a total concentrate containing 46.22 % Cr_2O_3 with 13.3 % wt. and 66.1 % total Cr_2O_3 recovery. The total tailings which is the sum of the tailings from the shaking table and the MGS was 86.7 wt. % of the head sample. The Cr_2O_3 content of the total tailings was 3.6 % Cr_2O_3. In the light of the experimental data gathered, the flowsheet proposed for the enrichment plant is given in Figure 5.

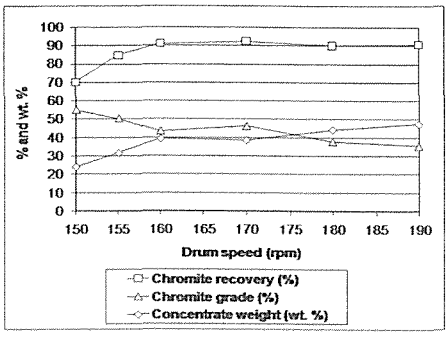

Figure 3. The graphical representation of MGS test results.

Table 4. The results of MGS test

Test no.	Drum speed (rpm)	Feed Cr_2O_3 (%)	Concentrate Cr_2O_3 (%)	Tailings Cr_2O_3 (%)	Concentrate Weight (%)	Tailings Weight (%)	Cr_2O_3 recovery (%)
1	150	18.84	55.00	7.39	24.04	75.96	70.2
2	155	18.80	50.40	4.20	31.60	16.70	84.7
3	160	18.82	43.46	2.82	39.37	65.34	90.9
4	170	19.30	46.11	2.46	38.57	61.43	92.2
5	180	18.61	37.81	3.39	44.23	55.77	89.8
6	190	18.56	35.44	3.31	47.45	52.55	90.6

4. CONCLUSIONS

In this laboratory research work, the feasibility of the beneficiation of a low grade chromite ore from Adana-Karsantı region of Turkey by the combination of shaking table and MGS was investigated. The results were as follows:

- A chromite concentrate with 46.2 % Cr_2O_3 grade and 66.1 % Cr_2O_3 recovery was obtained from the ore containing 9.3 % Cr_2O_3 by the combination of shaking table and MGS.
- The results of the shaking table test were not satisfactory due to the low recoveries that might arise from the gangue minerals such as olivine with high specific gravity and insufficient particle liberation.
- It was clearly seen that MGS was ideal beneficiation equipment for a low grade chromite ore. A high quality concentrate containing 50.4 % Cr_2O_3 was obtained at remarkably high chromite recovery of 84.7 %.
- On the basis of the experimental results, a principal flowsheet for the enrichment plant was proposed. According to the flowsheet, the plant that will process a low grade Cr_2O_3 ore with a capacity of 1 million tons/ year will produce 133 000 tons of chromite concentrate annually.

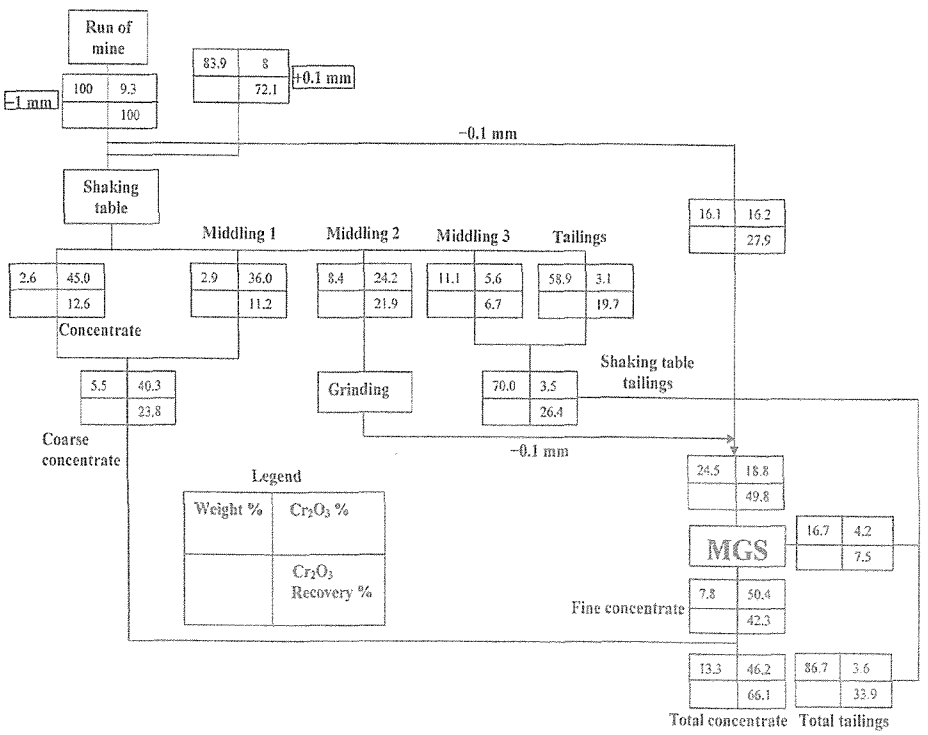

Figure 4. The mass/metal balance of the laboratory tests.

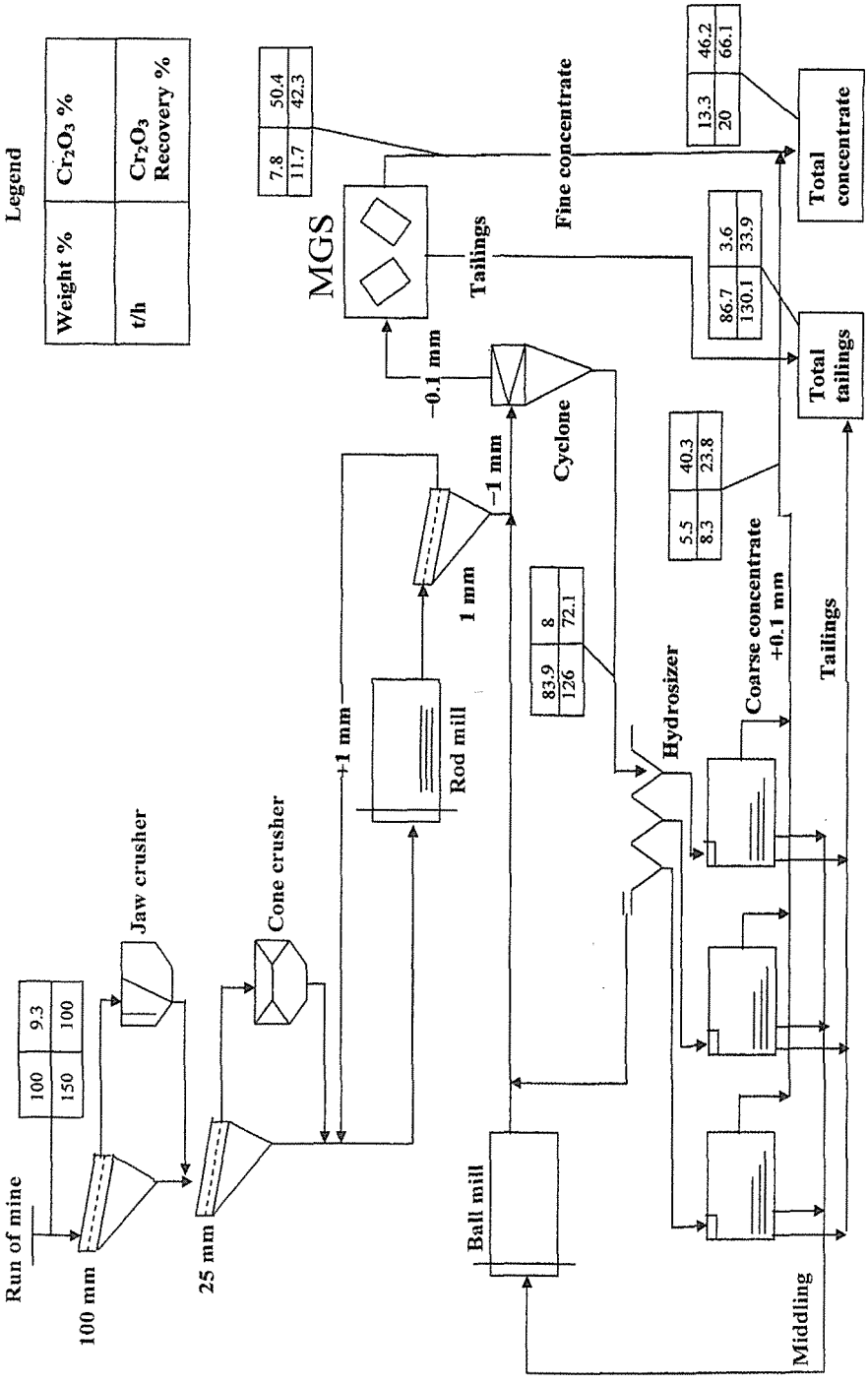

Figure 5. The proposed flowsheet of the chromite concentrator.

REFERENCES

Atalay, U., 1986. Surface Properties of Chromite and Concentration of Chromite Gravity Tailings, *PhD thesis*, Middle East Technical University, Ankara, Turkey.

Bayat, O., Cöcen, I., Çiçek, T., Özsever, V., Vapur, H. and Inan, S., 14-18 September 1999. Concentration of Aladağ-Adana chromite tailings by gravitational methods, *Proc. 8th Balkan Mineral Processing Conf.*, Herceg Novi, Yugoslavia.

Belardi, G., Sheau, N., Plescia, P. and Veglio, F., 1995. Recent developments in gravity treatment of chromite fines, *Minerals and Metallurgical Processing Journal*, pp.161-165.

Boci, S., Kondi, O., Demi, G. and Mati, S., 24-26 September 1996. Recycle of tailing of the chromium dressing plant of Bulgiza, *Proc. 6th Int. Mineral Processing Symp., Changing Scopes in Mineral Processing,* pp.107-110, Kuşadası, Turkey.

Chan,S. K., Mozley, R. H. and Childs, G. J.C., 1991 a. The Multi-Gravity Seperator (MGS)-A Mine Scale Machine', Richard Mozley Limited, *Private Report*, Redruth, Cornwall, UK.

Chan, B.S., Mozley, R.H. and Childs, G.J.C, 1991b. Extended trials with the high tonnage multi-gravity separator technology, *Minerals Engineering*, 4, pp.489-496.

Chan, B.S., Mozley, R.H., Childs, G.J.C. and Tucher, P., 1992c. Modelling the multi-gravity separator', Ind. Miner. Techniques, (*Proc. XVII Int. Mineral Processing Conf.*, Dresden, Germany,
Vol. III, Fine particle processing), 74 (5/92), pp.45-49.

Çiçek, T., Cöcen, I.and Samanli, S., 15-17 September 1998a. Gravimetric concentration of fine chromite tailings, *Proc. Int. 7th Mineral processing Symp., Innovations in Mineral and Coal Processing,* pp.731-736, İstanbul, Turkey.

Çiçek, T., Cöcen, I. and Birlik, M., 16-18 October 2000b. Applicability of Multi Gravity Separation to Kop Chromite Concentration Plant, *Proc. 8th Int. Mineral Processing Symp., Mineral Processing on the Verge of the 21st Century*, pp.87-92, Antalya, Turkey.

Çiçek, T. and Cöcen, I., 2002c. Applicability of Mozley multi gravity separator (MGS) to fine chromite tailings of Turkish chromite concentrating plants, *Minerals Engineering*, 15, pp.91-93.

Çiçek,T., Cöcen, İ., Engin, V. T., Cengizler, H. and Şen, S., 2008d. Technical and economical applicability study of centrifugal force gravity separator (MGS) to KEF chromite concentration plant, *Mineral Processing and Extractive Metallurgy* (TIMM C), 117, 4, pp.248-255(8).

DPT Report, 2001. '8th five year development plan', Report of private specialty commission of mining, *Metallic minerals subcommittee, Report of chromite group*, Report DPT 2626, ÖİK 637, Ankara, Turkey, 2001 (in Turkish).

Gence, N., 1999. Beneficiation of Elazığ-Kefdağ chromite by multi-gravity separator, *Turkish Journal of Engineering and Environmental Science*, 23, pp.473-475.

Gül, A., Yüce, A. E., Güney, A., Gürkan, V., Arslan, F. and Önal, G., 6-9 June, 1995. Beneficiation of low grade chromite ores from Adana-Karsantı region, *14th Mining Congress of Turkey*, pp.419-424, Ankara, Turkey.

Güney A. and Önal, G., '16-18 October

2000a. Application of a new beneficiation method to ultrafine-size chromite, *Proc. 8th Int. Mineral Processing Symp., Mineral Processing on the Verge of the 21st Century*, pp.299-303, Antalya, Turkey.

Güney, A., Önal, G. and Atmaca, T., 2001b. New aspect of chromite gravity tailings reprocessing, *Minerals Engineering*, 14, pp.1527-1530.

Kurşun, H., Canbazoğlu, M., Aydoğan, S. and Cebeci, Y., 6-8 September 1994. Beneficiation studies of Karanlıkdere chromite ore, *Proc. 5th Int. Mineral Processing Symp.*, pp.77-80, Cappadocia, Turkey.

Özdağ, H., Ucbas, Y. and Koca, S., 6-8 June 1994. Recovery of chromite from slime and table tailings by Multi-Gravity Separator, *Int. Conf. on 'Innovations in mineral processing'*, pp.267-278, Sudbury, Ontario, Canada.

Sarıiz, K., 1997. The potential of Mineral Resources of Turkey, *Metal Mine, İMMİB Export Journal*, 7, pp.39-40 (in Turkish).

Uçbas, Y. and Özdağ, H., 6-8 September 1994. Relationships between shake frequency and amplitude in the concentration of chromite fines by multi-gravity separator, *Proc. 5th Int. Mineral Processing Symp., Progress in Mineral Processing Technology*, pp.71-76, Cappadocia, Turkey.

Veglio, F., Forlano, P., Belardi G. and Sheau, N., 24-26 September 1996a. Factorial experiments and principal component analysis in the optimization study of a multi-gravity separator, *Proc. 6th Int. Mineral Processing Symp., Changing Scopes in Mineral Processing*, pp.91-96, Kuşadası, Turkey.

Veglio, F. and Gelardi, G., 2000b. Multivariate analysis supporting factorial experiments: A case study in the physical separation of chromite fines by a multi-gravity separator, *Separation Science and Technology*, 35, pp.109-132.

Use of Natural Sorbents to Purify Stratal Water

N.Jalgasuly, A.S.Tyshkanbaeva, B.N.Djubaniyazov, B.G.Almatova, B.Burkhanov
Mining Institute after D.A.Kunaeva, Almaty, the Republic of Kazakhstan

ABSTRACT The results of studies on rehabilitation of stratal water after underground borehole metal leaching with the use of natural sorbents are given.

1 INTRODUCTION

During the man-caused impact of various types on the stratal water as a result of physical and chemical interaction in it a complex anionic and cationic content is formed, a concentration of heavy metals and other harmful substances far exceeds the maximum permissible concentrations for water used for drinking and household consumption. A significant quantity of sulfates, chlorides, iron, aluminium bicarbonates, nitrates, radioactive nuclides other trace elements is accumulated. Ingress of hazardous elements in potable water can result in serious environmental consequences.

In the course of the man-caused chemical impact the natural epigene geochemical zoning is disturbed and new contrast oxidation-reduction barriers are formed. Its limits become the boundaries of man-caused impact. At these barriers the elements of the zone are settled passed to the solute state (Grabovnikov V. A. & Rubeikin V. Z., 1977).

In this same zone of reduction of pH value due to the settled solute elements with the prevailing iron and aluminium hydroxides, a so-called mudding barrier is formed. At this barrier the filtration capacity of water-bearing stratum is reduced due to the decrease of porous space.

The worsening of filtration properties as a result of a set of above-mentioned barriers results in the fact that the natural filtration flow with very slow speed of movement can't destroy the formed closed circuit and flows around the enclosed lens of man-caused solutions along the edges not moving it toward the proper direction.

Restoration of underground water is one of the main and essential tasks. This issue is especially vital when water-bearing stratum serves as a source of potable water.

For instance the industrial experience of the underground borehole metal leaching shows that natural restoration of stratal water is possible.

At that the reduction of mineralization of residual solutions is a result of hydraulic depression, molecular diffusion, physical and chemical reactions with adjoining rocks as well as mechanical sorption and simple ion exchange. However the practice shows

that natural demineralization of stratal water is very slow. To reach the complete restoration of original parameters 15-20 years are needed.

When the underground water needs to be restored in short time artificial methods of treatment should be used which in their turn can be divided into two groups.

The first groups stipulates the extraction of residual solutions from the groun and its purification from the harmful substances on land. At that the whole range of chemical methods is applied – sorption with ion exchange resins, extraction, electrodialysis, floatation and freezing, concentration with evaporation and many others. These methods are very expensive, and the recovery of individual valuable elements doesn't compensate all the costs. At that much volume of non-recovered harmful substances is accumulated on the surface (Smirnov A. D., 1982).

The second group of methods is directed at the neutralization of solutions directly underground. The following techniques are used: displacement of residual solutions with compressed air to the adjoining rocks and *in situ* electrochemical methods of purification; neutralization of solutions with soda at the place of deposition; reduction of metals with the solutions of sodium sulfate; microbiological methods of purification by means of implementation of natural microflora to the ore-bearing strata; pumping of residual solutions to the underlying strata with high neutralizing and reduction capacity of lithologic environment etc. Unfortunately, all these techniques are difficult to implement and require many expenses.

One of the methods of restoration of stratal water is the use of various sorbents. Natural minerals and rocks can sorb chemical compounds and metals (Tarasevich Yu. I., 1989).

2 DESCRIPTION OF THE METHOD

We have considered the opportunity to purify the residual solutions after the man-caused chemical impact on the stratal water by means of introduction of sorbents directly to the water-bearing strata.

The brown coal, schungite containing silica-alumina slates and bentonitic clay were used for research. Brown coal was used in natural form as well as the one exposed to pyrolysis (baking without oxygen access during 1 hour at the temperature 600-650^{0}C) to get rid of volatile substances and sulfur.

The studies was made on model solutions containing iron sulfate, copper sulfate and zinc sulfate.

The solutions (mg/cm^3) with different concentration of elements were prepared.

Solution (mg/cm^3) № 1: Fe - 250; Cu - 250; Zn - 250; ΣSO_4 - 2124.

Solution (mg/cm^3) № 2: Fe - 1000; Cu - 1000; Zn - 1000; ΣSO_4 - 8500.

The experiments were held in two stages. At the first stage the model solution with the concentration of 250 mg/cm^3 was used, at the second – the solution with the concentration of 1000 mg/cm^3.

The experiments were held in static conditions and the environmental temperature at that was in the limits of 25–30^{o}C, since such conditions can be observed in industry.

The relation of T:J during the experiments is assumed to be 1:2.

The time of sorption during the experiments was 3, 6, 12, 18 and 24 hours. The solution with sorbent was

mixed from time to time.

After this period the liquid phase was filtered under vacuum and its chemical analysis was made.

According to the results of the experiment the extent of solution purification from every element and the sorption capacity for various solution elements and total sorption capacity were identified.

The extent of purification was calculated with the formula:

$$\varepsilon = \frac{\alpha^i_{orig} - \alpha^i_{fin}}{\alpha^i_{orig}} \cdot 100,\% \qquad (1)$$

where a^i_{orig} - original concentration of i element in the solution, mg/cm³;

a^i_{fin} - final concentration of i element in the solution, mg/cm³.

Sorption capacity was calculated as follows:

$$N = \frac{(\alpha^i_{orig} - \alpha^i_{fin}) \cdot V}{Q}, \text{ cm}^3 \qquad (2)$$

where V - volume of the solution, cm³;

Q - weight of the sorbent, g.

The results of the experiments at the concentrations of heavy metals in the 250 mg/cm³ solution, relation T:J = 1:2 are shown in the table 1.

According to the tab. 1, iron, copper and zinc at the concentration of 250 mg/cm³ and relation of T:J = 1:2 are almost completely sorbed from the solution with the brown coal exposed to pyrolysis and bentonitic clay. Brown coal in natural form sorbs metals a little bit worse. The least figures of metal sorbtion from the solution were in case of sorbtion with shungite-containing silica-alumina slates. This can be explained with low content of shungite in the mineral rock which is as well known from the literature has good sorption properties (carbon content in the rock is only 5–8 %).

Table 1. Change of concentrations of ions in the solution depending on the time of sorption at the concentration of metals in the solution of 250 mg/cm³.

Type of sorbent, relation, T:J	Time of sorption, h	Content of ions in solution (mg/cm³)			
		Fe	Cu	Zn	Σ SO_4
Natural brown coal, 1:2	0	250,0	250,0	250,0	2124
	3	24,6	21,5	20,0	2760
	6	15,2	17,9	18,9	2850
	12	12,7	17,5	18,1	2775
	18	11,8	16,8	17,9	2682
	24	10,0	16,7	17,6	2555
Pyrolized brown coal, 1:2	0	250,0	250,0	250,0	2124
	3	<0,01	<0,01	<0,01	851
	6	<0,01	<0,01	<0,01	753
	12	<0,01	<0,01	<0,01	730
	18	<0,01	<0,01	<0,01	715
	24	<0,01	<0,01	<0,01	702
Shungitecontaining silica-alumina slates, 1:2	0	250,0	250,0	250,0	2124
	3	124,0	124,0	150,0	1379
	6	123,5	123,5	170,0	1285
	12	135,0	162,0	162,0	1340
	18	142,0	140,0	177,0	1380
	24	151,0	151,0	182,0	1406
Bentonitic clay, 1:2	0	250,0	250,0	250,0	2124
	3	<0,01	<0,01	<0,01	755
	6	<0,01	<0,01	<0,01	720
	12	<0,01	<0,01	<0,01	710
	18	<0,01	<0,01	<0,01	665
	24	<0,01	<0,01	<0,01	625

Sulfate ion is well sorbed with brown coal exposed to pyrolysis and with shungite-containing silica-alumina slates. At the sorption with natural brown coal in opposite the increase of concentration of sulfate-ion in the solution is observed initially. This can be possibly explained by the fact that brown coal contains readily soluble sulfates which transfer to solution. It is evident that right after the readily soluble sulfur compounds transfer to solution, the sulfate-ion sorption with coal released from the containing sulfur starts.

At the pyrolysis of brown coal the sulfur is removed along with the other volatile substances.

Since the first series of experiments show that sorption productivity with

shungite-containing silica-alumina slates is low, and natural brown coal doesn't rid the solution of the sulfate ion, the second stage of the experiments was made only with brown coal exposed to pyrolysis and with bentonitic clay.

The results of the experiments at the metal concentrations in the solution of 1000 mg/cm^3 are shown in the table 2.

Table 2. Change of concentrations of ions in the solution depending on the time of sorption at the concentration of metals in the solution of 1000 mg/cm^3.

Type of sorbent, relation, T:J	Time of sorption, h	Content of ions in solution, mg/cm^3 Fe	Cu	Zn	Σ SO_4
Pyrolized brown coal, 1:2	0	1000,0	1000,0	1000	8500
	3	185,18	106,5	750	5900
	6	120,61	42,0	515	5660
	12	106,32	32,1	465	5649
	18	94,05	22,4	405	5638
	24	80,41	11,5	340	5630
Bentonitic clay, 1:2	0	1000,0	1000,0	1000	8500
	3	330,00	375,0	410	5637
	6	310,00	345,0	380	5495
	12	300,00	330,0	352	5440
	18	295,00	315,0	343	5385
	24	290,00	306,0	328	5331

As it is seen from the charts brown coal exposed to pyrolysis and bent onitic clay well absorb either the metals either the sulfat-ion even at such metal concentrations in the solution.

The efficiency of water purification with natural sorbents depends on its sorption capacity.

The characteristics of the sorption capacity of brown coal exposed to pyrolysis and of bentonitic clay are shown in the charts of Figure 1 and

Figure 2

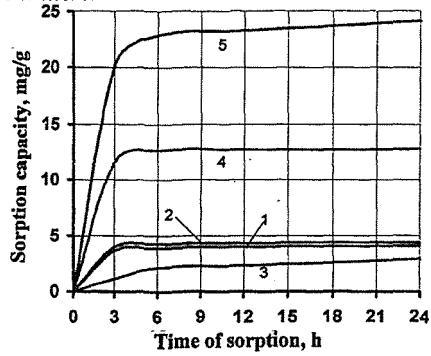

1- iron; 2 - copper; 3 - zinc; 4 - sulfate-ion; 5 - total sorption capacity.

Figure 1. Influence of time of sorption on sorption capacity of brown coal exposed to pyrolysis at the metal concentration in solutions of 1000 mg/cm^3.

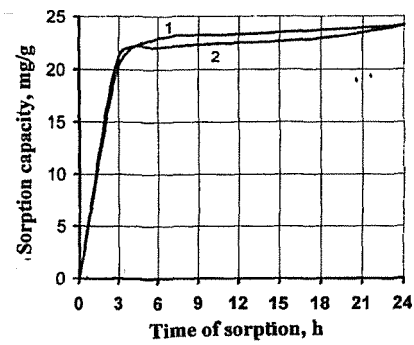

1 - iron; 2 - copper; 3 - zinc; 4 - sulfate-ion; 5 - total sorption capacity.

Figure 2. Influence of time of sorption on sorption capacity of bentonitic clay at the metal concentration in solutions of 1000 mg/cm^3.

Comparative total sorption capacity of pyrolized brown coal and bentonitic clay depending on the sorption time is shown in the charts of Figure 3.

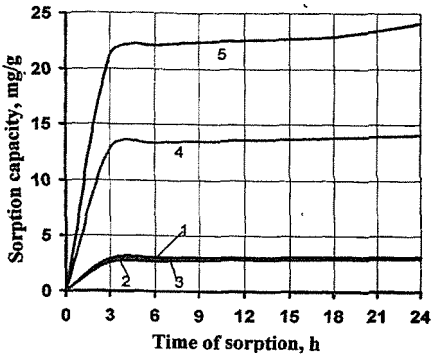

1 - brown coal exposed to pyrolysis;
2 - bentonitic clay.

Figure 3. Influence of time of sorption on total sorption capacity of natural sorbents.

As it is seen from the charts the total sorption capacity of brown coal exposed to pyrolysis and of bentonitic clay is almost the same.

The results of the researches allow to conclude that natural sorbents such as brown coal exposed to pyrolysis and bentonitic clay can be used for restoration of stratal water, exposed to man-caused impact by means of its introduction directly into the water-bearing stratum. At that the natural sorbent should be dispersed till granulation allowing the particles to move forward freely along the filtration channels of the water-bearing stratum.

The essence of the restoration of the stratal water is the absorption of harmful elements containing in residual solutions with the natural sorbents and the reaching the concentration of these elements equal to the original concentration before the man-caused impact or the concentration equal to maximum permissible concentration in potable water.

Quantity of natural sorbent needed for purification of 1 liter of residual solution can be calculated as follows

$$q_{n.c.} = \frac{\Sigma C_{resid} - \Sigma C_{mpc}}{N}, \qquad (3)$$

where ΣC_{resid} - total concentration of harmful elements in residual solution, mg/l;

ΣC_{mpc} - total concentration of harmful elements according to the MPC for potable water, mg/l;

N - maximal sorption capacity of natural sorbent, mg/g.

Consider an example. Total mineralization of residual solutions after the man-caused impact reaches 30000 mg/l. Total mineralization of natural water reaches 1000 mg/l. Total permissible mineralization according to MPC for potable water is 1000 mg/l.

Thus the total amount of harmful elements which should be removed from the residual solutions reaches 29000 mg/l.

In order to absorb the harmful elements containing in residual solutions the needed amount of sorbent should be introduced into the treated block.

As it is shown above the sorption capacity for the sum of elements reaches 24,13 mg/l for bentonitic clay and 24,16 mg/l for brown coal exposed to pyrolysis.

To absorb 29000 mg of the harmful elements containing in 1 liter of residual elements it is necessary to introduce 1208,3 g of sorbent.

At the value of specific weight of the bentonitic clay equal to 2,0-2,2 the volume of sorbent per 1 l of residual solution will amount to 0,5-0,6 cm^3. Therefore 40–50 % of porous space of stratum is free for filtration of stratal water.

3 CONCLUSIONS

The use of natural sorbents introduced into the zone of distribution of residual solutions is a perspective method of restoration of residual solutions after the underground borehole leaching.

Out of the studied natural sorbents for purification of residual solutions after UBL the most applicable are brown coal exposed to pyrolysis and bentonitic clay. According to the total sorption capacity they are almost equal (24,13 - 24,16 mg/g).

REFERENCES

Grabovnikov V. A. & Rubeikin V. Z., 1977. *Formation and structure of halations of substances spreading in underground water*. Nedra, Moscou. 184 p.

Smirnov A. D., 1982. *Sorption purification of water*. Chemistry, Leningrad. 168 p.

Tarasevich Yu. I., 1989. *Natural sorbents in water purification*. Naukova Dumka, Kiev. 292 p.

Variation In Coal Surface Wettability With Carbonization Temperature And Effect Of Pitch On Coal Fluidity

Kömür Yüzey Islanabilirliğinin Karbonizasyon Sıcaklığı ile Değişimi ve Ziftin Kömür Akışkanlığı Üzerindeki Etkisi

H. Cengizler,
Celal Bayar University, TMYO, Turgutlu

M. Kemal
Dokuz Eylül University, Mining Engineering Department, İzmir

ÖZET İkili karışımlarda ziftin (Z) kömür akışkanlığına ve karbonizasyon sıcaklığının kömür yüzeyi ıslanma davranışına olan etkisi Gieseler plastometresi ile yapılan deneyler ile araştırılmıştır. İkili karışımlar Tunçbilek linyit kömürü (TK) veya koktozları ile Z'nin farklı oranlarda karışımından oluşmuştur. TK200, TK400, TK600, TK800 ve TK1000 koktozları sırasıyla 200°, 400 °, 600 °, 800 ° and 1000 °C karbonizasyon sıcaklıklarında elde edilmiştir. İkili karışımlarda maksimum akışkanlık değerlerinin artan Z oranları ile arttığı tespit edilmiştir. En düşük maksimum akışkanlık değerleri TK400+Z ikili karışımlarında elde edilmiş ve TK400'ün en iyi yüzey ıslanma özelliğine sahip koktozu olduğu saptanmıştır. Maksimum akışkanlık değerlerinin TK400, TK200, TK, TK600, TK800 and TK1000 sırasına göre arttığı ve kömür yüzeyi ıslanma özelliğinin de aynı sıraya göre azaldığı tespit edilmiştir.

ABSTRACT The effect of pitch (Z) ratio on the fluidity of coal and of carbonization temperature on the wetting behaviour of coal surface in the binary mixtures have been investigated with the experimental runs performed by the constant-torque Gieseler plastometer. The binary mixtures consisted of Tunçbilek brown coal (TK) or its semicokes and Z in different ratios. TK200, TK400, TK600, TK800 and TK1000 semicokes were obtained at 200°, 400 °, 600 °, 800 ° and 1000 °C carbonization temperatures respectively. It was found that the maximum fluidity values of the binary mixtures increases with increasing Z ratios. The lowest maximum fluidity values were obtained in TK400+Z binary mixture and it was shown that TK400 is the semicoke which has the optimum surface wetting behaviour. It was determined that the maximum fluidity values increase in the order of TK400, TK200, TK, TK600, TK800 and TK1000. The surface wettability also decreases in the same order.

1 INTRODUCTION

The bituminous coals begin to soften and become fluid, when heated between 350-500 °C in an oxygen free atmosphere, known as the plastic behaviour of coal. The reason is the thermal decomposition of coal producing bituminous matters and their accumulation (Vankrevelen 1981). During the plastic stage, dense gas evolution occurs, plastic coal particles swell and the development of a stickiness or tackiness enables them to cohere or to adhere to inert particles. Therefore, when a coking coal is pulverized and heated in an oxygen free atmosphere, the coal particles begin to soften and the evolution of gas that may escape readily or may be effectively trapped in a tough and viscous mass (Elliot and Yohe 1981) leads to considerable swelling and formation of gas bubbles forcing the particles to adhere each other as temperature increases. Subsequently, the boundary among the coal particles vanish and a porous, carbon-rich firm solid coke mass is formed. As higher temperatures such as 950-1000 °C are attained, this solid mass of coke contracts and strengthens and settles as metallurgical coke consisting of strong and large pieces. In general, the development of a plastic state is limited to the bituminous coals of higher rank (Elliot and Yohe 1981), because at the plasticity range (350-500 °C) of the coals with high (dry ash free and with >40% volatile matter) and low (dry ash free and with<18% volatile matter) volatile matter, no coal tar accumulation occurs. Therefore, lignites and the high-rank anthracites, if pulverized and heated, remain as powders throughout the range of pyrolysis and gas evolution and these coals are not suitable for coke making.

To use non-coking coals in coke making, their particles must be firmly united by coking coal in the blend. In other words, the plastic and fluid mass formed by the softening bituminous coal must spread and adhere onto the inert coal or semicoke particles so as to hold them together firmly. Therefore, the surface of the non-coking coal particles and the plastic mass must have a specific wetting property and plasticity respectively. The agglomeration providing a strong bond among the coal particles is guided by these two factors.

In the production of metallurgical coke, it is known that the fluidity of a mixture increases when poorly coking or non-coking coals are mixed with Z. Z provides with the plasticity of the blend over a wide temperature range and the coke formation (Wilkinson 1960). Z also improves the coking and plasticity properties of coal blends and the wetting properties of the surface of non-softening inert particles, thus easing their binding and agglomeration. Furthermore, Z penetrates into the porous structure of the coal, delays the thermal decomposition of the blend's components, widens the plasticity range and ensures the re-arrangement of the micro structure (Bujnowska et al. 1994). Z also improves the coal blend's fluidity, reduces the sharpness of the interface between textural components of the resultant coke, increases the anisotropic carbon content and therefore ensures the formation of homogeneous, optically anisotropic coke structure with high mechanical strength (Bujnowska et al. 1994, Lin and Hong 1986, Maroto-Valer et al. 1998).

To study the variation in the surface wetting properties of poorly coking and non-coking coals and their semicokes, which are used in the production of coke, with the carbonization temperature; a number of studies have been carried out

with the Rhein region (Germany) brown coal or its semicokes + coking coal blends. The results revealed that, despite obtaining strong coke with semicokes of Rhein region brown coal carbonized at 500-600 °C, the cokes produced with the original Rhein region brown coal and its semicokes carbonized at 800-900 °C were not strong enough. The reason put forward was the oxidation of the coking coal affecting its fluidity adversely due to the water vapour driven off the brown coal's micro structure and the porous structure of the semicokes of the Rhein region brown coal carbonized at 800-900 °C absorbing the plastic mass and thus preventing the wetting of the inert particles' surfaces (Kemal 1974). In another work, the effect of carbonization temperature on the wetting behaviour of a lignite coal was studied and small differences were observed in the magnitudes of the contact angles of semicokes carbonized at the temperatures up to 900 °C and a sharp decrease was observed in the surface wettability of their semi-cokes carbonized above 900 °C. It was also put forward that the tendency of these semi-cokes to absorb Z in liquid and gas phase improves above 900 °C (Kemal 1989).

TK is a subbituminous hard brown coal and limited number of research work have been done on its utilization in selected ratios with coking coal for producing coke and some encouraging results were achieved employing different procedures (Kemal 1980). However, the two important factors enabling the utilization of poorly coking and non-coking coals in the production of coke have not yet been investigated. These factors are the effect of Z on the fluidity of a mixture and the variation in the surface wetting behaviour of TK with carbonization temperature. Therefore, this research work was carried out to fill in those gaps mentioned above.

2 EXPERIMENTAL

2.1 Sample Preparation

The air-dried Tunçbilek hard brown coal (TK), Zonguldak coking coal (ZK) and the coal tar pitch (Z) were used in the experimental work. The TK head sample received in large pieces and was primarily crushed down to 20-30 mm with a laboratory jaw crusher and was divided into seven individual samples each weighing 1 kg. One of them was crushed under 5 mm with a laboratory hammer mill and screened with a 0.425 mm screen in a closed circuit. This sample was denoted as the original TK. The ZK sample weighing 1 kg was also crushed through the same procedure.

The other five TK samples were carbonized at the temperatures of 200, 400, 600, 800, 1000 °C and the semicokes obtained were denoted as TK200, TK400, TK600, TK800, TK1000 respectively. The carbonization process adopted for each temperature was as follows: The coal sample was smoothly put into a steel box covered with a lid to prevent the air to get in. The box was then placed in a laboratory muffle furnace set to the selected temperature and heated. The dwelling time was four hours to ensure pyrolysis. After the furnace was cooled down, the carbonized coal sample (semicoke) was removed from the furnace. It was crushed and screened under 0.425 mm with the same procedure followed for the TK and ZK samples.

The cumulative undersize (CU) distributions of the samples used in the experimental runs are given in Table 1.

The Z was obtained from the coal tar pitch and its softening point is 70 °C. The solid Z sample primarily crushed with a small laboratory jaw crusher down to 1-2

Table 1. The cumulative undersize (C.U.) distribution of the samples used in the experimental runs.

Particle size	C.U. (%)						
(mm)	TK	TK200	TK400	TK600	TK800	TK1000	ZK
0.425-0.315	100.00	100.00	100.00	100.00	100.00	100.00	100.00
0.315-0.200	80.39	85.32	93.06	87.54	79.96	80.91	93.13
0.200-0.100	56.78	67.95	72.17	63.36	51.85	56.42	70.85
0.100-0.075	28.93	38.62	58.76	39.22	34.31	29.09	54.84
0.075-0.053	13.10	15.82	29.68	11.25	14.80	3.27	26.30
0.053-0.000	1.71	2.94	3.80	0.05	0.13	0.05	0.57

Table 2. The chemical analysis data of the samples used in the experimental runs.

	TK	TK200	TK400	TK600	TK800	TK1000	ZK
Moisture (%)	7.4	7.2	4.3	4.0	3.9	3.8	1.1
[a]Ash (%)	8.6	9.7	11.5	13.5	15.6	18.3	9.0
[b]Volatile matter (%)	46.1	44.9	30.9	15.2	5.2	1.4	32.5

[a]m.f. (moisture free)
[b]d.a.f. (dry ash free)

mm was ground with a pestle and mortar and screened with a 0.100 mm screen. The Z was added to the coal or semicoke samples in selected quantities during the experimental runs.

The ash, volatile matter and hygroscopic moisture analysis of the coal and semicoke samples are given in Table 2. The determination of the total moisture was performed according to the TS 690 (compatible Turkish standard with ISO). The determinations of the ash contents were performed according to the TS 330 and TS 1042 (compatible Turkish standards with ISO) and the volatile matter according to the TS 711 (compatible Turkish standard with ISO).

2.2 Experimental Procedure

The fluidity values of the binary mixtures consisting of Z and TK or its semicokes carbonized at different temperatures were measured by a constant-torque Gieseler plastometer according to the ASTM D-2639-74. Because an increase in the amount of Z spreading onto the coal surface would indicate an increase in the surface wettability and therefore lead to a decrease in the maximum fluidity values; the variation in the surface wettability was studied as a function of the variation in the maximum fluidity values.

The plastometer experiments were divided into two groups. Firstly, the effect of Z to the fluidity of the binary mixtures of TK or its semicokes + Z and ZK + Z was investigated. Secondly, the effect of carbonization temperature on the fluidity of the binary mixtures of TK or its semicokes + Z was studied.

In the experiments; 0.5, 1.5, 2.0, 2.5, 3.0, 3.5, 4.0, and 4.5 % Z additions were

tested for each sample, but it was not possible to measure the fluidity. Because the circular drum dial of the plastometer did not turn or turned too fast to read the fluidity in minute intervals. In both cases, it was impossible to take correct readings due to the insufficient Z ratio. In the first case, the circular drum dial remained stationary due to the particles in different geometry forced into a compact order when they were pressed tightly by the loading device. In other words, for some of the samples, the voids among the particles or under the rabble arms of the stirrer were more compacted than those of the other samples leading to a locked compact packing order. Such a tight packing and the friction among the particles created an opposite force against the torque applied to the rabble arms of the steel stirrer and this force cannot be related to the fluidity or the viscosity of the mixture. In the second case, the circular drum dial moved too fast to take correct readings immediately after a stationary position due to the insufficient Z ratios. Therefore, it was decided that the Z ratios up to 4.5 % could not reach a minimum critical amount to wet the surface of the coal particles and thus create a sufficiently viscous mass to apply an opposite force against the torque applied to the rabble arms of the steel stirrer.

Subsequently, the increased Z ratios of 5, 10, 15, 20, 25, and 30 % were tested. For some experiments, it was possible to take readings with 5 % Z content. However, a maximum fluidity value could not be measured for TK, TK200, TK400, TK600, TK800 and TK1000 samples with 30 % Z content due to the excess amount of Z except the amount wetting the surface of the coal particles. Furthermore, the re-solidification and termination of liquid state were not observed as in the case of coking coals. Briefly, the minimum and the maximum amount of Z in the experiments were determined to be 5 and 30 % respectively. A maximum amount of 28 % Z was reported for inert anthracite + Z mixtures and very high and immeasurable fluidity values were encountered when this ratio was exceeded (Stephens 1958). According to Stephens, the coal particles were liberated and a Z-coal suspension was formed above 28 % Z ratio which is in good agreement with the present study suggesting a maximum amount of 30 % Z for the TK and its semicokes. Furthermore, formation of a Z-coal suspension was also observed in the present study.

3 RESULTS AND DISCUSSIONS

3.1 Variation in Fluidity with Z Ratio

In Figure 1, the fluidity curves for TK200 with different Z ratios are seen. The highest maximum fluidity value was obtained at 25 % Z. The maximum fluidity decreased in the order of 20 %, 15 % and 10 % Z. For the mixture of 95% TK200+5% Z, a definite maximum fluidity value could not be measured due to the insufficient amount of Z not being

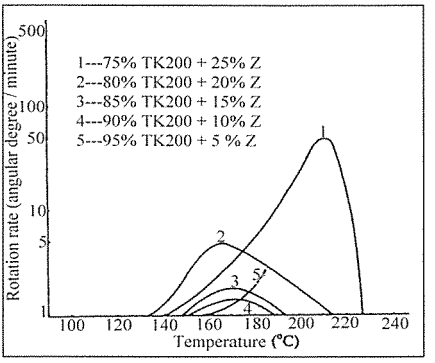

Figure 1. The curves obtained by the addition of Z in different ratios to TK200 in the Gieseler plastometer.

able to wet the surface of the TK200 particles. The torque applied to the rabble arms of the steel stirrer overcome the friction force among the coal particles and resulted in the extremely high and incorrect fluidity values. As mentioned before, it was possible to measure the fluidity values for some experiments carried out with different Z ratios. This can be explained with the example of flour and water mixture. When the amount of water added to the flour which is not at the critical sufficient limit, most of the flour particles will not be wetted. If the amount of water is increased, the flour, after a while, will transform into a thoroughly plastic state. The insufficient amount of Z (5 %) could not wet the surface of the TK200 particles properly at some points of the plastometer crucible and could not create an opposite force against the torque applied to the rabble arms of the steel stirrer. Therefore, apparently high fluidity state occurred. For verification, the sample in the plastometer crucible was checked after each experiment and was seen that a large part of the TK200particles was not wet due to the insufficient amount of Z. On the other hand, extremely high fluidity was observed in the experiments conducted with 30 % Z ratio. It was observed that the whole surface of the TK200 in the plastometer crucible was wetted and the mixture almost became fluid. But, the circular drum dial turned slower than those of the experiments carried out with 5 % Z ratio. Extremely high and immeasurable fluidities were due to the Z surplus of the TK200 sample in the plastometer crucible applying a very weak force onto the rabble arms of the steel stirrer.

In Figure 2, the fluidity curves for TK400 with different Z ratios are given. The highest maximum fluidity value

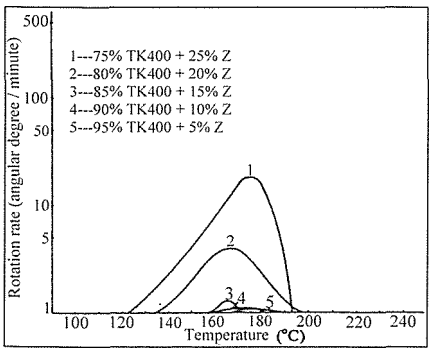

Figure 2. The curves obtained by the addition of Z in different ratios to TK400 in the Gieseler plastometer.

was obtained at 25 % Z ratio as in the case of TK200. The maximum fluidities decreased in the order of 20, 15, 10 and 5 % Z. However, a general decrease in the maximum fluidities was observed compared to those in Figure 1. The TK400 absorbed more Z in the mixture of %95 TK400+%5 Z contrary to the mixture of %95 TK200+%5 Z. In other words, the 5 % Z ratio in the mixture of %95 TK400+%5 Z reached the critical sufficient amount to wet a certain portion of the surface of the TK400 particles.

The increase in the fluidity with increasing Z is related to the Z surplus. The amount of Z absorbed by or spread onto the surface of inert coal particles varies according to the surface wetting behaviour. If coal and its semicokes have poor surface wettability, Z cannot wet the surface of the particles. Therefore, a surplus of Z as a separate phase causes to high fluidities. Because, the coal particles not wetted by Z are freed and a coal-Z suspension consisting of two separate phases is formed. In the regions where these two separate phases exists together in the plastometer crucible, an opposite force to the torque of the steel stirrer cannot be created and therefore very high fluidity values are measured. During the

runs, the retort barrel was opened and it was observed that the mixture, with increasing Z ratios, was in some kind of a muddy state. Nevertheless, contrary to the mixtures with 5 % Z ratio, the high fluidity observed with increasing Z ratio resulted in slower but continuous turns of the circular drum dial of the plastometer.

Consequently, the fluidity of the binary mixtures of TK200 or TK400 + Z with different Z ratios increases with increasing Z ratio as expected. The similar results were also gathered for TK, TK600, TK800 and TK1000 (Cengizler 1987).

The effect of Z on the fluidity of coking coals was studied and found that, in the range of 5 % to 15 % Z and for each 5 % Z addition, the fluidity of the coking coal increased by 15 fold (Stephens 1958). In the present study, the fluidity of ZK was increased 3 fold by 5 % Z addition in the binary mixtures and the plasticity range of ZK was also widened by 5 % Z addition (Figure 3) which is in good agreement with the literature (Wilkinson 1960, Bujnowska et al. 1994, Maroto-Valer et al. 1998, Stephens 1958).

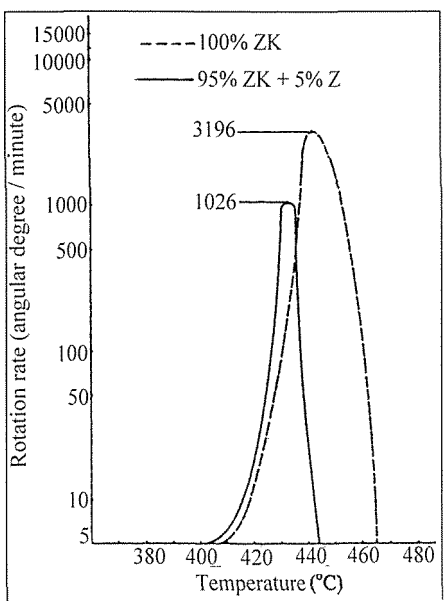

Figure 3. The effect of Z addition on the maximum fluidity of Zonguldak Coking coal.

3.2 The Variation in the Fluidity with Carbonization Temperature

In this group of experiments, Z ratios were kept constant while using different semicokes. The lowest maximum fluidity was measured in the binary mixtures of TK400. The maximum fluidity values increased following the order of TK400, TK200, TK, TK600, TK800 and TK1000.

As seen from Figure 4, the lowest maximum fluidity values were measured in the binary mixture of %75 TK400+%25 Z followed by %75 TK200+%25 Z. But, it was impossible to measure the maximum fluidities due to the extremely high fluid state in the experiments carried out with the binary mixtures of %75TK+%25 Z, %75 TK600+%25 Z, %75 TK800+% 25 Z and %75 TK1000+%25 Z as shown in Figure 4.

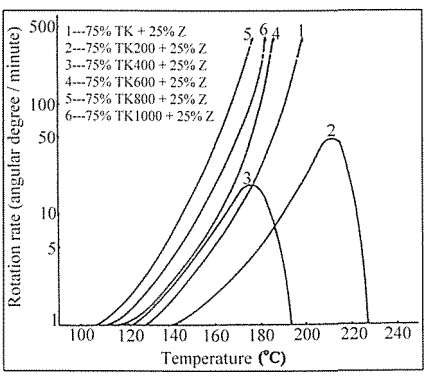

Figure 4. The curves obtained by 25% Z additions to TK, TK200, TK400, TK600, TK800, TK1000 in the Gieseler plastometer.

Figure 5 illustrates the fluidity curves for %20 Z additions. Again the lowest maximum fluidity values were determined in the binary mixture of %80 TK400+%20 Z followed by %80 TK200+%20 Z. Nevertheless, a general decrease in the maximum fluidity values compared to those in Figure 4 was observed. Due to an extremely high fluidity state similar to the experiments carried out at 25 % Z ratios, it was impossible to measure the maximum fluidities carried out with the binary mixtures of %80 TK+%20 Z, %80 TK600+% 20 Z, %80 TK 800+%20 Z and %80 TK1000+%20 Z. However, the curves are less bent and they go to infinity compared to those in Figure 4 (Figure 5).

It was possible to measure the maximum fluidity values for %85 TK+%15 Z and %85 TK600+%15 Z binary mixtures with decreasing Z ratio (Figure 6). Similarly, the lowest maximum fluidity was determined for the binary mixture of 85 TK400+%15 Z followed by higher values for %85 TK200+%15 Z, %85 TK+%15 Z and %85 TK600+%15 Z. But, the reliable fluidity values for the

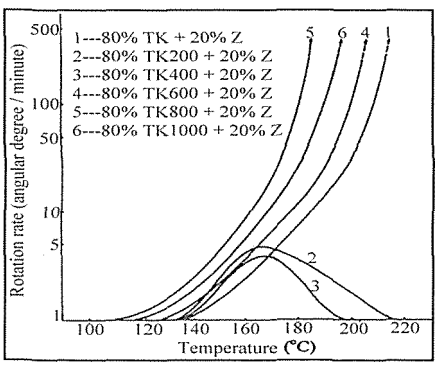

Figure 5. The curves obtained by 20% Z additions to TK, TK200, TK400, TK600, TK800, TK1000 in the Gieseler plastometer.

binary mixtures of %85 TK800+%15 Z and %85 TK1000+%15 Z at even 15 % Z ratio could not be measured due to an extremely high fluidity state.

As seen from all the figures, the rotation rate increases with increasing temperature for curves with a bell shape until a maximum is reached, after which a regular decrease sets in. As temperature increases, the viscosity of Z decreases, in other words, its fluidity increases leading to an increase in the fluidity of the mixture. During this stage, all of the inert semicoke particles cannot find sufficient time for their surfaces to get wet and therefore increasing fluidity with increasing temperature causes an increase in rotation rate. After a maximum is reached, the surfaces of the semicoke particles begin to absorb gradually more Z due to the sufficient time given and the amount of free Z in the mixture is reduced or consumed by this action. Therefore, a decrease in rotation rate with increasing temperature begins until the whole amount of Z is consumed for surface wetting in the mixture.

Consequently, the lowest maximum fluidity values were measured for only the binary mixtures containing TK400 (Figures 4, 5 and 6). The maximum fluidity values increased or the surface wetting behaviour deteriorated according to the order of TK400, TK200, TK and TK600, TK800 and TK1000. Therefore, it was clear that the best surface wetting behaviour was exhibited by TK400. Because, the liquid Z wetted and spread onto the surface of the TK400 particles in the binary mixtures containing TK400 better than any other binary mixture containing TK or other semicoke particles. Therefore, the amount of free Z in the surroundings decreased and the Z was completely absorbed by the surface of TK400 particles. As a result

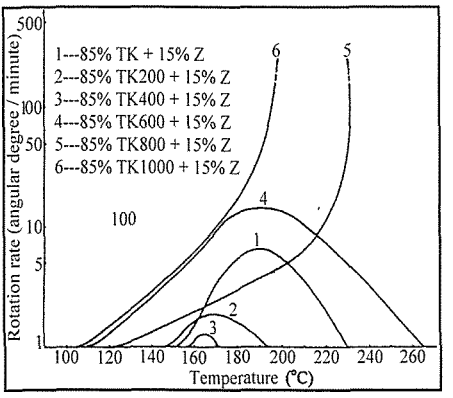

Figure 6. The curves obtained by 15% Z additions to TK, TK200, TK400, TK600, TK800 and TK1000 in the Gieseler plastometer.

of decreasing amount of Z, an opposite force is created against the torque applied to the rabble arms of the steel stirrer and the low maximum fluidity values were measured. The reason for TK to show poor surface wettability can be linked to the volatile matter released during heating probably preventing Z to be absorbed by the surface of the TK particles. On the other hand, the surface wetting behaviour of TK800 and TK1000 are worse compared to TK and other semicokes. In the binary mixtures of them, an opposite force against the torque applied to the rabble arms of the steel stirrer could not be created as the surface of the particles were not sufficiently wetted. Thus, misleadingly, extremely high fluidities were observed.

The reasons for the deterioration in the surface wetting property of TK and its some semicokes except TK400 were the variations in the physical and chemical properties of the surface of the particles due to different carbonization temperatures. It was reported that 800-900 °C semicokes represented a rather porous structure, absorbed Z and prevented the wetting of the surface of the inert particles (Kemal 1989). Different carbonization temperatures caused modifications in the physical and chemical properties of the semicoke surfaces and were effective in restructuring the micro structure. The present study can be supported by microscopic structural analysis and measurements of contact angles. Thus, significant quantitative data and information will be gathered on the surface wetting properties of TK and its semicokes. The data and information collected by the constant-torque Gieseler plastometer will also allow an interpretation in a broad sense.

4 CONCLUSION

The variation in the surface wettability properties of TK and its semicokes was studied as a function of the variation in the maximum fluidity values for the binary mixtures. It was clearly shown that the maximum fluidity values increase with increasing Z ratios as expected. The plastometer experiments performed with constant Z ratios and different semicokes obtained at different carbonization temperatures yielded different maximum fluidity values. The lowest maximum fluidity was determined in the binary mixtures containing TK400. The observations after the experiments showed that, in the mixtures with extremely high fluidities, Z could not spread onto the surface of the semicoke particles and remained in a muddy state as a separate phase. However, in the mixtures with low fluidity values, as in the case of the experiments carried out with TK400, Z was favorably absorbed by the surface of the semicoke particles. As a result, it was demonstrated that TK400 is the semicoke having

optimum surface wetting behaviour. The maximum fluidity values of the mixtures increased in the order of TK400, TK200, TK, TK600, TK800 and TK1000 while the surface wetting property deteriorated according to the same order. The present study also shows the necessity to improve the wetting property of the plastic mass in order to be able to use coals showing poor surface wetting behavior in coke production. The addition of Z to the mixture increases the coke strength when inert coal is incorporated in coke making.

REFERENCES

Bujnowska, B. and Collin, G., 1994. Co- carbonization of coals with coal-tar pitch, *Cokemaking International*, 6, 2, pp. 25-31.

Cengizler, H.: *The variation of the wettability properties of coal surfaces by temperature.* (1987), M.Sc. Dissertation, Dokuz Eylül University, Engineering Faculty, Mining Engineering Department , İzmir, Turkey.

Elliot, M. A. and Yohe, G. R., 1981. *Chemistry of coal utilization*, John Wiley & Sons, New York,

Second Supplementary Volume, pp. 1-55.

Kemal, M., 1974. *Herstellung von formkoks für metallurgische prozesse aus feinkörnigen schwelkoksen erdiger braun kohlen,* Ph.D. Thesis, Teknische Universitaet Clausthal, Germany.

Kemal, M., 1989. The effect of carbonization temperature on the wetting behaviour of the brown coal surface, *Braunkohle,* 41, heft 6, pp. 200-204.

Kemal, M., 1980. *The possibilities of using Tunçbilek coal in the production of metallurgical coke*, Thesis for Associated Professorship, Ege University, Faculty of Mechanical Engineering, İzmir, Turkey.

Lin, M.F. and Hong, M.T., 1986. The effect of coal blend fluidity on the properties of coke, *Fuel*, 65, pp. 307-311.

Maroto-Valer, M.M., Andrésen, J.M. and Snape,

C.E, 1998. In Situ ^{1}H NMR study of the fluidity enhancement for a bituminous coal by coal tar pitch and a hydrogen-donor liquefaction residue, *Fuel*, 77, 9/10, pp. 921-926.

Stephens, J. N. 1958. The effect of the pitch additions on the fluidity of coal, *Coke and Gas*, pp. 296-302.

Vankrevelen, D.W., (ed. Anderson L.L.), 1981.

Coal, Elsevier, Amsterdam, pp.263-264.

Wilkinson, H.C., 1960. The influence of the plasticity of coal on the quality of coke, *The Gas World-Coking*, pp. 39-46, Sheffield, U.K.

Investigation of the Breakage Kinetics of Gypsum as Dependent on Interstitial Filling in a Laboratory Ball Mill

Vedat Deniz
Amiroğlu Companies Group, Amiroğlu Mining Co., Denizli, Turkey
Gökhan Erdoğan
Metin Co., Aydın, Turkey

ABSTRACT Gypsum is an industrial material that is used in many applications such as building, chemical industry, fertilize, medicine and dental industries. In these industries, fine grinding of gypsum is generally needed. Energy necessity is very high in grinding processes. Therefore, the effects on breakage kinetics of powder filing and ball filling was investigated on the gypsum, taken Denizli-Honaz region (Turkey), at batch grinding conditions based on a kinetic model. For this purpose, firstly, eight different mono-size fractions were carried out between 1.7 mm and 0.106 mm formed by a $\sqrt{2}$ sieve series. Then, S_i and $B_{i,j}$ equations were determined from the size distributions at different grinding times, and the model parameters (S_i, a_i, α, γ and ϕ_j) were compared for four different powder filling (5%, 7.5%, 10% and 15%), three different ball filling (25%, 35% and 45%). Finally, model parameters are discussion for every test.
The result of tests, the effect of ball filling and powder filling on the grinding, it was found more different results than other investigators.

1 INTRODUCTION

For all dry grinding applications, chemical industries, mineral industries and cement production are certainly the most important. Energy necessity is very high in crushing and grinding process. There are many grinder manufactures and many varieties of machines made for grinding minerals. The correct selection between all alternative is a difficult problem (Deniz et al., 2005).

Gypsum is being produced in various region of Turkey, mainly in Denizli and Ankara that is widely used as special fillers, supplementary white pigment, as mould in dental and medicine, fertilize in farming, various constructions and a supplementary cementing material etc. In these industries, ultra fine grinding of gypsum is needed.

A number of researchers have shown that comminution of gypsum plays an important role in determining the cement properties, particularly setting times. An industrial Portland cement clinker, a by product gypsum with 42.4% SO_3 were

used as the base materials (Panigrahy et al., 2003).

Gypsum is added to clinker in grinding at the end of the fabrication process to control the hardening velocity of the cement. In an industrial process of cement fabrication, the use of mixtures of 95% clinker and 5% gypsum in grinding power consumption differences up to 15% (Iglesias et al., 1999). Gypsum and pozzolanic tuff used as grinding additional compounds improve energy efficiency by decreasing the specific energy for a given Blaine fineness (Touil et al, 2006).

In the design of grinding circuits in mineral processing and chemical plants, the Bond test method (Austin et al, 1984) is widely used to evaluate the performance and determine the power and mill size required for a given material. However, in recent years, mathematically models and simulation techniques have been developed by many investigators, to replace or expand the Bond design method.

The analysis of size reduction in tumbling ball mills using the concepts of specific rate of breakage and primary daughter fragment distributions has received considerable attention in recent years. Austin (1972) reviewed the advantages of this approach, and the scale-up of laboratory data to full-scale mills has also been discussed in a number of papers, summarized by Austin, Klimpel and Luckie in 1984.

The amount of powder in a mill relative to the amount of media is usually defined by "The fractional powder filling is the fraction of the interstices of the mill bed (at rest in a packed bed condition) that is filled with powder, calculated using a bulk density of the powder and assuming that the porosity of the bed is 0.4 for a bed of balls." This definition is easy to appreciate for dry grinding, but in wet grinding, it is the slurry that fills the interstices, so the amount of solid in the active breakage regions will depend on the slurry concentration as well as U (Austin et al., 1984).

In particular, Shoji et al. (1982) investigated the effects on the grinding of powder filling, for wet and dry grinding of quartz in a laboratory ball mill. The general shape of the curve of breakage rate vs. powder filling at a set ball load was explained as follows. A low filling of powder obviously gives a small rate of breakage. As the amount of powder increases, the collision spaces between the balls are filled and higher rates of breakage are obtained. When all the effective space in which collisions between tumbling balls are occurring is filled with powder, the rates of breakage reach a maximum. Further addition of powder increases the mill hold-up but does not give increased breakage because the collision zones are already saturated and further powder just enters a *reservoir* of powder. A plateau of almost constant breakage rates is obtained. Eventually, overfilling leads to deadening of the collions by powder cushioning, the ball-powder bed expands to give poor ball-ball powder nipping collions, and the breakage rates decrease. Defining the fraction of the interstitial spaces between the balls in the ball bed at rest that are filled with powder as U, it was concluded that $U = 0.6$ to 1.1 is the optimum filling condition for the maximum breakage rates at all ball loads.

Furthermore, Tangsathitkulchai (2003) was an investigated on the effect

of slurry concentration and powder filling on mill power for a small laboratory ball mill, with a constant ball load and rotational speed of the mill. In result of tests, grinding at about U= 1 gave the maximum in net mill power.

This paper will present some results on the effect of interstitial filling (U) on breakage parameters for a laboratory ball mill, with a constant ball diameter (25.4 mm) and rotational speed of mill (ϕ_c=0.75).

2 THEORY

Population balance modeling is a widely used tool for the quantitative analysis of comminution processes at the process length scale. The traditional size-discrete form of the population balance equation for batch comminution is linear and assumes first-order breakage kinetics (Austin, 1972).

$$\frac{dw_i(t)}{d_t} = -S_i W_i(t) + \sum_{j=1}^{i-1} b_{ij} S_j W_j(t), \qquad (1)$$

Thus, the breakage rate of material that is in the top size interval can be expressed as:

$$\frac{-dw_1}{dt} = S_1 w_1(t) \qquad (2)$$

Assuming that S_1 does not change with time (that is, a first-order breakage process), this equation integrates to

$$\log(w_1(t)) - \log(w_1(0)) = \frac{-S_1 t}{2.3} \qquad (3)$$

where $w_1(t)$ and is the weight fraction of the mill hold-up that is of size 1 at time t and S_1 is the specific rate of breakage. The formula proposed by Austin et al. (1984) for the variation of the specific rate of breakage S_i with particle size is

$$S_i = a_T X_i^{\alpha} \qquad (4)$$

where X_i is the upper limits of the size interval indexed by i, mm, and a_T and α are model parameters that depend on the properties of the material and the grinding conditions.

On breakage, particles of given size produce a set of primary daughter fragments, which are mixed into the bulk of the powder and then in turn have a probability of being refractured. The set of primary daughter fragments from breakage of size j can be represented by $b_{i,j}$, where $b_{i,j}$ is the fraction of size j material, which appears in size i on primary fracture, $n \geq i > j$. It is convenient to represent these values in cumulative form.

$$B_{i,j} = \sum_{k=n}^{i} b_{k,j} \qquad (5)$$

where $B_{i,j}$ is the sum fraction of material less than the upper size of size interval i resulting from primary breakage of size j material: $b_{i,j} = B_{i,j} - B_{i+1,j}$. Austin et al.(1981) have shown that the values of $B_{i,j}$ can be estimated from a size analysis of the product from short time grinding of a starting mill charge predominantly in size j (the one-size fraction BII method). The equation used is,

$$B_{i,j} = \frac{\log[(1-P_i(0))]/\log[(1-P_i(t))]}{\log[(1-P_{j+1}(0))]/\log[(1-P_{j+1}(t))]}, \quad n \geq i \geq j+1 \qquad (6)$$

where $P_i(t)$ is the fraction by weight in the mill charge less than size X_i at time t. $B_{i,j}$ can be fitted to an empirical function (Austin and Luckie, 1972).

$$B_{i,j} = \phi_j \left[X_{i-1}/X_j\right]^{\gamma} + (1-\phi_j)\left[X_{i-1}/X_j\right]^{\beta} \quad n \geq i) j \qquad (7)$$

where

$$\phi_j = \phi_1 \left[X_i / X_1\right]^{-\delta} \qquad (8)$$

where δ, ϕ_j, γ, and β are model parameters that depend on the properties of the material. If $B_{i,j}$ values are independent of the initial size, i.e. dimensionally normalizable, then δ is zero (Austin et al., 1984). .

3. EXPERIMENTAL STUDIES

3.1 Material

Gypsum samples taken from deposits belonging to the Özdenler Mining Co. in Denizli (the Honaz deposit), Turkey, were used as the experimental materials. The characterization of the raw material included chemical, mineralogical and morphological analysed with the XRF spectrometer to determine its chemical composition. Chemical properties of gypsum sample using experimentally are presented in Table 1.

Table 1. Chemical composites of gypsum sample using in experiments

Oxides	(%)
SO_3	40.90
CaO	34.73
MgO	1.37
SiO_2	0.50
Fe_2O_3	0.07
Na_2O	0.02
K_2O	0.02
Al_2O_3	0.01
H_2O	0.44
Loss on ignition	21.91

Mineralogical investigations were conducted using transmitted light microscopy and X-ray diffraction. Results indicate that samples prove to be mixtures of gypsum ($CaSO_4 \cdot 2H_2O$) and bassanite ($CaSO_4 \cdot \frac{1}{2}H_2O$). The sample had a gypsum content of about 75%, attributed to the presence of bassanite with very low quantities of clay minerals (Figure 1).

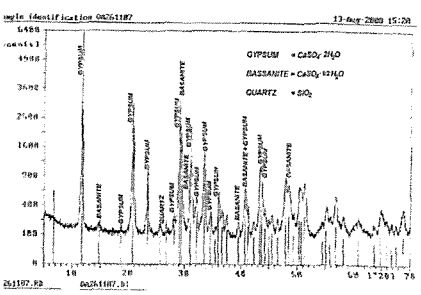

Figure 1. Characteristic X–ray diffractogram of gypsum sample

3.2 Grinding Tests

Firstly, Standard Bond Work index test was made for gypsum sample. Result of test, Bond Work index values of sample were appeared 13.85 kWh/t.

The standard set of grinding conditions used is shown in Table 2, for a laboratory mill of 6280 cm^3 volume. Eight mono-size fractions (-1.7+1.18, -1.18+0.850, -0.850+0.600, -0.600+0.425, -0.425 +0.300, -0.300+ 0.212, -0.212+0.150, -0.150+0.106 mm) were prepared and ground batch wise in a laboratory-scale ball mill for determination of the breakage functions. Samples were taken out of the mill and dry sieved product size analysis.

4. RESULT AND DISCUSSION

4.1 Determination of S Functions

The first-order plots for various feed sizes of gypsum samples are illustrated in Figures 2-8. The results indicated that grinding of all size fractions, samples could be described by the first-order law. In additional, parameters of specific rate of breakage to supply by first-order plots are present in Tables 3-4. The specific rates of breakage of each mono-size fraction that exhibited first-order grinding kinetic behaviuor were determined from the slope of straight-line of first-order plots. Additional, Figures 9-10 shows the values of *Si* for grinding of the three-ball filling and the four-powder filling studied as a function of size, respectively.

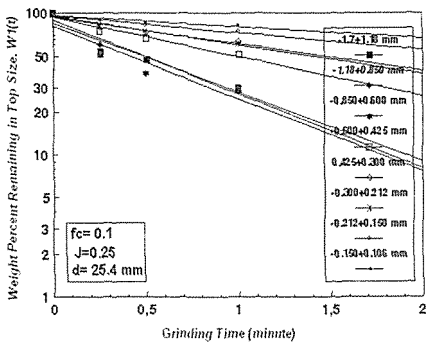

Figure 2. First-order plots for J=0.25

4.2. Determination of B functions

By definition, the values of B were determined from the size distributions at short grinding times. The parameters were determined according to the *BII* method (Austin et al, 1984), and show the graphical representation on Figures 11-12. Gypsum samples show a typical normalised behaviour, and the progeny distribution does not depend on the particle size, and it followed that the parameter δ was zero. Model parameters supply by cumulative distribution and these parameters are present in Tables 3-4.

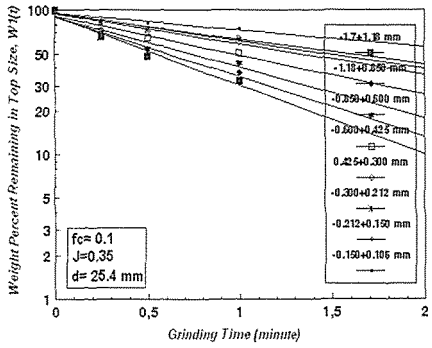

Figure 3. First-order plots for J=0.35

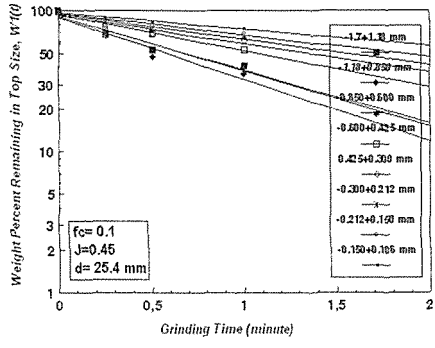

Figure 4. First-order plots for J=0.45

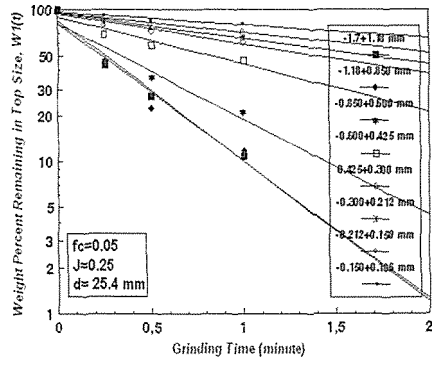

Figure 5. First-order plots for f_c=0.05

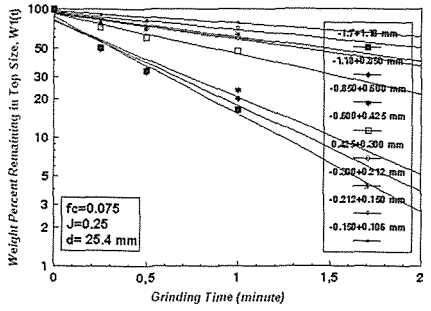

Figure 6. First-order plots for f_c=0.075

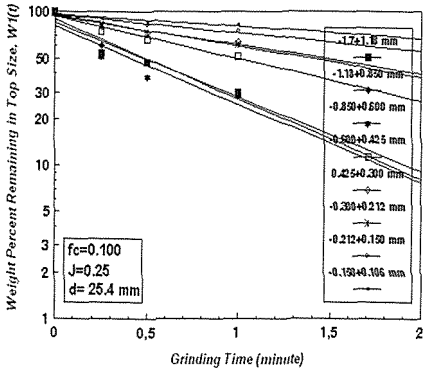

Figure 7 First-order plots for f_c= 0.10

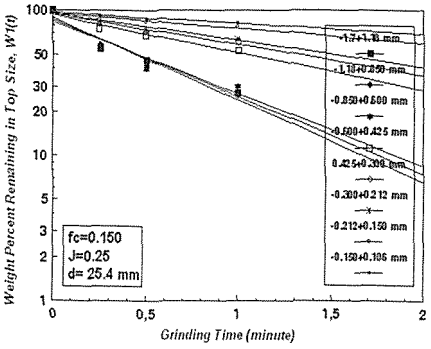

Figure 8. First-order plots for f_c=0.15

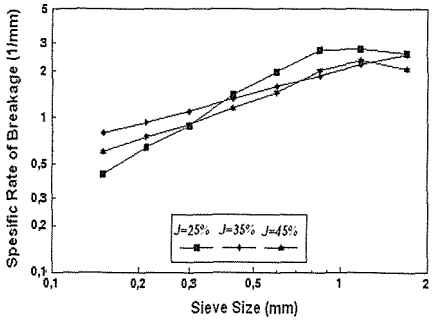

Figure 9. Specific rates of breakage for different ball filling

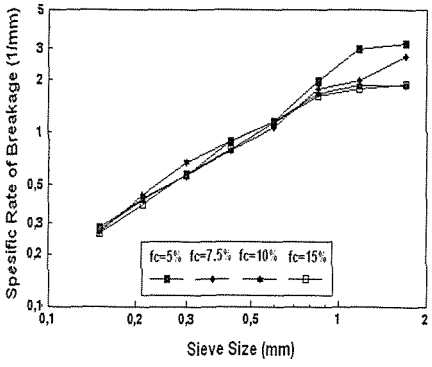

Figure 10 Specific rates of breakage for different powder filling

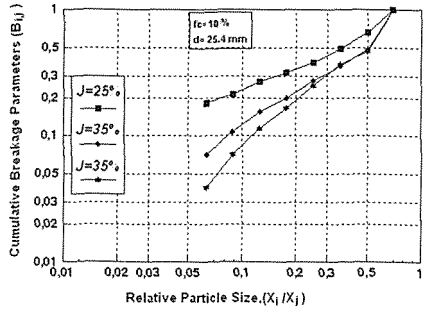

Figure 11. Cumulative breakage distribution functions for different ball filling

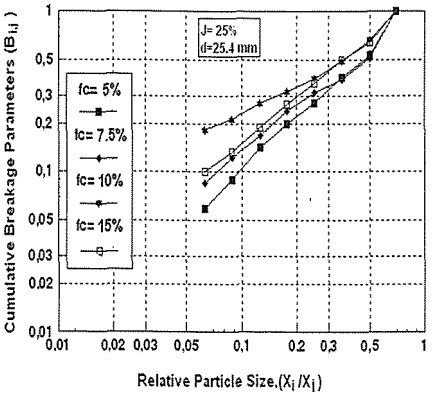

Figure 12. Cumulative breakage distribution functions for different powder filling

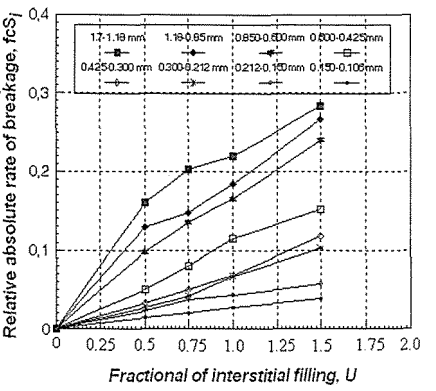

Figure 13. Variation of relative absolute of breakage with interstitial filling

4.3. The relationships between interstitial filling (U) and relative absolute rate of breakage (f_cS_i)

The product of S and f_c is called the "relative absolute rate of breakage", important because it is proportional to mill capacity. Differentiating f_cS_i with respect to U to obtain the maximum gives the highest capacity. Shoji et al. (1982) found the maximum at U= 0.83. A flat maximum occurred between U= 0.6 and 1.1. Tangsathitkulchai (2003) found that grinding at about U= 1 gave the maximum in net mill power. Furthermore, Deniz and Onur (2002) has been differently found that an interstitial filling fraction of U = 0.4 is a good powder–ball loading ratio to give efficient breakage in a ball mill for the pumice sample.

f_cS_i is plotted against for gypsum sample similar result as indicated by Shoji et al. (1982) and Deniz&Onur (2002), but this was not consistent with our data. The optimum value of U is $U\geq$ 1.5 (Fig. 13).

4.4. The relationships between interstitial filling (U) and first-order breakage constant (a_TU)

Figure 14 shows the effect of varying the mass of solid in the mill. From this limited amount of data it appeared that the results fitted this expression giving the optimum interstitial filling as $U\geq$ 1.5.

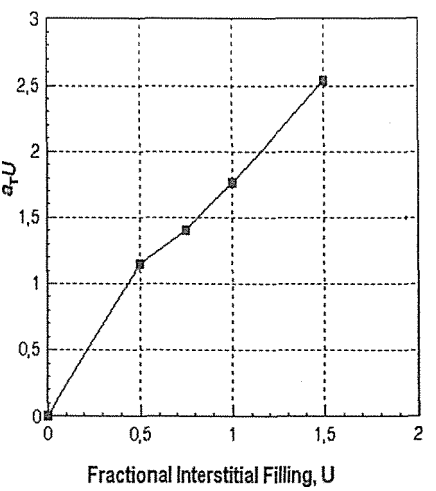

Figure 14. Variation of interstitial filling with first order breakage constant

Table 2. The standard set of grinding conditions

Mill	Diameter, mm		200		
	Length, mm		200		
	Volume, cm^3		6280		
Mill speed	Critical (N_c) [a], rpm		101		
	Operational $(\phi_c = 75\%)$, rpm		76		
Balls	Diameter range, mm		25.4		
	Specific gravity,		7.8		
	Quality		Alloy Steel		
	Assumed bed porosity		40%		
	Ball filling volume,$(J\%)$ [b]	25	35		45
Material	Formal bulk density,g/cm^3		1.676		
	(J=0.25)	50	75	100	150
	Interstitial filling $(U\%)$[d] (J=0.35)	35.7	53.5	71.4	107.1
	(J=0.45)	27.7	41.6	55.5	83.3
	Powder filling volume $(f_c\%)$[c]	5	7.5	10	15

[a] *Calculated from* $N_c = 42.3/\sqrt{D-d}$ (D, d *in metres*)

[b] *Calculated from* $J = \left(\frac{\text{mass of balls / ball density}}{\text{mill volume}} \right) \times \frac{1.0}{0.6}$

[c] *Calculated from* $f_c = \left(\frac{\text{mass of powder / formal bulk density}}{\text{mill volume}} \right)$

[d] *Calculated from* $U = \frac{f_c}{0.4J}$

Table 3. Model parameter values for different powder filling

f_c %	-0.850+0.600 mm S_i	α	a_T	γ	ϕ_j
5	0.417	2.49	1.067	1.501	0.64
7.5	0.410	1.84	0.995	0.774	0.48
10	0.433	1.76	1.150	0.571	0.64
15	0.382	1.69	1.075	1.165	0.99

Table 4. Model parameter values for different ball filling

J %	-0.850+0.600 mm S_i	α	a_T	γ	ϕ_j
25	0.433	1.76	1.151	0.571	0.64
35	0.513	1.67	0.580	1.139	0.78
45	0.505	1.41	0.599	1.367	0.89

5. CONCLUSIONS

Dry grinding of size intervals of gypsum samples showed that the interstitial filling followed the first-order breakage law with constant normalised primary breakage distributions. In additional, these samples do not depend on the particle size from cumulative breakage distribution function.

As the amount of S_i and α values (shown in Table 3 and Table 4) increased, expressed more effective breakage and broke as very fast in the undersize of original particle size. From S_i values experimentally obtained, grinding is faster grinding for J=0.35 as suitable value of ball filling for gypsum sample. Additional, it is given effective breakage for f_c=0.1 for powder filling.

The slope of the lower portion of the $B_{i,j}$ curve can be denoted by γ with smaller values of γ indicating that once particles of a certain size break, they produce many much smaller progeny fragments. Thus γ values tend to decrease with the decrease in the ball filling, which emphases that the grinding of gypsum produces finer material. It tend to decrease up to f_c =10% of powder filling and than start to show a increasing trend after f_c =10%. Therefore, the maximum of γ was found about 10% of powder filling.

The Values of the coefficient ϕ_j is related to coarse end of the breakage distribution function and show how fast fractions close to the feed size passes to smaller size interval. Higher value of ϕ_j for increase ball filling shows the rapid grinding of gypsum especially at sizes close to feed size.

The product of S and f_c is called the "relative absolute rate of breakage", important because it is proportional to mill capacity. Differentiating $f_c S_i$ with respect to U to obtain the maximum gives the highest capacity. Shoji et al. (1982) found the maximum at U= 0.83 for the quartz mineral. Tangsathitkulchai (2003) found that grinding at about U= 1 gave the maximum in net mill power, Deniz and Onur (2002) has been differently found that an interstitial filling fraction of U = 0.4 is a good powder–ball loading ratio to give efficient breakage in a ball mill for the pumice sample. In this research, it was found that $U \geq 1.5$ is a good ratio for the gypsum sample.

This study showed that grinding kinetic parameters could be different for different ball filling and powder filling. Therefore, it has appeared that the grinding kinetics for each material must be evaluated in order to lower the energy costs in grinding process.

REFERENCES

Austin, L.G., 1972. A Review Introduction to the Description of Grinding as a Rate Process, *Powder Technology*, 5, 1-7.

Austin, L.G. and Luckie, P.T., 1972. Methods for Determination of Breakage Distribution Parameters, *Powder Technology*, 5, 215-222.

Austin, L.G., Klimpel, R.R., Luckie, P.T. and Rogers, R.S.C., 1982. *Simulation of Grinding Circuits for Design, Design and Installation of Comminution Circuits,* S.M.E. , NewYork, USA, 301-324.

Austin, L.G., Klimpel, R.R. and Luckie, P.T., 1984. *Process Engineering of Size Reduction: Ball Milling*, A.I.M.E., S.M.E., NewYork, USA.

Deniz, V. and Onur, T., 2002. Investigation of the breakage kinetic

of pumice samples as dependent on powder filling in a ball mill, *Int. J. of Min. Processing*, 67, 71-78.

Deniz, V., Akkurt, Y. and Umucu, Y., 2005. A New Model on Breakage Behaviuor of A Laboratory Impact Mill, *The 19th International Mining Congress of Turkey*, Izmir, Turkey, 229-232.

Iglesias, J.G., Alvarez, M.M. and Rodrigues, J.E., 1999. Influence of gypsum's mineralogical characteristics on its grinding behaviuor applied to cement fabrication, *Cement and Concrete Research*, Vol.29, 727-730.

Panigrahy, P.K, Goswami, G., Panda, J.D. and Panda, R.K., 2003. Differential comminution of gypsum in cements ground in different mills, *Cement and Concrete Research*, 33, 945-947.

Prasher, C.L., 1987. *Crushing and Grinding Process Handbook,* John Wiley&Sons, Chichester, U.K.

Shoji, K., Austin, L.G., Smalia, F., Brame, K. and Luckie, P.T., 1982. Further Studies of Ball and Powder Filling Effects in Ball Milling, *Powder Technology*, 31, 121-126.

Tangsathitkulchai, C., 2003. Effects of slurry concentration and powder filling on the net mill power of a laboratory ball mill. Powder Technol. 137 131– 138.

Touil, D, Belaadi, S. and Frances, C., 2006. Energy efficiency of cement finishe grinding in a dry batch ball mill, *Cement and Concrete Research*, Vol.36, 416-421.

Enrichment and Processing of the Rare Earth Ores of Mongolia

A.Khaumdas, D. Sangaa
Institute of Physics and Technology of Mongolian Academy of Sciences
Rakaev A.I.
Mining Institute of Kola Scientific Center of Russian Academy of Sciences

ABSTRACT Synchisite is one of the main economic minerals of rare earth ores deposit on the territory in Mongolia. Research data on the opening and dressing processes of Synchisite was poor. The Synchisite mineral contains Rare earth elements (REE) of cerium group. Taking into account the existing rare publication and research materials on production technology that uses current mineral at the REE production, the Lugiin Gol rare earth elements deposit of our country may be considered without analogue world-wide.

Therefore, despite that in our country former was not carried out technology research work for enrichment and processing of REE ore, in result of research work was proved that Synchisite could be a raw material of REE production like bastnasite, monazite, parisite, xenotime.

1 INTRODUCTION

The Synchisite mineral of rare earth elements was established through combination of X-ray phase, derivatography, mass spectrometric analysis methods and comparison of etalon samples.

A possibility of raising the Synchisite dressing by 20-25% is shown. Its REO being raised by 8-10% at the expense of its total dressing from the particles with size of - 0.05 mm fractions by using a method of flotation and subsequent separation of the sediments produced .

The choice of a chemical process for processing the concentrates is stipulated by the physical and chemical characteristics of the raw material, the composition of the minerals and its compounds.

2 EXPERIMENTAL

The essence of our processed and containing REE method for enrichment of fluorine carbonated ore consists in 3 stages of enrichment of pyrite, calcite, REE. During the enrichment of calcite, in order to enrich and separate calcite and REE minerals, through change of REE ore surface enrichment activation with support of metal gel gumine acid, completion of classic conditions to

Table 1. Inter plane distances of some minerals and ores of Lugiin gol deposites

Literatura				Ore of Lugiin gol	
Bastnesite		Synchisite			
d(A°)	I	d(A°)	I	d(A°)	I
4.88	40	9.1	60	9.17	9
		4.53	50	4.58	10
				3.85	6
3.564	70	3.55	100	3.56	8
		3.32	40	3.34	2
				3.24	4
		3.97	30	3.04	100
				2.892	28
2.879	100			2.839	3
		2.80	100	2.802	9.5
2.610	1				
2.445	9			2.492	5
				2.4068	6
		2.30	20		
		2.28	20	2.283	13
2.273	3	2.06	50	2.0612	5
2.057	40	2.01	20	2.0179	6.5
				1.9244	3
		1.934	50	1.9209	16
		1.873	40	1.8732	17
		1.821	5		
1.783	9	1.777	10	1.7786	5
1.674	21			1.6234	5

set flotole-7.9 collector reagent, was established the possibility to extract REE concentration with REE 27-32 percent specific content and 72-80 percent recovery metal sample.

For the determination of the Synchisite concentrate there have been applied the following methods as infrared spectroscopy, X-ray diffractometry, differential thermal analysis and mass-spectrometry.

The infrared absorption of the Synchisite concentrates was registered by a two-ray spectrometer UR-20 within the range of 400-1600cm.

The differential thermal analysis was carried out at the derivatigraph of a Paulic-Erdey system at heating speed of 10^0/min to 1.000°C.

The concentrate was heated in the furnace resistance at constant speed while the gases being educed analyzed with a statistical mass-spectrometer MX1307M.

The X-ray analysis of the synchisite concentrate was carried out with the diffractometry DRON-2.

3 RESULTS AND DISCUSSION

In spite that there are discovered deposits and occurrences of rare-earth elements (REE), niobium, zirconium, tantalum at the alkaline granite, carbonatite, fluorine carbonatite, apatite rocks in the territory of Khovd, Uvs, Dornogobi, Umnugobi and Bayan-Ulgii provinces of our country, and preliminary explorations of some deposits (Khalzan burged, Tsakhiurt, Ulaan and Shar tolgoi, Maikhan tolgoi , Mushgai hudag) were at starting point, the ore reserve of the Lugiin gol deposit, that represents REE deposit and where the technological research had been done, counted by 500000 tons and the average content of synthesis oxide of REE was 3.3%.

The oxidized ore of that area is enriched with minerals of metal and manganese / hematite, magnetite, limonite, psilomelane/. In addition, it was established that current ore is a synthesis ore that contains such minerals as calcite, magnesite, quartz, pyrite, sphalerite, fluoric spar, ilmenite, galenite.

The deposit Lugiin gol is studied

Table 2. The maintenance of the basic components in investigated test of ore Lugiin gol deposite, %

1	Component	Content	1	Component	Content
1	SiO_2	4.0	9	CO_2	33.9
2	Al_2O_3	1.0	10	Na_2O	0.15
3	Fe_2O_3	5.3	11	K_2O	0.1
4	TR	8.6	12	Nb_2O_5	0.01
5	CaO	33.6	13	Ta_2O_5	0.02
6	MgO	5.3	14	P_2O_5	0.12
7	MnO	4.5	15	TiO_2	0.07
8	PbO	0.3	16	ThO_2	0.14

full enough in the geological attitude. The tentative estimation of stocks on ore and on the sum rare earth elements is executed.

The technology research work for ore enrichment of Lugiin gol REE deposit through the method of flotation was done in Poland. Regarding the technology, it was evident that there was used the technology of bastnasite ore enrichment of Mountain-Pass.

The method of drifting enrichment technology has such shortcomings in terms of technology as too much complex operation, number of stages, requiring much heating, as well as regarding the Polish technology has insufficient metal sampling and the application volume of vapor and water is high..

In order to carry out enrichment experiment through the gravitation method we have established newly the chemical and ore mineral content of present deposit.

Whereas the content of ore mineral were /%/: calcite-43.6, dolomite-25.9, Synchisite -11.05, monazite-0.36, parisite -0.71, pyrolysite-2.68, hematite-4.01, fluoric spar-6.05, nepheline-1.35, quartz-1.81, they were through chemical content /% oxide/: calcium-35.5, magnium-5.77, alluminium-1.69, iron-3.55, carbon-33.92, kalium-0.9, natrium-0.25, silicium-6.29, phosphor-0.14, titanium-0.08, sulphur-0.1, REE - 6.54.

Because the ore enrichment depends upon the amount of ore powdering, through the research to determine powdering kinetic regime was established the accumulation of REE Synchisite mineral in a fraction less than 0.4 mm, as well as in order to separate fully the Synchisite mineral at -0.05 mm from other minerals is effective the use of pivotal mill.

The main purpose of research work for enrichment of Lugiin gol REE ore consists in extracting 20-20% concentrate required for chemical-metallurgical processing and for this purpose about 2.0 ton ore of present deposit was enriched and tested in 2 versions on the semi production experimental equipment of Mining Institute by the Kola Scientific Center at the Russian Academy of Sciences.

The extracted REE concentrate was processed by the chemical-metallurgical method, at the technological research for extracting their synthesis acid was carried our the experiment of method for processing with nitrogen acid and

sulphur acid, as well as at research of extrcated prodsucts were used X-ray phase, derivatography, IK and mass-spectrometry methods.

Considering the publication materials, it would be widely used the technology process at which the REE would be melted by sulphur acid and sodium, the melt dissolved in water /in case, if the content of fluorine is high/ and REE transferred into water. But because in our country's Synchisite concentrate has less fluorine concentrate, in results of experiment was proved the possibility to extract REE synthesis oxides with 89-95% content and 97% metal by burning the concentrate and dissolving in 50% nitrogen acid.

The infrared spectroscopy analysis of the Synchisite was performed for the samples of gravity (1), flotation (2) concentrate and the concentrate being at a temperature of 800^{0}C (3) (fig.1).

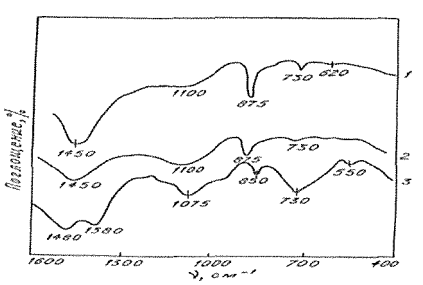

Figure 1. The infrared spectroscopy analysis

The absorption taken place at a 1480cm^{-1} might be apparently explained in connection with the fluctuations of a group pertaining to E (ν) (C-O). the absorption at a 1100cm^{-1}

Should be accounted for with the mixtures being contained in the samples studied. The absorptions at 630 and 550cm^{-1} are likely to be associated with M-O where M is REE or other components. The coincidence of the absorption range of the Synchisite concentrate with the standard samples of the Synchisite at 550 to 620.730. to 875. 1075 to 1100 and 1450 to1480 cm^{-1} evidences that the major carrier of the rare earths in ore is Synchisite.

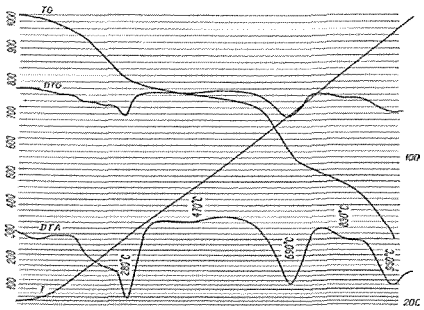

Figure 2. Differential Thermal analysis

Proceeding from the analysis of the derivatogramm the following conclusion is possible to be arrived at: the first effect in the range up to 280^{0}C is connected with a loss of the molecular water, the effect at a temperature of 470 to 600^{0}C signifies a decomposition of the Synchisite while the effect on temperature changes from 690 to 830^{0}C is to be characteristic the dissolution of carbonates of a bronerite (about 690^0) and calcite types together with dolomite (830^0). The step-by-step gradual character of the curves regarding the weight loss is much likely to evidence the hydration of the Synchisite and a partial substitute of CO_2 with hydroxyl groups. The total mass losses percentage under the heating accounts for 29.9 %.

On Fig.3 there are presented poly terms of the general pressure and ionic currents of gaseous components (CO_2 and CO) produced on a thermal decomposition of a Synchisite concentrate.

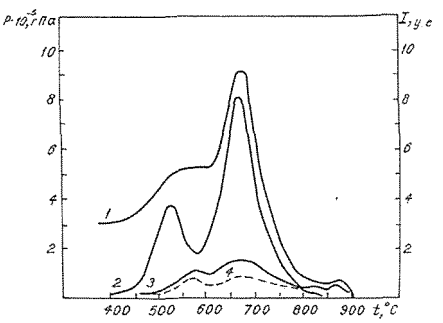

Figure 3. Mass specters

It was to be expected that CO_2 is educed in two stages: around 500 to 530°C and 670 to 700°C. In our opinion, the CO_2 an appear only due to the oxidation of cerium.

$$Ce_2(CO)_3 \rightarrow 2\,CeO_2 + 2\,CO_2 + CO$$

The fact of the cerium being subjected to oxidation is interesting in the respect that in the process of thermal treatment it is being transformed into a tetravalent form.

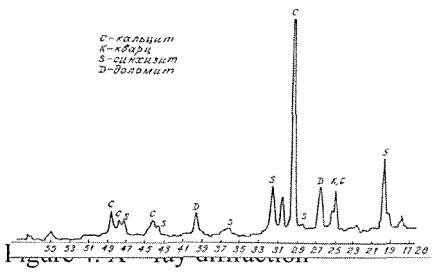

The results of the thermal analysis and infrared spectroscopy are in good agreement with the data of the X-ray phase analysis (Fig.4).

Taking into account the results of the thermal and mass spectrometric analysis the charring of the concentration was carried out in the range of temperatures from 400 to 800°C, during which it was proved that the mass loss of the concentrate amounted to approximately

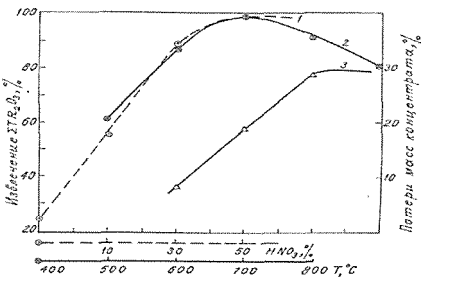

Figure 5. Concentration HNO3 and anneal temperature dependence of the REO recovery (1,2) and temperature dependence of loss mass (3).

Taking into account the results of the thermal and mass spectrometric analysis the charring of the concentration was carried out in the range of temperatures from 400 to 800°C, during which it was proved that the mass loss of the concentrate amounted to approximately 30% (Fig.5).

For the lixiviation of the Synchisite concentration charred there were utilized 10 to 50% solutions of HNO_3 prepared from 67% nitrogen acid.

At a temperature of the charring not exceeding 400°C recovery of the rare earth elements to the solution is not to be above 62% (Fig.5).

Which might be caused by the fact that a thin dissemination of Synchisite in minerals of the barren rocks is not being revealed due to a lack of its contact with acid.

The further raise of temperature leads to the opening of even those particles of the Synchisite and a temperature risen up to 600°C the recovery of ERT to the solution reaches its highest values (97.1%).

The reduction in the REO recovery while temperature being raised further is associated with the formation of heavily

soluble substances in particular cerium oxide in tetravalent form (CeO_2) and associates on a calcium basis. In order to dissolute them and thereby to increase the rate of recovery it is necessary to increase the time of dissolution or raise the acid concentration.

However an application of to much acid is not advisable for a following extraction of the REE.

As we have done an experiment to dissolve current concentrate by sulphur acid, we have extracted REE synthesis oxide with 76% content through dissolving sulphatized rests with water and sedimentation of solution with natrium alkaline. The following recovery of individual REE from nitrogen acid solution is executed as per a familiar technique by means of a liquid extraction with the utilization of different organic extra gents in the cascades of a few stage number.

Taking into account the preliminary geological exploration carried out in the Khalzan burged deposit located in the territory of Khovd province and containing rare metal, the content of rare metals and their preliminary established reserves, main minerals of present deposit are: zirconium silicate, pyrochlore, eudialyte, xenotime and REE fluorine carbonates.

The content of present deposit's rare metals as follows /%/: oxides of niobium 0.14, RE Elements -0.35, zirconium oxide-3.35.

We have carried out experiments to research possibilities for enrichment of present deposit's ore. In results of research work we have established that the ore of present deposit has much amount of radioactive substances, made conclusion that it is required to pay attention during the next technological experiments and put continual control over technological process.

4 CONCLUSION

Through the technology research of Lugiin gol ore enrichment, that represents REE deposit of our country was developed the technology for enrichment of present deposit's ore.

During the enrichment process of magnetite-apatite kind ore of the waved well was developed a version of technology for also possible enrichment of REE contained in it.

There were performed initial works to establish mineral and chemical content of ore of rare metals containing niobium, REE and zirconium of the Khalzan burged, as well as to research enrichment properties. It is required to establish geological and geochemical structure of present deposit, carry out large scale of technological research for ore enrichment and concentrate deep processing.

Through the research work was developed the technology for processing the concentrate by which was extracted the ore of the Lugiin gol by the chemical-metallurgical method and extraction of their synthesis oxide.

REFERENCES

Khaumdas Ashim. *" The technological features of dressing and processing of the rare earth ores of Mongolia"* (in Russian). Ulaanbaatar. "Sorkhon tsagaan" Publishing house. 2006, 127 pp.

Khaumdas Ashim, Rakaev A.I. and others. *" Synchisite – new resources of the rare earths"*. Proceedings of the 3 rd International Conference on Rare Earth Development and

Application. Batou, Inner Mongolia, China. August 21-25. 1995. Vol.2.p.834-837.

Khaumdas Ashim. *"Study of technological specific characteristic of the rare earth elements of Mongolia difficult of dressing"*. Dissertation for a degree of Ph.D., Almaty, 1995. 206pp

Khaumdas Ashim, Tuguldor N. *"Method of concentrating fluorcarbonate ores of Mongolia"*. Copyright N673, Ulaanbaatar. The first publication 4-7-1992.

Khaumdas Ashim, Rakaev A.I. and others. *"The developing of the rational technology of the Synchisite ore concentration"*. Proceedings of the 2 nd International Conference on Rare Earth Development and Application. Beijing, China. May 27-31. 1991. Vol.1.p.484-486.

Mihailichenko and others. *"Rare earth metals"*. Moscow.' Metallurgy' Publishing house. 1987, 232 pp.

The Correlations Between the Mean Particle Size in Grinding and Physico-Mechanical Properties of Igneous Rocks

S. Kahraman, M. Uçurum, E. Yoğurtçuoğlu
Nigde University, Mining Engineering Department, Nigde, Turkey

ABSTRACT

Igneous rocks are ground for different purposes. Mean particle size (d_{50}) can be a quantitative measure of grindability at the same grinding conditions. The prediction of d_{50} is useful for the mining engineers. For this reason, to investigate the relations between the d_{50} and physico-mechanical properties of igneous rocks, five different rocks including granite, basalt and andesite were tested in the laboratory. d_{50} values obtained from the size distribution plots were correlated with the corresponding physico-mechanical properties. Good correlations between the d_{50} and physico-mechanical properties could not be found using the simple regression analysis. However, the prediction equations having strong correlation coefficients were developed for the d_{50} using the multiple regression analysis. It was concluded that the d_{50} of igneous rocks can be predicted from the equations developed from the multiple regression analysis especially for preliminary investigations. The derived equations including index test values are also important for the practical consideration. Further research is necessary to check the validity of the derived equations for the other rock types.

1 INTRODUCTION

Grinding is widely used in mineral processing plants or some other industrial plants. The grinding process is a mechanical method and directly related with the physical and mechanical properties of rocks. Mean particle size (d_{50}) provides a quantitative measure of how thoroughly materials are ground. The prediction of d_{50} of rocks from the physico-mechanical properties will help the mining engineers especially for preliminary investigations.

Several researchers have investigated the effect of some rock properties on the grindability. Deniz et al. (1996) found an inverse relation between Bond grindability index and point load index for coals. Bearman et al. (1997) investigated the relations between some

mechanical properties and grindability, and they found a good correlation between indirect tensile strength and grindability. Deniz and Özdağ (2003) correlated dynamic elastic properties with Bond grindability and work index and found some statistical relations for sedimentary and volcanic rocks. Su et al. (2004) found some correlations between mechanical properties and Hardgrove grindability index for Zonguldak Coals. Similarly, Tiryaki (2005) derived correlations between mechanical properties and Hardgrove grindability index for Çayırhan Coals. Ozkahraman (2005) found some relations between Bond grindability, work index and friability value for some rocks. Şengün et al., (2006) developed some correlations between Bond grindability index and some rock properties for sedimentary rocks and marbles. They suggested some prediction equations including Shore hardness and point load index for Bond grindability.

Although some researchers have studied the relations between the grindability and some properties of coals and rocks, there is no investigation on the igneous rocks. In this study, the correlations between the d_{50} and physico-mechanical properties of igneous rocks were investigated.

2 SAMPLING

Five different igneous rocks were sampled and tested in this study. Granite factories and natural outcrops in Nigde area of Turkey were visited and rock blocks were collected. The name and location of the rocks are given in Table 1.

Table 1. The name and locations of samples.

Rock Code	Location	Rock type
1	Porrino/Spain	Granite (Rose Porrino)
2	Porrino/Spain	Granite (Pink Porrino)
3	Bor/Nigde/Turkey	Basalt
4	Yesilburc/Nigde/Turkey	Andesite-1
5	Yesilburc/Nigde/Turkey	Andesite-2

3 EXPERIMENTAL STUDIES

3.1 Uniaxial Compressive Strength Test

Uniaxial compressive strength tests were conducted on trimmed core samples, which had a diameter of 38 mm and a length-to-diameter ratio of 2.0. The stress rate was applied within the limits of 0.5-1.0 MPa/s. The tests were repeated at least five times for each rock type and the average value was recorded as the uniaxial compressive strength.

3.2 Brazilian Tensile Strength Test

Brazilian tensile strength tests were conducted on core samples having a diameter of 38 mm and a height to diameter ratio of 0.5-1.0. The tensile load on the specimen was applied continuously at a constant stress rate such that failure will occur within 5 minutes of loading. At least five samples were tested for each rock type and the results were averaged.

3.3 Point Load Test

The diametral point load test was carried out on the cores having a diameter of 38 mm and a length-to-diameter ratio of 1.2. The point load test results were corrected to a specimen diameter of 50

mm. The tests were repeated at least seven times for each rock type and the average value was recorded as the point load strength.

3.4 Schmidt Hammer Test

N-type Schmidt hammer tests were conducted in the field. All tests were made with the hammer held vertically downwards and at right angles to horizontal faces of large rock blocks. In the tests, twenty rebound values from single impacts separated by at least a plunger diameter were recorded and averaged the upper ten values. The test procedure was repeated at least three times for each rock type and the average value was recorded as the Schmidt hammer value.

3.5 Ultrasonic Test

P-wave velocities were measured on the samples having a diameter of 38 mm and a length of 76 mm. End surfaces of the core samples were polished sufficiently smooth plane to provide good coupling. In the tests, PUNDIT 6 instrument and two transducers (a transmitter and a receiver) having a frequency of 1 MHz were used. A good acoustic coupling between the transducer face and the soil surface is necessary for the accuracy of transit time measurement. Stiffer grease was used as a coupling agent in this study. Transducers were pressed to either end of the sample and the pulse transit time was recorded. The tests were repeated several times for each rock type and average value was taken as the P-wave velocity value.

3.6 Density Test

Trimmed core samples were used in the determination of dry density. The specimen volume was calculated from an average of several calliper readings. The dry weight of the specimen was determined by a balance, capable of weighing to an accuracy of 0.01 of the sample weight. The density values were obtained from the ratio of the specimen weight to the specimen volume.

3.7 Porosity Test

Porosity values were determined using saturation and calliper techniques. Pore volumes were calculated from dry and saturated weights and sample volumes were obtained from calliper readings for the trimmed core samples. The porosity values were obtained from the ratio of the pore volumes to the specimen volume.

3.8 Grinding Test

500 g material from each rock sample with a size of -2+1 mm was prepared for grinding tests. The samples were ground in a stainless steel ball mill under dry conditions for 5 minutes. The ball mill had the dimensions of 200x200 mm, and was charged with 5 kg of stainless steel balls. The size distribution plots of the individual fractions are shown in Fig. 1.

4 EVALUATION OF THE RESULTS

4.1 Simple Regression Analysis

All test results are given in Table 2. The test results were analyzed using the method of least squares regression. d_{50} values were correlated with corresponding physico-mechanical properties. As shown in Figs. 2-8, no significant correlation was found between d_{50} values and physico-mechanical properties. The reason for the lack of correlations is probably due

to the fact that grinding is a complex phenomenon and depends on more than one rock property. For this reason, multivariable analysis is necessary for the evaluation of d_{50}.

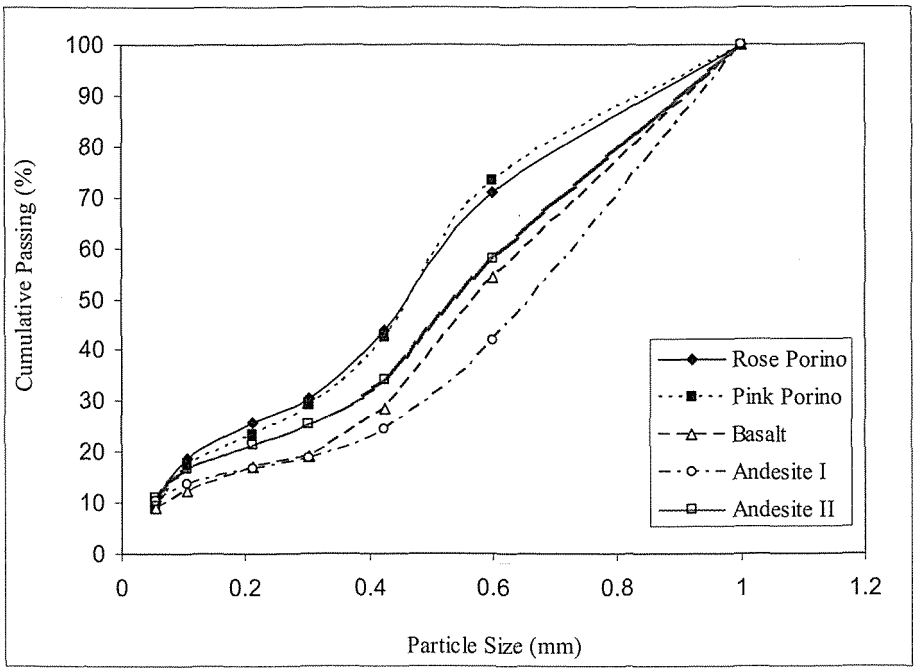

Fig. 1. The size distributions of the individual fractions.

Table 2. Test results.

Rock code	Uniaxial compressive strength (MPa)	Brazilian Tensile strength (MPa)	Schmidt hammer values	Point load index (MPa)	P-wave velocity (km/s)	Density (g/cm^3)	Porosity (%)	d_{50} (mm)
1	90.2	7.5	46.1	6.7	3.5	2.59	0.90	0.46
2	119.6	12.6	46.8	13.6	4.0	2.53	2.81	0.47
3	202.9	17.0	61.8	13.2	4.5	2.58	5.50	0.57
4	77.5	9.0	51.7	6.4	3.4	2.51	5.30	0.65
5	65.8	5.5	49.5	5.0	2.8	2.21	8.70	0.54

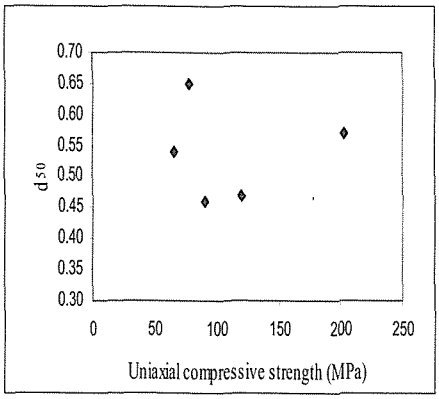

Fig. 2. The relation between uniaxial compressive strength and $d_{50.}$

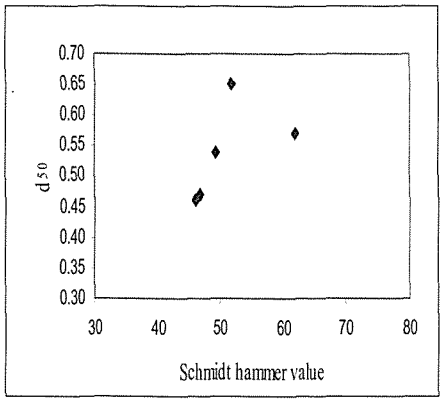

Fig. 5. The relation between Schmidt hammer value and $d_{50.}$

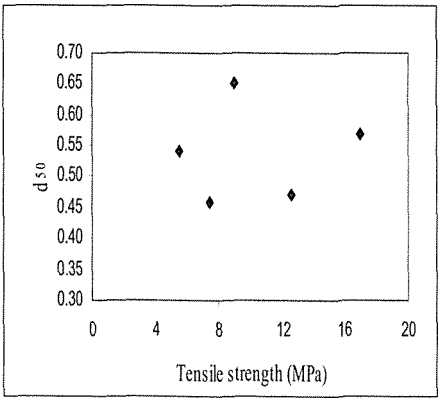

Fig. 3. The relation between tensile strength and $d_{50.}$

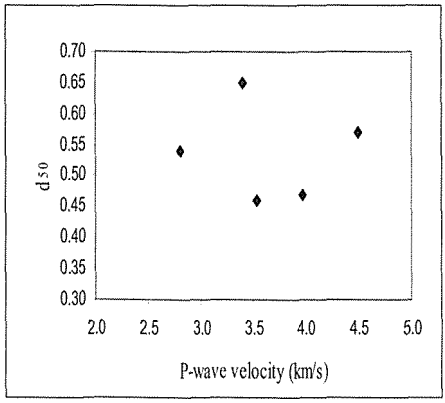

Fig. 6. The relation between P-wave velocity and $d_{0.}$

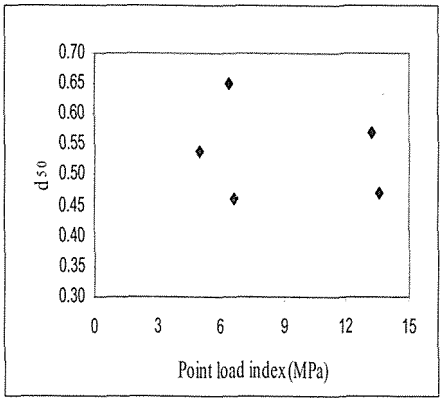

Fig. 4. The relation between point load index and $d_{50.}$

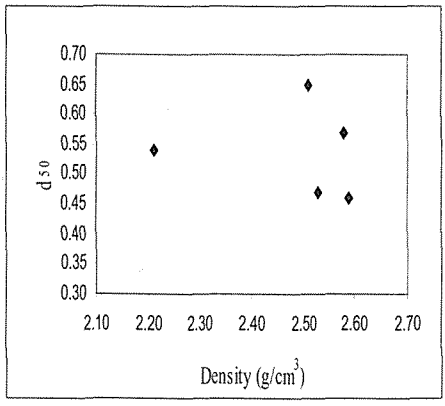

Fig. 7. The relation between density and $d_{50.}$

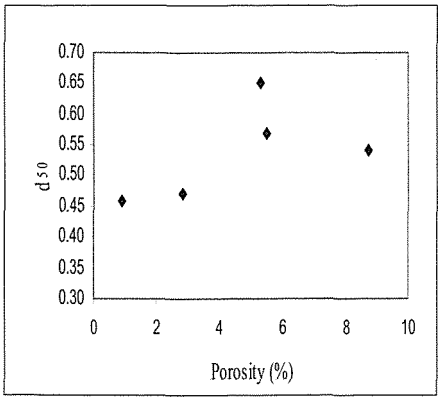

Fig. 8. The relation between porosity and d_{50}.

4.2 Multiple Regression Analysis

To develop the prediction equations having strong correlation coefficients for the d_{50}, the multiple regression analysis including three variables was performed. The alternative models produced are given following:

$$d_{50} = -2.28 - 0.001\sigma_c + 1.08\gamma + 0.059n \quad (1)$$

$r^2 = 0.999$

$$d_{50} = -2.33 - 0.016\sigma_t + 1.11\gamma + 0.059n \quad (2)$$

$r^2 = 0.916$

$$d_{50} = -2.76 - 0.018SHV + 1.52\gamma + 0.095n \quad (3)$$

$r^2 = 0.882$

$$d_{50} = -1.36 - 0.011I_s + 0.73\gamma + 0.042n \quad (4)$$

$r^2 = 0.855$

$$d_{50} = -2.15 - 0.134V_p + 1.18\gamma + 0.054n \quad (5)$$

$r^2 = 0.956$

where d_{50} is the mean particle size (mm), σ_c is the uniaxial compressive strength (MPa), σ_t is the uniaxial compressive strength (MPa), SHV is the Schmidt hammer value, I_s is the point load index (MPa), V_p is the P-wave velocity (km/s), γ is the density (g/cm^3) and n is the porosity (%).

As shown in Eqs.(1-5), all multiple regression models have very high correlation coefficients. Since the index tests are easy to carry out, economical and suitable for the field use, the derived equations including Schmidt hammer value point load index and P-wave velocity are valuable.

5 CONCLUSIONS

Five different igneous rocks including granite, basalt and andesite were tested in the laboratory and the relations between the d_{50} and physico-mechanical properties were investigated. The simple regression analysis showed that there were no correlations between the d_{50} and physico-mechanical properties However, as a result of multiple regression analysis, the prediction equations having strong correlation coefficients were developed for the d_{50}.

Concluding remark is that the d_{50} of igneous rocks can be predicted from the equations developed from the multiple regression analysis especially for preliminary investigations. In addition, the derived equations including index test values are important for the practical consideration. The validity of the derived equations should also be checked for the other rock types.

ACKNOWLEDGEMENT

This study has been supported by the Scientific Research Project Unit of Nigde University, under project number FEB 2008/10.

REFERENCES

Bearman, R.A., Briggs, C.A., Kojovic, T. 1997. The application of rock mechanics parameters to the prediction of comminution behavior, *Minerals Engineering*, 10, pp.255-264.

Deniz, V., Balta, G., Yamık, A. 1996. The interrelationships between bond grindability of coals impact strength index, point load index and friability index, *Proceedings of the 6th International Mineral Processing Symposium*, Kuşadası, Turkey, pp.15-19.

Deniz, V., Ozdag, H. 2003. A new approach to Bond grindability and work index: dynamic elastic parameters, *Minerals Engineering*, 16, pp. 211-217.

Ozkahraman, H.T. 2005. A meaningful expression between Bond work index, grindability index and friability value, *Minerals Engineering*, 18, pp. 1057-1059.

Şengün, N., Umucu, Y., Altındag, R., Deniz, V., Çayırlı, S., Oğuz, B. 2006. Kayaçların aşınma indeks değerlerinin fiziko-mekanik özelliklerle olan etkileşimlerinin değerlendirilmesi, *VIII. Bölgesel Kaya Mekaniği Sempozyumu*, İstanbul, Türkiye, pp.315-320.

Su, O., Akçın, N.A., Toroğlu, I. 2004. Kömürün öğütülebilirliği ile dayanım ve indeks özellikleri arasındaki ilişkiler. *Türkiye 14. Kömür Kongresi Bildiriler Kitabı*, pp. 77-86.

Tiryaki B. 2005. Practical assessment of the grindability of coal using its hardness characteristics, *Rock Mech. Rock Eng.*, 38 (2), pp. 145-151.

The Effect of $BaCO_3$ Addition on the Sintering Behavior of Lignite Coal Fly Ash

B. Ersoy, T. Kavas, A. Evcin, S. Başpınar, A. Sarışık
Afyon Kocatepe University, Engineering Faculty, Afyonkarahisar

S. Dikmen
Anadolu University, Applied Science Faculty, Eskişehir

ABSTRACT The effect of $BaCO_3$ (witherite) addition on the sintering behavior of lignite coal fly ash taken from the Seyitömer power plant of Kütahya/Turkey were examined at temperatures of 1100, 1150 and 1200°C in air atmosphere. Bloating of the fly ash samples sintered at 1150°C was prevented, that is, the decomposition temperature of $CaSO_4$ in the fly ash is shifted to a higher temperature, and their physico-mechanical properties (porosity, water absorption, bulk density and bending strength) were improved with $BaCO_3$ addition. Positive effects of $BaCO_3$, however, were not seen on the fly ash samples sintered at 1100°C. All the fly ash samples sintered at 1200°C were bloated due to the gas evolving and also they melted. During the thermal treatment at 1150°C a phase transformation from $CaSO_4$ (anhydrite) to $BaSO_4$ (Barite) occurred in the fly ash with $BaCO_3$ addition as seen from the X-ray diffraction (XRD) patterns and the bar shaped fly ash samples with $BaCO_3$ saved their structural integrity up to 1150°C.

ÖZET: Bu çalışmada Seyitömer termik santrali uçucu külünün 1100, 1150 and 1200°C'de sinterlenme davranışına $BaCO_3$ (witherite)'ın etkisi incelenmiştir. 1150 ^{0}C'de sinterlenen uçucu külün $CaSO_4$ içeriğinden dolayı meydana gelen yapısal bozunması (şişme) daha yüksek sıcaklığa ötelenmiş ve buna parallel olarak pişmiş ürünün fiziko-mekanik özellikleri (porozite, su emme, bulk yoğunluk ve eğilme dayanımı) iyileştirilmiştir. Fakat $BaCO_3$'ın olumlu etkisi 1100 ^{0}C'de görülmemiştir. 1200 ^{0}C'de sinterlenmiş numunelerin tamamı gaz çıkışı nedeniyle şişmiş ve erimişlerdir.1150 ^{0}C'deki ısıl işlem sırasında meydana gelen $CaSO_4$ (anhydrite) - $BaSO_4$ (Barite) faz dönüşümü $BaCO_3$ katkısıyla engellenmiş olup, bu durum xrd analizleriyle de desteklenmiştir. Sonuçda 1150 ^{0}C'de sinterlenen witerit katkılı çubuk numuneler yapısal bütünlüğünü korumuştur.

1. INTRODUCTION

Fly ash is the finely divided mineral residue resulting from the combustion of pulverized coal in thermal power plants. Every year a large quantity of fly ash is produced in the world. For instance,

only in Turkey more than 13 million tons of fly ash is produced annually and this amount is expected to reach 50 million tons per year by 2020 (Tütünlü, F., et.al. 2001; Özdemir, O., et.al. 2002). But, only a small amount of this waste fly ash in Turkey approximately 1 % is reused in construction industry particularly cement industry (Özdemir, O., et.al. 2001), the rest is disposed into ash dumps or landfill which is an inconvenient solution both from the environmental and economical point of view. Reusing ratio of fly ash generated in all the world is about 10-20 % of the total amount (Iyer, RS., et.al. 2001). Numerous studies have been performed in order to find out application areas for the waste fly ash. It has been pointed out that fly ash can be used as additive in cement industry (Sebök, T., et.al. 2001; Kula, İ., et.al. 2001; Alonso, JL., 1991) and building industry for brick making (Yılmaz, S., et.al. 1997; Pirmaksa, K., et.al. 2000; Kayali, O., 2005), for glass (Erol, M., 2000; Sheng, J., et.al. 2003; Sheng, J., 2001; Peng, F., et.al. 2004), light weight materials (Kumar, S., 2003; Ikeda, et.al. 1990), ceramic tableware and artware (Mukherji, SK., et.al. 1993), mullite (Hwang, JY., et.al. 1994), composite materials (Yıldırım, Ms., et.al. 1996), and sintered material (Ilic, M., et.al. 2003) production.

The fly ashes collected by electrostatic precipitators of power plants are usually finely sized (less than 100 μm) and spherical shaped particles, and consists of SiO_2, Al_2O_3, Fe_2O_3 as major components and alkali and earth alkali metal oxides (i.e. Na_2O, K_2O, CaO, MgO) (Alonso, JL., 1991). For this reason, sintering seems to be the most suitable way to convert the fly ash to useful fired products. The sintering behavior of powder materials such as fly ash is dependent on its chemical and mineralogical composition, physical properties i.e. particle size, shape, and thermal treatment conditions (Pirmaksa, K., 2000; Ilic, M., 2003; Rahaman, MN., 1995). Actually chemical and mineralogical components and physical properties of fly ashes vary depending on coal type (i.e. anthracite, bituminous coal, lignite and sub-bituminous coals) and combustion conditions of pulverized coal (i.e. dry combustion (1100–1400°C), high temperature combustion (1500–1700°C) and fluidized bed combustion (<900°C) and fly ash collection operations (i.e. cyclone, electrostatic precipitation, bag filters) (Alonso, JL., 1991;Ilic, M., 2003; Bayat, O., 1998). As a result, it is expected that the sintering behavior of each fly ash may be different from each other. Therefore, sintering behavior of each type fly ash needs to be investigated. On the other hand, sintering behavior becomes more important according to new approach of the production of bricks from 100% fly ash (Pirmaksa, K., et.al. 2000; Kayali, O., 2005). This approach is seemed to be a good way for consumption of the enormous fly ash waste and environmental protection. However, the existence of alkaline and alkaline earth metal salts such as $CaSO_4$ in ceramic raw materials might damage fired ceramic product (i.e.brick)'s structure due to its thermal decomposition during firing (Yılmaz, S., et.al. 1997; Ilic, M., et.al. 2003; Kingery, WD., 1960) and additionally the temperature of decomposition of $CaSO_4$ is lowered in the presence of SiO_2 (Ingo, GM., et.al. 1998).

$BaCO_3$ has many major commercial applications in glass, ceramic and building industries for various purposes i.e. fluxing agent, prevent the efflorescence

(Toydemir, N., 1991; Patnaik, P., 2002; Kingery, WD., 1960). Objective of this study is to see how $BaCO_3$ affects the sintering behavior of the Seyitömer fly ash including $CaSO_4$ (anhydrate) at relatively high temperatures of 1100, 1150 and 1200°C.

2. EXPERIMENTAL PROCEDURES

The fly ash used in the experiments was taken from the electrostatic precipitator bag of Seyitömer Power Station in Kütahya-Turkey, burning the pulverized lignite coal. Its chemical analysis by EDXRF (Energy-dispersive x-ray fluorescence) spectrometry technique (Spectro X-LAB 2000), carbon content using combustion and IR absorption technique (Multilab - CS Determinator), particle size using laser diffraction method (Malvern Mastersizer 2000), specific surface area using N_2 gas adsorption method by BET (Micromeriticies Gemini 2360) and specific gravity using helium-picnometer (Micromeriticies Autopycnometer 1320) were carried out. These analyses are given in Table 1. According to ASTM C618, which considers basically the chemical components of fly ash, the Seyitömer fly ash is a class F (SiO_2 + Al_2O_3 + $Fe_2O_3 \geq 70$ wt %) fly ash [34].

Table 1. Chemical composition and some physical properties of the Seyitömer fly ash (as- received).

Component	*wt %*
SiO_2	53,1
Al_2O_3	19,2
Fe_2O_3	10,4
CaO	4,6
K_2O	1,8
MgO	3,9
Na_2O	0,8
SO_3	3,0
LOI	3,2
Total	100
Specific Gravity (g/cm^3)	2,08
Carbon (wt %)	1,47
Specific Surface Area (m^2/g)	0,182
Particle Size (μm)	
D90	92
D50 (average particle size)	64
D10	16

LOI: Loss On Ignition

$BaCO_3$ (0,5 and 10 wt %) was added into the fly ash and the mixture was wet ground in a ball mill using alumina balls for 3 h. Subsequently, 10 ml of sample was taken from each suspension and their average particle size distributions were between 8,1–8,4 μm (Mastersizer 2000). The ground suspensions were dried in an oven at 105°C for 5 h and then passed from a blender for 10 min to comminute. Water was added into the powdered samples at the ratio of 15 wt % for shaping and then mixed. The moistened samples were passed from a sieve of 355 μm to obtain granulated particles. The bar shaped samples (or representative bricks) in dimensions of 10x10x50 mm were uniaxially pressed under the load of 98 MPa and dried at room temperature for two days followed by determining dimensions and weight of the samples. The samples were sintered at 1100, 1150 and 1200°C in air atmosphere with the heating rate of 240°C/h for 1 h in an electrical furnace. The cooling rate was 240°C/h. After firing linear shrinkage (%) of the samples were determined. Then, water absorption tests according to Archimedes principle were applied on the sintered samples and water absorption (wt %), bulk density (g/cm^3) and apparent porosity (vol. %) of the samples were calculated. Three-point bending strength was measured with 35 mm span length at the cross-head speed of 1mm/min (Instron 1150). In order to clarify the effect of $BaCO_3$ addition on the sintering behavior of the

fly ash, XRD (Rigaku miniflex) and electron microscopy (SEM, Leo-1430 VP) techniques were used.

3. RESULTS AND DISCUSSION

3.1. Appearance

The photographs of the fly ash samples without and with BaCO3 additive (5 and 10 wt %) sintered at 1100, 1150 and 1200 0C are seen in Fig.1. The photographs shows that considering their appearance; **(i)** all samples (without additive and with $BaCO_3$ additive) sintered at 1200°C were bloated totally due to the gas evolving and lost their structure entireness. A melting for the all samples is clearly seen at this temperature. That is, three separate bar shaped samples exist before firing but they turned a single piece after firing possibly as a result of melting as seen from the Fig. 1. Moreover, with increasing the amount of $BaCO_3$ additive, melting was promoted due to its fluxing effect. While the vitrified samples without $BaCO_3$ had heterogeneous large porous the $BaCO_3$ added samples resulted in samples with a small sized and homogenous porous caused by fluxing effect of $BaCO_3$. On the other hand homogeneity differences on the surfaces of both samples possibly dependent on unique decomposition behavior of $CaSO_4$ and $BaSO_4$ in the samples. Previous study indicated that thermal decomposition kinetics of metal sulphates vary significantly (L'vov, BV., et.al. 2004). Fluxing effect of barium in

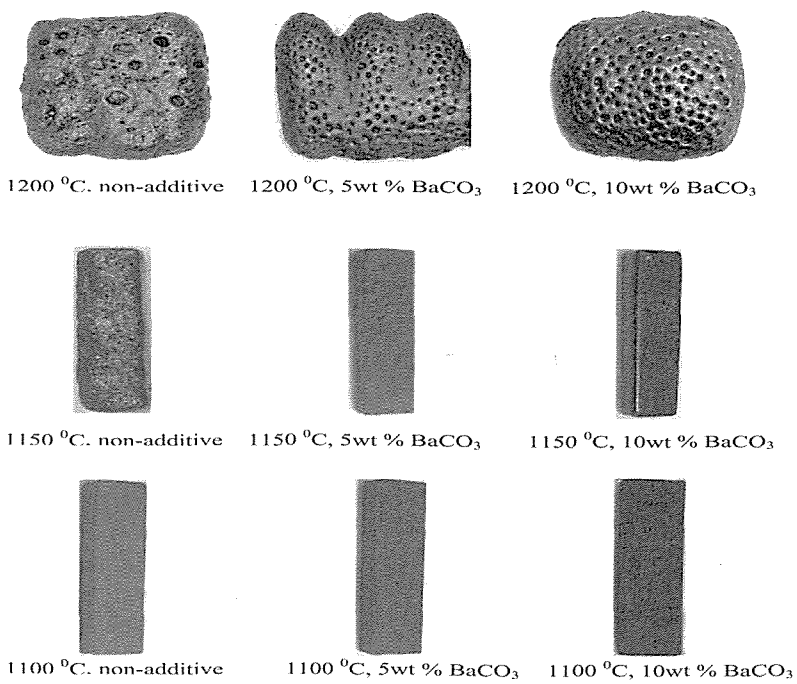

Figure 1. Photographs of the fly ash samples without and with $BaCO_3$ additive (5 wt and 10 wt %) sintered at 1100, 1150 and 1200°C for 1 h. (Note: For the sintered samples at 1200°C, there were 3 separate bar shaped samples in each formulation before the heat treatment, but after the heat treatment they became such a single piece of form as seen up).

production of ceramic and glass materials is also reported elsewhere (Peng, F., et.al. 2004; Toydemir, N., 1991). **(ii)** At 1150°C and under the working conditions, the samples with $BaCO_3$ additive saved their structural integrity, whereas the non-additive sample was bloated wholly because of the presence of $CaSO_4$ in the as-received fly ash as will be explained later. Moreover, a partly melting or liquid phase formation on the sample surface started. Especially, the surface of the sintered sample with 10 wt % $BaCO_3$ additive had a very smooth and a glassy appearance. (iii) At 1100°C, a significant difference on their structure was not seen, but only their color was getting darker with increasing the amount of additive.

3.2. Phase Analysis

X-ray diffraction patterns of the Seyitömer fly ash (as-received) and all the sintered fly ash samples are given in Fig. 2. The Seyitömer fly ash consists of those phases: quartz (SiO_2), hematite (Fe_2O_3), anorthite ($CaAl_2Si_2O_8$) and anhydrite ($CaSO_4$). After the sintering at 1100°C, in the non-additive sample cristobalite which is a high temperature phase of quartz and spinel [$Mg,(Al,Fe)_2O_4$] phases were occurred while the intensity of quartz peak was diminished. Moreover, cristobalite formation from quartz with increasing the temperature is encountered in the all sintered samples. Similar results on cristobalite formation have been obtained for different coal fly ashes (Ilic, M., et.al. 2003; Mollah, MYA., et.al. 1999). With

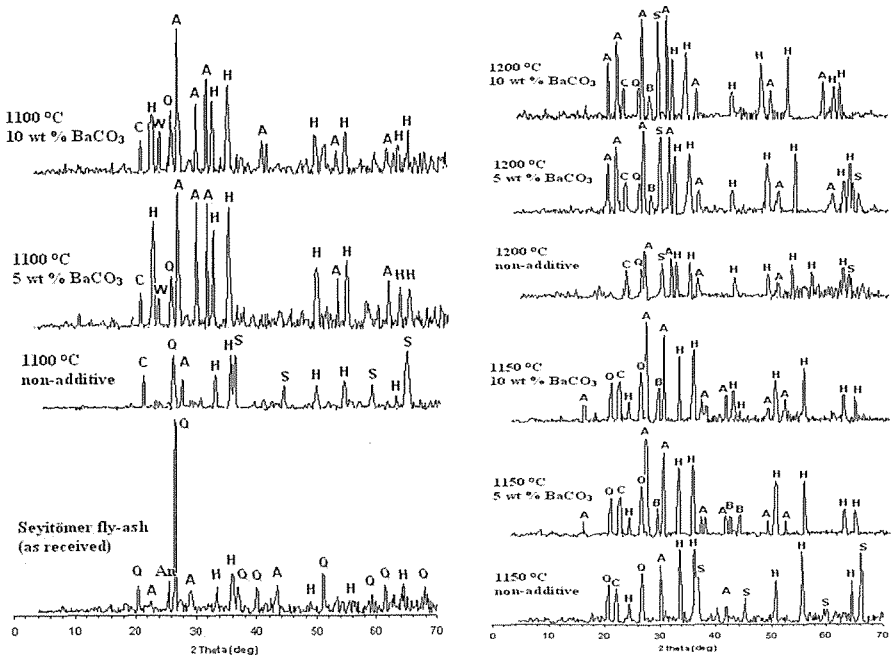

Figure 2. XRD patterns of the Seyitömer fly ash (as-received) and the fly ash samples without and with $BaCO_3$ additive sintered at 1100 and 1150 and 1200°C for 1 h. [Q:Quartz, H:Hematite, A:Anorthite, An:Anhydrite, C:Cristobalite, S:Spinel, W:Witherite, B:Barite]

$BaCO_3$ addition, peak intensities coming from anorthite and hematite increased and also witherite ($BaCO_3$) peaks were seen (Fig. 2). When considered the presence of witherite at 1100°C this might be expressed that this temperature is insufficient to occur barite through ion exchange between Ba^{+2} in witherite and Ca^{+2} in anhydrite.

Even though the anhydrite phase is present in both the as-received and the non-additive samples sintered at 1100°C, after their heat treatment at 1150°C it was disappeared as seen in Fig.2. This is due to the decomposition of anhydrite which leads to bloating of the non-additive sample. The bloating and also swelling of the sample sintered at 1150°C results from the evolved gases such as SO_2, SO_3 and O_2 during the thermal decomposition reaction of anhydrite. According to the literature (Ingo, GM., et.al. 1998) this reaction with two steps may be given as; $CaSO_4 \rightarrow CaO + SO_3$; $SO_3 \rightarrow SO_2 + ½\ O_2$

Essentially, pure anhydrite remains stable up to 1240°C in an atmosphere of air, but in the presence of 25 wt % SiO_2 the temperature of thermal decomposition of anhydrite $CaSO_4$ is lowered to about 1120°C (Ingo, GM., et.al. 1998). Similarly, Merwe et al. (1999) determined that Fe_2O_3 has a reducer effect on the decomposition temperature of anhydrite ($CaSO_4$) as in the case of alone. However, $BaCO_3$ addition caused a phase transformation from anhydrite ($CaSO_4$) to barite ($BaSO_4$) due to the exchange between Calcium and Barium in the sample during the sintering. Accordingly, $BaSO_4$ peaks are seen in Fig.2. As a result, it is assumed that $BaSO_4$ shows a better stability against to thermal decomposition at 1150°C than $CaSO_4$ under the working conditions. Therefore, the bar shaped samples with $BaCO_3$ additive saved their structural integrity at 1150°C (see Fig. 1) implying that bloating and swelling was inhibited by means of $BaCO_3$ addition. In other words, the decomposition temperature of $CaSO_4$ was shifted to a higher temperature above 1150°C.

After the sintering at 1200°C, the $BaSO_4$ peaks are also disappeared because of the decomposition of $BaSO_4$, whereas the peaks are seen at 1150°C (Fig.2). Indeed, it is reported that according to the XRD patterns the thermal stability of nearly pure $BaSO_4$ is above 1200°C (Torres J., et.al. 1999), which is sintered under the argon atmosphere, but in the presence of fly ash which includes fluxing metal oxides i.e., Na_2O, K_2O as well as complex mineralogical structure the thermal stability of barite might be decreased, e.g. anhydrite at 1150 °C. Consequently, both of the metal sulfates in the fly ash were decomposed at 1200 °C which leads to totally bloating of the sintered samples (see Fig.1).

3.3. SEM Investigations

The SEM micrographs taken from the fracture surface of the samples sintered at 1100 and 1150°C are given in Fig.3a and b, respectively. In general, the samples were poorly sintered at 1100°C comparing with the samples sintered at 1150 °C. This may be attributed to the heterogeneous packing of the fly ash powders. Likewise, Ilic et al (2003) reported poor sintering behavior of a fly ash without additive at 1130°C. At 1100°C, larger pores are seen in the samples containing $BaCO_3$ when compared with non-additive samples, however, pore amount and size distribution of both the samples with 5 and 10 wt % $BaCO_3$ were close to each other.

The structure of the non-additive samples sintered at 1150°C was totally bloated and expanded owing to gas evolving during thermal decomposition of anhydrite as mentioned above. As known from the literature (Rahaman, MN., 1995) some compounds become oxidized (or decomposed), generating gases as SO_3, CO_2, CO that are insoluble in the solid and the pressure of the gases can be sufficiently high to produce void in the solid. On the other hand, the sintering capability of the samples increased with $BaCO_3$ addition and consequently the amount of (open or apparent) pore of the sample reduced as supported by Fig.3b. This may results from the occurring of liquid phase and also promoting it with further increasing of $BaCO_3$ having fluxing property. The best sintering capability of the sample was obtained by 10 wt % $BaCO_3$ addition as seen from Fig.3b. In addition, in the SEM micrograph of 10 wt% $BaCO_3$ additive sintered at 1150°C fly ash only some spherical isolated (closed) pores which indicates enhancement of the microstructural property (reduced porosity or water absorption, and increased bulk density and bending

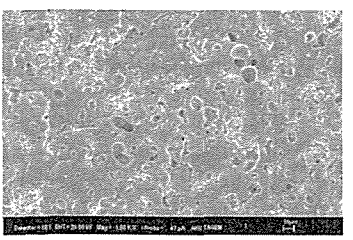

1100°C, non-additive

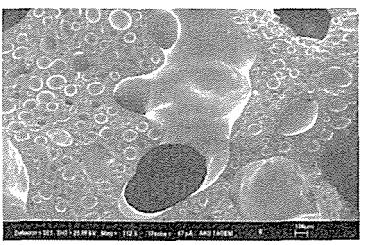

1150°C, non-additive

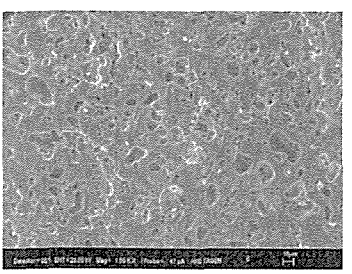

1100°C, 5wt % $BaCO_3$

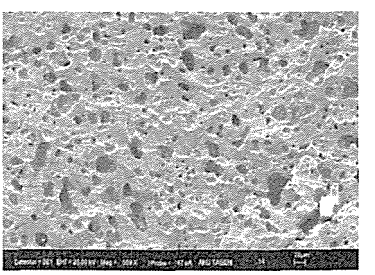

1150°C, 5 wt % $BaCO_3$

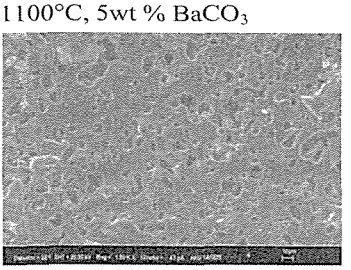

1100°C, 10 wt % $BaCO_3$

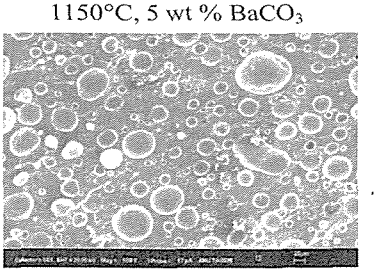

1150°C, 10 wt % $BaCO_3$

Figure 3. SEM micrographs of the fly ash samples without and with $BaCO_3$ additive (5wt and 10wt %) sintered at 1100 and 1150 ^{0}C for 1 h.

strength) with this ratio of the additive.

3.4. Physico-Mechanical Tests

In order to check the obtained results from the SEM and XRD analysis, some physico-mechanical tests were applied on the sintered samples. But those tests were not to be applied on the samples sintered at 1200°C due to their unsuitable forms as mentioned before (see Fig.1). The variation of water absorption (wt %) (Fig.4a), apparent (or open) porosity (% Vol) (Fig.4b), bulk density (g/cm^3) (Fig.4c) and bending strength (MPa) (Fig.4d) of the samples sintered at 1100 and 1150°C versus $BaCO_3$ addition (wt %) are given in Fig.4. At 1100°C, water absorption increases slightly with $BaCO_3$ addition but the further addition did not importantly affect the sintering behavior of the fly ash. At 1150°C, water absorption suddenly decreases to 2% ratio at 5 wt % $BaCO_3$, and to zero at 10 wt % $BaCO_3$ additions (Fig. 4a). Fig.4b shows that the apparent porosity (vol. %) of the sample sintered at 1100°C increased gradually while that of the samples sintered at 1150°C reduced sharply with $BaCO_3$ addition. As explained before the sharp decrease at 1150°C may results from the inhibiting of the bloating and the swelling due to the $BaSO_4$ formation, while the reason the small increase in the open porosity at 1100°C is unclear. The further addition resulted no significant change on the porosity of the sample sintered at 1100°C while that brings the porosity to zero after sintering at 1150°C. The amount of water absorption is a natural result of the amount of apparent porosity (Kingery, WD., 1960; Harnandez, MS., et.al. 2001). So, the porosity curves have exactly the same trends with the water absorption curves which indicates that when the apparent porosity increases (or decreases) the water absorption also increases (or decreases). The maximum porosity (as ~20 %) was obtained from the non-additive fly ash sample sintered at 1150°C due to the wholly decomposition of anhydrite present in the sample and the minimum porosity (as ~0 %) was obtained by the sample with 10 wt % BaCO3 additive sintered at 1150°C because of the good sintering process as well as the phase transformation from anhydrite to barite. The porosity results

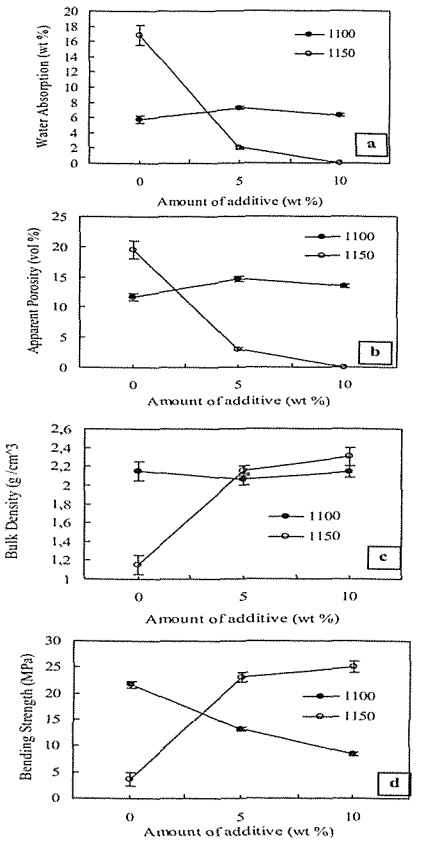

Figure 4. The variation of water absorption wt% (a), apparent porosity % (b), bulk density g/cm^3 (c), bending strength (MPa) (d) and linear shrinkage (e) of the samples sintered at 1100 and 1150°C versus $BaCO_3$ addition wt%.

for 1150°C in Fig.4b are in accordance with the photographs (Fig.1), the SEM micrographs (Fig. 3b) and the XRD patterns (Fig.2).

$BaCO_3$ addition significantly enhanced the bulk density at 1150°C whereas it causes to a little decrease in the bulk density at 1100°C (Fig.4c) agreeing with the results of apparent porosity and water absorption. As well known, bulk density is one of the most important properties of pressed powder since it directly influences bending strength, porosity, linear shrinkage and water absorption (Pirmaksa, K., et.al. 2000; Rahaman, MN., 1995). The highest (~2,3 g/cm^3) and the lowest (~1,2 g/cm^3) density in the experiments were obtained at the sintering temperature of 1150°C with the samples of 10 wt % $BaCO_3$ additive and the non-additive samples due to minimum and maximum apparent porosity, respectively. On the other hand, Yılmaz at. al. (1997) obtained ~1,7 g/cm^3 of bulk density at 1100°C for 1h using the seyitömer fly ash very similar to our fly ash samples, and this result is lower from the result ~2,1 g/cm^3 obtained in this study. This may be attributed to the differences, during the sample preparation i.e the moistened ratio of granulated powders which can lead to difference compacting causing different final density (Pirmaksa, K., et.al. 2000).

The variation of mechanical strength as bending strength of the sintered samples versus the amount of $BaCO_3$ additive is given in Fig.4d. The addition promotes the strength at 1150°C while it leads to decrease in the strength at 1100 0C similar to the bulk density. The highest strength (~25 MPa) was obtained with the sample of 10 wt % $BaCO_3$ additive sintered at 1150°C accompanying a decrease in the porosity and increase in the bulk density. These results at 1150°C were supported by SEM micrographs. The physico-mechanical properties of the Seyitömer fly ash with 5 and 10 wt % $BaCO_3$ additive sintered at 1150°C are in acceptable level to produce a fired building materials such as tile according to Turkish Standards adapted to European Norms (TS EN 14411, 2006).

4. CONCLUSIONS

The results of this study can be summarized as the following;

The Seyitömer fly ash without additive was bloated completely when sintered at 1150°C due to the thermal decomposition of anhydrite. $BaCO_3$ additions at levels of 5 and 10 wt % into the fly ash, inhibited the bloating and the swelling as a result of phase transformation from anhydrite ($CaSO_4$) to barite ($BaSO_4$) during sintering as supported by XRD analysis and photographs.

$BaCO_3$ addition had a significant positive effect on the sintering of the fly ash at 1150°C, whereas it indicated a negative effect on the sintering at 1100°C.

The all fly ashes without and with $BaCO_3$ addition sintered at 1200°C are totally bloated due to decomposition of metal sulfates ($CaSO_4$ and $BaSO_4$), and melted at this temperature. The further increase in $BaCO_3$ level leads to a more melting because of its fluxing effect.

Both bloating and swelling problems of the fired ceramic products made from the 100 % fly ashes including anhydrite, fired at about 1150°C, may be solved by $BaCO_3$ addition. Moreover, the reasonable physico-mechanical properties have been obtained from the sample containing 10 wt % $BaCO_3$ and sintered at 1150°C suggesting

the Seyitömer fly ash with the aid of $BaCO_3$ could be utilized as a possible raw material to produce fired ceramic materials.

REFERENCES

Alonso, JL, Wesche, K, 1991 Characterization of fly ash, in: Wesche K. editor. Fly ash in concrete (properties and performance), E&FN Spon/Chapman&Hall,

ASTM C 618, 1997, (American society for testing and materials). Fly ash and raw or calcined natural pozzolan for use as, mineral admixture in portland cement concrete, Philadelphia, PA ASTM,

Bayat, O, 1998 Characterization of Turkish fly ashes, Fuel 77 (9/10):1059-66.

Erol, M, Genç, A, Öveçoğlu, ML., Yücelen, E, Küçükbayrak, S, Taptık, Y, 2000, Characterization of a glass-ceramic produced from thermal power plant fly ashes. J Eur Ceram Soc 20:2209-214.

Hernandez-Crespo, MS., Rincon, JMa, 2001, New porcelainized stoneware materials obtained by recyling of msw incinerator fly ashes and granite sawing residues. Ceram.Int. 27:713-20.

Hwang, JY., Huang, X, Hein, AM., 1994, Synthesizing mullite from beneficiated fly ash. JOM, May 36-39.

Ilic, M, Cheeseman, C, Sollars, C, Knight, J, 2003, Mineralogy and microstructure of sintered lignite coal fly ash. Fuel 82:331-36.

Ikeda, K, Tomisaka, T, 1990, Physical properties of fgl, novel porous materials prepared from fly ash, gypsum and lime with special emphasis to the thermal conductivity. in: Proceedings Silicer'90 Silicate Ceramics, Ceramic Forum International, Nürnberg, p. 84-91.

Ingo, GM., Chiozzini, G, Faccenda, V, Bemporad, E, Riccucci, C, 1998, Thermal and microchemical characterizations of CaSO4-SiO2 investment materials for casting jewellery alloys. Thermochim. Acta 321:175-83.

Iyer, RS, Scott, JA., 2001, Power station fly ash-a review of value-added utilization outside of the construction industry. Resour Conserv & Recycl. 217-28.

Kayalı, O, 2005, High performance bricks from fly ash, International Ash Utilization Symposium, (http://www.flyash.info/2005/1kay.pdf)

Kingery, WD., 1960, Introduction to ceramics. John Wiley & Sons.Inc, New York,

Kula, İ, Olgun, A, Erdoğan, Y, Sevinç, V., 2001, Effects of colemanite waste, coal bottom ash, and fly ash on the properties of cement. Cem. Concr. Res. 491-94.

Kumar, S, 2003, Fly ash-lime-phosphogypsum hollow blocks for walls and partitions. Build. Environ. 38:291-95.

L'vov, BV., Ugolkov, VL., 2004, Kinetics of free-surface decomposition of magnesium and barium sulfates analyzed thermogravimetrically by the third law method. Thermochim. Acta 411:73-9

Merwe, EM., Strydom, CA., Potgieter, JH., 1999, Thermogravimetric analysis of the reaction between carbon and CaSO4.2H2O, gypsum and phosphogypsum in an inert atmosphere. Thermochim. Acta 340-341: 431-37.

Mollah, MYA., Promreuk, S, Schennach, R, Cocke, DL., Güler R, 1998, Crystobalite formation from thermal treatment of Texas lignite fly ash. Fuel 78:1277-282.

Mukherji, SK., Machhoya, BB., Savsani, RM., Vyas, DR., Dan, TK., 1993, The utilization of fly ash in the preparation of ceramic tableware and artware. British Ceram Trans. 92 (6): 254-57.

Özdemir, O, Çelik MS., 2002, Characterization and recovery of lignitic fly ash by products from the Tunçbilek Power Station. Canadian Metallurgical Quarterly; 41(2): 143-50.

Özdemir, O, Ersoy, B, Çelik, MS., 2001, Separation of pozzolonic material from lignitic fly ash of Tunçbilek power station, International Ash Utilization Symposium, Utah-USA, (www.flyash.info/2001/benef1/45ozdem.pdf).

Patnaik, P, 2002, Handbook of Inorganic Chemicals. Mc-Graw Hill, New York,

Peng, F, Liang, K, Hu, A, Shao, H, 2004, Nano-crystal glass-ceramics obtained by crystallization of vitrified coal fly ash. Fuel 83:1973-77.

Pirmaksa, K, Wilhelm, M, Wruss, W, 2000, A new approach to the production of bricks made of 100 % fly ash. Tile&Brick Int. 16 (6): 428-31.

Rahaman, MN., 1995, Ceramic Processing and Sintering, Marcel Dekker Inc., New York,

Sebök, T, Simonik, J, Kulisek K., 2001, The compressive strength of samples containing fly ash with high content of calcium sulfate and calcium oxide. Cem. Concr. Res. 1101-107.

Sheng, J, Huang, BX, Zhang, J, Zhang, H, Sheng, J, Yu, S, Zhang, M, 2003 Production of glass from coal fly ash. Fuel 82:181-85.

Sheng, J, 2001, Vitrification of borate waste from nuclear power plant using coal fly ash. (I) Glass formulation development, Fuel 80, 1365-69

Toydemir, N, 1991, Ceramic Building Materials (in Turkish). ITU-Publishing Center,

Torres, J, Mendez, J, Sukiennik, M, 1999, Transformation enthalpy of the alkali-earths sulfates (SrSO4, CaSO4, MgSO4, BaSO4). Thermochim. Acta 334:57-66.

TS EN 14411, 2006, Ceramic tiles-definitions, classification, characteristics and marking .

Tütünlü, F, Atalay Ü, 2001, Utilization of fly ash in manufacturing of building bricks. International Ash Utilization Symposium, Utah-USA, (http://whocares.caer.uky.edu/wasp/AshSymposium/AshLibraryAgenda.asp).

Yılmaz, S, Sen, S, Günay, V, Özkan, OT., 1997 Utilisation of power fly-ash as a building material. Tile&Brick Int. 3 (4): 297-00.

Yıldırım, MS., Yaşar, B, Cengiz, Y, 1996, Utilization of fly ash polypropylene waste in the production of a new porous composite material. J Porous Mater. 3:189-91.

An Example of the Application of Digital Image Processing Methods to Mineral Processing: Determination of Particle Size of Akpınar Quartz Sands

Dijital Görüntü İşleme Yöntemlerinin Cevher Hazırlamada Uygulamasına Bir Örnek: Akpınar Kuvars Kumlarının Tane Boyutlarının Belirlenmesi

Ilgin Kursun, Kagan Ozdemir

Istanbul University, Engineering Faculty, Mining Engineering Department, 34320, Avcılar, Istanbul, Turkey

ABSTRACT The determination of particle size distribution for several raw materials used in glass, cement, paper, plastic and ceramic industries and mineral processing operations which is reduced to small sizes through size reduction operations is important nowadays. During many stages of mining which includes successive operations, a proper identification of particle size distribution from blasting to mineral processing is important in terms of productivity and economy. By the recent development of computer and image obtaining technologies, the useage of digital image processing as a measurement tool has been popular. Digital image processing methods used in mineral processing are being employed in terms of saving time and providing accurate data. Operating at the same productivity level as conventional mineral processing methods and presenting the same results in far shorter time, these methods have proven themselves in the field of mineral processing. Within the scope of this study, a comparison on the results of sieve analysis and digital image processing technique was conducted in order to determine the size distribution of the sand samples taken from a private mining company in the district of Kemerburgaz-Akpınar. The P_{50} and P_{80} values of particle size distribution were obtained by using both methods and the results were compared and interpreted. As a result of analysis, both particle size distribution results of sieve and digital image processing methods are found out to be similar. Evaluating the results, it is understood that the digital image processing method can be used as a tool for assessing particle size distribution in mineral processing.

ÖZET Boyut küçültme işlemleri sonucunda, ince boyutlara indirilmiş cam, çimento, kâğıt, plastik, seramik endüstrilerinde ve cevher zenginleştirme işlemlerinde kullanılan

çeşitli hammaddelerinin boyut dağılımlarının belirlenmesi günümüzde önemli bir yer tutmaktadır. Ardışık işlemlerden oluşan madenciliğin pek çok evresinde patlatmadan cevher hazırlamaya tane boyut dağılımın doğru bir şekilde belirlenmesi gerek verimlilik gerekse ekonomiklik açısından önemlidir. Özellikle son yıllarda bilgisayar teknolojisindeki gelişmelere paralel olarak görüntü alma teknolojisin gelişmesi, görüntü işleme metotlarının ölçüm ve gözlem yöntemi olarak çeşitli disiplinlerde kullanımını yaygınlaşmıştır. Dijital görüntü işleme yöntemleri, zaman tasarrufu ve doğru veriler vermek açısından cevher hazırlamada uygulanmaktadır. Bu çalışma kapsamında Kemerburgaz-Akpınar bölgesinde bulunan bir maden ocağından alınan kum numunelerinin boyut dağılımının belirlenmesinde elek analizi yöntemi ile dijital görüntü işleme tekniği sonuçlarının karşılaştırılması yapılmıştır. Bu iki yöntem ile elde edilen d_{50} ve d_{80} değerleri karşılaştırılmış ve yorumlanmıştır. Yapılan analizler sonucunda elek analizi ile dijital görüntü işleme yöntemi ile elde edilen parça boyut dağılımları birbirine yakın değerler göstermiştir. Bu sonuçlardan yola çıkarak dijital görüntü işleme yönteminin, cevher hazırlamada parça boyut dağılımının tespitinde elek analizine alternatif olarak kullanılabileceği anlaşılmıştır.

1. INTRODUCTION

Size distribution, specific weight and specific surface are among important parameters during identification of particulate materials (Rona, D.2006). Each discipline has used methods of particle size measurement depending on their own conditions and priorities. Particle size analysis is a method used during every stage of mineral processing. It is included among chief tools used especially for identification of liberation, design of unit operations such as crushing, grinding, classification and dewatering, performance analysis or control and perception of the process. It is an obligation to conduct particle size analysis for a mineral during each stage from size reduction to classification; from dressing stages based on flotation or specific weight to thickener bottom current and even to identification of the qualities of the final product obtained (Saklara, S.et al. 2000).

Particle size analyses are generally conducted with the use of relatively oversized standard laboratory sieves up to 38 micron. The reason for this is that the method is very simple and economical; and furthermore the material can be divided into its fractions with ease. The main problem of particle size analysis is the analysis of fine particle. Although many methods have yielded reproducible results, there may be some differences among them. There are also advantages and disadvantages resulting from the physical ground on which different methods are used. (Saklara, S. et al..2000). Several methods are employed for determination of size distributions and shape factors of grains. The reliability of these methods applied is of great importance. Since each mineral in the nature has a different shape factor, one may encounter with errors during identification of grain-shape distributions. In parallel with the advance of technology, automatic devices which can carry out quick and precise measurements in very small sizes, have been developed. However, the high cost of these devices is an

handicap to become so much common in use (Kursun, 2009).

Within the scope of mineral processing, the size determination is generally made on the basis of sieve size through which particles can or cannot pass. In the simplest sense, the size distribution can be determined through the use of sieves. When the size or size range of the material is determined through sieves, the 3rd dimension is ignored depending on particle shape factor. Therefore, this sometimes may lead to errors. The sieving through standard sieves in laboratory with the aim of determining the size distribution of the material consisting of grains with different sizes, of finding out the relation between the particle size and its amounts in the sample, i.e. how much material is found in each dimension, is called laboratory sieving. It is the process of sieving according to dimension on the basis of the capabilities of grains to or not to pass through apertures or gaps with certain sizes. The grain size of minerals is highly important for the selection of separation method.

Advanced technology, laser imaging techniques are also being used for size determination. In laser imaging, all three dimensions of the grain are examined and size determination is carried out with ease. In natural materials, particles are rarely spherical. The effect of these particles which are not spherical on different technologies differs and may lead to variations in knowledge about the real properties of the sample. For practices in many fields, there is a need for an insight into the shape of grains as well as their sizes (Ulusoy et al, 2008).

Conventional size determination methods used in mineral processing such as sieve analysis, sedimentation,etc. have tended to be replaced by modern methods like laser diffraction. Also, it is an important alternative to study the practicability of digital image processing methods,which are used in different practices in mining sector, in mineral processing operations.

2. PARTICLE SIZE ANALYSIS BY DIGITAL IMAGE PROCESSING METHOD

An image is the radiation reflected or diffused from an object or scene. Images are stored in computers in the form of sets and they can be obtained from the following resources:

1-From an analogue resource (photographic film, video signal),or

2-Digitally in a direct manner (CCD camera,point-to-point measurement).

The first idea of digital image analysis (or digital image processing) was put forward in 1920s concerning the issue of transmitting the images through cable. The first processing with computer was used in Ranger-7 video images in 1964. These early studies were confined exclusively to space projects especially owing to high costs of imaging systems and computer systems. The first book on image processing method through a computer was written by A. Rosenfeld in 1969 and published by Academic Press. The principle of visual (direct) methods was put forward by sediment petrologists called Wadell and Wright for the first time and studies on this issue have been still progressing. Digital image processors developed for that purpose are powerful computer-based devices which enable the storage of information in more than one area (Makinacı, A et al. 2007).

In parallel with developments in computer technology in recent years,

imaging technology has also developed and image processing techniques have began to be used in different disciplines as measurement methods (Tovey, N. K.. and Hunslow, M.W. 1995) The study of image analysis techniques in geology, engineering geology and rock mechanics started in the last two decades. Especially in different areas which are difficult to measure such as physical properties of rocks and their engineering properties, researchers have considered image analysis methods as an alternative. Research has been conducted under the titles identification of minerals under microscope, determination of void ratio of rocks (porosity), analysis of transients, determination of the limits of minerals, determination of the limits of particles, particle size distribution and formal analysis. Image processing techniques have been also used for determining the sieve analysis of conglomeration of minerals with different sizes. These studies conducted research at a micro-level and made size determination on the images obtained from optical and electron microscope. Jenkins et al (1991) studied the industrial application of the image processing method with the same principle and the effect of particle sizes on refractory magnesite. (Goodchild, J. and S., Fueten, F.(1998).

2.1. Split Desktop Digital Image Analysis System

Split-Desktop software accepts both digital still and video images for analysis. There must be a mechanism (software and/or hardware) for downloading digital or video camera images onto the computer: for digital camera images only camera software is required and for video camera images a framegrabber board is required. The first step for the user is to acquire images in the field and download these images onto the computer. Split-Desktop then assists the user in properly scaling the images. Almost all of the programs accept images in compatible with file formats Jpeg, Tiff, Gif and Bmp (Ozdemir et.al.2003,2007).The basic principles followed by the software Split-Desktop for image processing are as follows:

-Taking images automatically or manually,

-Correcting the lighting-related problems images and preprocessing of unacceptable images for imaging,

-Description of pieces within each digital image processing algorithm,

Coprocessing of several images for average distribution (including the images taken in various sizes). Transferring the outcome data to screen, hard disc and network control systems. As it can be seen from Figure 1, the program opens the original picture in a "Grey Scale" form, i.e. in black and white.

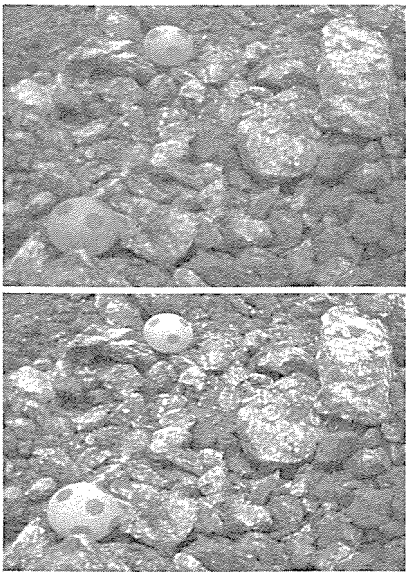

Figure 1. Original and Gray-Scale Image (Özdemir, et al. 2003)

Scaling of Picture: After the picture is transferred to the program, the length of the ball, which has a known length, or another object is entered into the program with the help of scaling bar (Figure 2).

Analysis of Particles : Several sensitivity adjustments are entered and the program is ordered to separate the particles one by one (Figure 3).

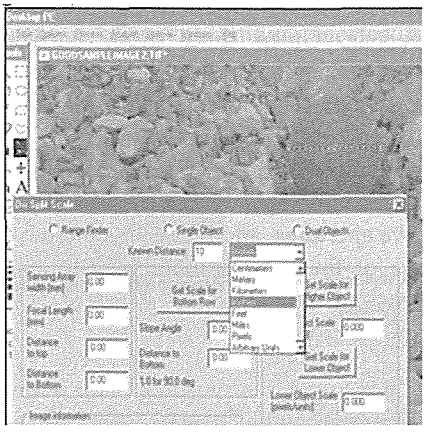

Figure 2. Scaling the image (Özdemir, et al. 2003)

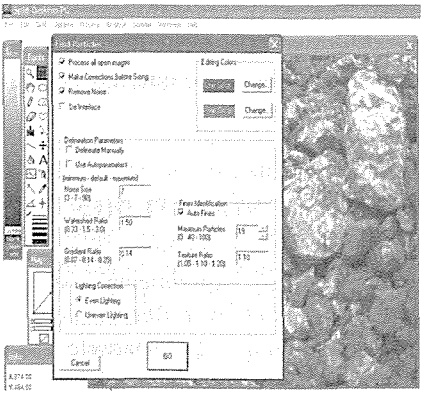

Figure 3. Delineation of the particles (Özdemir, et al. 2003)

The operation of the program is based on the principle of determining the limits among rock particles and measuring their lenghts. Following this operation, the program draws these boundaries among the particles in a two-dimensional form. At this stage, the user enters the color of the boundaries among particles and small substances which are too small to be taken into account into the program.

Correction of Boundaries by the User: Once the program has completed the separation, it provides the user with an opportunity to correct the errors and wrong boundaries. This is one of the most crucial stages of the program. The light of the environment in which the photograph is taken or the quality of the picture may not be decent under all circumstances.

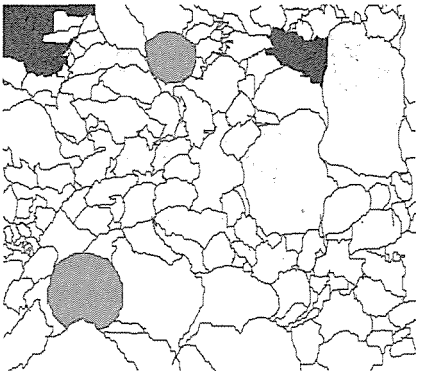

Figure 4. Processed Image (Özdemir, et al. 2003)

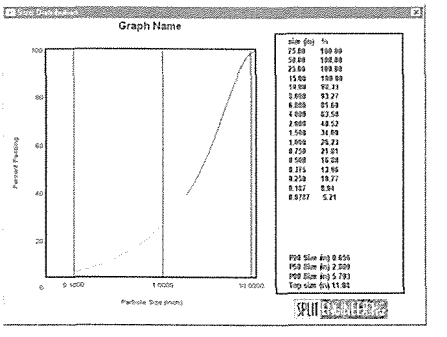

Figure 5 The results of particle size distribution analysis.

That is why the program is not able to perform a complete separation between some pictures. Each processed image should be examined with care, and wrong boundaries and errors should be eliminated by the user. What we have at the end of this operation is the processed picture shown in Figure 4 (Özdemir, et al. 2007).

Formation of Sizes and Reaching to Conclusions: At this stage of the program, the program calculates the size distribution in accordance with the processed picture and provides us with graphical conclusions (Figure 5).

3. SIEVE ANALYSIS

Particle size analysis by means of sieve analyses is one of the oldest methods and one of the most widespread even today. Sieve is accomplished by passing a known weight of sample material successively through finer sieves and weighing the amount collected on each sieve to determine the percentage weight in each size fraction (Bernhardt.,2000). Sieving is carried out with wet or dry materials and the sieves are usually agitated to expose all the particles to the openings (Wills 1985). The mechanical process of sieving consists of two parts:

1) In the first very short time, grains with a major axis smaller than the aperture size will pass through the sieve,

2) The grains with a size close to the size of the aperture are left on the sieve. These grains must be oriented in a particular way in order to pass the sieve or must find larger holes in the sieve (Dalsgaard et.al., 2007).

Sieving, when applied to irregularly shaped particles, is complicated by the fact that a particle with a size near that of the nominal size of the test sieve may pass only when presented in a favourable position. As there is inevitably a variation in the size of sieve sizes, due to irregularity of weaving, prolonged sieving will cause the larger sizes to exert an unduly large effect on the sieve analysis. Given time, every particle small enough could find its way through a very few such holes. The procedure is also complicated in many cases by the presence of "near-size" particles which cause "blinding", or obstruction of the sieve apertures, and reduce the effective area of the sieving medium. Blinding is most serious with test sieves of very small aperture size (Wills 1985).

Sieve analyses presents there major difficulties: with woven wire sieves the weaving process produces three dimensional apertures with considerable tolerances, particularly for fine-woven mesh. The mesh is easily damaged in use. The particles must be efficiently presented to the sieve apertures (Allen 1997).

4 EXPERIMENTAL STUDIES

With the aim of attaining the goals specified, the experimental studies were carried out by different methods for determining the particle size characteristics of Senkoy and Sarikum sand samples and assessing the particle size distribution and the comparison of the results from different methods are done. These samples are used in construction chemicals after they have been exposed to a series of washing and classification operations. It is important to accurately determine both the particle

size distribution of silica sand used in construction chemicals and their shape factor. A chemical analysis of the sand samples used in the experiment indicates that the sample Sarikum consists of 89.4% SiO_2, 2.02 %Fe_2O_3 and 4.2% Al2O3 while the sample Şenköy consists of 88.3% SiO_2, 2.01 %Fe_2O_3 and 4.4% Al2O3. The sample subjected to the experiments was taken from the sand pit of private mining located in the village Akpinar of Kemerburgaz. Satellite photograph of the area is shown in Figure 6.

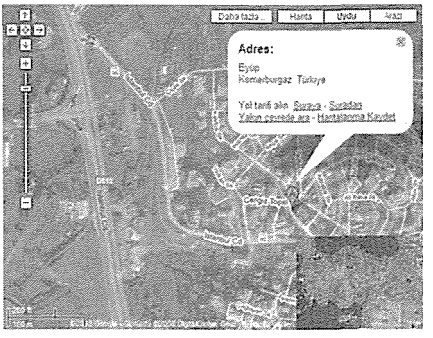

Figure 6. Satellite photograph of the Kemerburgaz-Akpınar

4.1 Sieve Analysis

The samples from Senkoy and Sarikum were exposed to a sieve analysis through the use of sieves from 500 μ to 38 μ with the Ro-Tap for one hour. Undersize-oversize curves of the sand samples are presented in Figure 7 and Figure 8.

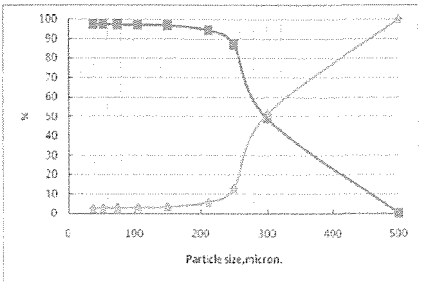

Figure 7. Sieve Analysis of Sarikum

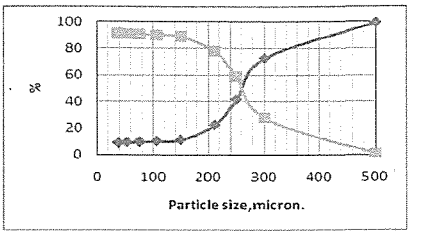

Figure 8.Sieve Analysis of Senkoy

4.2 Application of Split Desktop software for Sarikum and Senkoy Sand Samples

Although Split-Desktop software is used more in assessing the particle size distribution after blasting, it can also be used for samples with fine particle sizes. Since the particle sizes are very small, the photographs should be taken with a scale which can represent the size of the material. In order to analyse Sarikum sand sample in Split, a digital picture of the sample is taken by a digital camera through a microscope. Ruler is used as a scaling object in the image. The original image of Sarikum sample which is loaded into Split Desktop software is given in Figure 9. The image is converted into gray scale image, given in Figure 10. Manually processed image of the scaled image is given in Figure 11 and the result of the image is given in Figure 12.

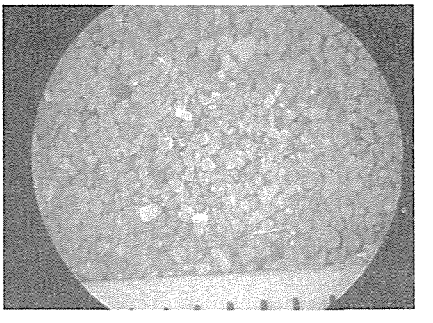

Figure 9. The image of Sarikum sample under microscop.

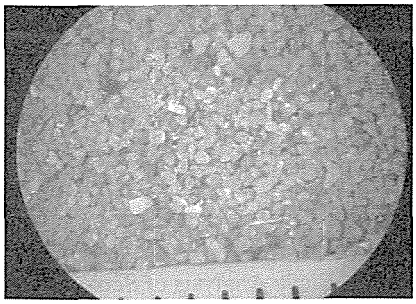

Figure 10 The image of the sample Sarıkum transferred to the program.

Same procedures were also done for Senkoy sample and the original, gary scale and manually processed images are given in Figure 13,14 and 15 respectively. Particle size distribution of Senkoy samples is presended in Figure 16.

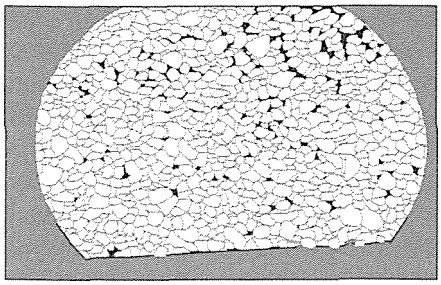

Figure 11.Manually processed image of the scaled image of the sample Sarikum.

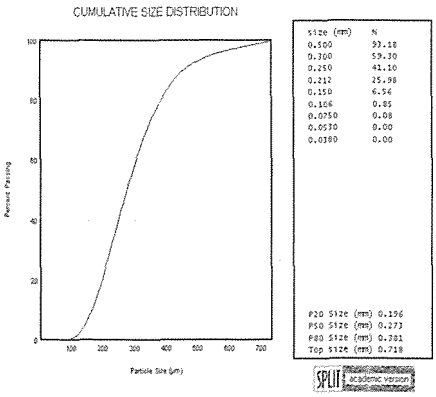

Figure 12.Cumulative particle size distribution of Sarıkum

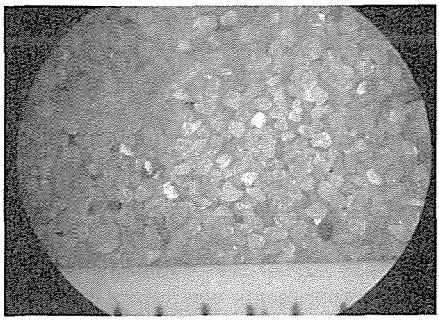

Figure 13.The image of Senköy sample

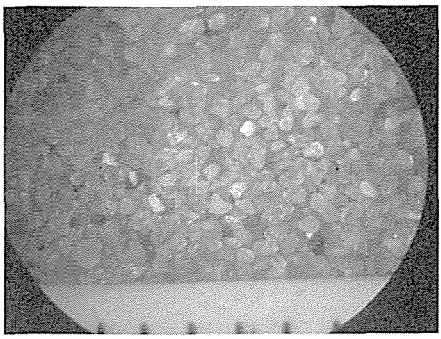

Figure 14 The image of the sample Senköy transferred to the program.

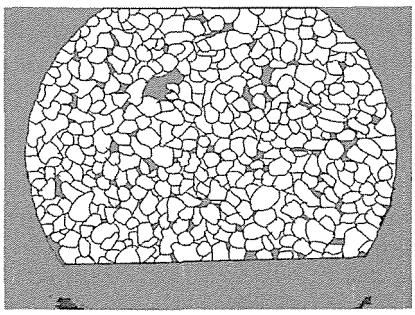

Figure 15.Manually processed image of the scaled image of the Senkoy sample.

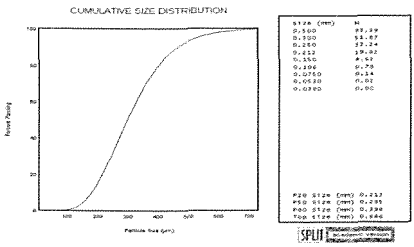

Figure 16 Cumulative particle size distribution of Senköy sample

Table 1. Comparison of the P_{50} and P_{80} results

Method	Senkoy Sample P_{50} (mm)	Sarıkum Sample P_{50} (mm)	Senkoy Sample P_{80} (mm)	Sarıkum Sample P_{80} (mm)
Digital Image Processing	0;273	0,295	0,381	0,398
Sieving	0,278	0,302	0,375	0,401

5 RESULTS AND DISCUSSIONS

In mineral processing particle size is one of the most important characteristics of the samples. There are many methods for particle size measurement which have been used in the past. With the advance of both time and technology, these methods have been changing and renewing themselves.

Split-Desktop is a program conducting sieve analysis through a digital imaging method.

After the samples of Sarikum and Senkoy were applied to the program Split-Desktop Engineering, it was measured that the sieve size through which 80 percent of the Sarikum sample passed was P_{80}=0.398mm, that its average particle size was P_{50}= 0.295mm,that the sieve size through which 80 percent of the Senkoy sample passed was P_{80}= 0.381mm, that its average particle size was P_{50}= 0.273 mm. On the other hand, according to the results obtained from the sieve analysis, it was observed that the sieve size through which 80 percent of the sample Sarikum passed was P_{80}=0.401mm, that its average particle size was P_{50}= 0.302mm,that the sieve size through which 80% of the sample Senkoy passed was P_{80}= 0.375mm, that its average particle size was P_{50}= 0.278mm. Comparison of the P_{50} and P_{80} values results obtained from the digital image processing and sieving is given Table 1. In comparison with the different techniques, there are not large differences in results. However digital image processing make on-line measuring of particle size defining possible. Besides, it completes the size distribution in a shorter time than sieving analysis.

REFERENCES

Allen,T., 1997, 'Particle Size Measurement', Volume 1, Chapman&Hall, ISBN: 0 412 2950 4 pp.156-157.

Bernhardt, C., 2000, 'Particle Size Analyses, Classification and Sedimentation Methods' ISBN: 0 412 55880 7, Chapman&Hall.

Dalsgaard, K., Jensen, L., Sorensen, M., 2007, 'Methodology of Sieving Small Samples and Calibration of Sieve Set' Edited by James P.M.SYVITSKI 'Principles Methods, and applications of particle size analyses' Cambridge University Press, ISBN: 0-521-364772-8.

Goodchild, J. S., Fueten, F. 1998, Edge detection in petrographic images using the rotating polarizer stage. *Computer Geoscience, 24* (8), 745–751.

Kursun.I., 2009,''Comparison of Digital Image Processing and Conventional Techniques in Coarse Particle Size Analysis' 7th International Industrial Minerals Symposium and Exhibition, İzmir,pp.355-362.

Makinacı, A. Topal, M. Sinecen, 2007, 'Determination of Aggregate shape with Digital Image Analysis' '6th International Industrial Minerals Symposium and Exhibition,İzmir.

Ozdemir, K., Tuncer, G., Kahriman, A., Ozer, U., Karadogan, A., 2007, 'The Relation between Excavator Bucket Loading Time and Particle Size Distribution of Shot Rock', Proceedings of The 33rd Annual Conference on Explosives and Blasting Technique, Nashville, Tennesse, USA., Volume I, pp. 303-313

Özdemir, K., Kahriman, A., Karadoğan, A., Tuncer, G., 2003, "Blast Fragmentation Assessment and Control Using The Split Digital Image Analysis System", International Conference on Earth Sciences and Electronics (ICESE-2003), Istanbul University, Avcılar, Istanbul, Turkey,

Rona, D., 2006, 'Measuring Methods of Particle Size' Adviser: Yrd.Doç.Dr. İlgin Kurşun, Bsc Thesis, University of Istanbul Department of Mining Engineering, Istanbul.

Saklara, S., Bayraktar, I., Oner M., 2000, The Methods Used In Analysis of Fine Particle Size, Mining Bulletin No: 39.

Tovey, N. K., Hunslow, M. W. 1995, Quantitative Micro-porosity and Orientation Analysis in Soils and Sediments. *Journal of the Geological Society Landon,* 752(1), 119–129.

Ulusoy, U., 2008, 'Application of ANOVA to Image Analysis Result of Particles Producd by Different Milling',Powder Technology,188 pp.133-138

Wills., B. A., 1985, Mineral Processing Techology', Oxford, Pergamon Press.

Main Conditions for Galena Flotation

M. Chettibi
Badji Mokhtar University, Annaba, Algeria. 53, cite du 19 juin guelma, Algeria

A. A. Abramov
Moscow State Mining University, Leninskii pr. 6, 117049 Moscow, Russia

F. Beladah

Badji Mokhtar University, mining Department, Annaba, Algeria

ABSTRACT As a result of theoretical and experimental investigations, it has been shown that the optimal pH values ensuring a complete flotation of galena are agree with the potential of zero or minimum charge of its surface, and the optimal composition of the collector sorption layer consisting both of chemisorbed xanthenes and physically adsorbed dixanthogenes. The pH values corresponding to the potential of zero or minimum charge on of the covered surface of mineral can be derived as a result of the thermodynamic analyses and complete chemical calculation of the mineral surface state in supposed flotation conditions.

1 INTRODUCTION

Sulphide minerals floatability and possibility of their separation from ores are defined by their surface properties, determining their behavior during flotation process. The processes, occurring at the contact of minerals with the liquid phase of flotation pulp, define the way of their surface electrochemical properties variation which is the major factor, directly influencing on sulphide minerals flotation efficiency. [Chettibi M., 2002]

Sulphide minerals flotate for three different reasons: elemental sulphur, metal-xanthenes and dixanthogen layer formation on the surface of minerals. Theses reactions are electrochemical in nature and the oxidation state of valuable minerals should be controlled in the process to maximize economic results. [Ruonala M., Heimala S., Jounela S., 1997]

The electrochemical nature of mineral/collector interaction also means that the processes that lead to mineral hydrophobicity are amenable to investigation by electro-chemical techniques. This is important not only because it allows a detailed knowledge of reactions that can occur in flotation systems to be established, but also because such knowledge is essential if effective potential monitoring and control methods are to be introduced

in practice. [Buckley A. N., Woods R., 1997].

Actually, it is established, that the surface state and the floatability of sulphide minerals are defined at the greatest degree by such factors, as red-ox potential (Eh), electrode potential and pulps pH. [Heifetz V.L., Krasikov B.S., 1959].

The purpose of the present work consists in determination of the main galena flotation conditions, by using the thermodynamic analyses, the electro-chemical techniques and the complete chemical calculation of the mineral surface state in supposed flotation conditions which consist in the optimal pH values ensuring a complete galena flotation agreed with the potential zero or minimum charge of its surface, and the optimal composition of the collector sorption layer consisting both of chemisorbed xanthenes and physically adsorbed dixanthogenes.

2 RESULTS AND DISCUSIONS

2.1 Lead floatability investigation in different conditions

Results of lead floatability of the carried out researches in the absence of collector (figure 1,(a) curve 1), at the presence of only frothier cyclohexanole (figure 1, (a) curve 3), the laurel alcohol (figure 1, (a) curve 4), pine oil (figure 1, (a) curve 5) and at the presence of no-polar collector as well (figure 1, (a) curve 2) which testify the maximal natural hydrophobicity of galena surface in neutral, strong acid and strong - alkaline conditions.

The increase of surface natural hydrophobicity and galena floatability with transition in strongly alkaline and strongly acid conditions can be due to the dissolution of lead polar oxidized

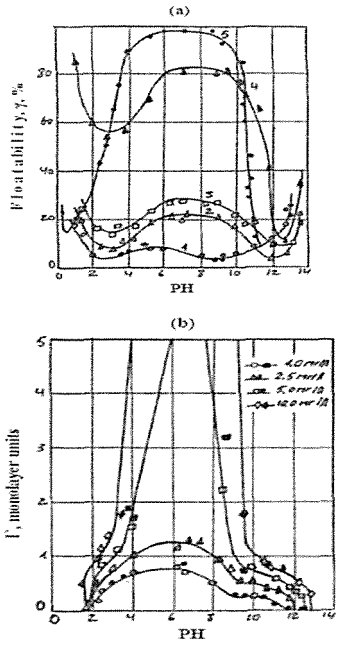

Figure 1. pH influence on galena floatability (fig. a) without collector (1) in the presence of kerosene 5mg/l (2); cyclohexanole 500mg/l (3); pine oil 10mg/l (4) and xanthenes 1,0mg/l (5), and also on sorption density of butyl xanthenes on galena surface (fig.b) at different of its concentrations in solution (mg/l): 1,0; 2,5; 5,0; 10,0.

connections and the uncovering of less polar sulphide mineral surface with the formation of elementary sulfur at last (figure 2, (a)).

At the presence of xanthenes (figure 1, (a) curve 5), galena floatability increasing preserves only in strong – acid and neutral conditions. However, there is no bibliography explaining the reasons "why only the neutral environment is characterized maximal collector sorption on galena surface (figure 1, (b)) and its floatability (figure 1, (a) curve 6)".

It is possible to suppose, that the

argumentation of observed condition of collector maximal sorption and galena floatability can be obtained as results of mineral surface state and its electrochemical characteristics changing analysis.

2.2 Analysis of galena surface state

Results of the thermodynamic analysis and experimental researches see (figure 2, (a)) show, that in usual conditions, galena surface is represented by products of its oxidation: $PbSO_4$ (pH = 1.6-6.07); $PbCO_3$ (pH = 6.07- 9.06); $Pb_3(OH)_2(CO_3)_2$ (pH = 9.06-12.00), at pH > 12 galena surface being oxidized is dissolved with formation of $HPbO_2^-$ and at pH<1,6 elementary sulfur formation (S^0) was observed on naked sulphide surface.

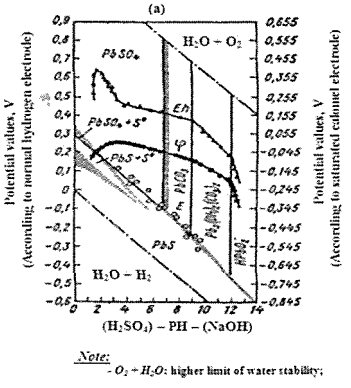

Figure 2. Influence of redox potential and pH values of solution on galena surface state at temperature 25°C and global depression 1 atm. (dissolved carbonic acid concentration in solution = 10^{-5}mol/l)

2.3 Estimation of electrochemical characteristics state of galena surface and its oxidation products

In order to estimate the electrochemical characteristics state of galena surface and its oxidation products was used the following reactions and equations see (table 1): reactions of dissociation (1.1-1:12), equations of balance (I.1 – I.7), electrode reactions (1.13 -1.16) and the equations (I.9 –I.12), particularly: for PbS - reactions and equations (1.1, 1.5 – 1.9, 1.13, I.1, I.5); for $PbSO_4$ - reactions and equations (1.2, 1.5 – 1.7, 1.10, 1.14, I.2, I.6); for $PbCO_3$ - reactions and equations (1.3, 1.5 – 1.7, 1.11- 1.15, I.6, I.7) and finally for $Pb_3(OH)_2(CO_3)_2$

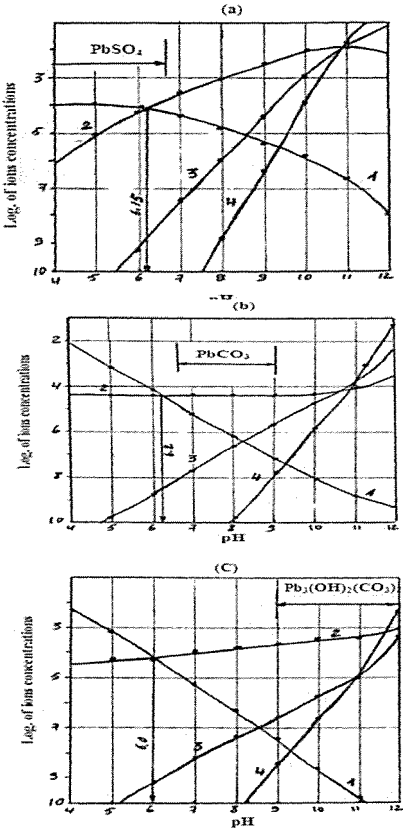

Figure 3. Influence of pH on the following ions concentrations: $[Pb^{2+}]$ (1); $[PbOH^+]$ (2); $[Pb(OH)_{2\ aq}]$(3) и $[PbO^-_2]$ (4), and equilibrium pH determination in the case of different galena oxidation products: $PbSO_4$ (fig. a); $PbCO_3$ (fig. b); $Pb_3(OH)_2(CO_3)_2$ (fig. c).

Table 1. The thermodynamic characteristics (K, ΔF°, E°) reactions and equations

№ react. & equat.	reactions and equations	K	ΔF° reaction Kcal.	E°, V.
1.1	$PbS \rightleftarrows Pb^{2+} + S^{2-}$	$K_1 = 6{,}592.10^{-29}$	38,44	
1.2	$PbSO_4 \rightleftarrows Pb^{2+} + SO_4^{2-}$	$K_2 = 1{,}34.10^{-8}$	10,74	
1.3	$PbCO_3 \rightleftarrows Pb^{2+} + CO_3^{2-}$	$K_3 = 1{,}11.10^{-13}$	17,67	
1.4	$Pb_3(OH)_2(CO_3)_2 \rightleftarrows 3\,Pb^{2+} + 2(OH)^- + 2CO_3^{2-}$	$K_4 = 2{,}1.10^{-42}$	60,94	
1.5	$Pb(OH)^+ \rightleftarrows Pb^{2+} + OH^-$	$K_5 = 1{,}3.10^{-8}$	10,67	
1.6	$Pb(OH)^+ + H_2O \rightleftarrows H^+ + Pb(OH)_{2\,aq}$	$K_6 = 1{,}24.10^{-11}$	14,875	
1.7	$Pb(OH)_{2\,aq} \rightleftarrows H^+ + HPbO_2^-$	$K_7 = 1{,}2.10^{-11}$	14,896	
1.8	$HS^- \rightleftarrows H^+ + S^{2-}$	$K_8 = 1{,}01.10^{-14}$	19,09	
1.9	$HSO_4^- \rightleftarrows H^+ + SO_4^{2-}$	$K_9 = 0{,}24.10^{-2}$	02,60	
1.10	$H_2CO_3 \rightleftarrows H^+ + HCO_3^-$	$K_{10} = 4{,}26.10^{-7}$	8,69	
1.11	$HCO_3^- \rightleftarrows H^+ + CO_3^{2-}$	$K_{11} = 4{,}677.10^{-11}$	14,09	
1.12	$H_2O \rightleftarrows H^+ + OH^-$	$K_w = 10^{-7}$	19,60	
I.1	$[Pb^{2+}] = [Pb(OH)^+] = [S^{2-}] + [HS^-]$			
I.2	$[Pb^{2+}] + [Pb(OH)^+] + [Pb(OH)_{2\,aq}] + [HPbO_2^-] = [SO_4^{2-}] + [HSO_4^-]$			
I.3	$[Pb^{2+}] + [Pb(OH)^+] = [CO_3^{2-}] + [HCO_3^-] + [H_2CO_3]$			
I.4	$2[Pb^{2+}] + 2[Pb(OH)^+] + 2[Pb(OH)_{2\,aq}] + 2[HPbO_2^-] = 3[CO_3^{2-}] + 3[HCO_3^-]$			
I.5	$2Pb^{2+} + Pb(OH)^+ + H^+ = 2S^{2-} + HS^- + OH^-$			
I.6	$2Pb^{2+} + Pb(OH)^+ + H^+ = 2SO_4^{2-} + HSO_4^- + HPbO_2^- + OH^-$			
I.7	$2Pb^{2+} + Pb(OH)^+ + H^+ = 2CO_3^{2-} + HCO_3^- + OH^-$			
I.13	$Pb - S^{2-} \rightleftarrows PbS - 2e$		-44,25	-0,959
I.14	$Pb - SO_4^{2-} \rightleftarrows PbSO_4 - 2e$		-16,55	-0,359
I.15	$Pb - CO_3^{2-} \rightleftarrows PbCO_3 - 2e$		-23,48	-0,509
I.16	$3\,Pb - 2(OH)^- + 2CO_3^{2-} \rightleftarrows Pb_3(OH)_2(CO_3)_2 - 6e$		-78,37	-0,291
I.9	$E = -0.959 - 0.0295 LOG[S^{2-}]$			reac.1.13
I.10	$E = -0.359 - 0.0295 LOG[SO_4^{2-}]$			reac.1.14
I.11	$E = -0.509 - 0.0295 LOG[CO_3^{2-}]$			reac.1.15
I.12	$E = -0.291 - 1/3 * 0.059 (PH - LOG[CO_3^{2-}])$			reac.1.16

- reactions and equations (1.4 – 1.7, 1.12, 1.16, I.4, I.7).

From result of full chemical computation were defined pH equilibrium values for each product see (figure 3), and corresponding to them the regularities of potential determining ions concentration at various pH values.

The pH equilibrium values of system [product – water] make: for PbS - 7,0; for $PbSO_4$ – 5,075; for $PbCO_3$ – 8,07 and for $Pb_3(OH)_2(CO_3)_2$ – 6,19. Thus, the equilibrium condition of system answers the minimal value of its free energy, so the obtained pH equilibrium values of systems can be considered as value of potential zero charge of oxidation product surface within galena oxidized surface.

Carried out potential values of each product surface (on the basis of values of potential determining ions concentrations corresponded to them) are illustrated on figure 4, (b).

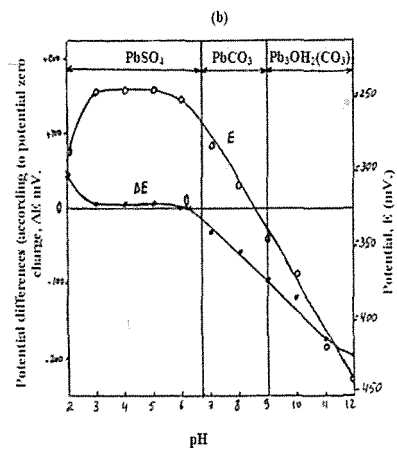

Figure 4. Also pH influence on potential values (E) and potential differences (ΔE) of galena oxidized surface (fig. b) at interval of following components formation: $PbSO_4$ (1); $PbCO_3$ (2); $Pb_3(OH)_2(CO_3)_2$.

Note. (E- Potential of fresh naked galena surface; φ – galena electrode potential after 10 min of being in solution of the fresh naked surface),

They show, that surface potentials values of minimal charge practically coincides on pH values with pH of maximal hydrophobicity and floatability of galena (figure 1, (a)), and collector sorption on its surface as well (figure 1, (b)).

Important to note, that stechiometric anions replacement (SO_4^{2-}, CO_3^{2-}, OH^-) of intermediate connection on galena surface by reactions (1) or (2): [Chettibi M., 2002].

$$Pb] - Pb\text{-}OH + X^- \leftrightarrow PbS] - Pb\text{–}X + OH^-; \quad (1)$$

$$PbS] - Pb\text{-}An + 2X^- \leftrightarrow PbX_2 + An^-; \quad (2)$$

Where: An- anions of SO_4^{2-} and CO_3^{2-}, equally charged with X^- anions, in result of their chemical sorption there is no change of global charge in Stern's layer, though can change the electro-kinetic potential values (in the negative side) due to layer thickness increasing by chemical sorption of xanthenes ions, having the much more size, in comparison with inorganic ions.

Results of experimental researches carried out with special applications illustrated in (figure 5, (a)) show, that galena surface interaction with xanthenes in usual conditions is accompanied as chemical interaction between them, that proves also the displacement of electrode potential ΔE in the negative side (fig. 3, Curve ΔE), and oxidation of a xanthenes part up to dexanthogenes, which will co-adsorbed on chemically fixed collector.

Thus it is observed that maximum values of collector sorption Γ_0, xanthenes chemical sorption Γ, electrode potential variation ΔE and galena floatability γ_0 and γ after and before removing dexanthogenes from its surface which coincide with pH values 6 -8, answering to galena surface potential zero charge.

Maximum dexanthogenes quantity in sorption layer at xanthenes accepted initial concentration - 10 mg / l, makes about 90 %. The last value of dexanthogenes quantity in sorption layer will be increased by increasing xanthenes

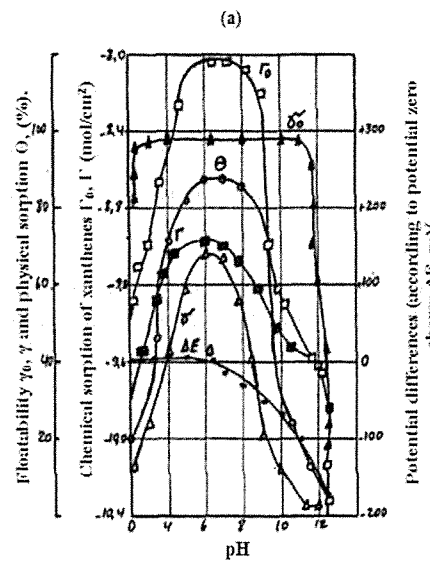

Figure 5. Influence of pH: (fig. a) on galena surface potential (E), xanthenes sorption (Γ_0, Γ) and galena floatability (γ_0,γ) before and after elimination of physically adsorbed dexanthogenes molecules from its surface (θ), initial concentration of potassium xanthenes of experiences – 10mg/l.

Presence of dexanthogenes in sorption layer renders rather essential influence on galena floatability. For example, at the same density of xanthenes global sorption, equal 0,65 mono layer, galena floats completely when about 20 % of adsorbed collector is presented in dexanthogenes (curves Γ_0, γ_0, θ at pH = 11), and only on 10-13 % when dexanthogenes is absented in sorption layer (curves Γ, γ at pH = 10).

2.4 Lead xanthenes surface behavior in solution and its equilibrium pH

For studying lead xanthenes surface state (PbX_2) in a solution, an equations system has been made from expressions of equilibrium constant of dissociation reactions (2.1 - 2.6), the equations of balance (II.1) and electro neutrality (II.2), electrode reactions (2.7, for butyl and ethyl xanthenes) and the equations corresponding to them (II.3, II.4) (see table. 2).

From result of full chemical calculation was determined the equilibrium pH values of lead xanthenes and variation regularities of ions determining potential concentration according to them, the carried out results are illustrated on figure 6, (b, c).

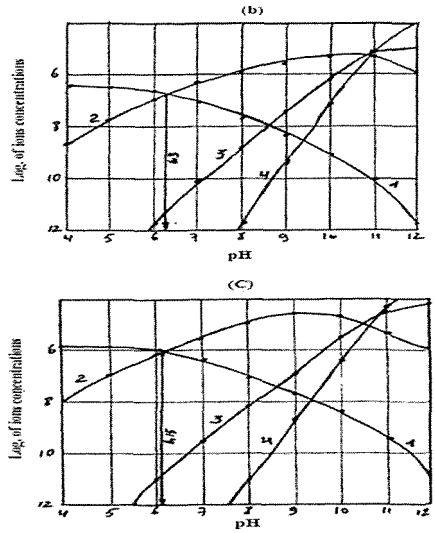

Figure 6. Influence of pH on the following ions concentration: $[Pb^{2+}]$ (1); $[PbOH^{+}]$ (2); $[Pb(OH)_{2\ aq}]$(3) и $[PbO^{-}_{2}]$ (4) and equilibrium pH determination in the case of butyl xanthenes (b) and ethyl xanthenes (c)

Table 2. The thermodynamic characteristics (K, ΔF^0, E^0) reactions and equations

№ react .& equat.	reactions and equations	K	ΔF^0 reaction Kcal.	E^0, V.
2.1	$PbX_{2\,but} \leftrightarrow Pb^{2+} + 2X^-$	$1{,}35.10^{-19}$		-0,100
2.2	$PbX_{2\,ethyl} \leftrightarrow Pb^{2+} + 2X^-$	$1{,}7.10^{-7}$		-0,037
2.3	$Pb(OH)^+ \leftrightarrow Pb^{2+} + OH^-$	$1{,}5.10^{-8}$	10,67	
2.4	$Pb(OH)^+ + H_2O \leftrightarrow H^+ + Pb(OH)_{2\,aq}$	$1{,}26.10^{-11}$		
2.5	$Pb(OH)_{2\,aq} \leftrightarrow H^+ + HPbO_2^-$	$1{,}2.10^{-11}$		
2.6	$H_2O \leftrightarrow H^+ + OH^-$	$K_w=10^{-14}$	19,095	
2.7	$2X^- \leftrightarrow X_2 + 2e$			
II.1	$2[Pb^{2+}]+2[Pb(OH)^+]+2[Pb(OH)_{2\,aq}]+2[HPbO_2^-] = [X^-]$			
II.2	$2\,Pb^{2+} + Pb(OH)^+ + H^+ = X^- + HPbO_2^- + OH^-$			
II.3	$E_1 = -0{,}100 - 0{,}059\log[X^-_{but}]$			r. 2.7
3.11	$E_2 = -0{,}037 - 0{,}059\log[X^-_{etyl}]$			r. 2.7

It was found, that balance pH value of system « Lead xanthenes - water » makes: for $PbX_{2\ but.}$ - 6,3 and for $PbX_{2\ ethyl.}$ - 6,15 see (figure 6, (b, c)). Since, the system equilibrium condition answers the minimal value of its free energy, so the obtained system equilibrium pH values can be considered as potential values of the minimal charge of lead xanthenes surface.

Practically, potential value of surface minimal charge of sulphide minerals coincides by pH values with pH corresponding maximal hydrophobicity and floatability of galena, that confirms results of lead xanthenes surface state calculation, as pH values maximal floatability of galena and equilibrium pH of lead xanthenes surface are similar and equal 6,0.

Thus, the received results testify that at potentials, answering minimal charge on galena surface floats optimum structure collector sorption layer, consisting from both kind of sorption; chemically fixed xanthenes and physically adsorbed dexanthogenes.

Chemically fixed collector insures the necessary hydrophobicity of mineral surface and the thermodynamic possibility of its fastening on bubbles.

Physically adsorbed collector (dexanthogenes) plays role of kinetic functions at flotation as providing effective destruction of hydro-layers between bubble and particle and hardening of contact bubble-particle [Abramov A. A., 1993]. In results effective flotation could be provided [Abramov A. A., 1993].

Conformity of optimal pH value at flotation to value of minimal charge potential of float ting mineral surface is caused by the following:

- insuring maximal surface hydrophobicity as consequence of its zero charge (it means its no polar states), and collector chemical sorption, which no polar radicals are directed towards the side of liquid phase;

- guarantee at a surface zero charge optimal conditions of physical adsorption of dexanthogenes uncharged molecules, carrying out kinetic functions while fastening and flotation of mineral [Abramov A. A., 1993].

3 CONCLUSIONS

From results of thermodynamic analysis and experimental researches we can conclude the following moments:

- Optimum pH values at galena flotation answer surface potential of minimal charge, guaranteeing the formation of collector optimum sorption coverings structure, consisting from both type of sorption, chemically fixed xanthenes and physically adsorbed dexanthogenes on its surfaces.

- pH value, answering to surface potential of a zero or minimal charge floating mineral can be defined as a result of thermodynamic calculation of the surface state in suggested conditions of flotation.

REFERENCES

Abramov A. A., 1993. Mineral processing by using flotation methods. Nedra, Moscow, 1993.

Buckley A. N., Woods R., 1997. Chemio-sorption- the thermodynamically favored process in the interaction of thiol collectors with sulphide minerals. Int. J. Miner. Process. 51 (1997) 15-26.

Chettibi M., 2002. Optimization of Lead and Zinc Mineral Sulfide flotation. 2002. PhD Thesis; Moscow Mining University. Russia.

Heifetz V. L., Krasikov B. S., 1959. Influence of surface active substances on kinetics of certain cations discharge. Scientific notes of LGU. 262, p.3-30.

Melik-Gaykazian V. I., Abramov A. A., 1990. Investigation methods of flotation process. Moscow, Nedra, 1990.

Puonala M., Heimala S., Jounela S., 1997. Different aspects of using electrochemical potential measurements in mineral processing. Int. J. Miner. Process. 51, (1997) 97-110.

Determination of Operation Parameters of a Mineral Processing Study Incorporating Multiple Regression Analysis and Multiobjective Genetic Algorithms

M.Birinci, M.Kumral, M.Sarıkaya
Department of Mining Engineering, Inonu University, 44280 Malatya - Turkey

ABSTRACT The design of a mineral processing plant dictates to determine optimal system parameters such as impeller speed, temperature, pH, process duration, solid % in pulp. The paper proposes a combination of multiple regression modelling and the multiobjective genetic algorithms (GA) to find the optimal system parameters simultaneously. In this research, impeller speed, process duration and solid % in pulp are considered as independent variables for the beneficiation of Al_2O_3 in pyrophyllite ore. Grade and electricity consumption are dependant variables. The multiple regression analysis is performed to relate dependant and independent variables to each other. The obtained models are used in optimisation procedure as objective functions. The first objective is to maximise the Al_2O_3 grade and the second one is to minimise electricity consumption. This is a multiobjective optimization problem and is solved by GA. The results showed that the proposed approach could be used to determine operation parameters in a mineral processing plant.

1 INTRODUCTION

When optimal operation parameters are determined in a mineral processing operation, many parameters should be considered. These parameters usually have a direct influence on the operation costs. Therefore, it is required that these costs should be minimized. On the other hand, main objective is, of course, is to maximize the recovery of variable under consideration. The problem has a multi-objective nature and can be seen as one in which there are several competing objectives such as minimizing operation costs and maximizing recovery. In this research, we recommend a methodology, which comprises multiple regression model and multiobjective GA. In literature there are some recent researches on the optimization of flotation circuits (Cisternas *et. al.*, 2004, Naik *et. al.*, 2004 and Kalyani *et. al.*, 2005). These studies have used mixed integer programming, steepest ascend, response surface methodology. On the other hand, there are increasing interests in the use of GA in mineral processing (Karr and Yeager, 1995, Aldrich *et. al.*, 2000, While *et. al.*, 2004, Svedensten

and Evertsson, 2005, Guria *et. al.*, 2005, Guria, *et. al.*, 2005).

2 METHODOLOGY

The research can be divided into three stages:

Independent variables or predictors are determined. These may be process duration, impeller speed, temperature, solid-to-liquid ratio, pH, reagent consumption or concentration. The pre-defined number of experiments is conducted with varying values of independent variables. Thus, the values of dependant variables or response are obtained. The dependant variables may be grade, recovery or energy consumption.

Each scenario is used to model the operation under consideration. The multiple regression analysis is performed to relate dependant and independent variables to each other.

The obtained model is an optimisation problem. For example, if dependant variable is recovery, the problem is a maximization problem or if dependant variable is electricity consumption, the problem is a minimization problem. Independent variables are now decision variables. When more than one objective exists simultaneously, this is a multiobjective optimisation problem and is solved by an appropriate method from operations research area. In this research, multiobjective GA is chosen to solve the problem.

The value of dependent variable can be predicted by multiple regression modeling that is a statistical methodology that is used to relate variables (Bowerman and O'Conell, 1990 and Tacq, 1997). A variable called dependant or response variable is related to one or more called predictor or independent variable(s). The objective is to construct a regression model relating dependant variable, y, to independent variable(s), $x_1, x_2, ..., x_p$.

The multiple regression model relating y to $x_1, x_2, ..., x_p$ is

$x_1, x_2, ..., x_p$ is

$$y_i = \mu_i + \varepsilon_i = \beta_0 + \beta_1 x_{i1} + \beta_2 x_{i2} + \cdots + \beta_p x_{ip} + \varepsilon_i \quad (1)$$

where:

μ_i is the mean value of the dependant variable when the values of the independent variable when are .

$x_1, x_2, \cdots, x_p$ are $x_{i1}, x_{i2}, \cdots, x_{ip}$.

$\beta_0, \beta_1, \cdots, \beta_p$ reunknownparameters relating μ_i to $x_{i1}, x_{i2}, \cdots, x_{ip}$

is an error term that determines the effect on y_i of all factors other than the values $x_{i1}, x_{i2}, \cdots, x_{ip}$ of the independent variables . $x_1, x_2, \cdots, x_p$.

The GA is a stochastic search algorithm that mimics the process of natural selection and genetics. The GA has presented considerable achievement in yielding good solution to many complex optimisation problems (Davis 1991, Goldberg 1989, Haupt and Haupt 1998). When the objective functions are multi-model or the search space is irregular, highly robust algorithms are required so as to avoid trapping at local optima. The GA can reach the global optimum fairly. Furthermore, the GA does not require the specific mathematical analysis of optimisation problem.

Simple algorithm of the GA consists of the following steps:

1. Generate an initial population of strings

2. Evaluate the string according to the fitness function

3. Apply a set of genetic operators to generate a new population of strings

4. Go Step 2 until a solution converges

The length of the vector of floating number is same as the solution vector. The chromosome $V=(x_1, x_2,...,x_n)$ represents a solution $x = (x_1, x_2, ..., x_n)$ of the problem where n is the dimension. In order to solve the problem by the GA, each solution is coded by a chromosome $V(x_1, x_2,...,x_n)$. A pre-defined integer *population-size*, which is the number of chromosomes, is initiated at random. Until the pre-determined population size is reached, the feasible solutions are accepted as chromosomes in the population. Then the fitness value of each chromosome is calculated. The chromosomes are rearranged in ascending order on the basis of the fitness values.

Now the parameter, a, is initiated in the genetic system. The rank-based evaluation function is defined as follows:

$$E(V_i)=a(1-a)^{i-1} \quad i = 1,2, ..., \text{population-size} \quad (2)$$

When $i = 1$ represents the best individual, i = *population-size* is the worst individual. The reproduction operator used herein is a biased roulette wheel, which is spun *population-size* time. A single chromosome is selected in each spinning for a new population. The roulette wheel is a fitness-proportional selection. The probability of being selected is given by modifying equation (2) to

$$P(V_i)=a(1-a)^{i-1} / [1-(1-a)^{\text{population-size}}. \quad (3)$$

This population is updated by the crossover and mutation operators. First of all, the crossover probability, P_c, is defined. P_c * *population-size* gives the expected value of number of chromosomes undergoing on the crossover process. In order to carry out this process, random numbers, r_i, are generated from interval [0, 1] in i = 1, *population-size*. If r_i is smaller than P_c, V_i is selected as a parent. The selected chromosomes are randomly grouped as pairs. If the number of selected chromosomes is odd, one of them is removed from the system. The crossover procedure is performed on each pair. Let the pair (V_1, V_2) be subjected to the crossover operation. Firstly, a random number, r, is generated from the interval (0, 1). Then the crossover operator will yield two children X and Y as follows:

$$X = r*V1 + (1-r)*V2 \text{ and } Y = (1-r)*V1+r*V2 \quad (4)$$

The feasibility of each child is checked. If so, the child is accepted.

The mutation operator is implemented on new version of population. Similar to the crossover operation, a mutation probability, P_m, is defined. P_m * *population-size* gives the expected value of number of chromosomes undergoing the mutation operation. In this procedure a random number, r_i, is generated $i=1$ to *population-size* from the interval [0, 1]. If r_i smaller than P_m, V_i is selected as a parent for the mutation. A random direction, d, is generated in $\Re^3$. The selected parent will be mutated by $V + M*d$ in this direction. If $V + M*d$ is not feasible to the constraints, M is set as a random number from interval $[0, M]$ until it is feasible. If this procedure does not manage to find a feasible solution in a pre-determined number of iterations, M is set to zero.

The key to multiobjective decision-making problems is the trade-off amongst competing objectives that may not have equal priority. On this point, the concept of non-dominated solutions emerges. Let f_1 and f_2 denote two objectives for a minimisation problem F. Imagine that F has two solutions, x_A and x_B in its

solution space. If $f_1(x_a)$ is smaller than $f_1(x_B)$ but if $f_2(x_a)$ is larger than $f_2(x_B)$, it cannot be decided which solution is better. Solutions x_A and x_B are non-dominated for the minimisation problem F. The non-dominated set generally includes many alternatives, all of which obviously cannot be selected. The non-dominated solution that is selected as the preferred alternative is called the best compromise solution. The concept of non-dominated solutions also appears in the literature under the names of Pareto optimum, efficient solutions or non-inferior solutions.

Binary or floating vector can be used as the representation structure in the GA. In this research a floating vector represents a real value of a decision variable as a chromosome because binary coding has received substantial criticism (Liu 1998). When the values of the decision variables are continuous, it is necessary to represent them by a floating vector. Furthermore, real-valued GA can ensure the values of decision variables to the full machine precision. The real valued GA also has the advantage of requiring less storage than the binary valued GA. As the number of bits in binary coding representation increases, the storage becomes important. The representation of the fitness function in real valued GA is also more accurate as a result.

3 CASE STUDY

The approach was demonstrated on a case study. Pyrophyllite ore ($Al_2Si_4O_{10}(OH)_2$) samples taken from Malatya-Pütürge region of Turkey were used in this research. The chemical analysis showed that the ore contains 13.90% Al_2O_3. However, ceramic, refractory and steel industries require pyrophyllite ore with higher Al_2O_3. Therefore, the beneficiation of Al_2O_3 in pyrophyllite ore was investigated. It was expected that the beneficiation could be achieved by flotation, comminution-classification and attrition-scrubbing methods. In this research, the important parameters affecting the beneficiation process were process duration (x_1) impeller speed (x_2) and the percentage of solid by weight in pulp (x_3). Fourteen experiments were conducted with varying parameters values (Birinci and Sarikaya, 2004). Grades (y_g) and electricity consumptions (y_e) were measured (Table 1).

Multiple regression analysis is performed to derive a model containing

Table 1. Experimental results

Process duration (x_1)	Impeller speed (x_2)	Solid % in pulp (x_3)	Grade (y_g) (experimental)	Electricity (y_e) (experimental)	Grade (y_g) (model)	Electricity (y_e) (model)
30.0	1000.0	50.0	21.960	0.101750	21.83506	0.104860
30.0	1000.0	60.0	22.790	0.104900	22.86928	0.107364
30.0	1000.0	65.0	23.140	0.106750	23.45682	0.109974
30.0	1000.0	70.0	24.930	0.110100	24.07969	0.114111
30.0	1000.0	75.0	23.010	0.118500	23.01482	0.120456
15.0	1000.0	70.0	20.380	0.055050	20.51830	0.059136
45.0	1000.0	70.0	25.980	0.165150	26.16297	0.169086
60.0	1000.0	70.0	28.130	0.220500	27.64108	0.224061
90.0	1000.0	70.0	30.090	0.330600	29.72436	0.334011
120.0	1000.0	70.0	31.230	0.441000	31.20247	0.443961
60.0	750.0	70.0	21.460	0.185000	21.64863	0.188519
60.0	1000.0	70.0	26.820	0.220500	27.64108	0.224061
60.0	1500.0	70.0	33.640	0.295000	33.91615	0.298973
60.0	1750.0	70.0	33.600	0.356000	33.50349	0.359447

all parameters. In order to compare all reasonable regression models, backward elimination procedure was used as the screening procedure. The model summary, ANOVA table and R values were given in Table 2, 3 and 4, respectively for grade. For grade, the best model was found as:

$$Y_{grade} = -147.345 - 4.71*10^{-33}* \exp(x_3) - 9.56*10^{-18}* x_2^{5.5} + 21.665* \ln(x_2) + 5.138* \ln(x_1) + 9.402*10^{-4}* x_3^2 \quad (5)$$

Then, the values of electricity consumption were estimated. The procedure described above was implemented for electricity consumption. The following model and the corresponding tables (Tables 5-7) are found as:

$$Y_{electricity} = -0.797 + 1.093*10^{-19}* x_2^{5.5} + 0.114* \ln(x_2) + 1.241*10^{-15}* x_3^7 + 3.665*10^{-3}* x_1 \quad (6)$$

For all parameter set experimental values versus model values were given in Figure 1 and 2. As seen from Table 1,

Table 2. Multiple regression results for grade

Variable	Estimated Coefficient	t-statistics	Variance Inflation Factor (VIF)	Beta
Constant	-147.345	-12.726		
$\exp(x_3)$	$-4.71*10^{-33}$	-2.845	1.358	0.104
$x_2^{5.5}$	$-9.56*10^{-18}$	-5.191	5.800	0.393
$\ln(x_2)$	21.665	13.051	5.628	0.973
$\ln(x_1)$	5.138	17.764	1.258	0.626
x_3^2	$9.402*10^{-4}$	4.262	1.409	0.159

Table 3. ANOVA for dependent variable (grade)

	Sum of squares	df	Mean square	F	Sig.
Regression	259.727	5	51.945	201.091	0.000
Residual	2.067	8	0.258		
Total	261.793	13			

Table 4. Model summary for dependant variable (grade)

R	R square	Adjusted R square	Standard error of the estimate
0.996[a]	0.992	0.987	0.5082

a. Predictors: Constant, $\exp(x_3)$, $x_2^{5.5}$, $\ln(x_2)$, $\ln(x_1)$ and x_3^2

Table 5. Multiple regression results for electricity consumption

Variable	Estimated Coefficient	t-statistics	Variance Inflation Factor (VIF)	Beta
Constant	-0.797	-49.479		
$x_2^{5.5}$	$1.093*10^{-19}$	42.489	5.628	0.174
$\ln(x_2)$	0.114	48.501	5.572	0.198
x_3^7	$1.241*10^{-15}$	17.837	1.059	0.032
x_1	$3.665*10^{-3}$	498.842	1.063	0.889

Table 6. ANOVA for dependent variable (electricity consumption)

	Sum of squares	df	Mean square	F	Sig.
Regression	0.174	4	$4.347*10^{-2}$	83756.724	0.000
Residual	$4.671*10^{-6}$	9	$5.190*10^{-7}$		
Total	0.174	13			

Table 7. Model summary for dependant variable (electricity consumption)

R	R square	Adjusted R square	Standard error of the estimate
1.000[a]	1.000	1.000	$7.20*10^{-4}$

b. Predictors: Constant, x_1, $\ln(x_2)$, x_3^7 and $x_2^{5.5}$

there were strong correlations between experimental and model values.

In the final stage of research, multiple regression models were treated as an optimisation problem. The first objective was to maximise the grade. The second

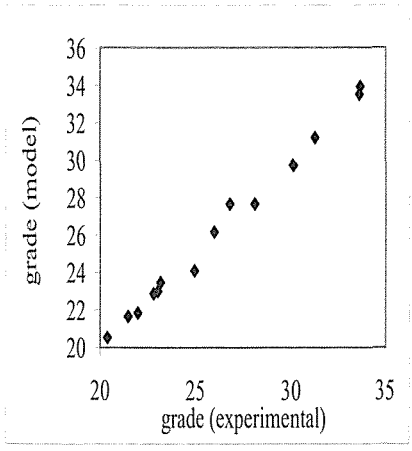

Figure1.Measured and predicted grade value

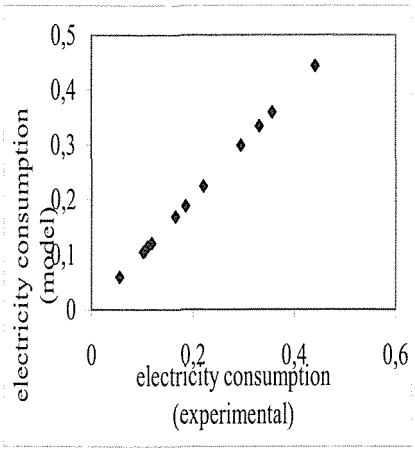

Figure 2. Measured and predicted electricity consumption values

Table 8. Parameter file used in the multiobjective GA

40	\number of chromosome
100000	\number of iterations
2	\number of objective
3	\number of variables
15.00 120.00	\lower and upper limits for process duration
750.00 1750.00	\lower and upper limits for impeller speed
50.00 75.00	\lower and upper limits for ratio
0.25	\crossover probability
500.0 25.0 25.0	\a large positive number used in mutation
0.20	\mutation probability

Table 9. Solution set

x_1 (process duration)	x_2 (impeller speed)	x_3 (solid % in pulp)	Y_{grade}	$Y_{electricity}$
71.321890	1556.72500	73.485150	35.067140	0.3561202
56.502900	1483.39500	72.236110	33.733440	0.2854944
61.451050	1299.37600	73.841290	32.442870	0.2750054
45.894290	1294.65800	68.817370	30.764020	0.2115024
36.958170	1348.77800	61.279800	29.304190	0.1819898
38.064260	1168.81000	66.793170	27.870690	0.1632834
22.689420	1341.64800	58.577200	26.423060	0.1274855
27.472810	1119.08100	62.375980	24.869000	0.1149745
23.394030	1117.68700	60.641090	23.819410	0.0990228
18.468820	1075.52900	51.807710	20.944170	0.0728748
18.677640	824.31810	68.926210	17.524690	0.0472793
15.001290	834.70420	65.768620	16.266300	0.0327515

objective was to minimise the electricity consumption. This was a multiobjective optimisation problem and was solved by multiobjective GA. The constraints were lower and upper limits of decision variables used in experiment stage. In order to solve the problem, a computer program in FORTRAN was written. The input parameter file of the program was given in Table 8. The procedure was repeated 100000 times in approximately ten minutes. A solution set on the Pareto curve (non-dominated solutions) was given in Table 9.

4 CONCLUSIONS

Low ore prices, increasing global competition and costs induce careful design of operation parameters of a mineral processing plant. The approach incorporating multiple regression modelling and multiobjective GA is a powerful method to determine operation parameters of a mineral processing plant. Multobjective GA yields a set of non-dominated solutions. As seen from Table 9, there were 12 solutions. The selection of solution to be used depends upon the preferences of the decision maker. If prevailing objective is maximum grade, the first solution can be selected. On the other hand, if one wishes to minimise electricity consumption, the last solution can be preferred. The approach can be used to determine operation parameters of any mineral processing plant.

REFERENCES

Aldrich C., Schmitz GPJ and Gouws FS, 2000. Development of fuzzy rule-based systems for industrial flotation plants by nse of inductive techniques and genetic algorithms, Journal of the South African Institute of Mining and Metallurgy, 100 (2): 129-134.

Birinci M. & Sarikaya M., 2004. An investigation on the beneficiation of pyrophyllite, in: A. Akar & A. Seyrankaya (Eds), Industrial Raw Material Symposium, Izmir, Turkey, pp. 69-75.

Bowerman B.L. and O'Conell R.T.,1990. Linear Statistical Models: An Applied Approach, 2nd edn., Duxbury Press, USA.

Cisternas L.A., Galvez E.D., Zavala M.F. and Magna J., 2004. A MILP model for the design of mineral flotation circuits, International Journal of Mineral Processing, 74 (1-4), 121-131.

Davis L., 1991. Handbook of Genetic Algorithms, V.N. Reinhold, New York

Goldberg D.E., 1989. Genetic Algorithms in Search, Optimization and Machine Learning, Addison Wesley Pub. Inc., Reading, MA.

Guria C., Verma M., Mehrotra SP and Gupta S.K., 2005. Multi-objective optimal synthesis and design of froth flotation circuits for mineral processing, using the jumping gene adaptation of genetic algorithm, Industrial & Engineering Chemistry Research, 44 (8), 2621-2633.

Guria C., Verma M., Gupta S.K. and Mehrotra SP, 2005. Simultaneous optimization of the performance of flotation circuits and their simplification using the jumping gene adaptations of genetic algorithm, to appear in International Journal of Mineral Processing.

Haupt R.L. & Haupt S.E., 1998. Practical Genetic Algorithms, John Wiley & Sons Inc., New York.

Kalyani V.K., Pallavika T., Gouri Charan T. and Chaudhuri S., 2005.

Optimization of a laboratory-Scale froth flotation process using response surface methodology, Coal Preperation, 25(3), 141-153.

Karr C.L. and Yeager D., 1995. Calibrating computer models of mineral processing equipment using genetic algorithms. Minerals Engineering, 8, 989-998.

Liu, B., 1999. Uncertain Programming, John Wiley and Sons Inc, New York.

Naik P.K., Reddy, P.S.R. and Misra V.N., 2004. Optimization of coal flotation using statistical technique, Fuel Processing Technology, 85 (13), 1473-1485.

Tacq J., 1997. Multivariate Analysis Techniques, Sage Publication, London.

Svedensten, P. and Evertsson C.M., 2005. Crushing plant optimisation by means of a genetic evolutionary algorithm. Minerals Engineering, 18(5), 473-479.

While L., Barone, L., Hingston, P., Huband, S., Tuppurainen, D. and Bearman, R., 2004, A multi-objective evolutionary algorithm approach for crusher optimisation and flowsheet design, Minerals Engineering, 17, 1063-1074.

Miscellaneous

3-D Seismic Travel Time Tomography in Bakhtyari Dam Site

Yousef Sharghi, Firooz Alinia, Parviz Moarefvand
Amirkabir University of technology, Tehran, Iran.
Hamidreza Siahkoohi
Tehran University, Tehran, Iran.

ABSTRACT Seismic traveltime tomography is presently one of the most used methods for calculating velocity distribution inside of the ground. Surveys of this method provide a technique for engineering site investigation capable of assessing beneath the existing structures without disturbing them. This paper describes the seismic tomography investigation performed at the abutments of Bakhtyari Dam site inorder to find the low velocity zones that may correspond to jointed media where seepage is most likely.

We performed 3-D tomographic inversion on Bakhtiari dam seismic data. To perform ray tracing and travel-time computation at each iteration, we used Um and Thurber (1987) method and for inversion step we used SIRT method. In most of the tomograms, average velocity was 3km/s. According to the results, main factor in velocity decrease in site is the presence of major joints.

1 INTRODUCTION

In seismic tomography, the aim is to provide a more detailed map of subsurface velocity variations, by using both surface and down-hole sources and receivers. It could be used to supplement drilling for complex geological interpretation, or to obtain a detailed distribution of strong and weak rock formations. It can also be used to detect time variation in formation velocity (Angioni et al., 2003).

Its use as a highly accurate method is expected to grow, particularly since a seismic tomography survey can be conducted using existing boreholes, adits and ground surface.(Takahashi, 2006)

This paper describes the seismic tomography investigation performed at the abutments of Bakhtyari Dam site. We performed 3-D tomographic inversion on Bakhtiari dam seismic data that has some important advantage.

The study aimed to find the low-velocity zones that may correspond to jointed media where seepage is most likely happens.

Bakhtyari dam site is Located in downstream of Bakhtyari river of Lorestan province and south- west of

Iran in folded zagros structured zone and 5 kilometers of north- west of Tang-e-Panj station in Tehran-Ahvaz railway. (Nicksiar et al., 2007) The concrete double arch dam has been designed thin with 330m height from river base that is considered the highest arch dam of the world.

2 DATA PROCESSING

In data processing of seismic tomography, an iterative inversion technique is commonly used because of its non-linear characteristics. In this method, for an initial velocity model firstly set up, theoretical traveltimes are calculated (Ray tracing) for all source and receiver pairs and compared against the observed ones. The model is modified (Inverse modeling) repeatedly until the residuals between calculated and observed traveltimes are minimized (Takahashia, 2006).

As an initial velocity model, a homogeneous velocity model or a velocity model made by a simple back projection of observed traveltimes is generally employed.

Ray tracing is a two point boundary value problem: the end points are specified (the source and receiver positions), and the propagation path and time must be determined. Ray theory is used in the development of some ray tracing algorithms. However, there are more general solutions. In all cases, ray tracing fulfills Fermat's principle (Gheshlaghi, 1997). This study ray tracing was performed with a revised form of ray bending, derived from the Um and Thurber (1987) method.

After raytracing, by the use of inversion techniques, we can update the model. In solving inverse problem, it is rare to directly perform the matrix calculations, as the size of the matrix in seismic tomography problems is usually very large.

In this study, we performed inversions with the simultaneous iterative reconstruction technique (SIRT) (Santamarina and Fratta, 2005).

Ray tracing and inversion are repeated until the residuals between calculated and observed traveltimes become acceptably small. It is necessary to monitor the variation of the residuals during calculation because the residual convergence strongly depends on the initial model and the inversion algorithm used.

3 GEOLOGICAL SETTING

The Bakhtyari Dam site has been considered in the gorge the Bakhtyari River has eroded, almost perpendicular to the Siah Kuh Anticline axis. This gorge is almost 1150 m long and 25 to 30 m wide at its bottom. Its width at the dam crest is about 340 m. The dam axis is almost 350 downstream of the gorge entrance, in the centre of the Siah Kuh Anticline and near its axial plane. The foundation rock consists of the second and third unit of Sarvak Formation (Sv2, Sv3) at the bottom and the main part of the dam abutments, and of Sv4 beds especially in the highest elevations of the abutments. The lithology of Sarvak is siliceous limestone. Sarvak formation was divided to seven units (SV1–SV7). (Dietler, et al., 2008)

The galleries that the seismic tomography has been performed, excavated in Siah-Kuh anticline, composed of limestone to marly limestone with shaley and siliceous limestone interbeds. A total of eight reconnaissance galleries were excavated in the dam site. Six of them are placed in dam area, galleries GR1 to GR3 in right

bank and GL1, GL2 and GL3 galleries are on the left bank (Fig. 1). Primary gallery observation and mapping indicate some open joints mainly with clay infilling and parallel to J1, one of the joint sets of the dam site (Table 1), which can enlarge and produce high seepage pathways after impounding. These open joints called major joints. Although the major joints are common in the right bank, their presence should not be neglected in the left.

Table 1. Major discontinuity surveyed at site

Discontinuity	Dip	Dip direction
Bedding	60–70	220
J1	70-80	310
J2	20-30	140
J3	15-20	50

4 RESULTS AND DISCUSSION

The Bakhtyari dam site tomography was performed using six galleries excavated at the dam site (GR1, GR2 and GR3, and GL1, GL2 and GL3). We performed 3-D tomographic inversion on Bakhtiari dam seismic data. The ability to perform 3-D analyses is an important advantage in counteracting the problem of nonuniqueness with cross-hole (or between gallery) data. After processing of data, 3D image of P wave velocity has been prepared.

Fig. 2 shows 3-D image velocity between GL2 and GL3. In this image in cells which seismic ray has not passed them, the average of seismic velocity (obtained by average travel time of fountain and receivers) has been used. Because lithology of region formed by limestone or its combinations, so seismic velocity in different units will be similar. The studies performed for

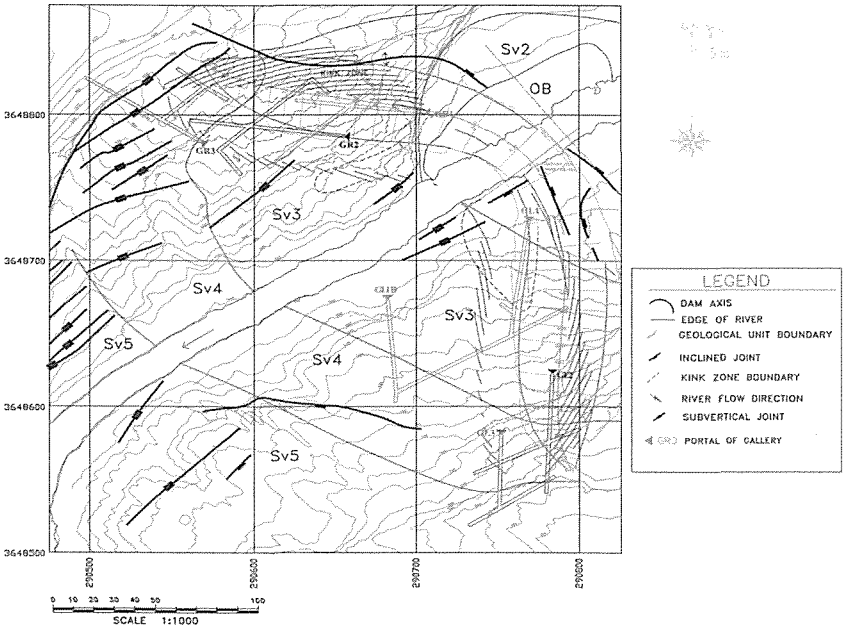

Fig. 1. Dam site geological map and galleries position (Nicksiar et al., 2007).

determining velocity of P wave in various samples show that average velocity of rock material (rock without joint) in different Sarvak formation units is near to 6.1 km/s. Also studies of performed hydrogeology and observations about galleries, exploration boreholes and superficial outcrops do not show any phenomenon of karst. According to the structural geology of dam construction, the most probable factor in velocity decrease of p waves in different parts is the presence of weak zones such as bedding surface, joints, fault zones and fragment zones resulting from folding function.

To study the reason of velocity changes, obtained velocity images have been compared with site geology. The images show good adaptation velocity with site geology. Fig. 3 shows 2-D section of velocity distribution between two inlet branches GL2, GL3 related to left abutment of site extracted from 3-D image. Velocity average in this part of site is about 3 km/s.

Major joints with wide aperture parallel with J1 in velocity section (Fig. 3) and other major joints shown by dash

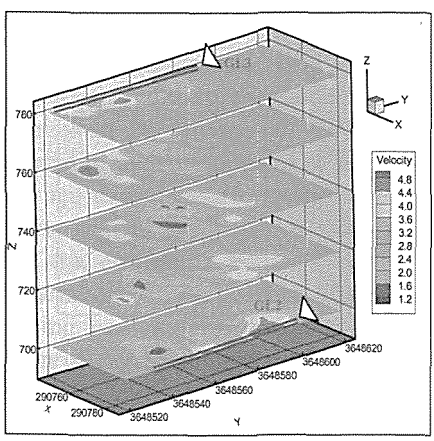

Fig. 2. 3-D velocity image from seismic tomography between inlet branches of GL2 and GL3

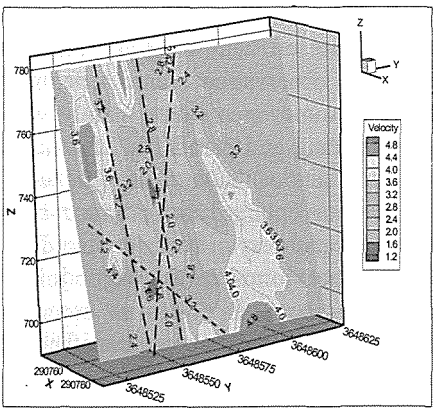

Fig. 3. 3-D velocity image from seismic tomography between inlet branches of GL2 and GL3

line. There is good adaptation between zones with low velocity and joints place. The width of fragment zones in geological survey of galleries GL2 and GL3 averagely measured 20 cm. So main factor in decreasing seismic velocity between these two galleries is fragment zones related to major joints.

According to the results, main factor in velocity decrease in site is the presence of major joints paralleled with J1. These joints are parallel with river axis (Fig. 1) and after dam construction can act as drain and transfer water of dam storage to downstream. Therefore, it is important to identify location, dip, persistence and aperture of these joints. With regard to seismic tomography in identifying fragment zones, tomography survey in new drilled boreholes can help to locate these zones in other parts of site.

5 CONCLUSION

Average velocity in most parts of Bakhtyari Dam Site which tomography survey performed in them is about 3km/s.

According to the results, main factor

in velocity decrease in site is the presence of major joints which are parallel to J1.

According to seismic capability in identifying fragment zones, tomography survey in new drilled boreholes can help to locate these zones in other parts of the site.

REFERENCES

Dietler, Th, Malekzadeh, L., Binazadeh, K. H., Novin, H., 2008. *Bakhtiari Dam and Hydrolic Power Project, Geological Report*, Iran Water and Power Resources Development Co (IWPC) Authority, Tehran, 121 P.

Gheshlaghi, F., 1997. *Tomographic Imaging in Civil Engineering Infrastructure*, Ph.D. Thesis university of waterloo,.

Santamarina, J. C., Fratta, D., Second Edition, 2005. *Discrete Signals and Inverse Problems: An Introduction for Engineers and Scientists*, Wiley, 350 P.

Angioni, T., Rechtien, R. D., Cardimono, S. J., Luna, R., vol. 368, 2003. Crosshole Seismic Tomography and Borehole Logging for Engineering Site Characterization in Sikeston , MO , USA, *Tectonophysics*, p.p.119 – 137.

Nicksiar M., Esfandiary M., Mehinrad A., Binazadeh K., vol. 44, 2007. Application of Seismic Tomography for Detecting Potential Seepage Paths in Bakhtyari Dam, Iran, *Int J Rock Mech Mining Sci.*

Takahashia, T., Takeuchib, T., Sassac, K., Vol. 43, 2006. ISRM Suggested Methods for borehole geophysics in rock engineering, *Int J Rock Mech Mining* Sci. p.p. 337-368.

Um, J., Thurber, C., vol. 77, 1987. A Fast Algorithm for Two-Point Seismic Ray Tracing, *Bull. Seismol. Soc. Am.*, p.p. 972-986.

Role of paleofluids and their evolution in iron oxide-copper-gold hydrothermal systems: a classic example from the Precambrian Mag Hill volcano-plutonic system, Northwest Territories, Canada

A. Karimzadeh Somarin
Department of Geology, Brandon University, Brandon, Manitoba, R7A 6A9, Canada

ABSTRACT The Mag Hill volcano-plutonic system is one of the Precambrian hydrothermal complexes in the Great Bear Magmatic Zone, Northwest Territories, Canada. The Mag Hill volcano-plutonic complex is the result of intrusion of syn-volcanic monzodioritic pluton into the andesitic rocks. As a result several types of hydrothermal alteration were formed including albitic, magnetite-actinolite-apatite, potassic, phyllic, and propylitic. The early stage of hydrothermal activity is marked with iron oxide (magnetite-actinolite-apatite) and alkali (albitic and potassic) alterations followed by phyllic-propylitic alteration and sulfide mineralization. Mineralization started at 560 °C at depth ~2.5 km by a magmatic fluid with 12.83 wt% NaCl equivalent average salinity, 0.833 g/cm3 density and 230.3 bars vapor pressure. Main sulfide and uranium mineralization started at 270 °C at very shallow depth by a high salinity (average 30wt% NaCl equivalent) fluid with 1.143 g/cm3 density and only 3.8 bars vapor pressure. Several types of paleofluids were involved in the formation of these assemblages.

1 INTRODUCTION

The Mag Hill system is one of several very large hydrothermal complexes developed within the ~1.86 Ga Echo Bay stratovolcano complex. The complex is located along the eastern shore of the Greta Bear Lake within the northern Great Bear Magmatic Zone (GBMZ), Northwest Territories, Canada. The Mag Hill volcano-plutonic system is part of the arc-related plutons of the Great Bear Batholith (Hoffman and McGlynn, 1977; Hoffman, 1978; Mumin et al., 2008). Volcanic and sedimentary units (not exposed at Mag Hill) occur as isolated bodies within the granitoid batholiths that dominate the Great Bear Magmatic Zone. These supracrustal sequences are generally interpreted as roof pendants to the larger and in part coeval intrusions (Hildebrand, 1984).

2 LOCAL GEOLOGY

At Mag Hill, andesite porphyry is the most common volcanic rock with some local dacite and possibly trachyte. These rocks are always altered to various

degrees and as a result the original texture and mineralogy has changed. In the least-altered samples of andesite, plagioclase, hornblende and locally biotite occur as phenocrysts. Large grains of hydrothermal K-feldspar are also found. Accessory minerals commonly include apatite and zircon.

The andesitic host rocks of Mag Hill are intruded by a series of microdiorite dikes. The least altered microdiorite is typically predominantly comprised of plagioclase, orthopyroxene and magnetite.

3 HYDROTHERMAL ALTERATION

Hydrothermal alteration covers an extensive area (>20 km2) at Mag Hill. The alteration is distinctly zoned with a core region comprising albite alteration in the contact of the Contact Lake monzodiorite pluton with andesitic volcanic rocks, and extensive zones of pervasive, vein and stockwork magnetite-actinolite-apatite alteration. In addition, assemblages progressively transition outwards to classic potassic (K-feldspar), phyllic (quartz-sericite-pyrite) and propylitic (chlorite-epidote± carbonate, sericite-albite) assemblage. This transition is visible at surface over a distance of ~3 km. A modest zone of pervasive hematitic alteration occurs between the potassic and phyllic zones. However, a stratiform hematite replacement body, up to 20 m thick and 300 m long, grading from a disseminated dusting to massive hematite occurs between potassic and phyllic zones.

Superimposed on any of the other alteration assemblages are suites of distal and/or late forming epithermal quartz-carbonate±hematite veins.

4 MICROTHERMOMETRIC STUDIES

The coexistence of various fluid inclusions, especially vapor-rich and vapor-poor ones, is considered as evidence of boiling (e.g. Roedder, 1984; Muntean and Einaudi, 2000; Karimzadeh Somarin and Lentz, 2008). Therefore, T_h (homogenization temperature) is considered to be the formation temperature (T_f) and no pressure correction was needed. High freezing temperature (2 °C) in one case suggests presence of liquid CO_2. No opaque solid phase was found in the studied fluid inclusions, although halide daughter crystals are relatively common in some types of inclusions. Depth, vapor pressure and density of fluid were calculated using Hass (1971) and average values of temperature and salinity for each mineral assemblage.

5 RESULTS

The early stage of hydrothermal activity is marked with iron oxide (magnetite-actinolite-apatite) and alkali (albitic and potassic) alterations followed by phyllic-propylitic alteration and sulfide mineralization. Various assemblages were formed during hydrothermal activity. Mineralization started at 560 °C at depth ~2.5 km by a magmatic fluid with 12.83 wt% NaCl equivalent average salinity, 0.833 g/cm3 density and 230.3 bars vapor pressure. Main sulfide and uranium mineralization started at 270 °C at very shallow depth by a high salinity (average 30wt% NaCl equivalent) fluid with 1.143 g/cm3 density and only 3.8 bars vapor pressure. This represents an epithermal formation conditions.

Several hydrothermal fluids were involved in the precipitation of various assemblages. Some assemblages, despite having similar mineralogical

composition, show different salinity and formation temperature. In addition, in some cases, younger assemblages show higher temperature than older assemblages indicating that the younger assemblages were precipitated from younger pulses of hydrothermal fluids which originated from possibly a new batch of magma. As a consequence, various hydrothermal fluids with different physico-chemical properties were responsible for the formation of these assemblages at Mag Hill. At deeper levels, the early-stage magnetite-actinolite- apatite hydrothermal assemblage formed by hot (560-434 °C) and moderately saline (11.70-13.9 wt% NaCl equivalent) magmatic paleofluid; at shallower levels, cooler mixed magmatic-meteoric fluids precipitated the younger assemblages including Cu-Co-U minerals. Each paleofluid experienced a different path during its evolution. These evolutionary paths are explained by boiling of hydrothermal fluid, mixing of high-temperature high-salinity magmatic paleofluid with cold low salinity groundwater, and simple cooling.

REFERENCES

Haas, J.L. Jr., 1971. The effect of salinity on the maximum thermal gradient of a hydrothermal system at hydrostatic pressure. Economic Geology 66, 940-946.

Hildebrand, R.S., 1984. Geology of the Rainy Lake-White Eagle Falls area, district of Mackenzie: Early Proterozoic cauldrons, stratovolcanos and subvolcanic plutons: Geological Survey of Canada, Paper 83-20, 42 pp.

Hoffman, P.F., 1978. Geology of the Sloan River map-area: Geological Survey of Canada, Open File 535, map scale 1:125,000.

Hoffman, P.F., McGlynn, J.C., 1977. Great Bear Batholith: volcano-plutonic depression, in Baragar, W.R.A., Coleman, L.C., and Hall, J.M., eds., Volcanic regimes in Canada: Geological Association of Canada Special Paper 16, 170–192.

Karimzadeh Somarin, A., Lentz, D., 2008. A fossil hydrothermal system in the Paleogene Mendejin volcanic sequence, East Azarbaijan, Iran: analysis of phase equilibria, geochemical mass-balance, and fluid evolution. Mineralogy and Petrology 94, 123-143.

Mumin, A.H., Somarin, A.K., Jones, B., Corriveau, L., Ootes, L., and Camier, J., 2008. The IOCG-porphyry-epithermal continuum of deposits types in the Great Bear Magmatic Zone, Northwest Territories, Canada, in Corriveau, L. and Mumin, A.H., eds., Exploring for iron oxide copper-gold deposits: Canada and global analogues: Geological Association of Canada, Mineral Deposits Division Short Course Volume, 57-76.

Muntean, J.L., Einaudi, M., 2000. Porphyry gold deposits of the Refugio district, Maricunga Belt, Northern Chile. Economic Geology 95, 1445-1472.

Roedder, E., 1984. Fluid inclusions. Min. Soc. Am., Reviews in Mineralogy 12, 644 pp.

Review of IOCG Style Polymetallic Mineralization in a Volcanic arc Setting of the Contact Lake Belt, Northwest Territories, Canada

A. Karimzadeh Somarin and A. Hamid Mumin
Department of Geology, Brandon University, Brandon, Manitoba, R7A 6A9, Canada

ABSTRACT
Wells conditions are different in wide range of temperature and depth. Cement slurries in such conditions have to remain pumpable and after setting to stay homogenous in production well life. For cementing operations in wide range of temperature and pressure and to accommodate cement slurries for individual well requirements more than 50 additives are now used for various API classes of cement. Laboratory in NIS - National Oil Company of Serbia provides cement analysis of dry cement, tests on cement slurries and cement stone in compliance with methods prescribed by API standard, whereby quality and type of equipment fully meet the requirements. Adaptation of the local cement to the well conditions has already been done by these additives and by numerous tests of pure cement and cement mixtures we developed a palette of typical cement mixtures for cementing oil wells in the south eastern region of the Pannonian basin.

1 INTRODUCTION

The Contact Lake Belt refers to the northwest-trending zone of volcanic and intrusive rocks in the Contact Lake area of the Great Bear Magmatic Zone (GBMZ east of Great Bear Lake, Northwest Territories, Canada (Fig. 1). This belt is located about 10 km southeast of the Port Radium-Echo Bay mining district, one of the historically (pre-1960) important sources of uranium in Canada, and a significant producer of silver plus lesser copper, nickel, cobalt, bismuth, radium, lead, and polonium between 1931–1982.

2 REGIONAL GEOLOGY

2.1 Great Bear Magmatic Zone

The Great Bear Magmatic Zone constitutes a 1.88–1.84 Ga Andean-type calc-alkaline volcano-plutonic arc complex, developed at the margin of the Archean Slave craton (Fig. 1; Hildebrand et al., 1987; Gandhi et al., 2001). The GBMZ was not recognized to be prospective for IOCG styles of mineralization until long after closure of the last producing mine in 1982 (Hildebrand, 1986; Gandhi and Bell, 1993).

The two best-known Canadian iron oxide-copper-gold (IOCG) deposits, the NICO Co-Au-Bi and the Sue-Dianne Cu-Ag-Au deposits (Goad et al., 2000a, b; Fig. 1), are located in the southern GBMZ. The northern GBMZ hosts past-producing vein-type U-Ag -Co-Cu mines, spectacular but weakly mineralized pyrite gossans, albite, magnetite-amphibole-apatite, potassic and phyllic alteration

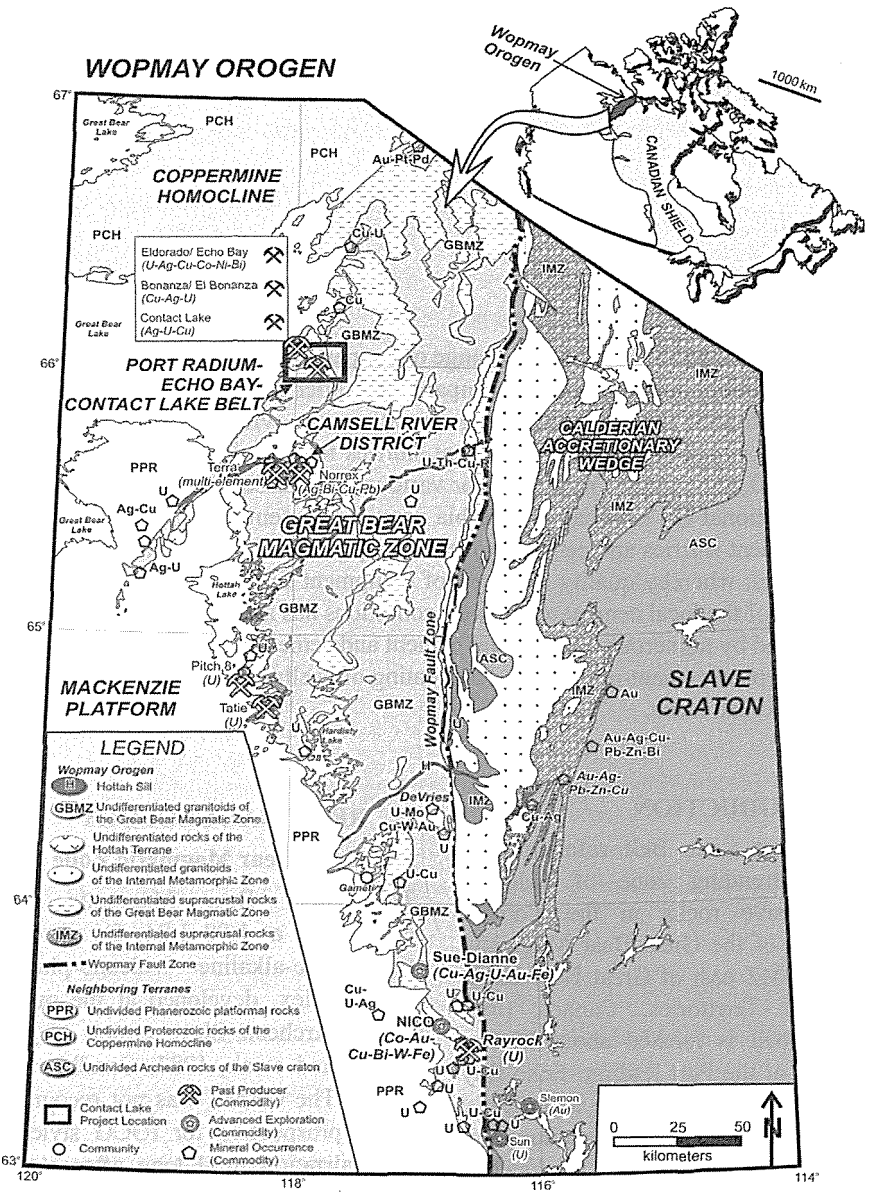

Fig. 1. Geological setting of the Contact Lake Belt within the Great Bear Magmatic Zone (Modified after Hoffman and Hall, 1993

zones (Robinson and Badham, 1974; Hildebrand, 1986; Reardon, 1992a, b, Mumin et al., 2007, 2008). Goad et al. (2000a, b) described the geology of the NICO Co-Bi-Au deposit discovered in themid-1990s, and demonstrated that it is hosted in iron- and potassium-altered, brecciated basement sedimentary rocks at and beneath a volcanic unconformity, some similarities with the Salobo IOCG deposit in Brazil (Requia et al., 2003). Camier (2002) reported on the geology and origin of the Sue-Dianne Cu-Ag-Au iron oxide-rich breccia complex, and demonstrated its many similarities to the Olympic Dam breccias. These and other exploration and geoscientific studies resulted in recognition that the Great Bear Magmatic Zone is host to several variants of the IOCG class of mineralization (Gandhi et al., 1996; Goad et al., 2000a, b; Camier, 2002; Gandhi, 2004; Mumin et al., 2007, 2008).

2.2 Port Radium and Echo Bay formations, northern GBMZ

The Port Radium and Echo Bay formations of the Echo Bay stratavolcano complex represent a single caldera fill sequence (Hildebrand et al., 1987; Mumin et al., 2007). The Port Radium Formation is composed of laminated volcanic tuff, pyroclastic breccia, and minor metasedimentary rocks, and is overlain by a thick sequence of andesitic volcanic rocks of the Echo Bay Formation. The lower part of this sequence (Mile Lake Member) consists of fine-grained to microporphyritic andesitic and trachytic flows intercalated with tuffaceous beds. The upper part of the sequence (Surprise Lake Member) consists of massive porphyritic trachyandesitic flows. To the north and northeast, the Echo Bay Formation is overlain by the Cameron Bay Formation, a succession of rhyodacitic ash-flow and ash-fall tuff intercalated with andesitic lava, arkose and conglomerate beds. The basal member of the Cameron Bay Formation is a crumbly-weathering, ferruginous conglomerate within extensive arkose that is overlain by poorly cemented sediments. The intercalated volcanic and sedimentary rocks are thought to result from several episodes caldera collapse and resurgence.

A number of intrusive rocks are emplaced into the volcanic succession including hornblende-plagioclase porphyry of the Cobalt Porphyry, diorite, monzodiorite and quartz monzonite of the Mystery Island Intrusive Suite, biotite-hornblende granite/quartz monzonite and diabase of variable age.

Geochemical studies of the altered volcanic rocks at Port Radium (Somarin and Mumin, 2008a) show extreme enrichment in a large suite of elements including Fe, P, Ti, Ca, Mn, Mg, Na, S, V, As, Ce, Y, Nb, Ta, Zn, Sc, Li, U, Co, Ni, Th, Cr, Cd and La. This enrichment is characteristic of at least some IOCG systems. It appears that such enrichment (particularly in Fe, P, V, Cr, Co, Ni and Ti) is caused by deeply sourced, highly fractionated melts with at least some mantle components, and probable mixing of mafic magma with more felsic crustal components.

2.3 Contact Lake Belt

The Contact Lake Belt comprises the southeast flank of the Echo Bay stratavolcano complex. The Belt is bounded, and presumably underlain to the south, southeastern, and southwestern extents by Granitic and syenogranitic batholiths of the Great Bear plutonic suite (Hildebrand, 1983; Mumin et al., 2007).

The central part of the belt is occupied by the Contact Lake pluton, which is mainly composed of a fine- to medium-grained, homogeneous monzonite/monzodiorite body with hypidiomorphic granular texture. It is comprised of plagioclase, K-feldspar, and 10 to 20% amphibole and biotite. Accessory minerals include pyroxene, quartz and secondary chlorite, epidote, and carbonate.

Collapse of the Echo Bay stratovolcano and associated lava flow and pyroclastic deposits is the most outstanding feature of volcanism in the Contact Lake Belt. These volcanic rocks, commonly andesitic in composition, and associated monzodiorite intrusions cover almost the entire of the belt (Fig. 2). Andesitic volcanic rocks vary from massive ash tuff, crystal tuff, lapilli tuff, to plagioclase and plagioclase-hornblende porphyritic and amygdaloidal lava flow and breccia. Plagioclase and hornblende

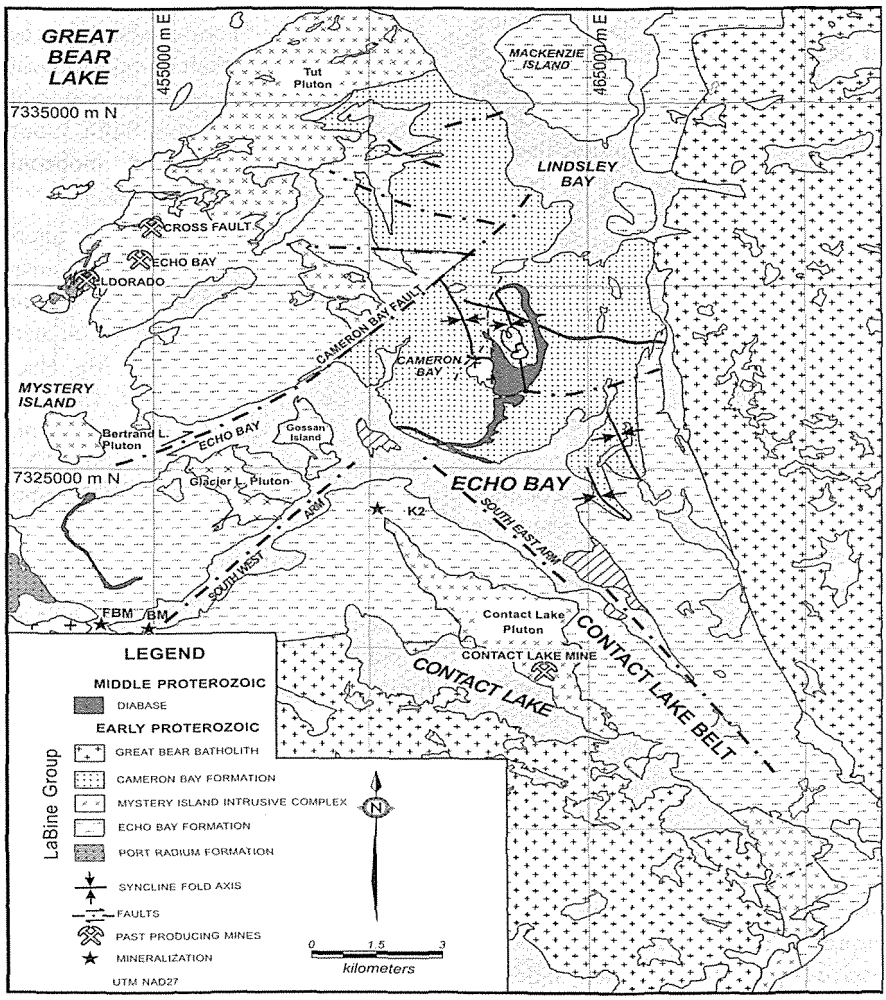

Fig. 2. Regional geology map of the Port Radium-Echo Bay district (modified after Hilderbrand, 1983; Reardon, 1992a)

phenocrysts, up to 8 mm long, are commonly replaced by epidote, sericite and chlorite. Amygdules are filled with quartz ± chlorite, carbonate, epidote, and hematite or pyrite, depending on the type of hydrothermal alteration affecting the immediate host rock.

Diorite and diabase dikes have intruded along SE- and E-trending structural zones.. These dikes are of limited width and length, although larger gabbroic dikes are exposed locally. The dikes are moderately magnetic and generally barren, and display only minimal to moderate hydrothermal alteration effects suggesting a syn-volcanic but slightly younger age for these dykes. However, they locally host vein-type mineralization such as the high-grade Thompson polymetallic showing. Some diorite dikes appear to be syn-volcanic, whereas gabbroic dikes that have intruded marginal syenogranite are clearly younger than the immediate host. The syenogranite may be genetically associated with the volcanic rocks.

One of the classic IOCG style mineralizations in the Contact Lake area is seen in the K2 hydrothermal system (Somarin and Mumin, 2008b). Two types of elemental association are found at K2: mafic-affinity (e.g. Fe, V, Cr, Co, Ni) and felsic-affinity elements (e.g. Zr, Hf, K, Na, Rb, U, Th). This bimodal association may indicate a mantle signature to the hydrothermal system, possibly by mixing of a mafic magma (having no or minimum crustal signature) at depth with the intermediate monzodioritic magma (fractionated with more crustal signature) that is immediately associated with the widespread hydrothermal alteration at K2.

3 ALTERATION AND MINERALIZATION

Vein type mineralization is common in the Great Bear Magmatic Zone where about ten past-producing mines are situated. They include the Rayrock U mine at its southern extent, the Terra and Norex Ag mines in the Camsell River district, and the Eldorado, Echo Bay, Contact Lake, Bonanza, and El Bonanza U-Ag-Cu ± Co-Ni-Bi mines in the Echo Bay district (Mursky, 1973; Kissin 1993a, b; Mumin et al., 2007). These deposits are structurally controlled, high-level, quartz or quartz-carbonate vein systems associated with varying degrees of iron oxide (hematite dominant) and alkali metasomatism. The presence of low-temperature mineral assemblages, vuggy nature, and open space-filling textures suggest an epithermal environment for formation of these deposits.

The deposits occur within regionally extensive IOCG alteration systems and are situated peripheral to the centers (source) of hydrothermal activity. Polyphase hydrothermal alteration affects all rocks of the belt. Various types of pervasive hydrothermal alteration are characterized based on dominant mineral assemblages including sodic (albite), magnetite-actinolite-apatite, potassic (K-feldspar), tourmalinization, hematitic, phyllic (quartz-sericite-pyrite), and propylitic (chlorite-epidote-carbonate±albite±sericite.

The high-level epithermal veins that constituted the economic ore were also enriched locally in one or more of the elements As, Ni, Co, Bi, Au, Zn, Pb, Sb, W, REE, and Ra, and many of these were episodically recovered, mostly as by-products of the Ag, U, and/or Cu mining. These ENE- and EW-striking economic veins show evidence of multiple hydrothermal events and brecciation during episodic ductile shearing to primarily brittle fracturing. Cumulative silver production from the Great Bear Magmatic Zone mining districts is >

50 Moz, of which 32 Moz are from the Port Radium-Echo Bay district (Normin, 2006). The Port Radium-Echo Bay district also reportedly yielded >5100 t Cu and ~15 million lbs U_3O_8.

More than forty different sulfide and arsenide minerals are reported from the Eldorado mine (Port Radium) alone (e.g., Mursky, 1973). Sulfide and arsenide minerals typically overprint quartz-hematite (± carbonate, chalcopyrite, pyrite, and pitchblende) veins. In the Port Radium district, sulfide-arsenide-quartz-carbonate-hematite veins occur in NE- and E-trending, steeply dipping fault and fracture zones. They are typically narrow veins averaging 1.2 m wide (but locally up to ~13 m) and form multiple sub-parallel veins within a ~1.6 km-long by ~600 m-wide NE-trending structural corridor that extends northeastward from the Eldorado mine (Fig. 2). These veins occur within an extensive halo of alkali-iron alteration that is similar to alteration throughout the district.

A second type of high-grade, but generally narrow (<2 m) and short (<100 m) vein, is found at several localities along the Contact Lake Belt. The best examples are the Contact Lake Mine, Thompson, Bornite Lake, South Contact, and Azurite showings. They are characterized by high-grade stringer to semi-massive chalcopyrite-bornite veins with quartz, carbonate, hematite ± arsenides, and are variably enriched in uranium, silver, cobalt, bismuth, zinc, and gold.

An early phase of albite and magnetite-actinolite-apatite alteration has a demonstrated special and probable genetic association with the Mystery Island suite of monzodioritic intrusions (Reardon, 1992b; Mumin et al., 2007, 2008), whereas late-stage polymetallic sulfide and arsenide mineralization may be genetically linked to the monzodiorite and/or to marginal granitic intrusions. The alkaline nature and spatial association of these granitic intrusions with altered and mineralized rocks in the belt raises as yet unresolved questions about their possible genetic relationship to various types of hydrothermal alteration and metal enrichment.

Similarities between the style and composition of alteration and mineralization, and the age of host rocks, in the Contact Lake area with those of the southern GBMZ and other IOCG districts worldwide clearly demonstrate its IOCG potential.

REFERENCES

Camier, J., 2002. The Sue-Dianne Fe-oxide Cu-Ag-Au breccia complex, southern Great Bear Magmatic Zone, Northwest Territories, Canada: M.Sc. thesis, University of Western Ontario, London, ON, 210 p.

Gandhi, S.S. (compiler), 2004. World distribution of iron oxide +/- Cu +/- Au +/- U deposits: World Minerals Geoscience Database, Geological Survey of Canada, unpublished database, http://gdr.nrcan.gc.ca/minres/data_e.php.

Gandhi, S.S., and Bell, R.T., 1993. Metallogenic concepts to aid exploration for the giant Olympic Dam-type deposits and their derivatives, in Maurice, Y.T., ed., Proceedings of the 8th Quadrennial International Association on the Genesis of Ore Deposits Symposium: E. Schweizerbart'sche Verlagsbuchhandlung, Stuttgart, Germany, 787–802.

Gandhi, S.S., Prasad, N., and Charbonneau, B.W., 1996. Geological and geophysical signatures of a

large polymetallic exploration target at Lou Lake, southern Great Bear magmatic zone, Northwest Territories: Geological Survey of Canada, Current Research Paper 1996-E, 147–158.

Gandhi, S.S., Mortensen, J.K., Prasad, N., and van Breemen, O., 2001. Magmatic evolution of the southern Great Bear continental arc, northwestern Canadian Shield: geochronological constraints: Canadian Journal of Earth Sciences, 38, 767–785.

Goad, R.E., Mumin, A.H., Duke N.A., Neale, K.L., and Mulligan, D.L. 2000a. Geology of the Proterozoic iron oxide-hosted NICO cobalt-gold-bismuth, and Sue Dianne copper-silver deposits, southern Great Bear Magmatic Zone, Northwest Territories, Canada, *in* Porter T.M., ed., Hydrothermal iron oxide copper-gold and related deposits: A global perspective: Australian Mineral Foundation, 1, 249–267.

Goad, R.E., Mumin, A.H, Duke, N.A., Neale, K.L., Mulligan, D.L., and Camier, W.J., 2000b. The NICO and Sue-Dianne Proterozoic, iron oxide-hosted, polymetallic deposits, Northwest Territories: application of the Olympic Dam model in exploration: Exploration and Mining Geology, 9, 123–140.

Hildebrand, R.S., 1983. Geology - Echo Bay-MacAlpine Channel area, district of Mackenzie, Northwest Territories: Geological Survey Canada, Map 1546A, scale 1:50,000.

Hildebrand, R.S., 1986. Kiruna-type deposits: their relationship to intermediate subvolcanic plutons in the Great Bear magmatic zone, northwest Canada: Economic Geology, 81, 640–659.

Hildebrand, R.S., Hoffman, P.F., and Bowring, S.A., 1987. Tectono-magmatic evolution of the 1.9 Ga Great Bear magmatic zone, Wopmay Orogen, northwestern Canada: Journal of Volcanology and Geothermal Research, 32, 99–118.

Kissin, S.A., 1993a. The geochemistry of transport and deposition in the formation of five-element (Ag-Ni-Co-As-Bi) veins, *in* Maurice, Y.T., ed., Proceedings of the Eight Quadrennial International Association on the Genesis of Ore Deposits Symposium: E. Schweizerbart'sche Verlagsbuchhandlung, Stuttgart, 773–786.

Kissin, S.A., 1993b. Five-element (Ni-Co-As-Ag-Bi) veins, in Sheahan, P.A. and Cherry, M.E., eds., Ore Deposit Models. Geoscience Canada Reprint Series 6, 87-98.

Mursky, G., 1973. Geology of the Port Radium map area, district of Mackenzie: Geological Survey of Canada, Memoir 374, 40 p. plus geology (Map 1349A) and aeromagnetic survey maps scale 1:50,0000.

Mumin, A.H., Somarin, A.K., Jones, B., Corriveau, L., Ootes, L., and Camier, J., 2008. The IOCG-porphyry-epithermal continuum of deposits types in the Great Bear Magmatic Zone, Northwest Territories, Canada, in Corriveau, L. and Mumin, A.H., eds., Exploring for iron oxide copper-gold deposits: Canada and global analogues: Geological Association of Canada, Mineral Deposits Division Short Course Volume, 57-76.

Mumin, A.H., Corriveau, L., Somarin, A.K., and Ootes, L., 2007. IOCG-type polymetallic mineralization

in the Contact Lake Belt, Great Bear Magmatic Zone, Northwest Territories. Exploration and Mining Geology, 16, 187-208.

Normin, 2006. Northwest Territories Geoscience website (http://www.nwtgeoscience.ca/normin/).

Reardon, N.C., 1992a. Altered rocks associated with the Mystery Island Intrusive Suite, Echo Bay, Northwest Territories: Geological Survey of Canada, Open File 2507, map scale 1:25,000.

Reardon, N.C., 1992b. Magmatic-hydrothermal systems and associated magnetite-apatite-actinolite deposits, Echo Bay, Northwest Territories: Unpublished MSc thesis, University of Ottawa, 154 p.

Requia, K., Stein, H., Fontboté, L., and Chiaradia, M., 2003. Re–Os and Pb–Pb geochronology of the Archean Salobo iron oxide copper-gold deposit, Carajás mineral province, northern Brazil: Mineralium Deposita, 38, 727–738.

Robinson, B.W., and Badham, J.P.N., 1974. Stable isotope geochemistry and the origin of the Great Bear Lake silver deposit, Northwest Territories, Canada: Canadian Journal of Earth Sciences, 11, 698–711.

Somarin, A.K., and Mumin, H., 2008a. Geochemistry and possible source of metals and alkalies for the Port Radium IOCG style hydrothermal system, Great Bear Magmatic Zone, Northwest Territories, Canada. Geological Association of Canada and Mineralogical Association of Canada Annual Meeting, Quebec City, Quebec, May 2008.

Somarin, A.K., and Mumin, H., 2008b. Geochemical evidence of a mafic contribution to IOCG style hydrothermal systems: evidence from the K2 system, Great Bear Magmatic Zone, Northwest Territories. Geological Association of Canada and Mineralogical Association of Canada Annual Meeting, Quebec City, Quebec, May 2008.

Application of local Cement for Cementing Oil Wells in the South Eastern Region of the Pannonian Basin

Zvonimir Bošković
NIS - Naftagas, Novi Sad, Serbia
Eldar Husejnagić
Faculty of Mining and Geology, Tuzla, Bosnia and Herzegovina
Vladimir Čebašek
Faculty of Mining and Geology, Belgrade, Serbia
Slobodan Stanić
NIS - Naftagas, Novi Sad, Serbia

ABSTRACT Wells conditions are different in wide range of temperature and depth. Cement slurries in such conditions have to remain pumpable and after setting to stay homogenous in production well life. For cementing operations in wide range of temperature and pressure and to accommodate cement slurries for individual well requirements more than 50 additives are now used for various API classes of cement. Laboratory in NIS - National Oil Company of Serbia provides cement analysis of dry cement, tests on cement slurries and cement stone in compliance with methods prescribed by API standard, whereby quality and type of equipment fully meet the requirements. Adaptation of the local cement to the well conditions has already been done by these additives and by numerous tests of pure cement and cement mixtures we developed a palette of typical cement mixtures for cementing oil wells in the south eastern region of the Pannonian basin.

1 INTRODUCTION

As basis for preparation of cement mixtures, NIS Naftagas – Serbia uses cements E, F, and G API class, as well as local cements. Adaptation of local cements is done with additives for regulation of cement slurry and cement stone characteristics manufactured by leading world servicing companies for conductor pipe, intermediate and production casing. Laboratory test of cements, additives for cements and cement mixtures have a huge importance for successful cementing of casing. Tests include quality control of supplied components, design of cement mixtures, control of cement mixture samples in the preparatory phase. Bringing physical-mechanical values of cement slurries and cement stone within the parameters prescribed by API Standard – API Specification 10 - (thickening time,

filtrate loss, unbound water, reological parameters, development of compressive strength) has lead to creation of several standardized mixtures based on local cements.

2 TESTING OF LOCAL CEMENTS

Principal requirements set for cement slurry based on local cements are: thickening time, filtrate loss, reology, development of compressive strength of cement stone, volume mass, mixability and special requirements (gas migration control, thixotropy, expansion, bond tightness with casing and formation). All tests have been executed in compliance with recommendations of API Standard, Specification 10 and with application of standard laboratory equipment as defined in this Specification.

2.1 Thickening time

Thickening time of cement slurries is one of the critical elements in designing of cement mixtures in general. Adjusting adequate thickening time of cement mixtures based on local cement, required a large number of laboratory tests and corresponding selection from retarder program. HTHP consistometers Chandler Engineering, models 8-25-10 and 7-1, as well as Halliburton model 800.6605 were used. Test tables have been made as recommended by API Standard and with application of well data (temperature and pressure gradient, type, volume mass and working fluid characteristics, cementing type and available equipment).

When conducting acceptance tests on local cements we also apply our internal quality control procedure which includes determination of thickening time at test temperatures from 50 °C to 90 °C with application of standard retarder – lignosulphonate type, determination of optimal water-cement ratio, determination of diffusion and compressive strength of cement stone of standardized mixtures. Table 1 presents certain physical values of several standardized cement mixtures based on local cements.

Table 1. Standardized cement mixtures based on local cements and their application

Mixture	w/c	Density (kg/m^3)	Diffusion (mm)	Thickening time	Application
I cement, pucolan and accelerator	0.50	1830	210	80'/50°C	Primary cementing of conductor pipe and intermediate casing
II cement, pucolan, gypsum, retarder	0.50	1830	220	168'/50°C	Primary cementing of intermediate casing and cement bridges
III cement, pucolan, retarder, dispergator and filtration regulator	0.55	1770	240	136'/90°C	Primary cementing production casing, cementing under pressure and cementing of „liner" casing
IV cement, pucolan, fly ash (dia. earth, dispergator and filtration regulator	0.68	1620	230	147'/90°C	Primary cementing of production casing (lead cement)
V cement, pucolan, retarder, dispergator and filtration regulator	0.55	1750	240	110'/110°C	Cementing under pressure, cement plugs and bridges
VI cement, quartz flour, retarder, dispergator, filtration regulator and anti- moussant	0.50	1780	220	90'/125°C	Primary cementing of production casing, "liner", cement plugs and bridges

2.2 Filtrate loss

According to API Specification 10, filtrate loss for cement G class is not precisely defined, but it is recommended to apply approximate values depending on type of cementing operations:

For cementing intermediate casing	up to 1000 ml/30min
For cementing production casing	up to 500 ml/30min
For cementing "liner" casing	≤ 100 ml/30min
For gas wells cementing and cementing under pressure	from 30 to 50 ml/30min

Excessive filtrate loss of cement slurry negatively influences on cementing operation during pumping in, displacement, and during waiting on cement – WOC because density of cement slurry is increased, reological properties are changed, cement bridges of dehydrated material are created. As per their chemical nature, additives for filtrate loss regulation are cellulose derivates, synthetic polymers, asphaltenes, thermoplastic resin, bentonite etc, and they act by increase of viscosity of bound water, creating polymer layer on filter cake and particles of cement, and by packing of particles according to their size. Filtrate loss values of standardized cement mixtures based on local cement are presented in Table 2.

Table 2. Filtrate loss of standardized cement mixtures based on local cements

Mix.	w/c	ΔP (psi)	ΔT (°C)	Temp. (°C)	Filtration
I	0.50	500	-	50	600+ ml/30'
II	0.50	500	-	50	500+ ml/30'
III	0.55	1000	2.5	90	180 ml/30'
IV	0.68	1000	2.5	90	300+ ml/30'
V	0.55	1000	3.0	110	80 ml/30'
VI	0.50	1000	3.0	125	45 ml/30'

2.3 Reology

Reology of cement slurries has a great importance for design, execution and quality of primary cementing. It is necessary to be familiar with reology properties in order to estimate mixability and pumpability of cement slurries, determination of pressure - depth ratio during and after displacement, calculation of return circulation in the "free fall" phase, anticipation of temperature profile during pumping cement slurry in and designing capacity required for obtaining optimal displacement of cement slurry. Chemical composition, specific area of supplied local cement, relatively high water-cement ratio and presence of additives of various chemical composition for various purposes in cement mixture influenced on reological behavior of cement slurries (Table 3).

Table 3. Reological properties of standardized cementing mixtures based on local cements

Mix	w/c	PV (mPas)	GT (Pa)	n'	K' ($Pas^{n'}$)	Gel (MPa)
I	0.50	47	11.0	0.75	0.3276	7.5/31.5
II	0.50	73	7.5	0.98	0.1550	5.5/8.5
III	0.55	39	5.0	0.90	0.0020	3.5/15.0
IV	0.68	31	5.5	0.79	0.5330	5.0/19.0
V	0.55	120	20.0	0.81	0.0870	3.5/7.5
VI	0.50	87	13.0	0.82	0.3400	5.5/15.0

Due to the fact that dispergators play an important role in fine defining of reological properties, local cements required application of dispergators of different chemical nature such as complex sulphonate polymers, lignosulphonates, organic acid salts etc. Mixing and test procedures from API Specification 10 have been followed during measuring reological properties of cementing slurries, and rotating viscometer Chan 35 and Fann 35 were used.

2.4 Compressive strength

Destructive methods have been done (Table 4) in accordance with API Specification Section 7, Appendix D of Specification 10, procedure and tables for determination of compressive strength, chambers for cement maturation Chandler model 7-00 and Chandler model 19-90-10 in addition to tester for measuring compressive strength of

cement stone Chandler model 4207.

Table 4. Compressive strength of standardized cement slurries of local cements

Mix.	w/c	Temp. (°C)	Pressure (MPa)	Time (h)	Compr. strength (MPa)
I	0.50	50	-	24	16.10
II	0.50	50	-	24	11.00
III	0.55	110	21	24	14.52
IV	0.68	110	21	24	6.80
V	0.55	127	21	16	10.40
VI	0.50	138	21	20	19.70

Also, we have applied UCA (ultrasonic cement analyzer). Its advantage is reflected in elimination of a large number of tests using traditional, destructive method, continuous tracking and determining development trend of compressive strength more precisely and therewith determining WOC (waiting on cement) more accurately.

3 CONDUCTOR PIPE CEMENTING

On some oil fields in the south eastern region of the Pannonian basin, conductor pipe OD 355.6mm is set in the wells with nominal drilling diameter 444.5mm up to 20m, and cement mixture properties for cementing conductor pipe are presented in Table 5.

Table 5. Properties of cement mixture for conductor pipe cementing

Composition of cement mixture	w/c	Density (kg/l)	Thickening time start/final (min)	Compressive strength (MPa)	WOC (h)
Local cement + 2% CaCl2	0.50	1.83	48/64	14.95	16

4 INTERMEDIATE CASING CEMENTING

Some intermediate casing ID 244.5 mm is set up to 450 m in hole bit size 311.15 mm and annulus from bottom to the top is cemented. Since temperatures at the well bottom do not exceed 50 °C local cement without additives is applied (Table 6).

Table 6. Properties of local cement for cementing intermediate casing

Composition of cement mixture	w/c	Density (kg/l)	Thickening time start/final (min)	Compressive strength (MPa)	WOC (h)
Local cement	0.50	1.78 – 1.81	114/123	7.2	24

5 PRODUCTION CASING CEMENTING

On some oil fields in the south eastern region of the Pannonian basin, where temperatures at the bottom of the well do not exceed 120 °C, and layer fracturing pressure gradient is from 0.148 – 0.18 bar/m, through adaptation of local cements successful cementing operations of annulus between production casing OD 139.7 mm and hole size 215.9 mm are executed, with application of lead and tail cement slurries (Table 7 and 8).

Reological properties of such cement mixtures (Table 9) do not allow turbulent displacement regime (displacement capacity more than 1800 l/min), yet the displacement of cement slurry is done in highly laminar regime – Re = 2000.

Table 7. Properties of lead cement slurry

Composition of cement mixture	w/c	Density (kg/l)	Thickening time start/final (min)	Compressive strength (MPa)	WOC (h)
Local cement, volume mass regulator, dispergator, retarder, fluid loss	0.70	1.59	120/129	10.15	24

Table 8. Properties of tail cement slurry

Composition of cement mixture	w/c	Density (kg/l)	Thickening time start/final (min)	Compressive strength (MPa)	WOC (h)
Local cement, dispergator, retarder, fluid loss	0.55	1.77	139/153	12.4	48

Table 9. Reological properties of fluid

Fluid	Density (kg/l)	PV (mPas)	GT (Pa)	Gel (Pa)
Mud	1.13	16	7	4/12
Lead cement	1.59	23	4	4/13
Tail cement	1.77	33	12	5/12

6 CONCLUSION

Thickening time regulation of cement mixtures with local cements is possible for majority of primary and secondary operations for temperatures up to 120 °C. With partially increased demand of additives for filtrate loss regulation in comparison to API cements it is possible to bring filtrate loss of cement slurries within satisfactory limits for a particular type of cementing. Retarded development of compressive strength of cement stone i.e. longer WOC in comparison to API cements increases nonproductive time of drilling rigs, and costs accordingly. Densities of cement slurries up to 1849 kg/m^3 meet most of the requirements. There are challenges with densities above 1849 kg/m^3 due to high w/c ratio and increased retarder and dispergator concentrations which may threaten stability of the system.

REFERENCES

Technical documentation of NIS Naftagas

API Specification 10 A, Twenty-second edition, January 1, 1995.

Model for Analysing Cement Stone Stability After Cementing Production Strings in the Wells of the South Eastern Region of the Pannonian basin

Zvonimir Bošković
NIS - Naftagas, Novi Sad, Serbia
Eldar Husejnagić
Faculty of Mining and Geology, Tuzla, Bosnia and Herzegovina
Vladimir Čebašek
Faculty of Mining and Geology, Belgrade, Serbia
Slobodan Stanić
NIS - Naftagas, Novi Sad, Serbia

ABSTRACT The main function of the cement in the annulus of the well is to prevent any fluid communication between drilled formations, to provide long term zonal isolation and to bond and support the casing. In addition to isolating oil – gas – water producing zones, cement also aids in protecting the casing from corrosion, preventing blowout by quickly forming a seal and sealing off zones of lost circulation, or thief zones. Cement systems with low Young's modulus value compared to that of the rock are the best cements in term of mechanical durability. These requirements are function of the downhole specific well environment such as well geometry, casing properties, rock mechanical properties and expected loading history. Mechanical damage is caused by a large increase of wellbore pressure, a large increase of wellbore temperature or the formation loading. Model for selection adequate cement slurry and analyzing cement sheath integrity during well life is necessary.

1 INTRODUCTION

Exploration activities, up to present day, in the region of the south-eastern Pannonian basin resulted in founding over 230 deposits of hydrocarbons on 99 oil and gas fields on depths from 300 – 3600 m. According to the type of trap, most of the deposits belong to deposits with combined or stratigraphic trap. Majority of discovered deposits, as per the quantity of acquired reserves belong to group of marginal, while small deposits and deposits of medium size are the least in number. Main characteristic of the south-eastern region of the Pannonian basin is that the deposits of classical structure type occur up to

2200.m depth with favourable physical characteristics of reservoir rocks, with regular hydrodynamic ratio between the layers, and linear growth of temperature gradient without significant anomalies.

Deeper than 2200 m, occur zones with overbalance pressures. Reservoir rocks beside hydrocarbons are saturated with corrosive fluids (CO_2 and H_2S), and layer pressures and temperatures are extremely high. Such natural conditions of rock spreading in the south-eastern region of the Pannonian basin are becoming worse and more complex with larger depths, especially in the period of Mesozoic, while layer pressures on the certain locations reach even 800 bar, while temperatures reach over 200 °C. Geological explorations in the south-eastern region of the Pannonian basin are taking place for over two centuries. For a long time, geologists paid due attention to study of geology of the mountain ranges on the rims of the basin, as well as the Fruška gora mountain, fro which, from the very beginning, it was thought to represent a remarkable playground for development of fundamental geological disciplines. Intensive development in study of geological material in the south –eastern region of the Pannonian basin starts only in the second half of the 20th century and basically it is defined by development of petroleum-geological explorations. In geological studies, so far, it has been determined that geological material of the south-eastern region of the Pannonian basin consists of Paleozoic, Mesozoic and Cenozoic rocks.

2 COLLECTOR ROCKS OF THE SOUTH-EASTERN REGION OF THE PANNONIAN BASIN

In the south-eastern region of the Pannonian basin collector rocks, as carriers of hydrocarbons, are detected and examined in various lithological formations. The oldest reservoir rocks were drilled in metamorphous series of Paleozoic period which are lithologically presented with very hard and fractured schists and gneises. Young's modulus of elasticity ranges between 6550 – 8960 MPa and Poisson's coefficients from 0.25 – 0.29. Collector rocks are also represented by sediments from Mesozoic era: from Triassic until Cretaceous. Observed rocks of ophiolite complex are represented with periodites and serpentinites with secondary type of porosity. Young's modulus of elasticity ranges from 4550 – 8960 MPa and Poisson's coefficient from 0.22 – 0.29. Sandstones and metamorphic rocks from Cretaceous era have the same characteristics as above described rocks.

Neogene formations include Lower, Middle and Upper Miocene and Pliocene. Lithologically, they are presented with conglomerates and breccias of red-brown color. These are fractured series, and main repositories are gaps and cavities. Young's modulus of elasticity ranges from 4480 – 8960 MPa and Poisson's coefficients from 0.22 – 0.25.

In the Middle Miocene, reef, sub-reef and basin sediments were used as collector rocks that are represented by lime stones, marls and clastics. These are soft up to hard formations with secondary inter granular and combined porosity type. Marls and marl lime stones with inter layers of sandstones are Pannonian sediments and they have been used as collector rocks on almost entire area of the south-eastern region of the Pannonian basin with combined type of porosity in which sub-vertical cracks are major paths of hydrocarbons.

Besides Pannonian sediments, Pontian sediments from tertiary complex

of the Pannonian basin of Vojvodina have been analyzed. Pontian sediments as collectors and deposits of hydrocarbons, lithologically are represented by marl-clay-aleurolite- sandy associations. Main repositories of hydrocarbons are layers of sands and sandstones of various thickness. Sands and sandstones consist of quartz, muscovite and feldspat, and binder is either foully or carbon type. According to the hardness they belong to soft- medium hard formations. Young's modulus of elasticity is between 1580 – 4480 MPa, and Poisson's coefficient from 0.13 – 0.22. According to the type of porosity they belong to sediments with inter granular type and combine type of porosity is rarely noticed: inter granular and secondary.

Primary cementing mixtures for oil wells are becoming more complex and demanding due to extreme conditions which are expected during well life. Stress to which cement stone is exposed during well operations can be so strong to damage it and it has negative influence on safety and economical aspect of the well.

In the south-eastern region of the Pannonian basin there is a need for use of cement mixtures of lower specific density. Reason for that are formations with low gradient of fracturing, where, during cementing process, through use of medium heavy and heavy cement mixtures of specific density from 1.80 – 1.90 kg/dm^3, loss of circulation occurs or, during the process of hardening cement slurry in the annulus, up to decrease of cement slurry level in well annulus where conditions for fluid migration are created. Preparation of cement slurries of reduced specific density, with reference to type of additives added, vary in comparison to preparation of standard cement mixtures. The most extensively used cement mixture of reduced specific density in NIS Naftagas - Serbia is the one with additives which bind water (bentonit). This cement mixture for preparation and laboratory analysis does not require other equipment except for the standard one.

3 MODEL FOR ANALYZING STABILITY OF CEMENT STONE THICKENING TIME

Model for analyzing stability of cement stone is design in such manner to completely comply with the status and conditions existing in the well. Its formation through application of software package Phase^2 is divided into two entities such as:

- Graphical display of the model, and
- Defining characteristics of the model.

Models which are presented in figures 1, 2 and 3 represent typical constructions of production casing used in the wells of south-eastern region of the Pannonian basin.

Research and production wells on the territory of the south –eastern region of the Pannonian basin in their construction have production casing with outer diameter of 177.8 mm. Collector rocks where such casing is installed are medium hard and hard formations. Production casing P-110 (51.8 kg/m′) analyzed in this work is set in the wells with high thermo-bar conditions.

3.1 Model I - Model of the well with casing string 177.8 mm P-110 (51.8 kg/m′) set up to 2800 m

Bit diameter: 215.9 mm, TD=2800 m.
Casing: ***OD=177.8 mm,***
ID=152.9 mm,
GRAD P-110
Formation: ***medium and hard***

Besides previously mentioned construction, on the territory of the south-eastern region of the Pannonian basin non-standard construction is applied with use of production casing of outer diameter 139.7 mm in the wells of 215.9 mm diameter. Use of casing grade, K-55 (20.83 kg/m′) and K-55 (23.0 kg/m′) is standard for setting in collectors consisting of soft and medium hard formations.

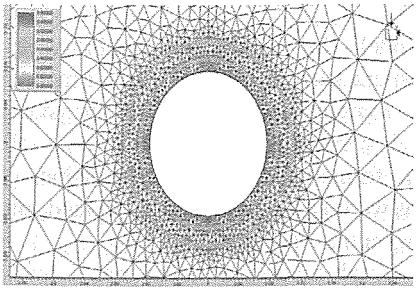

Figure 1. Model of the well with casing 177.8 mm P-110 (51.8 kg/m′) set up to 2800 m

3.2 Model II - Model of the well with casing string 139.7 mm K-55 (20.83 kg/m) set u to 1100 m

Bit diameter: 215.9 mm, TD=1100 m.
Casing: OD=139.7mm,
ID= 127.3mm,
GRAD K-55
Formation: soft and medium hard

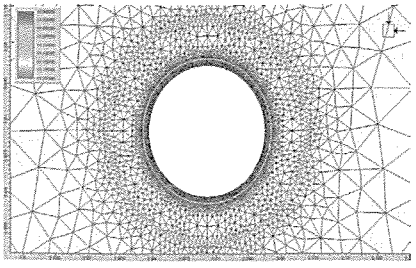

Figure 2. Model of the well with casing 139.7 mm K-55 (20.83 kg/m′) set up to 1100 m

3.3 Model III - Model of the well with casing string 139.7 mm K-55 (23,0 kg/m′) set up to 1100 m

Bit diameter: 215.9 mm, TD=1100m.
Casing: ID=125.73mm,
OD=139.7mm,
GRAD: K-55
Formation: soft and medium hard

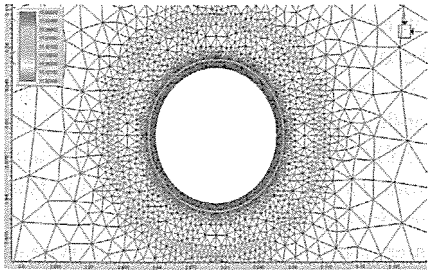

Figure 3. Model of the well with casing 139.7 mm K-55 (23.0 kg/m′) set up to 1100 m

In Table 1, list of number of finite elements and "nods" for certain well models with characteristic production casing.

Table 1. Finite elements number and "nods"

Production casing	Finite elements number	No. of nods
Grad:P-110 (51.8 kg/m′)	21872	11136
Grad:K-55 (20.83 kg/m′)	26464	13552
Grad:K-55 (23.0 kg/m′)	26280	13460

It is possible to execute detailed analysis of: stress condition ($\sigma_1 = \sigma_0$, $\sigma_3 = \sigma_r$), course and direction of deformations.

Model features, and their determination is divided into two groups:

- The first group includes determination of stress fields where analyzed model is located (permanently and gravitationally), sizes which determine the stress field, as well as determination of borderline conditions of the model. In this case, permanent stress field has been adopted with the following value of horizontal component σ_H = 28 MPa and 11 MPa. These values of stress field are adopted, since in the course of production casing string cementing process, displacement of cement slurry has been done with water.
- Within the second group, identification of physical-mechanical material characteristics is carried out. This program gives possibility to identify up to 10 various materials. Here, it is required to determine one out of three criteria for material fracturing (Mohr-Coulomb, Hoek-Brown, Drucker-Prager) and define a material, depending on available values, as flexible or plastic. Table 2 lists characteristics of materials used in these models, in accordance with Mohr-Coulomb criterion. All materials are considered to be flexible.

This software package enables simultaneous analysis of several models, so that changes in well conditions can be investigated at different well geometry, and optimal solution which would provide satisfactory stability of casing-cement stone-formation can be found.

Laboratory analysis of well cements in NIS Naftagas – Serbia up to now have covered, beside basic cement characteristics, analysis of mechanical compression strength. These laboratory data and their values represent a part of input, variable values used in technical-technological analysis and evaluation of sustainability of well cement stone quality and stability. Having reviewed laboratory tests, it has been determined that it is necessary to analyze parameter values of Young's modulus of elasticity as well as Poisson coefficients. Values of these mechanical parameters indicate borderline values of cyclic stress in situations of increased and reduced well pressure. Values of these coefficients indicate obtained quality of cement stone and its specific features in achieving its purpose when used in deep well

Tablo 2 Metarial Characteristics

Material	Flexible module E (MPa)	Poisson coefficient μ	Tensile strength σ_t (MPa)	Angle of inner friction φ (°)	Cohesion c (MPa)
Iron	200000	0.27	880	53.5	138.77
Cement stone: API Class G	9200	0.2	3	42.95	6.05
Cement stone: Spec. cement system (1)	4100	0.2	3	42.95	6.05
Cement stone: Spec. cement system (2)	2600	0.2	3	42.95	6.05
Formation: soft	1580	0.13	2.07	30	10.5
Formation: medium hard	4550	0.22	2.07	30	10.5
Formation: hard	8960	0.29	2.07	30	10.5

conditions.

Attention has to be paid to cement mixtures with flexibility parameters set to meet requirements of long term mechanical durability. These types of cement mixtures contain additives for volume increase which lead to optimal composition of cement mixture for preventing isolation loss when conditions in the well are changed. However, even though all prerequisites are fulfilled, and cement operation has been executed in technically correct manner, there are various operations in well system which lead to occurrence of stress and forces which are sufficient to destroy integrity of cement sheath. Permeability of the annulus may face a problem of long term gas migration as a consequence.

Cement mixtures, which after hardening, have tensile strength with lower Young's modulus of elasticity in comparison to formations, are the best from the aspect of retaining mechanical hardness. These requirements are in function of specific well environment such as well geometry, characteristics of casing, mechanical characteristics of formation and assumed load in the well.

4 CONCLUSION

Mechanical damages are caused by increase of well pressure (inspection of casing tightness, increase of specific mud density, perforation of casing, stimulation, gas production), considerable increase of temperature in the well (geothermal production, steam injection and wells with extreme thermo-bar conditions) or formation loading (creep, faulting, compaction...). More unfavorable condition is found with unconsolidated formations, since they do not have capacity to mechanically follow deformation of cement stone.

At this point, the only technique which can be applied for prevention of micro channels to occur, beside special cementing operations, is use of mixtures which do not shrink while hardening or even in some cases expanding cement mixtures. Results of experiment lead to conclusion that cased wells cemented by expanding cement mixtures in soft formations (weakly bonded sandstones) carry the risk of permeability between cement stone and line of casing, since expansion happens radially in the direction of the lowest resistance. Therefore, use of expanding cement mixture is the best in hard formations. In such case, cement is overstressed and good hydraulic impermeability has been achieved. Practically speaking, this means that cement stone has to be so flexible in comparison to rock, to enable expanding towards casing.

REFERENCES

Technical documentation of NIS Naftagas

Brady, B.H.G., Brown, E.T., 2002 *Rock Mechanics For Underground Mining*, George Allen&Unwin, London, 527 p.

Budavari, S., 1983 *Rock Mechanics In Mining Practice*, The South African Institute of Mining And Metallurgy, Johannesburg, 282 p

Rocscience Inc., 1999 *Phase² – 2D finite element program for calculating stress and estimating support around underground excavations, Tutorial Manual*, Rocscience Inc., Toronto, 163 p

Hoek, E., 2007 *Practical Rock Engineering*, Rocscience Inc., Toronto, 313 p

The Itacolomito Project – Mapping Rocks to Stonemasonry

Rodrigo Fina Ferreira, Issâmu Endo, Carlos Alberto Pereira
Universidade Federal de Ouro Preto, Ouro Preto, MG, Brazil
Antonio Liccardo
Univerdidade Federal do Paraná, Curitiba, PR, Brazil

ABSTRACT The ITACOLOMITO PROJECT, a mapping of quartzites used in stonemasonry in Ouro Preto, Brazil, is the result of Geology Science and Mining Engineering teamwork in the stonemasonry school. Among the objectives are data generation about rocks used in this craft for preservation and conservation; and valuation of "Cultural Heritage of the Humanity", the title given by UNESCO to Ouro Preto city, in Minas Gerais. The main purpose was to survey, to organize and to systemize geological data for supporting the "Oficina da Cantaria" with specific actions, including production of special pieces for restoration or even new artistic works. The main results of this research are presented in this excerpt and include: investigation into the origin of lithologic materials used in masonry works; a specific geological survey in Ouro Preto region; to build a thematic map of source materials used in masonry; and the location of old quartzite extraction sites used to build the city.

1 INTRODUCTION

The "Itacolomito Project - mapping rocks used in stonemasonry" has as an objective the preservation of Ouro Preto´s National Heritage and to show the importance of stonemasonry as a craft. The project intends to carry out the geological survey of a discrete area of Itacolomi quartzite, located in Itacolomi mountain, near Ouro Preto city, aiming to characterize the different kinds of quartzite with geological analysis. These rocks are used in stonemasonry in such a way as to replace pieces qualified by their geological characteristics; this can be done in an appropriate way without losing the characteristics of the work.

Ouro Preto´s historical heritage deserves not only our narrow specialist interest but international attention for being the world's biggest architectural Baroque collection. Preserving it is a way of recovering part of its history and art, which could be a source of culture and inspiration for future generations.

Quartzite is the geological material most often used in stonemasonry. By definition, it is a metamorphic rock constituted of 85% quartz. The remaining parts are formed of a variety of minerals,

such as muscovite, feldspar, zircon and opaque minerals such as hematite, ilmenite and magnetite. Quartzite, as has already been mentioned, belongs to Itacolomi Mountain and is a metamorphic rock of sedimentary origin. The composition is very simple - however, its structure is a complex setting of components; if shape and size of grains are considered, a great variation in different layers can be seen. The properties of this kind of rock can usually be evaluated by their visual aspects.

With the above in mind, the restoration process of the works in Ouro Preto's stonemasonry should follow, as the minimum standard of quality, the similarity of the materials. This procedure requires knowing the characteristics of the original materials, not only about their composition but also about their structural aspects and textures, as well as the material's colour. So, geological knowledge is the most appropriate tool for finding rocks with the same characteristics as the original masonry works.

Itacolomi Mountain is formed by rocks of the Itacolomi Group and is situated between Mariana and Ouro Preto, approximately between latitudes 43°23′ and 20°27′south. It consists of a physiographic element used as a point of reference in south-east Minas Gerais, with an average altitude of 1300m, a minimum of 750m rising to a maximum of 1762m, which corresponds to Itacolomi Peak. This mountain belongs to the southern portions of the Espinhaço mountain range (see Figure 1).

The control of quartzites in this mountain belongs to Itacolomi State Park whose legal power derives from the Instituto Estadual de Florestas (IEF) and is accessed from Ouro Preto by the Contorno highway, BR-356, in the direction of Passagem de Mariana.

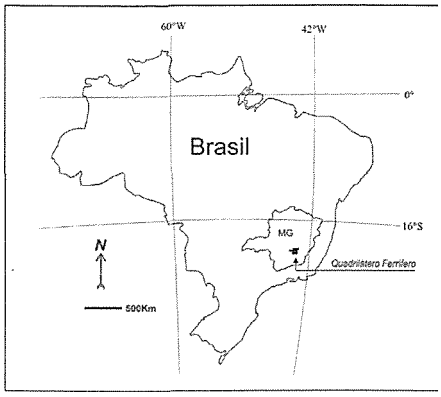

Figure 1 – Localization map of studied region showing Ouro Preto, the baroque city, considered international cultural heritage by UNESCO.

2 MATERIALS AND METHODS

Firstly, bibliographical research about the region's geology was undertaken, as shown above. Following this, field work was performed in order to define the area where the research should take place. This was located on the road to Itacolomi Peak.

To ensure the initial research was correct, a preliminary section of the specific region was made, in order to facilitate the study and to make it more detailed and reliable.

The section was constructed using aerial photography of the region to a scale of 1:25000 and supplemented and cross-checked with the detailed research from the field.

The following stages were developed:

- Research of stratigraphy;
- Rock sampling;

• Petrographical analysis of samples;

• Description of thin sections to characterize the composition of the rock, volumetric percentage of minerals, as well as texture determination and primary structures.

2.1 Geological Context

In regional terms, the investigated area is located in the centre-southeast sector of Quadrilátero Ferrífero (QFe) and includes large rocky clusters: a) Ancient Metamorphic Compounds; b) Rio das Velhas Supergroup c) Minas Supergroup d) Sabará Group e) Itacolomi Group (Fig. 2).

The metamorphic groups of QFe enclose different rocks with large exposure in the S-SE portion. These units are predominantly formed by striped gneisses, with or without amphibolitic inclusions, migmatites and granites of diverse compositions. The metamorphic behaviour of this unit is, generally, polyphasic and affected by a regional metamorphism in medium-high amphibolitic facies and, also, a retrograde metamorphism in greenschist facies.

On the textural and structural side, the rocks of these groups can be isotopic or foliated, as a result of the superimposing of tectono-metamorphic processes. Generally, the main foliation is a product of transposition, being the result of processes linked to the ductile non-coaxial cut. The orientation, with high deep angles, is mainly N-S, NE-SW and E-W.

Commonly, basic rocks fulfill discontinuities produced by crustal distension. The contacts of these groups are, normally, tectonical, showing a foliation from a medium to high angle (*e.g.* Gomes 1985; 1986 e 1989, Endo & Chemale 1991; Marshak *et al.* 1992; Costa 1992; Endo & Nalini 1992; Hippertt *et al.* 1992; Chemale *et al.* 1994) or also concordants (*e.g.* Herz 1970).

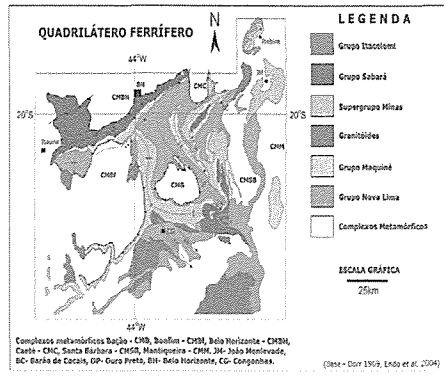

Figure 2 - Simplified geological map of Quadrilátero Ferrífero, where Ouro Preto city and studied area are included.

The Itacolomi Group, defined by Dorr (1969), is constituted of two facies: one called Itacolomi quartzite and the other is composed of phylite. The quartzite facies is constituted mainly of quartzite, sometimes with conglomerates, phylites and quartzites, with high contents of iron, similar to banded iron formations (BIF). The remaining rubble is composed of quartz, hematite, BIFs, phylites and granite. Hematite and martite fill vacancies often found in the matrix. A surface rich in iron is commonly found in the basis portion of the sequence. This unit is formed of many isolated quartzite masses and distributed along the south and east edges of the QFe. It is estimated that the unit exceeds two metres in thickness. In this area, the Itacolomi Group lies at angles over the Sabará, Barreiro and Fecho do Funil units. The

maximum angle between the layers is about 12°.

Santo Antônio facies has been described by Barbosa (1949) in Congonhas do Campo region. This unit is composed of phylite, quartzite-phylites, metaconglomerates, quartzites and iron-quartzites (BIF). Relations of contact between the two facies are uncertain.

Almeida *et al.* (2005) and Almeida (2004) propose Itacolomi Group is restricted to its locality-kind, *i.e.* Itacolomi mountain .

2.2 Stonemasonry

This special region has been used as quartzite source to build stonemasonry monuments in Ouro Preto (Fig. 3 and 4). To do so, traditional masons have more commonly used boulders and rarely organized a quarry for the extraction of this rock. Along the slope of Itacolomi mountain, many stonemason´s marks have been found, which are concentrated in the Pocinho region, appointed here as Pocinho´s archeological site.

Figure 3 - Ouro Preto Itacolomi´s peak. Quartzite in many different colours has been extracted from the slope of this mountain, in order to build Ouro Preto´s monuments - such as the St Francisco Church (on the right hand side). Photo: Antonio Liccardo.

The extraction of quartzite blocks was a drawn-out process. The stone-cutters made use of sound to choose more adequate blocks for masonry, tapping the hammer on the rock. If the sound was sharp, the block would be selected; if it was dull, the rock would be discarded.

Figure 4 - Traditional stonemasonry piece made in Stonemasonry School with Itacolomi quartzite by Master Juca mason. This is is a typical baroque style pieces that predominate in 18th Century in Ouro Preto. Photo: Antonio Liccardo.

At the time, the basic cutting was done at the place of extraction and the finishing done at the work place. Transport of great blocks was always a great challenge for builders and the pieces must be finished or, probably, semi-finished *in situ*.

Figure 5 - This block has been prepared for breaking by a wedging process, but has been left in the field for unknown reasons. Photo: Rodrigo Ferreira.

This is why we can observe various blocks partially worked and left at the place of origin, as showed in Figure 5. Often is possible to find abandoned blocks by ancient stonemasons, as shown in Figures 6 and 7.

Figure 6 - Portal lintel partially completed, found in Itacolomi mountain, in the ancient track road. Photo: Rodrigo Ferreira.

Figure 7 – Masonry pieces abandoned in the field by ancient craftsmen. It is possible to see the holes of wedges. Photo: Carlos Pereira.

3 RESULTS

The geological study undertaken in a segment of Itacolomi range, on the road to Itacolomi's Peak, has permitted the definition of six types of quartzite by their physical characteristics and by their composition:

Facies A: The rock is compounded by macroscopic crystals of quartz, sericite (white mica) and magnetite. The Mesh varies from thin to medium-thin. Among all types, this is the one which shows the smallest granulation. They are relatively homogeneous bodies with massif aspect and do not show crossed stratification. They present a thickness of 140 metres. The sericite's pallets show good preferential orientation. The rock contains about 5% magnetite.

Facies B: The rock consists of quartz, sericite and magnetite, from medium to thick Mesh, with bigger grains of magnetite, circa 2mm, dispersed in the rock. Crossed stratum from small to medium size may be present. Frequently, the presence of sparce thick fragments may be noticed in the matrix. In this case the sets show a magnetite track. It is about 125 metres thick.

Facies C: These are meta-conglomerates from thick to very thick granulation which consists of quartz rubbles and matrix sand, medium to thick. It contains in general euhedric magnetite crystals. It is about 35 metres thick.

Facies D: Rock constituted of quartz, sericite and magnetite, clearly presenting internal schist. The Mesh is variable, the grains are subangulous to subrounded and badly selected. There is much more quartz here than the other components, probably more than 70% of the rock composition - and magnetite less than 5%. It presents crossed strata from small to medium size, of consistent shape in all sections. The sets show a magnetite track. Decimetric levels of meta-conglomerates can be present. It is about 80 metres thick.

Facies E: Rock constituted by quartz, sericite and magnetite. The Mesh varies from thin to medium and the grains are found sub-rounded and more selectively.

It presents a stratification which is flat-parallel (tabular). Thickness is around 95 metres. The constituted minerals have a preferable orientation. Sericite is found in small quantities, about 15% of the rock composition; so less than 5% is magnetite and the rest is quartz.

Facies F: Rock constituted of quartz, sericite and magnetite; however, sericite is present, apparently in smaller quantity, consequently increasing the content of quartz on the rock. The grains of magnetite are found dispersed in the rock; sericite and quartz are found orientated, though. The mesh varies from medium to thick (the latter is predominant). Crossed strata from small to medium are frequent. Rare levels of thin conglomerates are found. Thickness is about 10 meters.

4 FINAL COMMENTS

Stonemasonry monuments in Ouro Preto city (built in the 18th Century using quartzite as the main rock) and the geology of region have been studied, in order to compare the rocks and understand traditional extraction criteria. Among the rocks found in Itacolomi mountain, six facies of quartzite were analysed and classified. The results can be useful to find sources of rock to maintain the stone monuments. The lithological characterization also facilitates the understanding of production process in the 18th Century. The materials left by ancient stonemasons in Itacolomi's slope may allow the creation of an archeological park, and this preliminary data must be useful as geological support.

The program is supported by private companies and government agencies, such as: PETROBRAS, Ministry of Culture (MINC), Fundação de Amparo à Pesquisa do Estado de Minas Gerais (FAPEMIG), Fundação Gorceix, Fundação de Apoio da Universidade Federal de São João Del Rei (FAUF), Conselho Nacional de Pesquisa (CNPq), Universidade Federal de Ouro Preto (UFOP) and Novelis S.A.

5 REFERENCES

ALMEIDA L. G. 2004. *Evolução Tectônica da porção central do sinclinal Dom Bosco, Quadrilátero Ferrífero - Minas Gerais.* Dep. de Geologia da Universidade Federal de Ouro Preto. Dissertação de Mestrado, 110p;

ALMEIDA L. G., CASTRO P. T., ENDO I., FONSECA M. A. 2005. O Grupo Sabará no Sinclinal Dom Bosco, Quadrilátero Ferrífero: Uma Revisão Estratigráfica. *Rev. Bras. Geoc.* 35(2):177-186;

BARBOSA O. 1949. Contribuição à geologia do centro de Minas Gerais. *Miner. Metal.*, 14(79): 3-19;

CHEMALE F. Jr., ROSIÈRE C. A., ENDO, I. 1994. The tectonic evolution of the Quadrilátero Ferrífero, Minas Gerais, Brazil. *Prec. Res.*, 65:25-54;

COSTA A. F. da. 1992. Feições microestruturais das rochas do Complexo Granito-Gnáissico Caeté no contato com o Grupo Nova Lima na região de Caeté, Quadrilátero Ferrífero, Minas Gerais. *Rev. Esc. Minas*, 45(1/2): 35-37;

DORR J. V. N. II. 1969. Physiographic, stratigraphic and structural development of the Quadrilátero

Ferrífero, Minas Gerais, Brazil. USGS/DNPM. *Professional Paper 641-A*. 110p;

ENDO I. & NALINI H. A. Jr. 1992. Geometria e cinemática das estruturas extensionais e compressionais na borda oeste do Sinclinal Moeda, Quadrilátero Ferrífero. *Rev. Esc. Minas*, 45(1/2): 15-17;

GOMES C. J. S. 1985. *Strukturelle und texturelle untersuchungen im Bação Komplex und seinen rahmengesteine, Eisernes Viereck*. Clausthal. 190p. (Tese de Doutoramento, Technischen Universität Clausthal);

GOMES C. J. S. 1986. Estudos estruturais e texturais no Complexo de Bação e nos metassedimentos adjacentes, Quadrilátero Ferrífero, Minas Gerais. In: CONGRESSO BRASILEIRO DE GEOLOGIA, 34. Goiânia, 1986. *Anais...* Goiânia, SBG. 3, p.1232-1245;

GOMES C. J. S. 1989. Estudos microtexturais nos xistos Nova Lima, na borda do Complexo Bação, Quadrilátero Ferrífero, Minas gerais. *Rev. Esc. Minas*, 42:3-6;

HIPPERTT J. F., BORBA, R. P., NALINI H. A. Jr. 1992. O contato Formação Moeda-Complexo Bonfim: Uma zona de cisalhamento normal na borda oeste do Quadrilátero Ferrífero, MG. *Rev. Esc. Minas*, 45(1/2): 32-34;

Tailing Impoundment Site Selection (TISS) by Fuzzy Multi-Attribute Group Decision Making

M. Golestanifar
Young Researchers Club, Science and Research branch, Islamic Azad University, Tehran, Iran.
A.Aghajani Bazzazi
Department of Mining Engineering, Savadkooh branch, Islamic Azad University, Polsefid, Iran.

ABSTRACT Tailing dam is one of the most important mining task interfaces with surrounding environment even as long as many years after ore reserve exhaust. Therefore appropriate design and management respect to future limitations of environmental regulations is required. Recently, multiple criteria effect on tailing impoundment site selection (TISS) makes it complex as the conventional procedures unable to answer. The systematic approach of multi attribute decision making helps decision makers select the most preferable decision and provides the basis of a decision support system. This paper developed new strategy based on Fuzzy Multi Attribute Group Decision Making (FMAGDM) methods include: Technique for Order Preference by Similarity to Ideal Solution, and Analytical Hierarchy Process in fuzzy group environment. To demonstrate the strategy's efficiency, a hypothetical case is processed and results are compared and ranked so that the most preferable option is identified.

1 INTRODUCTION

The increasing demand for minerals and ascending price make it possible to process ores in lower grade that means more tailing and more environmental disturbance. Tailing management apart from its necessary operating cost usually has a considerable portion in capital cost of a mining plan. On the other hand more countries enforce rigid rules to control the tailing dams' contaminations which in some cases shut the mines down (Akbari et.al 2007).

Tailings impoundments are probably the largest structures built by man. Unlike a water dam, they cannot be breached at the end of their serviceable life: they will exist for many centuries and may impact the environment as they respond to the same natural forces which erode and level the surrounding landscape (Caldwell et.al 1983). Because of their importance, a new tailings impoundment site selection (TISS) to completely undertaking many conflicting factors and represents is needed. These factors are both qualitative and quantitative. For the qualitative attributes, defining exact assessments is impossible. Also some of the quantitative factors are uncertain or

collection exact measures are not cost-effective. Judgments about preference effecting factors are often vague and complex so decision makers (DMs) cannot estimate their preferences with an exact scale. Hence, only linguistic assessments are applicable.

Formerly, TISS was a simple procedure using evaluating relative distances from mill location, in the function of the shortest was the best. Since last two-three decades the environmental impacts has been taking into a great consideration. The mine engineers and environmental agencies usually have different objects which come from their job and organization purposes. Mine engineers often interested in increasing the productivity, decreasing the costs and maximizing the profit, while environmental societies believe that public health is the highest goal (Osanloo et.al 2003).

The distinctions between the mining operation participants and such agencies are neither possible to solve nor eliminate completely. The best site is a location which meets both objectives.

To cover mentioned complexities, this paper performed a new strategy based on Fuzzy Multi Attribute Group Decision Making (FMAGDM) by two groups of mine engineers with different opinions: maximum profitability, and sustainable development.

Group decision is usually understood as the reduction of different individual preferences on a given set to a single collective preference (Lu et.al 2007).

Nowadays, there are few approaches such as Analytic hierarchy process (AHP) and Technique for Order Preference by Similarity to Ideal Solution (TOPSIS) which solve the group selection problem with multiple criteria in a widely acceptable way.

Major weaknesses of TOPSIS are in withholding for weight elicitation, and consistency checking for judgments (Shih et. al 2007). However, AHP's employment has been significantly restrained by the human capacity for information processing, and thus the number seven plus or minus two would be the ceiling in comparison (Saaty and Ozdemir, 2003). From this viewpoint, TOPSIS alleviates the requirement of paired comparisons and the capacity limitation might not significantly dominate the process. Hence, it would be suitable for cases with a large number of attributes and alternatives, and especially handy for objective or quantitative data given. Thus, for making the comprehensive strategy, integrated fuzzy Group Analytical Hierarchy Process (FGAHP) to weight up criteria in group environment and fuzzy Technique for Order Preference by Similarity to Ideal Solution (FTOPSIS) has been employed to ranking alternatives.

2 DEVELOPMENT A NEW STRATEGY

With respect to the mentioned regards, decision making about tailing dam location is one of the critical tasks in mine planning. Therefore unlike the past, the solution strategy should be fit to the problem appropriately. This paper, found FMAGDM as suitable tools to handle this problem. Steps of this strategy are shown in figure 1. There are two groups of mine engineers with different tendencies as DMs who interested in increasing the productivity, decreasing the costs, and maximizing the profit (group A) and another group rely on environmental sustainability (group B). In the first step, concerning criteria about decision making by group A and B are elucidated. Then, it refers to groups to evaluate relative importance of attributes by FGAHP.

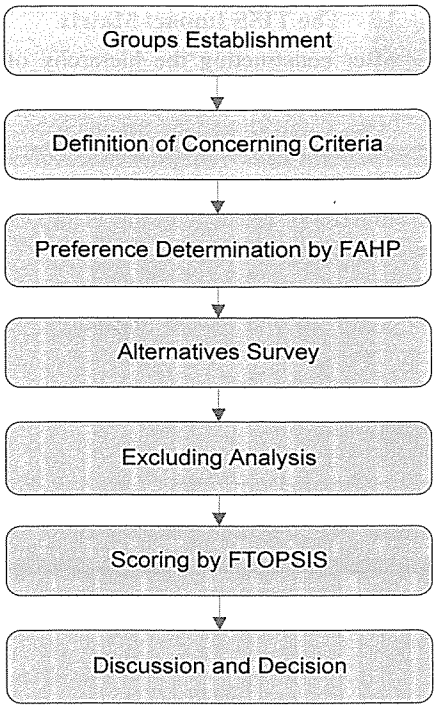

Figure 1. Structure of new TISS

To achieve possible options, alternatives that are known in survey step, process by excluding analysis. The final decision will be made by grading the possible alternatives using FTOPSIS method and discussing about that.

2.1 Possible Options Survey

A radius of 10km to 50km around the mill, depending on project specifics, should be considered in the alternative survey (Robertson et.al 1981). Candidate site may be possible for one or more embankment options: 1) Valley impoundments 2) Ring dikes 3) In-pit disposal (open pit mines) 4) Specially dug pits 5) Underground mines (mine backfilling) 6) Deep lake disposal (Vick 1990). Therefore, it may be possible to have more than an alternative in particular sites.

Some attention should be given to the capacity of the identified sites. It is preferable to have only one impoundment of adequate capacity instead of a cluster of small ones (Robertson et.al 1981).

Some of alternatives may take the top of ranking while being undesirable cause including unacceptable measures of an attributes that had been not very important. To tackle this error, excluding analysis should be done. Robertson et.al (1980) introduced unacceptable excluding regards consist: visual, land-use/ecological, airborne release, seepage release, stability release, and operational cost. For more detail see (Robertson et al. 1980). All remained alternatives are "possible alternative" and appointed to detail study.

2.2 Effecting factors in TISS

Sixty one numbers of extracted leading evaluation attributes from literatures were categorized into five main clusters as criteria to form first hierarchical level of overall goal that is optimum tailing dam site. The attributes level consists of Technical (T), Stability (St), Project economics (P), Environmental (E), and Social-Economic (S) factors (Figure 2).

Then each main criterion was protracted to a sub-attribute level (Figures 4 to 7). Note the rest on Saaty and Ozdemir (2003), number or attributes in each hierarchy cluster should be less than seven plus or minus two.

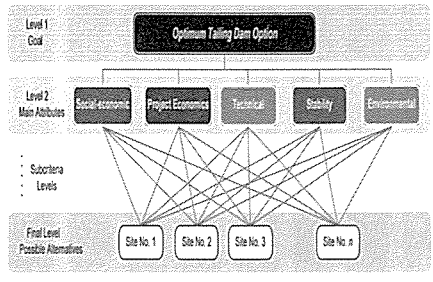

Figure 2. Hierarchy of TISS

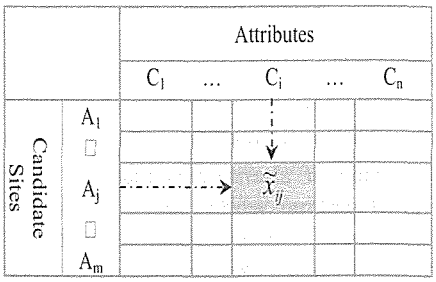

Figure 3. Representation of decision matrix

2.3 The TISS Impact Matrix

After constructing the hierarchy of TISS problem, to introduce MADM methods, candidate sites (A_j), attributes (C_i), and measures of performance of alternatives with respect to the attributes (x_{ij}) must be established during an impact matrix (Figure 3).

Here, it is supposed that experts of group A and B on measures of

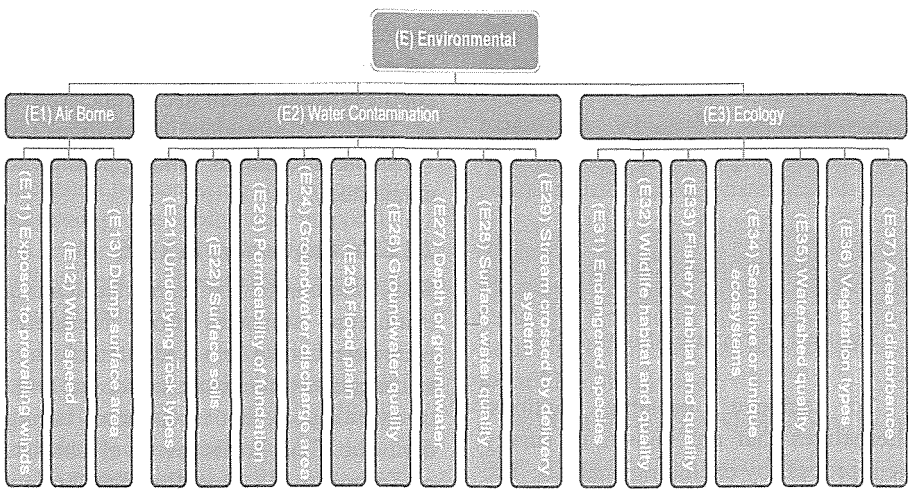

Figure 4. Environmental sub-criteria cluster

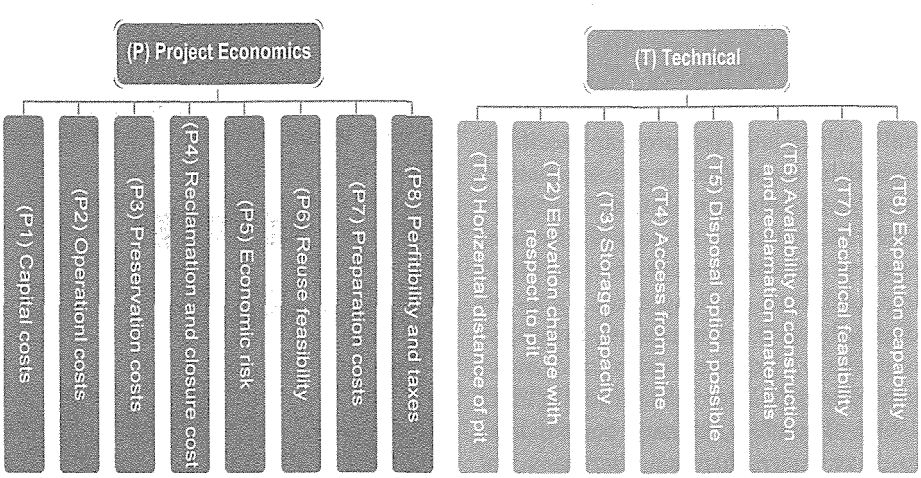

Figure 5. Project Economics & Technical sub-criteria clusters

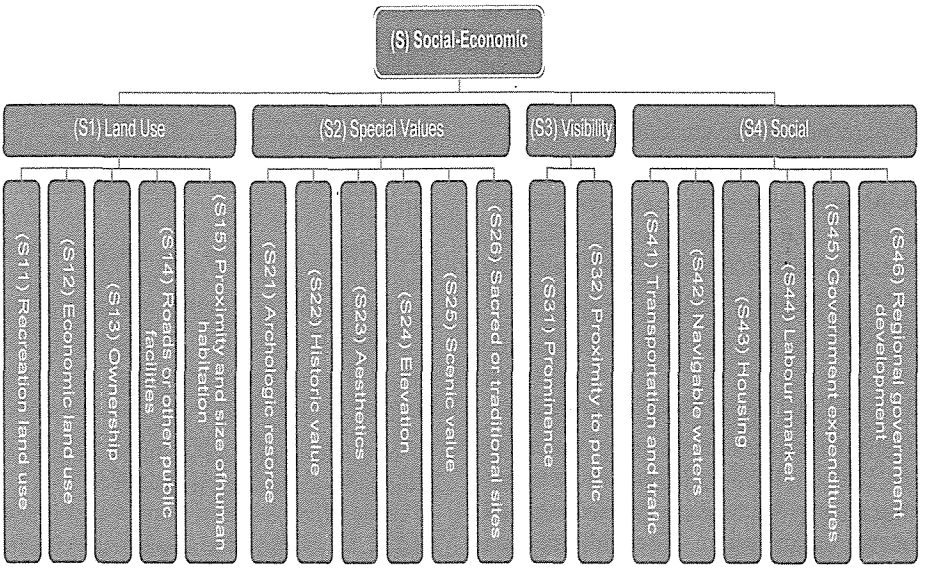

Figure 6. Social-Economic sub-criteria cluster

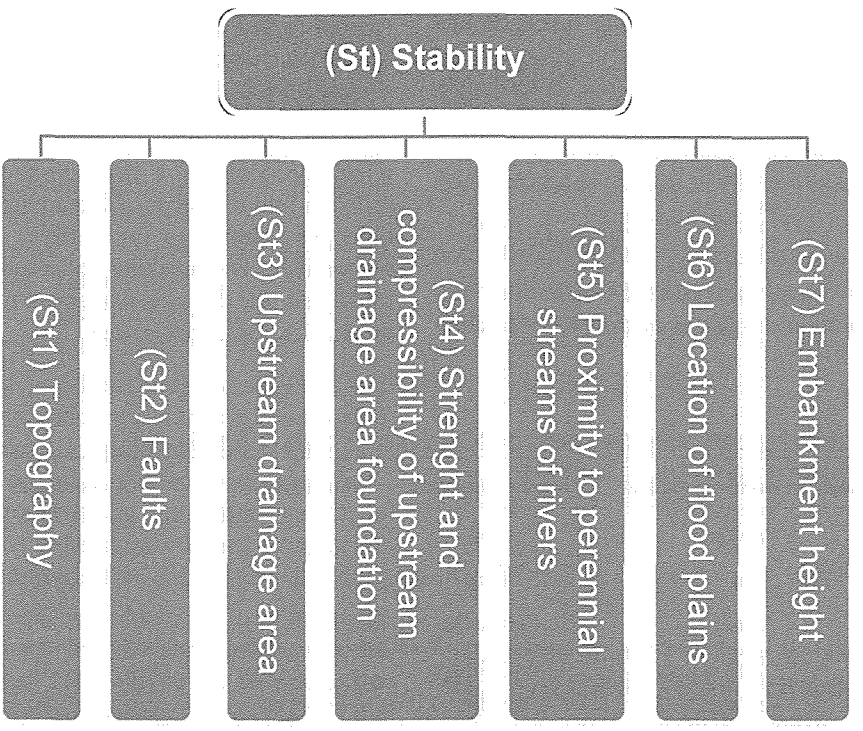

Figure 7. Stability sub-criteria cluster

performance in impact matrix have conjunct opinion. Impact matrix may consists of quantitative and qualitative measures of alternatives performance with respect to the attributes.

In this case qualitative measures must be exchanged to quantities. For this attempt, as it has been shown in Table 1, fuzzy subjective measure scale has been used to exchange subjective measure of attribute.

3 FUZZY SETS AND FUZZY NUMBERS

The concept of a fuzzy set was introduced by Zadeh (1965). He presented ideas concerning fuzzy decision-making and fuzzy optimization. The applications of the fuzzy set theory in this study are elaborated in uncertainly of impact matrix entries and linguistic variable judgments of DMs. They have been shown by triangular fuzzy number (TFN). TFN membership functions are usually described as:

$$\mu_{\tilde{a}}(x)=\begin{cases}\dfrac{x-a_1}{a_2-a_1} & a_1 < x \le a_2\\ \dfrac{a_3-x}{a_3-a_2} & a_2 < x \le a_3\\ 0 & \text{Otherwise}\end{cases} \quad (1)$$

Some of utilized operations in solution strategy according to researches by Zadeh (1965), Zimmermann (1991), and Kaufmann (1985) are described below:

Let and be two triangular fuzzy numbers, then:

a) Fuzzy numbers summation is defined by:

$$\tilde{a}+\tilde{b}=(a_1+b_1,a_2+b_2,a_3+b_3) \quad (2)$$

b) Also, fuzzy numbers multiplication is defined by:

$$\tilde{a}\times\tilde{b}=(a_1\times b_1,a_2\times b_2,a_3\times b_3) \quad (3)$$

c) On the other hand, fuzzy numbers division is defined as follows:

$$\frac{\tilde{a}}{\tilde{b}}=\left(\frac{a_1}{b_3},\frac{a_2}{b_2},\frac{a_3}{b_1}\right) \quad (4)$$

d) Vertex method is defined to calculate the distance between them, according to Equation (5):

$$d(\tilde{a},\tilde{b})=\sqrt{\frac{1}{3}[(a_1-b_1)^2+(a_2-b_2)^2+(a_3-b_3)^2]} \quad (5)$$

4 FGAHP METHOD

Saaty (1980, 2000) developed AHP, which decomposes a decision-making problem into a system of hierarchies of objectives, attributes (or criteria), and alternatives. By breaking the problem into levels, the decision maker can focus on smaller sets of decisions.

Table1: Fuzzy subjective measure scale (after Orlando & Aguilo 2008)

Subjective measure of attribute	Relative importance	Fuzzy symbol	Assigned value
Very low	Equal	$\tilde{1}$	(1, 1, 1)
Low	Weak	$\tilde{3}$	(2, 3, 4)
Average	Fairly strong	$\tilde{5}$	(4, 5, 6)
High	Very strong	$\tilde{7}$	(6, 7, 8)
Very high	Absolute	$\tilde{9}$	(9, 9, 9)
Intermediate values		$\tilde{2},\tilde{4},\tilde{6},\tilde{8}$	[(a-1), a, (a+1)]

Table1: Fuzzy subjective measure scale (after Orlando & Aguilo 2008)

AHP continues to be the most highly regarded and widely used decision-making method.

An essential feature of decision problems is the DM's preferences. Preferences on criteria refer to expressions of the relative importance of criteria. They are generally called weights; the weight for criterion j is w_j. It is usually assumed that $w_j > 0$ for all criteria. Usually weights are normalized to sum to 1 (Venkata 2007).

Eigenvector method probably is the best-known and most widely used in subjective weighing of attributes taking part in AHP method. The eigenvector method of AHP is commonly used to determine the relative normalized weights of the attributes, because of its *simplicity, easy determination of the* maximum Eigen value, and reduction in inconsistency of judgments (Saaty 2000). Especially where the subjective judgments of different individuals constitute an important part of the eigenvector method, it is a powerful weighing methodology in order to determine the priorities among different criteria. The eigenvector method by a group DMs encompasses six steps as summarized as follows:

Step 1: Determine the objective and the evaluation attributes by decomposing the decision problem into a hierarchy with a goal at the top, criteria and sub-criteria at levels and sub-levels of and decision alternatives at the bottom of the hierarchy (figure 2).

Step 2: construct the fuzzy judgment matrices. The decision makers use the defined scale (Table 1) to assess the priority score (Saaty 1980, 2000). If the decision making problem consists of n criteria, and K DMs; each fuzzy judgment matrices ($\widetilde{A}_1, \widetilde{A}_2, \widetilde{A}_3, ..., \widetilde{A}_k$) take the form:

$$\widetilde{A}^k_{n\times n} = \begin{array}{c} \{k\} \\ C_1 \\ C_2 \\ \vdots \\ C_n \end{array} \begin{array}{c} \begin{array}{cccccc} C_1 & C_2 & C_3 & \cdots & C_n \end{array} \\ \begin{bmatrix} \widetilde{a}^k_{11} & \widetilde{a}^k_{12} & \widetilde{a}^k_{13} & \cdots & \widetilde{a}^k_{1n} \\ \widetilde{a}^k_{21} & \widetilde{a}^k_{22} & \widetilde{a}^k_{23} & \cdots & \widetilde{a}^k_{2n} \\ \vdots & \vdots & \vdots & \ddots & \vdots \\ \widetilde{a}^k_{n1} & \widetilde{a}^k_{n2} & \widetilde{a}^k_{n3} & \cdots & \widetilde{a}^k_{nn} \end{bmatrix} \end{array} \quad (6)$$

$$\widetilde{a}^k_{n\times n} = 1, \widetilde{a}^k_{ji} = 1/\widetilde{a}^k_{ij}, \widetilde{a}_{ii} \neq 0$$

Where a_{ij} denotes the comparative importance of attribute i with respect to attribute j.

Step 3: Establish aggregate matrix ($\widetilde{P}_{ij}$) by mix the various judgment matrices from all decision makers. As for group decision making with multiple experts, there are two most widely employed ways to obtain group priorities in AHP, the aggregation of individual judgments (AIJ) and the aggregation of individual priorities (AIP) (Escobar et.al 2007). Herein AIJ method employed:

$$\widetilde{P}_{ij} = [\prod_{k=1}^{K} \widetilde{a}_{ij}^{\beta_k}]^{1/\sum \beta_k} \quad (7)$$

That β_k is relative importance of K^{th} decision maker (Sun & Li 2009).

Step 4: Find the fuzzy relative normalized weight ($\widetilde{V}_j$) of each attribute by calculating the geometric mean of the i^{th} row as follow:

$$\widetilde{V}_j = [\prod_{i=1}^{n} \widetilde{p}_{ij}]^{1/n} \quad (8)$$

And then normalize the geometric means of rows in the comparison matrix. This can be represented as:

$$\widetilde{W}_j = \frac{\widetilde{V}_j}{\sum_{j=1}^{m} \widetilde{V}_j} \quad (9)$$

Therefore a set of n fuzzy weights $\widetilde{W}_1, \widetilde{W}_1, \widetilde{W}_2, ..., \widetilde{W}_n$ $\widetilde{W}_2 \widetilde{W}_j$ is obtained.

Step 5: Do consistency analysis to ensure of results accuracy by following:

$$\tilde{A} \times \tilde{w}_j = \lambda_{max} \times \tilde{w}_j \ , \ i = 1,2,...,n \quad (10)$$

Then consistency index (CI) is calculated as:

$$CI = \frac{\lambda_{max} - n}{n - 1} \quad (11)$$

Step 6: The last ratio that has to be calculated is CR (consistency ratio).

The formulation of CR is:

$$CR = \frac{CI}{RI} \quad (12)$$

If the CR is less than 10%, the comparisons are acceptable, otherwise not. RI represents the average index for randomly generated weights. The table of random indexes of the matrices of order 1–15 can be seen in Saaty (1980).

Since $\lambda_{max}\lambda_{max}\lambda_{max}$ is a triangular number, it has to be defuzzified into a crisp number to compute the CI. *Orlando et al. (2008)* suggest here using the central value of $\lambda_{max}\lambda_{max}\lambda_{max}$, because of the symmetry of the triangular number, the central value corresponds to the center of the triangular area.

5 THE FTOPSIS METHOD

The TOPSIS method was developed by Hwang and Yoon (1981). Hwang explained that a Multiple Criteria Decision Making (MCDM) problem may be viewed as a geometric system. The m alternatives that are evaluated by *n* attributes are similar to *m* points in an n-dimensional space.

This method is based on the concept that the chosen alternative should have the shortest Euclidean distance from the "ideal" solution which consists of all best data attainable, and the farthest from the "worst" solution that consists of all worst data attainable.

The main procedure of the TOPSIS method for the selection of the best alternative from among those available is described below:

Step 1: The impact matrix components ($\tilde{X}_{ij}$ $\tilde{X}_{ij}$) need to be normalized in order to obtain the dimensionless environment ($\tilde{r}_{ij}$ $\tilde{r}_{ij}$) for inter-attribute comparison by equation 13.

$$\tilde{r}_{ij} = \frac{\tilde{x}_{ij}}{\sqrt{\sum_{i=1}^{m} \tilde{x}_{ij}^{\,2}}} \quad (13)$$

Step 2: A set of weights ($\tilde{w}_j$), where $\tilde{w}_j$ is the weight of the j^{th} attribute (from previous section), is incorporated to form a weighted normalized impact matrix of $\tilde{V}$ by equation 14.

$$\tilde{V} = [\tilde{v}_{ij}] = [\tilde{w}_j \tilde{r}_{ij}] \ , i = 1,2,...,m \ , j = 1,2,...,n \quad (14)$$

Step 3: Obtain the fuzzy positive ideal solution (PIS P) and fuzzy negative ideal solution (NIS) through equation 15 and 16.

$$PIS_j = \{(\max_j \tilde{V}_{ij} | i \in I), (\min_j \tilde{V}_{ij} | i \in I') | j = 1,2,...,n\}$$

$$NIS_j = \{(\min_j \tilde{V}_{ij} | i \in I), (\max_j \tilde{V}_{ij} | i \in I') | j = 1,2,...,n\} \quad (15, 16)$$

Where I and I' represent benefit and cost attributes respectively.

Step 4: Evaluate the separation measures. The separation of each alternative from the ideal one is given by the Euclidean distance in the following equations:

$$PD_i = \sum_{j=1}^{n} d(\tilde{v}_{ij}, PIS_j), \ i = 1,2,...,m \quad (17)$$

$$ND_i = \sum_{j=1}^{n} d(\tilde{v}_{ij}, NIS_j), \ i = 1,2,...,m \quad (18)$$

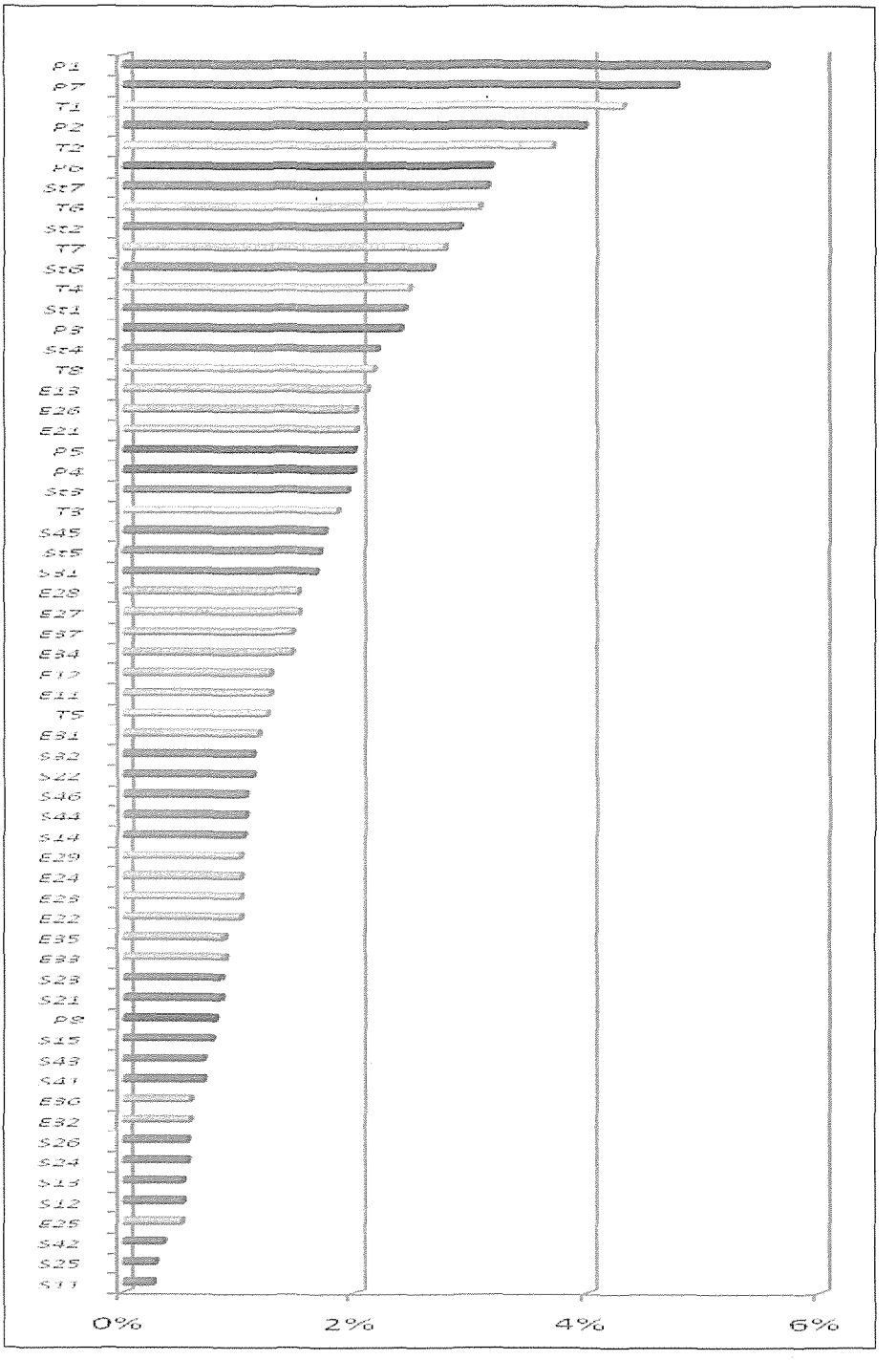

Figure 8. Global weights of the sub criteria calculated using FGAHP method

PD_i and ND_i represent Euclidean distance from positive and negative ideal solution respectively.

Step 5: The relative closeness of a particular alternative to the ideal solution (C_i) can be expressed in this step as follows.

$$C_i = \frac{ND_i}{ND_i + PD_i} \qquad (19)$$

Finally, the alternatives can be ranked according to descending order and the one with the maximum overall or composite performance score is the most preferable solution. Scope of obtained scores of alternatives is relative to 0% and 100% for hypothetical negative and positive ideal solutions respectively.

6 ILLUSTRATIVE CASE STUDY

In order to benchmark the proposed approach, a numerical example is illustrated herein. It is assumed that a company is looking for selecting a location to build a new tailing dam in five alternative sites. With consensus of two group DMs, entries of impact matrix obtained. Because of data largeness, it illustrated in a broken matrix (Table 2).

Some of entries are benefit attributes and another's are cost as superscripted with plus and minus in impact matrix respectively. Linguistic verbal measures of impact matrix have been converted to fuzzy numbers based on Table 1. Fit on FGAHP, Preferences of DMs on attributes started with establishing thirteen individual judgments matrix (Equation 2) respect to every sub-criteria cluster for each group (please see figures 3 to 8). AIJ method (equitation 7) is desirable to aggregate Individual opinions of DMs. Aggregation of different groups judgments done among equal their values ($\beta_A=\beta_B$) assumption. Then according to Equation 8 to 9, importance of attributes has been estimated. In final step of FGAHP, judgments inconstancy ratio verified. Results of FGAHP for lowest level in each cluster and main level of attributes are shown in figures 8 and 9, respectively. Note that for understanding the role of attributes in

Table 2. Impact matrix of case study (Linguistic terms)

Criteria			*Alternatives*				
Main Level	*Sub-L 1*	*Sub-L 2*	*Site 1*	*Site 2*	*Site 3*	*Site 4*	*Site 5*
Social-Economic (S)	S1	$^{-}$S11	M	VH	L	H	M
		$^{-}$S21	M	H	M	M	L
	⋮	⋮	⋮	⋮	⋮	⋮	⋮
	S4	$^{+}$S46	M-H	L	H	M	L
Environmental (E)	E1	$^{-}$E11	L	M	L	VH	L
		$^{-}$E12	M	H	VL	L-M	L
	⋮	⋮	⋮	⋮	⋮	⋮	⋮
	E3	$^{-}$E37	L-M	VL	M	H	H
Stability (St)	$^{-}$St1		L	M	M	L	VL
	$^{-}$St2		L-M	H	VH	VL-L	VL
	⋮		⋮	⋮	⋮	⋮	⋮
	$^{-}$St7		M	H	VH	VL-L	M
Project-Economics (P)	$^{-}$P1		H	VH	L	M-H	L
	$^{-}$P2		M	H	VL	H	L-M
	⋮		⋮	⋮	⋮	⋮	⋮
	$^{-}$P8		L-M	VH	VL-L	L	M-H
Technical (T)	$^{-}$T1		H	VH	L	VL	H
	$^{-}$T2		L-M	H-VH	L	VL	H
	⋮		⋮	⋮	⋮	⋮	⋮
	$^{+}$T8		M	VL	H-VH	VH	M-H

VL: very low L: low M: medium H: high VH: very high +: benefit attribute -: cost attribute

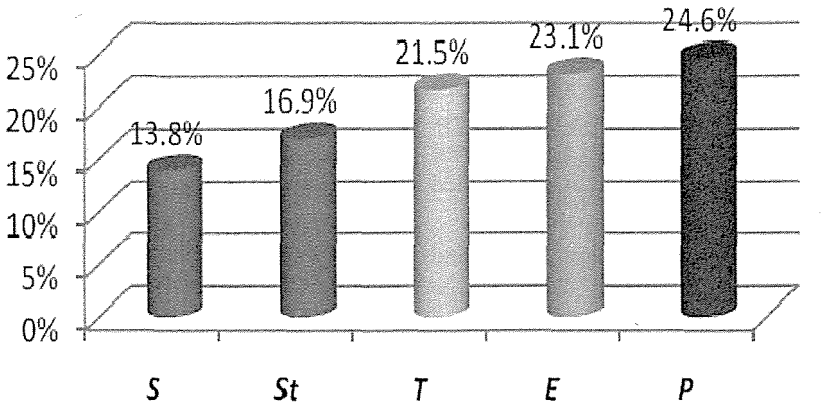

Figure 9. Global weights of the main criteria calculated using FGAHP method

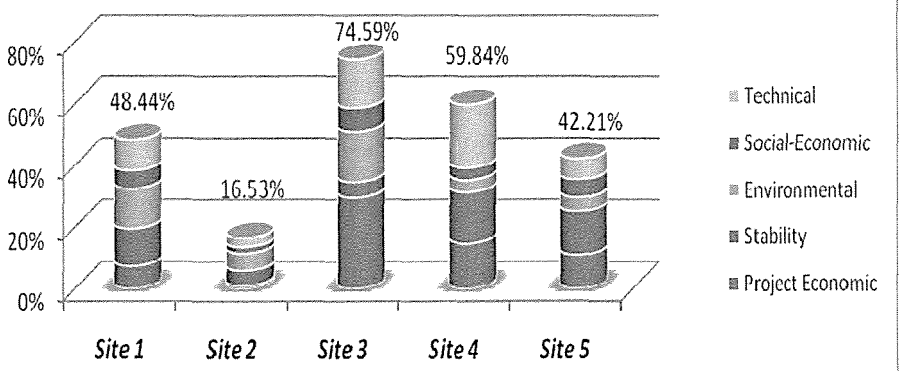

Figure 10. Preference order of alternatives by TISS method

Table 3. Impact matrix of case study (Fuzzy terms)

Criteria			*Alternatives*				
Main Level	*Sub-L 1*	*Sub-L 2*	*Site 1*	*Site 2*	*Site 3*	*Site 4*	*Site 5*
Social-Economic (S)	S1	$^{-}$S11	(4,5,6)	(9,9,9)	(2,3,4)	(6,7,8)	(4,5,6)
		$^{-}$S21	(4,5,6)	(6,7,8)	(4,5,6)	(4,5,6)	(2,3,4)
	⋮	⋮	⋮	⋮	⋮	⋮	⋮
	S4	$^{+}$S46	(5,6,7)	(2,3,4)	(6,7,8)	(4,5,6)	(2,3,4)
Environmental (E)	E1	$^{-}$E11	(2,3,4)	(4,5,6)	(2,3,4)	(9,9,9)	(2,3,4)
		$^{-}$E12	(4,5,6)	(6,7,8)	(1,1,1)	(3,4,5)	(2,3,4)
	⋮	⋮	⋮	⋮	⋮	⋮	⋮
	E3	$^{-}$E37	(3,4,5)	(1,1,1)	(4,5,6)	(6,7,8)	(6,7,8)
Stability (St)	$^{-}$St1		(2,3,4)	(4,5,6)	(4,5,6)	(2,3,4)	(1,1,1)
	$^{-}$St2		(3,4,5)	(6,7,8)	(9,9,9)	(1,2,3)	(1,1,1)
	⋮		⋮	⋮	⋮	⋮	⋮
	$^{-}$St7		(4,5,6)	(6,7,8)	(9,9,9)	(1,2,3)	(4,5,6)
Project-Economics (P)	$^{-}$P1		(6,7,8)	(9,9,9)	(2,3,4)	(5,6,7)	(2,3,4)
	$^{-}$P2		(4,5,6)	(6,7,8)	(1,1,1)	(6,7,8)	(3,4,5)
	⋮		⋮	⋮	⋮	⋮	⋮
	$^{-}$P8		(3,4,5)	(9,9,9)	(1,2,3)	(2,3,4)	(5,6,7)
Technical (T)	$^{-}$T1		(6,7,8)	(9,9,9)	(2,3,4)	(1,1,1)	(6,7,8)
	$^{-}$T2		(3,4,5)	(7,8,9)	(2,3,4)	(1,1,1)	(6,7,8)
	⋮		⋮	⋮	⋮	⋮	⋮
	$^{+}$T8		(4,5,6)	(1,1,1)	(9,9,9)	(9,9,9)	(5,6,7)

ranking results, cumulative effect of each cluster population should be regarded as well. After identification attributes weights, ranking process via FTOPSIS put forward. First, fuzzy impact matrix normalized by equation 13 and weighted normalized impact matrix is constructed (equation 14).

Positive ideal solution (*PIS*) and negative ideal solution (*NIS*) can be found during equations 15 and 16 and theirs separation measures from every alternative accomplished. In final step of FTOPSIS, relative closeness of a particular alternative to the ideal solution (C_i) C_i expressed by Equation 19. See final ranking result and cumulative portion of each main criterion in figure 10. Based on results from TISS method, "Site 3" with score 74.59% is the best alternative for designing tailing impoundment in this case. Figure 10 reflect useful information about decision making responses; "Site 3" interested in technical, project economic, and social-economic characters and should included it as main reasons of top ranking situation. However essential eliminating efforts about stability should be considered.

7 CONCLUSION

The TISS process is a technique for evaluating the suitable sites and selecting a limited number of sites by using a detailed evaluation. The consideration of the objective, subjective and critical factors can be more acquaint with the adoption of the mathematical model with the real world problems. The solution procedure was illustrated through a numerical example. At the beginning of the process the DMs had very strong opinions about the goodness of each alternative. These opinions, however, were based on only one or two points of view; namely economical versus environmental ways of thinking. The modeling of the problem through TISS framework provided a common language between actors with opposite views. This seemed to create discussion between DMs with different "right" opinions in the beginning. The multidimensional consideration of the problem broadened their views, decreasing the conflict.

REFERENCES

Akbari A., Osanloo M., Hamidian H., 2007, Suggested Method for Tailing Dam Site Selection with Analytical Hierarchy Processing (AHP): Case Study in Coal Washery Tailing Dam of Anjirtange Plant-Savadkooh-Iran, *Application of Computers and Operations Research in the Mineral Industry (APCOM), 2007*, Santiago, Chile, pp. 775-784.

Caldwell J.A., Robertson A.M.G., 1983, Selection of tailings impoundment sites, *Die Sivieleingenieur in Suid-Afrika*, pp. 537-552.

Escobar MT, Moreno-Jiménez JM., 2007, Aggregation of individual preference structures. *Group Decision and Negotiation*, 16, pp.287–301.

Hwang, C.L., Yoon, K., 1981. *Multiple Attribute Decision Making: Methods and Applications.* Springer, New York.

Kaufmann A., Gupta M.M., 1985, *Introduction to Fuzzy Arithmetic Theory and Application*, Van Nostrand Reinhold, New York.

Lu J., Zhang G., Ruan D., Wu F., 2007, *Multi-objective Group Decision Making: Methods, Software and Applications with Fuzzy Set Techniques*, Imperial College Press, London.

Orlando D., Aguilo J., 2008, "Computer-Aided Machine-Tool Selection Based on a Fuzzy-AHP approach", *Expert Systems with Applications*, 34, pp.1787–1794.

Osanloo M., Ataei M., 2003, Factors Affecting the Selection of Site for Arrangement of Pit Rock-Dump; *Journal of Mining Science*, 39, pp.148-153

Robertson A.M.G. and Moss, A., 1981, Site Selection and Optimization Studies for Mill Sites and Tailings Impoundments, *Asian Mining Conference*, pp.301-311

Robertson A.M.G., Shepherd T.A., Van Zyl D., 1980, Uranium Tailing Impoundment Site Selection, *Symposium on uranium mill tailing management*, Colorado, pp. 67-99

Saaty T. L., Ozdemir M.S., 2003, Why the Magic Number Seven Plus or Minus Two, *Mathematical and Computer Modeling*, 38, pp.233–244.

Saaty T.L., 1980, *the analytic hierarchy process*. McGraw Hill, New York.

Saaty T.L., 2000, *Fundamentals of decision making and priority theory with the AHP*. RWS Publications, Pittsburg.

Shih H.S., Shyur H.J., Lee E.S., 2007, An extension of TOPSIS for group decision making, *Mathematical and Computer Modeling*, 45, pp.801–813.

Sun J., Li H., 2009, Financial distress early warning based on group decision making, *Computers & Operations Research*, 36, pp.885 – 906.

Venkata Rao R., 2007, *Decision Making in the Manufacturing Environment*, Springer Publication.

Vick, S.G., 1990, *Planning, Design and Analysis of Tailings Dams*. BiTech Publishers Ltd.

Zadeh, L.A, 1965. Fuzzy sets. *Information and Control*, 8, pp. 338–353.

Zimmermann, H. J., 1991, *Fuzzy set theory and its applications*, Dordrecht, Kluwer.

Author Index